DESIGN OF STEEL STRUCTURES

2nd EDITION

ECCS EUROCODE DESIGN MANUALS

ECCS EDITORIAL BOARD
Luís Simões da Silva (ECCS)
António Lamas (Portugal)
Jean-Pierre Jaspart (Belgium)
Reidar Bjorhovde (USA)
Ulrike Kuhlmann (Germany)

DESIGN OF STEEL STRUCTURES – 2ND EDITION
Luís Simões da Silva, Rui Simões and Helena Gervásio

FIRE DESIGN OF STEEL STRUCTURES – 2ND EDITION
Jean-Marc Franssen and Paulo Vila Real

DESIGN OF PLATED STRUCTURES
Darko Beg, Ulrike Kuhlmann, Laurence Davaine and Benjamin Braun

FATIGUE DESIGN OD STEEL AND COMPOSITE STRUCTURES
Alain Nussbaumer, Luís Borges and Laurence Davaine

DESIGN OF COLD-FORMED STEEL STRUCTURES
Dan Dubina, Viorel Ungureanu and Raffaele Landolfo

DESIGN OF JOINTS IN STEEL AND COMPOSITE STRUCTURES
Jean-Pierre Jaspart and Klaus Weynand

DESIGN OF STEEL STRUCTURES FOR BUILDINGS IN SEISMIC AREAS
Raffaele Landolfo, Federico Mazzolani, Dan Dubina, Luís Simões da Silva and Mario d'Aniello

ECCS – SCI EUROCODE DESIGN MANUALS

DESIGN OF STEEL STRUCTURES, U. K. EDITION
Luís Simões da Silva, Rui Simões, Helena Gervásio and Graham Couchman

ECCS EUROCODE DESIGN MANUALS – BRAZILIAN EDITIONS

DIMENSIONAMENTO DE ESTRUTURAS DE AÇO
Luís Simões da Silva, Rui Simões, Helena Gervásio, Pedro Vellasco, Luciano Lima

INFORMATION AND ORDERING DETAILS
For price, availability, and ordering visit our website **www.steelconstruct.com**. For more information about books and journals visit **www.ernst-und-sohn.de**.

DESIGN OF STEEL STRUCTURES

Eurocode 3: Design of steel structures
Part 1-1 – General rules and rules for buildings

2nd Edition

Luís Simões da Silva
Rui Simões
Helena Gervásio

ECCS CECM E K S

WILEY
Ernst & Sohn
A Wiley Brand

Design of Steel Structures

2nd Edition, 2016

Published by:
ECCS – European Convention for Constructional Steelwork
publications@steelconstruct.com
www.steelconstruct.com

Sales:
Wilhelm Ernst & Sohn Verlag für Architektur und technische Wissenschaften GmbH & Co. KG, Berlin Sales:

All rights reserved. No parts of this publication may be reproduced, stored in a retrieval system, or transmitted in any form or by any means, electronic, mechanical, photocopying, recording or otherwise, without the prior permission of the copyright owner.

ECCS assumes no liability with respect to the use for any application of the material and information contained in this publication.

Copyright © 2016 ECCS – European Convention for Constructional Steelwork

ISBN (ECCS): 978-92-9147-134-8
ISBN (Ernst & Sohn): 978-3-433-0316-36

Legal dep.: Printed in Multicomp Lda, Mem Martins, Portugal
Photo cover credits: Wolfdream16499 / Shutterstock.com

TABLE OF CONTENTS

FOREWORD xiii

PREFACE xv

Chapter 1

INTRODUCTION 1

1.1. General Observations 1

1.2. Codes of Practice and Normalization 3

1.2.1. Introduction 3

1.2.2. Eurocode 3 6

1.2.3. Other standards 7

1.3. Basis of Design 8

1.3.1. Basic concepts 8

1.3.2. Reliability management 9

1.3.3. Basic variables 13

1.3.3.1. Introduction 13

1.3.3.2. Actions and environmental influences 13

1.3.3.3. Material properties 14

1.3.3.4. Geometrical data 15

1.3.4. Ultimate limit states 15

1.3.5. Serviceability limit states 16

1.3.6. Durability 18

1.3.7. Sustainability 19

1.4. Materials 21

1.4.1. Material specification 21
1.4.2. Mechanical properties 22
1.4.3. Toughness and through thickness properties 25
1.4.4. Fatigue properties 27
1.4.5. Corrosion resistance 27
1.5. Geometric Characteristics and Tolerances 28

Chapter 2
STRUCTURAL ANALYSIS 33
2.1. Introduction 33
2.2. Structural Modelling 34
2.2.1. Introduction 34
2.2.2. Choice of member axis 36
2.2.3. Influence of eccentricities and supports 38
2.2.4. Non-prismatic members and members with curved axis 39
2.2.5. Influence of joints 44
2.2.6. Combining beam elements together with two and three dimensional elements 51
2.2.7. Worked examples 52
2.3. Global Analysis of Steel Structures 75
2.3.1. Introduction 75
2.3.2. Structural stability of frames 77
2.3.2.1. Introduction 77
2.3.2.2. Elastic critical load 80
2.3.2.3. 2nd order analysis 86
2.3.3. Imperfections 88
2.3.4. Worked example 94
2.4. Classification of Cross Sections 108

Chapter 3

DESIGN OF MEMBERS 119

3.1. Introduction 119

3.1.1. General 119

3.1.2. Resistance of cross sections 120

3.1.2.1. General criteria 120

3.1.2.2. Section properties 121

3.1.3. Buckling resistance of members 125

3.2. Tension 125

3.2.1. Behaviour in tension 125

3.2.2. Design for tensile force 128

3.2.3. Worked examples 131

3.3. Laterally Restrained Beams 138

3.3.1. Introduction 138

3.3.2. Design for bending 139

3.3.2.1. Elastic and plastic bending moment resistance 139

3.3.2.2. Uniaxial bending 141

3.3.2.3. Bi-axial bending 142

3.3.2.4. Net area in bending 142

3.3.3. Design for shear 143

3.3.4. Design for combined shear and bending 144

3.3.5. Worked examples 146

3.4. Torsion 157

3.4.1. Theoretical background 157

3.4.1.1. Introduction 157

3.4.1.2. Uniform torsion 159

3.4.1.3. Non-uniform torsion 161

3.4.1.4. Cross section resistance in torsion 166
3.4.2. Design for torsion 173
3.4.3. Worked examples 176
3.5. Compression 186
3.5.1. Theoretical background 186
3.5.1.1. Introduction 186
3.5.1.2. Elastic critical load 186
3.5.1.3. Effect of imperfections and plasticity 192
3.5.2. Design for compression 198
3.5.3. Worked examples 204
3.6. Laterally Unrestrained Beams 212
3.6.1. Introduction 212
3.6.2. Lateral-torsional buckling 212
3.6.2.1. Introduction 212
3.6.2.2. Elastic critical moment 213
3.6.2.3. Effect of imperfections and plasticity 223
3.6.3. Lateral-torsional buckling resistance 225
3.6.4. Worked examples 229
3.7. Beam-Columns 242
3.7.1. Introduction 242
3.7.2. Classification of cross sections under bending and axial force 243
3.7.3. Cross section resistance 247
3.7.3.1. Theoretical background 247
3.7.3.2. Design resistance 249
3.7.4. Buckling resistance 253
3.7.4.1. Theoretical background 253
3.7.4.2. Design resistance 256
3.7.5. Worked examples 265

Chapter 4

ELASTIC DESIGN OF STEEL STRUCTURES 293

4.1. Introduction 293

4.2. Simplified Methods of Analysis 295

4.2.1. Introduction 295

4.2.2. Amplified sway-moment method 297

4.2.3. Sway-mode buckling length method 299

4.2.4. Worked example 300

4.3. Member Stability of Non-prismatic Members and Components 310

4.3.1. Introduction 310

4.3.2. Non-prismatic members 310

4.3.3. Members with intermediate restraints 316

4.3.4. General method 322

4.3.5. Worked example 325

4.4. Design Example 1: Elastic Design of Braced Steel-Framed Building 340

4.4.1. Introduction 340

4.4.2. Description of the structure 342

4.4.3. General safety criteria, actions and combinations of actions 344

4.4.3.1. General safety criteria 344

4.4.3.2. Permanent actions 345

4.4.3.3. Imposed loads 345

4.4.3.4. Wind actions 346

4.4.3.5. Summary of basic actions 353

4.4.3.6. Frame imperfections 353

4.4.3.7. Load combinations 356

4.4.3.8. Load arrangement 358

4.4.4. Structural analysis 359

4.4.4.1. Structural model 359

4.4.4.2. Linear elastic analysis 360

4.4.4.3. Susceptibility to 2nd order effects: elastic critical loads 361

4.4.4.4. 2nd order elastic analysis 362

4.4.5. Design checks 363

4.4.5.1. General considerations 363

4.4.5.2. Cross section resistance 365

4.4.5.3. Buckling resistance of beams 366

4.4.5.4. Buckling resistance of columns and beam-columns 366

Chapter 5

PLASTIC DESIGN OF STEEL STRUCTURES 367

5.1. General Principles for Plastic Design 367

5.1.1. Introduction 367

5.1.2. Plastic limit analysis: method of mechanisms 368

5.1.3. Code requirements for plastic analysis 372

5.2. Methods of Analysis 376

5.2.1. Introduction 376

5.2.2. Approximate methods for pre-design 376

5.2.3. Computational analysis 388

5.2.4. 2nd order effects 393

5.2.4.1. Introduction 393

5.2.4.2. Elastic critical load 394

5.2.4.3. 2nd order computational analysis 397

5.2.4.4. Simplified methods for analysis 397

5.2.5. Worked example 400

5.3. Member Stability and Buckling Resistance 410

5.3.1. Introduction 410

5.3.2. General criteria for the verification of the stability of members with plastic hinges 410

5.3.3. Bracings 411

5.3.4. Verification of the stability of members with plastic hinges 414

5.3.4.1. Introduction 414

5.3.4.2. Prismatic members constituted by hot-rolled or equivalent welded I sections 415

5.3.4.3. Haunched or tapered members made of rolled or equivalent welded I sections 417

5.3.4.4. Modification factors for moment gradients in members laterally restrained along the tension flange 420

5.3.5. Worked examples 423

5.4. Design Example 2: Plastic Design of Industrial Building 432

5.4.1. Introduction 432

5.4.2. General description 433

5.4.3. Quantification of actions, load combinations and general safety criteria 434

5.4.3.1. General criteria 434

5.4.3.2. Permanent actions 434

5.4.3.3. Imposed loads 434

5.4.3.4. Snow loads 435

5.4.3.5. Wind loads 435

5.4.3.6. Summary of basic actions 440

5.4.3.7. Imperfections 440

5.4.3.8. Load combinations 441

5.4.4. Pre-design 443

5.4.5. Structural analysis 446

5.4.5.1. Linear elastic analysis 446

5.4.5.2. 2nd order effects 448

5.4.5.3. Elastic-plastic analysis 449

5.4.6. Code checks 451

5.4.6.1. General considerations 451

5.4.6.2. Cross section resistance 451

5.4.6.3. Buckling resistance of the rafters 451

5.4.6.4. Buckling resistance of the columns 454

5.4.7. Synthesis 454

REFERENCES **455**

Annex A

FORMULAS FOR COMMON TORSIONAL CASES **465**

A.1. Cross Sectional Properties for Torsion 465

A.2. Solution of Differential Equation for Torsion 467

A.2.1 Concentrated torsional moment 467

A.2.2 Distributed torsional moment 474

Annex B

ELASTIC CRITICAL MOMENT **483**

B.1. Abacus to Calculate the Coefficients C_1, C_2 and C_3 483

B.1.1 Elastic critical moment in beams submitted to end moments simultaneously with transverse loads 483

B.1.2 Elastic critical moment of unbraced cantilevers 487

B.2. Alternative Equations for the Determination of the Elastic Critical Moment 490

FOREWORD

The development program for the design manuals of the European Convention for Constructional Steelwork (ECCS) represents a major effort for the steel construction industry and the engineering profession in Europe. Conceived by the ECCS Technical Activities Board under the leadership of its chairman, Professor Luis Simões da Silva, the manuals are being prepared in close agreement with the final stages of Eurocode 3 and its national Annexes. The scope of the development effort is vast, and reflects a unique undertaking in the world.

The publication of the first of the manuals, *Design of Steel Structures*, is a signal achievement which heralds the successful completion of the Eurocode 3 work and brings it directly to the designers who will implement the actual use of the code. As such, the book is more than a manual – it is a major textbook that details the fundamental concepts of the code and their practical application. It is a unique publication for a major construction market.

Following a discussion of the Eurocode 3 basis of design, including the principles of reliability management and the limit state approach, the steel material standards and their use under Eurocode 3 are detailed. Structural analysis and modeling are presented in a chapter that will assist the design engineer in the first stages of a design project. This is followed by a major chapter that provides the design criteria and approaches for the various types of structural members. The theories of behavior and strength are closely tied to the Eurocode requirements, making for a unique presentation of theory into practice. The following chapters expand on the principles and applications of elastic and plastic design of steel structures.

The many design examples that are presented throughout the book represent a significant part of the manual. These will be especially well received by the design profession. Without a doubt, the examples will facilitate the acceptance of the code and provide for a smooth transition from earlier national codes to the Eurocode.

Reidar Bjorhovde
Member, ECCS Editorial Board

PREFACE 2nd EDITION

The first edition of Design of Steel Structures was published by ECCS as a paperback in 2010. Since 2012, this publication is also available in electronic format as an e-book. The first edition was sold in over 100 countries and the interest for this publication was so high that a second edition would have to be printed.

The authors took the opportunity of this second edition to revise their manuscript. The standard that constitutes the object of this book, namely EN 1993-1-1, is still in application in the same versions as those that prevailed at the time of writing the first edition except for a minor amendment published in 2013. However, many comments were received by readers that resulted in the correction of some small mistakes and the rephrasing of some sentences or sections and the addition of some new material.

The new material comprises:

- A revised section dealing with the design for torsion of steel members, including a new worked example illustrating an open cross section beam subject to bending and torsional moments;
- A revised section on the elastic critical moment of beams;
- An improved explanation on the classification of cross sections subject to bending and axial force;
- An additional worked example of a beam-column with transversal loads and end moments;
- A new Annex containing formulas for common torsional cases;
- A revised and expanded Annex with formulas for elastic critical moment calculation.

The authors are indebted to Profs. E. Mirambell and K. Rasmussen for their thorough revision of the section on torsion.

Luís Simões da Silva
Rui Simões
Helena Gervásio
Coimbra, 2016

PREFACE 1st EDITION

The General rules and rules for buildings of part 1-1 of Eurocode 3 constitute the core of the code procedures for the design of steel structures. They contain the basic guidance for structural modeling and analysis of steel frameworks and the rules for the evaluation of the resistance of structural members and components subject to different loading conditions.

According to the objectives of the ECCS Eurocode Design Manuals, it is the objective of this book to provide mix of “light” theoretical background, explanation of the code prescriptions and detailed design examples. Consequently, this book is more than a manual: it provides an all-in-one source for an explanation of the theoretical concepts behind the code and detailed design examples that try to reproduce real design situations instead of the usually simplified examples that are found in most textbooks.

This book evolved from the experience of teaching Steel Structures according to ENV 1993-1-1 since 1993. It further benefited from the participation in Technical Committees TC8 and TC10 of ECCS where the background and the applicability of the various clauses of EN 1993-1-1 was continuously questioned. This book covers exclusively part 1-1 of Eurocode 3 because of the required level of detail. Forthcoming volumes discuss and apply most of the additional parts of Eurocode 3 using a consistent format.

Chapter 1 introduces general aspects such as the basis of design, material properties and geometric characteristics and tolerances, corresponding to chapters 1 to 4 and chapter 7 of EN 1993-1-1. It highlights the important topics that are required in the design of steel structures. Structural analysis is discussed in chapter 2, including structural modelling, global analysis and classification of cross sections, covering chapter 5 of EN 1993-1-1. The design of steel members subjected to various types of internal force (tension, bending and shear, compression and torsion) and their combinations is described in chapter 3, corresponding to chapter 6 of EN 1993-1-1. Chapter 4 presents the design of steel structures using 3D elastic analysis based on the case study of a

real building. Finally, chapter 5 discusses plastic design, using a pitched-roof industrial building to exemplify all relevant aspects.

Furthermore, the design examples provided in this book are chosen from real design cases. Two complete design examples are presented: i) a braced steel-framed building; and ii) a pitched-roof industrial building. The chosen design approach tries to reproduce, as much as possible, real design practice instead of more academic approaches that often only deal with parts of the design process. This means that the design examples start by quantifying the actions. They then progress in a detailed step-by-step manner to global analysis and individual member verifications. The design tools currently available and adopted in most design offices are based on software for 3D analysis. Consequently, the design example for multi-storey buildings is analysed as a 3D structure, all subsequent checks being consistent with this approach. This is by no means a straightforward implementation, since most global stability verifications were developed and validated for 2D structures.

The authors are indebted to Prof. Reidar Bjorhovde who carried out a detailed technical review of the manuscript and provided many valuable comments and suggestions. Warm thanks to Prof. David Anderson who carried out an additional detailed revision of the book and also made sure that the English language was properly used. Further thanks to Liliana Marques and José Alexandre Henriques, PhD students at the University of Coimbra, for the help with the design examples of chapter 4. Additional thanks to Prof. Tiago Abecasis who spotted innumerous “bugs” in the text. Finally, thanks to Filipe Dias and the staff of cmm and ECCS for all the editorial and typesetting work, making it possible to bring to an end two years of work in this project.

Luís Simões da Silva
Rui Simões
Helena Gervásio
Coimbra, 2010

Chapter 1

INTRODUCTION

1.1. GENERAL OBSERVATIONS

Steel construction combines a number of unique features that make it an ideal solution for many applications in the construction industry. Steel provides unbeatable speed of construction and off-site fabrication, thereby reducing the financial risks associated with site-dependent delays. The inherent properties of steel allow much greater freedom at the conceptual design phase, thereby helping to achieve greater flexibility and quality. In particular, steel construction, with its high strength to weight ratio, maximizes the useable area of a structure and minimizes self-weight, again resulting in cost savings. Recycling and reuse of steel also mean that steel construction is well-placed to contribute towards reduction of the environmental impacts of the construction sector (Simões da Silva, 2005).

The construction industry is currently facing its biggest transformation as a direct result of the accelerated changes that society is experiencing. Globalisation and increasing competition are forcing the construction industry to abandon its traditional practices and intensive labour characteristics and to adopt industrial practices typical of manufacturing. This further enhances the attractiveness of steel construction.

All these advantages can only be achieved with sound technical knowledge of all the stages in the life-cycle of the construction process (from design, construction and operation to final dismantling). The objective of the ECCS Eurocode Design Manuals is to provide design guidance on the use of the Eurocodes through a “light” overview of the theoretical background together with an explanation of the code’s provisions, supported

by detailed, practical design examples based on real structures. Each volume addresses a specific part of the Eurocodes relevant for steel construction.

This inaugural volume of the ECCS Eurocode Design Manuals addresses the Design of Steel Structures in terms of the General Rules and Rules for Buildings, covering all the topics of Part 1-1 of Eurocode 3 (CEN, 2005a), abbreviated in this book to EC3-1-1. These range from structural analysis of skeletal structures to design of members and components. More specifically, chapter 1 of this manual introduces general aspects such as the basis of design, material properties and geometric characteristics and tolerances, corresponding to chapters 1 to 4 and chapter 7 of EN 1993-1-1. It highlights the important topics that are required in the design of steel structures. Structural analysis is discussed in chapter 2, including structural modelling, global analysis and classification of cross sections, covering chapter 5 of EN 1993-1-1. The design of steel members subjected to various types of internal force (tension, bending and shear, compression and torsion) and their combinations is described in chapter 3, corresponding to chapter 6 of EN 1993-1-1. Chapter 4 presents the design of steel structures using 3D elastic analysis based on the case study of a real building. Finally, chapter 5 discusses plastic design, using a pitched-roof industrial building to exemplify all relevant aspects.

The design examples are chosen from real design cases. Two complete design examples are presented: i) a braced steel-framed building and ii) a pitched-roof industrial building. The chosen design approach tries to reproduce, as much as possible, real design practice instead of more academic approaches that often only deal with parts of the design process. This means that the design examples start by quantifying the actions. They then progress in a detailed step-by-step manner to global analysis and individual member verifications. The design tools currently available and adopted in most design offices are based on software for 3D analysis. Consequently, the design example for multi-storey buildings is analysed as a 3D structure, all subsequent checks being consistent with this approach. This is by no means a straightforward implementation, since most global stability verifications were developed and validated for 2D structures.

The scope of this manual is limited to those issues covered by Part 1-1 of EC3. Issues such as fire design and the design of joints, which are covered by Parts 1.2 and 1.8 of EN 1993, are not included in this manual. Other companion publications on fire design (Franssen and Vila Real, 2015) and

joint design (Jaspart and Weynand, 2016) address these. Seismic action is also not considered in this manual. This is because the many different options that could be adopted in the conceptual design phase would lead to completely different structures for the same architectural brief. A forthcoming manual dealing specifically with seismic design issues for buildings is planned (Landolfo *et al*, 2016).

This manual follows the code prescriptions of the Structural Eurocodes. This is done without loss of generality since the theoretical background, the design philosophy and the design examples are code independent, except when it comes to the specific design procedures.

1.2. CODES OF PRACTICE AND NORMALIZATION

1.2.1. Introduction

The European Union has spent several decades (since 1975) developing and unifying the rules for the design of structures. This work has culminated in a set of European standards called the Eurocodes which have recently been approved by member states. The foreword to each part of the set of Eurocodes contains the following statement:" *In 1975, the Commission of the European Community decided on an action programme in the field of construction, based on article 95 of the Treaty. The objective of the programme was the elimination of technical obstacles to trade and the harmonization of technical specifications. Within this action programme, the Commission took the initiative to establish a set of harmonized technical rules for the design of construction works which, in a first stage, would serve as an alternative to the national rules in force in the Member States and, ultimately, would replace them. For fifteen years, the Commission, with the help of a Steering Committee with Representatives of Member States, conducted the development of the Eurocodes programme, which led to the first generation of European codes in the 1980's. In 1989, the Commission and the Member States of the EU and EFTA decided, on the basis of an agreement between the Commission and CEN, to transfer the preparation and the publication of the Eurocodes to CEN through a series of Mandates, in order to provide them with a future status of European Standard (EN). This links de facto the Eurocodes with the*

provisions of all the Council's Directives and/or Commission's Decisions dealing with European standards (e.g. the Council Directive 89/106/EEC on construction products - CPD - and Council Directives 93/37/EEC, 92/50/EEC and 89/440/EEC on public works and services and equivalent EFTA Directives initiated in pursuit of setting up the internal market)."

The publication of the Construction Products Directive in 1989 (OJ L 040, 1989) established the essential requirements that all construction works must fulfil, namely: i) mechanical resistance and stability; ii) fire resistance; iii) hygiene, health and environment; iv) safety in use; v) protection against noise and vi) energy economy and heat retention.

The first two requirements are addressed by the following nine Structural Eurocodes. These have been produced by CEN (European Committee for Standardization) under the responsibility of its Technical Committee CEN/TC 250:

- EN 1990 Eurocode: Basis of Structural Design
- EN 1991 Eurocode 1: Actions on Structures
- EN 1992 Eurocode 2: Design of Concrete Structures
- EN 1993 Eurocode 3: Design of Steel Structures
- EN 1994 Eurocode 4: Design of Composite Steel and Concrete Structures
- EN 1995 Eurocode 5: Design of Timber Structures
- EN 1996 Eurocode 6: Design of Masonry Structures
- EN 1997 Eurocode 7: Geotechnical Design
- EN 1998 Eurocode 8: Design of Structures for Earthquake Resistance
- EN 1999 Eurocode 9: Design of Aluminium Structures

Each Eurocode contains provisions that are open for national determination. Such provisions include weather aspects, seismic zones, safety issues etc. These are collectively called Nationally Determined Parameters (NDP). It is the responsibility of each member state to specify each NDP in a National Annex that accompanies each Eurocode.

More recently (July 2013) the Construction Products Directive was replaced by the Construction Products Regulation (OJ L 088, 2013). This document adds an additional basic requirement: sustainability. This seventh basic requirement must follow the standards prepared by CEN/TC 350 and should be incorpared in future revisions of the Eurocodes.

The Structural Eurocodes are not, by themselves, sufficient for the construction of structures. Complementary information is required on: the

products used in construction (“Product Standards”, of which there are currently about 500);

- the tests used to establish behaviour (“Testing Standards”, of which there are currently around 900);
- the execution standards used to fabricate and erect structures (“Execution Standards”).

The flowchart in Figure 1.1 illustrates the full range of information required. It also illustrates the relationship between the Construction Products Regulation, the Eurocodes and their supporting standards. More detailed information on the development process of the Eurocodes can be found in Dowling (1992) and Sedlacek and Muller (2006).

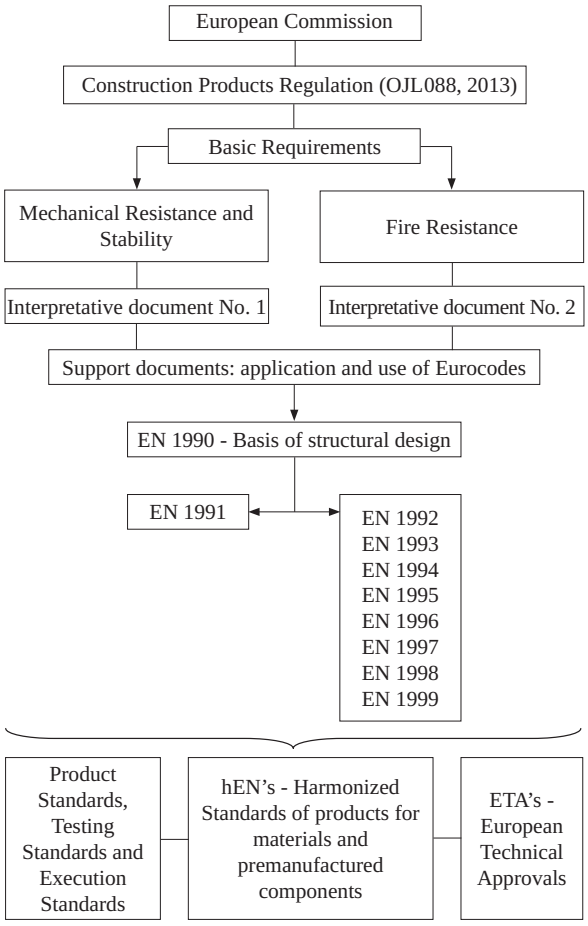


Figure 1.1 – European normative structure for the construction sector

Initially the Eurocodes were presented as Pre-Standards (ENVs), and between 2002 and 2007 were converted in to European Standards (ENs). This was followed by the development and publication of the National Annexes in each CEN country and the translation of the Eurocodes into the various national languages. After a period of coexistence the Eurocodes replaced all conflicting national standards from 2010.

The development of technical rules is also taking place outside Europe. Codes such as the North American AISC code, the Chinese code and the Australian code contain alternative design procedures that sometimes appear to be quite different, mostly because they reflect local engineering tradition.

1.2.2. Eurocode 3

EN 1993, Eurocode 3: Design of Steel Structures (abbreviated in this book to EC3) is divided in the following parts:

EN 1993-1	General rules and rules for buildings
EN 1993-2	Steel bridges
EN 1993-3	Towers, masts and chimneys
EN 1993-4	Silos, tanks and pipelines
EN 1993-5	Piling
EN 1993-6	Crane supporting structures

EN 1993-1, Eurocode 3: Design of Steel Structures - General rules and rules for buildings is further sub-divided in the following 12 sub-parts:

EN 1993-1-1	General rules and rules for buildings
EN 1993-1-2	Structural fire design
EN 1993-1-3	Cold-formed thin gauge members and sheeting
EN 1993-1-4	Stainless steels
EN 1993-1-5	Plated structural elements
EN 1993-1-6	Strength and stability of shell structures
EN 1993-1-7	Strength and stability of planar plated structures transversely loaded
EN 1993-1-8	Design of joints
EN 1993-1-9	Fatigue strength of steel structures
EN 1993-1-10	Selection of steel for fracture toughness and through-thickness properties

EN 1993-1-11	Design of structures with tension components made of steel
EN 1993-1-12	Supplementary rules for high strength steel

According to the normative framework described in section 1.2.1, EC3 is used together with a series of complementary standards. The execution standard for steel structures EN 1090-2 (CEN, 2011) guarantees an execution quality that is compatible with the design assumption in EC3. The product standards provide the characteristic properties of the materials used, that in turn must conform to the quality control procedures specified in the test standards. Finally, the EC3 National Annexes specify the national parameters relating to actions and safety levels, as well as some options concerning design methodologies.

1.2.3. Other standards

EN 1090: Execution of structures in steel and aluminium (CEN, 2011), establishes the execution conditions compatible with the design prescriptions of EC3. In particular, it establishes the execution classes and the tolerances of structural components. It is noted that the fulfilment of these tolerances and of the other requirements of EN 1090 constitutes necessary conditions for the validity of the EC3 rules. EN 1090 is organised in 3 parts:

- EN 1090-1: Steel and aluminium structural components – Part 1: General delivery conditions
- EN 1090-2: Technical requirements for the execution of steel structures
- EN 1090-3: Technical requirements for the execution of aluminium structures

Part 2 is divided in the following 12 chapters (including 12 annexes):

- Chapter 1: Scope
- Chapter 2: Normative references
- Chapter 3: Terms and definitions
- Chapter 4: Specifications and documentation
- Chapter 5: Constituent products
- Chapter 6: Preparation and assembly
- Chapter 7: Welding

- Chapter 8: Mechanical fastening
- Chapter 9: Erection
- Chapter 10: Surface treatment
- Chapter 11: Geometrical tolerances
- Chapter 12: Inspection, testing and correction

The other relevant standards for steel structures can be grouped into standards for materials (steel, steel castings, welding consumables, mechanical connectors, high-resistance steel cables and support devices), fabrication, welding, testing, assembly, protection against corrosion and other complementary standards.

1.3. BASIS OF DESIGN

1.3.1. Basic concepts

Eurocode 3 must be used in a consistent way with EN 1990 Eurocode: Basis of structural design, EN 1991 Eurocode 1: Actions on Structures, EN 1998 Eurocode 8: Normative rules for the design of earthquake resistant structures, and EN 1997 Eurocode 7: Geotechnical design.

Chapter 2 of EC3-1-1 introduces and complements the normative rules included in these standards. According to the basic requirements specified in EN 1990, a structure must be designed and executed so as to perform the functions for which it was conceived, for a pre-determined service life. This includes ensuring that the conditions that prevent failure (ultimate limit states) are verified, as well as conditions that guarantee proper performance in service (serviceability limit state) and those related to durability (among others, protection against corrosion). These basic requirements should be met by: i) the choice of suitable materials; ii) appropriate design and detailing of the structure and its components and iii) the specification of control procedures for design, execution and use.

The limit states shall be related to design situations, taking into account the circumstances under which the structure is required to fulfil its function. According to EN 1990 (CEN, 2002a) these situations may be: i) persistent design situations (conditions of normal use of the structure); ii) transient design situations (temporary conditions); iii) accidental design

situations (exceptional conditions, e.g. fire or explosion) and iv) seismic design situations. Time dependent effects, such as fatigue, should be related to the design working life of the structure.

The Ultimate Limit States (ULS) correspond to states associated with failure of the structure, endangering people's safety; in general, the following ultimate limit states are considered: loss of equilibrium considering the structure as a rigid body, failure by excessive deformation, transformation of the structure or any part of it into a mechanism, rupture, loss of stability and failure caused by fatigue or other time-dependent effects.

The Serviceability Limit States (SLS) correspond to a state beyond which the specific service conditions, such as the functionality of the structure, the comfort of people and acceptable appearance are no longer met; in steel structures, limit states of deformation and of vibration are normally considered.

The requirements for limit state design are, in general, achieved by the partial factor method as described in section 6 of EN 1990; as an alternative, a design directly based on probabilistic methods, as described in Annex C of EN 1990, may be used.

In a design process, the loading on the structure must be quantified and the mechanical and geometrical properties of the material must be accurately defined; these topics are described in the subsequent sub-chapters.

The effects of the loads for the design situations considered must be obtained by suitable analysis of the structure, according to the general requirements specified in section 5 of EN 1990. The different types of analysis for steel structures and all the main procedures involved are treated in detail in chapter 2 of this book.

For the design of a structure in circumstances where: i) adequate calculation models are not available; ii) a large number of similar components are to be used or iii) to confirm a design of a structure or a component, EN 1990 (Annex D) allows the use of design assisted by testing. However, design assisted by test results shall achieve the level of reliability required for the relevant design situation.

1.3.2. Reliability management

The design and execution of steel structures should be performed according to a required level of reliability. The levels of reliability should be

achieved by an appropriate choice of quality management in design and execution, according to EN 1990 and EN 1090. The levels of reliability relating to structural resistance and serviceability can be achieved by suitable combinations of the following measures:

- preventive and protective measures (e.g implementation of safety barriers, active or passive protective measures against fire, protection against risks of corrosion);
- measures related to design calculations (representative values of actions or partial factors);
- measures related to quality management;
- measures aimed to reduce human errors in design and execution;
- other measures related to aspects such as basic requirements, degree of robustness, durability, soil and environmental influences, accuracy of the mechanical models used and detailing of the structure;
- measures that lead to an efficient execution, according to execution standards (in particular EN 1090);
- measures that lead to adequate inspection and maintenance.

To ensure that the previous measures are verified, EN 1990, in Annex B, establishes three classes of reliability: RC1, RC2 and RC3, corresponding to values of the reliability index β for the ultimate limit state of 3.3, 3.8 and 4.3 respectively, taking a reference period of 50 years. The β index is evaluated according to Annex C of EN 1990, depending on the statistical variability of the actions, resistances and model uncertainties. The design of a steel structure according to EC3-1-1, using the partial factors given in EN 1990 - Annex A1, is considered generally to lead to a structure with a β index greater than 3.8 for a reference period of 50 years, that is, a reliability class not less than RC2.

According to the consequences of failure or malfunction of a structure, Annex B of EN 1990 establishes three consequence classes as given in Table 1.1 (Table B1 of Annex B of EN 1990). The three reliability classes RC1, RC2 and RC3 may be associated with the three consequence classes CC1, CC2 and CC3.

Depending on the design supervision level and the inspection level, Annex B of EN 1990 establishes the classes given in Tables 1.2 and 1.3 (Tables B4 and B5 of Annex B of EN 1990). According to Annex B of EN 1990, the design supervision level and the inspection level are also associated with the reliability classes, as given in Tables 1.2 and 1.3.

Table 1.1 – Definition of consequence classes

Consequence Classes	Description	Examples of buildings and civil engineering works
CC3	*High* consequence for loss of human life, or economic, social or environmental consequences *very great*.	Grandstands, public buildings where consequences of failure are high (e.g. a concert hall).
CC2	*Medium* consequence for loss of human life, economic, social or environmental consequences *considerable*.	Residential and office buildings, public buildings where consequences of failure are medium (e.g. an office building).
CC1	*Low* consequence for loss of human life, and economic, social or environmental consequences *small or negligible*.	Agricultural buildings where people do not normally enter (e.g. storage buildings), greenhouses.

Table 1.2 – Design supervision levels

Design Supervision Levels	Characteristics	Minimum recommended requirements for checking of calculations, drawings and specifications.
DSL3 relating to RC3	Extended supervision	Third party checking: Checking performed by an organisation different from that which has prepared the design.
DSL2 relating to RC2	Normal supervision	Checking by different persons than those originally responsible and in accordance with the procedure of the organisation.
DSL1 relating to RC1	Normal supervision	Self-checking: Checking performed by the person who has prepared the design.

The reliability classes are also associated with the execution classes defined in EN 1090-2 (CEN, 2011). Four execution classes, denoted EXC1, EXC2, EXC3 and EXC4, are defined, with increased requirements from EXC1 to EXC4. The requirements related to execution classes are given in Annex A.3 of EN 1090-2. The choice of the execution class for a steel structure is related to production categories and service categories (defined in Annex B of EN 1090-2)

with links to consequence classes as defined in Annex B of EN 1990 and consequently with reliability classes defined in the same standard.

Table 1.3 – Inspection levels

Inspection Levels	Characteristics	Requirements
IL3 relating to RC3	Extended inspection	Third party inspection.
IL2 relating to RC2	Normal inspection	Inspection in accordance with the procedures of the organisation.
IL1 relating to RC1	Normal inspection	Self inspection.

Annex B of EN 1090-2 defines two service categories: SC1 – Structures submitted to quasi-static actions or low seismic and fatigue actions and SC2 – Structures submitted to high fatigue load or seismic action in regions with medium to high seismic activity. The same standard defines two production categories: PC1 – Structures with non welded components or welded components manufactured from steel grade below S 355, and PC2 – Structures with welded components manufactured from steel grades S 355 and above or other specific components such as: components essential for structural integrity assembled by welding on a construction site, components hot formed or receiving thermal treatment during manufacturing and components of CHS lattice girders requiring end profile cuts. The recommended matrix for the determination of the execution class of a steel structure, after the definition of the production category, the service category and the consequence classes, is given in the Table 1.4 (Table B.3 of Annex B in EN 1090-2).

One way of achieving reliability differentiation is by distinguishing classes of γ_F factors (partial safety factors for the actions) to be used in fundamental combinations for persistent design situations. For example, for the same design supervision and execution inspection levels, a multiplication factor K_{FI}, given by 0.9, 1.0 and 1.1 for reliability classes RC1, RC2 and RC3 respectively, may be applied to the partial factors given in EN 1990 - Annex A1. Reliability differentiation may also be applied through

the partial factors γ_M on resistance; however, this is normally only used for fatigue verifications.

Table 1.4 – Determination of execution classes in steel structures

Consequence classes		CC1		CC2		CC3	
Service categories		SC1	SC2	SC1	SC2	SC1	SC2
Production categories	PC1	EXC1	EXC2	EXC2	EXC3	EXC3 [a)]	EXC3 [a)]
	PC2	EXC2	EXC2	EXC2	EXC3	EXC3 [a)]	EXC4
[a)] EXC4 should be applied to special structures or structures with extreme consequences of a structural failure as required by national provisions.							

The working life period should be taken as the period for which a structure is expected to be used for its intended purpose. This period may be specified according to Table 2.1 of EN 1990 (CEN, 2002a).

1.3.3. Basic variables

1.3.3.1. Introduction

The basic variables involved in the limit state design of a structure are the actions, the material properties and the geometric data of the structure and its members and joints.

When using the partial factor method, it shall be verified that, for all relevant design situations, no relevant limit state is exceeded when design values for actions or effects of actions and resistances are used in the design models.

1.3.3.2. Actions and environmental influences

The actions on a structure may be classified according to their variation in time: i) permanent actions (self weight, fixed equipment, among others); ii) variable actions (imposed loads on building floors, wind, seismic and snow loads); and iii) accidental loads (explosions or impact loads). Certain actions, such as seismic actions and snow loads may be classified as either variable or accidental depending on the site location. Actions may also

be classified according to: i) origin (direct or indirect actions); ii) spatial variation (fixed or free) and iii) nature (static or dynamic).

For the selected design situations, the individual actions for the critical load cases should be combined according to EN 1990, as described in the sections 1.3.4 and 1.3.5. Load combinations are based on the design values of actions. The design values of actions F_d are obtained from the representative values F_{rep}. In general, their characteristic values F_k are adopted, considering adequate partial safety factors γ_f, through the equation:

$$F_d = \gamma_f \, F_{rep}. \tag{1.1}$$

The characteristic values of actions (permanent, variable or accidental actions) shall be specified as a mean value, an upper or a lower value, or even a nominal value, depending on the statistical distribution; for variable actions, other representative values shall be defined: combination values, frequent values and quasi-permanent values, obtained from the characteristic values, through the factors ψ_0, ψ_1 and ψ_2, respectively. These factors are defined according to the type of action and structure.

The design effects of an action, such as internal forces (axial forces, bending moments, shear forces, among others), are obtained by suitable methods of analysis, using the adequate design values and combinations of actions as specified in the relevant parts of EN 1990.

The environmental influences that could affect the durability of a steel structure shall be considered in the choice of materials, surface protection and detailing.

The classification and the quantification of all actions for the design of steel structures, including more specific examples such as the seismic action or the fire action, shall be obtained according to the relevant parts of EN 1990 and EN 1991.

1.3.3.3. Material properties

The material properties should also be represented by upper or lower characteristic values; when insufficient statistical data are available, nominal values may be taken as the characteristic values. The design values of the material properties are obtained from the characteristic values divided by appropriate partial safety factors γ_M, given in the design standards of each

material, Eurocode 3 in the case of steel structures. The values of the partial safety factors γ_M, may vary depending on the failure mode and are specified in the National Annexes.

The recommended values in EC3-1-1 for the partial safety factors γ_{Mi} are the following: $\gamma_{M0} = 1.00$; $\gamma_{M1} = 1.00$ and $\gamma_{M2} = 1.25$.

The values of the material properties shall be determined from standard tests performed under specified conditions, as described in sub-chapter 1.4.

1.3.3.4. Geometrical data

The geometry of a structure and its components must be evaluated with sufficient accuracy. Geometrical data shall be represented by their characteristic values or directly by their design values. The design values of geometrical data, such as dimensions of members that are used to assess action effects and resistances, may be, in general, represented by nominal values. However, geometrical data, referring to dimensions and form, must comply with tolerances established in applicable standards, the most relevant being described in sub-chapter 1.5.

1.3.4. Ultimate limit states

For a structure, in general, the ultimate limit states to be considered are: loss of static equilibrium, internal failure of the structure or its members and joints, failure or excessive deformation of the ground and fatigue failure. In a steel structure, the ultimate limit state referring to internal failure involves the resistance of cross sections, the resistance of the structure and its members to instability phenomena and the resistance of the joints.

In general, the verification of the ultimate limit states consists of the verification of the condition:

$$E_d \leq R_d\,, \tag{1.2}$$

where E_d is the design value of the effect of actions, such as internal forces and R_d represents the design value of the corresponding resistance.

The design values of the effects of actions E_d shall be determined by combining the values of actions that are considered to occur simultaneously.

EN 1990 specifies the following three types of combinations, and each one includes one leading or one accidental action:

i) combinations of actions for persistent or transient design situations (fundamental combinations);
ii) combinations of actions for accidental design situations;
iii) combinations of actions for seismic design situations.

The criteria for the establishment of these combinations and the values of all the relevant factors are defined in EN 1990 and its Annex A.

The verification of the ultimate limit state of loss of static equilibrium of the structure, considered as a rigid body, shall be verified comparing the design effect of destabilising actions with the design effect of stabilising actions. Other specific ultimate limit states, such as failure of the ground or fatigue failure, have to be verified according to the relevant rules specified in EN 1990 (EN 1997 and EN 1993-1-9).

1.3.5. Serviceability limit states

As defined before, the serviceability limit states correspond to a state beyond which the specific service conditions are no longer valid; in steel structures limit states of deformation and of vibration are normally considered.

The verification of the serviceability limit states consists of the verification of the condition:

$$E_d \leq C_d \,, \tag{1.3}$$

where E_d is the design value of the effect of actions specified in the serviceability criterion, determined by the relevant combinations, and C_d is the limiting design value of the relevant serviceability criterion (e.g. design value of a displacement).

The design values of the effects of actions E_d in the serviceability criterion shall be determined by one of the following three types of combinations specified in EN 1990 and its Annex A:

i) characteristic combinations;
ii) frequent combinations;
iii) quasi-permanent combinations.

The limit values of the parameters for the verification of the serviceability limit states, according to EC3-1-1, section 7 and to EN 1990 – Basis of Structural Design, must be agreed between the client and the designer, and can also be specified in the National Annexes. Typical recommended values[1] for the verification of the deformation limit state in steel structures are described below, for vertical deformations in beams (Figure 1.2 and Table 1.5) and for horizontal deformations in multi-storey structures (Figure 1.3).

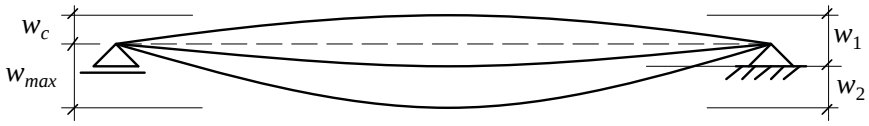


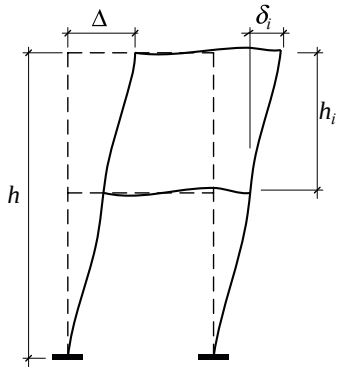
Figure 1.2 – Vertical deformations in beams

In Figure 1.2, w_c is the precamber in the unloaded state of the beam, w_1 is the deflection of the beam due to permanent actions, immediately after their application, w_2 is the deflection of the beam due to variable actions, increased by the long term deformations due to permanent actions and w_{max} is the final maximum deflection measured from the straight line between supports.

Table 1.5 – Limiting values for the vertical displacements in beams (span L)

	w_{max}	w_2
Roofs in general	$L/200$	$L/250$
Roofs often used by people	$L/250$	$L/300$
Floors in general	$L/250$	$L/300$
Floors and roofs supporting plaster or other fragile finishes or non-flexible partition walls	$L/250$	$L/350$
Floors that bear columns (unless the displacement has been included in the global analysis for the ultimate limit state)	$L/400$	$L/500$
When w_{max} may affect the appearance of the building	$L/250$	-
Cantilever beam ($L = 2\ L_{cantiliver}$)	Previous limits	

[1] Portuguese National Annex of EC3-1-1



$$\delta_i \leq h_i / 300$$

$$\Delta \leq h / 500$$

Figure 1.3 – Limiting values for horizontal displacements in frames

The limit state of vibration for steel-framed buildings has become more relevant in recent years because of the increased demand for buildings that are fast to construct, have large uninterrupted floor areas and are flexible in their intended final use (Smith *et al*, 2007). The subject of floor vibration is complex. In general, the designer should make realistic predictions of the floor's response in service by considering the excitation directly and comparing this with acceptability criteria (ISO, 2006). Smith *et al* (2007) provides a practical method for assessing the likely vibrational behaviour of floors in steel-framed buildings. However, in many situations, simpler deemed-to-satisfy criteria are traditionally applied that should ensure adequate designs. For example, the Portuguese National Annex for EC3-1-1 (IPQ, 2010) establishes in clause NA-7.2.3(1)B that the verification of the maximum vertical accelerations may be ignored whenever the eigen frequencies associated with vertical modes are higher than 3 Hz, in the case of residential or office buildings, or 5 Hz, in the case of gyms or other buildings with similar functions. Additionally, if the vertical deflections due to frequent load combinations are lower that 28 mm (office or residential buildings) or 10 mm (gyms or other buildings with similar functions), the calculation of the natural frequencies is not required.

1.3.6. Durability

Clause 2.4 of EN 1990 defines the requirements for the durability of structures. For steel structures (chapter 4 of EC3-1-1), the durability depends

on the effects of corrosion, mechanical wear and fatigue; consequently, the parts most susceptible should be easy to access, inspect, operate and maintain.

When building structures are not subjected to relevant cyclic loads it is not necessary to consider the resistance to fatigue, as it would be in the case of loads resulting from lifts, rolling bridges or vibrations of machines.

The durability of a steel structure depends essentially on its protection against corrosion. Corrosion is a chemical process of degradation of the steel, which grows in the presence of humidity, oxygen and existing pollutant particles in the environment. Independent of the anticorrosion protection system adopted (e.g. organic painting, metal coating), the conception and design of steel structures should take precautions to avoid the accumulation of water and debris, as illustrated in Figure 1.4.

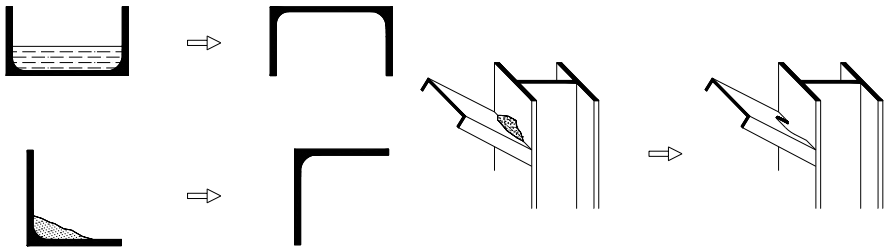


Figure 1.4 – Anti-corrosion details

1.3.7. Sustainability

Steel is one of the most sustainable materials on earth due to its natural properties. Steel is the most recyclable material in the world. It can be recycled over and over again without losing its properties, saving natural resources and reducing construction waste in landfills, thus minimizing two major problems faced by the construction sector.

However, it is not only the environmentally-friendly properties of steel that contribute to its sustainability credentials. Steel structures also have an important role to play. Steel structures are durable. With proper design, a

steel structure can last for many years beyond its initial service life. The durability of steel, associated with the adaptability of steel structures, avoids the need for demolition and new construction.

The other advantages of steel structures are briefly outlined below.

The construction stage has a significant impact on the environment. Waste generated by construction accounts for a large proportion of landfill volumes. Emissions, dust, particles and other airborne contaminants generated during the construction process may cause health problems. In this regard, steel structures have major advantages:

- the prefabrication of steel frames provides a safer and cleaner working environment and minimizes the pollution and noise on the construction site;
- frame elements are delivered in time for installation minimizing the area needed for storage and contributing to an efficient construction site;
- prefabrication ensures accurate dimensions and ease of erection;
- waste during construction is reduced to a minimum and most waste is recyclable.

During the building's life, the main environmental impacts result from the operational energy needed to heat and cool the building. In the European Union, buildings are responsible for more than 40 % of the total energy consumption (of which 70 % is for heating) and for the production of about 35 % of all greenhouse gas emissions (Gervásio *et al*, 2010). Steel framed buildings provide efficient solutions to minimize this problem:

- lightweight steel systems provide well-insulated envelope panels contributing to the energy efficiency of buildings;
- alternative and renewable sources of energy are easily installed in steel buildings.

At the end-of-life of a structure, the major source of concern is the construction waste. Buildings and the built environment are the source of 450 MT of construction and demolition waste per year (over a quarter of all waste produced). The advantages of steel structures are:

- steel structures are easily dismantled, allowing the removal and collection of parts of the steel frame;
- steel frames can be re-used and are easily removed from one place to another.

1.4. MATERIALS

1.4.1. Material specification

Constructional steel used in steel structures consists of alloys of iron with carbon and various other elements (e.g. manganese, silicon, phosphorus, sulphur, …). Some of these are unavoidable impurities while others are added deliberately. The mechanical and technological properties depend on the steel's chemical composition. The carbon content exerts the biggest influence on the microstructure of the material and, consequently, on the mechanical properties, such as yield, ultimate strength and ductility and also on technological properties, like weldability and corrosion resistance.

Hot-rolled steel is the most widespread type of steel used in structural members and joints. When made using the electric arc furnace process and continuous casting, this steel has carbon contents of between 0.06 % to 0.10 %. This increases to between 0.20 % to 0.25 % for steel made using the basic oxygen process (Bjorhovde, 2004).

Cold-formed members are produced by forming steel plates of small thickness, in general with a pre-applied zinc coating. Members are available in several types of section, leading to lightweight structures mainly used in low-rise residential buildings or as secondary components.

Connecting devices, such as bolts, nuts, are in general manufactured from high strength steels.

All steel is produced in several grades and according to different production processes and chemical compositions, as specified in EN 10020 (CEN, 2000). In Europe, hot-rolled steel plating or profiles for use in welded, bolted or riveted structures must be produced in conformity with EN 10025-1 (CEN, 2004b). The first part of this European standard specifies the general technical delivery conditions for hot-rolled products. The specific requirements, such as classification of the main quality classes of steel grades in accordance with EN 10020 (CEN, 2000), is given in parts 2 to 6 of EN 10025; these parts refer to the technical delivery conditions of the following steel products: non-alloy structural steels; normalized/normalized rolled weldable fine grain structural steels; thermo-mechanical rolled weldable fine grain structural steels; structural steels with improved atmospheric

corrosion resistance; flat products of high yield strength structural steels in the quenched and tempered condition. Structural hollow sections and tubes must be specified in accordance with EN 10210-1 (CEN, 2006a) and EN 10219-1 (CEN, 2006b). According to EN 10025, the steel products are divided into grades, based on the minimum specified yield strength at ambient temperature, and qualities based on specified impact energy requirements. EN 10025 also specifies the test methods, including the preparation of samples and test pieces, to verify the conformity relating to the previous specifications.

The main material specifications imposed by EN 10025 for hot rolled products are: i) the chemical composition determined by a suitable physical or chemical analytical method; ii) mechanical properties: tensile strength, yield strength (or 0.2 % proof strength), elongation after failure and impact strength; iii) technological properties, such as weldability, formability, suitability for hot-dip zinc-coating and machinability; iv) surface properties; v) internal soundness; vi) dimensions, tolerances on dimensions and shape, mass.

1.4.2. Mechanical properties

The behaviour under monotonic loading is obtained, in general, by uniaxial tensile tests, performed according to EN ISO 6892-1 (CEN, 2009). The location and orientation of samples and pieces for tensile tests for common structural sections are described in Figure 1.5, according to Annex A of EN 10025-1 (CEN, 2004b).

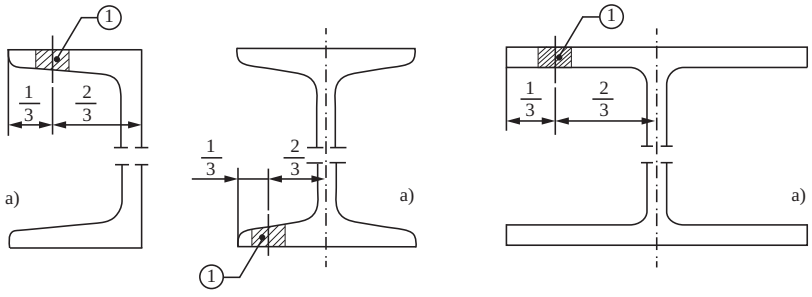
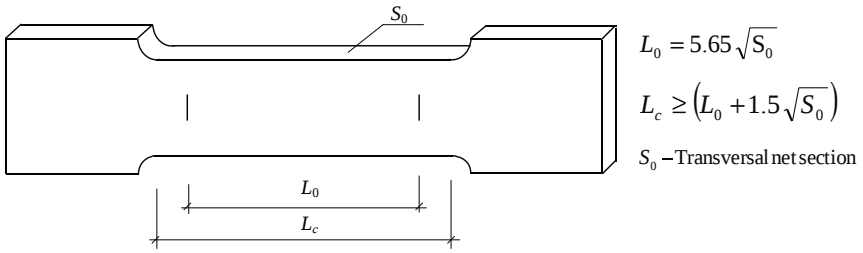


Figure 1.5 – Location and orientation of samples and pieces for tests

Samples for plates, bars, wide strips, among others, are also specified in EN 10025-1 (CEN, 2004b). Since the thickness has a significant influence on the yield and tensile strength of steel, samples are taken from the flanges

to establish the conformity of the steel grade, in accordance with EN 10025. Despite the greater yield strength of the web, this procedure gives an adequate estimate of the resistance of a cross section.

According to EN ISO 6892-1, the geometry of the samples may be proportional or non-proportional. In the case of proportional flat samples, the main geometrical dimensions, including the gauge initial length (L_0) and the transversal net section (S_0), are illustrated in Figure 1.6. In this test, the sample is submitted to an increasing deformation until rupture, in a room with a temperature between 10 and 35 ºC. From the resulting stress-strain curve, shown schematically in Figure 1.7 for the case of a mild steel (steel with ductile behaviour), it is possible to obtain the key mechanical properties of steel: yield stress (upper yield stress R_{eH} or lower yield stress R_{eL}), tensile strength (R_m), maximum load strain (A_{gt}) and strain after failure (A). If these properties are evaluated using the initial dimensions (initial length L_0 and initial transversal net section S_0) they are called engineering stresses and engineering strains; alternatively, if they are obtained with the instantaneous dimensions they are called true stresses and true strains.



a) Geometry



b) Sample after test

Figure 1.6 – Geometry of proportional flat test samples

Table 1.6 lists the main mechanical properties of the hot-rolled steel grades of the qualities covered by EN 10025-2 (CEN, 2004c) (non-alloy structural steel), for the most common thicknesses. As the thicknesses is increased, the tensile properties such as the yield stress and ultimate tensile stress decrease.

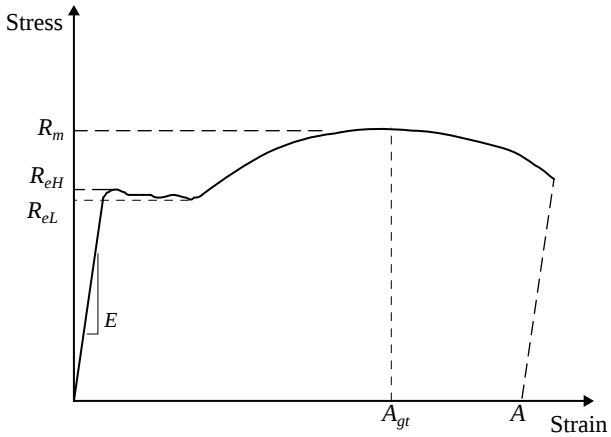


Figure 1.7 – Schematic stress-strain curve

Table 1.6 – Hot-rolled steel grades and qualities according to EN 10025-2

Steel grades and qualities	Minimum yield strength R_{eH} (MPa)				Tensile strength R_m (MPa)		Minimum percentage elongation after fracture $L_o = 5.65\sqrt{S_0}$		
	Nominal thickness (mm)				Nominal thickness (mm)		Nominal thickness (mm)		
	≤ 16	>16 ≤ 40	>40 ≤ 63	>63 ≤ 80	< 3	≥3 ≤ 100	≥3 ≤ 40	>40 ≤ 63	>63 ≤ 100
S 235JR	235	225	215	215	360 to 510	360 to 510	26	25	24
S 235J0	235	225	215	215	360 to 510	360 to 510			
S 235J2	235	225	215	215	360 to 510	360 to 510	24	23	22
S 275JR	275	265	255	245	430 to 580	410 to 560	23	22	21
S 275J0	275	265	255	245	430 to 580	410 to 560			
S 275J2	275	265	255	245	430 to 580	410 to 560	21	20	19
S 355JR	355	345	335	325	510 to 680	470 to 630	22	21	20
S 355J0	355	345	335	325	510 to 680	470 to 630			
S 355J2	355	345	335	325	510 to 680	470 to 630			
S 355K2	335	345	335	325	510 to 680	470 to 630	20	19	18
S 450J0	450	430	410	390	-	550 to 720	17	17	17

In clause 3.2 of EC3-1-1 the following mechanical and physical properties are specified:

- Modulus of elasticity E = 210 GPa;
- Poisson's ratio in elastic range ν = 0.3;
- Coefficient of linear thermal expansion $\alpha = 12 \times 10^{-6}$ / ºC;
- Shear modulus G = 81000 N/mm^2

With the volumetric mass ρ defined in EN 1991-1-1 (CEN, 2002b) within the range 7700 – 7850 kg/m^3.

1.4.3. Toughness and through thickness properties

Steel may present acceptable properties when submitted to monotonic loading but may fail in a brittle way under rapid loading. Resistance to fast fracture is commonly defined as material toughness. Part 1-10 of Eurocode 3 (CEN, 2005d) supplies design guidance for the selection of steel (grades S 235 to S 690) according to material toughness for use in welded elements in tension and fatigue elements in which some portion of the stress cycle is tensile. This property is quantified by the energy absorbed by a test specimen in an impact test. The most common is the Charpy test (CEN, 1990). According to this, the material toughness is quantified by the value of the impact energy $A_v(T)$ in Joules required to fracture a Charpy V – notch specimen at a given temperature. Steel product standards generally specify that test specimens should not fail at impact energy lower than 27 Joules at a specified test temperature T. In general, the toughness-temperature diagram of a structural steel presents a transition region in which the material toughness decreases with decreasing temperature and the failure mode changes from ductile to brittle; the temperature values T27J required by the product standard are located in the lower part of this region (Figure 1.8). EN 10025-2 (CEN, 2004c) specifies four classes of quality in terms of impact strength: classes JR, J0 and J2 corresponding to an impact energy not lower than 27 Joules at temperatures 20 ºC, 0 ºC and -20 ºC, respectively, and class K2 corresponding to an impact energy not lower than 40 Joules at a temperature of -20 ºC. The maximum permitted thickness for a steel element may be specified according to Table 2.1 of EC3-1-10 depending on the steel grade, its toughness quality in terms of K_V-value, the reference stress level σ_{Ed} and the reference temperature T_{Ed}.

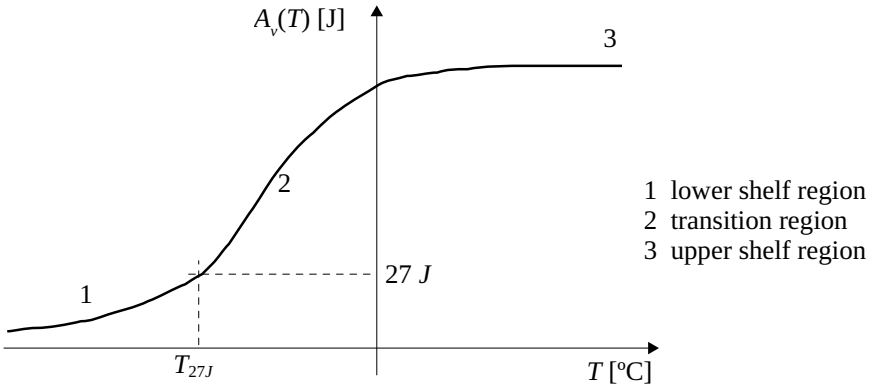


Figure 1.8 – Relationship between impact energy and temperature

The selection of the through-thickness properties of materials should prevent lamellar tearing in steel assemblies (Figure 1.9). The susceptibility of the material should be determined by measuring the through-thickness ductility quality according to EN 10164 (CEN, 2004d), which is expressed in terms of quality classes identified by *Z*-values. According to EC3-1-10, lamellar tearing may be neglected in a detail if $Z_{Ed} \leq Z_{Rd}$, Z_{Ed} being the required design *Z*-value resulting from the magnitude of strains from restrained metal shrinkage under the weld beads obtained as given in Table 3.2 of EC3-1-10 and Z_{Rd} is the available design *Z*-value for the material according to EN 10164 (Z15, Z25 and Z35 classes are established). The appropriate Z_{Rd} class according to EN 10164 may be obtained by applying a suitable classification. According to EC3-1-1, the classification described in Table 1.7 may be adopted for buildings structures.

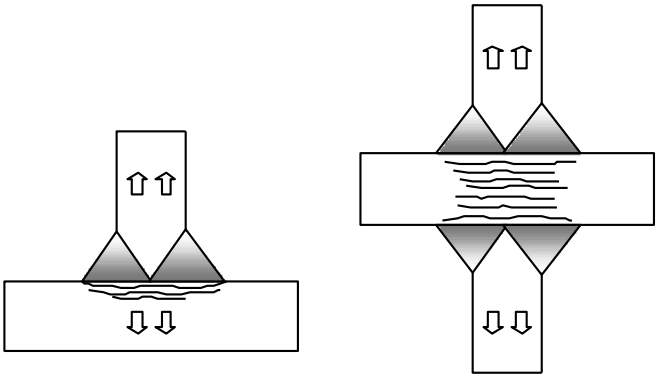


Figure 1.9 – Lamellar tearing

Table 1.7 – Choice of quality class according EN 10164

Target value of Z_{Ed} obtained according to EN 1993-1-10	Required value of Z_{Rd} obtained according to EN 10164
$Z_{Ed} \leq 10$	-
$10 < Z_{Ed} \leq 20$	Z 15
$20 < Z_{Ed} \leq 30$	Z 25
$Z_{Ed} > 30$	Z 35

1.4.4. Fatigue properties

The fatigue properties are important when the structure and its members and joints are submitted to cyclic loading. Fatigue may cause premature failure of a structural detail at stress levels much lower than those required for failure under a steadily applied stress. The fatigue strength depends on the material but essentially on the detail category. The fatigue strength of a detail, in general obtained by extensive testing, is expressed as a $\Delta\sigma_R$-N curve, where $\Delta\sigma_R$ is the stress range and N is the number of cycles to failure. In a particular detail, the fatigue strength depends essentially on the design stress range and the mean stress of the cycles. The stress range below which failure does not occur is designated as the endurance limit. The fatigue strength for the majority of details in steel structures should be obtained according to Part 1-9 of Eurocode 3 (CEN, 2005c).

1.4.5. Corrosion resistance

Steel materials in aggressive environments, in presence of water and oxygen, have a tendency to develop processes of corrosion that can be very damaging for the durability of the structure. In order to prevent these phenomena, it is essential to ensure that the surface of steel elements exhibits sufficient corrosion resistance. According to clause 2.1.3.1(1) of EC3-1-1, this may be provided by: i) the modification of the properties of the parent metal or alloy, producing a surface film which is stable in most corrosive environments (in stainless steel this is achieved by producing a passive chromic oxide surface film); or ii) by the application of protective coatings that can be either metallic or non-metallic.

1.5. GEOMETRIC CHARACTERISTICS AND TOLERANCES

The main hot-rolled products are: I and H sections, box sections, channels, tees, angles, plates, among others (Figure 1.10). Alternatively it is possible to obtain welded sections with various cross section configurations, including those shown in Figure 1.10. By the cold-form process it is possible to make a wide variety of sections (Figure 1.10 and Figure 1.11).

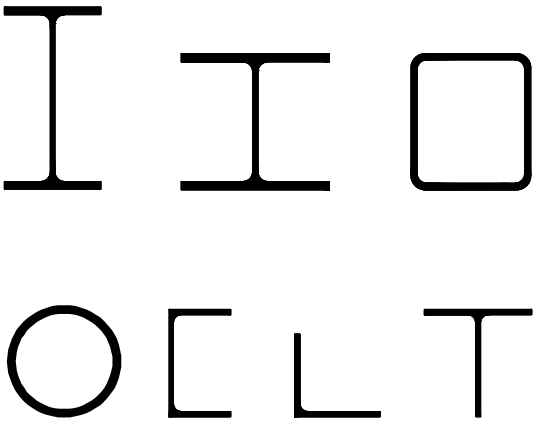


Figure 1.10 – Rolled sections

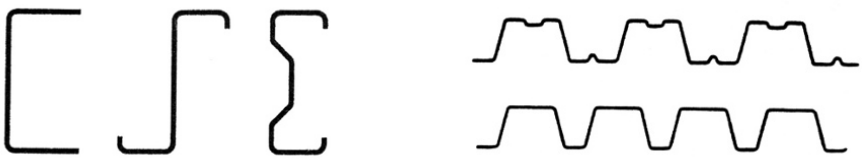


Figure 1.11 – Cold formed sections

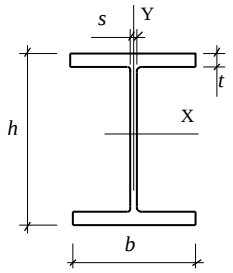
All the steel products to be used in steel structures should fulfil geometrical tolerances (on dimensions and shape) dependent on the forming process. EN 1090-2 (2011) establishes two types of tolerances: i) essential tolerances – applicable for a range of criteria that are essential for the

mechanical resistance and stability of the structure and ii) functional tolerances – required to fulfil other criteria such as fit-up and appearance of the structure. In specific cases special tolerances may be specified.

According to EN 1090, hot-rolled, hot-finished or cold-formed structural products shall conform to the permitted deviations specified by the relevant product standards. The most relevant applicable standards are supplied in EN 10025-1 (clause 2.2). In the case of hot-rolled products with I or H sections, the maximum permitted values specified in EN 10034 (CEN, 1993) are given in Tables 1.8 to 1.10. The deviation from the nominal mass of a piece shall not exceed ± 4 %. The tolerances on length of pieces are ± 50 mm or, where minimum lengths are requested, + 100 mm.

Table 1.8 – Dimensional tolerances for structural steel I and H sections (EN 10034)

Section height h (mm)	Tol. (mm)	Flange width b (mm)	Tol. (mm)	Web thickness s (mm)	Tol. (mm)	Flange thickness t (mm)	Tol. (mm)
$h \leq 180$	+3.0 -3.0	$b \leq 110$	+4.0 -1.0	$s < 7$	+0.7 -0.7	$t < 6.5$	+1.5 -0.5
$180 < h \leq 400$	+4.0 -2.0	$110 < b \leq 210$	+4.0 -2.0	$7 \leq s < 10$	+1.0 -1.0	$6.5 \leq t < 10$	+2.0 -1.0
$400 < h \leq 700$	+5.0 -3.0	$210 < b \leq 325$	+4.0 -4.0	$10 \leq s < 20$	+1.5 -1.5	$10 \leq t < 20$	+2.5 -1.5
$h > 700$	+5.0 -5.0	$b > 325$	+6.0 -5.0	$20 \leq s < 40$	+2.0 -2.0	$20 \leq t < 30$	+2.5 -2.0
				$40 \leq s < 60$	+2.5 -2.5	$30 \leq t < 40$	+2.5 -2.5
				$s \geq 60$	+3.0 -3.0	$40 \leq t < 60$	+3.0 -3.0
					--	$t \geq 60$	+4.0 -4.0



h - Height measured at the centre line of web thickness
b - Flange width
s - Web thickness measured at the mid-point of dimension *h*
t - Flange thickness measured at the quarter flange width point

Table 1.9 – Tolerances on out-of-square and web off-centre of structural steel I and H sections (EN 10034)

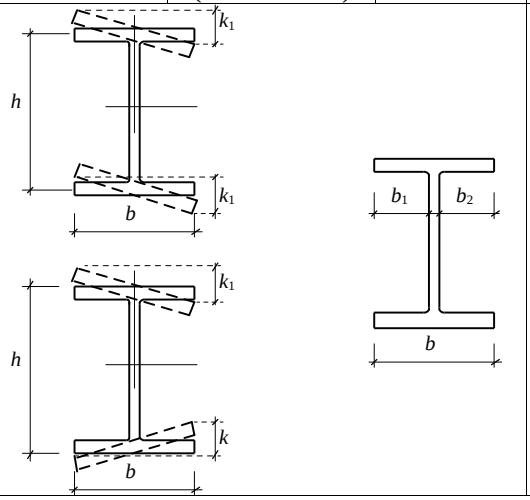
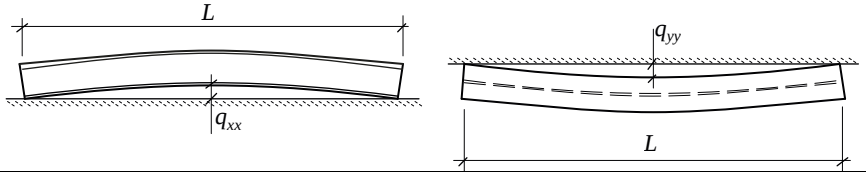
Out-of-square $k + k_1$	Tol. (mm)	Web off-centre e		Tol. (mm)
$b \leq 110$	1.50	$t < 40$ mm	$b \leq 110$	2.50
			$110 \leq b < 325$	3.5
			$b > 325$	5.0
$b > 110$	2 % of b (max. 6.5 mm)	$t \geq 40$ mm	$110 < b \leq 325$	5.0
			$b > 325$	8.0
				b – Flange width t – Flange thickness $e = \frac{b_1 - b_2}{2}$

Table 1.10 – Tolerances on straightness of structural steel I and H sections (EN 10034)

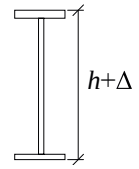
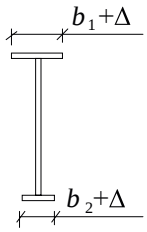
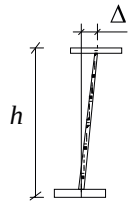
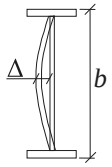
Section height h (mm)	Tolerance on straightness q_{xx} and q_{yy} on length L (%)
$80 < h < 180$	0.30 L
$180 < h \leq 360$	0.15 L
$h > 360$	0.10 L
	

Annex D of EN 1090-2 specifies geometrical tolerances for other products, such as welded sections, cold formed sections, plates, sheets and

shells. For example, Table 1.11 describes some of the main essential tolerances for welded sections. Essential erection and functional tolerances are also specified in Annex D of EN 1090.

The tolerances on mass must be evaluated from the nominal dimensions of profiles using a volumetric mass of 7850 kg/m^3 as specified in clause 7.7.2 of EN 10025-1.

Table 1.11 – Essential manufacturing tolerances – welded sections (EN 1090-2)

Criterion	Parameter	Tolerance Δ
Depth 	Overall depth h	$\Delta = -h/50$ No positive value given
Flange width 	Width $b = b_1$ or b_2	$\Delta = -b/100$
Squareness at bearings 	Verticality of web at supports for components without bearing stiffeners	$\Delta = \pm 200$ but $\Delta \geq t_w$ (t_w = web thickness)
Plate curvature 	Deviation Δ over plate height b	$\Delta = \pm b/100$ but $\Delta \geq t$ (t = plate thickness)

Finally, Figure 1.12 illustrates the main notation used in Eurocode 3 for the geometric definition of steel sections. In general, the following axis convention is used: *xx* – piece axis; *yy* – section axis, parallel to the flanges; *zz* – section axis, perpendicular to the flanges. However, it should be noted that this notation is not always in agreement with other standards, namely with EN 10034 concerning the geometric tolerances of steel sections.

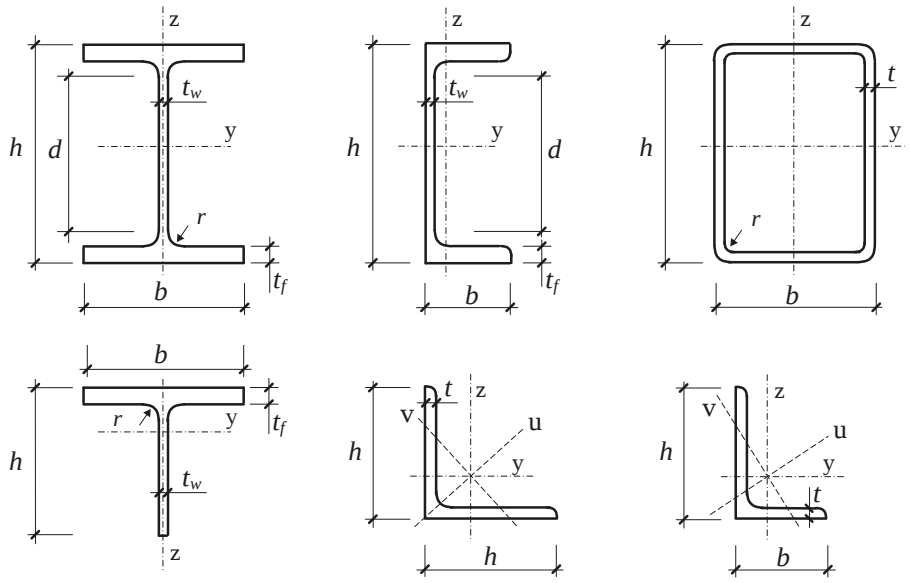


Figure 1.12 – Conventions for dimensions and axes of steel cross sections

Chapter 2

STRUCTURAL ANALYSIS

2.1. INTRODUCTION

The design of steel structures classically consists of a two-step analysis and verification procedure: i) internal forces and displacements are first evaluated based on the principles of equilibrium and compatibility; ii) subsequently, these internal forces and displacements are compared against corresponding resistance, stiffness and ductility values to ensure structural safety and fitness-for-purpose.

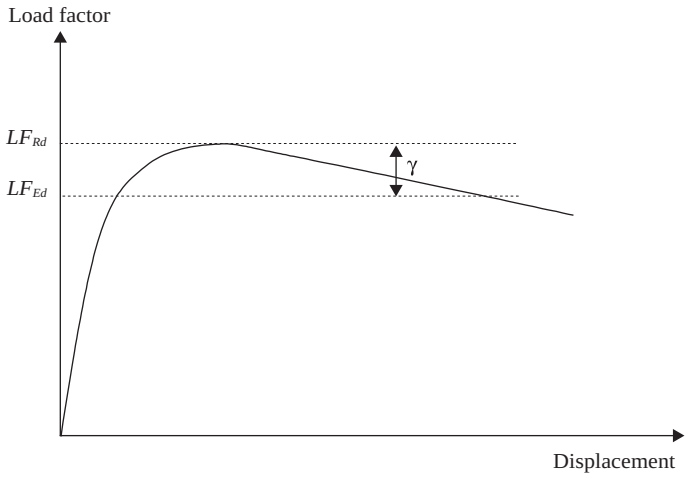


Figure 2.1 – Nonlinear analysis

The growing understanding of the behaviour of steel structures, coupled with the development of more and more sophisticated and

user-friendly design tools, means that the two-steps described above progressively become more coupled. Nonlinear design of steel structures provides a good example of these developments: the results of the structural analysis are directly compared with applied loads (Figure 2.1), thus allowing a one-step evaluation of the structure.

Current practice still consists of a two-step procedure for most design situations, leading to the best compromise between accuracy and time. This chapter thus focuses on the analysis step, presenting and discussing the relevant aspects for standard XXI century design practice, in the framework of the Structural Eurocodes. Firstly, in sub-chapter 2.2, the modelling of steel structures is discussed. Next, the various methodologies for structural analysis are presented, directly related to the susceptibility of the structure to nonlinear phenomena. Finally, the classification of cross sections and its implications in the choice of design procedures is described. Throughout the chapter, several worked examples are presented in detail.

2.2. STRUCTURAL MODELLING

2.2.1. Introduction

Steel structures are very often composed by linear members. The following figures illustrate the structural framework of a steel industrial building (Figure 2.2) and a multi-storey office building (Figure 2.3).

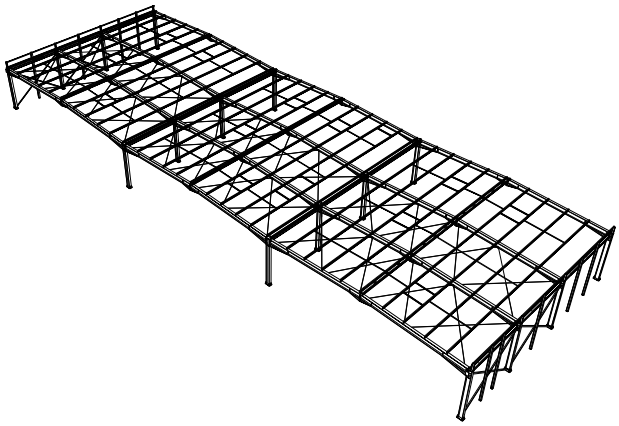


Figure 2.2 – Industrial building

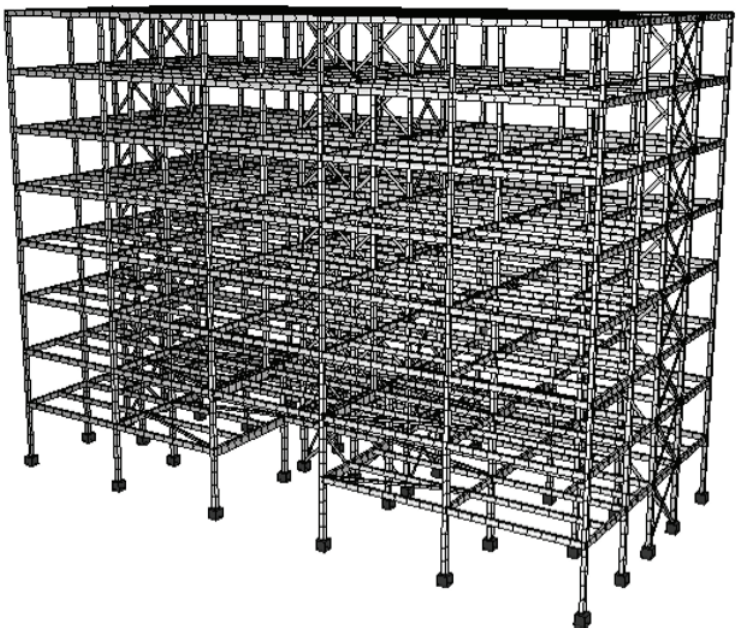


Figure 2.3 – Multi-storey building

In many applications two-dimensional elements, such as slabs in buildings, coexist with linear members, as can be seen in Figure 2.4. The slabs may be reinforced concrete, composite steel-concrete or prestressed concrete. Other common two-dimensional elements are concrete walls in buildings and slabs in decks of composite steel-concrete bridges (in reinforced concrete or steel orthotropic solutions).



Figure 2.4 – Structural model with two-dimensional elements

The modelling of steel structures using linear elements involves the consideration of several specific aspects (discussed in sections 2.2.2 to 2.2.5) such as the choice of the structural axis of a member, the influence of eccentricities, non-prismatic and curved members and the modelling of joints. This option is obviously adequate for linear members (beams, columns, bracing and cables). With a degree of approximation it may also be possible to model two-dimensional elements in this way, provided that the analysis results are sufficiently accurate for the intended purpose. Whenever it is intended to analyse and design steel structures using the finite element method (FEM), combining in the modelling of the structure linear elements with two and three-dimensional elements, it is necessary to connect them adequately. This aspect will be discussed in section 2.2.6.

2.2.2. Choice of member axis

In modelling linear members it is usual to choose the element's axis to coincide with the centroidal axis. In this case, the internal forces (e.g. bending moment, torsional moment) resulting from the structural analysis are referred to the centroid of the section. Though this is the usual option, this is not compulsory, as long as all subsequent calculations take the chosen option into account (Ghali and Neville, 1997). This comment is particularly important when applied forces are compared to resistant forces determined from normative expressions (EC3-1-1, for example) derived with respect to the centroid of the section.

To illustrate this aspect, consider the H-section column in Figure 2.5.

Consider, in addition, that the column bears a vertical concentrated load P that acts in the mid-plane of the web, with an eccentricity e with respect to the centroid. If the axis of the element coincides with the centroid (CC'), the forces at the base plate are:

$$\begin{cases} M_{C'} = P\,e \\ N_{C'} = P' \end{cases}, \tag{2.1}$$

while if the axis of the element coincides with AA', the forces at the base plate will be given by:

$$\begin{cases} M_{A'} = 0 \\ N_{A'} = P \end{cases}. \tag{2.2}$$

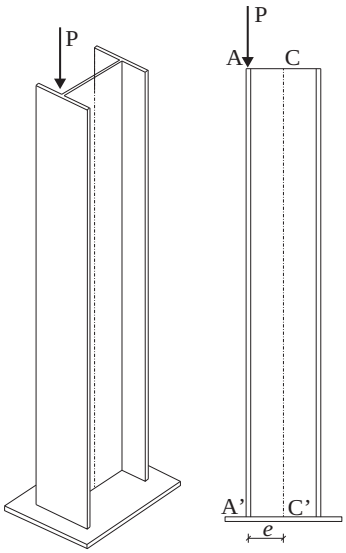
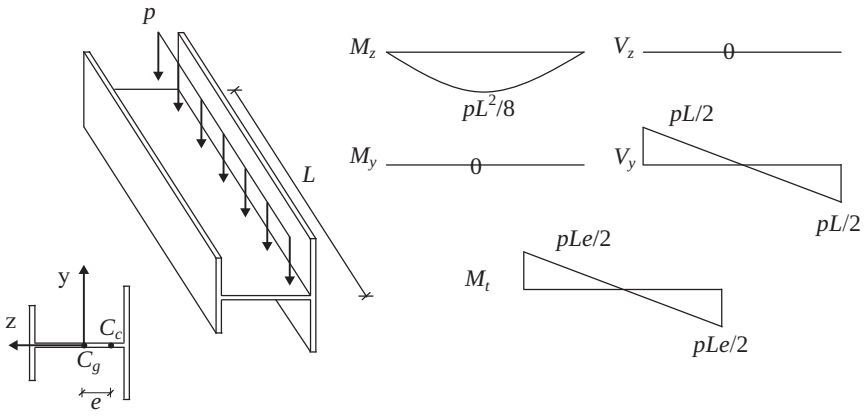


Figure 2.5 – Influence of the choice of member axis

For asymmetric or monosymetric sections, in which the centroid does not coincide with the shear centre, bending loads not aligned with the shear centre lead to torsional moments. These should be considered in design (CEN, 2005a). As an example, consider the beam with a monosymetric I-section, Figure 2.6a. The ends are simply supported , with rotation around its axis restricted but with freedom to warp. A uniformly distributed transverse load *p* acts at the centroid of the cross section. The resulting stress resultants (i.e. moments and shear forces) are represented in Figure 2.6b.



a) b)

Figure 2.6 – Influence of load eccentricity in relation to the shear centre

2.2.3. Influence of eccentricities and supports

A structural model of linear members presents differences between the real length of the elements (beams and columns) and the corresponding system length. This is because the structural nodes at the intersection of converging members normally correspond to their centroid, as is illustrated in Figure 2.7. These differences affect the evaluation of both forces and displacements, and may result in significant over-estimation of these effects. To illustrate this, consider first (Figure 2.7) the evaluation of the maximum negative moment acting in the beam. This should be evaluated at points A' and B' and not at points A and B, as would result directly from the structural model. For a uniformly distributed load, the difference reaches 19 % when h/L_C = 0.1 (that is, for a 6 m span between axes and IPE 600 columns, for example) [1]. Secondly, the maximum displacement is also significantly lower, due to the rigid behaviour in bending of sections AA' and BB'. For a uniformly distributed load, the difference reaches 34.4 % when $h/L_C = 0.1$ [2].

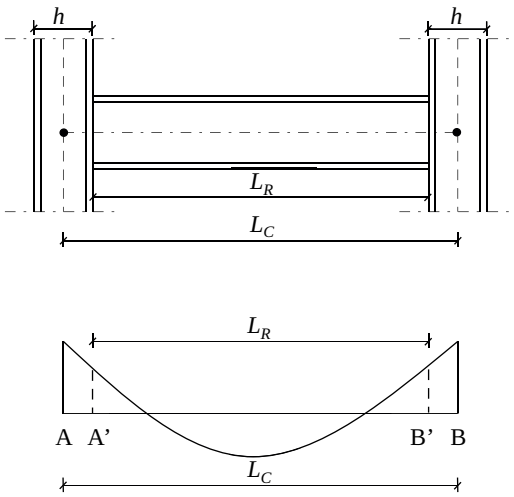


Figure 2.7 – Influence of eccentricities

[1] For h/L_c = 0.05 or h/L_c = 0.2 the differences would be of, respectively, 9.75 % or 36 %.

[2] For h/L_c = 0.05 or h/L_c = 0.2, the differences would be of, respectively, 18.5 % or 59 %.

In practical terms, with the use of computer programs, it is necessary to introduce rigid links and eccentricities in order to obtain the correct values of forces and displacements. This aspect is explored in detail in example 2.1.

The existence of eccentricities is not limited to the case described above. In many situations there is a discontinuity at an intermediate section of a beam, as illustrated in Figure 2.8. In that case, the structural model should consider a node at that section and the elements to the left and to the right have different geometrical properties. In addition, due to the vertical discontinuity of the centroids, a rigid link should connect them. Normally, the forces on the left section will be different from the forces on the right section (in the case of the bending moment and axial force, for example), This is because the forces are determined in relation to different centroidal axes, as can be seen in Figure 2.8. Finally, in the generic case of an arbitrary intersection of several elements in space, with non-coincident centroids, rigid links must be considered, oriented in space. Equilibrium will be satisfied taking account of the eccentricity between centroids.

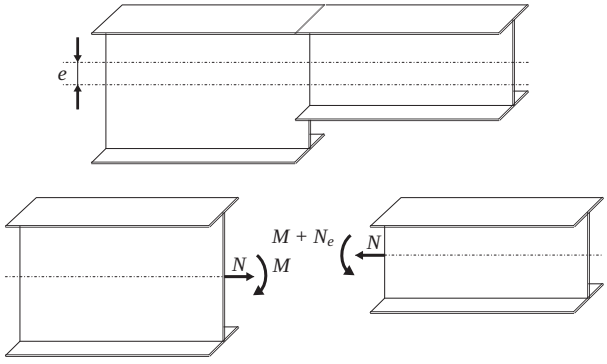


Figure 2.8 – Influence of discontinuities at intermediate sections

2.2.4. Non-prismatic members and members with curved axis

The modelling of non-prismatic members, typically illustrated in Figure 2.9, must follow specific modelling rules.

The first situation (Figure 2.9a), corresponding to a discrete variation of cross section, was already discussed in section 2.2.3.

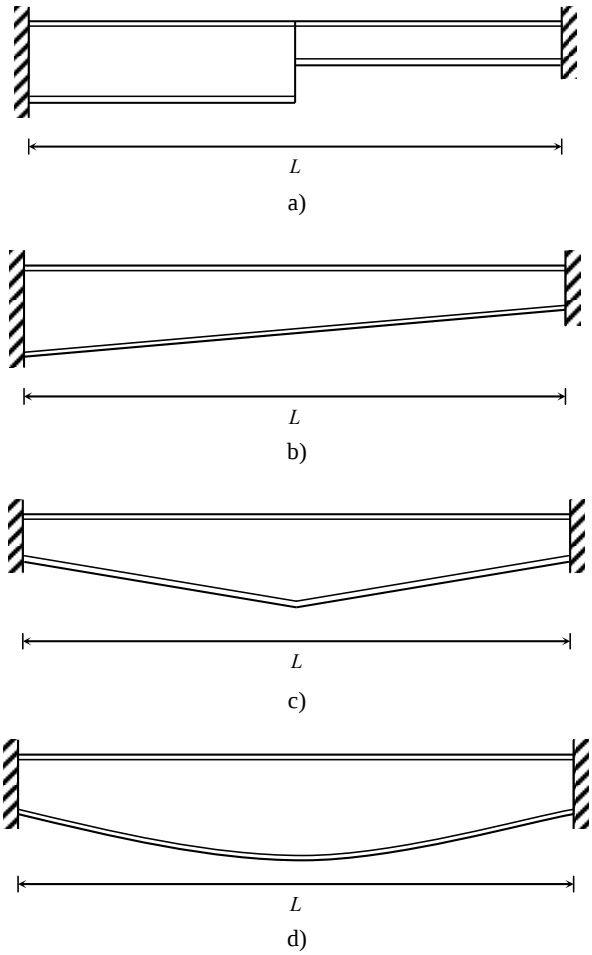


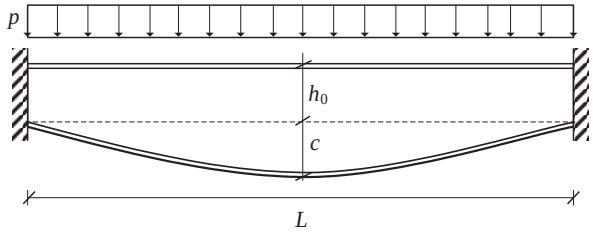
Figure 2.9 – Examples of elements with variable cross section

The second situation (Figure 2.9b) corresponds to a continuous variation of the cross section. The usual modelling consists of considering nodes at the ends of the element and a linear variation of the depth of section of the cross section between those points. In this case, the accuracy of the results will vary significantly from program to program, depending on how the stiffness matrix of the element is calculated.

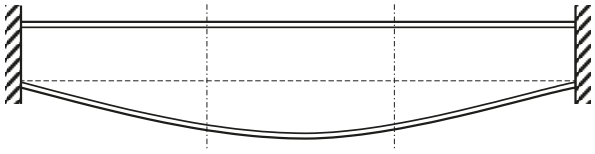
The third case (Figure 2.9c) corresponds to a combination of the previous case with a discontinuity at a specific cross section. An intermediate node must be considered and it is required to know the variation of the properties of the cross section between the nodes of the element.

Finally, in the fourth case (Figure 2.9d), as the variation of the cross section is not linear (parabolic, in this case), it is necessary to consider a tighter discretization, with a reasonable number of intermediate nodes so that the linear approximation between nodes does not introduce a significant error. Alternatively, the calculation of the stiffness matrix of the element could be done considering the real variation of the cross section along the member.

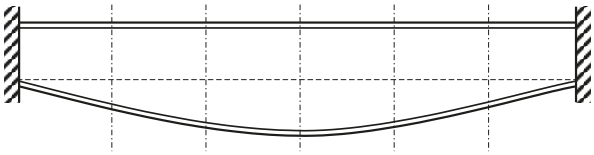
Figure 2.10 illustrates several discretizations for the determination of forces and displacements in a beam, for a uniformly distributed load and fixed supports.



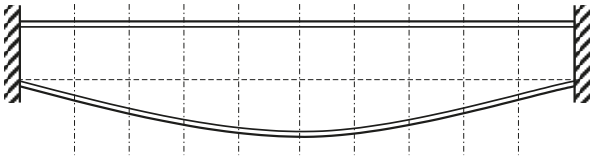
a) Real system



b) Mesh 1 – with 3 elements



c) Mesh 2 – with 6 elements



d) Mesh 3 – with 10 elements

Figure 2.10 – Alternative discretizations for a beam with parabolic variation of the depth of the cross section

where L = 10 m; p = 10 kN/m; E = 210 GPa and h_0 = 0.50 m. In order to explore the influence of the ratio c/h_0, two cases were considered: c/h_0 = 1 (c = 0.50 m) and c/h_0 = 2 (c = 1.0 m). Figure 2.11 illustrates the bending moment diagram and the vertical displacements of the beam (c/h_0 = 1).

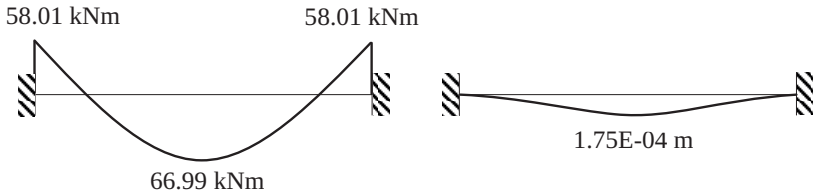


Figure 2.11 – Bending moment diagram and vertical displacements of the beam

Numerically, using a computer program, Tables 2.1 and 2.2 summarize the various results obtained for the different mesh discretizations, which are compared with the analytical solution.

Table 2.1 – Comparison of results for c/h_0 = 1

c/h_0 = 1		n	$M_{support}$ (kNm)		$M_{midspan}$ (kNm)		$\delta_{midspan}$ (mm)	
				Error		Error		Error
Analytical sol.		-	- 58.01	-	+ 66.99	-	0.175	-
Numerical solution	Mesh 1	3	- 71.90	23.9 %	+ 44.43	33.7 %	0.116	33.7 %
	Mesh 2	6	- 60.19	3.8 %	+ 52.79	21.2 %	0.135	22.9 %
	Mesh 3	10	- 61.73	6.4 %	+ 63.37	5.4 %	0.171	2.3 %
	Mesh 4	20	- 59.06	1.8 %	+ 66.05	1.4 %	0.171	2.3 %
	Mesh 5	40	- 58.28	0.5 %	+ 66.83	0.2 %	0.174	0.6 %
	Mesh 6	80	- 58.07	0.1 %	+67.03	0.1 %	0.175	0.0 %

In order to obtain an error lower than 5 %, a discretization with a minimum of 10 elements is required as the the continuous variation of the member is replaced by a series of elements of uniform but different depth, separated by discontinuities as shown in Fig. 2.8. This requirement increases with an increasing ratio c/h_0.

In case of a member with a curved axis, the curvature influences the results (Timoshenko, 1956; Weaver and Gere, 1990), and the classic theory

of linear members should include a correction to consider this effect. Since most of the commercial programs do not usually contemplate this correction, the solution to minimize this problem is to consider a tighter element discretization. To illustrate this aspect, consider a curved beam (in the horizontal plan) with R radius, subjected to a concentrated vertical load P applied at an arbitrary point C, normal to ACB, represented in Figure 2.12.

Table 2.2 – Comparison of results for $c/h_0 = 2$

$c/h_0 = 2$		n	$M_{support}$ (kNm)		$M_{midspan}$ (kNm)		$\delta_{midspan}$ (mm)	
				Error		Error		Error
Analytical sol.		-	- 43.32	-	+ 81.68	-	0.077	-
Numerical solution	Mesh 1	3	- 66.28	53.0 %	+ 42.07	48.5 %	0.043	44.0 %
	Mesh 2	6	- 49.14	13.4 %	+ 51.33	37.2 %	0.051	33.3 %
	Mesh 3	10	- 52.22	20.5 %	+ 73.21	10.4 %	0.072	6.2 %
	Mesh 4	20	- 46.17	6.6 %	+ 79.24	3.0 %	0.073	5.3 %
	Mesh 5	40	- 44.08	1.8 %	+ 81.33	0.4 %	0.076	0.8 %
	Mesh 6	80	- 43.50	0.4 %	+ 81.92	0.3 %	0.077	- 0.5 %

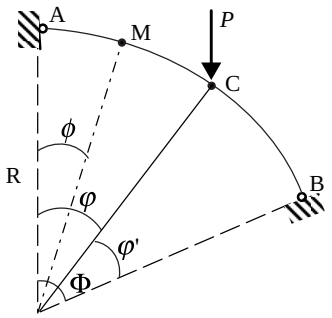


Figure 2.12 – Influence of the elements' curvature

Table 2.3 summarizes the results obtained for the analytical solution (Nakai and Yoo, 1988) and the several numerical results obtained for various discretizations (n = 5, 10, 20, 40 and 80), considering R = 6.366 m, L = 10 m, P = 50 kN, $\Phi = 90^o$, $\phi = 18^o$ and $\varphi = \varphi' = 45^o$. For the various

discretizations each element is assumed straight, with a change in member direction at each node. M_o and T_o are the bending moment and the torsional moment at an arbitrary point M.

Table 2.3 – Moments in curved beam

	M_o (kNm)	T_o (kNm)	M (kNm)	T (kNm)
	R-F		R-R	
Analytical solution	69.55	11.02	69.55	54.91
Model 1 (n = 5)	69.56	-	62.38	59.68
Model 2 (n = 10)	70.21	5.53	65.03	60.20
Model 3 (n = 20)	69.93	8.28	67.35	57.60
Model 4 (n = 40)	69.76	9.65	68.46	56.27
Model 5 (n = 80)	69.66	10.33	69.01	55.59

The first two columns present the results for the situation in which one of the supports does not restrain torsional deformations (R-F) and the two last columns present the same results for the situation in which both supports restrain torsional deformations (R-R).

2.2.5. Influence of joints

Steel joints exhibit a behaviour that ranges from rigid to extremely flexible. Obviously, the deformability of joints varies in accordance with the applied loading: a joint may behave very rigidly when subjected to shear force or torsion but show a flexible response when subjected to bending. Figure 2.13 illustrates this statement for a typical bolted end-plate beam-to-column steel joint: rigid in torsion or shear, semi-rigid under major axis bending or axial force and flexible under minor axis bending (Simões da Silva, 2008). The corresponding moment (force) – rotation (displacement) curves are clearly non-linear, a typical feature of joint behaviour. The incorporation of joint behaviour into the structural analysis is thus complex.

In general terms, a steel joint can be modelled as a six degree-of-freedom non-linear spring. This representation is adequate whenever the

behaviour of the joint can be uncoupled into six independent internal forces (two bending moments, a torsional moment, an axial force and two shear forces). This assumption is not always adequate, in which case the consideration of interaction formulae becomes necessary. The *M-N* interaction is a typical example (Simões da Silva *et al*, 2004; Cerfontaine, 2003).

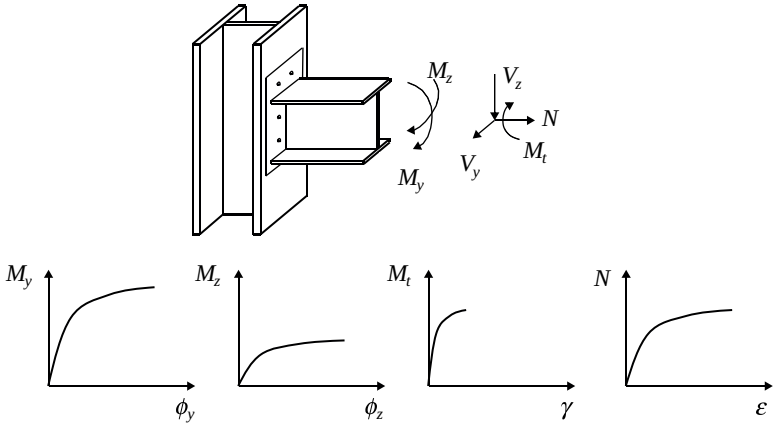


Figure 2.13 – Typical 3D behaviour of bolted end-plate beam-to-column steel joint

Deformability in bending is usually critical and mostly influences the results from structural analysis (Simões da Silva, 2008). Figure 2.14 reproduces the typical non-linear bending moment-rotation curve (M_j-ϕ_j), as well as the usual idealized curve characterized by three fundamental properties: stiffness (S_j), in particular initial stiffness ($S_{j,ini}$), moment resistance ($M_{j,Rd}$) and rotation capacity (ϕ_{Cd}).

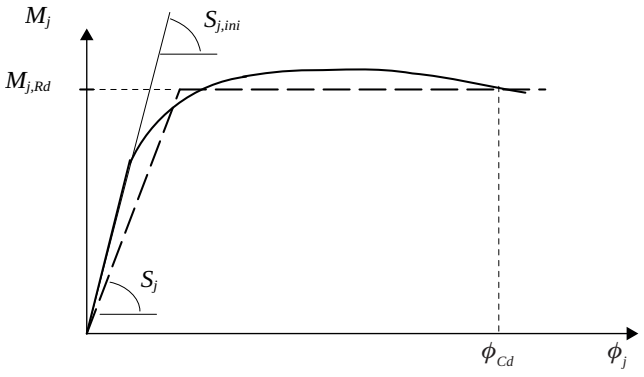
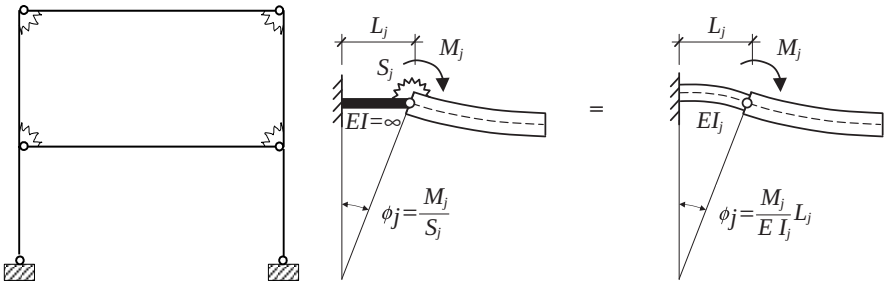


Figure 2.14 – Bending-rotation moment curve of a joint

Part 1-8 of Eurocode 3 (CEN, 2005b), based on the so-called component method (Weynand *et al*, 1995), provides procedures for the characterization of the rotational behaviour of joints, allowing the specification of the corresponding moment-rotation curve or some representative properties. Normally, the deformability corresponding to the remaining degrees of freedom is either much lower or the global behaviour of the structure does not induce significant internal forces in the other directions (as it is the case, for example, of the resistance of a beam-to-column joint around the beam's minor axis). In this case, the corresponding degrees of freedom can be safely modelled with either infinite or zero stiffness. Figure 2.15a illustrates the modelling of a plane frame where it is assumed that the shear deformability is negligible, as well as the level of axial force acting in the beams. In case of less sophisticated computer programs that do not allow spring elements, the bending flexibility of a joint can still be modelled using an equivalent beam stub, as shown in Figure 2.15b.



a) b)

Figure 2.15 – Modelling of joints in structural analysis

It should be pointed out that including non-linear springs makes it necessary to perform a non-linear analysis, which significantly increases the complexity of the structural analysis. In fact, Figure 2.14 shows that the moment-rotation curve presents initially an elastic behaviour, followed by a plastic response resulting from the progressive yielding of some components. Thus, the modelling of joints invariably requires the consideration of a non-linear analysis with non-linear springs (unless all joints are designed as full-strength, with an adequate overstrength level to ensure that they remain elastic for all load combinations). As an alternative to performing a non-linear analysis, it is possible to approximate the results of a non-linear analysis (with

respect to the behaviour of the joints) by a linear elastic analysis with linear springs. These linear springs should be representative of the joint behaviour up to loading levels corresponding to ULS, in an average sense. EC3-1-8 defines such an equivalent elastic stiffness (equation (2.3)), called secant stiffness, illustrated in Figure 2.16, and provides estimates of its value for the most usual major axis joint typologies.

$$S_j = \frac{S_{j.ini}}{\eta} . \tag{2.3}$$

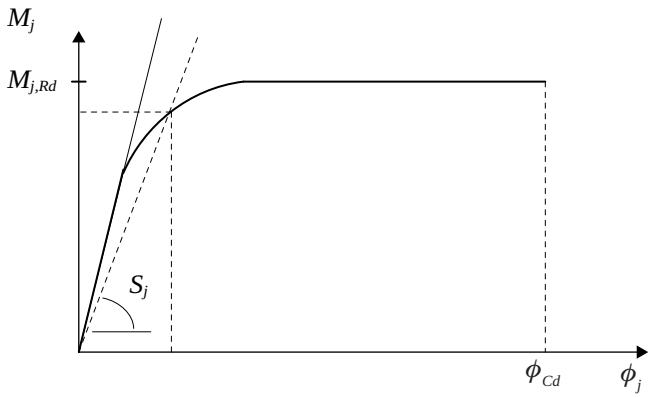


Figure 2.16 – Definition of the secant stiffness of a joint

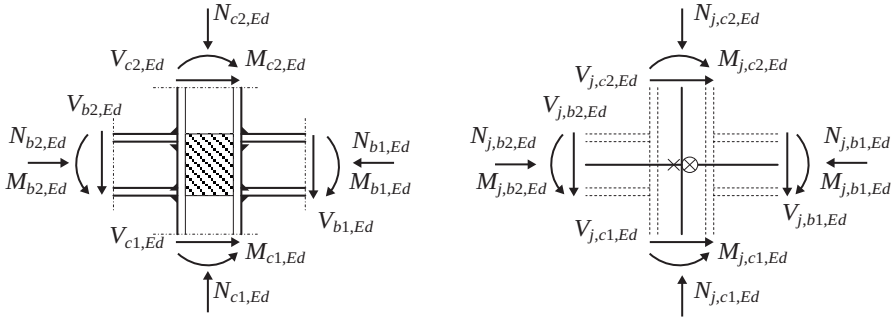
Table 2.4 illustrates the values of η for some cases.

Table 2.4 – Stiffness modification coefficient η

Type of joint	Beam-to-column joints	Other types of joints (beam-to-beam, beam splices, column bases)
Welded	2	3
Bolted end plates	2	3
Bolted flange angles	2	3.5
Base plates	-	3

Example 2.1 illustrates the various aspects discussed above.

The modelling of internal node joints is substantially more complex than joints to external columns (Figure 2.15). This is because the contribution of the deformability of the column web panel must be distributed between the left and right springs of the structural model (see Figure 2.17).



a) Forces outside the web panel

b) Forces in the intersection of the members' axes

Figure 2.17 – Modelling of joints in the internal node of a frame

In this case, in a simplified manner, EC3-1-8 divides this contribution between the two springs, according to the transformation parameter β (CEN, 2005b):

$$\beta_1 = \left|1 - M_{j,b2,Ed} / M_{j,b1,Ed}\right| \leq 2\,; \tag{2.4}$$

$$\beta_2 = \left|1 - M_{j,b1,Ed} / M_{j,b2,Ed}\right| \leq 2\,, \tag{2.5}$$

where

β_1, (β_2) is the value of the transformation parameter for the right (left) connection;

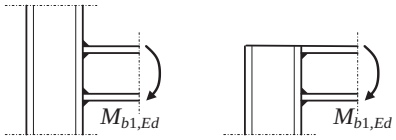
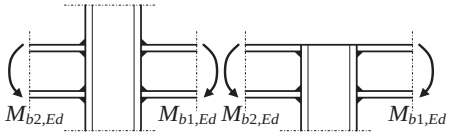
$M_{j,b1,Ed}$, ($M_{j,b2,Ed}$) is the applied bending moment on the right (left) beam, at the intersection of the centre lines of the elements.

Approximate values of β_1 and β_2 based on the values of the moments on the beams $M_{1,Ed}$ and $M_{2,Ed}$ on the periphery of the column web panel are indicated in Table 2.5 (CEN, 2005b). This approximate distribution assumes

a previous knowledge of the bending moments in the left and right beams. This requires, in practical terms, an extensive iterative procedure, as the properties of the structural model must be altered for each load combination.

Although it is not the aim of this book to present a deep treatment of this subject, nor is it intended to include the quantification of the properties of joints, two methodologies to deal with this aspect are indicated next[3].

Table 2.5 – Transformation parameter β

Type of configuration of the joint	Action	Value of β
	$M_{b1,Ed}$	$\beta \approx 1$
	$M_{b1,Ed} = M_{b2,Ed}$	$\beta = 0$ *)
	$M_{b1,Ed} / M_{b2,Ed} > 0$	$\beta \approx 1$
	$M_{b1,Ed} / M_{b2,Ed} < 0$	$\beta \approx 2$
	$M_{b1,Ed} + M_{b2,Ed} = 0$	$\beta \approx 2$

*) *In this case, the value of β is the exact value, not the approximate value*

The first, included in the simplified approach of EC3-1-8, comprises the following steps:

i) initial structural analysis, assuming, for the characterization of the rotational springs representing the joints and for all load combinations, β equal to one for the joints in external nodes and β equal to zero (equal and opposed moments) for the joints in internal nodes;
ii) for each load combination, verification and correction of the assumed values of β and the properties of the joints;
iii) structural analysis with the corrected values;

[3] Note that the interested reader may find in ECCS Eurocode Design Manuals (Jaspart and Weynand, 2016) a thorough treatment of the design of steel and steel-concrete composite joints.

iv) repetition of steps ii) and iii) until convergence.

The second approach avoids, on one hand, the iterative process and, on the other, perhaps most importantly, the necessity of analysing distinct structural models for each load combination by a more sophisticated modelling of the nodal zone. Based on Figure 2.18, it can be seen that, in reality, the node embraces three contributions for the deformability of that zone: the left connection, the right connection and the column web panel.

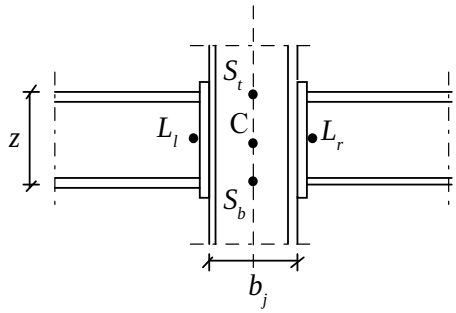


Figure 2.18 – Internal node steel beam-to-column joint

The representative springs for the left and right connections should be placed as indicated in Figure 2.18, with an eccentricity equal to half the depth of the cross section of the column and with stiffnesses $S_{j,ini}^{L_l}$ and $S_{j,ini}^{L_r}$, respectively. The spring modelling the shear deformation of the column web panel is characterized by a stiffness (axial and rotational) given by:

$$k_1 = \frac{0.38 A_{vc}}{\beta z}; \tag{2.6}$$

$$S_{j,ini}^{S} = E\, z^2\, k_1, \tag{2.7}$$

where A_v is the shear area of the column and z is the lever arm of the joint. Several alternative models are possible, such as indicated in Figure 2.19. In this case, the value of β is not considered in the characterization of this component. More detailed information on this matter can be found in Jaspart (1991) or Jordão *et al* (2013). Example 2.2 illustrates the aspects of modelling of joints in internal nodes.

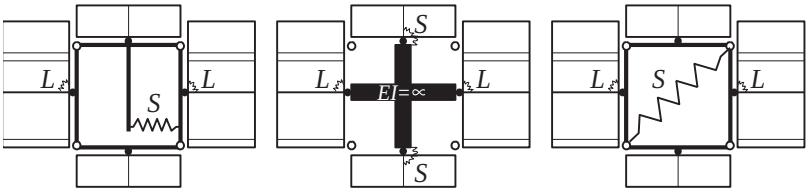


Figure 2.19 – Alternative models for the representation of the column web panel in shear

2.2.6. Combining beam elements together with two and three dimensional elements

Figure 2.20 illustrates a 3D frame composed of steel beams and columns and a concrete slab. Since most computer programs currently allow the combination of beam and shell elements, it becomes necessary to discuss specific modelling aspects related to the connection of these two element types.



Figure 2.20 – Beam and shell structural model

Firstly, it should be highlighted that the concrete slab usually fulfils a dual role: supporting the vertical loads and transmitting them to the steel structure but also providing in-plane stiffness that ensures rigid in-plane floor behaviour. In some computer programs, this may be implemented using constraint equations that impose equal in-plane displacements for a given slab. Alternatively, equivalent diagonal bracing may be used to achieve the same result, as illustrated in Figure 2.21.

The concrete slab may also be connected to the steel beams, resulting in composite action between steel and concrete. If composite action occurs and full interaction is assumed, the shell elements are rigidly connected to the beam nodes. For non-composite action the shell elements should be allowed to slip freely in the beam's longitudinal direction.

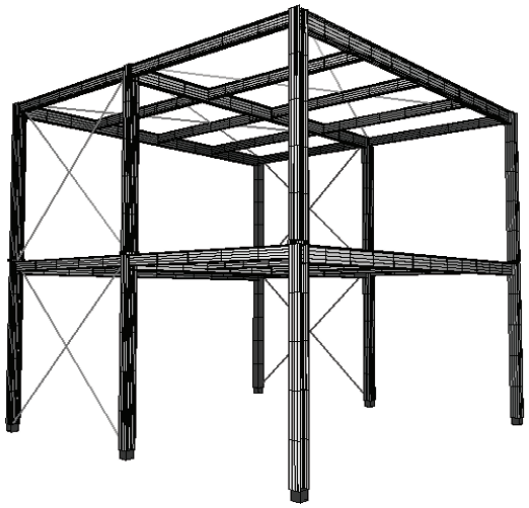


Figure 2.21 – Modelling of in-plane rigid slab behaviour

For all cases, the results are very sensitive to the modelling of the eccentricities between the mid-plane of the slab and the centroid of the beam elements. Also, in the case of non-composite action, even for reduced thicknesses of the slab, its bending stiffness is still sufficient to absorb non-negligible bending moments, therefore reducing the bending moments in the beams. All these aspects are illustrated in example 2.3.

2.2.7. Worked examples

Example 2.1: Consider the steel frame (E = 210 GPa and S 275) represented in Figure 2.22, subjected to the indicated loading, already factored. Assume that the column bases are fixed. Determine the design internal forces and displacements considering the following situations.

a) Full-strength rigid joints between the beams and the columns:
a.1) without considering the effect of eccentricities;

a.2) considering the effect of eccentricities;

b) Full-strength semi-rigid joints between the beams and the column;

c) Partial-strength semi-rigid joints.

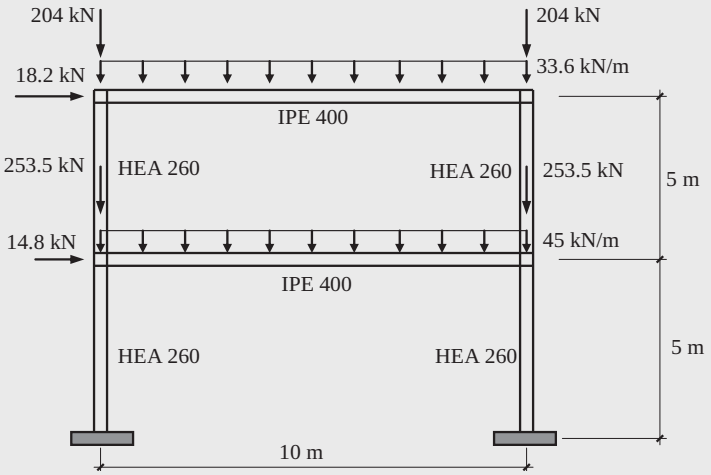


Figure 2.22 – Steel frame

a) Evaluation of the design internal forces and displacements assuming full-strength rigid beam-to-column joints.

Assuming full-strength rigid beam-to-column joints, the calculation model for the structure is shown in Figure 2.23 that represents the critical cross sections and the reference displacements to consider in the analysis of the results.

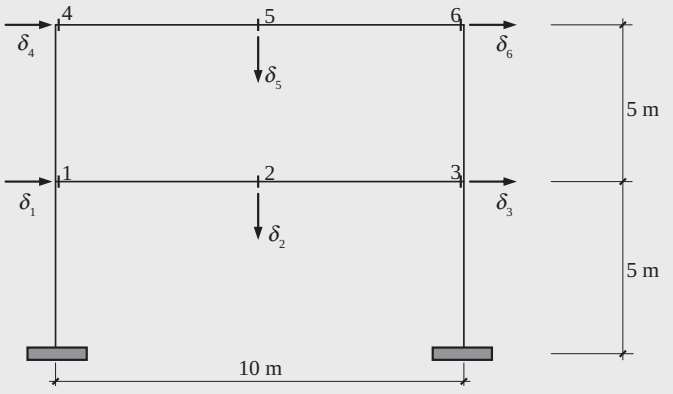


Figure 2.23 – Calculation model without eccentricities

The following diagrams of internal forces are obtained (Figures 2.24 to 2.26).

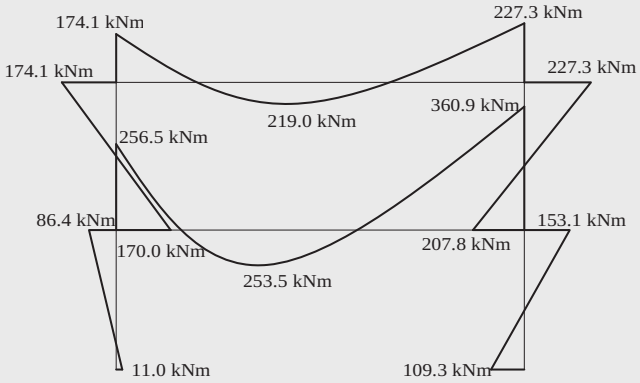


Figure 2.24 – Bending moment diagram

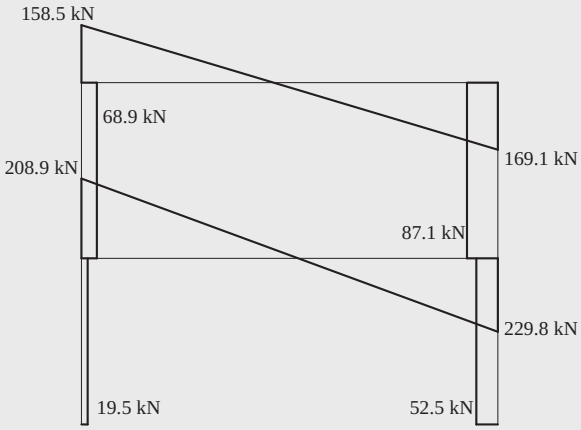


Figure 2.25 – Transverse shear diagram

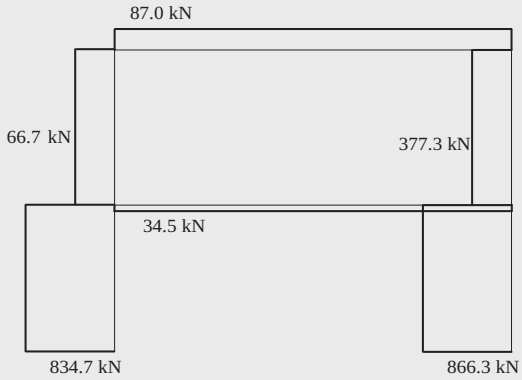


Figure 2.26 – Axial force diagram

Table 2.6 indicates the forces and displacements obtained at the critical cross sections.

Table 2.6 – Results at the critical cross sections

	M_y (kNm)	V_z (kN)	N_x (kN)	δ (mm)
1	256.5	208.9	34.5	12.2
2	253.5	10.5	34.5	43.4
3	360.9	229.8	34.5	12.4
4	174.1	158.5	87.0	23.7
5	219.0	5.3	87.0	41.7
6	227.3	169.1	87.0	23.2

In reality, the relevant design internal forces should be calculated taking into account the eccentricities that result from the finite dimensions of the cross sections, as illustrated in Figure 2.27.

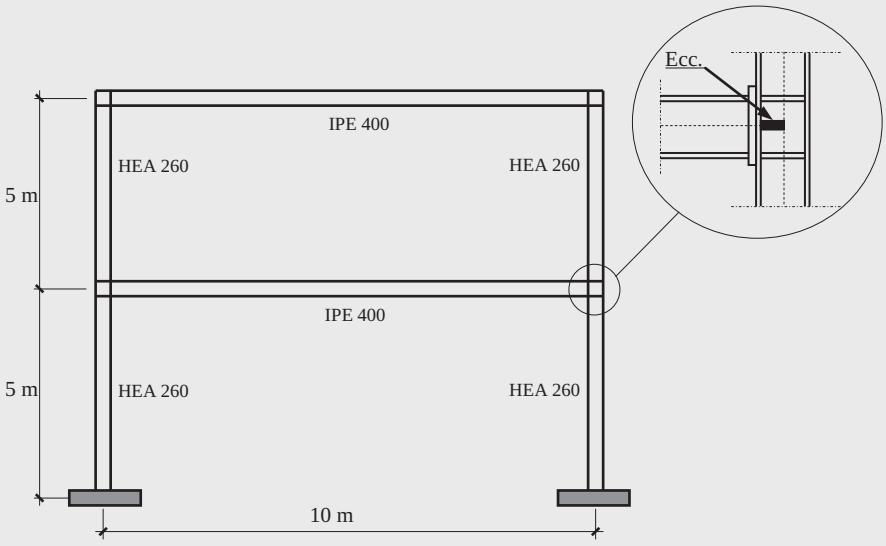


Figure 2.27 – Definition of the frame's eccentricities

The calculation model is illustrated in Figure 2.28. Table 2.7 summarizes the internal forces and displacements at the critical cross sections.

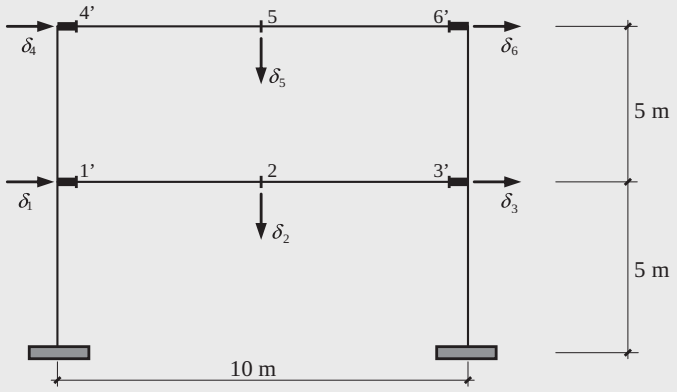


Figure 2.28 – Calculation model with eccentricities

Table 2.7 – Results at the critical cross sections with eccentricities

	M_y (kNm)	V_z (kN)	N_x (kN)	δ (mm)
1	-	-	-	-
1’	235.9	208.8	35.2	12.0
2	247.3	10.6	35.2	41.9
3’	339.0	230.0	35.2	12.2
3	-	-	-	-
4	-	-	-	-
4’	158.0	158.5	88.5	23.0
5	215.5	5.3	88.5	40.8
6’	209.6	169.1	88.5	22.5
6	-	-	-	-

Comparing the results in Tables 2.6 and 2.7, a decrease of 2.4 % and 1.6 % at the midspan moments of both beams and of 3.6 % and 2.1 %, respectively, for the vertical displacements, is noted, as a consequence of the consideration of rigid sections. These differences are small in this case, as the ratio $h/L_C = 0.025$ is low (see section 2.2.3).

However, the bending moment at 1’ compared to 1, 3’ compared to 3, etc., shows real benefits i.e lower design moments, when the designer bothers to account for eccentricity by including rigid links 1-1’, 3-3’, etc. These reductions reach 9.2 %.

Based on the design internal forces of Table 2.6, two different joints are considered, one at the intermediate beam level and another at the top beam. The joints at both ends of each beam have the same characteristics. The joints were calculated according to EC3-1-8, using a commercial program (Weynand *et al*, 2014).

Figures 2.29 and 2.30 represent the chosen full-strength joints. The joint at the intermediate beam consists of an extended end plate with a thickness of 16 mm, a haunch at the bottom flange and transverse and diagonal stiffeners in the column's web. The dimensions are shown in Figure 2.29. The bolts are M20, class 10.9. For this joint an initial stiffness ($S_{j,ini}$) of 416125 kNm/rad and a secant stiffness (S_j) of 208062 kNm/rad were obtained, and the joint is classified as rigid according to EC3-1-8. The joint exhibits a moment resistance $M_{j,Rd}$ = 366.2 kNm, corresponding to a relative resistance of $M_{j,Rd} \big/ M_{pl,y,Rd}^{beam} = 1.02$.

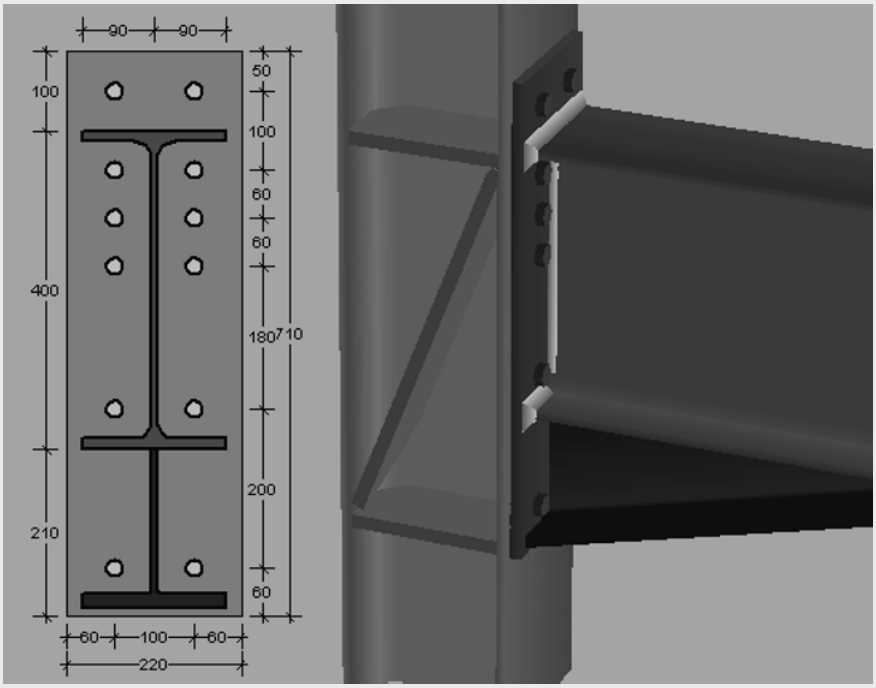


Figure 2.29 – Full-strength joint at intermediate beam level

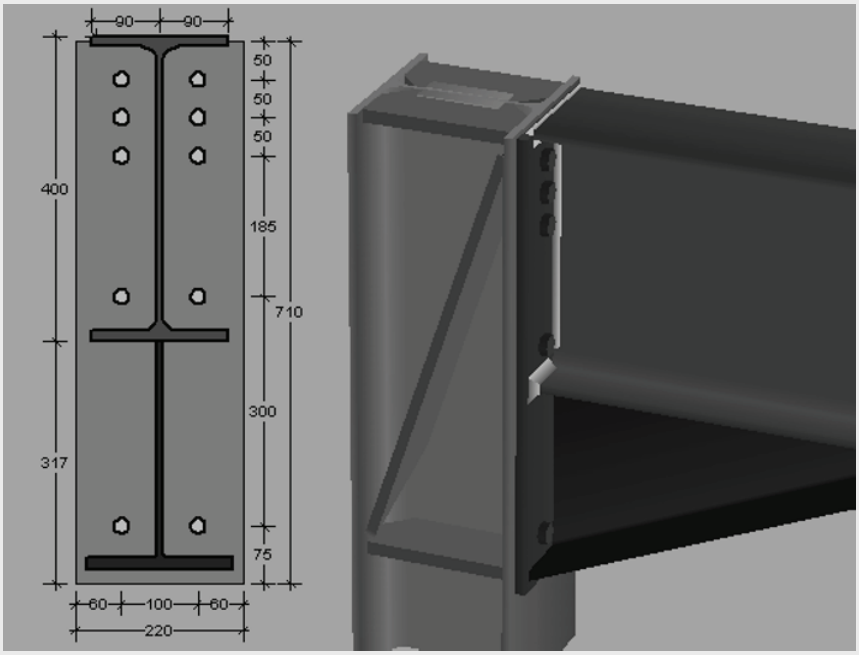


Figure 2.30 – Full-strength joint at top beam level

At the level of the top beam of the frame, the joint also consists of an extended end plate with a thickness of 16 mm, a haunch at the bottom flange of the beam and transverse and diagonal stiffeners in the column's web, with the dimensions shown in Figure 2.30. The bolts are also M20, class 10.9. In this case the initial stiffness ($S_{j,ini}$) is 389646 kNm/rad and the secant stiffness (S_j) is 194823 kNm/rad, the joint also being classified as rigid. The joint presents a moment resistance of $M_{j,Rd}$ = 360.0 kNm, and $M_{j,Rd} \big/ M_{pl,y,Rd}^{beam} = 1.00$.

Although both joints are classified as rigid according to EC3-1-8, it is interesting to assess the relevance of the real stiffness of the joints. The calculation model of Figure 2.23 with rigid joints between beams and columns, is replaced by the calculation model shown in Figure 2.31. In this structural model, the joints are represented by rotational springs, with an elastic behaviour characterized by the initial stiffness of the joint or the secant stiffness.

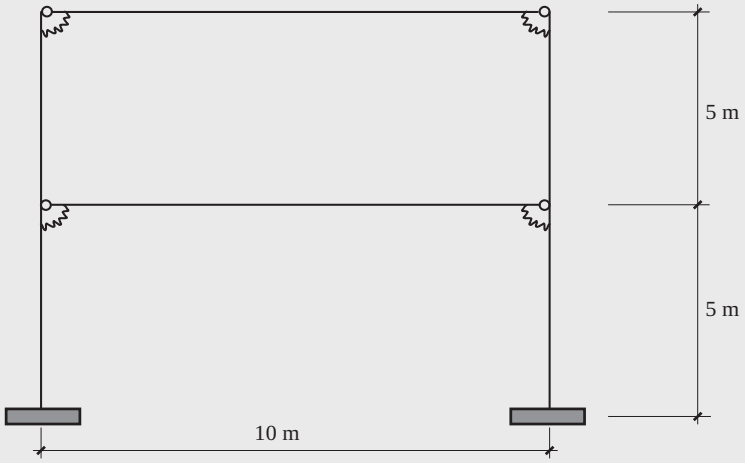


Figure 2.31 – Steel frame with semi-rigid joints

Table 2.8 represents the internal forces and displacements at the critical cross sections, which were calculated considering the secant stiffness of the joints.

Table 2.8 – Results for full-strength joints, evaluated using the secant stiffness

	M_y (kNm)	V_z (kN)	N_x (kN)	δ (mm)
1	246.2	209.2	33.1	12.8
2	264.9	10.2	33.1	46.3
3	348.4	229.6	33.1	12.9
4	166.9	158.4	84.3	25.1
5	226.0	5.4	84.3	43.5
6	220.6	169.2	84.3	24.6

Because the joints are full-strength, the critical cross sections occur in the beam and not at the joints. So it is not necessary to consider in the analysis the non-linear behaviour of the joint but just assess the effect of its flexibility. However, in this case, as the joint is full-strength but with a resistance only slightly larger than the plastic moment of the beam, at a load level close to ultimate limit state the bending moment developed in the joint will be close to its moment resistance. It follows that it will be adequate to perform the analysis with the secant stiffness and not with the initial stiffness (CEN, 2005b).

The consideration of the flexibility of the joints leads to a decrease of 4.0 %, 3.5 %, 4.1 % and 2.9 % in the negative moments of cross sections 1, 3, 4 and 6, respectively, when compared to the rigid model without eccentricities and to an increase of 4.5 % and 3.2 % in the mispan moments of the beams (cross sections 2 and 5, respectively) and of 6.8 % and 4.3 % of the corresponding vertical displacements. Rigid links are not considered to simulate the finite dimension of the cross sections as, in this case, its influence is negligible.

b) Evaluation of the design internal forces and displacements considering full-strength semi-rigid beam-to-column joints.

Considering a secant stiffness (S_j) of 85000 kNm/rad for the joint at the intermediate beam level and a secant stiffness (S_j) of 70000 kNm/rad for the joint at the top beam, Table 2.9 presents the internal forces and displacements at the critical cross sections, which were calculated using the structural model of Figure 2.31.

Table 2.9 – Results for partial-strength joints and secant stiffness

	M_y (kNm)	V_z (kN)	N_x (kN)	δ (mm)
1	232.4	209.4	30.7	13.6
2	280.1	9.9	30.7	50.3
3	331.7	229.3	30.7	13.6
4	155.6	158.4	80.1	27.1
5	237.1	5.4	80.1	46.3
6	209.7	169.2	80.1	26.7

c) Evaluation of the design internal forces and displacements considering partial-strength semi-rigid beam-to-column joints.

In the case of joints with partial resistance, consider the configurations that are represented in Figures 2.32 and 2.33 for the joints at the intermediate and top beam levels, respectively.

The joint at the intermediate beam level consists of an extended end plate with a thickness of 15 mm, a haunch at the bottom flange and transverse stiffeners in the column's web, with the dimensions indicated in Figure 2.32 and 2.33. The bolts are M20, class 10.9. For this joint, again using a commercial program

(Weynand *et al*, 2014), an initial stiffness ($S_{j,ini}$) of 86728 kNm/rad and a secant stiffness (S_j) of 43364 kNm/rad were obtained, and so the joint is classified as semi-rigid. The moment resistance of the joint is $M_{j,Rd}$ = 236.1 kNm, and so the joint is of partial resistance $\left(M_{j,Rd} / M_{pl,y,Rd}^{beam} = 0.66\right)$. The non-linear moment-rotation curve is shown in Figure 2.34.

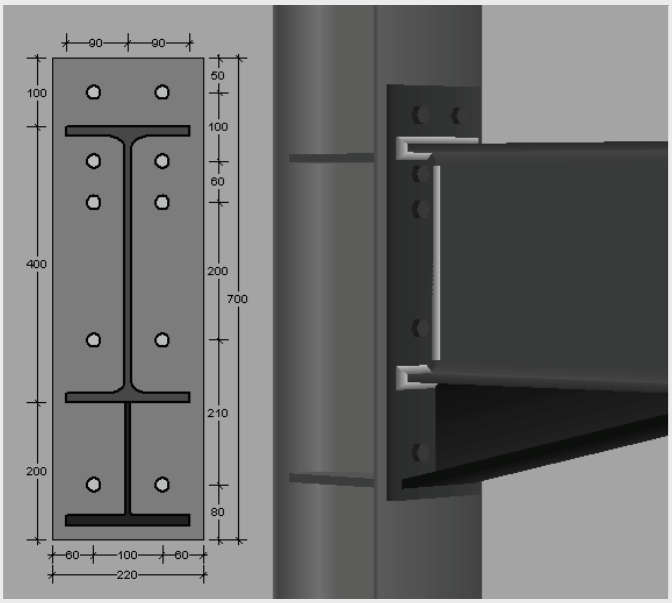


Figure 2.32 – Partial-strength joint at the intermediate beam level

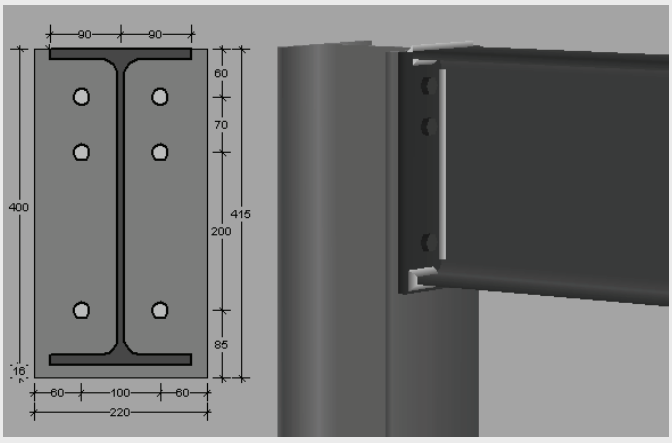


Figure 2.33 – Partial-strength joint at top beam level

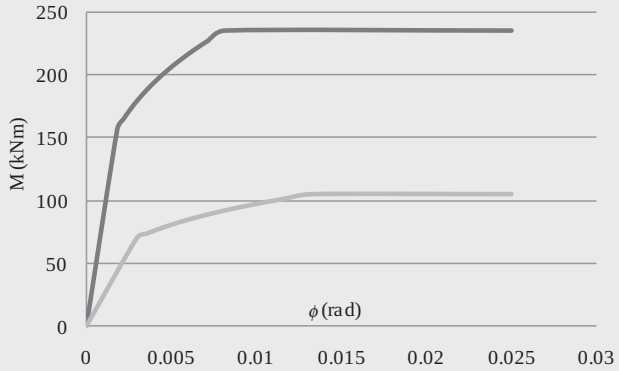


Figure 2.34 – M-ϕ curve of the joints of the intermediate and top beams

At the top beam, the joint also consists of an extended end plate with the dimensions indicated in Figure 2.33 and with a thickness of 15 mm. The bolts are also M20, class 10.9. In this case the initial stiffness ($S_{j,ini}$) is 23544 kNm/rad and the secant stiffness (S_j) is 11772 kNm/rad, and so the joint is classified as semi-rigid. The moment resistance is $M_{j,Rd}$ = 104.7 kNm, and the joint is of partial resistance $\left(M_{j,Rd} \big/ M_{pl,y,Rd}^{beam} = 0.29\right)$. The non-linear moment-rotation curve is represented in Figure 2.34.

Using partial-strength joints requires a non-linear analysis as the level of the bending moment at the joints will certainly reach their plastic resistance. Table 2.10 presents the internal forces and displacements in the structure, considering the real behaviour of joints, simulated by non-linear springs, according to Figure 2.34. Finally, Table 2.11 compares the results of the various models (FS/R: full-strength rigid joints; FS/SR: full-strength semi-rigid joints; PS/SR: partial-strength semi-rigid joints) with the reference case of an elastic analysis with rigid joints (Table 2.6), denoted by *R* in the table .

Table 2.10 – Results for partial-strength joints and real behaviour

	M_y (kNm)	V_z (kN)	N_x (kN)	δ (mm)
1	177.7	213.5	6.2	33.3
2	355.2	5.8	6.2	69.6
3	236.1	225.2	6.2	33.3
4	79.0	161.2	50.4	94.3
5	327.9	2.6	50.4	69.7
6	104.7	166.4	50.4	94.0

Table 2.11 – Comparative summary of results

	FS/R	*FS/SR*	*PS/SR*	M_{pl}^{beam}/M_i^R
M_1/M_1^R	0.96	0.91	0.69	1.4
M_2/M_2^R	1.04	1.10	1.40	1.4
M_3/M_3^R	0.96	0.92	0.65	1.0
M_4/M_4^R	0.96	0.89	0.45	2.1
M_5/M_5^R	1.03	1.08	1.50	1.6
M_6/M_6^R	0.97	0.92	0.46	1.6

The analysis of column $M_{pl,y,Rd}^{beam}/M_i^R$ in Table 2.11 shows that, neglecting the deformability of the joints, the resistance of the beams is governed by the hogging moment in section 3. For the full-strength joints of Figures 2.29 and 2.30, classified as rigid according to EC3-1-8, the maximum influence of the flexibility of the joints on the results is 4.1 % (inside the 5 % maximum difference allowed by EC3). Realistic full-strength semi-rigid joints for this example are classified according to stiffness close to the rigid boundary. Therefore, a limited effect is noted, with maximum variation of 11 % on the results. Finally, for the partial-strength joints of Figures 2.32 and 2.33, large differences are noted. The critical cross sections in terms of cross sectional-resistance are now located at mid-span of the beams, with moment increases of 40 % for the intermediate beam and 50 % for the top beam, with respect to the rigid solution. The maximum hogging moments are reduced by up to 55 %. This example highlights the potential advantages of using partial strength joints, potentially leading to more balanced and economical solutions as long as the rotation capacity of the joints is ensured.

Example 2.2: Consider the frame represented in Figure 2.35 (E = 210 GPa and steel grade S 275), under the indicated loading. Consider pinned column base joints, and full-strength rigid joints at the external nodes. At the internal node, the joint to be used is shown in Figure 2.36. It has an end plate 20 mm thick, and M24 class 10.9 bolts.

Using an elastic analysis and neglecting eccentricities in the nodes, determine the forces and displacements, considering the following situations:

a) rigid internal node joint;

b) internal node joint modelled by two rotational springs;
c) internal node joint modelled by three rotational springs.

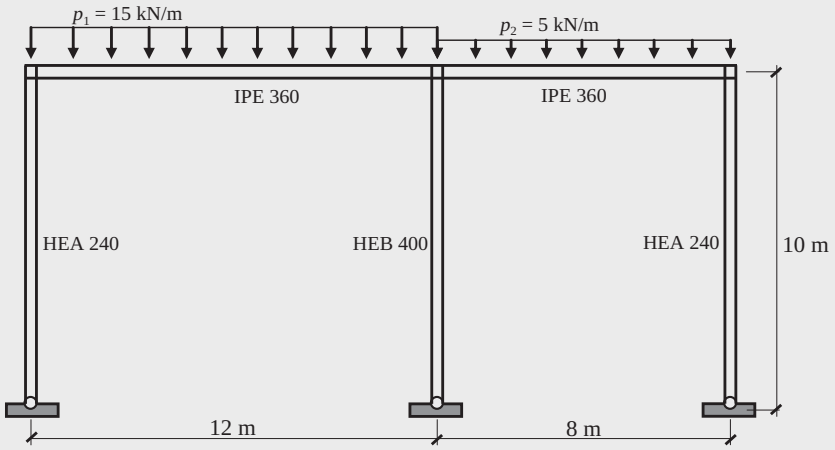


Figure 2.35 – Steel frame

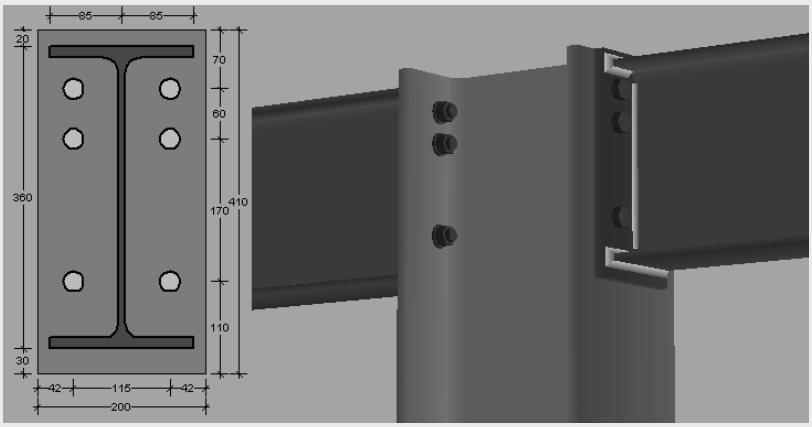


Figure 2.36 – Detail of the internal node joint

Figure 2.37 illustrates the critical cross sections to consider in the analysis, as well as the three modelling alternatives for the internal node beam-to-column joint. Because of the asymmetry of the structure and of the loading, the maximum sagging moment will not occur at points 2 or 4 (mid-span of the beams). Points 2’ and 4’ have an undefined location and correspond to the points of maximum sagging moment.

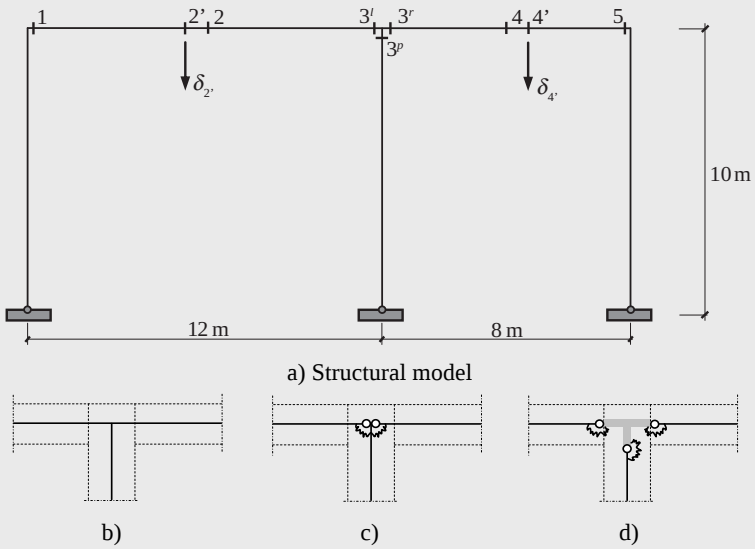


Figure 2.37 – Modelling of the internal node joint

a) Determination of the forces and displacements for rigid connections.

Based on Figure 2.37a and modelling the internal node according to Figure 2.37b, the bending moment diagram of Figure 2.38 is obtained.

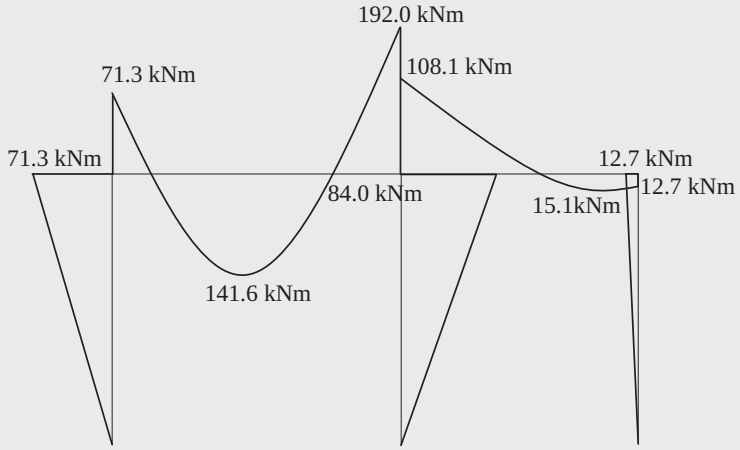


Figure 2.38 – Bending moment diagram

b) Determination of the forces and displacements for an internal node joint modelled by two rotational springs.

In this case, the modelling of the joint at the internal node corresponds to the simplified approach of EC3-1-8 (see section 2.2.5).

Using a commercial program (Weynand *et al*, 2014), the initial stiffness of the left and right joints, for $\beta^l = \beta^r = 0$ (equal and opposed moments) is given by:

$S_{j,ini}^l = S_{j,ini}^r = 42590 \text{ kNm/rad}$.

An elastic analysis of the structure leads to M_3^l = 162.0 kNm and M_3^r = 78.8 kNm, and so the assumed values for β must be corrected. Application of the iterative procedure described in section 2.2.5 yields the results of Table 2.12.

Table 2.12 – Iterative process

	Number of iteration			
	(0)	(1)	(2)	(3)
β_l	0	0.51	0.53	0.53
β_r	0	1.06	1.14	1.14
$S_{j.ini}^l$	42590	36698	36515	36505
$S_{j.ini}^r$	42590	32020	31419	31385
M_3^l (kNm)	162.0	157.3	157.0	157.0
M_3^r (kNm)	78.8	73.6	73.3	73.3

c) Determination of forces and displacements for an internal node joint modelled by three rotational springs.

In this case, the modelling of the internal node joint, schematically represented in Figure 2.37d, corresponds to the non-iterative approach (see section 2.2.5).

Using a commercial program (Weynand *et al*, 2014), it is necessary to determine the secant stiffness of the left and right joints without considering the contribution of the column web panel in shear (which is equivalent, in this case, to consider $\beta^l = \beta^r = 0$). So, the value of the initial stiffness is identical to the value of initial iteration of the previous case:

$S_{j,ini}^l = S_{j,ini}^r = 42590 \text{ kNm/rad}$.

Additionally, it is necessary to determine separately the stiffness of the column web panel in shear, without considering the parameter β. According to equations (2.6) and (2.7), where *z* is the level arm obtained from Figure 6.15 of EC3-1-8:

$$k_1 = \frac{0.38 A_{vc}}{z} = \frac{0.38 \times 69.98 \times 10^2}{273.6} = 9.72 \text{ mm};$$

$$S_{j,ini}^{S} = \frac{E \times z^2}{1/k_1} = 152789 \text{ kNm/rad}.$$

An elastic analysis of the structure yields M_3^l = 161.3 kNm and M_3^d = 79.9 kNm.

Table 2.13 summarises the results (absolute values) for the three approaches, for the critical cross sections of Figure 2.37a. Neglecting the stiffness of the two joints in the internal node (case (a)), errors of 19 %, 35 % and 3 % in the bending moments in the left and right beams and column, respectively, are noted. Using the simplified model of EC3 (case (b)), those errors are reduced to 3 %, 8 % and 3 %, for the same cross sections. This example highlights the importance of taking into account the flexibility of the joints. Additionally, the simplified approach of EC3-1-8 yields reasonable results when compared to the non-iterative approach.

Table 2.13 – Synthesis of results

M (kNm)	a)	b)			c)
		(0)	(1)	(3)	
1	71.3	75.7	76.7	76.7	74.9
2’	141.6	152.9	154.5	154.6	153.6
2	138.3	151.1	153.0	153.1	151.9
3^l	192.0	162.0	157.3	157.0	161.3
3^p	84.0	83.3	83.6	83.7	81.5
3^r	108.1	78.8	73.6	73.3	79.9
4	7.7	4.4	6.7	6.8	3.4
4’	15.1	16.0	16.8	16.9	15.0
5	12.7	7.5	7.0	6.9	6.6

Example 2.3: Consider the two-storey steel framed building (*E* = 210 *GPa* and S 275) of Figure 2.39, subject to the following factored loads:

- a uniformly distributed load on the 1st floor of 9.0 kN/m^2 and on the 2nd floor of 6.7 kN/m^2 (these loads are applied directly on the primary beams);
- vertical linearly distributed loads on the secondary beams of 50.7 kN/m and 40.8 kN/m, respectively on the 1st floor and on the 2nd floor as shown in Figure 2.40;

- horizontal linearly distributed loads of 2.96 kN/m and 3.64 kN/m, applied at the level of the 1st floor and of the 2nd floor respectively, and only in one side of the structure (see Figure 2.40).

The columns consist of HEA 260 profiles and the primary beams (*x*-direction) are IPE 400 profiles. The secondary beams (*y*-direction) are constituted by IPE 300 and the vertical bracing consists of CHS 26.9×2.3. The concrete slab is 13 cm thick and the spacing of the frames in the *y* direction is 5.0 m. Consider rigid beam-to-column joints and column bases. Also assume that the beams are non-composite.

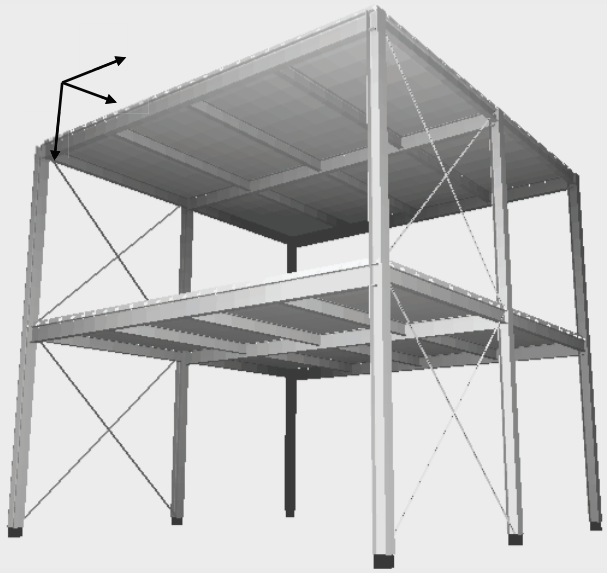


Figure 2.39 – Two-storey steel framed building

Determine the design internal forces and displacements corresponding to ULS for the following modelling alternatives:

a) structure modelled with beam elements only, neglecting the slab;
b) structure modelled with beam elements only, considering the in-plane contribution of the slab by applying equivalent diagonal bracing;
c) structure modelled with beam elements for the beams and columns and shell elements for the slab.

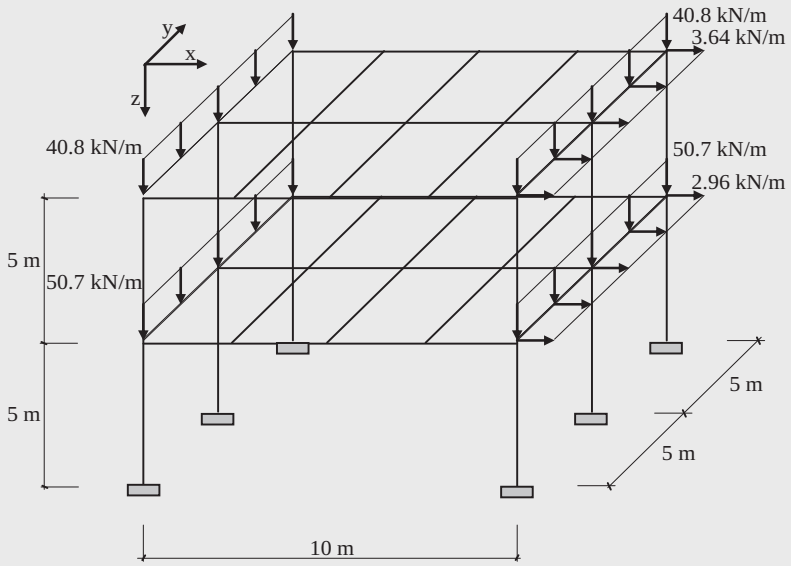


Figure 2.40 – Loads on secondary beams

The internal forces and displacements are calculated for three different structures, corresponding to the three modelling options. The results presented are related to the critical cross sections represented in Figure 2.41, and for the middle frame only.

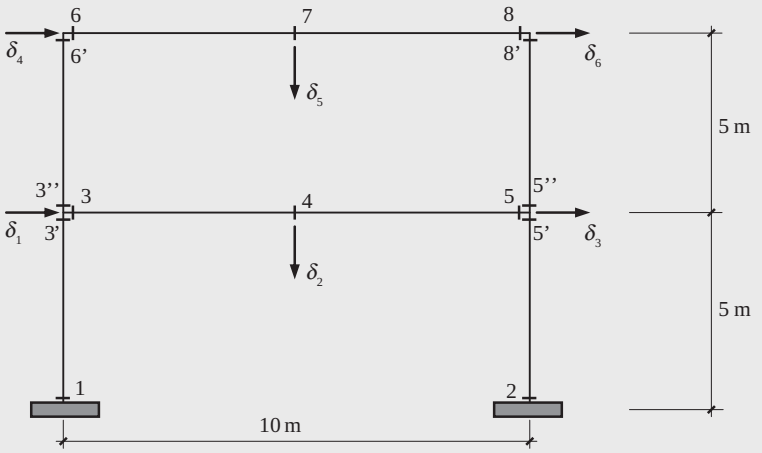


Figure 2.41 – Critical cross sections in the middle frame

a) Structure modelled with beam elements only, neglecting the slab (model 1).

Neglecting the slab, the calculation model considers only the bare steel frame, as illustrated in Figure 2.42. The joints between the primary beams and the columns are rigid. The secondary beams are pinned at both ends.



Figure 2.42 – Structural steel model (neglecting the slab)

b) Structure modelled with beam elements only, considering the in-plane contribution of the slab by applying equivalent diagonal bracing (model 2).

In this model, represented in Figure 2.43, the in-plane contribution of the slab is simulated by an equivalent diagonal bracing. Hence, the steel structure is similar to the previous case, apart from the horizontal diagonal bracing system, which is introduced in order to provide the equivalent stiffness corresponding to a concrete slab 13 cm thick. Bracing members are pinned at both ends.



Figure 2.43 – Structural steel model with horizontal bracing

c) Structure modelled with beam elements for the beams and columns and shell elements for the slab (model 3).

In this case the model is illustrated in Figure 2.39. The beams are non-composite, so that the slab is simply supported on the beams.

For model 1, the bending moment, shear force and axial force diagrams are illustrated in Figures 2.44 to 2.46. The torsional and beam minor axis bending moment diagrams are not represented because they yield negligible values.

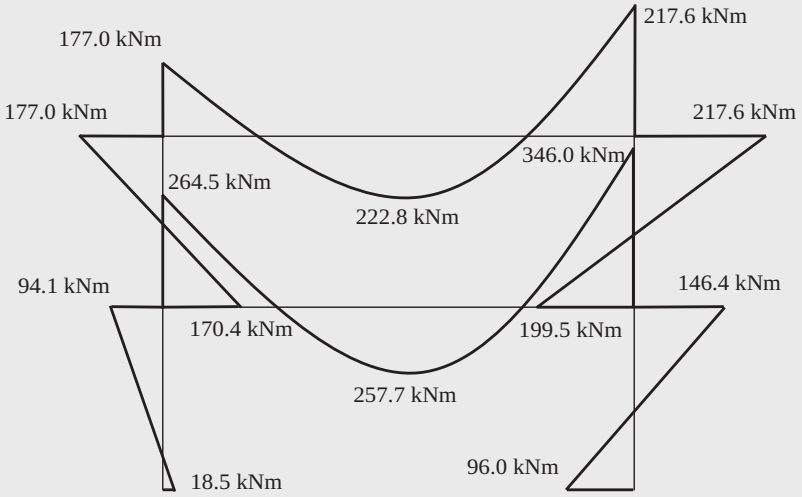


Figure 2.44 – Bending moment diagram

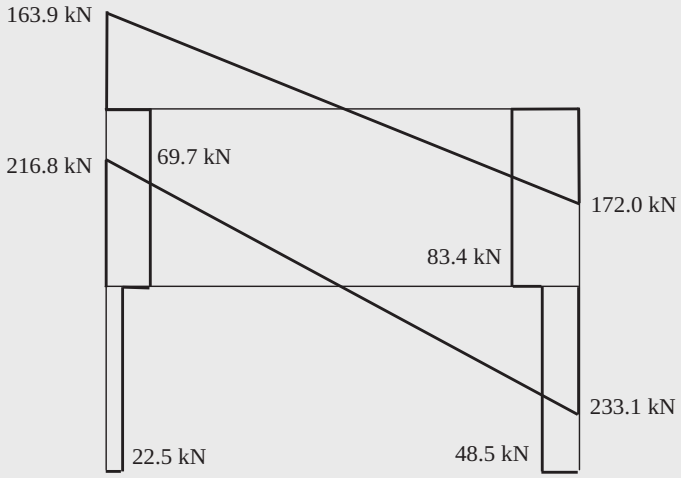


Figure 2.45 – Shear force diagram

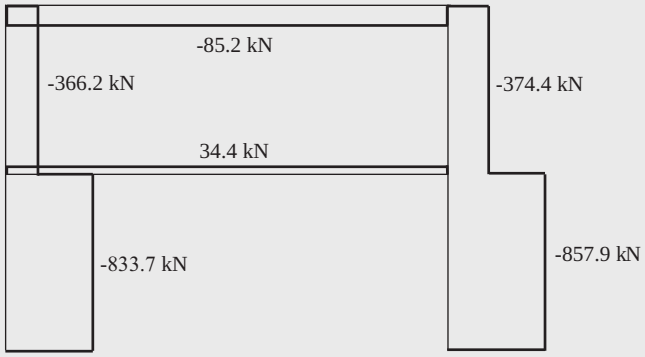


Figure 2.46 – Axial force diagram

Table 2.14 compares the results (bending moment and axial force) for the three models at the critical cross sections. Compared to model 2, the mid-span moments show maximum variations of + 6.7 % and - 37.3 % for model 1 and model 3, respectively. A similar comparison for the hogging moments yields maximum variations of + 5.8 % and - 28 % for model 1 and model 3, respectively.

Table 2.14 – Bending moments and axial forces at the critical cross sections (beam elements)

	Model 1		Model 2		Model 3	
	M_y (kNm)	N_x (kN)	M_y (kNm)	N_x (kN)	M_y (kNm)	N_x (kN)
1	18.5	833.7	20.8	829.9	14.4	854.9
2	96.0	857.9	86.9	854.9	79.4	885.2
3	264.5	34.4	251.7	19.0	179.9	109.1
3’	94.1	833.7	89.9	829.9	73.3	854.9
3’’	170.4	366.0	161.7	365.8	127.1	381.2
4	257.7	34.4	241.6	19.0	151.5	109.1
5	346.0	34.4	327.1	19.0	251.3	109.1
5’	146.4	857.9	136.7	854.9	121.0	885.2
5’’	199.5	374.1	190.4	371.8	154.7	392.3
6	177.0	84.2	170.4	42.1	132.3	70.8
6’	177.0	366.0	170.4	365.8	132.3	381.2
7	222.8	84.2	211.4	42.1	130.1	70.8
8	217.6	84.2	207.0	42.1	169.4	70.8
8’	217.6	374.4	207.0	371.8	169.4	392.3

Table 2.15 compares the displacements for the three models. Compared with model 2, the maximum vertical displacement of the beams differs by + 20.2 % and - 29.5 % for models 1 and 3, respectively.

Table 2.15 – Displacements δ (mm), at the critical cross sections

	Model 1	Model 2	Model 3
3	11.8	9.9	9.2
4	51.1	48.3	34.3
5	11.3	9.4	9.3
6	21.2	17.7	17.0
7	48.6	46.5	32.8
8	20.7	17.4	16.5

Comparing model 1 with model 2, the differences in bending moment, are less than 10 %. At almost all critical sections, model 1 gives larger values than model 2 and are on the safe side compared to model 2. On the contrary, model 3 (apparently the most sophisticated model) presents differences of up to 37.3 % compared to model 2. Model 3 gives lesser values. These differences can be explained by the influence of the bending stiffness of the concrete slab itself, as can be seen in Table 2.16.

Table 2.16 – Moments at the critical cross sections (slab elements)

	Model 3		
	M_y (kNm)	M_z (kNm)	M_{yz} (kNm)
3	81.1	9.6	0.14
4	23.4	28.9	0.01
5	93.2	10.3	0.52
6	18.7	3.5	0.002
7	19.8	24.3	0.002
8	21.9	3.4	0.002

However, the results of model 3 are not realistic at ultimate limit state because no account is taken of the cracking of concrete in the hogging regions. A proper simulation would require a non-linear analysis with

cracked concrete or an approximate iterative procedure. Since this is not a practical approach for common building frames, a good compromise is to use a reduced thickness of the slab. This solution keeps the modelling advantages (direct application of the loading on the shell elements, therefore reducing significantly the amount of pre-processing work), and also simulates the in-plane stiffness of the slab. Table 2.17 compares the results for three slab thicknesses. The model with the thinnest slab shows maximum differences of 8 % when compared with model 2 and the bending moments in the slab along the beam direction virtually vanish.

Table 2.17 – Bending moments in the critical sections (beam and shell elements)

	Model 3		Model 3* (7.5 cm)		Model 3** (2.5 cm)	
	Beam M_y(kNm)	Shell M_y(kNm)	Beam M_y(kNm)	Shell M_y(kNm)	Beam M_y(kNm)	Shell M_y(kNm)
1	14.4	-	20.6	-	21.7	-
2	79.4	-	86.1	-	89.7	-
3	179.9	81.1	238.5	27.3	268.8	1.4
3’	73.3	-	88.4	-	96.3	-
3’’	127.1	-	150.1	-	172.5	-
4	151.5	23.4	215.3	8.1	253.6	0.5
5	251.3	93.2	309.4	29.6	338.6	1.5
5’	121.0	-	133.4	-	140.6	-
5’’	154.7	-	176.1	-	198.0	-
6	132.3	18.7	160.3	10.8	177.3	0.6
6’	132.3	-	160.3	-	177.3	-
7	130.1	19.8	185.8	7.0	220.5	0.4
8	169.4	21.9	196.7	11.6	212.6	0.7
8’	169.4	-	196.7	-	212.6	-

Table 2.18 compares the critical buckling loads for the three models. The critical modes are similar for all models but the model with beam and shell elements is much stiffer for the first two (torsional) modes. This reflects the contribution of a stiff 13 cm thick concrete slab. The third mode is a sway mode in the global *x* direction and good agreement is observed for the critical buckling load between the three models (differences of only - 12.6 % and - 4.7 % when compared to model 3).

Table 2.18 – Critical buckling loads and buckling modes

	Model 1	Direction	Model 2	Direction	Model 3	Direction
1	7.37	T	7.42	T	10.30	T
2	7.57	T	7.61	T	10.65	T
3	**9.93**	X	**10.83**	X	**11.36**	X
4	13.30	T	13.36	T	13.48	T
5	13.90	T	13.84	T	14.82	T
6	14.82	T	14.89	T	15.44	T
7	14.96	T	15.01	T	16.24	X
8	15.23	T	15.30	T	19.33	T
9	15.56	T	15.50	T	19.81	T
10	16.15	X	16.67	T	20.30	T

2.3. GLOBAL ANALYSIS OF STEEL STRUCTURES

2.3.1. Introduction

The global analysis of a steel structure should provide with sufficient accuracy the internal forces and moments and the corresponding displacements. Analysis is to be based on appropriate calculations models (clause 5.1.1(1)) and the model and the basic assumptions should reflect the structural behaviour (clause 5.1.1(2)). In particular, it should ensure that the relevant non-linearities for a given limit state are adequately taken into account.

The internal forces and displacements may be determined using either a global elastic analysis or a global plastic analysis (clause 5.4.1(1)). Finite element analysis is also possible but it is not specifically covered in EC3-1-1, reference being made to EC3-1-5 (CEN, 2006c).

Global elastic analysis is based on the assumption of a linear stress-strain relation for steel, whatever the stress level in the structure is (clause 5.4.2(1)). In practical terms, global elastic analysis assumes that the reference stress caused by the applied forces is lower than the yield stress of steel anywhere in the structure. Elastic global analysis may be used in all cases (clause 5.4.1(2)), provided that the provisions in clause 5.1 are met. It is noted that even though the internal forces and displacements are obtained using elastic analysis, the design resistance of the members may be evaluated on the basis of the plastic cross section resistance (clause 5.4.2(2)).

Specific procedures and a detailed practical example of a multi-storey building designed using global elastic analysis are presented in chapter 4.

Global plastic analysis assumes progressive yielding of some cross sections of the structure, normally leading to plastic hinges and a redistribution of forces within the structure. In this type of analysis it is mandatory that the cross sections where plastic hinges occur possess sufficient rotation capacity. Usually, the adopted stress-strain relation for steel is a bi-linear elastic-plastic relationship, although more precise relationships may be adopted (clause 5.4.3(4)). The use of plastic global analysis is subjected to several conditions. These are detailed in chapter 5, together with a detailed practical example of an industrial building designed using global plastic analysis.

Global analysis may also be of 1st or 2nd order. In a first order analysis, the internal forces and displacements are obtained with reference to the undeformed structure (clause 5.2.1(1)). In a 2nd order analysis, the influence of the deformation of the structure is taken into account. This should be considered whenever it increases the action effects significantly or modifies significantly the structural behaviour (clause 5.2.1(2)). The presence of compressive forces or stresses may induce 2nd order effects, amplifying internal forces and displacements. In terms of global analysis, it is then required to assess the structural stability of the frame, an aspect that will be detailed in the next section. A second situation where the deformed geometry of the structure must be taken into account occurs whenever the structure or parts of it present low stiffness, such as is the case of structures containing cables. In this case, a large-displacement analysis (or third-order analysis in german terminology) should be carried out. This case will not be covered in this book, EC3-1-11 (CEN, 2006e) being specifically devoted to this.

Global analysis must also explicitly model imperfections, both at global level and member level, although some simplified procedures exist to avoid direct modelling of some imperfections (section 2.3.3 and chapter 3). Also, the effects of shear lag and of local buckling on the stiffness should be taken into account if this significantly influences the global analysis (clause 5.2.1(5)). EC3-1-5 presents detailed procedures for such situations, although for rolled sections and welded sections with similar dimensions, shear lag effects may be neglected. The ECCS Eurocode Design Manual “Design of Plated Structures” (Beg *et al*, 2010) covers shear lag and local buckling in detail. Finally, the

effects on the global analysis of slip in bolt holes and similar deformations of connection devices like studs and anchor bolts should be taken into account, where relevant and significant (clause 5.2.1(6)).

The choice of the analysis procedure (elastic or plastic, clause 5.4.1(1)), should take into account all the aspects discussed above (non-linear material behaviour, 2nd order effects and imperfections), aiming to achieve a good compromise between safety and simplicity of the calculation procedures. All of these aspects are discussed and detailed in the following sections. Elastic 1st order analysis is the usual choice for most practitioners. However, in many cases, it does not ensure results on the safe side. A number of simplified procedures based on 1st order analysis were therefore developed to incorporate non-linearities and imperfections, described in chapters 4 and 5.

2.3.2. Structural stability of frames

2.3.2.1. Introduction

Steel structures are usually slender structures when compared to alternatives using other materials. Instability phenomena are potentially present, so that it is normally necessary to verify the global stability of the structure or of part of it. This verification leads to the need to carry out a 2nd order analysis, with the consideration of imperfections (clause 5.2.2(2)). There is a multiplicity of ways to assess 2nd order effects including imperfections. In general terms and according to clause 5.2.2(3), the different procedures can be categorized according to the following three methods (clause 5.2.2(3)):

- global analysis directly accounts for all imperfections (geometrical and material) and all 2nd order effects (method 1);
- global analysis partially accounts for imperfections (global structural imperfections) and 2nd order effects (global effects), while individual stability checks on members (clause 6.3) intrinsically account for member imperfections and local 2nd order effects (method 2);
- in basic cases, individual stability checks of equivalent members (clause 6.3), using appropriate buckling lengths corresponding to the global buckling mode of the structure (method 3).

Normally, it is usual to sub-divide the 2nd order effects into *P*-δ effects (for members) and *P*-Δ effects (for the structure). *P*-δ effects correspond to the effects of the displacements along the length of a member (Figure 2.47), while *P*-Δ effects correspond to the effects of the displacements at the ends of the members, also illustrated in Figure 2.47.

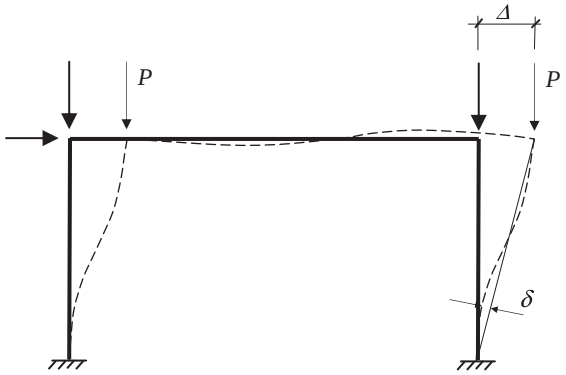


Figure 2.47 – Typical displacements Δ and δ

This subdivision helps to understand the three methods described above. In fact, both the *P*-δ and the *P*-Δ effects can be approximately accounted for, through individual verifications of the stability of equivalent members (method 3). However, especially with respect to *P*-Δ effects, this method requires an accurate determination of the buckling modes and the corresponding equivalent lengths, as well as a structural behaviour in which the first buckling mode is dominant. It is therefore understandable that EC3 limits the application of this method to simple cases (that correspond to standard cases in which the effective lengths are normally established by inspection[4]). It must also be pointed out that, in this method, imperfections are exclusively considered in the context of clause 6.3 in the verification of the stability of members.

Method 1 is the most sophisticated method because the global analysis, commonly called GMNIA (Geometrical and Material Non-linear

[4] Note that EC3 allows the more generalized use of this methodology, method of the equivalent column (clause 5.2.2(8)), leaving as a national option the definition of its scope.

Analysis with Imperfections), accounts for the 2nd order effects, as well as the global imperfections of the structure and local imperfections of the members. According to clause 5.2.2(7), if 2nd order effects in individual members and relevant member imperfections are totally accounted for in the global analysis of the structure, no individual stability check for the members according to clause 6.3 is necessary. However, either because of its complexity, or for the volume of work that it requires, this method still does not constitute the preferential option in design.

Method 2 constitutes the usual design procedure. The P-δ effects and the local member imperfections are incorporated in the normative expressions for the stability of members, whereas the P-Δ effects are directly evaluated by global analysis and the global imperfections are explicitly considered in the analysis of the structure. The individual stability of members should be checked according to the relevant criteria in clause 6.3 for the effects not included in the global analysis (clause 5.2.2(7)). This verification may be based on a buckling length equal to the system length as a safe estimate, although the non-sway buckling length may also be used. So, from this point forward in this chapter, unless explicitly indicated otherwise, only the procedures for the determination of P-Δ effects will be described.

2nd order effects increase not only the displacements but also the internal forces, in comparison to 1st order behaviour. It is thus necessary to assess if this increase is relevant and, if so, to calculate (exactly or approximately) the real forces and displacements in the structure.

Usually, the sensitivity of a structure to 2nd order effects is assessed indirectly using the elastic critical load of the structure, F_{cr}. This assessment must be done for each load combination, through the ratio between the critical load and the corresponding applied loading (F_{cr}/F_{Ed}). EC3 requires the consideration of 2nd order effects whenever (clause 5.2.1(3)):

$$\alpha_{cr} = F_{cr} / F_{Ed} \leq 10 \quad \text{(in elastic analysis);} \tag{2.8a}$$

$$\alpha_{cr} = F_{cr} / F_{Ed} \leq 15 \quad \text{(in plastic analysis).} \tag{2.8b}$$

It is noted that a greater limit for α_{cr} for plastic analysis is given because structural behaviour may be significantly influenced by non-linear material properties in the ultimate limit state (e.g. where a frame forms

plastic hinges with moment redistribution or where significant non-linear deformations arise from semi-rigid joints). EC3 allows National Annexes to give a lower limit for α_{cr} for certain types of frames where substantiated by more accurate approaches.

2.3.2.2. Elastic critical load

The elastic critical load of a structure (Timoshenko and Gere, 1961; Chen and Lui, 1987) plays a very important role in the evaluation of the sensitivity of a structure to 2nd order effects. According to King (2001a), the critical load of a structure, although a theoretical value, is of great practical interest, as it:

- shows the sensitivity of the structure to 2nd order effects through the ratio $\alpha_{cr} = F_{cr} / F_{Ed}$;
- can be calculated much more easily than a 2nd order analysis;
- constitutes the basis for a series of approximate methods for the evaluation of 2nd order effects, that can be applied to a large proportion of cases (except when $\alpha_{cr} \leq 3.0$);
- reflects the relative sensitivity of each load combination with respect to 2nd order effects.

The determination of the critical loads of a framed structure can be carried out analytically, using the stability functions of Livesley and Chandler (1956) or, in an equivalent way, using commercial software. Alternatively, the critical loads can be calculated using approximate methods. Both procedures are discussed in detail in the following paragraphs.

Nowadays, the numerical calculation of the elastic critical loads of a structure is a standard feature of most commercial software for structural analysis. However, in order to obtain reliable results, the following rules should be obeyed:

- the structural model shall adequately reproduce the structure's elastic behaviour. In the modelling of joints, the initial stiffness should be used;
- the discretization of the members must be adequate, with a minimum number of elements for each sinusoidal half-wave of the buckling mode (Figure 2.48);

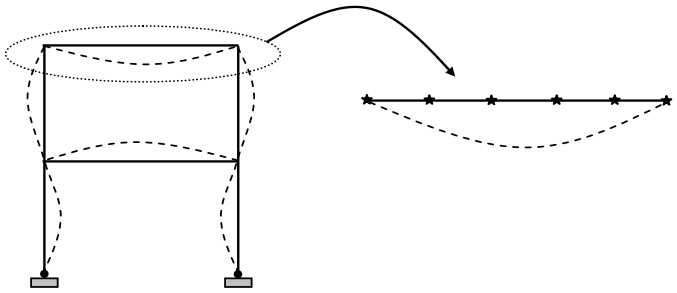


Figure 2.48 – Recommended discretization for the evaluation of critical loads

– the determination of the critical loads should be done for each load combination and the actions must be specified for a level of loading that corresponds to ultimate limit state. So, the program will directly provide the quotient α_{cr}, without being necessary to evaluate explicitly F_{Ed}. Note that $F_{Ed,}$ defined in EC3 (clause 5.2) as the design load, corresponds in reality to the axial force distribution in the structure (Figure 2.49)[5];

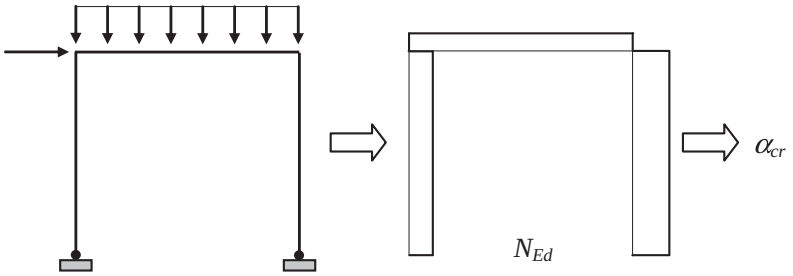


Figure 2.49 – Definition of the axial loading for the determination of critical load

– because any structure has more than one buckling mode, and the 2nd and higher critical loads can be relevant to the 2nd order effects, more than just the 1st critical load and buckling mode should be calculated. In particular, it is convenient to always calculate the lowest critical load for a "sway mode" and for a "non-sway mode", illustrated in Figure 2.50. In the case of three-

[5] Some authors define F_{Ed} as the sum of the (gravity) vertical reactions in the structure, which creates difficulties in the interpretation of results for loadings in which the total vertical reaction is zero (wind action, for example).

dimensional frames, this requirement must be widened to the lowest critical loads and buckling modes in each direction.

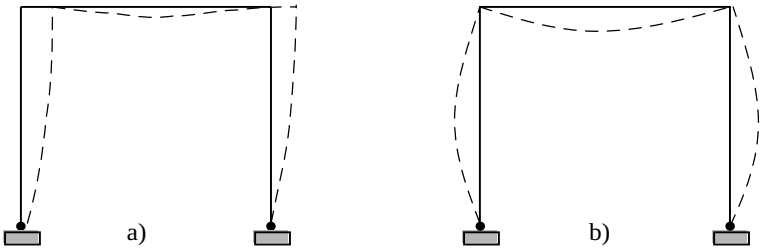


Figure 2.50 – "Sway mode" (a)) and "Non-sway mode" (b))

Example 2.4, presented at the end of this sub-chapter, shows in detail the determination of critical loads and buckling modes.

The approximate calculation of critical loads evolved in days where computational tools were not readily available to allow exact analysis. Nowadays, they still remain quite useful, either for the pre-design phase, or for checking to eliminate gross errors in numerical results. The most widespread approximate method was developed by Horne (1975) and it is applicable to regular frames for the determination of the lowest critical load in a "sway mode". According to this method, α_{cr} is given by:

$$\alpha_{cr} = \frac{1}{200\phi_{\max}}, \tag{2.9}$$

in which ϕ_{max} is the maximum value of the "sway" index for each floor, $\phi_{s,}$ given by:

$$\phi_s = \frac{\delta_U - \delta_L}{h}, \tag{2.10}$$

and h is the height of the floor, δ_U and δ_L are the horizontal displacements at the top and at the bottom of the floor, respectively, calculated on the basis of a linear elastic analysis of the frame under fictitious horizontal forces applied at the level of each floor, equal to 0.5 % of the factored total vertical loads applied to that floor. This procedure requires therefore the calculation of α_{cr}

for each floor and each load combination. Note that, in Horne's original work, equation (2.9) presents 222.2 instead of 200, in order to ensure a safe estimate of the critical load[6].

EC3 also suggests this method for sway mode failure (clause 5.2.1(4)B), for beam-and-column type plane frames in buildings or portal frames with shallow roof slopes[7], provided that the axial compression in the beams or rafters is not significant[8]. In this case, parameter α_{cr}, that corresponds to the instability mode with lateral displacements (as illustrated in Figure 2.50a) can be evaluated by the following simplified equation:

$$\alpha_{cr} = \left(\frac{H_{Ed}}{V_{Ed}} \right) \left(\frac{h_i}{\delta_{H,Ed}} \right), \tag{2.11}$$

where H_{Ed} is the total horizontal reaction at the top of the storey[9], V_{Ed} is the total vertical reaction at the bottom of the storey, $\delta_{H,Ed}$ is the relative horizontal displacement between the top and the bottom of a given storey, when the frame is loaded with the design horizontal loads, increased with the horizontal forces equivalent to the imperfections and h_i is the height of the storey, such as illustrated in Figure 2.51.

[6] Except for frames with a single floor, in which in that same case the estimates can present unsafe results. That is why BS 5950 (BSI, 2000) does not allow the application of this method for frames with a single floor.

[7] In Note 1B of clause 5.2.1(4)B it is stated that in the absence of more detailed information a roof slope may be taken to be shallow if it is not steeper than 1:2 (26º).

[8] In Note 2B of clause 5.2.1(4)B it is stated that in the absence of more detailed information the axial compression in the beams or rafters may be assumed to be significant if

$$\overline{\lambda} \geq 0.3 \sqrt{\frac{A f_y}{N_{Ed}}}$$

where N_{Ed} is the design value of the compression force and $\overline{\lambda}$ is the in-plane non dimensional slenderness calculated for the beams or rafters considered as hinged at the ends of the system length measured along the beams or rafters.

[9] EC3-1-1 originally defined it as the reaction at the bottom of the storey, now corrected in a corrigenda.

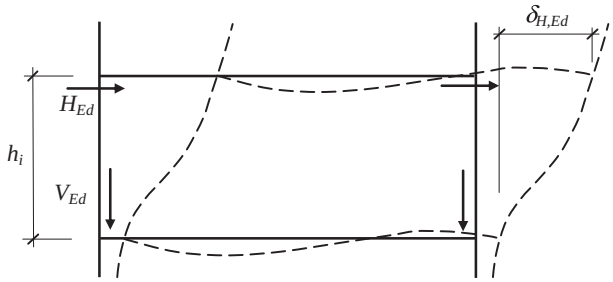


Figure 2.51 – Lateral displacements in an unbraced frame

As an alternative to Horne's method, Wood (1974) suggested a method for the calculation of critical loads based on a beam-and-column equivalent system, illustrated in Figure 2.52. According to Wood's method, the relation (L_E/L) between the buckling length L_E and the real length L is evaluated according to distribution coefficients η_1 and η_2, given by:

$$\eta_1 = \frac{K_c + K_1}{K_c + K_1 + K_{11} + K_{12}}; \tag{2.12a}$$

$$\eta_2 = \frac{K_c + K_2}{K_c + K_2 + K_{21} + K_{22}}, \tag{2.12b}$$

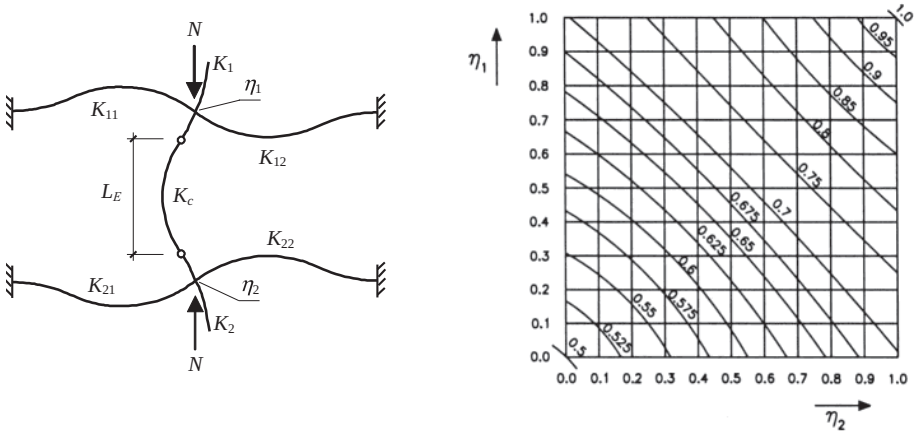
where K_c is the column stiffness coefficient, given by I/L, K_1 and K_2 are the stiffness coefficients for the adjacent columns, also given by I/L and K_{ij} represent the effective stiffness coefficients of the adjacent beams. I denotes the moment of inertia (second moment of area) and L is the length of the member.

The K_{ij} stiffness coefficients of the beams depend on the conditions of support at the opposite end, presented in Table 2.19 for beams without axial force, working in the elastic range. Other situations can be found in Boissonnade *et al* (2006).

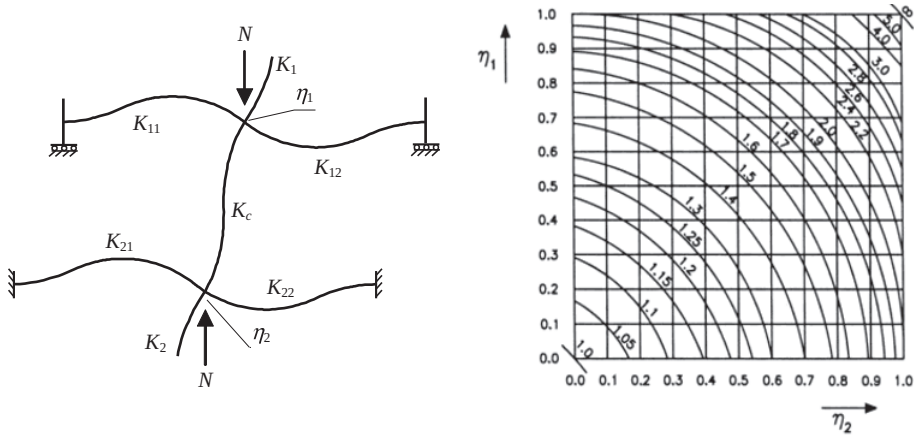
In the case of columns in which the lower end is a connection to the exterior, η_2 coefficient is zero if the connection is fixed, and equal to 1.0 if it is pinned. Similar graphs for elastically restrained columns to horizontal displacements can be found in Gonçalves (2000).

Table 2.19 – K_{ij} stiffness coefficients in beams

Restriction to rotation at the opposite end	K_{ij}
Fixed	1.0 *I/L*
Pinned	0.75 *I/L*
Equal rotation (single curvature)	0.5 *I/L*
Equal rotation but in the opposite way (double curvature)	1.5 *I/L*
General case (θ_a next to the column and θ_b at the opposite end)	$1+0.5(\theta_b/\theta_a))I/L$



a) Frame with no lateral displacements



b) Frame with lateral displacements

Figure 2.52 – Wood's equivalent frame

The application of this method consists of the following steps:

- determination of the equivalent length (L_e) for the column to be studied, using equation (2.12) and the graphs of Figure 2.52;
- determination of the critical load of the column (N_{cr}), using equation (2.13)

$$N_{cr} = \frac{\pi^2 EI}{L_e^2}; \tag{2.13}$$

- calculation of α_{cr} by:

$$\alpha_{cr} = \frac{N_{cr}}{N_{Ed}}. \tag{2.14}$$

This process must be repeated for all columns in order to find the lowest critical load multiplier.

2.3.2.3. 2nd order analysis

The 2nd order analysis of structures invariably requires the use of computational methods, including step-by-step or other iterative procedures (clause 5.2.2(4)). In this case, to ensure reliable results, the guidance described in sub-section 2.3.2.2 for the numerical evaluation of the elastic critical loads should be followed[10]. Also, convergence of the results should be explicitly checked by imposing adequate error limits on the geometrical non-linear calculations. Finally, the results should be compared with a reference first order elastic analysis to ensure that the amplified internal forces and displacements are within expected limits. Example 2.4 exemplifies the application of 2nd order elastic analysis in the context of a simple two-storey plane frame.

In order to allow quicker approaches, approximate methods have been developed which, in many cases, estimate the exact results with acceptable

[10] This depends on the implementation of second-order effects in each structural analysis software. The reader should carefully check the user manual of each program.

error. Generically, the approach is through a linear combination of buckling modes of the structure[11] to provide amplification methods of 1st order results (Horne, 1985), illustrated in the following equation:

$$E_{Ed}^{II} = \sum \left(1 - \frac{1}{\alpha_{cr.i}} \right)^{-1} A_i q_i . \tag{2.15}$$

E_{Ed}^{II} denotes 2nd order values (only P-Δ effects), q_i denotes buckling mode i and A_i is a constant. It is important to highlight that the results converge to the exact solution as long as a sufficient number of buckling modes is used and the loading does not approach too much the lowest critical load. In practical terms, given the resemblance between buckling modes and deformations of the structure under appropriate loading, equation (2.15) can be re-written in the following more practical format:

$$E_{Ed}^{II} = \sum \left(1 - \frac{1}{\alpha_{cr,i}} \right)^{-1} a_i \, d_i^I , \tag{2.16}$$

where superscripts $()^{I}$ and $()^{II}$ denote, respectively, 1st and 2nd order values and d_i^I is the 1st order displacement that corresponds to a loading causing a deformation similar to the corresponding buckling mode.

In the particular case of frames that are susceptible of instability in a sway mode, the amplification involves only the lowest buckling mode and is given by:

$$d_{ap}^{II} = \left(d^I - d_{AS}^I \right) + \left(1 - \frac{1}{\alpha_{cr.AS}} \right)^{-1} d_{AS}^I ; \tag{2.17a}$$

$$M_{ap}^{II} = \left(M^I - M_{AS}^I \right) + \left(1 - \frac{1}{\alpha_{cr.AS}} \right)^{-1} M_{AS}^I ; \tag{2.17b}$$

[11] Note the analogy with the amplification of 2nd order moments and displacements of a member under bending and compression (Boissonnade *et al*, 2006).

$$V_{ap}^{II} = \left(V^{I} - V_{AS}^{I}\right) + \left(1 - \frac{1}{\alpha_{cr.AS}}\right)^{-1} V_{AS}^{I}; \qquad (2.17c)$$

$$N_{ap}^{II} = \left(N^{I} - N_{AS}^{I}\right) + \left(1 - \frac{1}{\alpha_{cr.AS}}\right)^{-1} N_{AS}^{I}, \qquad (2.17d)$$

where index *ap* means approximate, *index AS* denotes the anti-symmetric "sway" mode, *d*, *M*, *V* and *N* denote, respectively, displacement, bending moment, shear force and axial force.

This procedure provides the general framework for several simplified methods to assess 2nd order effects, allowing if necessary for the development of plasticity. These are described in more detail in chapters 4 and 5.

2.3.3. Imperfections

In steel structures, irrespective of the care taken in their execution, there are always imperfections, such as: residual stresses, eccentricities in joints, eccentricities of load, lack of verticality and lack of linearity in members (clause 5.3.1(1)). These imperfections are responsible for the introduction of additional secondary forces that must be taken into account in the global analysis and in the design of the structural elements. The type and amplitude of all imperfections are bounded by the tolerances specified in the execution standards such as EN 1090-2 (CEN, 2011), as described in chapter 1.

According to EC3-1-1, the imperfections should be incorporated in the analysis preferably in the form of *equivalent geometric imperfections*[12] , with values which reflect the possible effects of all types of imperfections (clause 5.3.1(2)). Unless these effects are already included in the resistance formulae for member design, the following imperfections should be taken into account: i) global imperfections of the frame and ii) local imperfections of the members (clause 5.3.1(3)).

Imperfections for global analysis should be considered with the shape and direction that lead to the most adverse effects. So, the assumed shape of global

[12] That include all imperfections (residual stresses, etc.) exclusively as geometrical imperfections.

and local imperfections may be derived from the elastic buckling mode of a structure in the plane of buckling considered (clauses 5.3.2(1)). Account should be taken of both in-plane and out-of-plane buckling including torsional buckling with symmetric and asymmetric buckling shapes (clause 5.3.2(2)).

For frames sensitive to buckling in a sway mode, the effect of imperfections should be allowed for in frame analysis by an equivalent imperfection in the form of an initial sway imperfection and individual bow imperfections of the members (clause 5.3.2(3)). The global initial sway imperfection corresponds to a lack of verticality of the structure, defined by an angle ϕ (illustrated in Figure 2.53), given by (clause 5.3.2(3)a)):

$$\phi = \phi_0 \alpha_h \alpha_m, \tag{2.18}$$

ϕ_0 is the basic value, given by

$$\phi_0 = 1/200,$$

and α_h is the reduction factor for height h applicable to columns and α_m is the reduction factor for the number of columns in a row, given by:

$$\alpha_h = \frac{2}{\sqrt{h}} \quad \text{but} \quad \frac{2}{3} \le \alpha_h \le 1.0; \qquad \alpha_m = \sqrt{0.5\left(1+\frac{1}{m}\right)},$$

where h is the total height of the structure in metres and m is the number of columns in a row, including only those columns which carry a vertical load N_{Ed} not less than 50 % of the average value of the axial force in the columns in the vertical plane considered.

It is noted that for building frames (clause 5.3.2(4)B) sway imperfections may be neglected whenever

$$H_{Ed} \ge 0.15\, V_{Ed}, \tag{2.19}$$

where H_{Ed} is the total horizontal design force and V_{Ed} is the total vertical design force. The initial sway imperfections should be applied in all relevant horizontal directions, but need only be considered in one direction at a time (clause 5.3.2(8)).

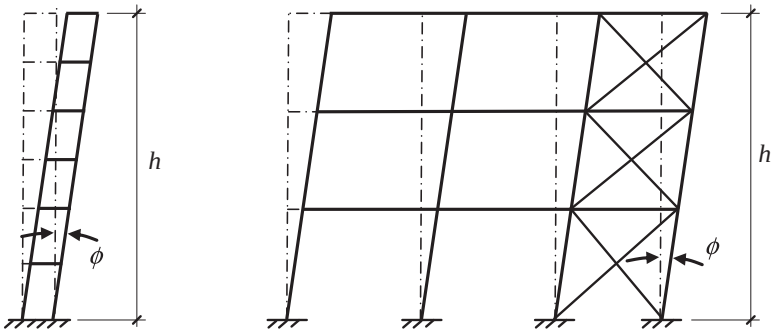


Figure 2.53 – "Equivalent geometric imperfection" in framework structures

The relative initial local bow imperfections of members for flexural buckling in a bending mode are given by

$$e_0/L, \tag{2.20}$$

where e_0 is the maximum amplitude of the initial lateral displacement and L is the length of the member (see Figure 2.54). Table 2.20 summarizes the recommended design values for the equivalent initial local bow imperfections for the various buckling curves and types of analysis.

Table 2.20 – Initial local bow imperfections

Buckling curve	Elastic analysis	Plastic analysis
	e_0/L	e_0/L
a_0	1/350	1/300
a	1/300	1/250
b	1/250	1/200
c	1/200	1/150
d	1/150	1/100

It is recalled from 2.3.2.1 above that when performing the global analysis for determining end-forces and end moments to be used in member checks according to clauses 6.3, local bow imperfections may be neglected because they are already built-in the resistance formulae. However, they should not be neglected for frames sensitive to second-order effects in which, for the compressed members, there is at least one moment-resisting joint at one member end, and

$$\overline{\lambda} > 0.5\sqrt{\frac{A f_y}{N_{Ed}}}\,. \tag{2.21}$$

N_{Ed} is the design value of the compressive force and $\overline{\lambda}$ is the in-plane non-dimensional slenderness calculated for the member considered as pinned at its ends (clause 5.3.2(6)). Whenever the stability of members is accounted for by second-order analysis (method 1, clause 5.2.2(3)(a) or clause 5.2.2(7)a)), the member imperfections e_0 given in Table 2.20 should be considered (clause 5.3.4(2)). For a second-order analysis taking account of lateral torsional buckling of a member in bending, the imperfections may be adopted as $ke_{0,d}$, where $e_{0,d}$ is the equivalent initial bow imperfection of the weak axis of the profile considered (clause 5.3.4(3)). A value of k = 0.5 is recommended, although the National Annexes may choose different values. In general, an additional torsional imperfection need not be allowed.

For simplicity, the effects of initial sway imperfections and local bow imperfections may be replaced by systems of equivalent horizontal forces, introduced for each column, as shown in Figure 2.54 (clause 5.3.2(7)). In case of multi-storey buildings, the equivalent horizontal forces representing the initial sway imperfections should be applied at each floor and roof level, in proportion to the vertical loads applied to that level (clause 5.3.2(9)).

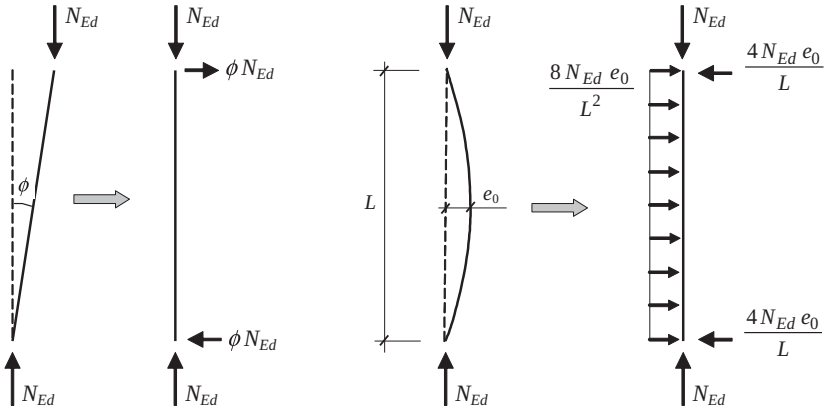


Figure 2.54 – Imperfections and corresponding equivalent horizontal forces

Imperfections leading to torsional effects on a structure caused by anti-symmetric sways at two opposite faces should also be considered (clause 5.3.2(10)).

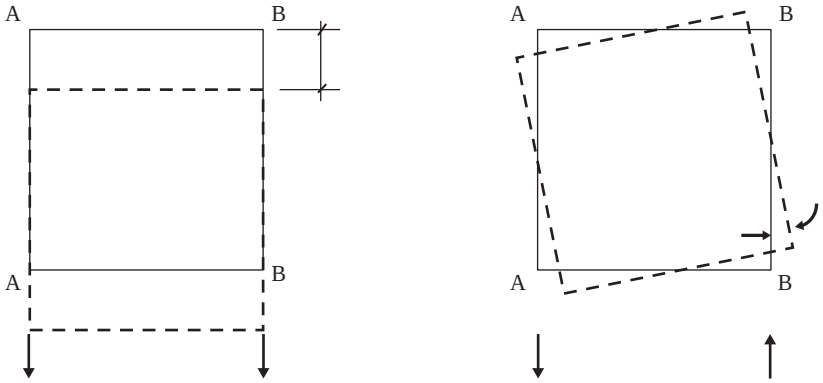


Figure 2.55 – Plan view of translational and torsional effects

In the analysis of bracing systems which are required to provide lateral stability within the lengths of beams or compression members, the effects of imperfections should be included by means of an equivalent geometric imperfection of the members to be restrained, in the form of an initial bow imperfection (clause 5.3.3(1)), given by:

$$e_0 = \alpha_m L/500\,, \tag{2.22}$$

where L is the span of the bracing system and

$$\alpha_m = \sqrt{0.5\left(1+\frac{1}{m}\right)}\,, \tag{2.23}$$

in which m is the number of members to be restrained.

For simplicity, the effects of the initial bow imperfections of the members to be restrained by a bracing system may be replaced by the equivalent stabilizing force q_d, illustrated in Figure 2.56 (clause 5.3.3(2)),

$$q_d = \sum N_{Ed} 8\frac{e_0+\delta_q}{L^2}\,, \tag{2.24}$$

where δ_q is the in-plane deflection of the bracing system due to q plus any external loads calculated from first order analysis (δ_q may be taken as 0 if second order theory is used).

Where the bracing system is required to stabilize the compression flange of a prismatic beam, the force N_{Ed} in Figure 2.56 may be obtained from:

$$N_{Ed} = \frac{M_{Ed}}{h}, \tag{2.25}$$

where M_{Ed} is the maximum moment in the beam and h is the overall depth of the beam (clause 3.2.2(3)). It is noted that where a beam is subjected to external compression, N_{Ed} should include a part of the compression force.

At points where beams or compression members are spliced, it should also be verified that the bracing system is able to resist a local force equal to:

$$2\Phi N_{Ed} = \alpha_m \frac{N_{Ed}}{100}, \tag{2.26}$$

where $\Phi = \alpha_m \Phi_0$ and Φ_0 = 1/200, applied to it by each beam or compression member which is spliced at that point, see Figure 2.57. It should be further verified that the bracing system is able to transmit this force to the adjacent points at which that beam or compression member is restrained (clause 5.3.3(4)). For checking for this local force, any external loads acting on the bracing systems should also be included, but the forces arising from the imperfection given in equation (2.26) may be omitted (clause 5.3.3(5)).

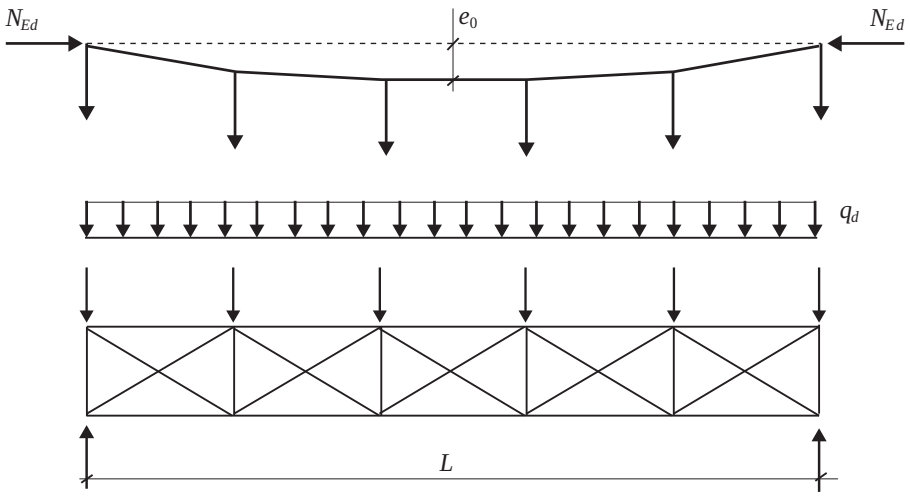


Figure 2.56 – Imperfections for bracing systems

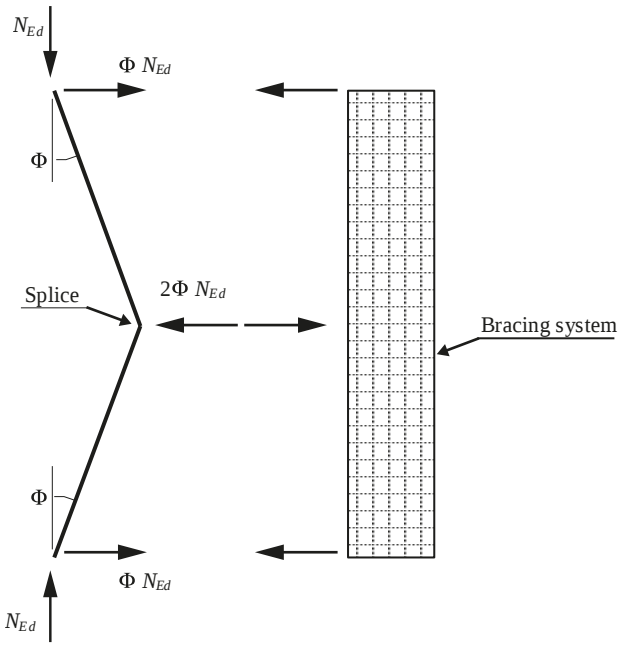


Figure 2.57 – Bracing forces at splices in compression elements

2.3.4. Worked example

94

Example 2.4: Consider the steel frame of example 2.1 (E = 210 GPa) subjected to the unfactored loadcases illustrated in Figure 2.58, where:

AP – permanent load (γ_G = 1.35);
AV_1 – imposed load (γ_Q = 1.50, $\psi_{0,1}$ = 0.7, $\psi_{1,1}$ = 0.5, $\psi_{2,1}$ = 0.3);
AV_2 – wind load (γ_Q = 1.50, $\psi_{0,2}$ = 0.6, $\psi_{1,2}$ = 0.2, $\psi_{2,2}$ = 0.0).

Calculate by elastic analysis the design internal forces for the verification of the Ultimate Limit State (ULS), and the displacements for the verification of the Serviceability Limit State (SLS), according to EC3-1-1. Assume rigid joints between the beams and the columns and column bases fully restrained.

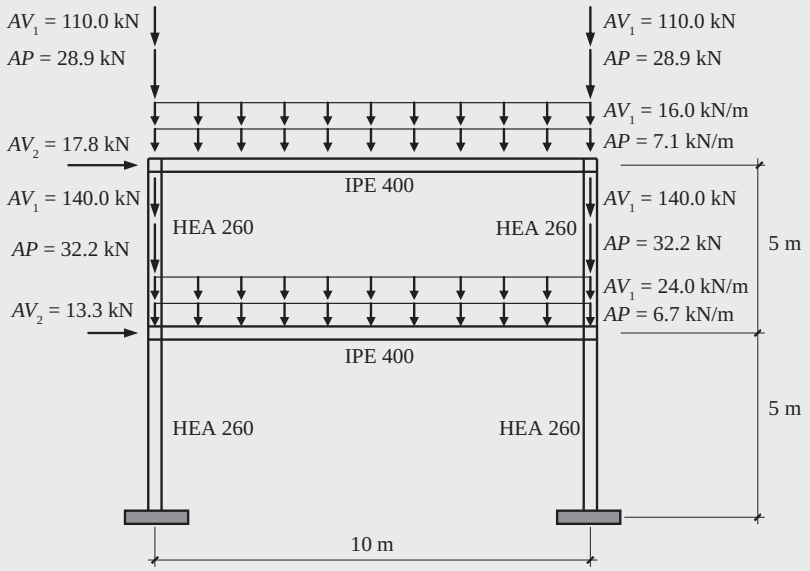


Figure 2.58 – Steel frame

i) Calculation of the *design internal forces*

There are two independent variable loads (AV_1 and AV_2), therefore the structure is analysed for two load combinations (according to EN 1990) as follows:

Combination 1 – Permanent load plus imposed load (AV_1) as leading variable action.

$$Ed_1 = \gamma_G AP + \gamma_Q \left(AV_1 + \psi_{0,2} AV_2 \right).$$

Combination 2 – Permanent load plus wind load (AV_2) as leading variable action.

$$Ed_2 = \gamma_G AP + \gamma_Q \left(AV_2 + \psi_{0,1} AV_1 \right).$$

First, additional horizontal forces are calculated due to the imperfections defined in clause 5.3.2. In the analysis only global imperfections are considered, assuming that local imperfections will be included in the buckling design of the members (as stated in clause 6.3).

The "equivalent geometric imperfection", corresponding to global imperfections of the frame, is given by the angle ϕ and: $\phi = \phi_0 \alpha_h \alpha_m$.

Assuming: $\phi_0 = 1/200$;

$$\alpha_h = \frac{2}{\sqrt{h}} = \frac{2}{\sqrt{10}} = 0.63 < \frac{2}{3} = 0.67 \Rightarrow \alpha_h = 0.67 \text{ and}$$

$$\alpha_m = \sqrt{0.5\left(1+\frac{1}{m}\right)} = \sqrt{0.5\times\left(1+\frac{1}{2}\right)} = 0.87,$$

hence, $\phi = \phi_0\, \alpha_h\, \alpha_m = 1/200 \times 0.67 \times 0.87 = 0.0029$ rad.

The lack of verticality of the columns, given by imperfection ϕ, may be simulated by equivalent horizontal forces, applied at the level of each floor and proportional to the vertical loads applied at that level. These forces are then added to the specified horizontal loads, as described in the following paragraphs, for the two load combinations.

Combination 1 (permanent load plus AV_1 as leading variable action).

The vertical design load applied at the 1st floor, is given by:

$$1.35\times\left(6.7\times10+2\times32.2\right)+1.50\times\left(24.0\times10+2\times140.0\right)=957.4 \text{ kN},$$

hence, $F_{i1,comb1} = 0.0029\times957.4 = 2.8$ kN.

Similarly, the vertical design load applied at the 2nd floor is given by:

$$1.35\times\left(7.1\times10+2\times28.9\right)+1.5\times\left(16.0\times10+2\times110.0\right)=743.9 \text{ kN},$$

hence, $F_{i2,comb1} = 0.0029\times743.9 = 2.2$ kN.

Adding these forces to the remaining horizontal loads, the horizontal design loads are obtained for combination 1, as follows:

$$F_{H1,comb1} = 1.50\times0.6\times13.3+2.8 = 14.8 \text{ kN}.$$

$$F_{H2,comb1} = 1.50\times0.6\times17.8+2.2 = 18.2 \text{ kN}.$$

Combination 2 (permanent load plus AV_2 as leading variable action).

Applying the same procedure for combination 2, the vertical design load applied at the 1st floor is given by:

$1.35\times\left(6.7\times10+2\times32.2\right)+1.5\times0.7\times\left(24.0\times10+2\times140.0\right)=723.4$ kN,

hence, $F_{i1,comb2}=0.0029\times723.4=2.1$ kN.

The vertical design load applied at the 2nd floor is given by:

$1.35\times\left(7.1\times10+2\times28.9\right)+1.5\times0.7\times\left(16\times10+2\times110.0\right)=572.9$ kN,

hence, $F_{i2,comb2}=0.0029\times572.9=1.7$ kN.

Adding these forces to the remaining horizontal loads, the horizontal design loads are obtained for combination 2, as follows:

$F_{H1,comb2}=1.5\times13.3+2.1=22.1$ kN.

$F_{H2,comb2}=1.5\times17.8+1.7=28.4$ kN.

Finally, in Figures 2.59 and 2.60 the loadcase arrangements for both combinations are presented. The loadcase arrangements already include the global imperfections of the frame.

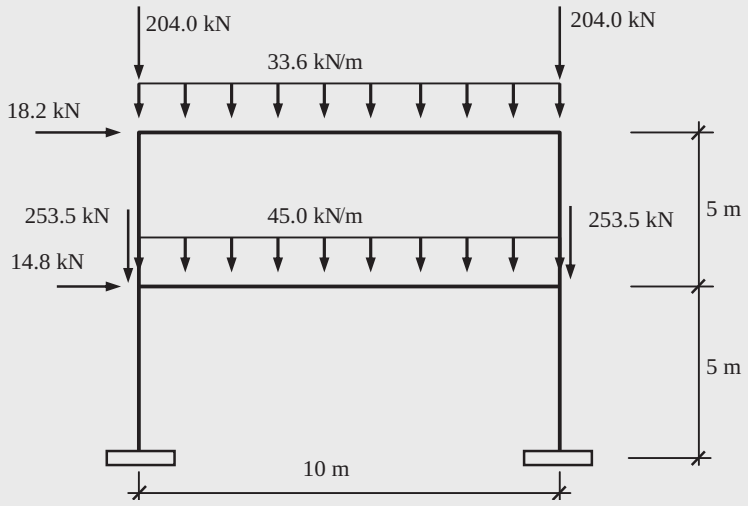


Figure 2.59 – Loadcase arrangement for combination 1

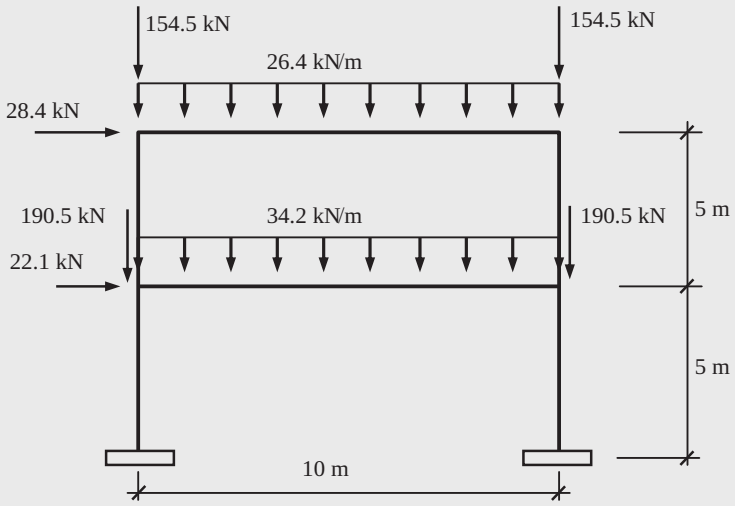


Figure 2.60 – Loadcase arrangement for combination 2

i-1) Internal forces for *combination* 1

From a 1st order elastic analysis the internal force diagrams due to vertical loads (Figures 2.61 to 2.63) and due to horizontal loads (Figures 2.64 to 2.66) are obtained. There are no horizontal displacements due to vertical loads because of the symmetry of the structure. Thus, Figure 2.68 illustrates the structural displacements due only to horizontal loads.

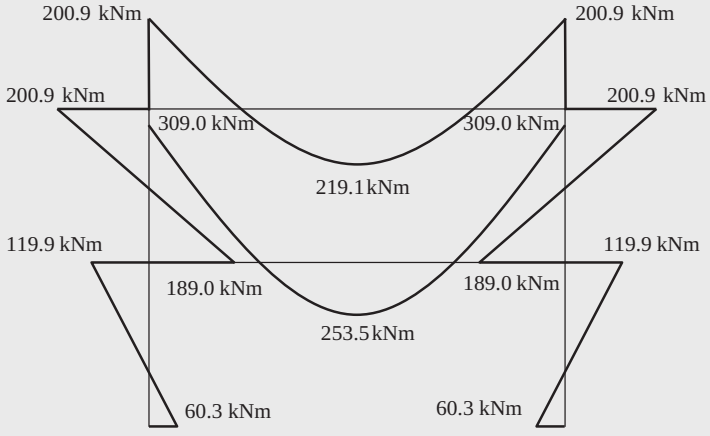


Figure 2.61 – Bending moment due to vertical loads (comb. 1)

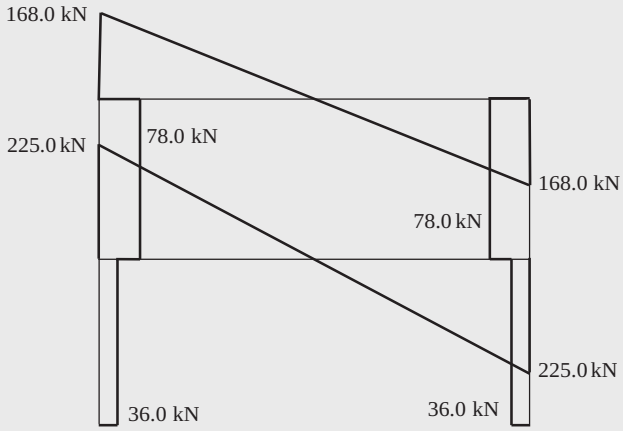


Figure 2.62 – Shear force due to vertical loads (comb. 1)

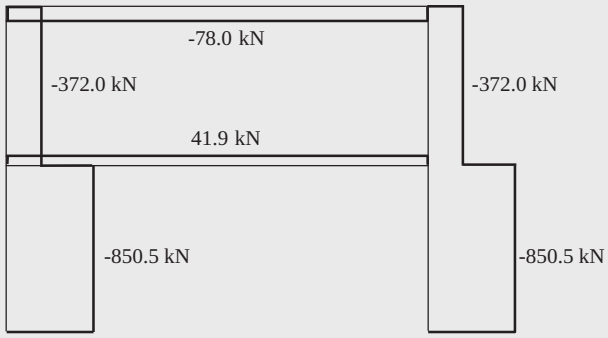


Figure 2.63 – Axial force due to vertical loads (comb. 1)

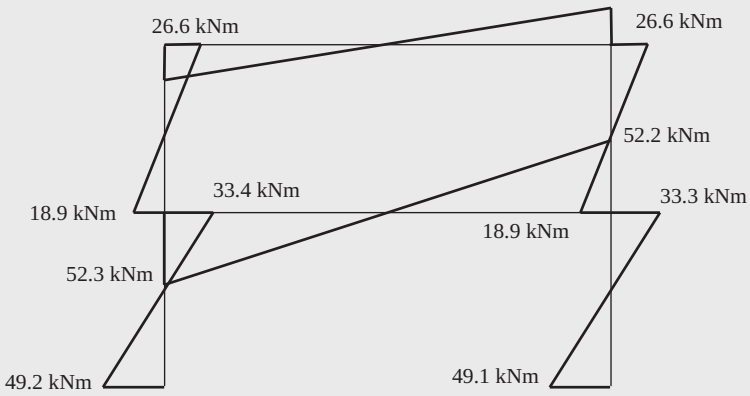


Figure 2.64 – Bending moment due to horizontal loads (comb. 1)

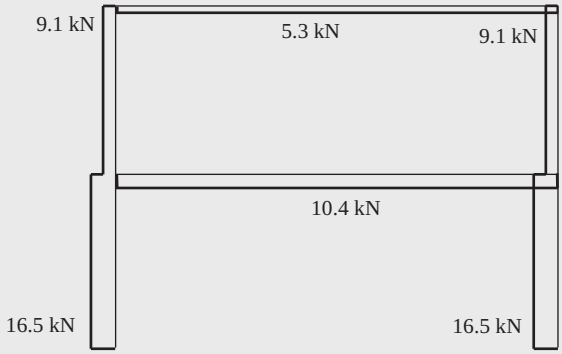


Figure 2.65 – Shear force due to horizontal loads (comb. 1)

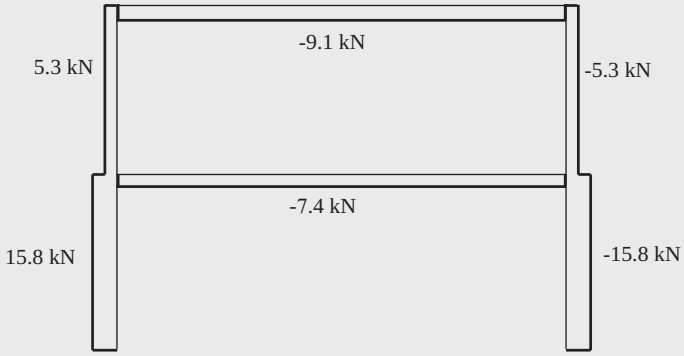


Figure 2.66 – Axial force due to horizontal loads (comb. 1)

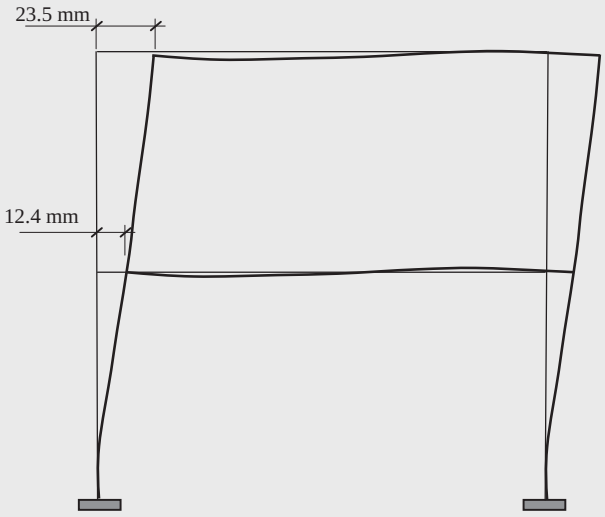


Figure 2.67 – Structural displacements for combination 1 (horizontal loads)

It is now required to check whether 2nd order effects should be taken into account in the structural analysis. Being a plane frame with a regular structure, the simplified method proposed in clause 5.2.1(4)B is considered. The horizontal displacements calculated in the previous paragraph allow to assess the factor α_{cr} , for each floor and for combination 1, as follows:

1st floor: H_{Ed} = 33.0 kN, V_{Ed} = 1701.0 kN, h = 5.00 m and $\delta_{H,Ed}$ = 12.4 mm.

$$\alpha_{cr} = \left(\frac{33.0}{1701.0}\right) \times \left(\frac{5.00}{12.4 \times 10^{-3}}\right) = 7.82.$$

2nd floor: H_{Ed} = 18.2 kN, V_{Ed} = 744.0 kN, h = 5.00 m and $\delta_{H,Ed}$ = 11.1 mm.

$$\alpha_{cr} = \left(\frac{18.2}{744.0}\right) \times \left(\frac{5.00}{11.1 \times 10^{-3}}\right) = 11.02.$$

As α_{cr} is less than 10 (although only for the 1st floor), the design internal forces should include global second order effects (P-Δ effects). Alternatively, performing a linear eigenvalue analysis, a value of α_{cr} = 7.2, would be obtained. Figures 2.68 to 2.70 illustrate the resulting 2nd order internal forces.

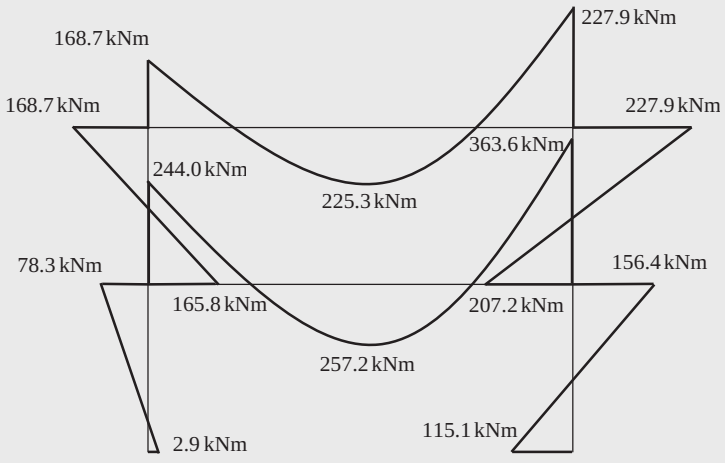


Figure 2.68 – Elastic 2nd order bending moment diagram

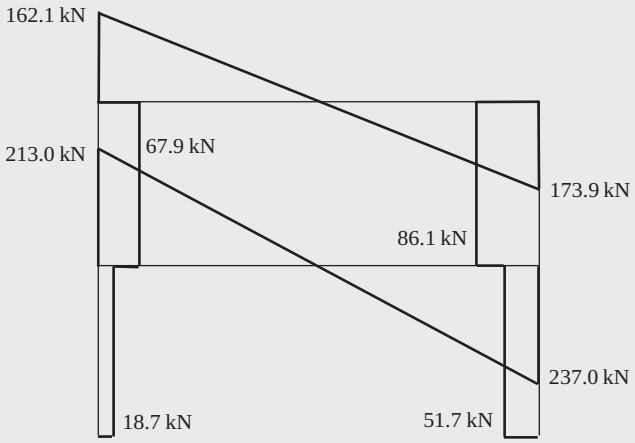


Figure 2.69 – Elastic 2nd order shear force diagram

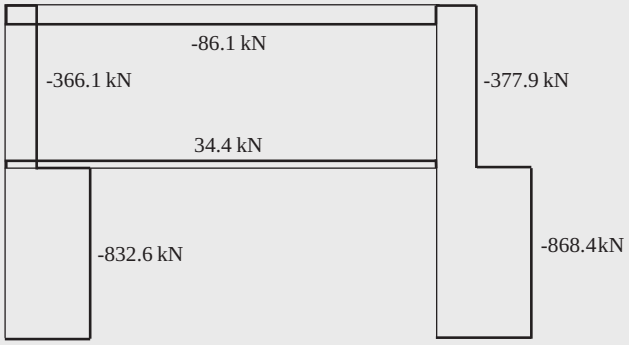


Figure 2.70 – Elastic 2nd order axial force diagram

As expected, because of the relatively high value of α_{cr} (= 7.2), the influence of 2nd order effects is low, resulting in a maximum increase of the bending moment in the columns of 5.2 %. These design internal forces should now be directly used to perform the cross section resistance checks and the buckling resistance checks according to chapter 6 of EC3-1-1, as it will explained in detail in chapter 3. Alternatively, to use method 1 (clause 5.2.2(3)), local bow imperfections should also be considered in the evaluation of the design internal forces.

i-2) Internal forces for *combination* 2

Following a similar procedure for combination 2 yields the linear elastic results for the vertical loads (Figures 2.71 to 2.73) and the horizontal loads

(Figures 2.74 to 2.76). Figure 2.77 illustrates the structural displacements due to horizontal loads, exclusively.

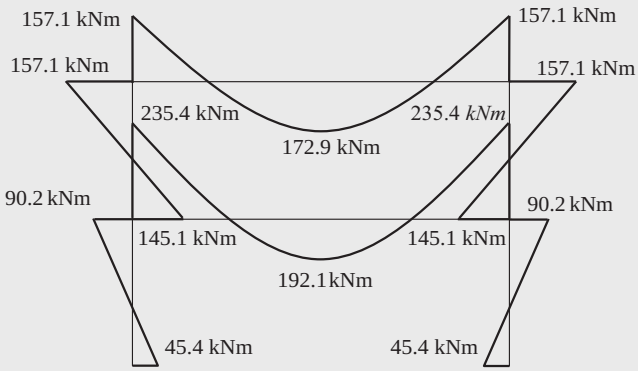


Figure 2.71 – Bending moments due to vertical loads (comb. 2)

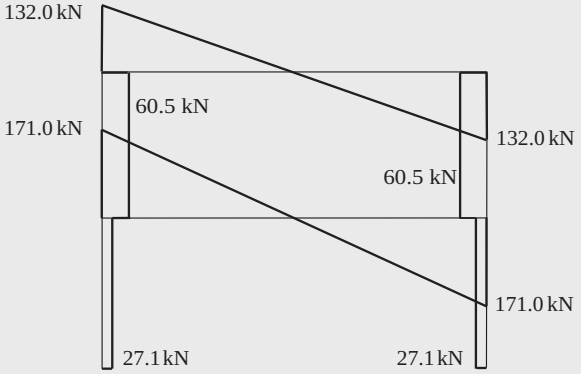


Figure 2.72 – Shear forces due to vertical loads (comb. 2)

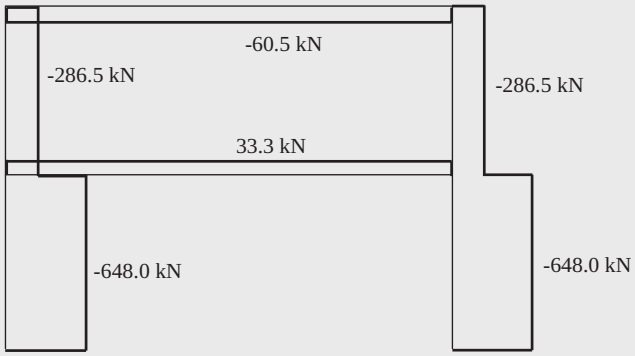


Figure 2.73 – Axial forces due to vertical loads (comb. 2)

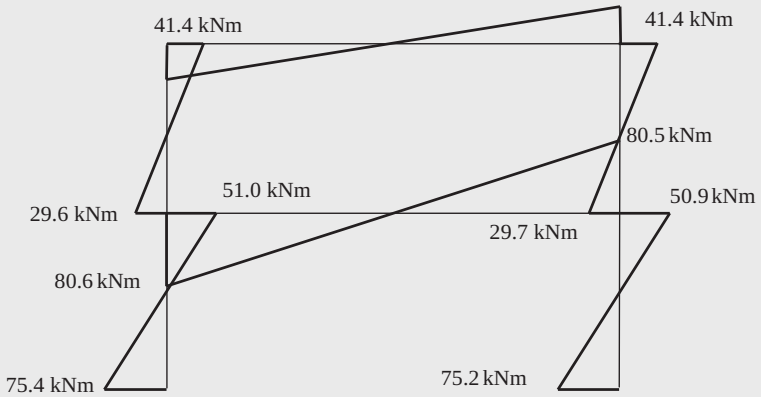


Figure 2.74 – Bending moments due to horizontal loads (comb. 2)

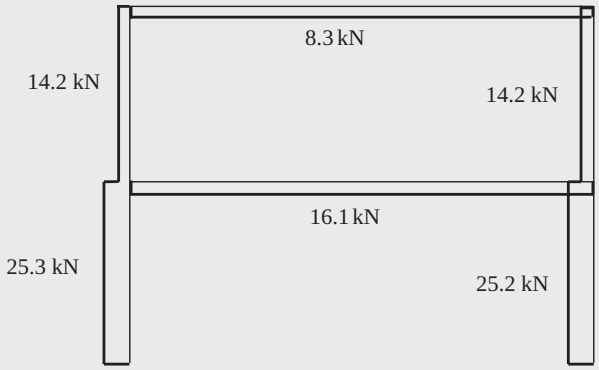


Figure 2.75 – Shear forces due to horizontal loads (comb. 2)

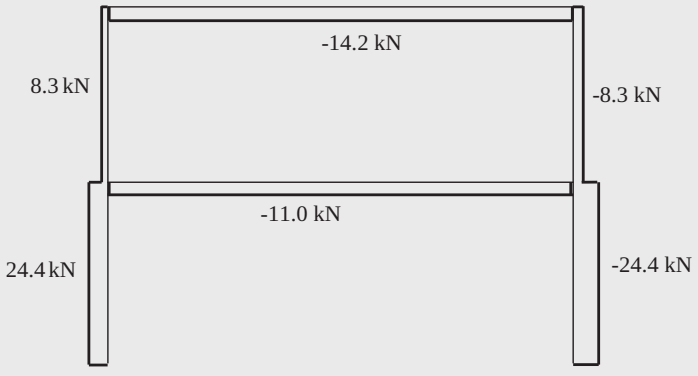


Figure 2.76 – Axial forces due to horizontal loads (comb. 2)

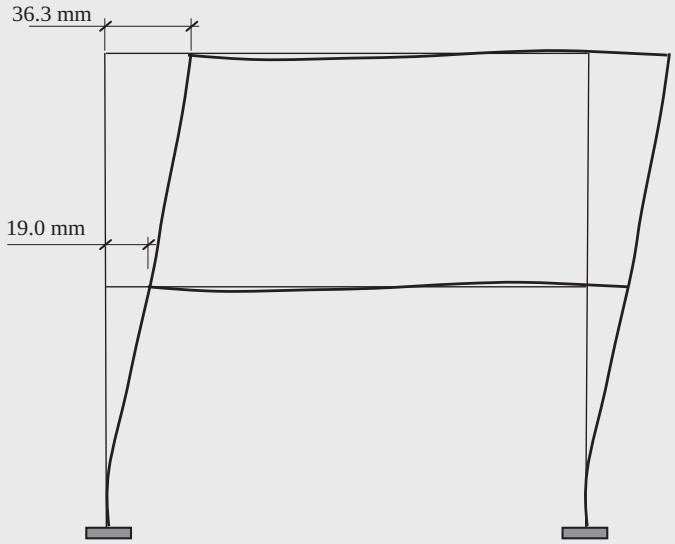


Figure 2.77 – Structural displacements due to combination 2 (horizontal loads)

The horizontal displacements calculated in the previous paragraph allow to assess the factor α_{cr} , for each floor.

1st floor: H_{Ed} = 50.5 kN, V_{Ed} = 1296.0 kN, h = 5.00 m and $\delta_{H,Ed}$ = 19.0 mm.

$$\alpha_{cr} = \left(\frac{50.5}{1296.0}\right) \times \left(\frac{5.00}{19.0 \times 10^{-3}}\right) = 10.25.$$

2nd floor: H_{Ed} = 28.4 kN, V_{Ed} = 573.0 kN, h = 5.00 m and $\delta_{H,Ed}$ = 17.3 mm.

$$\alpha_{cr} = \left(\frac{28.4}{573.0}\right) \times \left(\frac{5.00}{17.3 \times 10^{-3}}\right) = 14.32.$$

so that 2nd order effects can be neglected for this load combination. Alternatively, a linear eigenvalue analysis yields a value of α_{cr} = 9.95, approximately confirming the previous conclusion. Figures 2.78 to 2.80 illustrate the final (first order) results for this load combination.

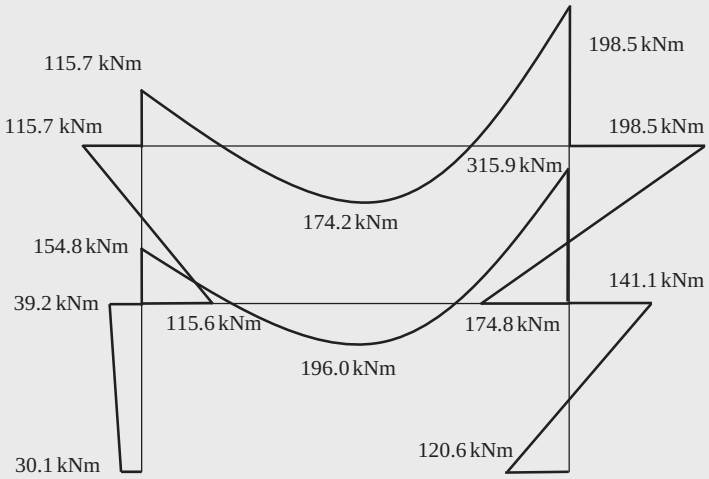


Figure 2.78 – Design bending moments

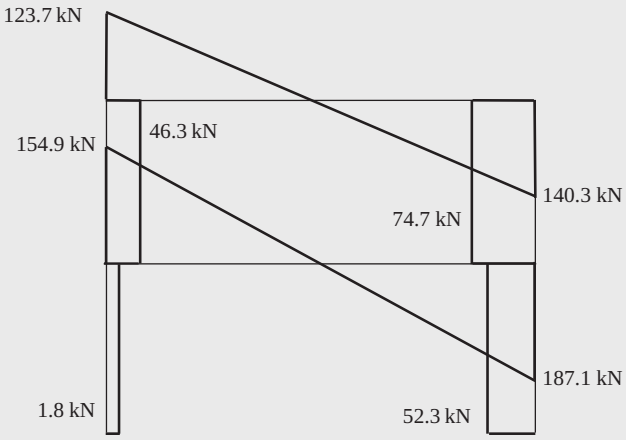


Figure 2.79 – Design shear forces

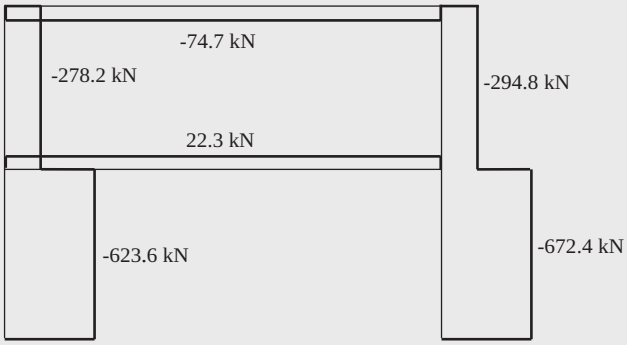


Figure 2.80 – Design axial forces

ii) Structural *displacements*

Considering, for example, frequent combinations for the verification of the serviceability limit state with respect to excessive deformation yields the two following combinations for the two imposed loads (AV_1 e AV_2):

Combination 1 – Permanent load plus AV_1 as leading variable action

$$Ed_1 = AP + \psi_{1,1} AV_1 + \psi_{2,2} AV_2 = AP + 0.5 \times AV_1 + 0.0 \times AV_2.$$

Combination 2 – Permanent load plus AV_2 as leading variable action

$$Ed_2 = AP + \psi_{1,2} AV_2 + \psi_{2,1} AV_1 = AP + 0.2 \times AV_2 + 0.3 \times AV_1.$$

Figures 2.81 and 2.82 illustrate the corresponding displacements. These do not include the effects of imperfections nor second order effects, as account for is not required. According to section 7 of EC3-1-1, these displacements should comply with limit values specified for each project and agreed with the client. Adopting the following values (Table 1.5 and Figure 1.4 in chapter 1): for vertical deflections (beams in general floors), $w_{max} = L/250$; for horizontal deflections between the top and the bottom of storey *i*, $\delta_{max} = h_i/300$; and for total horizontal deflection, $\Delta_{max} = h/500$, where L is the beam span, h_i is the height of storey i and h is the total height of the frame, gives, for vertical deflections:

$$w = 19.3 \text{ mm} < 10000/250 = 40 \text{ mm} \ \left(\text{combination } 1\text{ - SLS}\right);$$

$$w = 15.9 \text{ mm} < 10000/250 = 40 \text{ mm} \ \left(\text{combination } 2\text{ - SLS}\right).$$

For the maximum horizontal deflections (combination 2 - SLS):

δ = 2.4 mm < 5000/300 = 16.7 mm (relative displacement);

Δ = 4.4 mm < 10000/500 = 20.0 mm (total displacement).

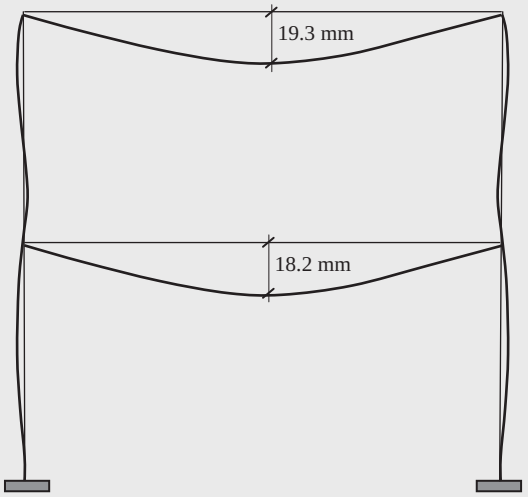


Figure 2.81 – Structural displacements for combination 1 (SLS)

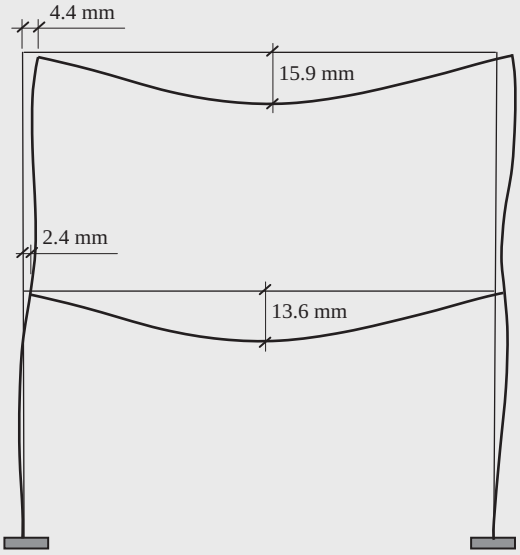


Figure 2.82 – Structural displacements for combination 2 (SLS)

2.4. CLASSIFICATION OF CROSS SECTIONS

The local buckling of cross sections affects their resistance and rotation capacity and must be considered in design. The evaluation of the influence of

local buckling of a cross section on the resistance or ductility of a steel member is complex. Consequently, a deemed-to-satisfy approach was developed in the form of cross section classes that greatly simplify the problem.

According to clause 5.5.2(1), four classes of cross sections are defined, depending on their rotation capacity and ability to form rotational plastic hinges:

- **Class 1** cross sections are those which can form a plastic hinge with the rotation capacity required from plastic analysis without reduction of the resistance;
- **Class 2** cross sections are those which can develop their plastic resistance moment, but have limited rotation capacity because of local buckling;
- **Class 3** cross sections are those in which the stress in the extreme compression fibre of the steel member, assuming an elastic distribution of stresses, can reach the yield strength. However, local buckling is liable to prevent development of the plastic resistance moment;
- **Class 4** cross sections are those in which local buckling will occur before the attainment of yield stress in one or more parts of the cross section.

The bending behaviour of members with cross sections of classes 1 to 4 is illustrated in Figure 2.83, where M_{el} and M_{pl} are, respectively, the elastic moment and the plastic moment of the cross section.

The classification of a cross section depends on the width to thickness ratio c/t of the parts subjected to compression (clause 5.5.2(3)), the applied internal forces and the steel grade. Parts subject to compression include every part of a cross section which is either totally or partially in compression under the load combination considered (clause 5.5.2(4)). The limiting values of the ratios c/t of the compressed parts are indicated in Tables 2.21 to 2.23 that reproduce Table 5.2 of EC3-1-1. In these tables, the various columns refer to the different types of stress distributions in each part of the cross section (webs or flanges); the steel grade is taken into account through the parameter $\varepsilon = \sqrt{235/f_y}$, where f_y is the nominal yield strength.

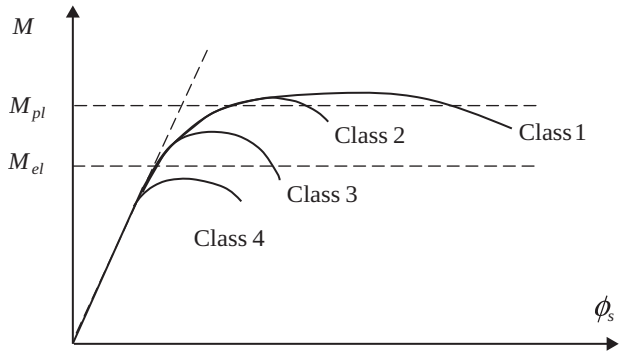


Figure 2.83 – Cross section behaviour in bending

The various compressed parts in a cross section (such as a web or flange) can, in general, be in different classes (clause 5.5.2(5)). In general, a cross section is classified according to the highest (least favourable) class of its compressed parts (clause 5.5.2(6)). For I or H cross sections and rectangular hollow sections, two types of compressed parts are defined: internal compressed parts (classified according to Table 2.21) and outstand flanges (classified according to Table 2.22); angles and tubular sections are classified according to Table 2.23. A cross section which fails to satisfy the limits for class 3 should be taken as class 4 (clause 5.5.2(8)).

EC3-1-1 envisages some exceptions to the general procedure for the classification of cross sections described in the previous paragraph: i) cross sections with a class 3 web and class 1 or 2 flanges may be classified as class 2 cross sections with an effective web in accordance with 6.2.2.4 (clause 5.5.2(11)); ii) whenever the web is considered to resist shear forces only and is assumed not to contribute to the bending and normal force resistance of the cross section, the section may be designed as class 2, 3 or 4, depending only on the flange class (clause 5.5.2(12)).

According to EC3, the classification of a cross section is based on its maximum resistance to the type of applied internal forces, independent from their values. This procedure is straightforward to apply for cross sections subject to compression forces or bending moment, acting separately. However, in the case of bending and axial force, there is a range of *M*-*N* values that correspond to the ultimate resistance of the cross section. Consequently, there are several values of the parameter α (limit for classes 1 and 2) or the parameter ψ (limit for class 3), both being dependent on the position of the

neutral axis. Bearing in mind this additional complexity, simplified procedures are often adopted, such as: i) to consider the cross section subjected to compression only, being the most unfavourable situation (too conservative in some cases); or ii) to classify the cross section based on an estimate of the position of the neutral axis based on the applied internal forces. Depending on whether only M_y is incremented or proportional loading is adopted, for I or H sections subject to major-axis bending and axial force with the neutral axis in the web (the usual case), the parameter α is given by the following alternative equations (Gardner and Nethercot, 2005; Greiner *et al*, 2011):

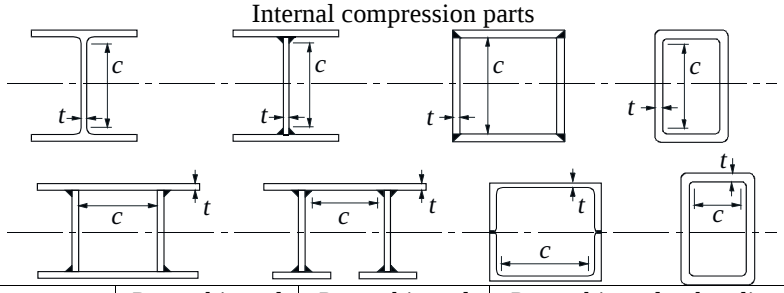
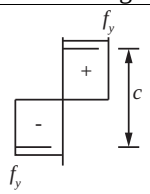
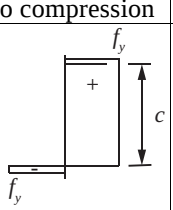
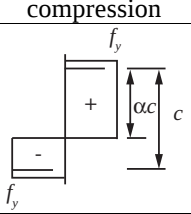
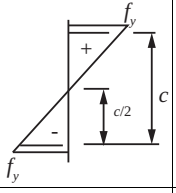
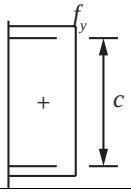
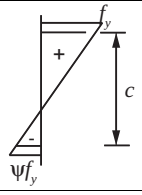
$$\alpha = \frac{1}{c}\left(\frac{h}{2} + \frac{1}{2}\frac{N_{Ed}}{t_w f_y} - \left(t_f + r\right)\right) \leq 1.0; \tag{2.27a}$$

$$\alpha = \frac{1}{2} + \frac{\left|M_{y,Ed}\right|}{N_{Ed}}\left(\frac{1}{c} - \frac{1}{2c}\sqrt{\left(c\frac{N_{Ed}}{M_{y,Ed}}\right)^2 + \frac{N_{Ed}^2\left(4\,W_{pl,y} - c^2 t_w\right)}{M_{y,Ed}^2\,t_w} + 4}\right) \leq 1.0, \tag{2.27b}$$

where c is the width of the web (defined in Table 2.21), h is the depth of the section, t_f is the thickness of the flange, t_w is the thickness of the web, r is the flange-to-web radius and $W_{pl,y}$ is the plastic modulus; this procedure corresponds to the classification of the cross section either for a pair of values consisting on the applied axial force N_{Ed} and a bending moment (Equation 2.27a) or for a pair of values consisting on the applied axial force N_{Ed} and the applied bending moment $M_{y,Ed}$, incremented proportionally (Equation 2.27b), such that the cross section is totally yielded. In case of class 3 cross sections, a similar procedure could be developed to determine the parameter ψ by superimposing the direct stresses resulting from N_{Ed} with a linear stress diagram resulting from bending such that the maximum normal stress equals f_y. The classification of cross sections subjected to bending and axial force will be exemplified in examples 3.13 to 3.15 in chapter 3.

Rolled sections of usual dimensions (HEA, HEB, IPE, etc...) belong, in general, to classes 1, 2 or 3. Class 4 cross sections are typical of plate girders and cold-formed sections. Class 4 cross sections are characterized by local buckling phenomena, preventing the cross section from reaching its elastic resistance. The usual procedure to deal with structures consisting of members of class 4 section is through the use of an effective section, as briefly explained in sub-chapter 3.1.

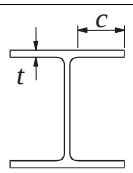
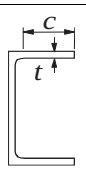
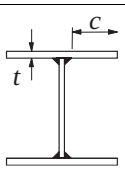
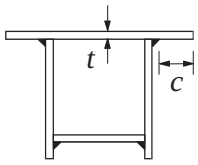
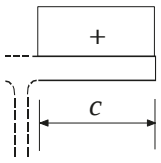
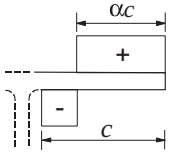
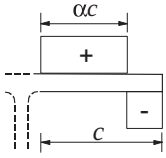
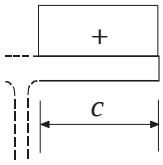
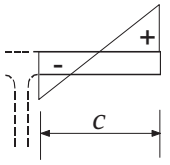
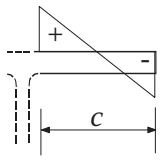
Table 2.21 – Maximum width-to-thickness ratios for internal compression parts

Internal compression parts			
			
Class	Part subjected to bending	Part subjected to compression	Part subjected to bending and compression
Stress distribution (compression +ve)			
1	$c/t \le 72\varepsilon$	$c/t \le 33\varepsilon$	if $\alpha > 0.5,\ c/t \le \dfrac{396\varepsilon}{13\alpha - 1}$ if $\alpha \le 0.5,\ c/t \le \dfrac{36\varepsilon}{\alpha}$
2	$c/t \le 83\varepsilon$	$c/t \le 38\varepsilon$	if $\alpha > 0.5,\ c/t \le \dfrac{456\varepsilon}{13\alpha - 1}$ if $\alpha \le 0.5,\ c/t \le \dfrac{41.5\varepsilon}{\alpha}$
Stress distribution (compression +ve)			
3	$c/t \le 124\varepsilon$	$c/t \le 42\varepsilon$	if $\Psi > -1$, $c/t \le \dfrac{0.42\varepsilon}{0.67 + 0.33\Psi}$ if $\Psi \le -1$*), $c/t \le 62\varepsilon(1-\Psi)\sqrt{(-\Psi)}$

$\varepsilon = \sqrt{235/f_y}$	f_y (N/mm^2)	235	275	355	420	460
	ε	1.00	0.92	0.81	0.75	0.71

*) $\Psi \le -1$ applies where either the compression stress $\sigma < f_y$ or the tensile strain $\varepsilon_y > f_y/E$.

Table 2.22 – Maximum width-to-thickness ratios of outstand flanges

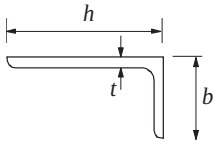
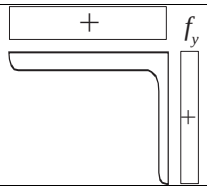
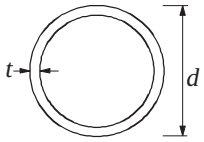
<table>
<tr><td colspan="7">Outstand flanges</td></tr>
<tr><td colspan="2"> 
</td><td colspan="2"> 
</td><td colspan="2"> 
</td><td> 
</td></tr>
<tr><td colspan="2">Rolled sections</td><td colspan="3">Welded sections</td></tr>
<tr><td rowspan="2">Class</td><td rowspan="2">Part subjected to compression</td><td colspan="3">Part subjected to bending and compression</td></tr>
<tr><td colspan="2">Tip in compression</td><td>Tip in tension</td></tr>
<tr><td>Stress distribution (compression +ve)</td><td> 
</td><td colspan="2"> 
</td><td> 
</td></tr>
<tr><td>1</td><td>$c/t \le 9\varepsilon$</td><td colspan="2">$c/t \le \dfrac{9\varepsilon}{\alpha}$</td><td>$c/t \le \dfrac{9\varepsilon}{\alpha\sqrt{\alpha}}$</td></tr>
<tr><td>2</td><td>$c/t \le 10\varepsilon$</td><td colspan="2">$c/t \le \dfrac{10\varepsilon}{\alpha}$</td><td>$c/t \le \dfrac{10\varepsilon}{\alpha\sqrt{\alpha}}$</td></tr>
<tr><td>Stress distribution (compression +ve)</td><td> 
</td><td colspan="2"> 
</td><td> 
</td></tr>
<tr><td>3</td><td>$c/t \le 14\varepsilon$</td><td colspan="3">$c/t \le 21\varepsilon\sqrt{k_\sigma}$
For k_σ see EN 1993-1-5</td></tr>
<tr><td rowspan="2">$\varepsilon = \sqrt{235/f_y}$</td><td>$f_y$ (N/mm^2)</td><td>235</td><td>275</td><td>355</td><td>420</td><td>460</td></tr>
<tr><td>ε</td><td>1.00</td><td>0.92</td><td>0.81</td><td>0.75</td><td>0.71</td></tr>
</table>

The design of structures with class 4 cross sections is outside the scope of this Manual. The ECCS Eurocode Design Manual “Design of Plated Structures” specifically addresses this issue (Beg *et al*, 2010). However, class 4 cross sections may be treated as class 3 if the width-to-thickness ratios are less than the limiting proportions for class 3 when ε is multiplied by the ratio (2.28):

$$\sqrt{\frac{f_y / \gamma_{M0}}{\sigma_{com,Ed}}}, \tag{2.28}$$

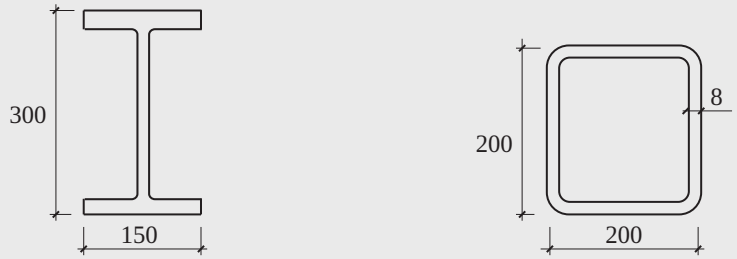
where $\sigma_{com,Ed}$ is the maximum design compressive stress in the part resulting from first order or, if necessary, second order analysis (clause 5.5.2(9)). This possibility is not allowed when verifying the design buckling resistance of a member using clauses 6.3, where the limiting proportions for class 3 should always be obtained from Tables 2.21 to 2.23 (clause 5.5.2(10)).

Table 2.23 – Maximum width-to-thickness ratios of angles and tubular sections

Angles See also Table 2.22	 Does not apply to angles in continuous contact with other components					
Class	Section in compression					
Stress distribution (compression +ve)						
3	$h/t \le 15\varepsilon : \frac{b+h}{2t} \le 11.5\varepsilon$					
Tubular sections 						
Class	Section in bending and/or compression					
1	$d/t \le 50\varepsilon^2$					
2	$d/t \le 70\varepsilon^2$					
3	$d/t \le 90\varepsilon^2$ NOTE: For $d/t > 90\varepsilon^2$ see EN 1993-1-6					
$\varepsilon = \sqrt{235/f_y}$	f_y (N/mm^2)	235	275	355	420	460
	ε	1.00	0.92	0.81	0.75	0.71
	ε^2	1.00	0.85	0.66	0.56	0.51

Example 2.5: Classify the cross sections of Figure 2.84 (dimensions in mm), according to EC3-1-1.

a) IPE 300 in steel grade S 235: i) subjected to bending; ii) subjected to compression.
b) Square hollow section SHS 200×200×8 mm in steel grade S 275, subjected to compression.



IPE 300 SHS 200×200×8 mm

Figure 2.84 – Classification of cross sections

---

a-i) Web in bending (Table 2.21):

$c/t = 248.6/7.1 = 35.0 < 72\varepsilon = 72 \times 1.0 = 72.0.$ (Class 1)

Flange in compression (Table 2.22):

$c/t = \left(150/2 - 7.1/2 - 15\right)/10.7 = 5.3 < 9\varepsilon = 9 \times 1.0 = 9.0.$ (Class 1)

The cross section is class 1.

a-ii) Web in compression (Table 2.21):

$c/t = 248.6/7.1 = 35.0 > 33\varepsilon = 33 \times 1.0 = 33.0,$

but, $c/t = 248.6/7.1 = 35.0 < 38\varepsilon = 38 \times 1.0 = 38.0.$ (Class 2)

Flanges in compression (Table 2.22):

$c/t = \left(150/2 - 7.1/2 - 15\right)/10.7 = 5.3 < 9\varepsilon = 9 \times 1.0 = 9.0.$ (Class 1)

The cross section is class 2.

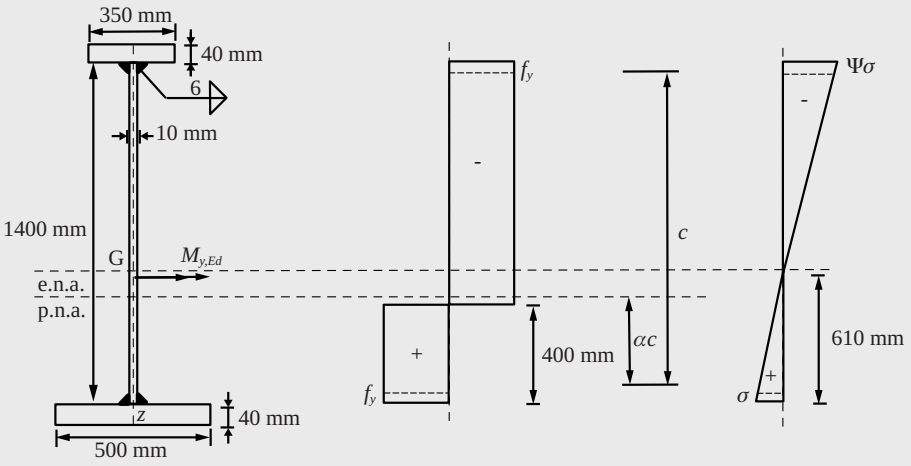
b) Web in compression (Table 2.21):

In a rectangular or square hollow section, the net length of a web can be approximated by $c \approx b - 3t$

$$c/t \approx \left(b - 3t\right)/t = \left(200 - 3\times 8\right)/8 = 22.0 < 33\varepsilon = 33\times 0.92 = 30.4.$$

The cross section is class 1.

Example 2.6: Considering the cross section with unequal flanges of Figure 2.85 (dimensions in mm) subject to a bending moment $M_{y.Ed}$, determine the cross section classification assuming steel grade S 275.



a) Cross section b) Plastic stress-distribution c) Elastic stress distribution

Figure 2.85 – Classification of a welded cross section

Flange in compression (Table 2.22):

$$c/t = \left[\left(500 - 10\right)/2 - 6\sqrt{2}\right]/40 = 5.91 < 9\varepsilon = 8.28 \qquad \text{(Class 1).}$$

Web in bending (Table 2.21):

Determination of the plastic neutral axis (p.n.a.):

$$A_c = A_t \Leftrightarrow 350\times 40 + \left(1400 - z_{pla}\right)\times 10 = 500\times 40 + z_{pla}\times 10 \Leftrightarrow z_{pla} = 400 \text{ mm}.$$

Considering a plastic distribution (Figure 2.85b)

$$\alpha = \frac{400 - 6\sqrt{2}}{1400 - 2 \times 6\sqrt{2}} = 0.28 < 0.50.$$

$$c/t = \frac{1400 - 2 \times 6\sqrt{2}}{10} = 138.30 > \frac{36\varepsilon}{\alpha} = 118.3. \qquad \text{(Not class 1)}$$

$$c/t = 138.30 > \frac{41.5\varepsilon}{\alpha} = 136.4. \qquad \text{(Not class 2)}$$

Determination of the elastic neutral axis (e.n.a.):

$$z_g = \frac{(350 \times 40) \times (1400 + 40/2) + (1400 \times 10) \times (1400/2) + (500 \times 40)(-40/2)}{350 \times 40 + 1400 \times 10 + 500 \times 40}$$

$$= 610 \text{ mm}.$$

Considering an elastic distribution (Figure 2.85c)

$$\Psi = -\frac{1400 - 610}{610} = -1.29 < -1.0.$$

$$c/t = 138.30 < 62\varepsilon(1 - \Psi)\sqrt{(-\Psi)} = 148.4. \qquad \text{(Class 3)}$$

The cross section is class 3.

Chapter 3

DESIGN OF MEMBERS

3.1. INTRODUCTION

3.1.1. General

According to the general framework established in EN 1990 for the safety of structures, the safety of steel members at ultimate limit state is ensured by applying partial safety factors γ_M to the various characteristic values of resistance. The safety factors are defined in accordance with the potential failure modes. For steel members, the following three failure modes are considered (clause 6.1(1)): i) resistance of cross sections, whatever the class; ii) resistance of members to instability assessed by member checks and iii) resistance of cross sections in tension to fracture. Specific partial safety factors γ_{M0}, γ_{M1} and γ_{M2}, deemed to guarantee the reliability targets of EN 1990, correspond to each failure mode, respectively. The following values of the partial safety factors γ_{Mi} are recommended for buildings[1]: $\gamma_{M0} = 1.00$; $\gamma_{M1} = 1.00$ and $\gamma_{M2} = 1.25$ and will be used throughout this book. It is noted that for other types of structures, recommended values are given in Parts 2 to 6 of EN 1993. For structures not covered by Parts 2 to 6 of EN 1993, the National Annexes may define the partial factors γ_{Mi}; it is recommended in this case to take the partial factors γ_{Mi} from EN 1993-2 (CEN, 2006d).

This chapter describes the basic theoretical concepts, as well as the normative design rules (according to EC3-1-1) concerning the verification of the resistance of steel members. In particular, the evaluation of the resistance

[1] These values were adopted by the majority of the National Annexes.

of cross sections of classes 1 to 3 subjected to the various combinations of internal forces is presented in accordance with clauses 6.2. Additionally, the assessment of the resistance of members subject to instability phenomena is also covered in accordance with clauses 6.3. Finally, as in the previous chapter, several detailed worked examples are presented.

3.1.2. Resistance of cross sections

3.1.2.1. General criteria

The resistance of cross sections depends on their class (clause 6.2.1(3)). According to the definition of the four cross section classes (see sub-chapter 2.4), cross section classes 1 and 2 reach their full plastic resistance, while class 3 cross sections only reach their elastic resistance. Class 4 cross sections are not able to reach their elastic resistance because of local buckling and they are outside the scope of EC3-1-1 and of this book. Nevertheless, using the concept of effective section (CEN, 2006c), they are effectively treated as class 3 cross sections and their resistance is evaluated as an elastic resistance.

The design value of an action effect, at each cross section, should not exceed the corresponding design resistance, and if several action effects act simultaneously, the combined effect should not exceed the resistance for that combination (clause 6.2.1(1)). Shear lag effects and local buckling effects should be included according to the concept of effective section of EC3-1-5 (CEN, 2006c). Shear buckling effects should also be considered according to EC3-1-5 (clause 6.2.1(2)).

An elastic verification according to the elastic resistance may be carried out for all cross sectional classes provided that the effective cross sectional properties are used for the verification of class 4 cross sections (clause 6.2.1(4)). In the most general case and as a conservative approach, where local longitudinal, transverse and shear stresses coexist at the critical point of the cross section, the following yield criterion may be used in the context of an elastic verification (clause 6.2.1(5)).

$$\left(\frac{\sigma_{x,Ed}}{f_y/\gamma_{M0}}\right)^2+\left(\frac{\sigma_{z,Ed}}{f_y/\gamma_{M0}}\right)^2-\left(\frac{\sigma_{x,Ed}}{f_y/\gamma_{M0}}\right)\left(\frac{\sigma_{z,Ed}}{f_y/\gamma_{M0}}\right)+3\left(\frac{\tau_{Ed}}{f_y/\gamma_{M0}}\right)^2\le 1, \qquad (3.1)$$

where $\sigma_{x,Ed}$ is the design value of the local longitudinal stress, $\sigma_{z,Ed}$ is the design value of the local transverse stress and τ_{Ed} is the design value of the local shear stress, all values at the point of consideration.

For classes 1 or 2, the resistance of cross sections may be evaluated on the basis of their plastic resistance by finding a stress distribution which is in equilibrium with the internal forces and moments without exceeding the yield strength. This stress distribution should be compatible with the associated plastic deformations (clause 6.2.1(6)).

For class 3 cross sections, where all the compression parts of a cross section are class 3, its resistance should be based on an elastic distribution of strains across the cross section. Compressive stresses should be limited to the yield strength at the extreme fibres (clause 6.2.1(9)). These extreme fibres may be assumed at the midplane of the flanges for ULS checks. However, whenever yielding first occurs on the tension side of the cross section, the plastic reserves of the tension zone may be utilized by accounting for partial plastification when determining the resistance of a class 3 cross section (clause 6.2.1(10)).

For both plastic and elastic verifications of safety, interaction formulae on the basis of resistances (N_{Rd}, M_{Rd}, V_{Rd}) are favoured since they may lead to less conservative results. As a conservative approximation for all cross section classes, a linear summation of the utilization ratios for each stress resultant may be used. For class 1, class 2 or class 3 cross sections subjected to a combination of N_{Ed}, $M_{y,Ed}$, $M_{z,Ed}$ this method may be applied by using the following criterion (clause 6.2.1(7)):

$$\frac{N_{Ed}}{N_{Rd}} + \frac{M_{y,Ed}}{M_{y,Rd}} + \frac{M_{z,Ed}}{M_{z,Rd}} \leq 1 . \qquad (3.2)$$

Class 3 cross sections exhibit a gradual transition from plastic to elastic resistance because of residual stress effects and local yielding. This is not currently recognized by Eurocode 3 whose provisions result in a sudden transition from plastic resistance to elastic resistance. Extensive research was recently carried out to provide a safe smooth transition between classes 2 and 3 (Greiner *et al*, 2011).

3.1.2.2. Section properties

The properties of the gross cross section should be determined using the nominal dimensions. Holes for fasteners need not be deducted, but

allowance should be made for larger openings. Splice materials should not be included (clause 6.2.2.1(1)).

Because of the existence of holes and other openings, it is necessary to define the net area of a cross section. Generally, it is defined as its gross area less appropriate deductions for all holes and other openings (clause 6.2.2.2(1)). For calculating net section properties, the deduction for a single fastener hole should be the gross cross sectional area of the hole in the plane of its axis. For countersunk holes, appropriate allowance should be made for the countersunk portion (clause 6.2.2.2(2)).

In the case of multiple fastener holes, provided that the fastener holes are not staggered, the total area to be deducted for fastener holes should be the maximum sum of the sectional areas of the holes in any cross section perpendicular to the member axis (clause 6.2.2.2(3)). Where the fastener holes are staggered (Figure 3.1), the net area A_{net} should be the minimum of (clause 6.2.2.2(4)):

$$A - n_p\, t\, d_0 \qquad \text{(fracture section 1)}; \tag{3.3}$$

$$A - n\, t\, d_0 + t\sum\left(\frac{s^2}{4p}\right) \qquad \text{(fracture section 2)}, \tag{3.4}$$

where:

- A is the gross area of the section;
- n_p is the number of non-staggered holes in any cross section perpendicular to the member axis;
- n is the number of holes extending in any diagonal or zig-zag line progressively across the member or part of the member, see Figure 3.1;
- t is the thickness;
- d_0 is the hole diameter;
- s is the staggered pitch, the spacing of the centres of two consecutive holes in the chain measured parallel to the member axis;
- p is the spacing of the centres of the same two holes measured perpendicular to the member axis.

The summation in expression (3.4) represents the number of segments between staggered holes, as it is exemplified in example 3.1.

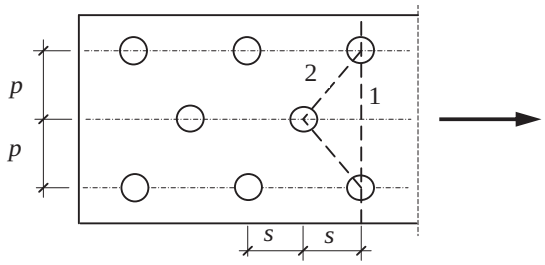


Figure 3.1 – Definition of the net area of a cross section

In the case of angles, or other member with holes in more than one plane, the spacing p should be measured along the mid-plane of the legs, as illustrated in Figure 3.2.

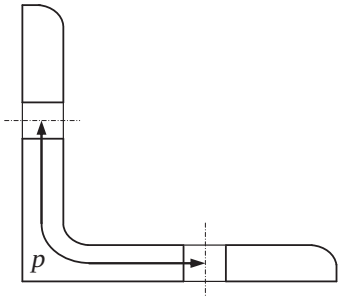
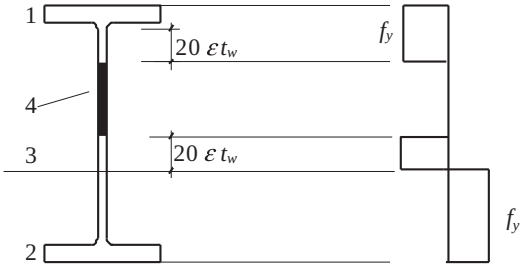


Figure 3.2 – Angle with holes in both legs

Cross sections with a class 3 web and flanges with class 1 or 2 may be classified and designed as class 2, considering a reduced effective area for the web. The effective area is obtained according to Figure 3.3 and the following iterative procedure: by replacing the portion of the web in compression by a part of 20 εt_w adjacent to the compression flange and another equal part adjacent to the plastic neutral axis of the effective cross section. Iteration results from the definition of the neutral axis as being that of the effective section (Figure 3.3).

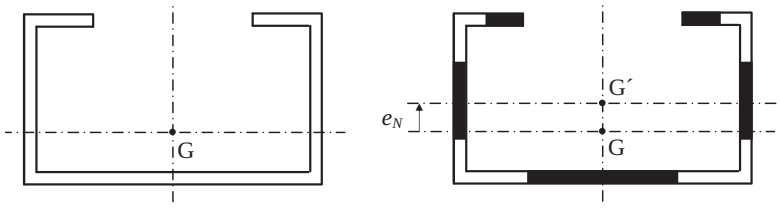
The resistance of class 4 cross sections is limited by local instability phenomena that prevent the development of the elastic resistance of the cross section. According to EC3-1-1, local instability phenomena, in class 4 cross

sections, should be taken into account by replacing the gross section by an effective cross section, obtained from a reduced area of the compression parts. The effective cross section should be based on effective widths, according to EC3-1-5. The effective cross section of circular hollow sections should be obtained from EC3-1-6 (CEN, 2007). Figures 3.4 and 3.5 represent, in a qualitative way, the effective cross section of a U section subject to compression and an I section subject to major axis bending, respectively. In these figures, the portions of the gross area to be deducted are indicated in black. For the I section, it is assumed that only the web is class 4.



1 - compression; 2 - tension; 3 - plastic neutral axis; 4 - neglected part

Figure 3.3 – Effective class 2 web



Gross cross section Effective cross section

Figure 3.4 – Class 4 cross section submitted to a compressive axial force



Gross cross section Effective cross section

Figure 3.5 – Class 4 cross section submitted to bending moment

An axial compression force in a cross section in class 4 due to the possible shift, e_N, of the centroid of the effective area, A_{eff}, relative to the centre of gravity of the gross cross section, results in an additional bending moment $\Delta M_{Ed} = N_{Ed} e_N$.

The analysis of cross sections with class 4 is not included in the scope of this book. The analysis may be performed according to EC3-1-3, for cold formed sections; according to EC3-1-5, for hot rolled sections and welded sections; and according to EC3-1-6, for circular hollow sections.

3.1.3. Buckling resistance of members

In addition to verification of the cross section resistance, the buckling resistance of members must also be checked, according to clauses 6.3 and 6.4. The buckling phenomenon depends on the presence of compressive stresses and therefore it must be checked for all members subjected to axial compression, bending moment or a combination of both. Shear buckling effects should also be considered according to EC3-1-5.

For a member under pure compression the buckling modes to take into account are: i) flexural buckling; ii) torsional buckling and iii) torsional-flexural buckling. A member under bending moment must be checked against lateral-torsional buckling. A member under a combination of compression force and bending moment must be checked against all the buckling modes mentioned above. The theoretical background, the design rules and several applications relating to the buckling resistance of steel members are presented in the sub-chapters 3.5, 3.6 and 3.7.

3.2. TENSION

3.2.1. Behaviour in tension

Figure 3.6 illustrates various examples of structures with some members that are commonly assumed to be loaded only in tension. Figure 3.7 shows typical cross sections of tension members. Simple or built-up rolled sections are commonly used in trusses, lattice girders and as bracing members. Cables, flats or bars are used in bracing systems. Cables,

flats or bars are some times used in bridges or long-span roofs; such member types are discussed in detail in EC3-1-11 (CEN, 2006e).

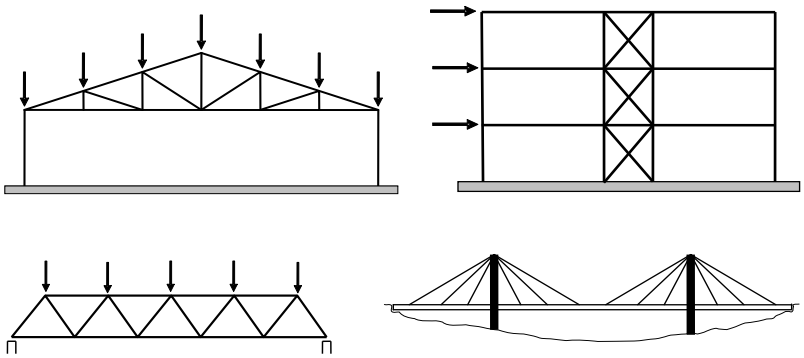


Figure 3.6 – Structures with some members in tension

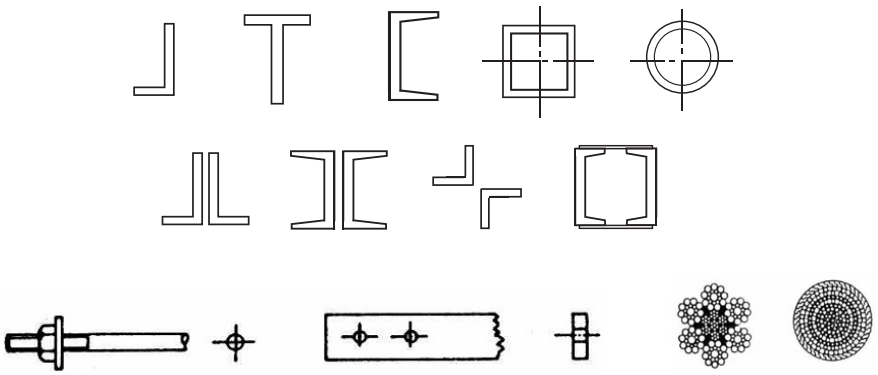


Figure 3.7 – Typical cross sections of members in tension

The behaviour of members in tension is closely related to the stress-strain behaviour of steel subjected to uniaxial tensile forces. Recalling the stress-strain relationship shown in Figure 1.7, the ultimate cross section resistance corresponds to the tensile strength R_m, although the plastic resistance is also often considered as the ultimate tensile resistance of the member, especially when ductility is of concern.

Typically, the governing design situation for members subject to tension corresponds to the location of the joints (either the connection to other parts of the structure or splices within the tension member). In these cross sections, either because of bolting or because of a change of cross sectional shape, the net area of the cross section must be taken into account.

The calculation of the net area in tension was described in section 3.1.2.2. In addition, it is noted that stress concentrations occur in the neighbourhood of holes or discontinuities, as shown in Figure 3.8.

Bolted or welded connections often induce second-order moments because of small eccentricities, as shown in Figure 3.9. These second-order effects should be taken into account. Alternatively, careful detailing should be specified to eliminate these eccentricities, as illustrated in Figure 3.10.

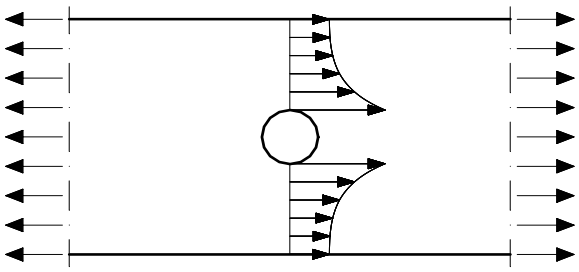


Figure 3.8 – Concentration of tension next to a hole

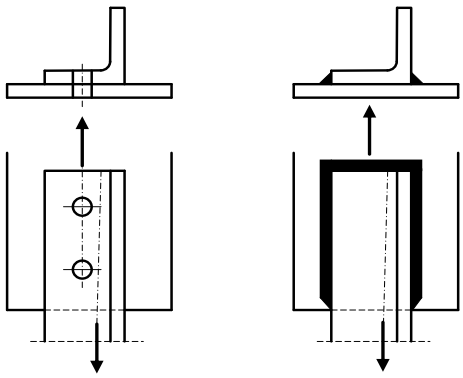


Figure 3.9 – Eccentric connections

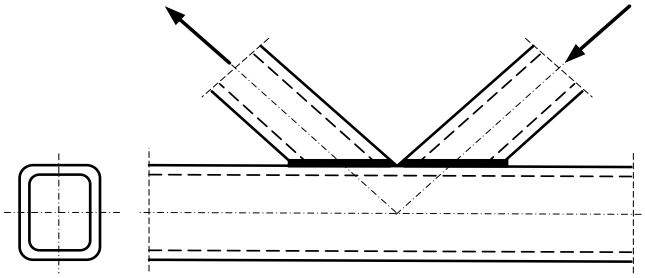


Figure 3.10 – Welded connections between hollow sections

3.2.2. Design for tensile force

A member exclusively subject to a tension force is under a uniaxial stress state. According to clause 6.2.3(1), the design value of the tension force N_{Ed} at each cross section, including cross sections in the vicinity of the connections, should satisfy:

$$\frac{N_{Ed}}{N_{t,Rd}} \leq 1.0\,, \tag{3.5}$$

where $N_{t,Rd}$ is the design tension resistance. For sections with holes the design tension resistance $N_{t,Rd}$ should be taken as the smallest of:

- design plastic resistance of the gross cross section,

$$N_{pl,Rd} = A\, f_y / \gamma_{M0}\,, \tag{3.6}$$

where:

A is the gross cross section area,
f_y is the yield strength of steel and
γ_{M0} is the partial safety factor.

- design ultimate resistance of the net cross section at holes for fasteners,

$$N_{u,Rd} = 0.9\, A_{net}\, f_u / \gamma_{M2} \tag{3.7}$$

where:

A_{net} is the net cross section area,
f_u is the ultimate strength of steel and
γ_{M2} is the partial safety factor.

Whenever dissipative behaviour is required under cyclic loading, such as in the case of capacity design (CEN, 2004a), the design plastic resistance $N_{pl,Rd}$ should be less than the design ultimate resistance of the net section at fasteners holes $N_{u,Rd}$ (clause 6.2.3(3)), that is,

$$N_{u,Rd} > N_{pl,Rd} \Leftrightarrow \frac{A_{net}}{A} > \frac{f_y}{0.9\, f_u}\frac{\gamma_{M2}}{\gamma_{M0}}\,. \tag{3.8}$$

In the case of members with Category C preloaded bolted connections loaded in shear[2], the design tension resistance $N_{t,Rd}$ at the cross section with holes for fasteners should be taken as $N_{net,Rd}$ (clause 6.2.3(4)):

$$N_{net,Rd} = A_{net} f_y / \gamma_{M0} \ . \tag{3.9}$$

For angles connected by one leg and other unsymmetrically connected members in tension (such as T sections or channel sections), the eccentricity in joints and the effects of the spacing and edge distances of the bolts should be taken into account in determining the design resistance (clause 3.10.3(1) of EC3-1-8). According to clause 3.10.3(2) of EC3-1-8, a single angle in tension connected by a single row of bolts, see Figure 3.11, may be treated as concentrically loaded over an effective net section for which the design ultimate resistance should be determined as follows:

$$N_{u,Rd} = \frac{2.0\left(e_2 - 0.5\, d_0\right) t\, f_u}{\gamma_{M2}}; \qquad \text{(1 bolt)} \tag{3.10}$$

$$N_{u,Rd} = \frac{\beta_2\, A_{net}\, f_u}{\gamma_{M2}}; \qquad \text{(2 bolts)} \tag{3.11}$$

$$N_{u,Rd} = \frac{\beta_3 A_{net}\, f_u}{\gamma_{M2}}. \qquad \text{(3 bolts or more)} \tag{3.12}$$

In these equations,

- t is the thickness of the leg of an angle;
- f_u is the ultimate strength of steel;
- d_o is the hole diameter;
- e_2 is the distance of the centre of the fastener holes to the adjacent edge of the angle, perpendicular to the direction of load transfer (as illustrated in Figure 3.11);
- γ_{M2} is a partial safety factor, defined according to EC3-1-8.

[2] Connections slip-resistant at ultimate limit state (clause 3.4.1(1)c of EC3-1-8).

The net area, A_{net}, is calculated according to sub-section 3.1.2.2 (clause 6.2.2); in angles of unequal legs, connected by the smaller leg, A_{net} should be taken as equal to the net section area of an equivalent equal-leg angle of leg size equal to that of the smaller leg. Parameters β_2 and β_3 are reduction factors which are defined depending on the distance between holes (pitch p_1), according to Table 3.1; for values of $2.5d_0 < p_1 < 5d_0$, these parameters can be determined by linear interpolation.

Table 3.1 – Reduction factors β_2 and β_3

Pitch	p_1	$\leq 2.5\ d_0$	$\geq 5.0\ d_0$
2 bolts	β_2	0.4	0.7
3 bolts or more	β_3	0.5	0.7

It is reminded that no matter what value is given by equations (3.10) to (3.12), the resistance is limited by equation (3.6).

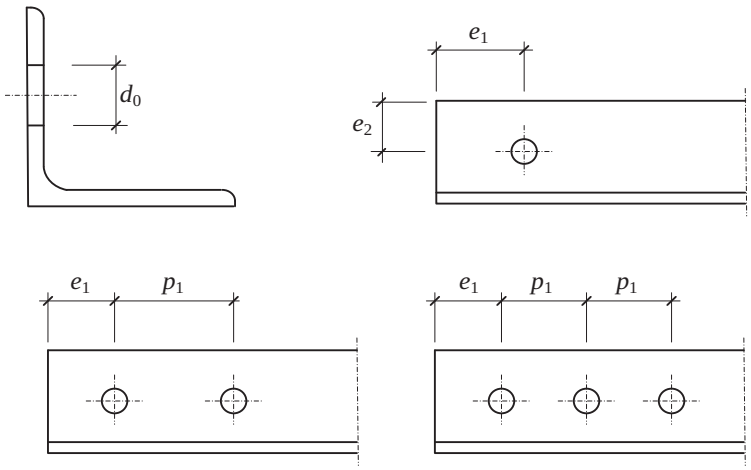


Figure 3.11 – Angles connected by one leg

Members that comprise angles connected by welding only in one leg can be treated as being concentrically loaded. Resistance is determined using equation (3.6), but based on an effective cross section area. The area of the effective cross section, according to clause 4.13 of EC3-1-8, must be evaluated as follows: i) for angles of equal legs or unequal legs that are

connected by the larger leg, the area of the effective section may be considered as equal to the gross area; ii) for angles of unequal legs, connected by the smaller leg, the area of the effective section should be taken as equal to the gross area of an equivalent angle, with legs that are equal to the smaller of the legs.

3.2.3. Worked examples

Example 3.1: Calculate the net area A_{net} of the bolted section of the plate represented in Figure 3.12. Assume a plate with thickness t and the remaining dimensions (in mm), as indicated in Figure 3.12.

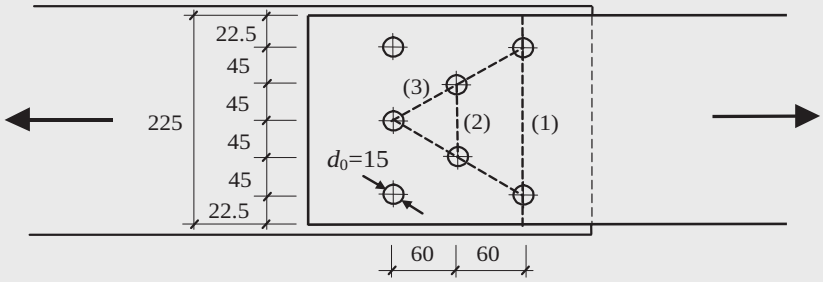


Figure 3.12 – Net area of a plate

The connection is loaded by a concentric axial force, therefore the load may be assumed to be uniformly distributed amongst the fasteners. Due to the position of the fasteners, the net area is evaluated considering fracture sections 1, 2 and 3, as illustrated in Figure 3.12. Fracture section 1 is perpendicular to the direction of the force, whereas fracture sections 2 and 3 include staggered pitches. However, all of these sections correspond to net sections subjected to the totality of the applied axial force. Hence, from expressions (3.3) and (3.4):

Fracture section 1 $\rightarrow A_{net}^{(1)} = 225 \times t - 2 \times t \times 15 = 195\, t$.

Fracture section 2 $\rightarrow A_{net}^{(2)} = 225 \times t - 4 \times t \times 15 + 2 \times t \times \dfrac{60^2}{4 \times 45} = 205\, t$.

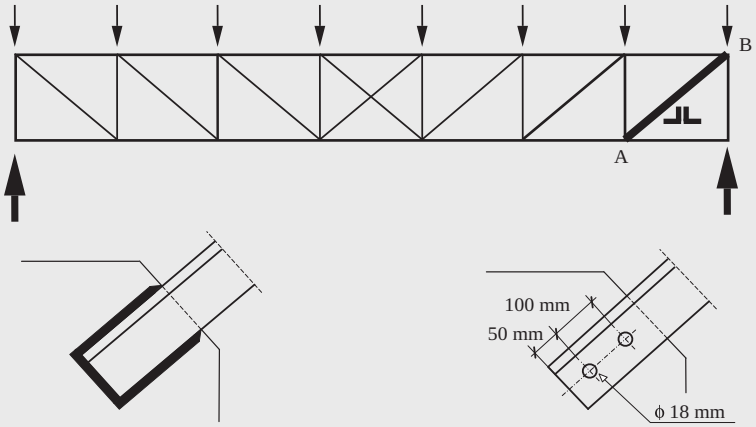
Fracture section 3 $\rightarrow A_{net}^{(3)} = 225 \times t - 5 \times t \times 15 + 4 \times t \times \dfrac{60^2}{4 \times 45} = 230\, t$.

The net area of the plate is given by the minimum value, $A_{net} = 195\ t$.

Example 3.2: Consider the chord AB of the steel truss, indicated in Figure 3.13, assuming it is submitted to a design tensile axial force of N_{Ed} = 220 kN. The cross section consists of two angles of equal legs, in steel grade S 235. Design chord AB assuming two distinct possibilities for the connections:

a) welded connections;

b) bolted connections.



a) Welded connections b) Bolted connections

Figure 3.13 – Steel truss

a) *Welded connections*

The chord is made up by two angles of equal legs, but the connection is made only in one leg of the angle. Thus, according to clause 4.13 of EC3-1-8, the effective area can be considered equal to the gross area. Therefore, the following conditions must be satisfied:

$$N_{Ed} \le N_{t,Rd} = \frac{A f_y}{\gamma_{M0}},$$

where $\gamma_{M0} = 1.0$, f_y = 235 MPa and A is the gross area of the section.

Considering the design axial force, N_{Ed} = 220 kN, then:

$$220\ \text{kN} \le \frac{A \times 235 \times 10^3}{1.0} \Rightarrow A \ge 9.36 \times 10^{-4}\ \text{m}^2 = 9.36\ \text{cm}^2 .$$

From a table of commercial profiles, a solution with two angles 50×50×5mm, with a total area of $2 \times 4.8 = 9.6\ \text{cm}^2$, satisfies the above safety requirement.

b) *Bolted connections*

In this case, the chord, made up by angles of equal legs, is connected by 2 bolts only in one leg. According to clause 3.10.3 of EC3-1-8, the following design conditions must be ensured:

$$N_{Ed} \le N_{t,Rd}, \text{ with } N_{t,Rd} = \min\left[N_{pl,Rd} = \frac{A f_y}{\gamma_{M0}}; N_{u,Rd} = \frac{\beta_2 A_{net} f_u}{\gamma_{M2}} \right],$$

where, γ_{M0} = 1.0, γ_{M2} = 1.25, f_y = 235 MPa, f_u = 360 MPa, A is the gross area of the cross section, A_{net} is the net area of the bolted section, and β_2 is a factor obtained from Table 3.1 (or Table 3.8 of EC3-1-8). A first check based on the plastic design of the gross cross section leads to:

$$220\ \text{kN} \le \frac{A \times 235 \times 10^3}{1.0} \Rightarrow A \ge 9.36 \times 10^{-4}\ \text{m}^2 = 9.36\ \text{cm}^2.$$

Hence, the section obtained in the previous design, two angles 50×50×5 mm (A = 9.6 cm^2), also satisfies this safety requirement.

The second condition (equation (3.11), reproduced above) requires the evaluation of the net area A_{net}, (illustrated in Figure 3.14) and the factor β_2, both evaluated according to clause 3.10.3 of EC3-1-8.

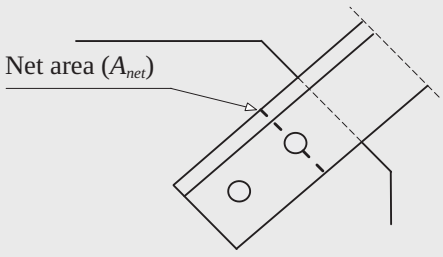


Figure 3.14 – A_{net} in the bolted connection

For $d_0 = 18$ mm, $2.5d_0 = 45$ mm and $5d_0 = 90$ mm.

As $p_1 = 100$ mm > 90 mm, then $\beta_2 = 0.70$.

The net area of the bolted section made up of two angles is given by:

$$A_{net} = A - 2\,t\,d_0 = 9.6 - 2 \times 0.5 \times 1.8 = 7.8 \text{ cm}^2.$$

Thus, the design ultimate resistance is given by:

$$N_{u,Rd} = \frac{0.7 \times 7.8 \times 10^{-4} \times 360 \times 10^3}{1.25} = 157.2 \text{ kN}.$$

However, N_{Ed} = 220 kN > $N_{u,Rd}$ = 157.2 kN; therefore, the chosen cross section is not appropriate. By adopting a cross section with enhanced resistance, for example, two angles 60×60×6 mm (A = 13.82 cm^2 and A_{net} =11.66 cm^2), then:

$$N_{pl,Rd} = 13.82 \times 10^{-4} \times 235 \times 10^3 / 1.0 = 324.8 \text{ kN} > N_{Ed} = 220 \text{ kN};$$

$$N_{u,Rd} = \frac{0.7 \times 11.66 \times 10^{-4} \times 360 \times 10^3}{1.25} = 235.1 \text{ kN} > N_{Ed} = 220 \text{ kN}.$$

As $N_{pl,Rd}$ = 324.8 kN > $N_{u,Rd}$ = 235.1 kN, failure is non-ductile; however, since this is not a design condition, the section defined by two angles 60×60×6 mm can be accepted.

Example 3.3: Figure 3.15 represents a lattice girder in steel grade S 275, supporting a reinforced concrete floor. The loading, applied on the floor and transmitted to the truss as concentrated loads applied in the nodes, is defined by the following distributed loads:

Permanent action on the floor = 5.75 kN/m^2 (γ_G = 1.35);

Variable action on the floor = 4.00 kN/m^2 (γ_Q = 1.50).

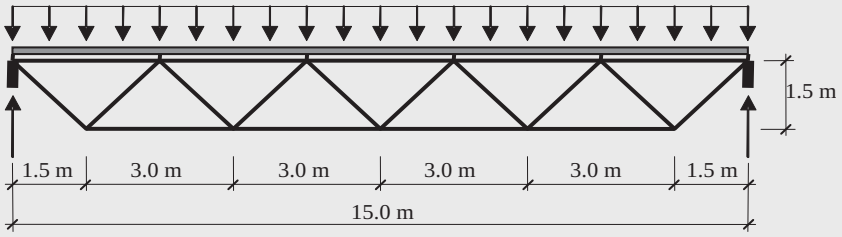


Figure 3.15 – Lattice girder

The distance between lattice girders is 3.00 m; the nodes of the truss are braced in the perpendicular direction to the plane of the structure; the loading already includes the selfweight of the steel truss. Design the tension members of the truss, assuming the following alternatives:

a) Square hollow sections (SHS), and welded connections for the members of the structure.

b) HEA profiles in the upper and lower chords (horizontal members) and 2 UPN channel profiles for the diagonal members. The diagonal members are bolted to gusset plates, which are welded to the HEA profiles in the upper and lower chords.

For design at the ultimate limit state, the following combination of actions is considered (according to EN 1990):

$$p_{Ed} = 1.35 \times 5.75 + 1.5 \times 4.00 = 13.76 \text{ kN/m}^2,$$

where p_{Ed} is the design load, uniformly distributed on the floor.

The concentrated loads, represented in Figure 3.16, were calculated based on the influence areas of each node, and considering a distance of 3.00 m between the lattice girders. In the same figure, the internal forces in the members, obtained by node equilibrium or any other appropriate method, are represented.

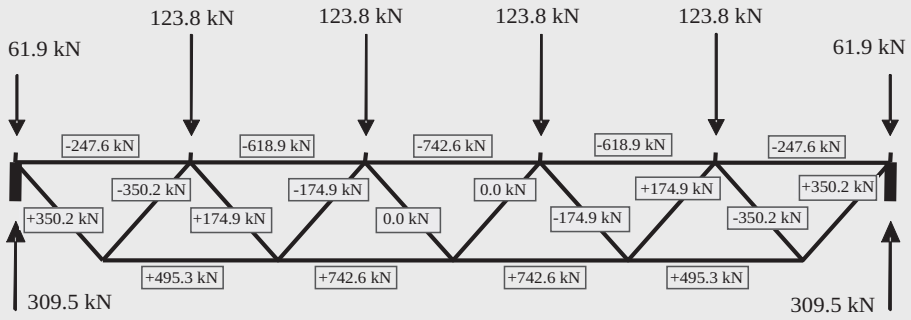


Figure 3.16 – Actions and internal forces on the structure

a) According to the distribution of internal forces illustrated in Figure 3.16, two distinct cross sections are adopted: one for the bottom tension chord,

designed for an axial force of N_{Ed} = 742.6 kN, and another for the diagonal tension members, designed for an axial force of N_{Ed} = 350.2 kN.

The members comprise square hollow sections with welded connections. Assuming that the axis of the members, in each node, converges in a point, there is no reduction of the resistance due to eccentricities in the connections (note, however, that reductions of the resistance due to local stresses in the connection may be necessary, as given in EC3-1-8). Hence, the design of the tension members is given by:

$$N_{Ed} \le N_{t,Rd} = \frac{A f_y}{\gamma_{M0}},$$

where γ_{M0} = 1.0, f_y = 275 MPa and A is the gross area of the cross section.

Considering the design axial forces leads to:

- for the bottom chord,

$$742.6 \le \frac{A \times 275 \times 10^3}{1.0} \Rightarrow A \ge \frac{742.6 \times 1.0}{275 \times 10^3} = 27.0 \times 10^{-4}\,\text{m}^2 = 27.0\,\text{cm}^2,$$

- for the diagonal members,

$$350.2 \le \frac{A \times 275 \times 10^3}{1.0} \Rightarrow A \ge \frac{350.2 \times 1.0}{275 \times 10^3} = 12.7 \times 10^{-4}\,\text{m}^2 = 12.7\,\text{cm}^2.$$

From a table of commercial profiles for square hollow cross sections (SHS), the following solution is adopted: a SHS 120×120×6.3 mm (A = 28.5 cm^2) cross section for the bottom chord and a SHS 80×80×5 mm (A = 14.9 cm^2) cross section for the diagonal members.

b) Taking into account the type of connection, the bottom tension chord is designed for an axial force N_{Ed} = 742.6 kN, considering the gross cross section; while the diagonals in tension are designed for an axial force N_{Ed} = 350.2 kN, but considering a possible reduction of the resistance in the bolted cross section, due to the holes. The design plastic resistance of the bottom chord, considering the gross cross section, is given by:

$$742.6 \le \frac{A \times 275 \times 10^3}{1.0} \Rightarrow A \ge \frac{742.6 \times 1.0}{275 \times 10^3} = 27.0 \times 10^{-4}\,\text{m}^2 = 27.0\,\text{cm}^2.$$

Similarly, for the diagonal members:

$$350.2 \le \frac{A \times 275 \times 10^3}{1.0} \Rightarrow A \ge \frac{350.2 \times 1.0}{275 \times 10^3} = 12.7 \times 10^{-4}\,\text{m}^2 = 12.7\,\text{cm}^2.$$

Hence, a HEA 140 (A = 31.42 cm^2) cross section is adopted for the bottom chord, and a 2 UPN 80 (A = 22.00 cm^2) cross section is initially proposed for the diagonal members. The overdesign of the section of the diagonal members is due to the fact that the dimensions of the bolts required to resist the applied axial force (considering the connection illustrated in Figure 3.17) are not compatible with the dimensions of smaller UPN cross sections.

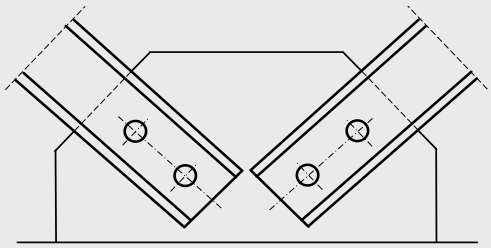


Figure 3.17 – Connection of the diagonal bars of the truss

In the case of the diagonal members, considering the connection with M20 bolts (d_0 = 22 mm) illustrated in Figure 3.17, the design ultimate resistance of the bolted cross section should also be checked. The net area of the bolted cross section made up of two UPN is given by:

$$A_{net} = A - 2td_0 = 22.0 - 2 \times 0.6 \times 2.2 = 19.36\,\text{cm}^2\,.$$

The design ultimate resistance is given by:

$$N_{u,Rd} = \frac{0.9 \times 19.36 \times 10^{-4} \times 430 \times 10^3}{1.25} = 506.5\,\text{kN} > N_{Ed} = 350.2\,\text{kN}.$$

As the design ultimate resistance in the bolted section exceeds the applied axial force, the section defined by two UPN 80 satisfies the safety criterion. However, as $N_{pl,Rd}$ = 605 kN > $N_{u,Rd}$ =506.5 kN, the failure of the diagonal members would be non-ductile. This situation often occurs in tension members with bolted connections.

3.3. LATERALLY RESTRAINED BEAMS

3.3.1. Introduction

The resistance of a steel beam in bending depends on the cross section resistance or the occurrence of lateral instability. The latter, typical of steel members composed of I or H sections bent about the major axis, will be discussed in sub-chapter 3.6.

Whenever one of the following situations occurs in a beam, lateral-torsional buckling cannot develop and assessment of the beam can be based just on the cross section resistance:

- the cross section of the beam is bent about its minor *z* axis;
- the beam is laterally restrained by means of secondary steel members, by a concrete slab or any other method that prevents lateral displacement of the compressed parts of the cross section;
- the cross section of the beam has high torsional stiffness and similar flexural stiffness about both principal axes of bending as, for example, closed hollow cross sections.

The bending resistance of a cross section can be obtained from its plastic resistance, if the section is compact (class 1 or 2 section), and made from material with a ductile behaviour, as in the case of mild steel. On the other hand, in a slender cross sections (class 3 or 4 section) the bending resistance must be based on its elastic resistance.

The web provides most of the shear resistance, as one can see from Figure 3.18. A common and conservative treatment assumes that the shear stress is uniformly distributed over the depth of the web, and any shear resistance of the flanges can be ignored, unless dealing with very thick flanges. EC3-1-1 recommends that whenever possible, the shear resistance of a steel section should be evaluated based on a plastic distribution of shear stress.

In a section subject to bending and shear force, the bending moment resistance may have to be reduced to account for the presence of shear.

I or H sections and rectangular hollow sections are usually chosen for beams because they possess high major axis bending resistance and bending stiffness.

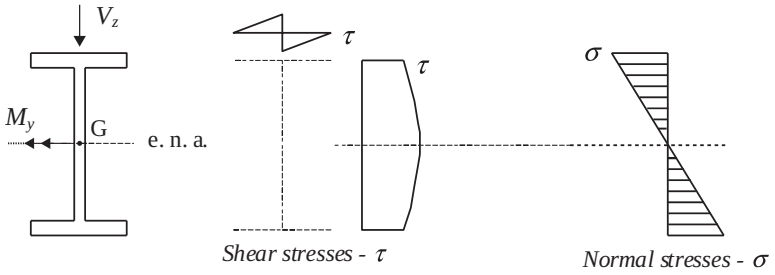


Figure 3.18 – Elastic distributions of normal stresses and shear stresses

3.3.2. Design for bending

3.3.2.1. Elastic and plastic bending moment resistance

The elastic bending resistance of a cross section is attained when the normal stress in the point furthest away from the elastic neutral axis (e. n. a.) reaches the yield strength f_y; the corresponding bending moment is denoted the elastic bending moment M_{el}. The bending moment that is able to totally plastify a section is denoted as the plastic bending moment M_{pl}.

In the calculation of the plastic bending moment of a steel cross section (assuming equal yield strengths in tension and compression), the plastic neutral axis (p.n.a.) is located at the centroid only if the section is symmetrical, as for the case of rectangular sections, I sections or H sections with equal flanges. In case of non-symmetric cross sections, such as a T-section, the neutral axis moves in order to divide the section in two equal areas. Figure 3.19 represents, for two distinct cross sections (I section with equal flanges and T section), the diagrams of normal stresses that correspond to the elastic limit (elastic bending moment) and to complete plastification (plastic bending moment). For both cross sections, the elastic bending moment and the plastic bending moment around the horizontal axis are given by:

$$M_{el} = \frac{I}{v} f_y = W_{el}\, f_y ; \tag{3.13}$$

$$M_{pl} = A_c\, f_y\, d_c + A_t\, f_y\, d_t = \left(S_c + S_t\right) f_y = W_{pl}\, f_y , \tag{3.14}$$

where:

I	is the second moment of area about the elastic neutral axis (coincident with the centroid of the cross section);
v	is the maximum distance from an extreme fibre to the same axis;
$W_{el} = I/v$	is the elastic bending modulus;
A_c and A_t	are the areas of the section in compression and in tension, respectively (of equal value);
f_y	is the yield strength of the material;
d_c and d_t	are the distances from the centroid of the areas of the section in compression and in tension, respectively, to the plastic neutral axis;
W_{pl}	is the plastic bending modulus, given by the sum of first moment of areas A_c and A_t, in relation to the plastic neutral axis ($W_{pl} = S_c + S_t$).

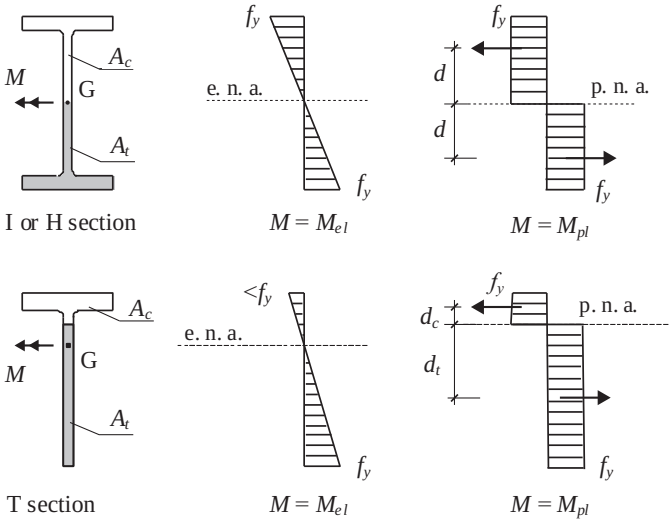


Figure 3.19 – Elastic and plastic bending moment cross sectional resistance

For symmetric sections the previous calculations are simpler because the plastic neutral axis coincides with the elastic neutral axis and, consequently, $d_c = d_t$.

When a cross section is subjected to bi-axial bending, an interaction formula between the two bending moments must be obtained. Such formulae

can be found in the literature for the majority of standard cross sectional shapes. In general, these were obtained as particular cases of interaction formulae between axial force (N) and bi-axial bending (M_y - M_z); therefore only a brief description and discussion of these formulae will be presented in sub-chapter 3.7. For practical applications, EC3-1-1 provides interaction formulae for bi-axial bending, in the elastic and plastic ranges, which are applicable for the design of usual cross sections in steel structures.

3.3.2.2. Uniaxial bending

In the absence of shear forces, the design value of the bending moment M_{Ed} at each cross section should satisfy (clause 6.2.5(1)):

$$\frac{M_{Ed}}{M_{c,Rd}} \leq 1.0 \ , \tag{3.15}$$

where:

$M_{c.Rd}$ is the design resistance for bending. The design resistance for bending about one principal axis of a cross section is determined as follows (clause 6.2.5(2)):

– Class 1 or 2 cross sections

$$M_{c,Rd} = W_{pl} \, f_y \big/ \gamma_{M0} \ ; \tag{3.16}$$

– Class 3 cross sections

$$M_{c,Rd} = W_{el,\min} \, f_y \big/ \gamma_{M0} \ ; \tag{3.17}$$

– Class 4 cross sections

$$M_{c,Rd} = W_{eff,\min} \, f_y \big/ \gamma_{M0} \ , \tag{3.18}$$

where:

W_{pl} is the plastic section bending modulus;

$W_{el,\min}$ is the minimum elastic section bending modulus;

$W_{eff,\min}$ is the minimum elastic bending modulus of the reduced effective section;

f_y is the yield strength of the material;
γ_{M0} is the partial safety factor.

3.3.2.3. Bi-axial bending

Design for bi-axial bending can be verified by plastic (class 1 or 2 cross sections) or elastic (class 3 and 4 cross sections) interaction formulae, according to clause 6.2.9, as described next:

Class 1 or 2 sections $$\left[\frac{M_{y,Ed}}{M_{pl,y,Rd}}\right]^{\alpha}+\left[\frac{M_{z,Ed}}{M_{pl,z,Rd}}\right]^{\beta}\le 1.0 \qquad (3.19)$$

where: α and β are parameters that are dependent of the cross section's shape and $M_{pl,y,Rd}$ and $M_{pl,z,Rd}$ are the plastic moments of resistance about *y* and *z*, respectively. Parameters α and β can conservatively take the value 1.0; in alternative, they can take the values defined in clause 6.2.9(6), that is, $\alpha = 2$ and $\beta = 1$ for I or H sections, $\alpha = \beta = 2$ for circular hollow sections and $\alpha = \beta = 1.66$ for rectangular hollow sections.

Class 3 or 4 sections $$\sigma_{x,Ed}\le\frac{f_y}{\gamma_{M0}}, \qquad (3.20)$$

where $\sigma_{x,Ed}$ is the design value of the longitudinal stress evaluated by elastic theory, based on the gross cross section, for class 3 sections, and on a reduced effective cross section, for class 4 sections. The holes for bolts or other connection elements must be considered according to the next sub-section.

3.3.2.4. Net area in bending

Holes in the tension flange for bolts or other connection members may be ignored if condition $A_{f,net}\ 0.9\ f_u / \gamma_{M2} \ge A_f\ f_y / \gamma_{M0}$ is satisfied, where $A_{f,net}$ and A_f are the net section and the gross area of the tension flange, respectively, and γ_{M2} is a partial safety factor (defined according to EC3-1-8). A similar procedure must be considered for holes in the tensioned part of a web, as described in clause 6.2.5(5). The holes in the compressed parts of a section may be ignored, except if they are slotted or oversize, provided that they are filled by fasteners (bolts, rivets, etc...).

3.3.3. Design for shear

According to clause 6.2.6, the design value of the shear force, V_{Ed}, must satisfy the following condition:

$$\frac{V_{Ed}}{V_{c,Rd}} \leq 1.0\,, \tag{3.21}$$

where $V_{c,Rd}$ is the design shear resistance.

Considering plastic design, in the absence of torsion the design shear resistance, $V_{c,Rd}$, is given by the design plastic shear resistance, $V_{pl,Rd}$, given by the following equation:

$$V_{pl,Rd} = A_v \left(f_y \Big/ \sqrt{3} \right) \Big/ \gamma_{M0}\,, \tag{3.22}$$

where A_v is the shear area, defined in a qualitative manner for an I section subjected to shear in Figure 3.20. The shear area corresponds approximately to the area of the parts of the cross section that are parallel to the direction of the shear force. Clause 6.2.6(3) provides expressions for the calculation of the shear area for standard steel sections; additionally, the shear area is specified in the tables of commercial profiles.

Considering elastic design, the verification of resistance to shear force is given by the following criterion:

$$\frac{\tau_{Ed}}{f_y \Big/ \left(\sqrt{3} \gamma_{M0} \right)} \leq 1.0\,, \tag{3.23}$$

where:

- τ_{Ed} is the design value of the local shear stress at a given point, obtained from: $\tau_{Ed} = V_{Ed} S \big/ I\, t$;
- V_{Ed} is the design value of the shear force;
- S is the first moment of area about the centroidal axis of that portion of the cross section between the point at which the shear is required and the boundary of the cross section;
- I is the second moment of area about the neutral axis;
- t is the thickness of the section at the given point.

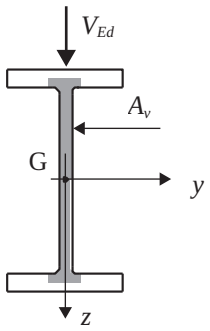


Figure 3.20 – Shear area for a I cross section

For some I or H sections, the shear stress in the web τ_{Ed} can be calculated more simply from clause 6.2.6(5).

The shear buckling resistance of webs should be verified, for unstiffened webs when (h_w / t_w) > 72 ε/η, where h_w and t_w represent the depth and the thickness of the web, respectively, η is a factor defined in EC3-1-5, which may be conservatively taken as 1.0, and ε is given by the relation $\sqrt{\left(235/f_y\right)}$.

Fastener holes need not be allowed for in the shear verification except in verifying the design shear resistance at connection zones as given in EC3-1-8 (clause 6.2.6(7)).

3.3.4. Design for combined shear and bending

In an elastic stress analysis, the interaction between bending and shear force may be verified by applying a yield criterion. This procedure, valid for any type of cross section, requires calculation of elastic normal stresses (σ) and elastic shear stresses (τ), based on formulas from the theory of the elasticity, at the critical points of the cross section. The following condition (from von Mises criterion for a state of plane stress) has then to be verified:

$$\sigma_{von-Mises} = \sqrt{\sigma^2 + 3\tau^2} \le \frac{f_y}{\gamma_{M0}}. \qquad (3.24)$$

For plastic analysis, there are several models for combining shear and bending. The model used by EC3-1-1 evaluates a reduced bending moment obtained from a reduced yield strength (f_{yr}) along the shear area. Figure 3.21

illustrates the model for bending moment–shear force interaction for a I or H section of equal flanges, considering bending about the *y*-axis); Figure 3.22 illustrates graphically the interaction curves for the same combination of forces and for the same cross section.

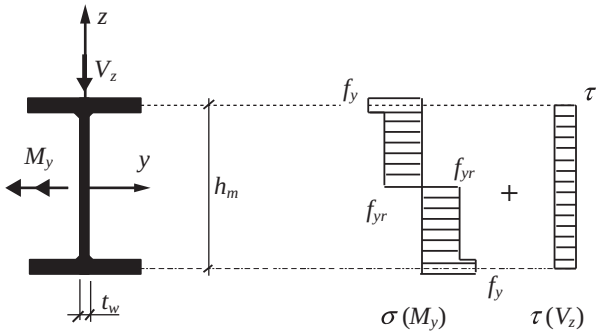


Figure 3.21 – Model for bending moment - shear force interaction in a I or H section

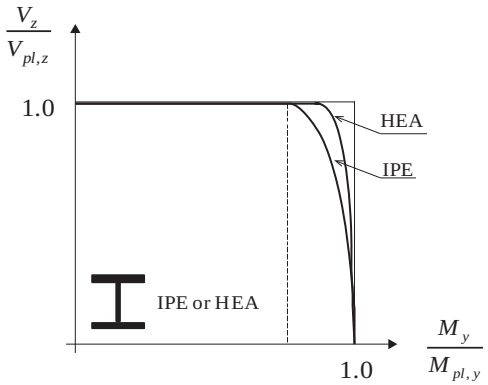


Figure 3.22 – Bending moment – shear force interaction diagrams for I or H sections

In general, when a section is subjected to bending moment and shear force, the design plastic bending resistance should be reduced to allow for the presence of the shear force. However, for low values of shear force, this reduction is not very significant, (as seen from the interaction curves represented in Figure 3.22). Also, as this reduction is counterbalanced by strain- hardening of steel, it may be assumed that for low values of shear it is not necessary to reduce the design plastic bending resistance. Thus, clause 6.2.8 establishes the following interaction criterion between bending moment and shear force:

- When V_{Ed} < 50 % of the plastic shear resistance $V_{pl,Rd}$, it is not necessary to reduce the design moment resistance $M_{c,Rd}$, except where shear buckling reduces the cross section resistance.
- When $V_{Ed} \geq 50$ % of the plastic shear resistance $V_{pl,Rd}$, the value of the design moment resistance should be evaluated using a reduced yield strength $(1-\rho)\, f_y$ for the shear area, where $\rho = (2V_{Ed} / V_{pl,Rd} - 1)^2$.

In I or H sections with equal flanges, under major axis bending, the reduced design plastic moment resistance $M_{y,V,Rd}$ may be obtained from:

$$M_{y,V,Rd} = \left(W_{pl,y} - \frac{\rho A_w^2}{4t_w} \right) \frac{f_y}{\gamma_{M0}}, \quad \text{but} \quad M_{y,V,Rd} \leq M_{y,c,Rd} \,, \tag{3.25}$$

where $A_w = h_w\, t_w$ is the area of the web (h_w is the depth of the web and t_w is the thickness) and; $M_{y,c,Rd}$ is the design resistance for bending moment about the y axis.

3.3.5. Worked examples

Example 3.4: The beam represented in Figure 3.23, with a length L = 6.0 m, is laterally restrained along its length by a floor. Assume a design load for the ultimate limit state comprising two concentrated loads P = 70.0 kN, as indicated in Figure 3.23. Design the beam using a HEA section (and alternatively an IPE section) in grade S 235 steel, according to EC3-1-1. Verify also the serviceability limit state of deformation for a characteristic combination (according to EN 1990), considering $\delta_{max} \leq L/300$ and assuming that the 70.0 kN loads were factored for the ultimate limit state with a factor of 1.50. The beam-column joints, with web cleats, may be assumed as pinned.

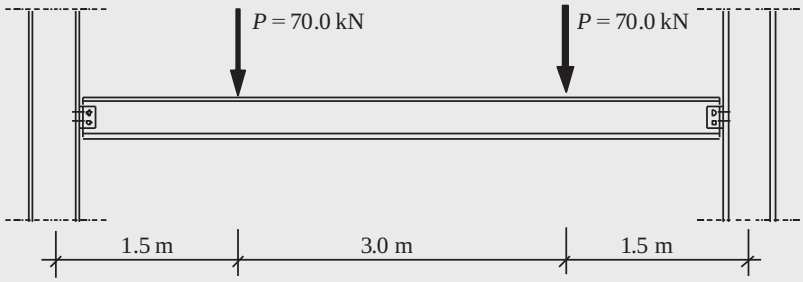


Figure 3.23 – Simply supported steel beam

i) *Diagrams of internal forces*

Figure 3.24 illustrates the bending moment and shear force diagrams corresponding to design loads for ULS (disregarding the eccentricities at the supports). The beam is laterally restrained. Therefore its design depends on the verification of the resistance of the cross sections and the verification of the serviceability limit state of deformation. From Figure 3.24, the critical cross sections are those where the concentrated loads are applied. Hence, the design values are M_{Ed} = 105.0 kNm and V_{Ed} = 70.0 kN.

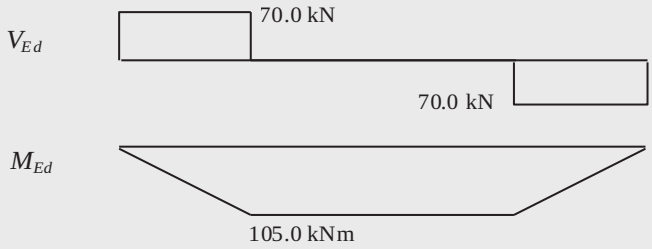


Figure 3.24 – Diagrams of internal forces

ii) *Preliminary design for bending*

Assuming class 1 or 2 cross sections, the following solution is obtained:

$$M_{Ed} = 105.0\ \text{kNm} \le W_{pl,y} \times 235 \times 10^3 / 1.0 \Rightarrow W_{pl,y} \ge 446.8 \times 10^{-6}\ \text{m}^3 = 446.8\ \text{cm}^3.$$

In order to satisfy this condition, a HEA 220 section ($W_{pl,y}$ = 568.5 cm^3) and, alternatively, a IPE 270 section ($W_{pl,y}$ = 484 cm^3) are selected.

iii) *Cross section classification* (*Tables 2.21 and 2.22*)

For the HEA 220:

Web in bending $\quad \dfrac{c}{t} = \dfrac{152}{7} = 21.7 < 72\varepsilon = 72 \times 1 = 72.0.$

Flange in compression $\quad \dfrac{c}{t} = \dfrac{220/2 - 7/2 - 18}{11} = 8.0 < 9\varepsilon = 9 \times 1 = 9.0.$

Hence, as previously assumed, the HEA 220 cross section in bending is class 1 (the IPE 270 cross section is also class 1).

iv) *Verification of shear force*

The shear area of the HEA 220 section is given by A_v = 20.67 cm^2, hence:

$$V_{Ed} = 70.0 \text{ kN} < V_{c,Rd} = V_{pl,Rd} = \frac{20.67 \times 10^{-4} \times 235 \times 10^3 / \sqrt{3}}{1.0} = 280.4 \text{ kN}.$$

As $h_w / t_w = 26.9 < 72\varepsilon/\eta = 72 \times 1.0/1.0 = 72.0$ (conservatively taking η = 1.0), it is not necessary to verify the shear buckling resistance of the web. Therefore the HEA 220 cross section meets the requirements concerning shear force. The alternative solution, constituted by a IPE 270 section, with $V_{c,Rd} = V_{pl,Rd}$ = 300.4 kN, also satisfies the same condition.

v) *Bending – shear force interaction*

As $V_{Ed} = 70.0 \text{ kN} < 50\ \% V_{pl,Rd} = 140.2 \text{ kN}$, it is not necessary to reduce the bending resistance to account for the shear force. The alternative solution, constituted by an IPE 270 section, also satisfies this condition.

vi) *Verification of the serviceability limit state of deformation*

The verification of the maximum vertical deflection is performed for the following load: 70/1.50 = 46.7 kN (as the 70 kN load was factored for the ultimate limit state with a coefficient of 1.50). For a simply supported beam with length L subjected to two concentrated loads, as indicated in Figure 3.23, the maximum vertical deflection, at mid-span, is given by $\delta_{\max} = 11PL^3 / (384EI)$, where EI is the bending stiffness of the cross section. For the HEA 220 cross section, the vertical deflection is $\delta_{\max} = 25.4 \text{ mm} > L/300 = 20 \text{ mm}$, therefore the cross section is not acceptable. By adopting a HEA 240 cross section, then

$$\delta_{\max} = \frac{11 \times 46.7 \times 6^3}{384 \times 210 \times 10^6 \times 7763 \times 10^{-8}} = 1.77 \times 10^{-2} \text{m} = 17.7 \text{ mm} < \frac{L}{300} = 20 \text{ mm}.$$

For the alternative solution, constituted by an IPE 270 cross section, a value of δ_{max} = 23.8 mm is obtained, which is also not acceptable. Thus, assuming an IPE 300 cross section, then $\delta_{\max} = 16.5 \text{ mm} < L/300 = 20 \text{ mm}$. Therefore

a HEA 240 cross section (A = 76.84 cm^2) or, alternatively, an IPE 300 cross section (A = 53.81 cm^2), is suitable for this application. It is noted that the limitation of deflection might be overcome by applying suitable precamber, as long as part of the applied loads are permanent.

Example 3.5: The continuous beam represented in Figure 3.25 is laterally restrained along its length by a composite floor. It is assumed that this restraint is sufficient to prevent lateral-torsional buckling in both positive and negative moment regions.

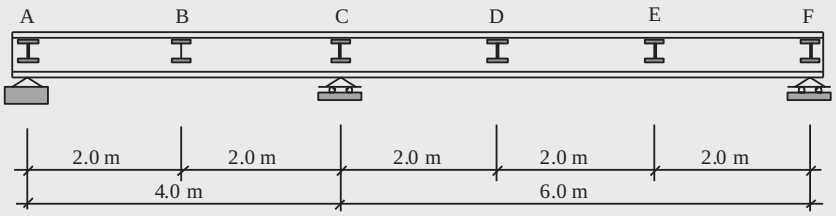


Figure 3.25 – Continuous beam

The beam is subjected to the following loads that include an estimate of the self-weight of the beams:

Dead loads: Uniformly distributed = 70 kN/m (γ_G = 1.35);
Concentrated in section B = 260 kN (γ_G = 1.35).
Live loads: Uniformly distributed = 60 kN/m (γ_Q = 1.50).

These loads are applied in a floor supported by secondary beams, shown in section in Figure 3.25. Therefore, the loads are transmitted to the continuous main beam as point loads, applied at the support sections of the secondary beams. Design the main beam assuming a HEA cross section, in grade S 275 steel, in accordance with table 3.1 of EC3-1-1.

For the design of the beam consider an elastic analysis and a redistribution of the negative moments with a maximum value of 15 %, as indicated in clause 5.4.1(4)B.

---

i) *Diagrams of internal forces* **–** Assuming that the live load may be applied in one span or in both spans simultaneously, and that the bending moment is the

critical load effect, three load combinations are defined for the verification of the ultimate limit state of resistance, as indicated in Figures 3.26 to 3.28.

Load combination 1 – Maximum negative moment at the intermediate support.

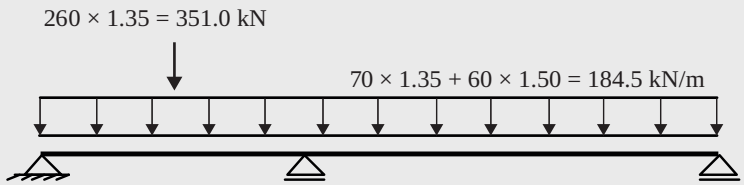


Figure 3.26 – Load combination 1

Load combination 2 – Maximum positive moment in the first span.

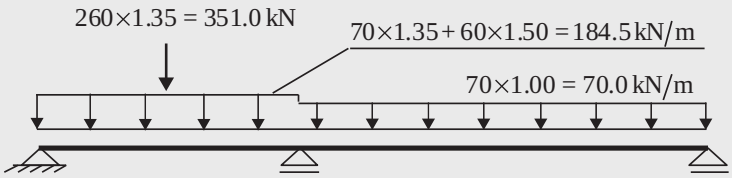


Figure 3.27 – Load combination 2

Load combination 3 – Maximum positive moment in the second span.

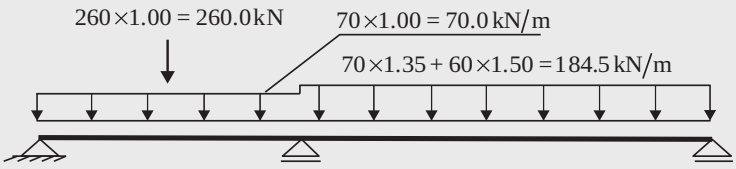


Figure 3.28 – Load combination 3

Considering the reactions of the secondary beams on the main beam and by performing an elastic analysis it is observed that the most unfavourable combination, regarding the maximum bending moment, is load combination 1. The arrangements for load combination 1 and the corresponding internal forces are indicated in Figure 3.29.

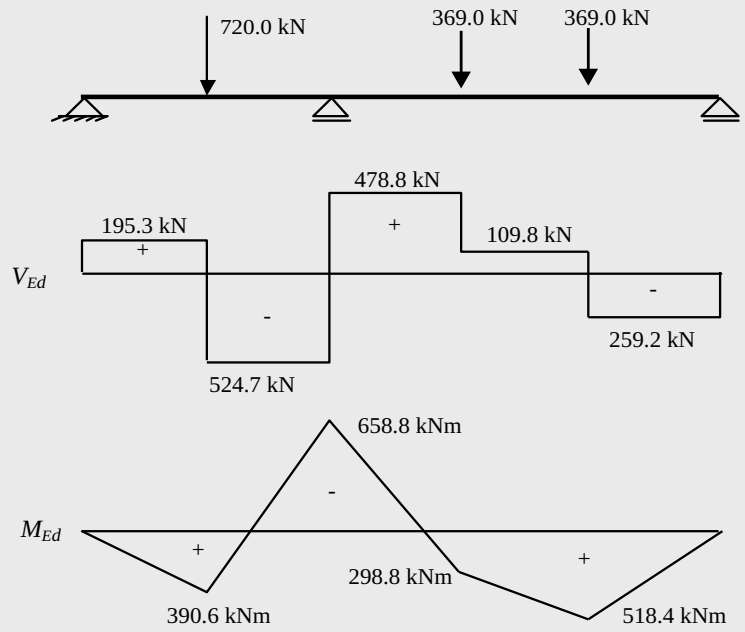


Figure 3.29 – Diagrams of elastic internal forces for load combination 1

The redistribution of the negative bending moment, at the intermediate support, is based on the elastic bending moment diagram. Hence, in order to optimize the bending moments a maximum redistribution of 15 % is allowed, according to clause 5.4.1(4)B. The redistribution of internal forces corresponds to an additional system of internal forces, self-equilibrated, which is represented in Figure 3.30.

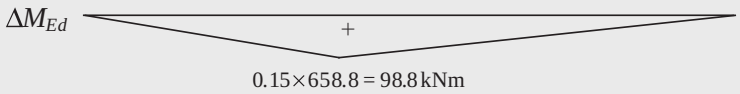


Figure 3.30 – Redistribution of bending moments

The resulting design internal force diagrams are represented in Figure 3.31. By inspection, it is observed that the maximum values of the bending moment and the shear force occur in Section C (intermediate support). The design values are thus: M_{Ed} = 560.0 kNm and V_{Ed} = 500.0 kN.

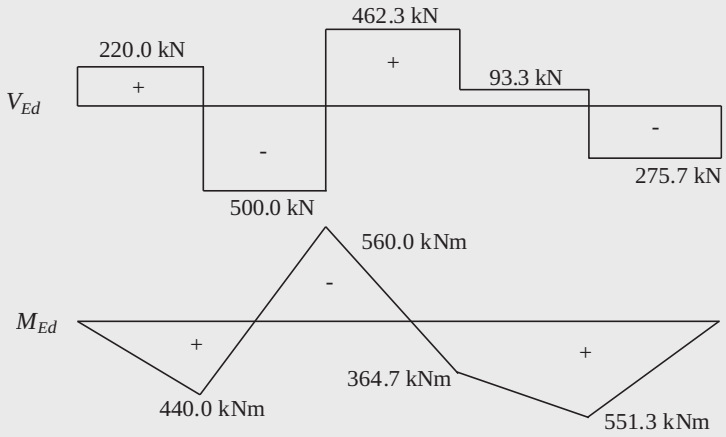


Figure 3.31 – Design internal forces after redistribution

ii) *Preliminary design for bending*

Assuming that the cross section is class 1 or 2, then:

$$M_{Ed} = 560.0\ \text{kNm} \le W_{pl,y} \times 275 \times 10^3 \big/ 1.0$$

$$\Rightarrow W_{pl,y} \ge 2036.4 \times 10^{-6}\,\text{m}^3 = 2036.4\,\text{cm}^3 .$$

152

Using a table of commercial profiles, a HEA 360, with $W_{pl,y}$ = 2088 cm^3 and shear area A_{vz} = 48.96 cm^2, is selected.

iii) *Verification of the cross section class* (*Tables 2.21 and 2.22*)

Web in bending

$$c/t = 261/10 = 26.1 < 72\varepsilon = 72 \times 0.92 = 66.2. \qquad \text{(Class 1)}$$

Flange in compression

$$\frac{c}{t} = \frac{300/2 - 10/2 - 27}{17.5} = 6.7 < 9\varepsilon = 9 \times 0.92 = 8.3. \qquad \text{(Class 1)}$$

Thus, the cross section is class 1 and the initial assumption in the preliminary design is correct.

iv) *Verification of the shear force*

The shear area of the HEA 360 cross section is A_v = 48.96 cm^2, hence:

$$V_{Ed} = 500.0 \text{ kN} < V_{c,Rd} = V_{pl,Rd} = \frac{A_v f_y}{\gamma_{M0}\sqrt{3}} =$$

$$= \frac{48.96 \times 10^{-4} \times 275 \times 10^3}{1.0 \times \sqrt{3}} = 777.3 \text{ kN}.$$

Shear buckling (for unstiffened webs) needs not be considered (clause 6.2.6(6)) provided that (conservatively assuming η=1.0):

$$\frac{h_w}{t_w} = \frac{315}{10} = 31.5 < 72\frac{\varepsilon}{\eta} = 72 \times \frac{0.92}{1.0} = 66.2.$$

Thus, the resistance to shear force is satisfied.

v) *Bending – shear force interaction*

The section to the left of the intermediate support (section C) is subjected to the maximum bending moment and the maximum shear force. Therefore, it is clearly the most critical cross section in terms of bending-shear force interaction. However, as

$$V_{Ed} = 500.0 \text{ kN} > 0.5 \times V_{pl,Rd} = 0.5 \times 777.3 = 388.7 \text{ kN},$$

then according to clause 6.2.8, it is necessary to reduce the bending moment resistance of the cross section. Therefore, for the HEA 360 cross section, as $\rho = \left(2V_{Ed}/V_{pl,Rd} - 1\right)^2 = \left(2 \times 500.0/777.3 - 1\right)^2 = 0.082,$ the design plastic bending resistance of the cross section is given by:

$$M_{y,V,Rd} = \left(W_{pl,y} - \frac{\rho A_w^2}{4t_w} \right) \frac{f_y}{\gamma_{M0}} =$$

$$= \left(2088 \times 10^{-6} - \frac{0.082 \times \left(315 \times 10^{-3} \times 10 \times 10^{-3}\right)^2}{4 \times 10 \times 10^{-3}} \right) \times \frac{275 \times 10^3}{1.00} =$$

$$= 568.6 \text{ kNm} \qquad \left(< M_{c,y,Rd} = W_{pl,y} f_y / \gamma_{M0} = 574.2 \text{ kNm} \right).$$

As M_{Ed} = 560.0 kNm < $M_{y,V,Rd}$ = 568.6 kNm, the bending resistance is verified.

vi) *Verification of the serviceability limit state of deformation*

By inspection of the continuous beam, the maximum vertical deflection occurs in the span of 6 m. Considering a load combination similar to load combination 3 (see Figure 3.28), but with the loads unfactored (corresponding to the characteristic combination of actions), a deflection of 14.9 mm is obtained. Considering a maximum allowable vertical deflection of L/300, then

$$\delta_{\max} = 14.9 \text{ mm} < L/300 = 6/300 = 2 \times 10^{-2} \text{ m} = 20 \text{ mm}.$$

Therefore, a HEA 360 in grade S 275 steel is suitable for this application.

It is noted that if EN 10025-2 (CEN, 2004c) is used, this cross section no longer satisfie the design.

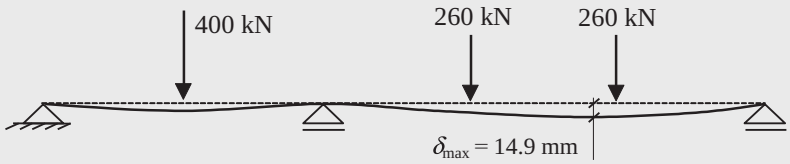


Figure 3.32 – Deformation of the beam for the characteristic combination of actions

Example 3.6: The beam represented in Figure 3.33 is subjected to a vertical concentrated load of 20.0 kN and a horizontal concentrated load of 6.0 kN, both already factored. Both loads are applied at the free end of the cantilever. Assuming that the deformation is not critical, design the cantilever beam using a rectangular hollow section in grade S 275 steel, considering:

a) plastic design;
b) elastic design.

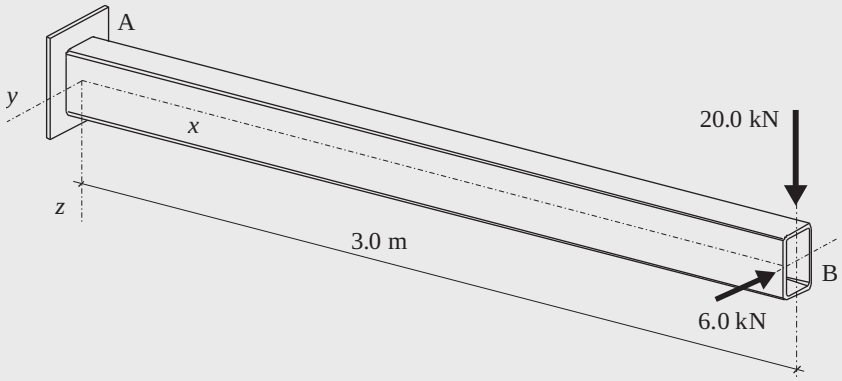


Figure 3.33 – Cantilever beam

As a rectangular hollow section has high resistance and bending stiffness about both axis (*y* and *z*) and high torsional stiffness, it is assumed that the beam is not susceptible to lateral-torsional buckling. Being a cantilever beam, with a considerable length, it is also assumed that resistance to shear force is not critical. As deformations are also not critical in this example, the design of the beam is based only on resistance to bi-axial bending of the most critical cross section (section A at the support). The design bending moments are $M_{y,Ed}$ = 60.0 kNm and $M_{z,Ed}$ = 18.0 kNm.

a) As the design is based on the plastic bending resistance, the section should be class 1 or 2. Because the cross section is subject to bi-axial bending, a preliminary design for bending about each axis separately is performed first:

$$M_{y,Ed} = 60\ \text{kNm} \le M_{c,Rd} = \frac{W_{pl,y} f_y}{\gamma_{M0}} = \frac{W_{pl,y} \times 275 \times 10^3}{1.00}$$

$$\Rightarrow W_{pl,y} \ge 218.2 \times 10^{-6}\ \text{m}^3 = 218.2\ \text{cm}^3.$$

$$M_{z,Ed} = 18\ \text{kNm} \le M_{c,Rd} = \frac{W_{pl,z} f_y}{\gamma_{M0}} = \frac{W_{pl,z} \times 275 \times 10^3}{1.00}$$

$$\Rightarrow W_{pl,z} \ge 65.5 \times 10^{-6}\ \text{m}^3 = 65.5\ \text{cm}^3.$$

Based on these results and bearing in mind that both bending moments $M_{y,Ed}$ and $M_{z,Ed}$ act simultaneously, a RHS 200×100×8 mm is proposed with $W_{pl,y}$ = 286.0 cm^3, $W_{pl,z}$ = 174.0 cm^3 and A = 45.10 cm^2.

For this cross section, the plastic verification of the bi-axial bending resistance is given by clause 6.2.9.1(6). With

$$M_{pl,y,Rd} = W_{pl,y} f_y / \gamma_{M0} = 286.0 \times 10^{-6} \times 275 \times 10^3 / 1.00 = 78.7 \text{ kNm},$$

$$M_{pl,z,Rd} = W_{pl,z} f_y / \gamma_{M0} = 174.0 \times 10^{-6} \times 275 \times 10^3 / 1.00 = 47.9 \text{ kNm},$$

and $\alpha = \beta = 1.66$ (rectangular hollow section), the following condition must be satisfied:

$$\left[\frac{M_{y,Ed}}{M_{pl,y,Rd}}\right]^{\alpha} + \left[\frac{M_{z,Ed}}{M_{pl,z,Rd}}\right]^{\beta} \le 1.0 \Leftrightarrow \left[\frac{60}{78.7}\right]^{1.66} + \left[\frac{18}{47.9}\right]^{1.66} = 0.83 < 1.0.$$

The classification of the section in bi-axial bending can be done considering the most unfavourable situation, where the longest side is totally compressed:

$$\frac{c}{t} \approx \frac{200 - 3 \times 8}{8} = 22 < 33\varepsilon = 33 \times 0.92 = 30.36. \qquad \text{(Class 1)}$$

The cross section is class 1, therefore the design can be made considering the plastic resistance and a RHS 200×100×8 mm cross section is acceptable.

b) An elastic design is based on the elastic bending resistance, therefore the cross section need not be higher than class 3. If the cross section is class 4, the resistance should be obtained from a reduced effective cross section. As the section is under bi-axial bending, a preliminary design about each axis separately is performed first:

$$M_{y,Ed} = 60 \text{ kNm} \le M_{c,Rd} = \frac{W_{el,y} f_y}{\gamma_{M0}} = \frac{W_{el,y} \times 275 \times 10^3}{1.00}$$
$$\Rightarrow W_{el,y} \ge 218.2 \times 10^{-6} \text{m}^3 = 218.2 \text{ cm}^3.$$

$$M_{z,Ed} = 18 \text{ kNm} \le M_{c,Rd} = \frac{W_{el,z} f_y}{\gamma_{M0}} = \frac{W_{el,z} \times 275 \times 10^3}{1.00}$$
$$\Rightarrow W_{el,z} \ge 65.5 \times 10^{-6} \text{m}^3 = 65.5 \text{ cm}^3.$$

Based on the previous conditions and as $M_{y,Ed}$ and $M_{z,Ed}$ act simultaneously, a RHS 250×150×6.3 mm is adopted with $W_{el,y}$ = 334.0 cm^3, $W_{el,z}$ = 252.0 cm^3 and A = 48.60 cm^2.

The elastic resistance to bi-axial bending, according to clause 6.2.9.2, requires the verification of the following condition:

$$\sigma_{x,Ed} \le \frac{f_y}{\gamma_{M0}} = \frac{275\times10^3}{1.00} = 275\times10^3 \text{ kPa} = 275 \text{ MPa}.$$

where $\sigma_{x,Ed}$ is the design value of the local longitudinal stress, given by:

$$\sigma_{x,Ed} = \frac{M_{y,Ed}}{W_{el,y}} + \frac{M_{z,Ed}}{W_{el,z}}$$

$$= \frac{60}{334.0\times10^{-6}} + \frac{18}{252.0\times10^{-6}} = 251.1\times10^3 \text{ kPa} = 251.1 \text{ MPa}.$$

As $\sigma_{x,Ed}$ = 251.1 MPa < 275 MPa, the safety of the cross section is verified.

The classification of the cross section is made under a conservative assumption, which considers that the longest side is totally under uniform compression (as would happen in plane bending around *z*), hence:

$$\frac{c}{t} \approx \frac{250-3\times6.3}{6.3} = 36.7 < 42\varepsilon = 42\times0.92 = 38.64.$$

Thus, cross section RHS 250×150×6.3 mm is class not higher than 3, and elastic design is appropriate for this application.

3.4. TORSION

3.4.1. Theoretical background

3.4.1.1. Introduction

Torsion results from lateral forces that do not pass through the shear centre of the cross section. Although torsion is not a predominant internal force in steel structures (compared to bending moment, shear or axial force), the analysis and design of steel members under torsion is covered by EC3-1-1. On the other hand, some of the instability phenomena that may occur in steel members (particularly lateral-torsional buckling of beams) depend on the behaviour in torsion. Consequently, the general concepts of the behaviour of steel members subjected to torsion are presented, including the main formulations for the calculation of stresses and deformations.

Generally, when a member is subjected to a torsional moment *T*, the cross sections rotate around the longitudinal axis of the member (axis that is defined by the shear centre of the cross sections) and warp, that is, they undergo differential longitudinal displacements, and plane sections no longer remain plane. If warping is free, which happens when the supports do not prevent longitudinal displacements and the torsional moment is constant, the member is said to be under uniform torsion or St. Venant torsion. Conversely, if the torsional moment is variable or warping is restrained at any cross section (usually at the supports), the member is under *non-uniform torsion* (Kollbrunner and Basler, 1969; Hirt *et al*, 2006).

Uniform torsion induces distortion that is caused by the rotation of the cross sections around the longitudinal axis. As a consequence, shear stresses appear which balance the applied torsional moment *T*; under these circumstances, the resistance to the torsional moment *T* exclusively results from St. Venant's torsion, T_t. Although longitudinal warping displacements may exist, they may occur unrestrained and do not introduce stresses.

In non-uniform torsion, besides the St. Venant shear stresses, longitudinal strains also exist (because warping varies along the member). These longitudinal strains generate self-equilibrating normal stresses at the cross sectional level that, depending on the level of restriction to warping, vary along the member. The existence of varying normal stresses implies (by equilibrium in the longitudinal direction) the existence of additional shear stresses that also resist to torsional moments, leading to:

$$T = T_t + T_w \tag{3.26}$$

The applied torsional moment *T* is thus balanced by two moments, one due to the torsional rotation of the cross section (T_t) and the other caused by the restraint to warping, designated by warping torsion (T_w).

In cross sections of circular shape, because they exhibit rotational symmetry with respect to the shear centre C (that coincides with the centroid G), only uniform torsion exists (Figure 3.34).

In thin-walled closed cross sections (the most appropriate type of cross section to resist torsion), uniform torsion is predominant. Therefore, in the analysis of thin-walled closed cross sections subjected to torsion, the warping torsion (T_w) is normally neglected.

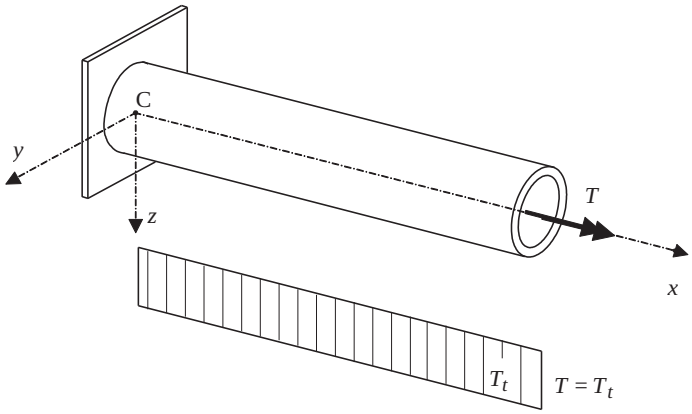


Figure 3.34 – Member under uniform torsion

In members with thin-walled open cross sections (such as I or H sections), so that only the uniform torsion component appears, it is necessary that the supports do not prevent warping and that the torsional moment is constant. On the contrary, if the torsional moment is variable or warping is restrained at some cross sections (usual situation), the member is under non-uniform torsion (Figure 3.35).

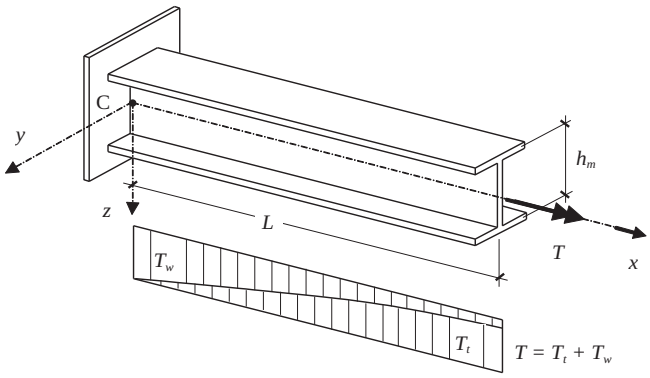


Figure 3.35 – Member with I section under non-uniform torsion

3.4.1.2. Uniform torsion

For a member under uniform torsion, the change of the angle of rotation per unit length $\left(d\varphi/dx\right)$ is related to the torsional moment through the following equation:

$$\frac{d\varphi}{dx} = \frac{T_t}{G\, I_T}, \tag{3.27}$$

where:

G is the shear modulus;
I_T is the torsion constant;
GI_T is the torsional stiffness;
x is the coordinate in the direction of the longitudinal axis of the member.

The shear stresses due to uniform torsion are obtained according to different methodologies (some are exact and others approximate), depending on the shape of the cross section. For cross sections with circular shape, the shear stresses vary linearly with the distance to the shear centre. In thin-walled closed cross sections (such as square or rectangular hollow sections), Bredt's theory is used, the shear stresses (τ) varying along the cross section such that the shear flow ($q = \tau t$) is constant. In thin-walled open cross sections (sections composed by rectangles with $h_i / t_i > 10$, where h_i and t_i are the height and the thickness of the rectangles that constitute the section) approximate expressions are used for the evaluation of the maximum stress.

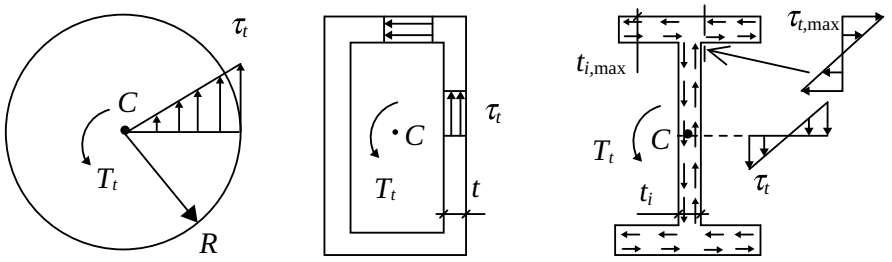
Table 3.2 indicates the equations for the calculation of the shear stresses τ_t due to uniform torsion and for the calculation of the torsion constant I_T for typical steel cross section shapes. Figure 3.36 illustrates the corresponding distributions of shear stresses.

Table 3.2 – Shear stresses and torsion constant for typical steel cross section shapes

Section	Shear stress	Torsion constant
Circular (solid or hollow)	$\tau_t = \frac{T}{I_p} r$	$I_T = I_p$
Thin-walled closed	$\tau_t = \frac{T}{2\, A_m t}$	$I_T = \frac{4A_m^2}{\oint \frac{ds}{t}}$
Thin-walled open	$\tau_{t,\max} \approx \frac{T}{I_T} t_{i,\max}$	$I_T \approx \frac{1}{3}\sum_{i=1}^{n} h_i\, t_i^3$

The nomenclature used in the Table 3.2 has the following meaning:

- I_p is the polar moment of inertia, given by $\pi R^4/2$ in the case of a circular solid section and by $\pi\left(R_e^4 - R_i^4\right)/2$ in the case of a circular hollow section;
- R is the radius of the circular solid section and R_e and R_i are the external and internal radius of the circular hollow section, respectively;
- r is the distance to the shear centre in a circular shaped cross section;
- A_m is the area defined by the middle line in a thin-walled closed cross section;
- t is the thickness at a point on a thin-walled closed section;
- s is a coordinate that is defined along the middle line of a thin-walled closed section;
- t_i and h_i represent the thickness and the height of the i^{th} rectangle, which composes a thin-walled open cross section; h_i may be measured between the middle lines of the adjacent rectangles.



a) Solid circular section b) Rectangular hollow section c) I section

Figure 3.36 – Shear stresses due to uniform torsion for typical steel cross section shapes

3.4.1.3. Non-uniform torsion

Consider again the I section cantilever beam, fixed at one end and free at the other, subjected to a torsional moment T, constant along its length, illustrated in Figure 3.35. As the fixed end cannot warp, the cross sections along the member undergo different longitudinal deformations, generating the torsional component which results from the restriction to warping, the warping torsion T_w. Because cross sections also rotate around the

longitudinal axis (especially next to the free end), there is also uniform torsion. Thus, in this case, the resistance to torsion is given by the sum of both effects ($T = T_t + T_w$), the warping torsion component, T_w, being significantly larger than the uniform torsion component, T_t, in sections near the built-in end. Close to the free end the opposite occurs (see diagram of torsional moments illustrated in Figure 3.35).

In short, a generic section at a distance x from the support is subjected to the following deformations:

- $\varphi(x)$ rotations around the longitudinal axis of the member, due to uniform torsion T_t;
- transverse displacements of the upper flange ($v_{top}(x)$) and lower flange ($v_{bot}(x)$) due to bending in its own plane (around z), due to the additional component T_w, as it is illustrated in Figure 3.37.

In the cross section of a member under non-uniform torsion, shear stresses τ_t also appear due to $\varphi(x)$ rotations, which are obtained according to the uniform torsion theory. Because of the lateral bending of the flanges, normal stresses σ_w appear and additional shear stresses τ_w, as it is illustrated in Figure 3.38. The normal stresses σ_w are calculated from the pair of moments M_{top} or M_{bot}, based on the so-called bimoment $B = M_{top}\, h_m$ ($= M_{bot}\, h_m$). Shear stresses τ_w, which develop in the flanges, are due to the pair of shear forces V_{top} and V_{bot}, statically equivalent to the warping torsion, T_w, as $T_w = V_{top}\, h_m$ ($= V_{bot}\, h_m$).

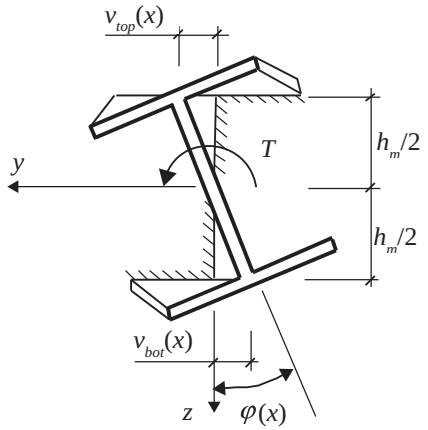


Figure 3.37 – Deformation in an I section under non-uniform torsion

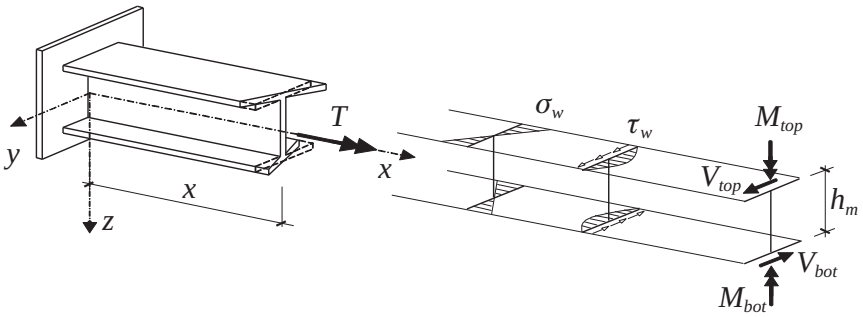


Figure 3.38 – Stresses due to warping torsion T_w

To derive the differential equation of a member subject to torsion, consider again the cantilever beam illustrated in Figure 3.35. For a generic section at a distance x from the built-in end and the deformed configurations illustrated in Figure 3.37, the following relations can be established:

$$\frac{d^2 v_{top}(x)}{dx^2} = -\frac{M_{top}}{E\,I_{fz}}; \tag{3.28}$$

$$v_{top}(x) = \varphi(x)\frac{h_m}{2}; \tag{3.29}$$

$$V_{top} = \frac{dM_{top}}{dx} = -\frac{d^3 v_{top}(x)}{dx^3} E\,I_{fz}, \tag{3.30}$$

where I_{fz} is the second moment of the flange area with respect to the z axis.

As this is a member with uniform cross section, equations (3.28) to (3.30) lead to:

$$M_{top} = -\frac{d^2\varphi(x)}{dx^2} E\,I_{fz}\frac{h_m}{2}; \tag{3.31}$$

$$V_{top} = -\frac{d^3 v_{top}(x)}{dx^3} E\,I_{fz} = -\frac{d^3\varphi(x)}{dx^3} E\,I_{fz}\frac{h_m}{2}. \tag{3.32}$$

The warping torsion, T_w, given by the couple of forces V_{top} and V_{bot}, which are h_m distance apart, is given by the following equation:

$$T_w = V_{top} h_m = -\frac{d^3\varphi(x)}{dx^3} E\, I_{fz} \frac{h_m^2}{2} = -E\, I_w \frac{d^3\varphi(x)}{dx^3}, \tag{3.33}$$

where:

$I_w = I_{fz}\left(h_m^2/2\right)$ is the warping constant and EI_w is the warping rigidity of the section.

Neglecting the second moment of the web area in relation to z axis (which implies $I_{fz} \approx I_z/2$), the warping constant of a I or H section of equal flanges can be obtained through the simplified equation $I_w = I_z h_m^2/4$. The warping constant of a I or H section of unequal flanges can be obtained from the following general equation:

$$I_w = \beta_f\left(1-\beta_f\right) I_z\, h_m^2, \tag{3.34}$$

where $\beta_f = I_{fc}\big/\left(I_{fc}+I_{ft}\right)$, I_{fc} and I_{ft} are the second moments of area in relation to the minor axis z of the compression and tension flanges, respectively, and h_m is the distance between the shear centres of the flanges. For the calculation of the warping constant of a generic section the reader is referred to Trahair (1993) or Hirt *et al* (2006); for usual cross sections the expressions indicated in Annex A.1 may be used.

Combining equations (3.27) and (3.33) yields the differential equation of non-uniform torsion:

$$T = T_t(x) + T_w(x) = G\, I_T \frac{d\varphi(x)}{dx} - E\, I_w \frac{d^3\varphi(x)}{dx^3}. \tag{3.35}$$

In case of a distributed torsional moment,

$$m_T(x) = -\frac{dT}{dx}, \tag{3.36}$$

the following differential equation is obtained:

$$m_T(x) = GI_T \frac{d^2\varphi}{dx^2} - EI_W \frac{d^4\varphi}{dx^4}. \tag{3.37}$$

The general solution of the differential equations (3.35) and (3.37), based on a concentrated torsional moment T or a uniformly distributed torsional moment $m_T(x)$, the shape of the cross section and the support conditions, leads to the rotation $\varphi(x)$ at each cross section along the member, given by (Chen and Atsuta, 1977):

$$\varphi(x) = C_1 + C_2 \cosh kx + C_3 \sinh kx + \frac{T}{k^2 E I_w} x; \tag{3.38a}$$

$$\varphi(x) = C_4 + C_5 x + C_6 \cosh kx + C_7 \sinh kx - \frac{m_T(x)}{2k^2 E\, I_w} x^2, \tag{3.38b}$$

with

$$k = \sqrt{\frac{G\, I_t}{E\, I_w}}, \tag{3.39}$$

and C_1 to C_7 are constants of integration that depend on the boundary conditions. Equations (3.40) represent the most common boundary conditions for torsion:

- zero twist $\varphi = 0;$
- free twist $\frac{d^3\varphi}{dx^3} - k^2 \frac{d\varphi}{dx} = 0;$
- zero warping $\frac{d\varphi}{dx} = 0;$
- free warping $\frac{d^2\varphi}{dx^2} = 0.$

(3.40)

From equations (3.38), the components of uniform torsion T_t, torsion due to the restriction to warping T_w and bimoment B_w are obtained as follows:

$$\begin{aligned} T_t &= GI_T \frac{d\varphi}{dx} = T\left(C_2 \sinh kx + C_3 \cosh kx + 1\right); \\ T_w &= -EI_w \frac{d^3\varphi}{dx^3} = -T\left(C_2 \sinh kx + C_3 \cosh kx\right); \\ B_w &= -EI_w \frac{d^2\varphi}{dx^2} = -\frac{T}{k}\left(C_2 \cosh kx + C_3 \sinh kx\right), \end{aligned} \tag{3.41a}$$

for a concentrated torsional moment and

$$T_t = GI_T \frac{d\varphi}{dx} = km_T(x)\left(C_5 + C_6 \sinh kx + C_7 \cosh kx + kx\right);$$

$$T_w = -EI_w \frac{d^3\varphi}{dx^3} = -km_T(x)\left(C_6 \sinh kx + C_7 \cosh kx\right); \quad (3.41b)$$

$$B_w = -EI_w \frac{d^2\varphi}{dx^2} = -m_T(x)\left(C_6 \cosh kx + C_7 \sinh kx + 1\right),$$

for a distributed torsional moment.

Annex A.2 presents solutions for standard cases of beams subjected to torsion (Roark and Young, 1976).

The normal stresses σ_w and the shear stresses τ_w are given by:

$$\sigma_w(y,z) = -\frac{B_w}{I_w}\omega(y,z); \quad (3.42)$$

$$\tau_w(y,z) = \frac{T_w}{t_f I_w} S_\omega(y,z), \quad (3.43)$$

where:

$\omega(y,z)$ is the warping function and $S_\omega(y,z)$ is the static moment with respect to the warping function, given by

$$S_\omega = \int_0^S \omega(y,z)\, t\, ds. \quad (3.44)$$

Annex A.1 presents expressions for the shear centre, torsional constant, warping constant, warping function and static moment with respect to the warping function for common thin-walled cross sectional shapes.

3.4.1.4. Cross section resistance in torsion

The elastic torsional resistance of a cross section is attained when the von Mises yield criterion is met at any point of the cross section:

$$\sigma_{von-Mises} = \sqrt{\sigma^2 + 3\tau^2} \leq \frac{f_y}{\gamma_{M0}}, \tag{3.45}$$

where σ and τ are obtained from equations (3.42), (3.43) and Table 3.2.

The plastic torsional resistance of class 1 and 2 cross sections requires, in general, the combination of normal stresses due to warping torsion, σ_w, and shear stresses due to uniform torsion (T_t) and warping torsion (T_w), τ_t and τ_w.

In case of a thin-walled closed cross section subjected to a torsional moment T (Figure 3.39), only shear stresses τ_t are present, given by:

$$\tau_t = \frac{T}{2A_m t}, \tag{3.46}$$

where:

A_m is the area limited by the middle line of the cross section;

t is the thickness of the wall.

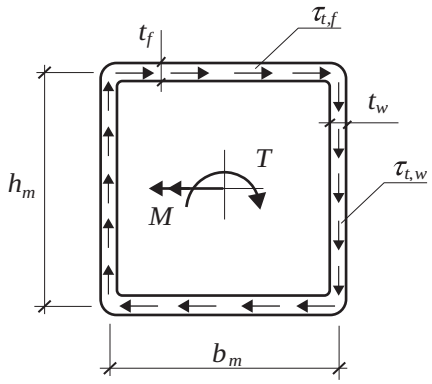


Figure 3.39 – Thin-walled closed rectangular hollow section

The torsional moment of a rectangular hollow section, obtained as the moment of the resultant of the shear stresses in relation to the shear centre of the section (in this case, it coincides with the centroid), is given by:

$$T = 2\,\tau_{t,f}\,t_f\,b_m\frac{h_m}{2} + 2\,\tau_{t,w}\,t_w\,h_m\frac{b_m}{2} = b_m\,h_m\left(\tau_{t,f}\,t_f + \tau_{t,w}\,t_w\right). \tag{3.47}$$

As $\tau_{t,f}\, t_f = \tau_{t,w}\, t_w$, the applied torsional moment T is given by:

$$T = 2\, \tau_{t,w}\, t_w\, h_m\, b_m . \tag{3.48}$$

Setting $\tau_{t,w} = f_y \big/ \sqrt{3}$, the torsional moment resistance T_{pl} is given by:

$$T_{pl} = 2\, t_w\, h_m\, b_m f_y \big/ \sqrt{3} . \tag{3.49}$$

In case of a thin-walled open cross section, both St. Venant and warping stresses are present. However, in most practical situations of a member subject to torsion (e.g. a cantilever subject to a torsional moment), at the cross section where the bimoment, B_w, is maximum, the St. Venant's torsional moment, T_t, is zero and vice-versa (see Figure 3.35). Hence, it is reasonable to quantify the plastic torsional resistance of an open cross section for these two limiting cases.

The plastic torsional moment resistance of an open cross section subject to St. Venant's stresses only is given by:

$$T_{pl} = \frac{3}{2} T_{el} = \frac{3}{2} \frac{I_T}{t_{\max}} \frac{f_y}{\sqrt{3}}. \tag{3.50}$$

Figure 3.40 illustrates the stress distribution in an open cross section that corresponds to plastic conditions. Equation (3.50) may be obtained from Nadai's sand-hill analogy (Nadai, 1950).

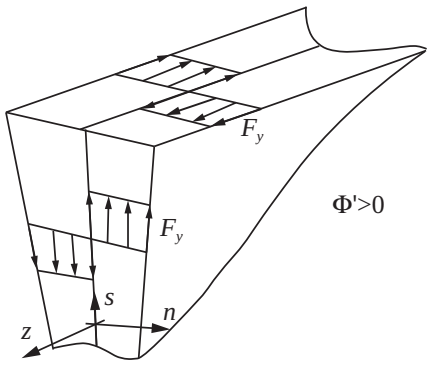


Figure 3.40 – Plastic stress distribution in thin-walled open cross section (Gjelsvik, 1981)

For a cross section subject to warping stresses only, the plastic normal stress distribution is shown in Figure 3.41 for a I-section profile.

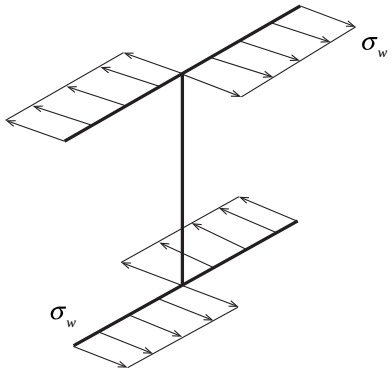


Figure 3.41 – Plastic normal warping stress distribution in I-section

The plastic bi-moment is obtained as the moment of the resultant of the normal warping stresses in relation to the shear centre of the section, leading to:

$$B_{w,pl} = \frac{1}{4} b^2 t_f \left(h - t_f\right) f_y, \tag{3.51}$$

and the plastic torsional moment resistance follows from the equations in Annex A.2. As an example, in the case of the cantilever of Figure 3.35 subject to a concentrated torsional moment, the plastic torsional moment resistance is given by:

$$T_{pl} = \frac{k}{\tanh kL} B_{w,pl}. \tag{3.52}$$

It is noted that "*a simple plastic theory can only be obtained by decoupling (…) the torsional moment T_t from the remaining active forces*" (Gjelsvik, 1981). Nevertheless, a more exact theory would require the combination of warping and St. Venant's deformations, leading to a slight reduction of the torsional plastic resistance (Gjelsvik, 1981).

For the majority of cross sectional shapes, the torsional stresses are obtained according to elastic theory. Therefore the interaction with other internal forces, such as axial force, bending moment and shear force may be performed by the application of the von Mises criterion on the critical points of the cross section, usually the web to flange junctions. A general procedure consists of the evaluation of the:

- elastic normal stresses σ due axial force N and bending moments M_y and M_z;
- normal stresses σ_w due to the warping torsion T_w in open cross sections;
- shear stresses due to shear forces V_z and V_y;
- shear stresses due to uniform torsion T_t;
- shear stresses due to warping torsion T_w,

followed by the subsequent comparison of the equivalent stress, obtained at the critical points of the cross section by the von Mises criterion (as described in clause 6.2.1(5)), with the yield stress f_y of the material.

In more compact cross sections (class 1 or 2 cross sections) a plastic interaction formula may be used; however, these formulae are quite complex, due to the large number of cross sectional shapes and combinations of internal forces. The procedures prescribed in EC3-1-1 for the interaction between torsion and other internal forces for standard cross sections are presented in the following section.

As an example, the derivation of an interaction formula between bending moment and a torsional moment in a thin-walled closed cross section with dimensions $b_m \times h_m$ is presented next (see Figure 3.39). In a thin-walled closed cross section subjected to a torsional moment T, as the warping stresses are negligible, the shear stresses $\tau_{t,w}$ are given by (equation (3.48)):

$$\tau_{t,w} = \frac{T}{2\, t_w\, h_m\, b_m} \tag{3.53}$$

so that the reduced resistant normal stresses, $\sigma_{b,w}$ and $\sigma_{b,f}$ can be obtained by the application of the von Mises criterion, along the flanges and webs of the cross section through the following equations:

$$\sigma_{b,w}^2 = f_y^2 - 3\tau_{t,w}^2; \tag{3.54}$$

$$\sigma_{b,f}^2 = f_y^2 - 3\tau_{t,f}^2 = f_y^2 - 3\left(\frac{t_w}{t_f}\right)^2 \tau_{t,w}^2 . \tag{3.55}$$

The bending moment is given by:

$$\begin{aligned} M &= \sigma_{b,f}\, t_f\, b_m\, h_m + \sigma_{b,w} \frac{1}{2} t_w\, h_m^2 = \\ &= t_f\, b_m\, h_m \left(f_y^2 - 3\left(\frac{t_w}{t_f}\right)^2 \tau_{t,w}^2 \right)^{1/2} + \frac{1}{2} t_w\, h_m^2 \left(f_y^2 - 3\,\tau_{t,w}^2 \right)^{1/2} . \end{aligned} \tag{3.56}$$

After several mathematical transformations, the following formula is obtained:

$$M = t_f\, b_m\, h_m\, f_y \left(1 - \left(\frac{t_w}{t_f}\right)^2 \left(\frac{T}{T_{pl}}\right)^2 \right)^{1/2} + \frac{1}{2} t_w\, h_m^2\, f_y \left(1 - \left(\frac{T}{T_{pl}}\right)^2 \right)^{1/2} . \tag{3.57}$$

This equation corresponds to the plastic interaction formula between bending moment M and torsional moment T, applicable to the cross sectional shape of Figure 3.39. For a rectangular hollow section with constant wall thickness, $t_w = t_f$, equation (3.57) may be rewritten as:

$$\left(\frac{M}{M_{pl}}\right)^2 + \left(\frac{T}{T_{pl}}\right)^2 = 1. \tag{3.58}$$

For open cross sections, warping normal stresses cannot be neglected and the plastic bending moment resistance must be reduced. Assuming that at every point of the cross section the normal warping stress is equal to the maximum normal warping stress $\sigma_{w,Ed,\max}$ leads to the following interaction equation (Mirambell *et al*, 2016):

$$M = \left(1 - \frac{\sigma_{w,Ed,\max}}{f_y}\right) M_{pl}. \tag{3.59}$$

This expression is over conservative, as noted by Mirambell *et al* (2016) who proposed a more accurate and realistic formulation for the determination of the plastic bending resistance of double-symmetric I-sections subject to major axis bending and warping torsion, given by:

$$M = \left(\sqrt{1 - \frac{\sigma_{w,Ed,\max}}{1.25\, f_y}}\right) M_{pl}. \tag{3.60}$$

The interaction between shear force and torsion is also required to check the resistance of a cross section. Similarly to the bending-torsion interaction, the formulae to evaluate the plastic cross section capacity under shear and torsion are also specific for each cross section shape. Considering a double symmetric I-section subject to torsional moment T_{Ed} and shear force V_{Ed}, it is noted that linear varying shear stresses $\tau_{t,Ed}$ due to St. Venant torsion (uniform torsion) and constant shear stresses $\tau_{z,Ed}$ due to the shear force are induced in the web, while the shear stresses due to warping torsion are null in the web. Following Mirambell *et al* (2016), analysing the interaction between both shear stress distributions as an analogy with the normal stress distributions induced in a rectangular cross section by axial force and bending moment leads to:

$$V_{pl,T} = \sqrt{1 - \frac{\tau_{t,Ed}}{1.25\left(f_y / \sqrt{3}\right) / \gamma_{M0}}}\, V_{pl}, \tag{3.61}$$

where the coefficient 1.25 represents an average value between plastic (1.0) and elastic (1.5) for the shear stress distribution of the St. Venant torsional shear stress across the thickness of the web.

Similar interaction expressions may be derived for channel cross sections or hollow sections.

3.4.2. Design for torsion

The design of members subjected to a torsional moment should comply with the following condition (clause 6.2.7(1)):

$$\frac{T_{Ed}}{T_{Rd}} \leq 1.0 \,, \tag{3.62}$$

where T_{Ed} is the design value of the torsional moment and T_{Rd} is the design torsional resistance of the cross section, evaluated according to the formulations presented previously.

For the verification of equation (3.62) in cross sections under non-uniform torsion, the design value of the torsional moment, T_{Ed}, should be decomposed into two components (clause 6.2.7(2)):

$$T_{Ed} = T_{t,Ed} + T_{w,Ed} \,, \tag{3.63}$$

where $T_{t,Ed}$ is the internal component of uniform torsion (or St. Venant's torsion) and $T_{w,Ed}$ is the internal component of warping torsion. The decomposition of the design value of the torsional moment T_{Ed} into the $T_{t,Ed}$ and $T_{w,Ed}$ components, described in sub-section 3.4.1.3, depends fundamentally on the support conditions, on the diagram of torsional moments and on the shape of the cross section. This decomposition may be determined from T_{Ed} by elastic analysis (clause 6.2.7(3)), by solving the differential equations (3.35) or (3.37).

In the cross section of a member under non-uniform torsion, the following stresses appear and should be taken into account (clause 6.2.7(4)):

- Shear stresses $\tau_{t,Ed}$ due to the component of uniform torsion $T_{t,Ed}$.
- Shear stresses $\tau_{w,Ed}$ due to the component of warping torsion $T_{w,Ed}$ and also normal stresses $\sigma_{w,Ed}$, due to bimoment B_{Ed}.

The resistance to torsion should be verified by combining the previous stresses (and all other stresses that result from other internal forces) using the von Mises yield criterion, according to expression (3.1), given in clause 6.2.1(5). Alternatively, for cross section classes 1 and 2, a plastic verification may be used, whereby T_{Rd} is calculated according to sub-section 3.4.1.4.

In general, for all cross sectional classes, an elastic verification of the safety of the cross sections under combined forces (e.g. bending moment, shear force, axial force and torsional moment) may be used by combining all the stresses that result from the internal forces and applying the von Mises yield criterion (expression (3.1)).

The stresses due to bimoment B_{Ed} should be taken into account in the evaluation of the plastic moment resistance of a cross section under the combination of bending moment and torsional moment (clause 6.2.7(6)). Additionally, the warping normal stresses due to bimoment B_{Ed} should be derived from elastic analysis (clause 6.2.7(6)). Equation (3.59) may be used to calculate the reduced plastic bending moment resistance for class 1 or 2 cross sections in this case.

Clause 6.2.7(7) proposes as a simplification that for closed hollow cross sections (the most appropriate type of cross sections to resist torsion), the effect of the warping torsion, $T_{w,Ed}$, can be neglected, whereas in open cross sections (like I or H sections) the effect of the component of uniform torsion, $T_{t,Ed}$, can be neglected.

For the verification of the safety of cross sections under shear force V_{Ed} and torsional moment T_{Ed}, clause 6.2.7(9) gives the following criterion:

$$\frac{V_{Ed}}{V_{pl,T,Rd}} \le 1.0\,, \tag{3.64}$$

where*:*

$V_{pl,T,Rd}$ is the reduced design plastic shear resistance, to account for the torsional moment.

For I or H sections:

$$V_{pl,T,Rd} = \sqrt{1-\frac{\tau_{t,Ed}}{1.25\left(f_y \big/ \sqrt{3}\right)\big/\gamma_{M0}}}\,V_{pl,Rd}\,, \tag{3.65}$$

for channel sections,

$$V_{pl,T,Rd} = \left[\sqrt{1-\frac{\tau_{t,Ed}}{1.25\left(f_y \big/ \sqrt{3}\right)\big/\gamma_{M0}}} - \frac{\tau_{w,Ed}}{\left(f_y \big/ \sqrt{3}\right)\big/\gamma_{M0}}\right] V_{pl,Rd}, \tag{3.66}$$

and for hollow sections,

$$V_{pl,T,Rd} = \left[1 - \frac{\tau_{t,Ed}}{\left(f_y / \sqrt{3}\right) / \gamma_{M0}}\right] V_{pl,Rd} \,. \tag{3.67}$$

In these equations, $V_{pl,Rd}$ is the design plastic shear resistance, evaluated according to clause 6.2.6.

The resistance of sections simultaneously under bending moment, shear force and torsional moment, must be evaluated in accordance with clause 6.2.8, as described in section 3.3.4, by replacing the design plastic shear resistance, $V_{pl,Rd}$, with the reduced design plastic shear resistance, $V_{pl,T,Rd}$, to account for the torsional moment. However, as the reduced yield strength $\left(1-\rho\right) f_y$ for the shear area or equation (3.25) do not account for the normal warping stresses $\sigma_{w,Ed}$, the reduced design plastic moment resistance should be taken as the design resistance of the cross section calculated using a reduced yield strength whenever $V_{Ed} \geq 50$ % of the reduced plastic shear resistance, as follows:

$$\left(1-\rho\right) f_y \frac{M_{c,B,Rd}}{M_{c,Rd}} \qquad \text{for the shear area;} \tag{3.68a}$$

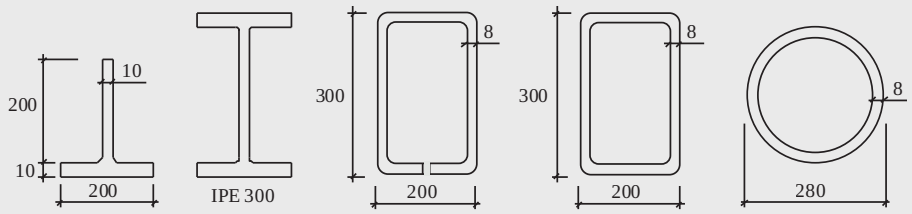
$$f_y \frac{M_{c,B,Rd}}{M_{c,Rd}} \qquad \text{for the rest of the cross section,} \tag{3.68b}$$

where $M_{c,B,Rd}$ is given by equation (3.59) and $\rho = \left(2V_{Ed} / V_{pl,T,Rd} - 1\right)^2$. Alternatively, for class 1 or 2 I or H sections with equal flanges, under major axis bending:

$$M_{y,B,V,Rd} = \left(W_{pl,y} - \frac{\rho A_w^2}{4t_w}\right) \frac{f_y}{\gamma_{M0}} \frac{M_{c,B,Rd}}{M_{c,Rd}}, \quad \text{but } M_{y,B,V,Rd} \leq M_{y,c,B,Rd}. \tag{3.69}$$

3.4.3. Worked examples

Example 3.7: Calculate the constant for uniform torsion I_T, and the warping constant I_w, of the thin-walled steel cross sections illustrated in Figure 3.42 (dimensions in mm).



i) ii) iii) iv) v)

Figure 3.42 – Thin-walled steel cross sections

i) *T Section*

As $\left(h_i/t_i\right)_{web} = \left(205/10\right) = 25.0 > 10$ and $\left(h_i/t_i\right)_{flange} = \left(200/10\right) = 20.0 > 10$, the cross section can be considered a thin-walled section. As this is an open section, the torsion constant is given by:

176

$$I_T \approx \frac{1}{3}\sum_{i=1}^{n} h_i\, t_i^3 = \frac{1}{3}\times\left(205\times10^3 + 200\times10^3\right) = 0.135\times10^6 \text{ mm}^4.$$

For a T section, according to Table A.1, the warping constant is $I_w = 0$.

ii) IPE 300 S*ection*

As

$$\left(h_i/t_i\right)_{web} = \left(\left(300-10.7\right)/7.1\right) = 40.7 > 10,$$

and

$$\left(h_i/t_i\right)_{flange} = \left(150/10.7\right) = 14.0 > 10,$$

the IPE 300 can be considered a thin-walled section. Thus, the torsion constant is given by:

$$I_T \approx \frac{1}{3}\sum_{i=1}^{n} h_i t_i^3 = \frac{1}{3}\times\left(\left(300-10.7\right)\times 7.1^3 + 2\times 150\times 10.7^3\right) =$$

$$= 0.157\times 10^6 \text{ mm}^4.$$

The warping constant (I section of equal flanges) is given by:

$$I_w = \frac{t_f\, h_m^2\, b^3}{24} = \frac{10.7\left(300-10.7\right)^2\times 150^3}{24} = 125.9\times 10^9 \text{ mm}^6,$$

or, alternatively, by the simplified equation given after equation (3.33):

$$I_w = I_z \frac{h_m^2}{4} = 603.8\times 10^4 \times \frac{\left(300-10.7\right)^2}{4} = 126.3\times 10^9 \text{ mm}^6.$$

iii) *Thin-walled rectangular open section*

The open section can be considered thin-walled because $\left(h_i/t_i\right)_{shorterleg} = \left(\left(200-8\right)/8\right) = 24.0 > 10$; as such, the torsion constant is given by:

$$I_T \approx \frac{1}{3}\sum_{i=1}^{n} h_i t_i^3 = \frac{1}{3}\times\left(2\times\left(300-8\right)\times 8^3 + 2\times\left(200-8\right)\times 8^3\right) =$$

$$= 0.165\times 10^6 \text{ mm}^4.$$

The warping constant is given by: I_w = 2386×10^9 mm^6. This value is obtained by applying a general formulation described in Nakai and Yoo (1988) and not detailed here.

iv) *Thin-walled closed rectangular section*

The torsion constant for a thin-walled closed section is given by:

$$I_T = \frac{4A_m^2}{\oint \frac{ds}{t}} = \frac{4\times\left(\left(300-8\right)\times\left(200-8\right)\right)^2}{2\times\frac{300-8}{8}+2\times\frac{200-8}{8}} = 103.9\times 10^6 \text{ mm}^4,$$

and the warping constant is $I_w \approx 0$.

v) *Circular hollow section*

For a circular hollow section, the torsion constant is given by the polar moment of inertia:

$$I_T = I_P = \frac{\pi \times \left(\left(280/2\right)^4 - \left(\left(280 - 2\times 8\right)/2\right)^4 \right)}{2} = 126.5 \times 10^6 \text{ mm}^4.$$

Alternatively, the torsion constant can also be obtained from Table 3.2:

$$I_T = \frac{4A_m^2}{\oint \frac{ds}{t}} = \frac{4 \times \left(\pi \times \left(200 - 8\right)^2 / 4 \right)^2}{\pi \times \frac{\left(200 - 8\right)}{8}} = 126.4 \times 10^6 \text{ mm}^4.$$

For a circular hollow section the warping constant is $I_w = 0$.

Example 3.8: Verify the safety of the cantilever beam A-B, illustrated in Figure 3.43, according to EC3-1-1. The beam, constituted by a rectangular hollow section (RHS 300×200×8 mm) in grade S 355 steel, is subjected to a design load of 60.0 kN, applied with an eccentricity of 0.80 m. Calculate also the rotation about the *x*-axis of the section B of beam A-B.

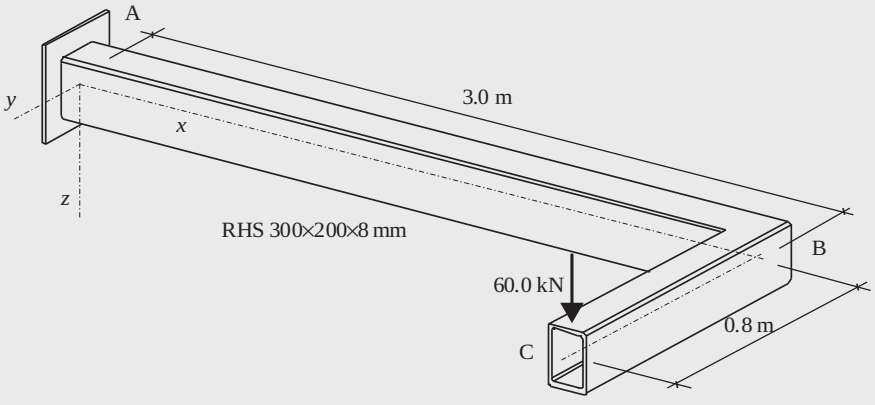


Figure 3.43 – Cantilever beam

For the given load arrangement, the beam is under bending moment, shear force and torsional moment. Despite the warping of the sections being prevented, particularly next to the clamping section, being a closed hollow section, the warping torsion, $T_{w,Ed}$, may be neglected. The applied torsional moment is then totally resisted by the component of uniform torsion or St. Venant's torsion. Because the beam is composed by a section with high torsional and lateral bending stiffness, it may be assumed that it is not susceptible to lateral-torsional buckling; thus, its resistance depends exclusively on the resistance of the cross sections. The critical cross section is section A, subjected to the following design internal forces:

$M_{y,Ed} = 60 \times 3 = 180$ kNm ,

$V_{z,Ed} = 60$ kN and $T_{Ed} = 60 \times 0.80 = 48$ kNm.

The main geometric characteristics of the RHS 300×200×8 mm cross section are:

A = 76.75 cm^2, I_y = 9717 cm^4, $W_{pl,y}$ = 779.3 cm^3, $W_{el,y}$ = 647.8 cm^3 and I_T = 10560 cm^4. The main characteristics of grade S 355 steel are: E = 210 GPa, G = 81 GPa and f_y = 355 MPa.

According to EC3-1-1, the interaction of forces can be checked by one of the following procedures: i) Elastic interaction as given by clause 6.2.7(5) or ii) Plastic interaction according to the criteria established in clauses 6.2.7 and 6.2.8.

A RHS 300×200×8 mm, in grade S 355 steel, is class 1 in bending:

$c/t \approx \left(200 - 3 \times 8\right)/8 = 22.0 < 33\varepsilon = 33 \times 0.81 = 26.7$, for the horizontal leg and $c/t \approx \left(300 - 3 \times 8\right)/8 = 34.5 < 72\varepsilon = 72 \times 0.81 = 58.3$, at the vertical leg.

i) *Elastic interaction*

According to this procedure, the elastic maximum stresses due to the three internal forces are calculated at the critical points of the cross section, and then they are combined using the von Mises yield criterion.

By inspection of the elastic stress diagrams of Figure 3.44, the critical points are the points of connection between the vertical legs and the horizontal legs.

At these points, the normal stresses due to bending and the shear stresses due to shear force and uniform torsion are given by:

$$\sigma_{x,Ed} = \frac{M_{y,Ed}}{W_{el,y}} = \frac{180}{647.8 \times 10^{-6}} = 277863.5 \text{ kPa} = 277.9 \text{ MPa};$$

$$\tau_{v,Ed} = \frac{V_{z,Ed}\, S_y}{I_y\, t} = \frac{60 \times \left(\left(200-8\right)/2 \times 8 \times \left(300-8\right)/2\right) \times 10^{-9}}{9717 \times 10^{-8} \times 8 \times 10^{-3}} =$$

$$= 8654.5 \text{ kPa} = 8.7 \text{MPa};$$

$$\tau_{t,Ed} = \frac{T_{Ed}}{2\, A_m\, t} = \frac{48}{2 \times \left(\left(300-8\right) \times \left(200-8\right)\right) \times 10^{-6} \times 8 \times 10^{-3}} =$$

$$= 53510.3 \text{ kPa} = 53.5 \text{ MPa}.$$

The shear stress at the critical points is given by:

$$\tau_{Ed} = \tau_{v,Ed} + \tau_{t,Ed} = 8.7 + 53.5 = 62.2 \text{ MPa}.$$

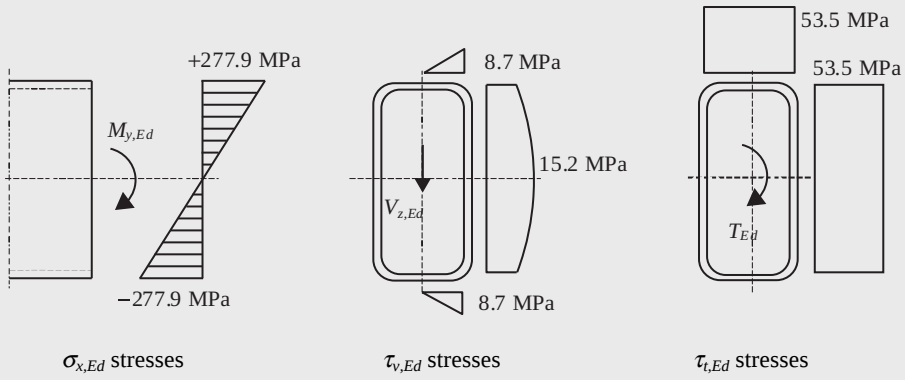


Figure 3.44 – Distributions of stresses at section A

From the von Mises yield criterion, according to clause 6.2.7(5):

$$\left(\frac{\sigma_{x,Ed}}{f_y/\gamma_{M0}}\right)^2 + 3\left(\frac{\tau_{Ed}}{f_y/\gamma_{M0}}\right)^2 = \left(\frac{277.9}{355/1.0}\right)^2 + 3 \times \left(\frac{62.2}{355/1.0}\right)^2 = 0.70 < 1.0.$$

Therefore, the RHS 300×200×8 mm, in grade S 355 steel, satisfies the condition.

ii) *Plastic interaction*

The procedure is according to clauses 6.2.7 and 6.2.8. The design plastic torsional resistance (equation (3.49)) is given by:

$$T_{Rd} = 2\,t_w\,A_m\frac{f_y}{\sqrt{3}} = 2\times 8\times 10^{-3}\times 292\times 10^{-3}\times 192\times 10^{-3}\times 355\times\frac{10^3}{\sqrt{3}} =$$

$$= 183.8\ \text{kNm} > T_{Ed} = 48\ \text{kNm}.$$

The design plastic moment resistance of the cross section, not reduced by shear, is given by:

$$M_{c,Rd} = M_{pl,Rd} = W_{pl,y}\,f_y/\gamma_{M0} = 779.3\times 10^{-6}\times 355\times 10^3/1.0 =$$

$$= 276.7\ \text{kNm} > M_{y,Ed} = 180\ \text{kNm}.$$

The shear area is given by:

$$A_{vz} = \frac{A\,h}{b+h} = \frac{76.75\times 300}{200+300} = 46.05\ \text{cm}^2.$$

The design plastic shear resistance is given by:

$$V_{pl,Rd} = \frac{A_{vz}\left(f_y/\sqrt{3}\right)}{\gamma_{M0}} = \frac{46.05\times 10^{-4}\times\left(355\times 10^3/\sqrt{3}\right)}{1.0} = 943.8\ \text{kN}.$$

The reduced plastic shear resistance of a rectangular hollow section, to account for the presence of a torsional moment, is given by:

$$V_{pl,T,Rd} = \left[1-\frac{\tau_{t,Ed}}{\left(f_y/\sqrt{3}\right)/\gamma_{M0}}\right]V_{pl,Rd} = \left[1-\frac{53.5}{\left(355/\sqrt{3}\right)/1.0}\right]\times 943.8 = 697.4\ \text{kN}.$$

As $V_{Ed} = 60\ \text{kN} < 0.5V_{pl,T,Rd} = 0.5\times 697.4 = 348.7\ \text{kN}$, it is not necessary to reduce the design plastic moment resistance due to shear force and torsional moment. Thus, a RHS 300×200×8 mm, in grade S 355 steel, is suitable for this application.

iii) *Calculation of the rotation about the x-axis of the section B of the beam A-B*

For the beam under uniform torsion ($T_{Ed} = T_t$), the rotation of section B is obtained by the integration of equation (3.27). As the torsional moment is constant and section A does not rotate, the rotation is given by:

$$\varphi = \frac{T_t}{G\, I_T} L = \frac{48}{81\times10^{6}\times10560\times10^{-8}}\times 3.0 = 1.68\times10^{-2}\,\text{rad.}$$

Example 3.9: Verify the safety of the beam that supports an overhang, illustrated in Figure 3.45, according to EC3-1-1. The beam consists of a IPE 500 in grade S 355 steel and it is subjected to the design loads shown in Figure 3.45. Neglect lateral-torsional buckling.

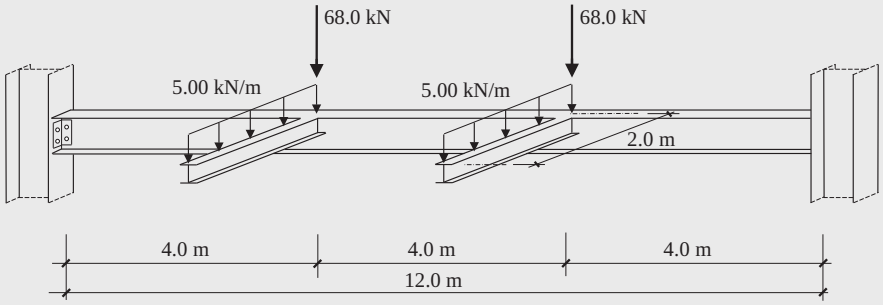


Figure 3.45 – Cantilever overhang structure

The geometric properties of the IPE 500 cross section are:

h =500 mm, b =200 mm, t_w =10.2 mm, t_f =16 mm, A = 115.52 cm^2, A_{vz} = 59.9 cm^2, I_y = 48198.5 cm^4, $W_{pl,y}$ = 2194.12 cm^3, $W_{el,y}$ = 1927.94 cm^3, I_T = 89.29 cm^4 and I_w = 115520 cm^6. The main characteristics of grade S 355 steel are: E = 210 GPa, G = 81 GPa and f_y = 355 MPa.

The main beam is subject to bending moment, shear and torsion. The internal force diagrams for the critical load combination are illustrated in Figure 3.46.

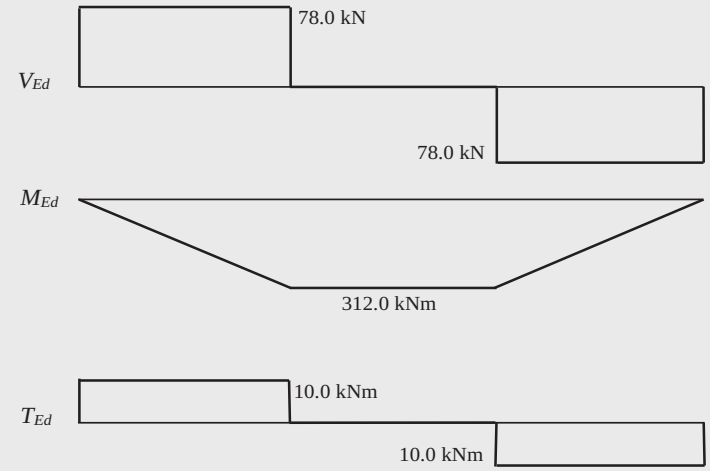


Figure 3.46 – Design internal forces

As the beam is composed of an open cross section, warping stresses must be considered. From equations (3.41) and applying directly the formulas for a doubly-supported beam subject to concentrated torsional moments at intermediate sections from Table A.4 for zero torsional rotation and free warping at the ends, the diagrams of Figure 3.47 are obtained.

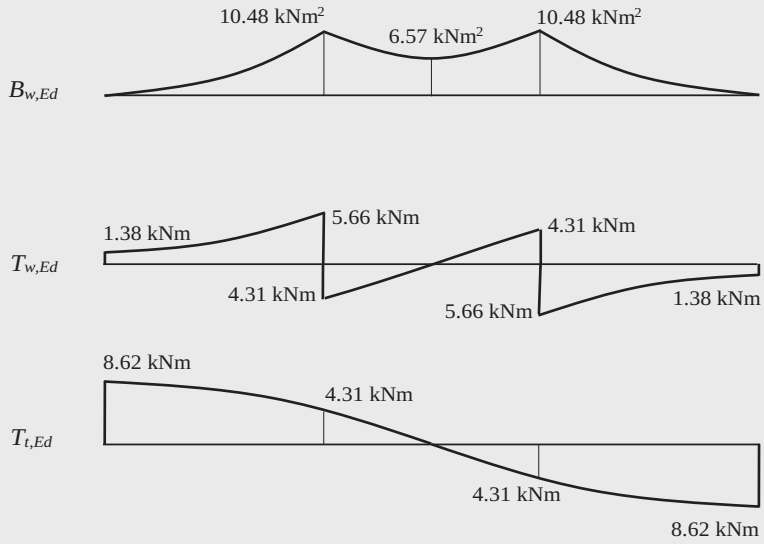


Figure 3.47 – Bimoment, warping torsion and St. Venant's torsion diagrams

The maximum bimoment occurs at the sections where the cantilevers are connected (x = 4.8), given by (Table A.4):

$$B_{w,Ed,max}\left(x=4.8\right)=-10.48\ \text{kNm}^2$$

and

$$T_{w,Ed}=\left(x=4.8\right)=\pm 5.66\ \text{kNm};$$

$$T_{t,Ed}\left(x=4.8\right)=\pm 4.31\ \text{kNm};$$

$$M_{y,Ed}\left(x=4.8\right)=312\ \text{kNm};$$

$$V_{y,Ed}\left(x=4.8\right)=\pm 78\ \text{kN},$$

while the maximum St. Venant torsional moment occurs at the supports, given by:

$$T_{t,Ed,\max}\left(x=0.12\right)=\pm 8.62\ \text{kNm}$$

and

$$B_{w,Ed}\left(x=0.12\right)=0\ \text{kNm}^2;$$

$$T_{w,Ed}\left(x=0.12\right)=\pm 1.38\ \text{kNm};$$

$$M_{y,Ed}\left(x=0.12\right)=0\ \text{kNm};$$

$$V_{y,Ed}\left(x=0.12\right)=\pm 78\ \text{kN},$$

A IPE 500, in grade S 355 steel, is class 1 in bending:

$c/t=426/10.2=41.76<72\varepsilon=72\times 0.81=58.32$, for the web and $c/t=\left(200/2-10.2/2-21\right)/16=4.62<9\varepsilon=9\times 0.81=7.29$, for the flanges.

Hence, a plastic verification may be performed. The design torsional moment resistance is given by (equation (3.51) and Table A.4):

$$T_{pl,Rd}=26.3\,\text{kNm}>T_{Ed}=10\ \text{kNm}.$$

The design plastic bending moment resistance of the cross section, is given by:

$$M_{c,Rd} = M_{pl,Rd} = W_{pl,y} f_y \big/ \gamma_{M0} = 2194.12 \times 355 \times 10^3 \big/ 1.0 =$$

$$= 778.9 \text{ kNm} > M_{c,Rd} = 312 \text{ kNm}.$$

The reduced plastic bending moment resistance due to the presence of warping normal stresses is given by (equation (3.59)):

$$M_{c,B,Rd} = \left(1 - \frac{\sigma_{w,Ed,max}}{f_y} \right) M_{pl,Rd} = \left(1 - \frac{209.5 \times 10^3}{355 \times 10^3} \right) \times 778.9 =$$

$$= 319.2 \text{ kNm} > 312 \text{ kNm},$$

with $\sigma_{w,Ed,\max}$ obtained from equation (3.42) and Table A.2:

$$\sigma_{w,Ed,\max} = -\frac{B_w}{I_w} \omega \left(x, y \right)_{\max} = 209.5 \text{ MPa}.$$

The design plastic shear resistance is given by:

$$V_{pl,Rd} = \frac{A_{vz} \left(f_y \big/ \sqrt{3} \right)}{\gamma_{M0}} = \frac{59.9 \times 10^3 \times \left(355 \times 10^3 \big/ \sqrt{3} \right)}{1.0} = 1227.7 \text{ kN}.$$

The reduced plastic shear resistance of a I-section, to account for the presence of a torsional moment, is given by:

$$V_{pl,T,Rd} = \left[1 - \frac{\tau_{t,Ed}}{\left(f_y \big/ \sqrt{3} \right) \big/ \gamma_{M0}} \right] V_{pl,Rd} = \left[1 - \frac{154.5 \times 10^3}{\left(355 \times 10^3 \big/ \sqrt{3} \right) \big/ 1.0} \right] \times 1227.7 =$$

$$= 773.4 \text{ kN} > 78 \text{ kN},$$

with $\tau_{t,Ed}$ = 154.5 MPa at x = 0.12 m.

Finally, as V_{Ed} > 50 % $V_{pl,T,Rd}$, it is not necessary to check the bending moment – shear force – torsional moment interaction, so that the design is OK.

3.5. COMPRESSION

3.5.1. Theoretical background

3.5.1.1. Introduction

The resistance of a steel member subject to axial compression depends on the cross section resistance or the occurrence of instability phenomena, such as flexural buckling, torsional buckling or flexural-torsional buckling. In general, the design for compression is governed by the second condition (instability phenomena) as steel members are usually of medium to high slenderness.

The cross section resistance to axial compression should be based on the plastic capacity (plastic axial force) in compact sections (class 1, 2 or 3), but taking into account the local buckling resistance through an effective elastic capacity in class 4 sections.

The buckling resistance should be evaluated according to the relevant buckling mode and relevant imperfections of real members, as described in the following sections.

3.5.1.2. Elastic critical load

Buckling is an instability phenomenon that is characterized by the occurrence of transverse deformations in members under compression forces. In steel structures, instability phenomena assume particular importance, because of the relatively high slenderness of compressed members.

The elastic critical load (Euler's critical load) is derived from the theory of elastic stability, as the value of the axial force at which an initially-perfect elastic member may start exhibiting deformations that are not exclusively axial. Buckling of a compressed member, free from imperfections, is illustrated in a simplified way in Figure 3.48; the critical load corresponds to the point of bifurcation of equilibrium. This phenomenon, rigorously called buckling due to compression in a bending mode, will be simply referred in this book as flexural buckling.

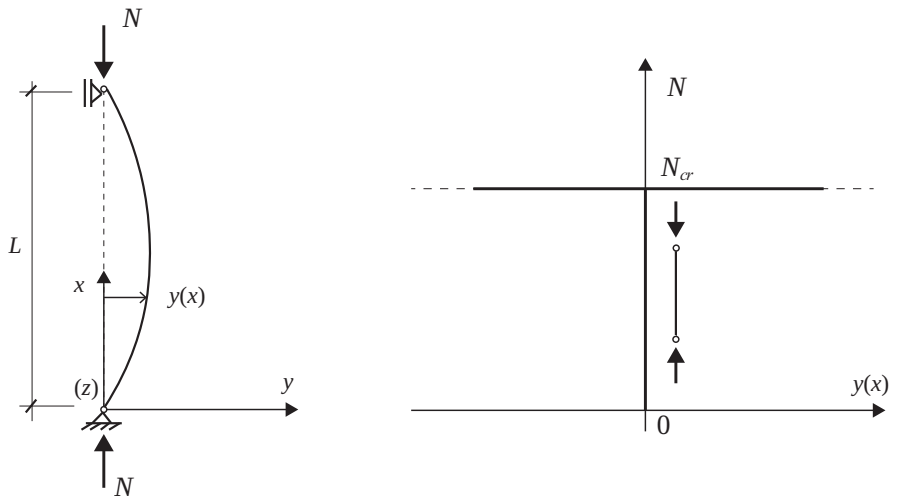


Figure 3.48 – Buckling in a pinned member (Euler's column)

The elastic critical load of a pinned column, with uniform cross section and subjected to constant axial force, is evaluated as shown below. In this formulation the following conditions (ideal design conditions) are assumed:

- material with linear elastic behaviour;
- member free from geometric imperfections and from residual stresses;
- perfectly centred load;
- small displacement theory.

For small deformations, the condition for equilibrium of moments (around z), along the member in Figure 3.48, is given by the following equation:

$$E\,I\frac{d^2y}{dx^2}+N\,y=0, \tag{3.70}$$

where:

E is the modulus of elasticity of the material and

I is the second moment of area with respect to the z axis, perpendicular to the plane where the deformation occurs. Equation (3.70) is a linear homogeneous differential equation of constant coefficients. The solution of this equation is:

$$y=D_1\sin\left(kx\right)+D_2\cos\left(kx\right), \tag{3.71}$$

with $k^2 = N/(E\,I)$. From the support conditions:

$$y(x=0)=0 \Rightarrow D_2 = 0; \tag{3.72}$$

$$y(x=L)=0 \Rightarrow D_1 \sin(k\,L)=0 \Rightarrow D_1 = 0 \text{ or } k\,L = n\,\pi. \tag{3.73}$$

The critical load is obtained from:

$$k\,L = n\,\pi \Rightarrow k^2 = \frac{n^2\pi^2}{L^2} = \frac{N}{E\,I}, \tag{3.74}$$

and $N_{cr} = \dfrac{n^2\,\pi^2\,E\,I}{L^2}$ (with n = 1, 2, …). The lowest critical load, which corresponds to the deformed configuration illustrated in Figure 3.48, is given by:

$$N_{cr} = \frac{\pi^2\,E\,I}{L^2}. \tag{3.75}$$

It can be concluded that for a perfect member, the resistance to buckling depends on the bending stiffness of the cross section, on its length and on the support conditions.

For other support conditions, the critical load is obtained by the solution of a fourth-order differential equation (similar to equation (3.70)), considering adequate support conditions. As an alternative to solving the differential equation, the critical load may be obtained from equation (3.75), replacing the real length L by the buckling length L_E. The buckling length L_E of a member is defined as the length of a fictitious equivalent pinned member with the same critical load. Figure 3.49 illustrates the buckling lengths for isolated members, for several support conditions.

By dividing Euler's critical load by the area of the cross section (A), the critical stress is obtained:

$$\sigma_{cr} = \frac{\pi^2 E\,I}{A\,L_E^2} = \frac{\pi^2 E}{\lambda^2}, \tag{3.76}$$

where: $\lambda = L_E / i$ is the slenderness coefficient and $i = \sqrt{I/A}$ is the radius of gyration of the section.

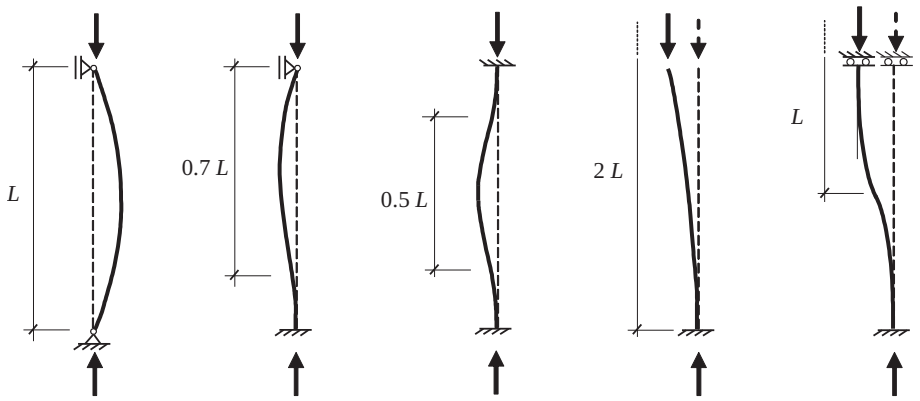


Figure 3.49 – Buckling length L_E as a function of the real length L of the column

In a member without imperfections, composed of a material with elastic-perfectly plastic behaviour (such as may be assumed for mild steel), failure will only occur by buckling in the elastic range if Euler's critical stress is lower than the yield stress f_y. For a short member (with a low slenderness coefficient λ), failure occurs by yielding of the cross section, when the applied stress equals the yield stress, that is, when $\sigma = N/A = f_y$.

The limit between the two types of behaviour is defined by a value of the slenderness coefficient, denoted as λ_1, given by:

$$\sigma_{cr} = \frac{\pi^2 E}{\lambda_1^2} = f_y \Rightarrow \lambda_1 = \pi \sqrt{\frac{E}{f_y}}. \tag{3.77}$$

Based on the slenderness coefficient λ_1, the non-dimensional slenderness coefficient $\bar{\lambda}$ is defined as:

$$\bar{\lambda} = \frac{\lambda}{\lambda_1} = \sqrt{\frac{A f_y}{N_{cr}}}. \tag{3.78}$$

The behaviour of a compressed member, without imperfections, for the full slenderness range, is represented in Figure 3.50.

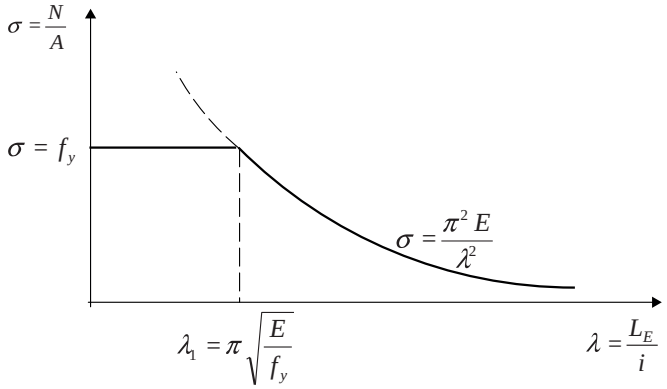
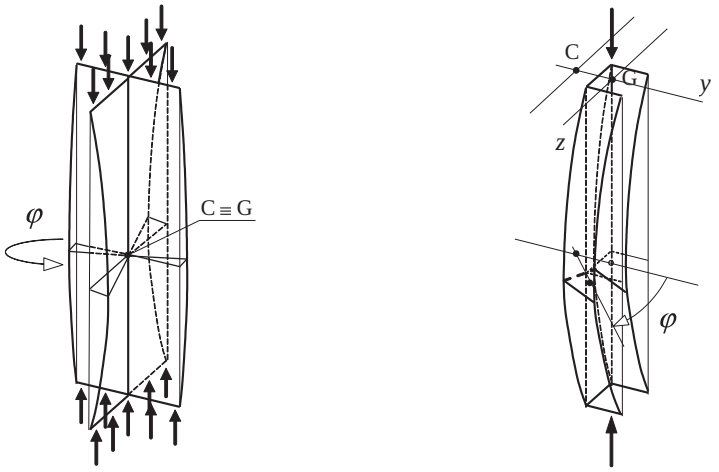


Figure 3.50 – σ - λ relationship of a compressed member

In compressed members of thin-walled open cross section (and hence low torsional stiffness), other instability phenomena may also occur – torsional buckling or flexural-torsional buckling (Trahair, 1993; Hirt *et al*, 2006). Torsional buckling is due to the rotation of cross sections around the axis of the member, as illustrated in Figure 3.51a; flexural-torsional buckling consists of the simultaneous occurrence of torsional and bending deformations along the axis of the member (Figure 3.51b).



a) Torsional buckling b) Flexural-torsional buckling

Figure 3.51 – Torsional buckling and flexural-torsional buckling

The instability phenomena illustrated in Figure 3.51 are characteristic of thin-walled open cross sections, such as channels, L sections or cruciform cross sections. For compressed members constituted by I or H sections, the most critical instability mode is usually flexural buckling.

For members with symmetric cross section with respect to the *y* axis, the torsional buckling critical load is given by:

$$N_{cr,T} = \frac{1}{i_C^2}\left(G\, I_T + \frac{\pi^2 E\, I_w}{L_{ET}^2} \right). \tag{3.79}$$

For the same type of cross sections, the flexural-torsional buckling critical load is given by:

$$N_{cr,TF} = \frac{1}{2\beta}\left[\left(N_{cr,y} + N_{cr,T} \right) - \sqrt{\left(N_{cr,y} + N_{cr,T} \right)^2 - 4\beta\, N_{cr,y}\, N_{cr,T}} \right], \tag{3.80}$$

where:

i_C is the radius of polar gyration given by $i_C^2 = y_C^2 + \left(I_y + I_z \right) / A$;

$G\, I_T$ is the stiffness of the section in uniform torsion;

I_T is the torsion constant;

$E\, I_w$ is the warping stiffness;

I_w is the warping constant;

L_{ET} is an equivalent length that depends on the restrictions to torsion and warping at the end sections;

$N_{cr,y}$ is the critical load for flexural buckling about the *y* axis;

β is a factor given by $\beta = 1 - \left(y_C / i_C \right)^2$, where y_C is the distance along the *y* axis between the shear centre and the centroid of the section.

The calculation of the critical loads in compressed non-prismatic members and/or for variable axial force is briefly addressed in chapter 4. Further guidance can be found in Allen and Bulson (1980) or Hirt *et al* (2006).

3.5.1.3. Effect of imperfections and plasticity

In real structures, imperfections are unavoidable and result in deviations from the theoretical behaviour previously described; under these circumstances, the critical load, in general, is not reached. Imperfections can be divided into two types: i) geometrical imperfections (lack of linearity, lack of verticality, eccentricity of the loads) and ii) material imperfections (residual stresses).

To assess the effect of geometrical imperfections, consider the slender pinned member of Figure 3.52a, with a sinusoidal initial deformed configuration, represented by the following equation:

$$y_0 = e_0 \sin\left(\frac{\pi x}{L}\right). \tag{3.81}$$

The differential equation for equilibrium of a pinned member with an initial deformation is given by:

$$E\,I\,\frac{d^2 y}{dx^2} + N\left(y + y_0\right) = 0. \tag{3.82}$$

Introducing equation (3.81) in equation (3.82) and considering the boundary conditions $y(0) = 0$ and $y(L) = 0$, leads to the following solution:

$$y = \frac{e_0}{\frac{N_{cr}}{N} - 1} \sin\left(\frac{\pi x}{L}\right), \tag{3.83}$$

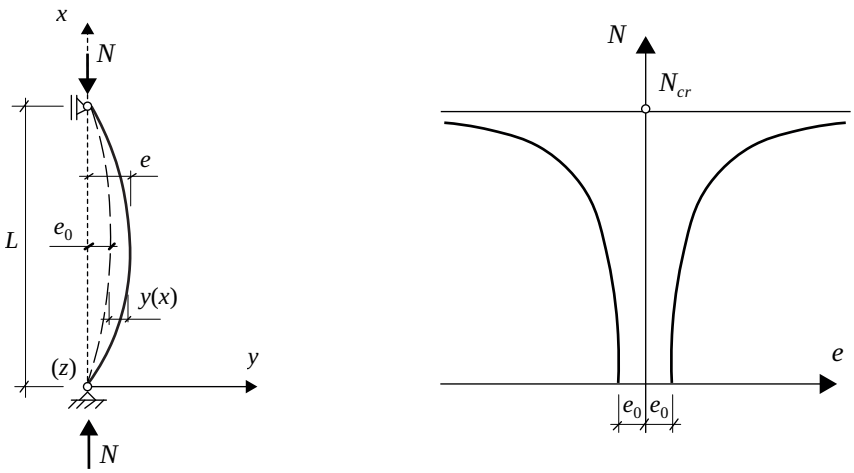
where: N_{cr} is the Euler critical load.

The total deformation of the member is obtained as a function of the applied axial force N:

$$y_t = y + y_0 = \frac{1}{1 - \frac{N}{N_{cr}}} e_0 \sin\left(\frac{\pi x}{L}\right), \tag{3.84}$$

Its maximum value, denoted by e, and obtained for $x = L/2$, is given by:

$$e = \frac{e_0}{1 - \frac{N}{N_{cr}}}. \tag{3.85}$$



a) Initial sinusoidal configuration b) Load – lateral displacement relation

Figure 3.52 – Column with initial geometrical imperfection

An initial deformation, even for low values of the axial force N, generates bending moments given by:

$$M(x) = N(y + y_0) = N\frac{1}{1 - \frac{N}{N_{cr}}} e_0 \sin\left(\frac{\pi x}{L}\right), \tag{3.86}$$

193

which cause a progressive increase of the lateral displacements. The relation between the maximum lateral displacement e and the applied axial force N (equation (3.85)) is represented in Figure 3.52b. For a member with a deformed initial configuration, the transverse displacements start to increase for low values of the axial force N (without bifurcational behaviour) and asymptotically approach infinity as the applied load tends to the critical load.

Residual stresses develop due to differential cooling after hot rolling and any other kind of process involving heat (like welding and flame cutting, for example), shearing and cold-forming and cold-bending; despite being a self-equilibrated system, as illustrated in Figure 3.53 for an I section, these

stresses change the load-deformation relationship for the cross section as a whole.

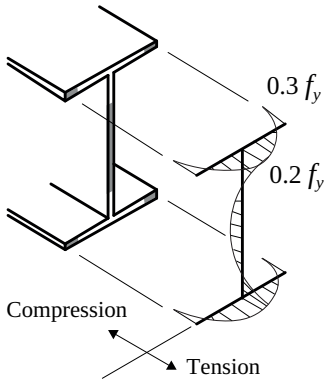


Figure 3.53 – Typical residual stresses in a rolled member with a I cross section

Figure 3.54 illustrates the results of experimental tests on axially compressed members with several slenderness coefficients $\overline{\lambda}$ and compares them with the theoretical behaviour (ECCS, 1976). It can be observed that for low values of $\overline{\lambda}$, failure occurs essentially by plastification of the section and values of σ/f_y higher than 1.0 are obtained experimentally due to strain-hardening. For high values of $\overline{\lambda}$, failure occurs by buckling in the elastic range, the imperfections not having much influence. For intermediate values of $\overline{\lambda}$, failure occurs by elastic-plastic instability, and it is in this slenderness domain that imperfections have more influence (the experimental results deviate most from the theoretical curve).

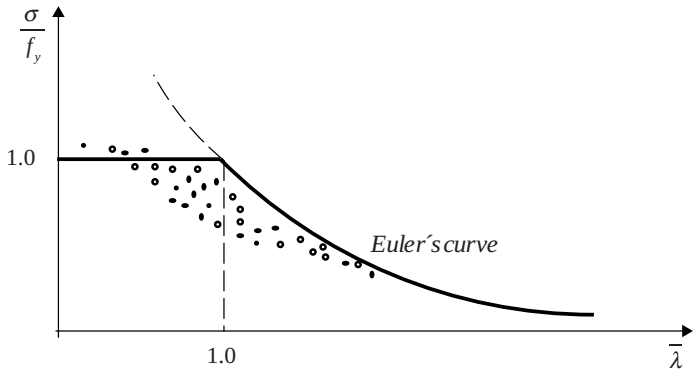


Figure 3.54 – Results of experimental tests in real members

The resistance of compressed members is based on the "European design buckling curves" (ECCS, 1977) that relate the ratio $\chi = \sigma / f_y$ with the non-dimensional slenderness $\overline{\lambda}$. These (five) curves were the result of an extensive experimental and numerical research programme (ECCS, 1976) that accounted for all imperfections in real compressed members (intial out-of-straightness, eccentricity of the loads, residual stresses). These imperfections were defined statistically following an extensive measurement campaign (Strating and Vos, 1973) that justified the adoption of a sinusoidal geometrical imperfection of amplitude *L*/1000 in the numerical simulations[3]. The analytical formulation of the buckling curves, briefly explained in the following paragraphs, was derived by Maquoi and Rondal (1978), based on the Ayrton-Perry formula, considering an initial sinusoidal deformedconfiguration corresponding to an "*equivalent initial deformed configuration*" where the amplitude is calibrated in order to reproduce the effect of all the imperfections.

Consider the compressed column of Figure 3.52a with a sinusoidal initial deformed configuration given by equation (3.81). Assuming that the column is free from residual stresses, plastification of the fibres that are most distant from the neutral axis occurs when the following condition is met:

$$\frac{N_{\max}}{A} + \frac{N_{\max} e}{W_{el}} = f_y, \tag{3.87}$$

where:

- $N_{\max}$ is the maximum value of axial compression N (limited by the resistance to buckling);
- e is the maximum lateral deformation;
- A is the area;
- W_{el} is the elastic bending modulus.

Equation (3.87) can be written in a non-dimensional form, by replacing e with the equation given by (3.85) and dividing all terms by f_y:

[3] This geometrical imperfection accounts for initial out-of-straightness (Gaussian distribution with an average $e_0 = L/1176.5$ and coefficient of variation of 23.5 %) and eccentricity of the loads (Gamma distribution with $\lambda = 2.798$ and $k = 1.663$).

$$\frac{N_{\max}}{N_{pl}} + \frac{N_{\max}\, e_0\, A}{W_{el}\left(1 - \frac{N_{\max}}{N_{pl}}\frac{N_{pl}}{N_{cr}}\right)N_{pl}} = 1. \tag{3.88}$$

Defining $\chi = N_{\max}/N_{pl}$ yields:

$$\chi + \frac{\chi}{\left(1 - \chi\overline{\lambda}^2\right)}\frac{e_0\, A}{W_{el}} = 1, \tag{3.89}$$

or

$$\left(1-\chi\right)\left(1-\chi\overline{\lambda}^2\right) = \frac{e_0\, A}{W_{el}}\chi = \eta\,\chi, \tag{3.90}$$

which constitutes the basic form of the Ayrton-Perry equation (Maquoi and Rondal, 1978). η represents the generalized initial imperfection that can be used to estimate the effects on the buckling phenomenon of initial imperfections such as residual stresses, initial out-of-straightness or eccentrically applied forces. Because the influence of some of these initial imperfections is linked with the length of the member, it has been chosen to express η as follows (Maquoi and Rondal, 1978):

$$\eta = \alpha\left(\overline{\lambda} - 0.2\right), \tag{3.91}$$

where the imperfection factor α depends on the shape of the cross section, buckling plane, etc., and 0.2 defines the length of the plateau along which χ = 1.0. Based on the previous relations, the Ayrton-Perry equation (3.88) can be written in the form:

$$\left(1-\chi\overline{\lambda}^2\right)\left(1-\chi\right) = \eta\,\chi = \alpha\,\chi\left(\overline{\lambda} - 0.2\right). \tag{3.92}$$

Equation (3.92) is a quadratic equation in χ, and its minimum solution is given by:

$$\chi = \frac{\phi - \sqrt{\phi^2 - \overline{\lambda}^2}}{\overline{\lambda}^2}, \tag{3.93}$$

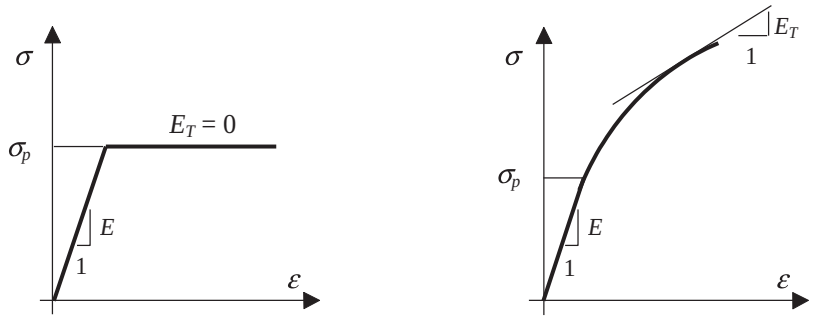
with

$$\phi = 0.5\left[1 + \alpha\left(\overline{\lambda} - 0.2\right) + \overline{\lambda}^2\right]. \tag{3.94}$$

By multiplying the numerator and the denominator of the previous equation by the conjugated term $\phi + \sqrt{\phi^2 - \overline{\lambda}^2}$, the equation from EC3-1-1 is obtained, which gives the χ factor (reduction factor accounting for the risk of flexural buckling) as a function of the non-dimensional slenderness coefficient $\overline{\lambda}$ and of the imperfection factor α:

$$\chi = \frac{1}{\phi + \sqrt{\phi^2 - \overline{\lambda}^2}}. \tag{3.95}$$

Metals present, in general, an elastic-plastic behaviour, and in the case of mild steel (except for the effect of residual stresses) a perfect elastic-plastic behaviour is normally adopted (Figure 3.55a). However, in materials like stainless steel or aluminium the behaviour is closer to the one illustrated in Figure 3.55b.



a) Perfect elastic-plastic b) Elastic-plastic

Figure 3.55 – Behaviour of metals

For members with low slenderness and of stainless steel or aluminium (or other material with similar behaviour), failure can occur when some points of the section have already exceeded the limit stress of proportionality

σ_p ($\sigma_p \approx f_y$ in case of mild steel); in these cases, the stability analysis must include the interaction between the geometric and material non-linearities (plasticity effect). The plasticity effect in the study of instability in the elastic-plastic range can be taken into account by the reduction of the modulus of elasticity. If the limit stress of proportionality is exceeded, the modulus of elasticity E must be replaced by the tangent modulus E_T, as illustrated in Figure 3.55b, the critical load being defined by:

$$N_{cr} = \frac{\pi^2 E_T I}{L_E^2}. \tag{3.96}$$

If E_T is variable, an iterative process is necessary.

3.5.2. Design for compression

According to clause 6.2.4(1), the cross section resistance of axially compressed members is verified by the following condition:

$$\frac{N_{Ed}}{N_{c,Rd}} \leq 1.0, \tag{3.97}$$

where:

N_{Ed} is the design value of the axial compression force and

$N_{c,Rd}$ is the design resistance of the cross section for uniform compression, given by (clause 6.2.4(2)):

– Class 1, 2 or 3 cross sections

$$N_{c,Rd} = A f_y / \gamma_{M0}; \tag{3.98}$$

– Class 4 cross section

$$N_{c,Rd} = A_{eff} f_y / \gamma_{M0}, \tag{3.99}$$

where:

A is the gross area of the cross section,

A_{eff} is the effective area of a class 4 cross section,

f_y is the yield strength of steel and

γ_{M0} is a partial safety factor.

In evaluating $N_{c,Rd}$, holes for fasteners can be neglected, provided they are filled by fasteners and are not oversize or slotted (clause 6.2.4(3)).

In compression members it must also be verified that:

$$N_{Ed} \le N_{b,Rd}, \tag{3.100}$$

where:

$N_{b,Rd}$ is the design buckling resistance of the compression member (clause 6.3.1.1(1)) and this generally controls design.

The design flexural buckling resistance of prismatic members is given by:

– Class 1, 2 or 3 cross sections

$$N_{b,Rd} = \chi A f_y / \gamma_{M1}; \tag{3.101}$$

– Class 4 cross sections

$$N_{b,Rd} = \chi A_{eff} f_y / \gamma_{M1} \ , \tag{3.102}$$

where:

χ is the reduction factor for the relevant buckling mode and

γ_{M1} is a partial safety factor (clause 6.3.1.1(3)).

The reduction factor χ is obtained from the following equation:

$$\chi = \frac{1}{\phi + \sqrt{\phi^2 - \overline{\lambda}^2}}, \quad \text{but } \chi \le 1.0. \tag{3.103}$$

In this equation, $\phi = 0.5\left[1 + \alpha\left(\overline{\lambda} - 0.2\right) + \overline{\lambda}^2\right]$ and $\overline{\lambda}$ is the non-dimensional slenderness coefficient, given by:

– Class 1, 2 or 3 cross sections

$$\overline{\lambda} = \sqrt{A f_y / N_{cr}} = \frac{L_{cr}}{i}\frac{1}{\lambda_1}; \tag{3.104}$$

– Class 4 cross sections

$$\overline{\lambda} = \sqrt{A_{eff} f_y / N_{cr}} = \frac{L_{cr}}{i}\frac{\sqrt{A_{eff}/A}}{\lambda_1}, \tag{3.105}$$

where:

α is the imperfection factor;

N_{cr} is the elastic critical load (Euler's critical load) for the relevant buckling mode;

L_{cr} is the length of the corresponding buckling mode;

i is the radius of gyration of the cross section;

$$\lambda_1 = \pi\sqrt{\left(E/f_y\right)} = 93.9\varepsilon;$$

$$\varepsilon = \sqrt{235/f_y} \quad \text{with } f_y \text{ in N/mm}^2.$$

The effect of imperfections is included by the imperfection factor α, which assumes values of 0.13, 0.21, 0.34, 0.49 and 0.76 for curves a_0, a, b, c and d (European design buckling curves), respectively. These curves, mathematically represented by equation (3.103), are illustrated in Figure 3.56. The imperfection factor α and the associated buckling curve to be adopted in design of a given member depends on the geometry of the cross sections, on the steel grade, on the fabrication process and on the relevant buckling plane, as described in Table 3.3.

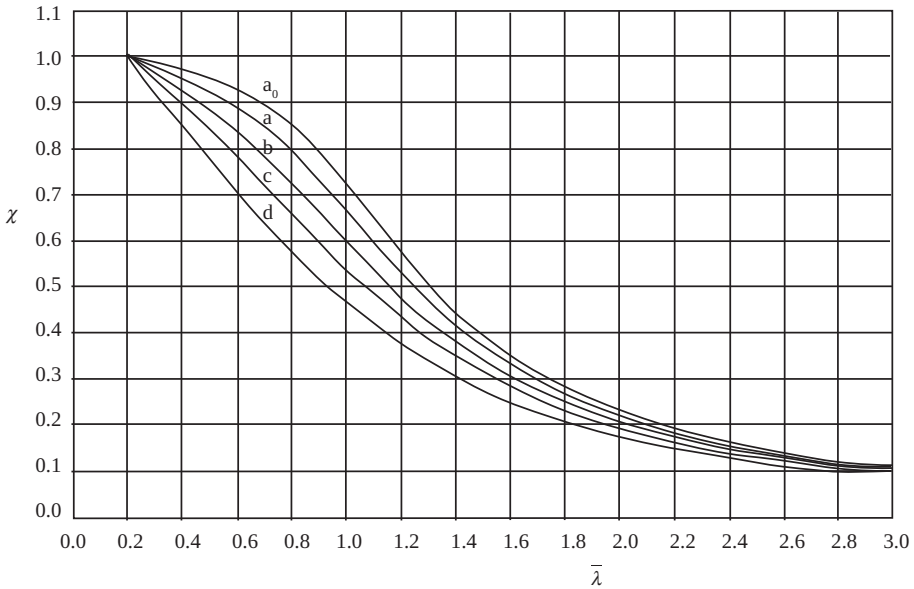
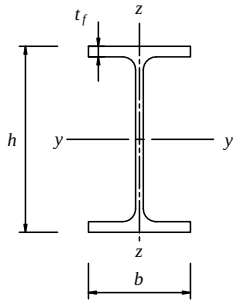
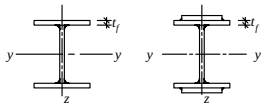
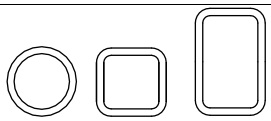
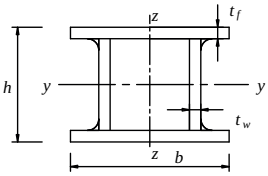
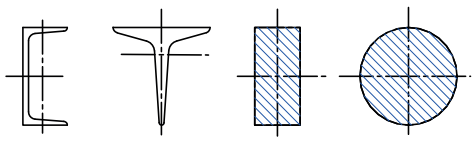
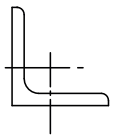


Figure 3.56 – Buckling curves according to EC3-1-1

Table 3.3 – Selection of the buckling curve

Cross section		Geometry limits		Buckling about axis	Buckling curve	
					S 235 S 275 S 355 S 420	S 460
Rolled I or H sections		$h/b > 1.2$	$t_f \le 40$ mm	y-y z-z	*a* *b*	a_0 a_0
			40 mm< $t_f \le$ 100 mm	y-y z-z	*b* *c*	*a* *a*
		$h/b \le 1.2$	$t_f \le 100$ mm	y-y z-z	*b* *c*	*a* *a*
			$t_f > 100$ mm	y-y z-z	*d* *d*	*c* *c*
Welded I or H sections		$t_f \le 40$ mm		y-y z-z	*b* *c*	*b* *c*
		$t_f > 40$ mm		y-y z-z	*c* *d*	*c* *d*
Hollow sections		hot finished		any	*a*	a_0
		cold formed		any	*c*	*c*
Welded box sections		Generally (except as below)		any	*b*	*b*
		thick welds: $a > 0.5\ t_f$ $b/t_f < 30$ $h/t_w < 30$ (*a* – throat thickness)		any	*c*	*c*
U, T and solid sections				any	*c*	*c*
L sections				any	*b*	*b*

According to clause 6.3.1.2(4), for values of the non-dimensional slenderness $\overline{\lambda} \le 0.2$ or if $N_{Ed}/N_{cr} \le 0.04$, the effect of buckling can be neglected, and members are designed based only on the cross section resistance.

In compression members with open cross sections, then according to clause 6.3.1.4(1), account should be taken of the possibility that resistance to torsional or flexural-torsional buckling could be less than the resistance to flexural buckling. The design process for these members is very similar to that for flexural buckling, the non-dimensional slenderness coefficient $\overline{\lambda}$ being replaced by the non-dimensional slenderness coefficient $\overline{\lambda}_T$, evaluated by the following equations (clause 6.3.1.4(2)):

- Class 1, 2 or 3 cross sections

$$\overline{\lambda}_T = \sqrt{A f_y / N_{cr}}; \tag{3.106}$$

- Class 4 cross sections

$$\overline{\lambda}_T = \sqrt{A_{eff} f_y / N_{cr}}, \tag{3.107}$$

where:

N_{cr} is the lower of the values $N_{cr,T}$ and $N_{cr,TF}$;

$N_{cr,T}$ is the elastic critical load for torsional buckling (equation (3.79)) and

$N_{cr,TF}$ is the elastic critical load for flexural-torsional buckling (equation (3.80)).

For both phenomena, the imperfection coefficient α can be taken as corresponding to flexural buckling about the *z* axis, obtained from Table 6.2 of EC3-1-1, reproduced in Table 3.3 above.

Annex BB.1 provides guidelines that allow quantification of the buckling length for members in triangulated and lattice structures. In general, for the evaluation of the buckling resistance of chord members, a buckling length equal to the real length *L* may be adopted, for both in-plane and out-of-plane buckling; in some particular cases lower values can be adopted, provided that they are properly justified. In the case of chord members with I or H sections, the in-plane buckling length of the

structure can be reduced to 0.9 *L*. In the case of chords with tubular sections, a buckling length equal to 0.9 *L* may be considered, for in-plane and out-of-plane buckling.

For web members, in general a buckling length equal to the real length *L* should be considered. For some types of members (except for those made of angles, for which clause BB.1.2 is applicable) a lower value can be adopted (equal to 0.9 *L*) for the in-plane buckling length of the structure, as long as the chords supply appropriate end restraint and the end connections provide adequate fixity (at least two bolts, in case of bolted connections) in accordance with clause BB.1.1(3).

In the definition of the real length *L*, particularly for chord members, the following rules should be followed: i) in the plane of the structure, the real length *L* of a bar is the distance between connections, or more generally as the distance between structural nodes, depending on the structural modeling; ii) for out-of-plane buckling, the real length *L* corresponds to the distance between connections (or structural nodes), but only if the nodes are braced in the perpendicular direction to the plane of the structure; otherwise a longer length should be considered, in the limit, the total length of the chord between supports.

Uniform built-up compression members must be analysed and designed according to clause 6.4. Closely spaced built-up members, shown in Figure 3.57 (clause 6.4.4), can be designed against buckling as a single member, as long as interconnection is provided (by bolts or welding) along its length, with a maximum spacing of 15 i_{min} (or 70 i_{min} in the case of members connected by pairs of battens as specified in the same clause 6.4.4), where i_{min} is the minimum radius of gyration of the cross section of one chord or one angle.

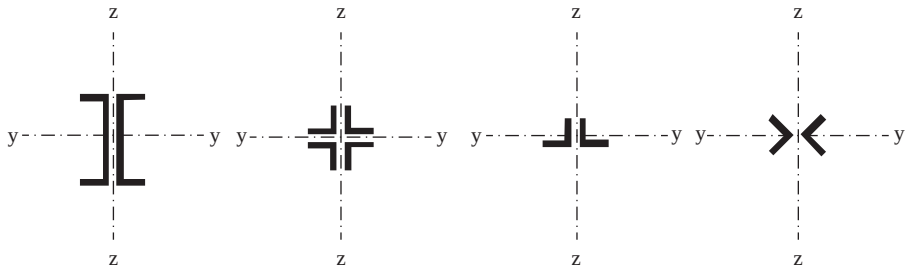


Figure 3.57 – Closely spaced built-up members

3.5.3. Worked examples

Example 3.10: Design the column BD of the steel structure represented in Figure 3.58, using a HEB cross section in S 355 steel, according to EC3-1-1. The column is fixed at the base and hinged at section B (with respect to the two principal axis of the cross section). Cross section B is fixed in both horizontal directions, in the plane of the structure (due to the beam itself) and in the perpendicular plane (because of secondary bracing members). Loading is already factored for ULS.

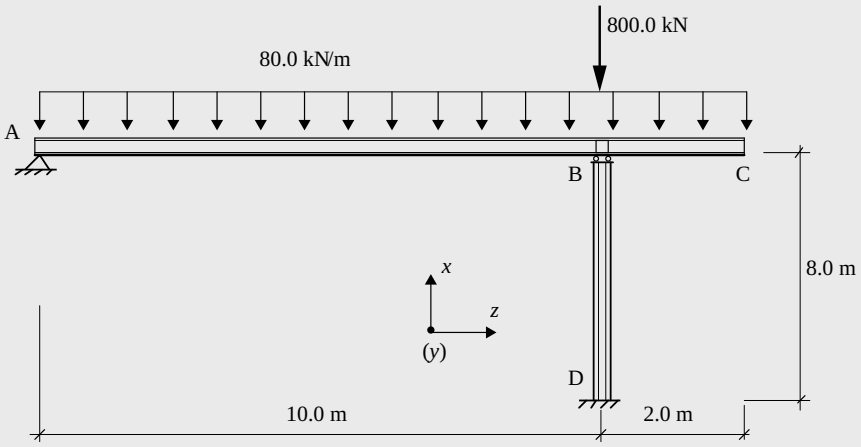


Figure 3.58 – Design of a column

i) *Design value of the applied compressive axial force* N_{Ed}

$$N_{Ed} = \frac{80.0}{10} \times \frac{12^2}{2} + 800 = 1376.0 \text{ kN}.$$

ii) *Preliminary design* – Assuming class 1, 2 or 3 cross sections, yields:

$$N_{Ed} = 1376.0 \text{ kN} \le N_{c,Rd} = A f_y / \gamma_{M0} = A \times 355 \times 10^3 / 1.0$$
$$\Rightarrow A \ge 38.76 \times 10^{-4} \text{ m}^2 = 38.76 \text{ cm}^2.$$

As it is expected that buckling resistance will govern the member design, a HEB 240 in S 355 steel is proposed (class 1 in pure compression), with the following properties (geometrical and mechanical):

A = 106 cm^2, b = 240 mm, h = 240 mm, t_f = 17 mm, t_w = 10 mm, I_y = 11260 cm^4, i_y = 10.31 cm, I_z = 3923 cm^4, i_z = 6.08 cm, f_y = 355 MPa and E = 210 GPa.

iii) *Buckling lengths* – According to the support conditions, the buckling lengths are equal in both planes, given by:

Buckling in the plane of the structure (plane x-z) - $L_{Ey} = 0.7 \times 8.0 = 5.6$ m.

Buckling in the perpendicular plane (plane x-y) - $L_{Ez} = 0.7 \times 8.0 = 5.6$ m.

Because the buckling lengths are equal in both planes, the orientation of the cross section is arbitrary. For constructional reasons, the section is placed as shown in Figure 3.58, with the strong axis (y axis) in the perpendicular direction to the plane of the structure.

iv) *Determination of the slenderness coefficients*

$$\lambda_1 = \pi\sqrt{\frac{210\times10^6}{355\times10^3}} = 76.4;$$

$$\lambda_y = \frac{L_{Ey}}{i_y} = \frac{5.6}{10.31\times10^{-2}} = 54.32; \qquad \overline{\lambda}_y = \frac{\lambda_y}{\lambda_1} = 0.71;$$

$$\lambda_z = \frac{L_{Ez}}{i_z} = \frac{5.6}{6.08\times10^{-2}} = 92.11; \qquad \overline{\lambda}_z = \frac{\lambda_z}{\lambda_1} = 1.21.$$

v) *Calculation of the reduction factor* $\chi_{\min}$

$$\frac{h}{b} = 1.0 < 1.2 \quad \text{and} \quad t_f = 17 \text{ mm} < 100 \text{ mm}$$

$$\Rightarrow \begin{array}{l} \text{bending around } y - \text{curve } b\left(\alpha = 0.34\right) \\ \text{bending around } z - \text{curve } c\left(\alpha = 0.49\right). \end{array}$$

As $\overline{\lambda}_z > \overline{\lambda}_y$ and $\alpha_{\text{curve } c} > \alpha_{\text{curve } b} \Rightarrow \chi_{\min} \Rightarrow \chi_z$.

$$\phi_z = 0.5\times\left[1 + 0.49\times\left(1.21 - 0.2\right) + 1.21^2\right] = 1.48;$$

$$\chi_z = \frac{1}{1.48 + \sqrt{1.48^2 - 1.21^2}} = 0.43;$$

$$\chi_{\min} = \chi_z = 0.43.$$

vi) *Safety verification*

$$N_{b,Rd} = \chi A f_y / \gamma_{M1} = 0.43 \times 106 \times 10^{-4} \times 355 \times 10^3 / 1.0 = 1618.1 \text{ kN}.$$

As $N_{Ed} = 1376.0 \text{ kN} < N_{b,Rd} = 1618.1 \text{ kN}$,

safety is verified. The solution for the problem consists of a HEB 240 in S 355 steel.

Example 3.11: Consider the lattice beam of example 3.3, in S 275 steel, with the internal forces represented in Figure 3.59. In order to complete its design, design the compressed members, considering the same types of cross sections, that is:

a) Square hollow sections (SHS), with welded connections between the members of the structure.

b) HEA sections in the chords (horizontal members) and sections built up from 2 channels in the diagonals, bolted to gusset plates welded to the HEA profiles in the upper and lower chords.

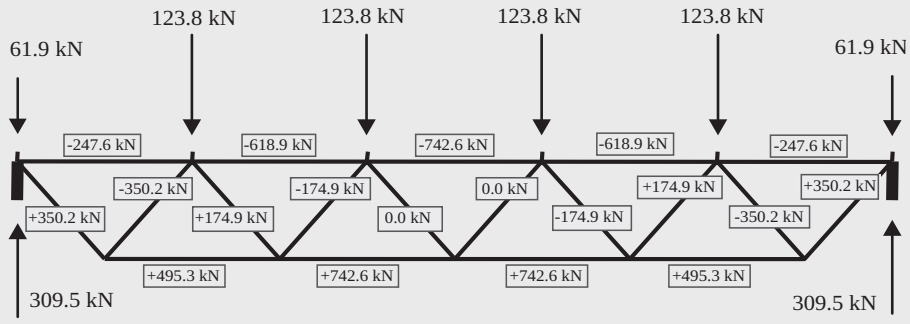


Figure 3.59 – Actions and internal forces on the lattice girder of example 3.3

Based on the axial force diagrams represented in Figure 3.59, the most compressed chord member is under an axial force of 742.6 kN and it is simultaneously one of the longest members, with L = 3.00 m; concerning the diagonals, the most compressed member, with a length L = 2.12 m, is under an axial force of 350.2 kN. For the definition of the buckling lengths of the members, it is assumed that all the nodes of the truss are braced in the direction perpendicular to the plane of the structure.

a) *Design with square hollow section (SHS) profiles*

i) *Preliminary design*, assuming a class 1, 2 or 3 cross section, gives:

Upper chord,

$$742.6 \leq \frac{A \times 275 \times 10^3}{1.0} \Rightarrow A \geq \frac{742.6 \times 1.0}{275 \times 10^3} = 27.0 \times 10^{-4}\,\text{m}^2 = 27.0\,\text{cm}^2.$$

Diagonals,

$$350.2 \leq \frac{A \times 275 \times 10^3}{1.0} \Rightarrow A \geq \frac{350.2 \times 1.0}{275 \times 10^3} = 12.7 \times 10^{-4}\,\text{m}^2 = 12.7\,\text{cm}^2.$$

Based on a table of commercial profiles of square hollow sections (SHS), a SHS 120×120×8 mm (A = 35.5 cm^2) is proposed for the upper chord and a SHS 80×80×6.3 mm (A = 18.4 cm^2) is proposed in the diagonals, with areas slightly above the minimum required by the above conditions; this is because verification of resistance to buckling is expected to govern. The following additional geometrical properties apply to the proposed sections:

SHS 120×120×8 mm: I = 738 cm^4, i = 4.56 cm;

SHS 80×80×6.3 mm: I = 165 cm^4, i = 3.00 cm.

ii) *Cross section classification*

For the proposed sections (square hollow sections of constant thickness), in S 275 steel, in compression:

SHS 120×120×8 mm: $c \approx h - 3t = 120 - 3 \times 8 = 96$ mm.

$$\Rightarrow \frac{c}{t} = \frac{96}{8} = 12 < 33\varepsilon = 33 \times 0.92 = 30.4. \qquad \text{(Class 1)}$$

SHS 80×80×6.3 mm: $c \approx h - 3t = 80 - 3 \times 6.3 = 61.1$ mm

$$\Rightarrow \frac{c}{t} = \frac{61.1}{6.3} = 9.7 < 33\varepsilon = 33 \times 0.92 = 30.4. \qquad \text{(Class 1)}$$

Therefore both cross sections are class 1.

iii) *Verification of the buckling resistance*

iii-1) Upper chord using a SHS 120×120×8 mm

$$\lambda_1 = \pi \sqrt{\frac{210 \times 10^6}{275 \times 10^3}} = 86.81;$$

$L_E = 0.9\, L = 0.9 \times 3.00 = 2.70$ m (according to Annex BB.1);

$$\lambda = \frac{L_E}{i} = \frac{2.70 \times 10^2}{4.56} = 59.21; \qquad \overline{\lambda} = \frac{\lambda}{\lambda_1} = 0.682;$$

Hot-finished square hollow section $\Rightarrow$ Curve *a*, so $\alpha = 0.21$;

$$\phi = 0.5 \times \left[1 + 0.21 \times \left(0.682 - 0.2\right) + 0.682^2\right] = 0.783;$$

$$\chi = \frac{1}{0.783 + \sqrt{0.783^2 - 0.682^2}} = 0.856;$$

$$N_{b,Rd} = \frac{\chi A f_y}{\gamma_{M1}} = \frac{0.856 \times 35.5 \times 10^{-4} \times 275 \times 10^3}{1.0} = 835.7 \text{ kN}.$$

As $N_{Ed} = 742.6$ kN $< N_{b,Rd} = 835.7$ kN, a SHS 120×120×8 mm, in S 275 steel, is adopted.

iii-2) Compressed diagonals using SHS 80×80×6.3 mm

$$\lambda_1 = \pi \sqrt{\frac{210 \times 10^6}{275 \times 10^3}} = 86.81;$$

$L_E = L = 2.12$ m (according to Annex BB.1);

$$\lambda = \frac{L_E}{i} = \frac{2.12 \times 10^2}{3.00} = 70.67; \qquad \overline{\lambda} = \frac{\lambda}{\lambda_1} = 0.814;$$

Hot-finished square hollow section $\Rightarrow$ Curve *a*, so $\alpha = 0.21$;

$$\phi = 0.5 \times \left[1 + 0.21 \times \left(0.814 - 0.2\right) + 0.814^2\right] = 0.896;$$

$$\chi = \frac{1}{0.896 + \sqrt{0.896^2 - 0.814^2}} = 0.787;$$

$$N_{b,Rd} = \frac{\chi A f_y}{\gamma_{M1}} = \frac{0.787 \times 18.4 \times 10^{-4} \times 275 \times 10^3}{1.0} = 398.2 \text{ kN}.$$

As N_{Ed} = 350.2 kN < $N_{b,Rd}$ = 398.2 kN a SHS 80×80×6.3 mm, in S 275 steel, is adopted.

b) *Design with HEA profiles for the chords and* sections built up from 2 channels *for the diagonals.*

i) Preliminary design assuming a class 1, 2 or 3 cross section, yields the same result as for the previous case, that is, for the upper chord $A \geq 27.0$ cm^2 and for the diagonals $A \geq 12.7$ cm^2.

Based on a table of commercial profiles, a HEA 180 (A = 45.25 cm^2) cross section is proposed for the upper chord and a cross section built-up from 2 UPN 100 (A = 27.00 cm^2), 10 mm apart (thickness of the gusset plate) is proposed for the diagonals (see Figure 3.60). The areas of the cross sections are larger than the minimum areas required by the above conditions, because the verification of the buckling resistance is expected to govern. The relevant geometrical properties of the HEA 180 section and of the UPN 100 section are as follows:

HEA 180: I_y = 2510 cm^4, i_y = 7.45 cm; I_z = 924.6 cm^4, i_z = 4.52 cm.

UPN 100: I_y = 206 cm^4, i_y = 3.91 cm; I_z = 29.3 cm^4, i_z = 1.47 cm; b = 50 mm; h = 100 mm; y_s = 1.55 cm (distance from the centroid to the outer face of the web).

ii) *Cross section classification*

HEA 180 in S 275 steel, under pure compression:

Web: $c/t = 122/6 = 20.3 < 33\varepsilon = 33 \times 0.92 = 30.36,$ (Class 1)

Flanges: $c/t = 72/9.5 = 7.6 < 9\varepsilon = 9 \times 0.92 = 8.28.$ (Class 1)

Therefore the section is class 1.

UPN 100 in S 275 steel, under pure compression:

Web: $c/t = 64/6 = 10.7 < 33\varepsilon = 33 \times 0.92 = 30.36,$ (Class 1)

Flanges: $c/t = 35.5/8.5 = 4.2 < 9\varepsilon = 9 \times 0.92 = 8.28.$ (Class 1)

Therefore the cross section is class 1.

iii) *Verification of the buckling resistance*

iii-1) Upper chord with a HEA 180

$$\lambda_1 = \pi\sqrt{\frac{210 \times 10^6}{275 \times 10^3}} = 86.81;$$

$L_E = L = 3.00$ m (for out-of-plane buckling, according to Annex BB.1);

$$\lambda = \frac{L_E}{i} = \frac{3.00 \times 10^2}{4.52} = 66.37; \qquad \overline{\lambda} = \frac{\lambda}{\lambda_1} = 0.765;$$

$h/b < 1.2$; bending around $z \Rightarrow$ curve $c\left(\alpha = 0.49\right)$;

$$\phi = 0.5 \times \left[1 + 0.49 \times \left(0.765 - 0.2\right) + 0.765^2\right] = 0.931;$$

$$\chi = \frac{1}{0.931 + \sqrt{0.931^2 - 0.765^2}} = 0.684;$$

$$N_{b,Rd} = \frac{\chi A f_y}{\gamma_{M1}} = \frac{0.684 \times 45.25 \times 10^{-4} \times 275 \times 10^3}{1.0} = 851.2 \text{ kN}.$$

As $N_{Ed} = 742.6$ kN $< N_{b,Rd} = 851.2$ kN, a HEA 180, in S 275 steel, is adopted.

iii-2) Diagonals with a cross section built-up from 2 UPN 100

In order to avoid buckling of the individual members the members must be connected with a maximum spacing of $15\, i_{\min} = 15 \times 1.47 \text{ cm} = 22.05 \text{ cm}$ (clause 6.4.4).

The second moment of area about *z* of the built-up cross sections (Figure 3.60) is obtained as follows:

$$I_z = 2\times\left(29.3+13.5\times\left(1.55+0.5\right)^2\right)=172.07\ \text{cm}^4\,.$$

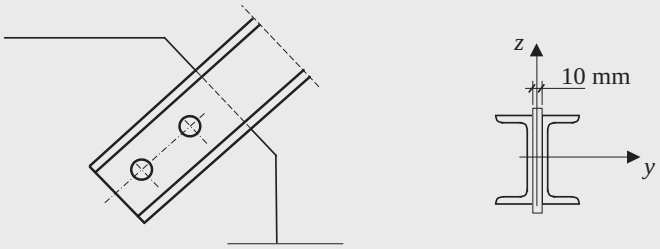


Figure 3.60 – Detail in the diagonals of the truss

As this is less than I_y for the built-up section, as the buckling lengths in-plane and out-of-plane are, in this case, equal (according to Annex BB.1) and the relevant buckling curve (curve *c*) is the same, it is concluded that out-of-plane buckling is critical (buckling about *z)*. Continuing the calculation:

$$i_z = \sqrt{I_z/A} = \sqrt{172.07/\left(2\times13.5\right)} = 2.52\ \text{cm};$$

$$\lambda_1 = \pi\sqrt{\frac{210\times10^6}{275\times10^3}} = 86.81;\ L_E = L = 2.12\ \text{m};$$

$$\lambda = \frac{L_E}{i} = \frac{2.12\times10^2}{2.52} = 84.13; \qquad \bar{\lambda} = \frac{\lambda}{\lambda_1} = 0.969;$$

Cross section built-up from 2 UPN $\Rightarrow$ Curve *c*, so $\alpha = 0.49$;

$$\phi = 0.5\times\left[1+0.49\times\left(0.969-0.2\right)+0.969^2\right] = 1.158;$$

$$\chi = \frac{1}{1.158+\sqrt{1.158^2-0.969^2}} = 0.558;$$

$$N_{b,Rd} = \frac{\chi\, A\, f_y}{\gamma_{M1}} = \frac{0.558\times27.0\times10^{-4}\times275\times10^3}{1.0} = 414.3\ \text{kN}.$$

As $N_{Ed} = 350.2\ \text{kN} < N_{b,Rd} = 414.3\ \text{kN},$ the section built-up from 2 channels UPN 100, in S 275 steel, is adopted.

3.6. LATERALLY UNRESTRAINED BEAMS

3.6.1. Introduction

The design of a beam subject to bending and shear must be performed in two steps: i) verification of the resistance of the cross section and ii) check on member stability. The cross section resistance, depending of cross sectional shape and cross section class, has already been explained in the sub-chapter 3.3; in the same sub-chapter, the local cross section instability (including verification of the class of the section) and instability caused by shear forces were also discussed. In this sub-chapter, the resistance of members against instability phenomena caused by a bending moment will be presented. In standard cross sectional shapes, such as I or H bent around the major axis (*y* axis), the typical instability phenomenon is lateral-torsional buckling.

3.6.2. Lateral-torsional buckling

3.6.2.1. Introduction

Consider a member subject to bending about the strong axis of the cross section (the *y* axis). Lateral-torsional buckling is characterised by lateral deformation of the compressed part of the cross section (the compressed flange in the case of I or H sections). This part behaves like a compressed member, but one continuously restrained by the part of the section in tension, which initially does not have any tendency to move laterally. As seen in Figure 3.61, where this phenomenon is illustrated for a cantilever beam, the resulting deformation of the cross section includes both lateral bending and torsion. This is why this phenomenon is called lateral-torsional buckling.

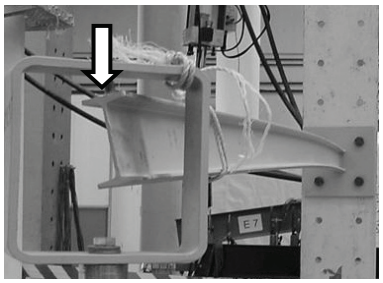
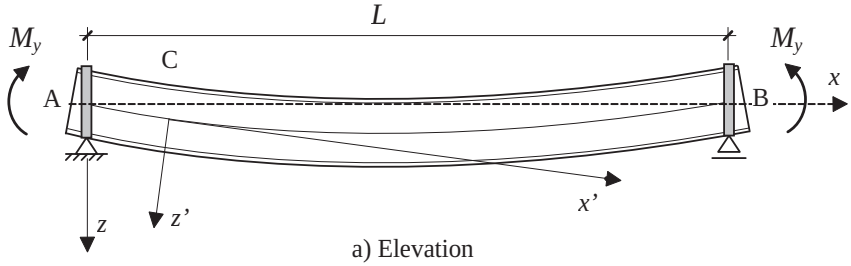


Figure 3.61 – Lateral-torsional buckling of a cantilever beam

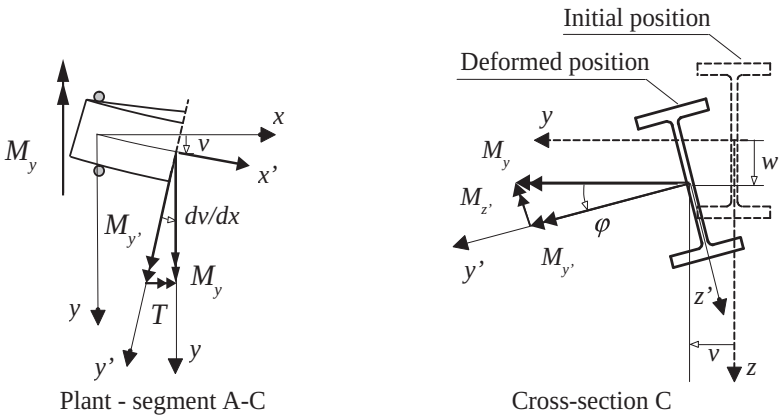
3.6.2.2. Elastic critical moment

To obtain the elastic critical moment, consider the simply supported beam of Figure 3.62, with the supports preventing lateral displacements and twisting but allowing warping and bending rotations around the cross sectional axes (*y* and *z*), submitted to a constant bending moment M_y. Consider the following assumptions:

- perfect beam, without any type of imperfections (geometrical or material);
- doubly symmetric cross section;
- material with linear elastic behaviour;
- small displacements ($\sin\phi \approx \phi; \cos\phi \approx 1$).



a) Elevation



b) Internal forces at-section C

Figure 3.62 – Lateral-torsional buckling in a doubly symmetric I section under constant bending moment

Consider the deformed configuration of Figure 3.62 and the set of three differential equations of equilibrium, defined in the system of axis *x'*, *y'*, *z'* (deformed position) where the unknown quantities are the displacements φ, *v*, *w*. According to small displacement theory, the properties of the cross sections in the undeformed position can be considered.

For bending about the *y'* axis, $M_{y'} = M_y \cos\varphi \approx M_y$, hence:

$$E\,I_y \frac{d^2 w(x)}{dx^2} + M_y = 0. \tag{3.108}$$

For bending around the *z'* axis, considering $M_{z'} = M_y \sin\varphi \approx \varphi M_y$, the following equation is obtained:

$$EI_z \frac{d^2 v(x)}{dx^2} + \varphi(x) M_y = 0. \tag{3.109}$$

For torsion around the *x'* axis, using equation (3.35) (differential equation for non-uniform torsion) and considering $T = M_y \sin(dv/dx) \approx M_y (dv/dx)$:

$$EI_w \frac{d^3 \varphi(x)}{dx^3} - G\,I_T \frac{d\varphi(x)}{dx} + M_y \frac{dv(x)}{dx} = 0. \tag{3.110}$$

Equation (3.108) is the usual differential equation for major-axis bending and depends only on the vertical displacement of the beam, *w*(*x*). Equations (3.109) and (3.110) are coupled. Differentiating equation (3.110) once with respect to *x* and replacing $d^2 v(x)/dx^2$ from equation (3.109), the following differential equation is obtained:

$$EI_w \frac{d^4 \varphi(x)}{dx^4} - G\,I_T \frac{d^2 \varphi(x)}{dx^2} + \frac{M_y^2}{E\,I_z} \varphi(x) = 0, \tag{3.111}$$

where $\varphi(x)$ is the rotation of a cross section at a distance *x* from the origin, around the axis of the beam. The solution of this fourth order differential equation, with constant coefficients, is of the type:

$$\varphi(x) = D_1 \sin mx + D_2 \cos mx + D_3 e^{nx} + D_4 e^{-nx}, \tag{3.112}$$

with

$$m = \sqrt{-a + \sqrt{a^2 + b}};\ n = \sqrt{a + \sqrt{a^2 + b}};\ a = \frac{G\,I_T}{2E\,I_w};\ b = \frac{M_y^2}{E\,I_z E\,I_w}, \tag{3.113}$$

where m and n are positive real quantities. Constants D_1, D_2, D_3 and D_4 in equation (3.112) are obtained from the boundary conditions of the problem. The cross sections at the supports cannot rotate around the axis of the beam and therefore $\varphi(x=0) = \varphi(x=L) = 0$. Since these sections are free to warp, moments M_{top} or M_{bot} (see Figure 3.38) do not develop. Considering $M_{top} = M_{bot} = 0$ in equation (3.28) and differentiating equation (3.29) twice, it is concluded that $\varphi''(x=0) = \varphi''(x=L) = 0$. Introducing the boundary conditions $\varphi(x=0) = \varphi''(x=0) = 0$ in equation (3.111), gives:

$$D_2 = 0;\quad D_3 = -D_4. \tag{3.114}$$

The conditions $\varphi(x=L) = \varphi''(x=L) = 0$ lead to the system of equations:

$$\begin{aligned} D_1 \sin mL - 2D_4 \sinh nL &= 0 \\ D_1\, m^2 \sin mL + 2D_4 n^2 \sinh nL &= 0. \end{aligned} \tag{3.115}$$

In order to obtain a non-trivial solution (D_1 and D_4 non-simultaneously equal zero), the determinant of the system of equations (3.115) must vanish, that is:

$$(\sin mL)(\sinh nL)(2m^2 + 2n^2) = 0. \tag{3.116}$$

As m and n are positive real quantities and as $\sinh nL = 0$ only if $nL = 0$, to obtain a non-trivial solution it is necessary that:

$$\sin mL = 0. \tag{3.117}$$

The lowest solution to equation (3.117) is given by $m = \pi / L$. Using the first of the equations (3.113), yields:

$$-a + \sqrt{a^2 + b} = \left(\frac{\pi}{L} \right)^2 . \tag{3.118}$$

Finally, introducing in equation (3.118) the values of *a* and *b* from equation (3.113), the critical value of the moment M_y, denoted as M_{cr}^E (critical moment of the "standard case") is obtained:

$$M_{cr}^E = \frac{\pi}{L} \sqrt{G\, I_T\, E\, I_z \left(1 + \frac{\pi^2 E\, I_w}{L^2\, G\, I_T} \right)}, \tag{3.119}$$

where*:*

I_z is the second moment of area in relation to *z* axis (weak axis),

I_T is the torsion constant,

I_w the warping constant,

L is the length between laterally braced cross sections of the beam and

E and G are the longitudinal modulus and the shear modulus of elasticity, respectively.

Equation (3.119), in spite of being derived for a member with an I or H cross section, is valid for members with other doubly symmetric cross sections.

The constant of uniform torsion I_T and the warping constant I_w for standard cross sections are usually supplied by steel producers, in tables of profiles. Alternatively, they can be obtained from Tables 3.2 and A.1 of Annex A.1.

By inspection of equation (3.119), it is observed that the critical moment of a member under bending depends on several factors, such as:

- loading (shape of the bending moment diagram);
- support conditions;
- length of the member between laterally braced cross sections;
- lateral bending stiffness;
- torsion stiffness;
- warping stiffness.

Besides these factors, the point of application of the loading also has a direct influence on the elastic critical moment of a beam. A gravity load applied below the shear centre C (that coincides with the centroid, in case of doubly symmetric I or H sections) has a stabilizing effect ($M_{cr,1}>M_{cr}$), whereas the same load applied above this point has a destabilizing effect ($M_{cr,2}<M_{cr}$), as illustrated in Figure 3.63. The calculation of the critical moment for design of a beam must also incorporate this effect.

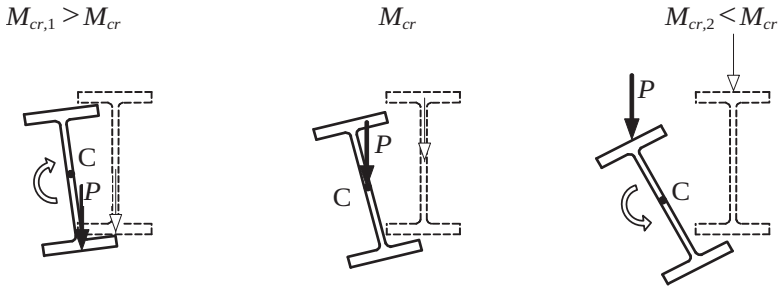


Figure 3.63 – Effect of the point of load's application

Equation (3.119) is valid for the calculation of the elastic critical moment of a simply supported beam, with a doubly symmetric cross section and subjected to a constant bending moment (the "standard case"). However, in reality, other situations often occur, such as beams with non-symmetrical cross sections, with other support conditions, subject to different loading patterns and, consequently, subject to different bending moment diagrams. The derivation of an exact expression for the critical moment for each case is not practical, as this implies the computation of differential equations of some complexity. Therefore, in practical applications approximate formulae are used, which are applicable to a wide set of situations. For the estimation of the elastic critical moment in situations not covered in this book, the user is advised to look at specific bibliography (Trahair, 1993; Boissonnade *et al*, 2006; Hirt *et al*, 2006) or to use other types of computational processes such as the finite element method.

According to Clark and Hill (1960) and Galéa (1981), the elastic critical moment can be estimated using equation (3.120). This is applicable to members subject to bending about the strong axis, with cross sections mono-symmetric about the weak *z* axis (see Figure 3.64), for several support conditions and types of loading.

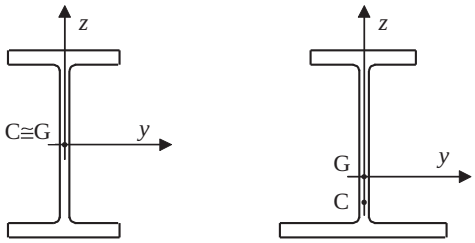


Figure 3.64 – Sections mono-symmetric about the weak axis

$$M_{cr} = C_1 \frac{\pi^2 E I_z}{\left(k_z L\right)^2} \left\{ \begin{array}{l} \left[\left(\frac{k_z}{k_w} \right)^2 \frac{I_w}{I_z} + \frac{\left(k_z L\right)^2 G I_T}{\pi^2 E I_z} + \left(C_2 z_g - C_3 z_j\right)^2 \right]^{0.5} \\ -\left(C_2 z_g - C_3 z_j\right) \end{array} \right\}, \qquad (3.120)$$

where,

C_1, C_2 and C_3 are coefficients depending on the shape of the bending moment diagram and on support conditions, given in Tables 3.4 and 3.5 for some usual situations (Boissonnade *et al*, 2006); in the Tables 3.4 and 3.5 the support conditions are those of the "standard case", however, lateral bending restraints and warping restraints may be taken into account through the parameters k_z and k_w described below;

k_z and k_w are effective length factors that depend on the support conditions at the end sections. Factor k_z is related to rotations at the end sections about the weak axis *z*, and k_w refers to warping restriction in the same cross sections. These factors vary between 0.5 (restrained deformations) and 1.0 (free deformations), and are equal to 0.7 in the case of free deformations at one end and restrained at the other. Since in most practical situations restraint is only partial, conservatively a value of $k_z = k_w = 1.0$ may be adopted;

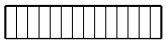
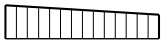
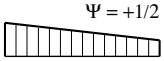
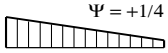
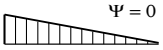
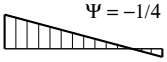
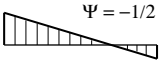
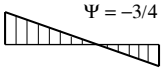
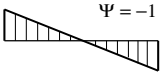
$z_g = \left(z_a - z_s\right)$, where z_a and z_s are the coordinates of the point of application of the load and of the shear centre, relative to the centroid of the cross section; these quantities are positive if located in the compressed part and negative if located in the tension part;

$z_j = z_s - \left(0.5 \int_A \left(y^2 + z^2\right)\left(z / I_y\right) dA \right)$ is a parameter that reflects the degree of asymmetry of the cross section in relation to the *y* axis. It is zero for

beams with doubly symmetric cross section (such as I or H cross sections with equal flanges) and takes positive values when the flange with the largest second moment of area about *z* is the compressed flange, at the cross section with maximum bending moment;

The remaining factors have the previous defined meanings.

Table 3.4 – Coefficients C_1 and C_3 for beams with end moments

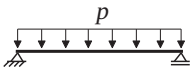
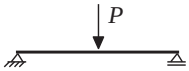
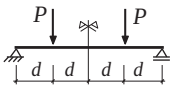
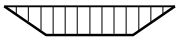
Loading and support conditions	Diagram of moments	k_z	C_1	C_3	
				$\psi_f \le 0$	$\psi_f > 0$
	Ψ = +1 	1.0 0.5	1.00 1.05	1.000 1.019	
	Ψ = +3/4 	1.0 0.5	1.14 1.19	1.000 1.017	
	Ψ = +1/2 	1.0 0.5	1.31 1.37	1.000 1.000	
	Ψ = +1/4 	1.0 0.5	1.52 1.60	1.000 1.000	
	Ψ = 0 	1.0 0.5	1.77 1.86	1.000 1.000	
	Ψ = −1/4 	1.0 0.5	2.06 2.15	1.000 1.000	0.850 0.650
	Ψ = −1/2 	1.0 0.5	2.35 2.42	1.000 0.950	$1.3 - 1.2\,\psi_f$ $0.77 - \psi_f$
	Ψ = −3/4 	1.0 0.5	2.60 2.45	1.000 0.850	$0.55 - \psi_f$ $0.35 - \psi_f$
	Ψ = −1 	1.0 0.5	2.60 2.45	$-\psi_f$ $-0.125 - 0.7\,\psi_f$	$-\psi_f$ $-0.125 - 0.7\,\psi_f$

- In beams subject to end moments, by definition $C_2 z_g = 0$.
- $\psi_f = \dfrac{I_{fc} - I_{ft}}{I_{fc} + I_{ft}}$, where I_{fc} and I_{ft} are the second moments of area of the compression and tension flanges respectively, relative to the weak axis of the section (z axis);
- C_1 must be divided by 1.05 when $\dfrac{\pi}{k_w L}\sqrt{\dfrac{EI_w}{GI_T}} \le 1.0$, but $C_1 \ge 1.0$.

In case of mono-symmetric I or H cross sections, Tables 3.4 and 3.5 must only be used if the following condition is verified: $-0.9 \leq \psi_f \leq 0.9$.

In practical applications, it is often necessary to calculate the elastic critical moment in beams or beams segments with bending moment distributions resulting from the combined effect of transverse loads applied along the segment and end moments (e.g. a span of a continuous beam).

Table 3.5 – Coefficients C_1, C_2 and C_3 for beams with transverse loads

Loading and support conditions	Diagram of moments	k_z	C_1	C_2	C_3
		1.0 0.5	1.12 0.97	0.45 0.36	0.525 0.478
		1.0 0.5	1.35 1.05	0.59 0.48	0.411 0.338
		1.0 0.5	1.04 0.95	0.42 0.31	0.562 0.539

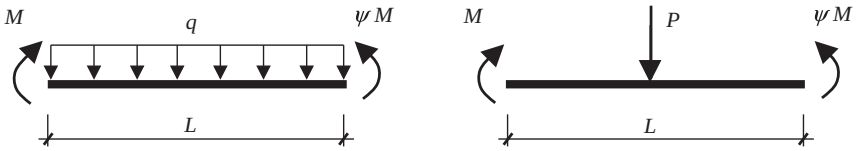
In the case of beams with double symmetrical cross section, subject to end moments combined with uniform distributed loads or point loads applied in mid-span (as shown in Figure 3.65), Boissonade *et al* (2006) includes a set of abacus (reproduced in Annex B.1.1) that provide the coefficients C_1 and C_2, necessary to calculate the elastic critical moment using equation (3.120).

In these abacus, coefficients C_1 and C_2 are calculated depending on the parameters ψ and μ. ψ is the ratio between the end moments evaluated so that $-1.0 \leq \psi \leq 1.0$, where M is the maximum moment in absolute value. μ is the ratio between the maximum moment due to the transverse load (assuming zero moments at the end sections) and M is the maximum end moment, given by the following equations for an uniformly distributed load and a concentrated load at mid-span, respectively:

$$\mu = \frac{q L^2}{8M}, \tag{3.121}$$

$$\mu = \frac{P\,L}{4M}. \tag{3.122}$$

It is noted that in the calculation of μ, the moments are taken with their algebraic value, so that $\mu > 0$ if M and the transverse load (q or P) lead to a bending curvature in the same direction (as shown in Figure 3.65); otherwise $\mu < 0$.



a) Uniformly distributed load b) Point load at mid span

Figure 3.65 – Beams with end moments and transverse loads

Equation (3.120) also allows to estimate the elastic critical moment of beams with other support or loading conditions, including cantilever beams. In the latter case, the coefficients C_1, C_2, C_3, k_z and k_w should be taken from Annex B.1.2.

In the case of a continuous beam with an overhang, the restraints at the supports are different from those of a fully fixed cross section. At the supports of the beam shown in Figure 3.66, although the rotation around the axis of the beam might be restrained, rotation by lateral bending and by warping will only be prevented if the beam in the adjacent span is infinitely rigid. As this generally does not happen, restraint to rotation by lateral bending and by warping at the supports should not be considered. Consequently, the critical moment of the segment comprising the overhang, subject to a concentrated load at the free end or under a linearly distributed load along its span, with the lateral displacement and rotation about beam axis restrained, can be estimated according to equations (3.123) and (3.124), respectively (Trahair, 1993).

$$M_{cr} = 6\frac{\sqrt{E\,I_z\,G\,I_T}}{L}\left[1+\frac{1.5\left(\varepsilon-0.1\right)}{\sqrt{1+2.25\left(\varepsilon-0.1\right)^2}}\right]+ 1.5\left(K-2\right)\frac{\sqrt{E\,I_z\,G\,I_T}}{L}\left[1+\frac{3\left(\varepsilon-0.3\right)}{\sqrt{1+9\left(\varepsilon-0.3\right)^2}}\right]; \tag{3.123}$$

$$M_{cr} = 15\frac{\sqrt{E\,I_z\,G\,I_T}}{L}\left[1+\frac{1.8\left(\varepsilon-0.3\right)}{\sqrt{1+3.24\left(\varepsilon-0.3\right)^2}}\right]+ \\ 4\left(K-2\right)\frac{\sqrt{E\,I_z\,G\,I_T}}{L}\left[1+\frac{2.8\left(\varepsilon-0.4\right)}{\sqrt{1+7.84\left(\varepsilon-0.4\right)^2}}\right], \tag{3.124}$$

where the parameters ε and K are defined by:

$$\varepsilon = \frac{2y_Q}{h_m}\frac{K}{\pi} \quad \text{and} \quad K = \sqrt{\frac{\pi^2 E\,I_w}{G\,I_T\,L^2}}, \tag{3.125}$$

and h_m is the distance between the centres of the flanges, see Figure 3.38, y_Q is the distance between the point of application of the loads and the centroid (in this case it coincides with the shear centre) and L is the distance between laterally braced sections. For gravity loads, the y_Q distance must be taken as negative or positive depending on the loads being applied above or below the shear centre. and the remaining symbols are as defined previously.

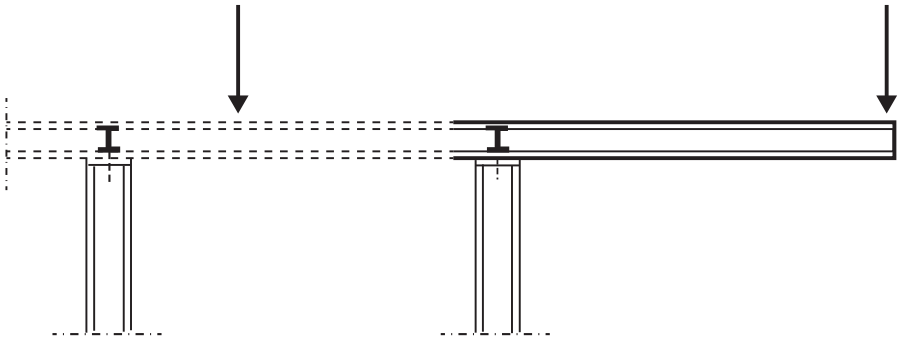


Figure 3.66 – Cantilever beam at the end of a continuous beam

Annex B.2 presents alternative equations for the calculation of the elastic critical moment.

Finally, it is noted that there are specific computer programs for the calculation of the elastic critical moment of beams under generic conditions such as LTBeamN (2015).

3.6.2.3 Effect of imperfections and plasticity

In the previous sub-section the elastic critical moment was obtained for an ideal member with constant bending moment (the "standard case"), and formulae were also presented, some exact and some approximate, for the calculation of the elastic critical moment in members with other support and/or loading conditions.

In the verification of the lateral-torsional buckling resistance, the effect of the following geometrical imperfections should be considered:

- the initial lateral displacements;
- the initial torsional rotations;
- the eccentricity of the transverse loads relative to the shear centre of the cross sections;
- residual stresses.

Due to the presence of geometrical imperfections the real behaviour of a member diverges from the theoretical behaviour and the elastic critical moment is never reached.

Considering the analogy between N_{cr} and M_{cr}, the lateral-torsional behaviour of beams in bending is similar to a compressed column. Therefore:

- The resistance of short members depends on the value of the cross section bending resistance (plastic or elastic bending moment resistance, depending of its cross section class).
- The resistance of slender members depends on the value of the critical moment (M_{cr}), associated with lateral-torsional buckling.
- The resistance of members with intermediate slenderness depends on the interaction between plasticity and instability phenomena.

The effect of geometrical imperfections may be introduced into the design procedure of a member under major axis bending in a similar way to that for design of a member under pure compression. Consider a single member with the end conditions of Figure 3.62 under pure bending $M_{y,Ed}$ constant along the span (the "standard case") and composed of a doubly-symmetric I or H cross section. Consider an initial lateral deformation of sinusoidal shape equivalent to the one represented by the equation (3.81)), with a maximum value $e_{0,d}$. Based on a second order elastic analysis

(Boissonnade *et al*, 2006), the buckling limit state may be defined by the first yield criterion of longitudinal stress as follows:

$$\frac{M_{y,Ed}}{M_{y,Rd}}+\frac{1}{\left(1-\dfrac{M_{y,Ed}^2}{M_{cr}^2}\right)}e_{0,d}\left(\frac{N_{cr,z}}{M_{z,Rd}}\frac{M_{y,Ed}^2}{M_{cr}^2}+\frac{N_{cr,z}^2}{M_{z,Rd}}\frac{h}{2}\frac{M_{y,Ed}}{M_{cr}^2}\right)\leq 1.0, \tag{3.126}$$

where M_{cr} is the elastic critical moment, $M_{y,Rd}$ and $M_{z,Rd}$ are the elastic bending moment resistances around y and z respectively, $N_{cr,z}$ is the elastic critical buckling load about the z axis and h is the depth of the cross section between flange centroids. In expression (3.126) the second and third terms represent the effect of the second order bending moments and the warping moments, respectively, due to the spatial member deformation (see Figure 3.62).

Setting $M_{y,Ed}$ equal to the lateral-torsional buckling resistance given by $\chi_{LT}M_{y,Rd}$, expression (3.126) yields the maximum value of the lateral imperfection $e_{0,d}$, as a function of the reduction factor χ_{LT}:

$$e_{0,d}=\frac{W_z}{A}\left(\frac{1}{\chi_{LT}}-1\right)\left(1-\chi_{LT}^2\overline{\lambda}_{LT}^4\right)\frac{\overline{\lambda}_z^2}{\overline{\lambda}_{LT}^4}\frac{1}{\chi_{LT}+\dfrac{A}{W_y}\dfrac{h}{2}\dfrac{1}{\overline{\lambda}_z^2}}, \tag{3.127}$$

where W_y and W_z are the elastic bending modulus about y and z, respectively, $\overline{\lambda}_z$ is the the slenderness for flexural buckling with respect to the z axis and $\overline{\lambda}_{LT}=\left(M_{y,Rk}/M_{cr}\right)^{0.5}$ is the slenderness for lateral-torsional buckling, where $M_{y,Rk}$ is the characteristic cross section bending resistance with respect to the y axis.

As for compressed members, residual stresses and other geometrical imperfections also affect the lateral-torsional resistance of beams. In a simplified way, all these imperfections are taken into account through the equivalent imperfection concept. The equivalent lateral imperfection given by equation (3.127) has an analogous meaning to that of equation (3.90) for flexural buckling, despite depending on different parameters. As a consequence, for lateral-torsional buckling, it is possible to define a similar

procedure to the one derived for flexural buckling under pure compression (expression (3.100)). To apply this procedure to the design of a member under pure bending it was necessary to calibrate the equivalent lateral imperfections for real members. Based on extensive numerical, experimental and parametric simulations (Boissonnade *et al*, 2006) it was concluded that the design of the majority of steel members (including members composed by rolled and welded I or H sections) could be done according to the European buckling curves, previously obtained for the design of members under pure axial compression. This is presented in the following section.

3.6.3. Lateral-torsional buckling resistance

The verification of resistance to lateral-torsional buckling of a prismatic member consists of the verification of the following condition (clause 6.3.2.1(1)):

$$\frac{M_{Ed}}{M_{b,Rd}} \leq 1.0, \tag{3.128}$$

where M_{Ed} is the design value of the bending moment and $M_{b,Rd}$ is the design buckling resistance, given by (clause 6.3.2.1(3)):

$$M_{b,Rd} = \chi_{LT}\, W_y\, f_y / \gamma_{M1}, \tag{3.129}$$

where:

$W_y = W_{pl,y}$ for class 1 and 2 cross sections;
$W_y = W_{el,y}$ for class 3 cross sections;
$W_y = W_{eff,y}$ for class 4 cross sections;
χ_{LT} is the reduction factor for lateral-torsional buckling.

In EC3-1-1 two methods for the calculation of the reduction coefficient χ_{LT} in prismatic members are proposed: a general method that can be applied to any type of cross section (more conservative) and an alternative method that can be applied to rolled cross sections or equivalent welded sections.

i) *General method*

According to the general method (clause 6.3.2.2), the reduction factor χ_{LT} is determined by the following equation:

$$\chi_{LT} = \frac{1}{\phi_{LT} + \left(\phi_{LT}^2 - \overline{\lambda}_{LT}^2 \right)^{0.5}}, \quad \text{but} \quad \chi_{LT} \leq 1.0, \tag{3.130}$$

with: $\phi_{LT} = 0.5\left[1 + \alpha_{LT}\left(\overline{\lambda}_{LT} - 0.2 \right) + \overline{\lambda}_{LT}^2 \right]$;

α_{LT} is the imperfection factor, which depends on the buckling curve;

$\overline{\lambda}_{LT} = \left[W_y f_y / M_{cr} \right]^{0.5}$;

M_{cr} the elastic critical moment.

The buckling curves to be adopted depend on the geometry of the cross section of the member and are indicated in Table 3.6. For the imperfection factors α_{LT} associated to the various curves, the values given in section 3.5.2 for members in compression should be adopted.

Table 3.6 – Buckling curves for lateral-torsional buckling (General method)

Section	Limits	Buckling curve
I or H sections rolled	$h/b \leq 2$	*a*
	$h/b > 2$	*b*
I or H sections welded	$h/b \leq 2$	*c*
	$h/b > 2$	*d*
Other sections	---	*d*

ii) *Alternative method – Rolled or equivalent welded sections*

According to this second method, defined in clause 6.3.2.3, the reduction factor χ_{LT} is determined by the following equation:

$$\chi_{LT} = \frac{1}{\phi_{LT} + \left(\phi_{LT}^2 - \beta\, \overline{\lambda}_{LT}^2 \right)^{0.5}}, \quad \text{but} \quad \begin{matrix} \chi_{LT} \leq 1.0 \\ \chi_{LT} \leq 1/\overline{\lambda}_{LT}^2 \end{matrix}, \tag{3.131}$$

with $\phi_{LT} = 0.5\left[1 + \alpha_{LT}\left(\overline{\lambda}_{LT} - \overline{\lambda}_{LT,0}\right) + \beta\,\overline{\lambda}_{LT}^{2}\right]$;

$\overline{\lambda}_{LT,0}$ and β are parameters to be defined in the National Annexes; the recommended values are: $\overline{\lambda}_{LT,0} \le 0.4$ (maximum value) and $\beta \ge 0.75$ (minimum value);

α_{LT} is the imperfection factor that depends on the appropriate buckling curve (defined as in the general method);

$\overline{\lambda}_{LT}$ the coefficient of non-dimensional slenderness (defined as in the general method);

M_{cr} the elastic critical moment.

The relevant buckling curves are indicated in Table 3.7.

Table 3.7 – Buckling curves for lateral-torsional buckling (Alternative method)

Section	Limits	Buckling curve (EC3-1-1)
I or H sections rolled	$h/b \le 2$	*b*
	$h/b > 2$	*c*
I or H sections welded	$h/b \le 2$	*c*
	$h/b > 2$	*d*

According to this second method, the shape of the bending moment diagram, between braced sections, can be taken into account by considering a modified reduction factor $\chi_{LT,\,mod}$:

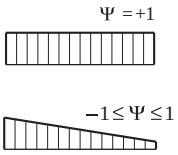
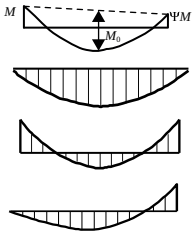
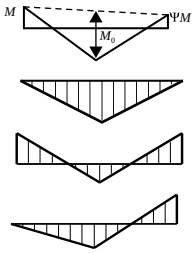
$$\chi_{LT,\mathrm{mod}} = \frac{\chi_{LT}}{f}, \quad \text{but} \quad \chi_{LT,\mathrm{mod}} \le 1.0. \tag{3.132}$$

The parameter *f* can be obtained from the following equation, or from an alternative process provided in the National Annexes:

$$f = 1 - 0.5\left(1 - k_c\right)\left[1 - 2.0\left(\overline{\lambda}_{LT} - 0.8\right)^{2}\right] \quad \text{but} \quad f \le 1.0, \tag{3.133}$$

where k_c is a correction factor, defined according to Table 3.8.

Table 3.8 – k_c correction factors

Diagram of bending moments	k_c
	1.0 $\frac{1}{1.33-0.33\Psi}$
	0.94 0.90 0.91
	0.86 0.77 0.82
Ψ - ratio between end moments, with -1 ≤ Ψ ≤ 1.	

In Table 3.8, three sets of bending moment diagrams are presented. The first refers to beam spans subject to concentrated bending moments applied in the extreme sections. The second set of diagrams may be induced by uniformly distributed load and moments in the extreme sections. For the third set, the diagrams correspond to central point loads and moments in the extreme sections. The support conditions are not relevant as they are reproduced in the bending moment diagrams. The values of k_c presented in Table 3.8 correspond to some typical situations; some are exact values and other are approximate. More detailed information on k_c values may be obtained from Boissonnade *et al* (2006).

iii) *Conditions for ignoring the lateral-torsional buckling verification*

The verification of lateral-torsional buckling for a member in bending may be ignored if at least one of the following conditions is verified: $\overline{\lambda}_{LT} \le \overline{\lambda}_{LT,0}$ or $M_{Ed} \big/ M_{cr} \le \overline{\lambda}^2_{LT,0}$ (clause 6.3.2.2(4)).

iv) *Methods for improving the lateral-torsional buckling resistance*

In practical situations, for given geometrical conditions, support conditions and assumed loading, the lateral-torsional buckling behaviour of a member can be improved in two ways:

- by increasing the lateral bending and/or torsional stiffness, by increasing the section or changing from IPE profiles to HEA or HEB or to closed hollow sections (square, rectangular or circular);
- by laterally bracing along the member the compressed part of the section (the compressed flange in the case of I or H sections).

Usually, the second option is more economical, although sometimes it is not feasible. The bracing members must connect the compressed zone of the cross sections with points with negligible transverse displacement.

Clause 6.3.2.4 presents a simplified methodology for the verification of lateral-torsional buckling in beams with discrete lateral restraint to the compression flange. This is based on the slenderness of that flange.

For non-prismatic members, the resistance to lateral-torsional buckling must be obtained according to clause 6.3.4, described in chapter 4.

3.6.4. Worked examples

Example 3.12: Consider the beam of example 3.4 (Figure 3.67), supported by web cleats and loaded by two concentrated loads, P = 70.0 kN (design loads). Design the beam using a HEA profile (and alternatively an IPE profile), in S 235 steel (E = 210 GPa and G = 81 GPa), according to EC3-1-1. Consider free rotation at the supports with respect to the y-axis and the z-axis. Also assume free warping at the supports but consider that the web cleats do not allow rotation around the axis of the beam (x axis). Assume:

a) unbraced beam;
b) beam braced at the points of application of the concentrated loads.

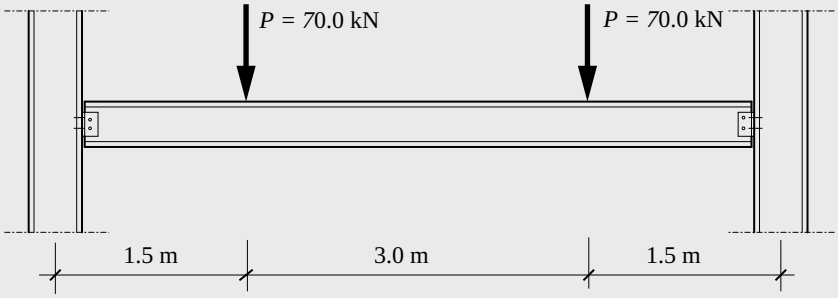


Figure 3.67 – Simply supported beam with two concentrated loads

i) *Diagrams of internal forces*

The internal forces diagrams are represented in the Figure 3.68.

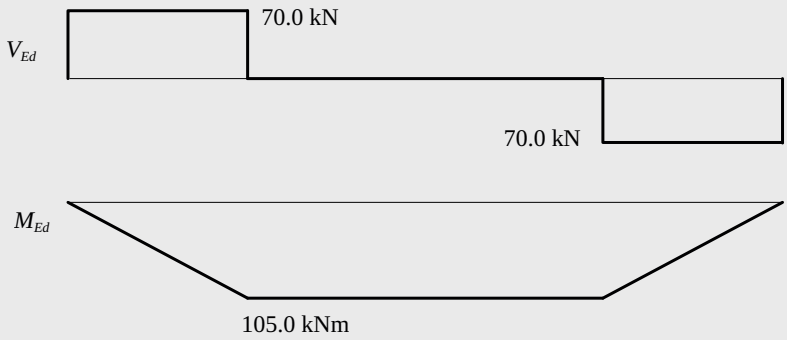


Figure 3.68 – Diagrams of internal forces

ii) *Bending and shear force*

In example 3.4, the verification of the cross section resistance to bending and shear force led to a HEA 220 with $W_{pl,y}$ = 568.5 cm^3 (or alternatively to a IPE 270 with $W_{pl,y}$ = 484 cm^3).

iii) *Lateral-torsional buckling without intermediate bracing*

iii-1) *General method*

Considering a HEA profile, a HEA 240 is adopted to allow for the effect of lateral-torsional buckling. The required geometric characteristics of this

cross section are: $W_{pl,y}$ = 744.6 cm^3, I_y = 7763 cm^4, I_z = 2769 cm^4, I_T = 41.55 cm^4 and I_w = 328.5 x 10^3 cm^6. The mechanical characteristics of the material are defined by: f_y = 235 MPa, E = 210 GPa and G = 81 GPa.

Since the support conditions correspond to the "standard case" and the loading is constituted by two concentrated loads, applied in the upper flange, the elastic critical moment can be obtained from equation (3.120). As L = 6.00 m, considering $k_z = k_w = 1.0$, C_1 = 1.04 and C_2 = 0.42 (Table 3.5), and z_g = 115 mm, equation (3.120) gives:

$$M_{cr} = 231.5 \text{ kNm} \qquad \Rightarrow \ \overline{\lambda}_{LT} = 0.87.$$

Since α_{LT} = 0.21 (H rolled section, with $h/b \le 2$),

$$\phi_{LT} = 0.95 \ \Rightarrow \ \chi_{LT} = 0.75.$$

The design buckling resistance is given by:

$$M_{b,Rd} = 0.75 \times 744.6 \times 10^{-6} \times \frac{235 \times 10^3}{1.0} = 131.2 \text{ kNm} > M_{Ed} = 105.0 \text{ kNm}.$$

Alternatively, using a IPE profile, a IPE 400 is required, giving a design buckling resistance of $M_{b,Rd}$ = 131.0 kNm.

The cross section class of a HEA 240 is obtained as follows (Table 2.21 and 2.22):

Web in bending, $\quad \frac{c}{t} = \frac{164}{7.5} = 21.9 < 72\varepsilon = 72 \times 1 = 72.0.$ (Class 1)

Flange in compression,

$$\frac{c}{t} = \frac{240/2 - 7.5/2 - 21}{12} = 7.9 < 9\varepsilon = 9 \times 1 = 9. \qquad \text{(Class 1)}$$

The HEA 240 is class 1 (IPE 400 is also class 1), confirming the use of $W_{pl,y}$.

iii-2) *Alternative method applicable to rolled or equivalent welded sections*

As the alternative method is less conservative, consider initially a HEA 220 profile in S 235 steel (pre-designed based on the cross section resistance). From L = 6.00 m, C_1 = 1.04, C_2 = 0.42, $k_z = k_w$ = 1.0, z_g = 105 mm, I_z = 1955 cm^4, I_T = 28.46 cm^4, I_w = 193.3 × 10^3 cm^6, $W_{pl,y}$ = 568.5 cm^3,

E = 210 GPa, G = 81 GPa and f_y = 235 MPa, the elastic critical moment, (equation (3.120)) is given by:

$$M_{cr} = 158.8 \text{ kNm} \quad \Rightarrow \quad \overline{\lambda}_{LT} = 0.92.$$

As α_{LT} = 0.34 (rolled H section, with $h/b \leq 2$),

$\phi_{LT} = 0.91 \Rightarrow \chi_{LT} = 0.74$, considering $\overline{\lambda}_{LT,0} = 0.4$ and β =0.75.

In addition, assuming k_c = 0.94 (approximate value, obtained from Table 3.8 for a beam span under a uniformly distributed load) $\Rightarrow f = 0.97$, giving $\chi_{LT,\text{mod}} = 0.76$.

The lateral-torsional buckling moment resistance is given by:

$$M_{b,Rd} = 0.76 \times 568.5 \times 10^{-6} \times \frac{235 \times 10^3}{1.0} = 101.5 \text{ kNm} < M_{Ed} = 105 \text{ kNm}.$$

Consequently, even with a less conservative method, the HEA 220 is not a solution to the problem. Using the alternative method, the HEA 240 profile gives $M_{b,Rd}$ = 140.2 kNm. By using an IPE profile, an IPE 360 would be sufficient, with a lateral-torsional buckling resistance of $M_{b,Rd}$ = 111.8 kNm. A HEA 240 and an IPE 360 are both class 1 in bending.

iv) *Lateral-torsional buckling with intermediate restraints*

If the beam is laterally braced at the points of application of the loads (through secondary beams or other devices that prevent the lateral displacement of the compressed flange and, consequently, the rotations of those sections around the axis of the beam), the lateral-torsional buckling behaviour is improved. The problem now consists on the evaluation of the resistance to lateral-torsional buckling of a beam segment 3.00 m long, under a constant bending moment (M_{Ed} = 105.0 kNm), as shown in Figure 3.69. The elastic critical moment of the beam is not aggravated by the fact that the loads are applied at the upper flange, because these are applied at sections that are laterally restrained.

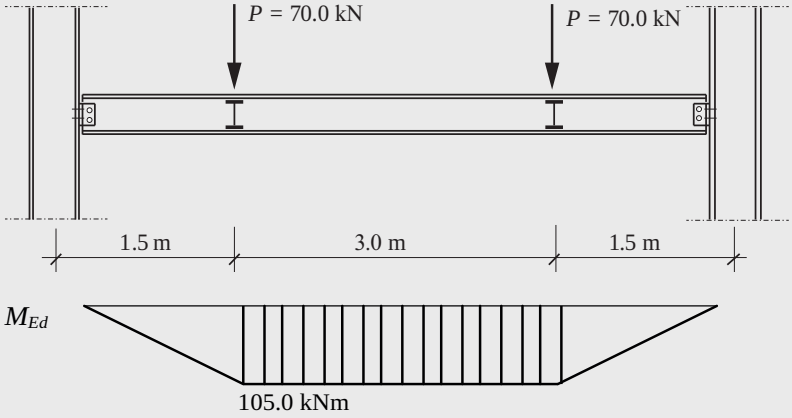


Figure 3.69 – Laterally braced beam

iv-1) *General method*

For the HEA 220 profile in S 235 steel (minimum section, governed by plastic resistance to bending), with L = 3.00 m, C_1 = 1.0, $k_z = k_w$ = 1.0, I_z = 1955 cm^4, I_T = 28.46 cm^4, I_w = 193.3 × 10^3 cm^6, $W_{pl,y}$ = 568.5 cm^3, E = 210 GPa, G = 81 GPa and f_y = 235 MPa, the elastic critical moment (equation (3.120) is given by:

$$M_{cr} = 551.3 \text{ kNm} \quad \Rightarrow \quad \overline{\lambda}_{LT} = 0.49.$$

As α_{LT} = 0.21 (rolled H section, with $h/b \leq 2$),

$$\phi_{LT} = 0.65 \;\Rightarrow\; \chi_{LT} = 0.93\,.$$

The lateral-torsional buckling resistance is given by:

$$M_{b,Rd} = 0.93 \times 568.5 \times 10^{-6} \times \frac{235 \times 10^3}{1.0} = 124.2 \text{ kNm} > M_{Ed} = 105.0 \text{ kNm},$$

and a HEA 220 is adequate. By using a profile from the IPE series, an IPE 300 is sufficient, with a lateral-torsional buckling resistance given by $M_{b,Rd}$ = 120.2 kNm. Both sections, in S 235 steel, are class 1.

iv-2) *Alternative method applicable to rolled or equivalent welded sections*

The application of this method leads to the same solution, with $M_{b,Rd}$ = 128.9 kNm for a HEA 220 and $M_{b,Rd}$ = 123.3 kNm for a IPE 300 profile.

v) *Final considerations*

By adding the verification of the deformation limit state, carried out in example 3.4, Table 3.9 summarizes the several possibilities for the design of the beam.

Table 3.9 – Summary table

Criteria	Unbraced beam	Braced beam
Cross section resistance	HEA 220 or IPE 270	
LTB (General method)	HEA 240 or IPE 400	HEA 220 or IPE 300
LTB (Alternative method)	HEA 240 or IPE 360	HEA 220 or IPE 300
Deformations	HEA 240 or IPE 300	
Solution	HEA 240 or IPE 360	HEA 240 or IPE 300

Example 3.13: Design the beam represented in Figure 3.70, using an IPE section in S 355 steel (E = 210 GPa and G = 81 GPa). Assume that the loading is already factored for ULS. Consider that the beam is free to rotate around its principal axes at sections A and C and also free to warp; also consider however that sections A, B, C and D are restrained from rotating around the axis of the beam (laterally braced sections by the secondary beams).

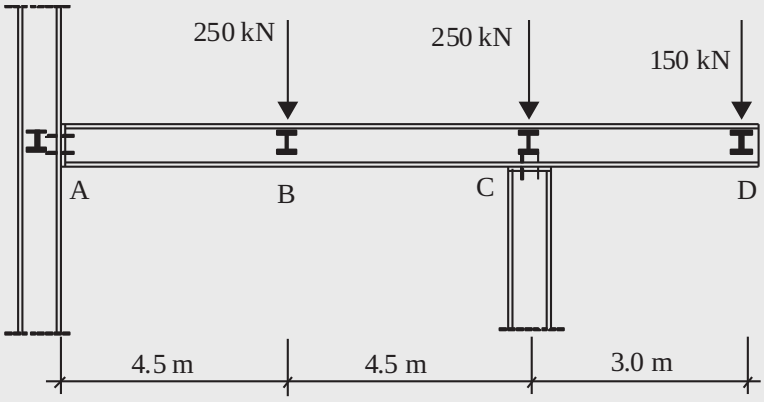


Figure 3.70 – Continuous beam with a cantilever span

i) *Diagrams of internal forces*

Figure 3.71 illustrates the internal force diagrams.

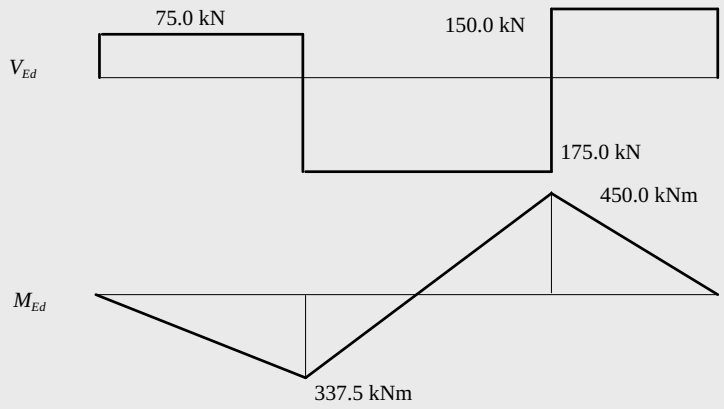


Figure 3.71 – Diagrams of internal forces

ii) *Resistance to bending and transverse shear*

Preliminary design for bending, assuming class 1 or 2 cross sections, gives:

$$M_{Ed} = 450\ \text{kNm} \le W_{pl,y} f_y / \gamma_{M0} = W_{pl,y} \times 355 \times 10^3 / 1.0$$

$$\Rightarrow W_{pl,y} \ge 1267.6 \times 10^{-6}\ \text{m}^3 = 1267.6\ \text{cm}^3.$$

From a table of commercial profiles, an IPE 450 is adopted, with $W_{pl,y} = 1702\ \text{cm}^3$.

Verification of the cross section class (Table 2.21 and 2.22):

Web in bending,

$$c/t = 378.8/9.4 = 40.3 < 72\varepsilon = 72 \times 0.81 = 58.3. \qquad \text{(Class 1)}$$

Compressed flange,

$$\frac{c}{t} = \frac{190/2 - 9.4/2 - 21}{14.6} = 4.7 < 9\varepsilon = 9 \times 0.81 = 7.3. \qquad \text{(Class 1)}$$

As both parts are class 1, the cross section is class 1.

The resistance to transverse shear leads to (shear area $A_v = 50.85\ \text{cm}^2$):

$$V_{Ed} = 175 \text{ kN} < V_{pl,Rd} = \frac{A_v f_y}{\gamma_{M0}\sqrt{3}} = \frac{50.85 \times 10^{-4} \times 355 \times 10^3}{1.0 \times \sqrt{3}} = 1042.2 \text{ kN}.$$

The verification of the shear buckling of the (unstiffened) web (clause 6.2.6(6)), conservatively considering η =1, is not required, since:

$$\frac{h_w}{t_w} = \frac{420.8}{9.4} = 44.8 < 72\frac{\varepsilon}{\eta} = 72 \times \frac{0.81}{1.0} = 58.3.$$

The interaction between bending moment and transverse shear must be verified at section C (left). However, according to clause 6.2.8,

$$V_{Ed} = 175.0 \text{ kN} < 0.50 \times V_{pl,Rd} = 0.50 \times 1042.2 = 521.1 \text{ kN},$$

it is not necessary to reduce the bending moment resistance.

iii) *Lateral-torsional buckling*

Lateral-torsional buckling is verified by the general method proposed in clause 6.3.2.2. According to the restraint conditions at sections A to D, three segments have to be considered. Examination of the shape and the maximum values of the bending moment diagrams, no segment should be excluded from the verification of lateral-torsional buckling. The elastic critical moments are calculated using equation (B.1) (they could equally be obtained from equation (3.120)). It is noted that for segment CD equations (3.123) and (3.124) are not applicable because they assume that the free end of the cantilever does not have restrictions to lateral bending and to warping.

The required geometrical characteristics of a IPE 450 are the following: I_z = 1676 cm^4, I_T = 66.87 cm^4, I_w = 791 x 10^3 cm^6 and $W_{pl,y}$ = 1702 cm^3. The mechanical properties of S 355 steel are: f_y = 355 MPa, E = 210 GPa and G = 81 GPa.

Segment A-B

Equation (B.1), yields:

$$\beta = 0.00 \Rightarrow \alpha_m = 1.75 \quad \Rightarrow M_{cr} = 842.5 \text{ kNm} \quad \Rightarrow \bar{\lambda}_{LT} = 0.85.$$

As α_{LT} = 0.34 (rolled I section, with $h/b > 2$),

$\phi_{LT} = 0.97 \Rightarrow \chi_{LT} = 0.70.$

The lateral-torsional buckling moment resistance is given by:

$$M_{b,Rd} = 0.70 \times 1702 \times 10^{-6} \times \frac{355 \times 10^3}{1.0} = 422.9 \text{ kNm}.$$

so that

$M_{b,Rd} = 422.9 \text{ kNm} > M_{Ed} = 337.5 \text{ kNm}.$

Segment B-C

According to Table B.5, $\beta = 337.5/450 = 0.75 \Rightarrow \alpha_m = 2.71$. As α_m must be smaller than or equal to 2.5, α_m = 2.50; equation (B.1) yields:

$M_{cr} = 1203.6 \text{ kNm} \Rightarrow \bar{\lambda}_{LT} = 0.71.$

As $\alpha_{LT} = 0.34$ (rolled I section, with $h/b > 2$),

$\phi_{LT} = 0.84 \Rightarrow \chi_{LT} = 0.78.$

The lateral-torsional buckling moment resistance is given by:

$$M_{b,Rd} = 0.78 \times 1702 \times 10^{-6} \times \frac{355 \times 10^3}{1.0} = 471.3 \text{ kNm},$$

so that

$M_{b,Rd} = 471.3 \text{ kNm} > M_{Ed} = 450.0 \text{ kNm}.$

Segment C-D

Equation (B.1) yields:

$\beta = 0.00 \Rightarrow \alpha_m = 1.75 \Rightarrow M_{cr} = 1671.4 \text{ kNm} \Rightarrow \bar{\lambda}_{LT} = 0.60.$

As $\alpha_{LT} = 0.34$ (rolled I section, with $h/b > 2$),

$\phi_{LT} = 0.75 \Rightarrow \chi_{LT} = 0.83.$

The lateral-torsional buckling moment resistance is given by:

$$M_{b,Rd} = 0.83 \times 1702 \times 10^{-6} \times \frac{355 \times 10^3}{1.0} = 501.5 \text{ kNm},$$

and

$$M_{b,Rd} = 501.5 \text{ kNm} > M_{Ed} = 450.0 \text{ kNm}.$$

It can be concluded that the IPE 450 section in S 355 steel is satisfactory.

Example 3.14: Consider the frame of a catwalk ilustrated in Figure 3.72 composed by one column and one beam, both members with the same cross section. The beam is simple supported at the left end and connected to the column by a rigid joint at right end; the column is double supported at the base. The design loading is composed by a vertical uniform distributed load of 12 kN/m applied at the top flange level and a horizontal point load of 20 kN applied at section B. Design the beam A-B for the ultimate limite state of resistance and stability, using an IPE section in steel S 275, assuming that the cross sections A and B are laterally braced by the secondary beams.

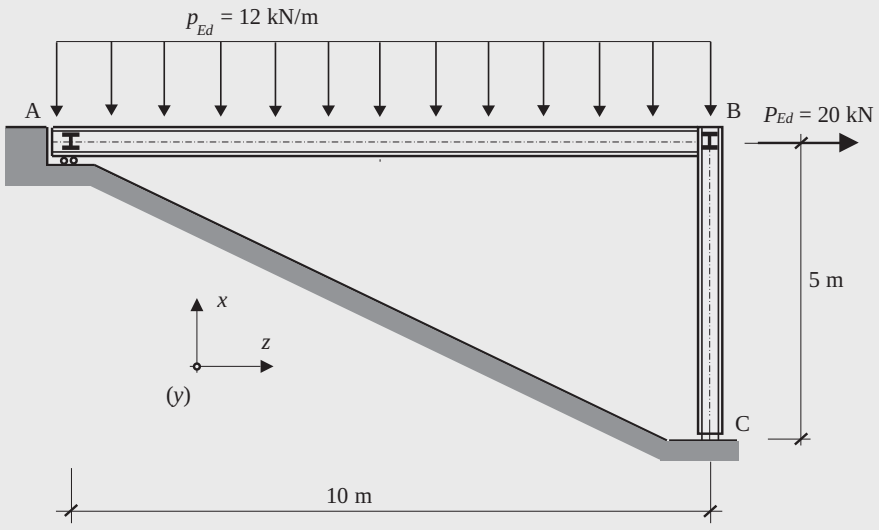


Figure 3.72 – Frame of a catwalk (vertical cut)

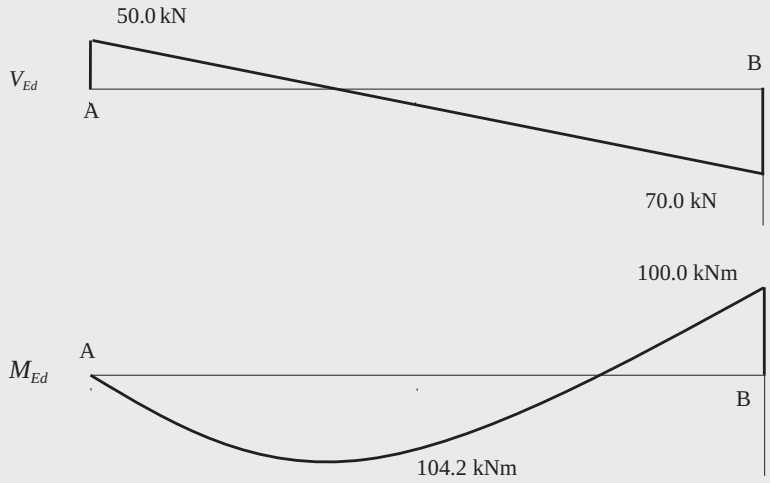


Figure 3.73 – Design internal forces for beam A-B with 10 m span

i) *Design of internal forces*

From Figure 3.73, the design values of shear force and bending moment are the followings: V_{Ed} = 70.0 kN and M_{Ed} = 100 kNm at end section B and M_{Ed} = 104.2 kNm in a section with V_{Ed} = 0.0 along the span.

ii) *Verification of the bending and shear force cross section resistance*

Assuming that the class of the cross section is 1 or 2, the required plastic modulus of the cross section is given by:

$$M_{Ed} = 104.2 \text{ kNm} \le W_{pl,y} f_y / \gamma_{M0} = W_{pl,y} \times 275 \times 10^3 / 1.0$$

$$\Rightarrow \; W_{pl,y} \ge 378.9 \times 10^{-6} \text{m}^3 = 378.9 \text{ cm}^3 .$$

This leads to a IPE 270 section with $W_{pl,y}$ = 484.0 cm^3. Since the beam is long and braced only at the ends, lateral-torsional buckling will probably be the critical failure mode. By trial and error, according to the calculations performed in iii), a IPE 450 with $W_{pl,y}$ = 1702 cm^3 is adopted.

Verification of the cross section class (according to clause 5.5 of EC3-1-1)

Web of the section in bending (Table 2.21)

$$\frac{c}{t} = \frac{378.8}{9.4} = 40.3 < 72\varepsilon = 72 \times 0.92 = 66.2 \,. \qquad \text{(Class 1)}$$

Compressed flange of the section (Table 2.22)

$$\frac{c}{t} = \frac{190/2 - 9.4/2 - 21}{14.6} = 4.7 < 9\varepsilon = 9 \times 0.92 = 8.3 \,. \qquad \text{(Class 1)}$$

As both parts are class 1, the cross section is class 1.

The shear area is given by A_v = 50.85 cm^2, leading to (clause 6.2.6):

$$V_{Ed} = 70.0 \text{ kN} < V_{pl,Rd} = \frac{A_v f_y}{\gamma_{M0}\sqrt{3}} = \frac{50.85 \times 10^{-4} \times 275 \times 10^3}{1.0 \times \sqrt{3}} = 807.4 \text{ kN} \,.$$

The verification of the web buckling (without stiffeners) by shear force (according to clause 6.2.6 (6) of EC3-1-1), considering conservatively η = 1 may be neglected, since:

$$\frac{h_w}{t_w} = \frac{420.8}{9.4} = 44.8 < 72\frac{\varepsilon}{\eta} = 72 \times \frac{0.92}{1.0} = 66.2 \,.$$

The interaction between the bending moment and the shear force at the right end of the beam may be disregarded, as:

$$V_{Ed} = 70.0 \text{ kN} < 0.50 \times V_{pl,Rd} = 0.50 \times 807.4 = 403.7 \text{ kN} \,,$$

iii) *Lateral torsional buckling verification*

In this example lateral torsional buckling is verified by the general method (clause 6.3.2.2). Assuming free lateral bending and free warping at the end sections, the elastic critical moment may be evaluated using equation (3.120), calculating the cofficients C_1 and C_2, using Annex B.1.1.

The main geometric characteristics of the pre-designed section (IPE 450) are the following: I_z = 1676 cm^4, I_T = 66.87 cm^4, I_w = 791 x 10^3 cm^6 and $W_{pl,y}$ = 1702 cm^3. The main mechanical properties of the steel S 275 are: f_y = 275 MPa, E = 210 GPa and G = 81 GPa.

Based on the bending moment diagram illustrated in Figure 3.73, ψ = 0.0; from equation (3.121), the parameter μ (with a negative value) is given by:

$$\mu = \frac{qL^2}{8M} = \frac{12 \times 10^2}{8 \times \left(-100.0\right)} = -1.50 .$$

From figures B2 and B4 of Annex B, $C_1 \approx 1.20$ and $C_2 \approx 0.70$ are obtained respectively.

From equation (3.120), with L = 10 m, considering $k_z = k_w = 1.0$ and z_g = 225 mm, it follows that:

$$M_{cr} = 133.4 \text{ kNm} \quad \Rightarrow \overline{\lambda}_{LT} = 1.87.$$

It is noted that a similar value of M_{cr} could be obtained using either the software LTBeam on the ECCS Steel Member Calculator.

As α_{LT} = 0.34 (I rolled section, with $h/b > 2$), the reduction factor χ_{LT} is given by:

$$\phi_{LT} = 2.53 \;\Rightarrow\; \chi_{LT} = 0.24 .$$

The design value of the resistant moment to lateral buckling is given by:

$$M_{b,Rd} = 0.24 \times 1702 \times 10^{-6} \times \frac{275 \times 10^3}{1.0} = 112.3 \text{ kNm} .$$

As $M_{b,Rd} = 112.3 \text{ kNm} > M_{Ed} = 104.2 \text{ kNm}$, the section IPE 450 in steel S 275 satisfies safety at ULS.

Based in this example, it is verified that the difference between the smaller section necessary to satisfy cross section resistance (IPE 270 section) and the smaller section necessary to satisfy lateral stability (IPE 450 section), in a beam with high slenderness, submitted to a descending load applied at the top flange level is very large.

From an economic point of view, it would certainly be advantageous to introduce lateral bracings (if possible) in one or more intermediate cross sections along the beam; with this option, the slendernesss could be reduced and consequentelly increase the resistance of the beam to lateral buckling, and in the limit, the section IPE 270 might be sufficient. Nevertheless, if the beam was laterally braced at some intermediate cross sections, the SLS (deformation or even vibration), might become the governing design condition.

3.7. BEAM-COLUMNS

3.7.1. Introduction

Figure 3.74 shows examples of members subject to bending and axial force. The behaviour of such members results from the combination of both effects and varies with slenderness. At low slenderness, the cross sectional resistance dominates. With increasing slenderness, pronounced second-order effects appear, significantly influenced by both geometrical imperfections and residual stresses. Finally, in the high slenderness range, buckling is dominated by elastic behaviour, failure tending to occur by flexural buckling (typical of members in pure compression) or by lateral-torsional buckling (typical of members in bending) (Boissonnade *et al*, 2006).

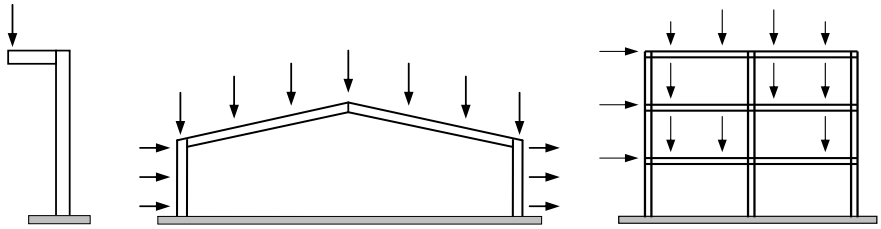


Figure 3.74 – Steel members subjected to bending and axial force

The behaviour of a member under bending and axial force results from the interaction between instability and plasticity and is influenced by geometrical and material imperfections. The behaviour is therefore very complex, a thorough explanation being outside the scope of this book. An excellent and detailed overview of the behaviour of beam-columns and the background to the interaction stability rules presented in EC3-1-1 can be found in Boissonnade *et al* (2006). The verification of the safety of members subject to bending and axial force is made in two steps:

- Verification of the resistance of cross sections.
- Verification of the member buckling resistance (in general governed by flexural or lateral-torsional buckling).

These two aspects are treated in the following sections.

3.7.2. Classification of cross sections under bending and axial force

The classification of a cross section based on EC3-1-1 is strictly not performed with respect to an applied loading, but instead to an equivalent loading, that corresponds to its full elastic or plastic capacity. This concept is of simple application for double-symmetric sections under pure compression or pure bending, because, whatever the values of the applied loading, the shape of the normal stresses diagram in the section (corresponding to its full capacity) and the corresponding position of the neutral axis remain the same. The same is not the case for a section under bending and axial force, because it is possible to define a multitude of strategies of load incrementation for M and N to reach the cross sectional resistance, as referred already in sub-chapter 2.4. Detailed guidance for the classification of cross sections subject to bending and axial free is presented in this section, closely following the guidance from the RFCS research project Semi-Comp + (Greiner *et al*, 2011).

The classification of a section is performed by comparing the relation c/t of several parts of the section with the limits defined in Tables 2.21 to 2.23. In the presence of bending moments and axial force, the section should be classified for the set of applied of loads, but increased until the section reaches its capacity (elastic or plastic, according to the class) in terms of resistance to normal stresses.

The limits between class 3 and class 4 can be established from the normal stresses diagram, evaluated on the basis of the applied loading (N_{Ed} + $M_{y,Ed}$ + $M_{z,Ed}$) using equation (3.134), since the elastic neutral axis and the necessary parameters to define the shape of the normal stresses diagram (such as parameter ψ, defined in Table 2.21) remain constant whenever the applied loading is proportionally increased.

$$\sigma = \frac{N_{Ed}}{A} + \frac{M_{y,Ed}}{I_y} z - \frac{M_{z,Ed}}{I_z} y \,, \tag{3.134}$$

where A, I_y e I_z represent the area and the moments of inertia of the cross section.

Figure 3.75 represents the elastic normal stresses diagram for the generic case of biaxial bending and axial force (sign convention according to EC3-1-1), from which the classification limits for the boundary between

class 3 and class 4 may be obtained. In this figure the definition of the parameter ψ for one semi flange and web is exemplified.

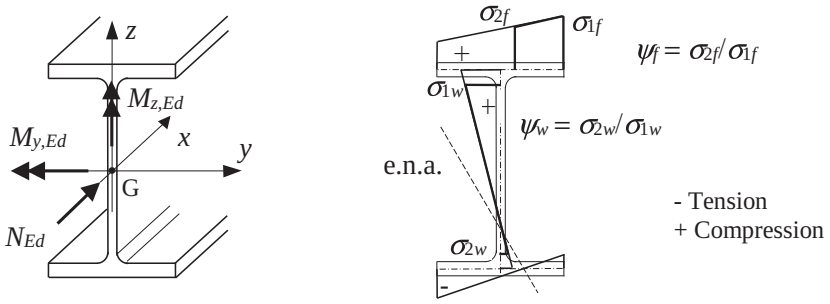
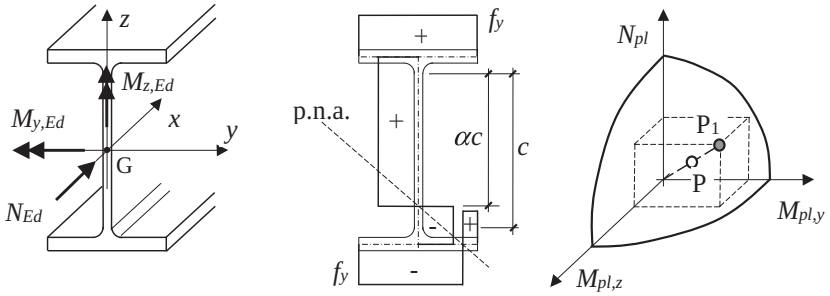


Figure 3.75 – Normal elastic stresses in a section with bi-axial bending combined with axial force

To establish the limits between classes 3 and 2 and between classes 2 and 1 it is necessary to increase the applied loads (N_{Ed} + $M_{y,Ed}$ + $M_{z,Ed}$) until a set of equivalent loads that plastifies the entire cross section is obtained. For cross sections under bi-axial bending and axial force, this procedure is generally too complex for hand calculation. Assuming proportional loading, Figure 3.76 illustrates this procedure: P_1 represent the set of applied loading that fully plastify the cross section, obtained as the point of intersection of a line defined by the origin and the point P with coordinates (N_{Ed}, $M_{y,Ed}$, $M_{z,Ed}$), and the plastic interaction surface (see Figure 3.76c).



a) Acting forces b) Plastification of the entire section c) Plastic interaction curve

Figure 3.76 – Complete plastification of an I or H section with bi-axial bending combined with axial force

In the previous paragraphs, proportional increase of loading was assumed. However this is not a compulsory requirement. Using the simple

case of uniaxial bending and axial force for exemplification, this issue is discussed in detail in this paragraph. Considering first the classification limits between classes 3 and 2 and between classes 2 and 1 it is necessary to determine the parameter α defined in Tables 2.21 to 2.23. Figure 3.77 illustrates a I or H section subject to uni-axial bending around y and an axial compressive force and the corresponding plastic interaction curve. The applied loading is represented by point P, with coordinates (N_{Ed}, $M_{y,Ed}$). Points P_1, P_2 and P_3 represent three possible loading pairs that fully plastify the entire cross section. Classification based on point P_1 corresponds to proportional incrementation of the applied loading until the plastic interaction curve is reached for a pair of forces (N_1, $M_{y,1}$) such that $N_1/N_{Ed} = M_{y,Ed} / M_{y,1} = U_F$. U_F denotes the utilization factor of the cross section, and it is illustrated in Figure 3.78, representing the ratio between the applied loading, generally denoted as R_{Ed} and the cross section resistance, denoted as R_{Rd}.

The classification based on point P_2 assumes that the axial force remains constant and only the bending moment is incremented until the yield curve is reached for a pair of forces (N_{Ed}, $M_{y,2}$). Finally, as a third alternative, point P_3 corresponds to the assumption of fixed bending moment and the incremetation of the axial force until full yielding is reached for a pair of forces (N_3, $M_{y,Ed}$). It is noted that all cases are possible, the real incrementation being very difficult to compete without a full nonlinear analysis as it depends on the relative contribution of the various permanent, variable and accidental actions for each load combination, as well as on the structural response of the steel structure, including the effects of redundancy and progressive yielding.

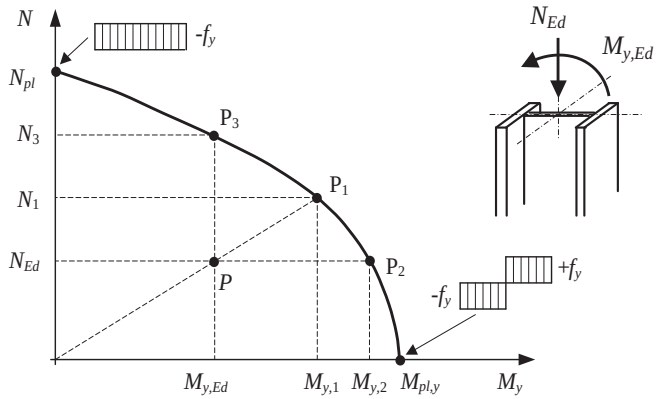


Figure 3.77 – Classification of the sections based on plastic stress diagrams

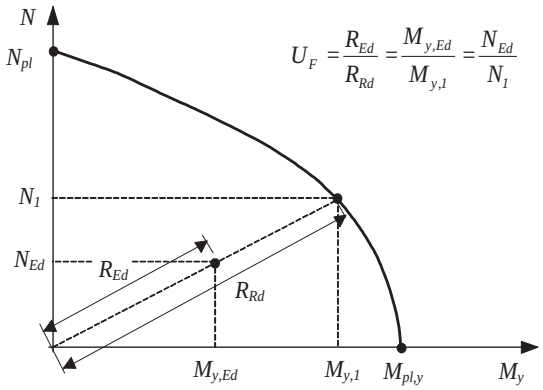


Figure 3.78 – Concept of utilization factor U_F

For a double-symmetric I or H section, subject to axial bending and axial force, the parameter α may be obtained from equation (2.27a), for incrementation of bending moment only (point P_2) or equation (2.27b) for proportional incrementation (point P_1).

The classification limits between classes 3 and 4 also depend on the choice of load incrementation. However, in this case, proportional incrementation is significantly simpler for the reasons explained above. If it is desired to use bending moment incrementation only (or axial force incrementation only), linear superposition is possible because of the assumed linear elastic behaviour.

In practical terms, for a section subject to bi-axial bending and axial force, the use of software is recommended, such as the program "SemiComp Member Design", developed under the research project Semi-Comp+ (Greiner *et al*, 2011).

Member classification is also required for the verification of the buckling resistance of beam-columns. However, for a member subject to bending (uni-axial or bi-axial) and axial force it is common to have a variation of the cross section class along the member. Although the consideration of the highest cross section class along the member would lead to a safe design, it would be excessively conservative for the majority of cases (see example 3.14). Hence, since the member class should be stricktly based on the second order critical cross section of the beam-column, the project Semi-Comp+ (Greiner *et al*, 2011) proposes, in a simplified way, that the member classification is established on the basis of the class of the cross section with the highest utilization factor for the purpose of checking the buckling resistance of the member.

3.7.3. Cross section resistance

3.7.3.1. Theoretical background

The cross section resistance is based on its plastic capacity (class 1 or 2 sections) or on its elastic capacity (class 3 or 4 cross sections). When a cross section is subjected to bending moment and axial force ($N + M_y$, $N + M_z$ or even $N + M_y + M_z$), the bending moment resistance should be reduced, using interaction formulas. The interaction formulae to evaluate the elastic cross section capacity are the well known formulae of simple beam theory, valid for any type of cross section. However, the formulae to evaluate the plastic cross section capacity are specific for each cross section shape.

For a cross section subjected to $N + M$, a general procedure may be established to evaluate the plastic bending moment resistance $M_{N,Rd}$, reduced by the presence of an axial force N. This method, applied to a cross section with a generic shape and gross area A, composed by a material with a yield strength f_y (Figure 3.79), involves the definition of an area $A_c = N/f_y$ in compression, located in such a way that the areas A_1 and A_2 are equal ($A_1 = A_2 = (A - N / f_y) / 2$). The reduced plastic bending moment resistance $M_{N,Rd}$ is given by the product of the force $F_t = A_1 f_y$ (equal to $F_c = A_2 f_y$) and the distance d between the centroid of areas A_1 and A_2, as shown in Figure 3.79.

$$M_{N,Rd} = A_1 f_y d . \qquad (3.135)$$

247

The application of the general procedure allows the derivation of exact interaction formulae for specific cross sectional shapes. Although the interaction formulae are easy to obtain by applying the general method, the resulting formulae differ for each cross sectional shape and are often not straightforward to manipulate.

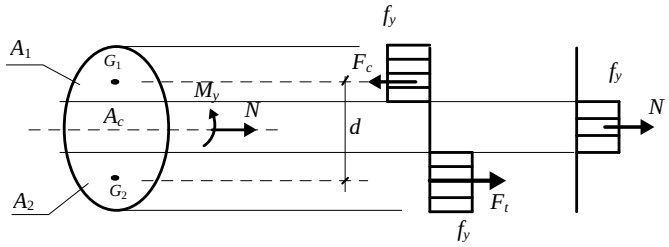


Figure 3.79 – Bending moment-axial force plastic interaction

Historically, several approximate formulae have been developed, a thorough review being found in Villette (2004). Recently, Villette (2004) proposed an accurate general formula, applicable to most standard cross sections, with an axis of symmetry with respect to the axis of bending, given by:

$$\frac{M_{Ed}}{M_{pl,Rd}}+\left(\frac{N_{Ed}}{N_{pl,Rd}}\right)^{\alpha,plan}=1.0\,, \tag{3.136}$$

where,

$$\alpha_{plan}=1.0+1.82\sqrt{\left(\frac{k}{w_{pl}}-1.01\right)\frac{k-1}{w_{pl}-1}}\,. \tag{3.137}$$

$w_{pl}=\left(W_{pl}/W_{el}\right)$ is the ratio between the plastic bending modulus and the elastic modulus and $k=\left(v/i\right)$ is the ratio between the maximum distance v from an extreme fibre to the elastic neutral axis and the radius of gyration i of the section about the axis of bending. In equation (3.136), M_{Ed} and N_{Ed} are the design bending moment and the design axial force, respectively; $M_{pl,Rd}$ and $N_{pl,Rd}$ are the plastic bending moment resistance and the plastic resistance to axial force, respectively; these symbols have the same meaning throughout this sub-chapter.

For a circular hollow section, the following exact equation may be established (Lescouarc'h, 1977):

$$M_{N,Rd}=M_{pl,Rd}\sin\frac{\pi\left(1-n\right)}{2}\,, \tag{3.138}$$

where $n = N_{ed}/N_{pl,Rd}$; this symbol has the same meaning throughout this sub-chapter.

For sections under axial force and bi-axial bending ($N + M_y + M_z$) the interaction is substantially more complex. Villette (2004) reports several approximate formulae available in the literature. Interaction formulae for axial force and bi-axial bending have usually the following general format:

$$\left[\frac{M_{y,Ed}}{M_{N,y,Rd}}\right]^{\alpha}+\left[\frac{M_{z,Ed}}{M_{N,z,Rd}}\right]^{\beta}=1.0\,, \tag{3.139}$$

where $M_{N,\,y,\,Rd}$ and $M_{N,\,,z,\,Rd}$ are the plastic moments of resistance reduced due to the design axial force, for bending about the y and z axes, respectively.

For I or H cross sections subjected to $N + M_y + M_z$, Villette (2004) proposed an accurate formula, where the parameters α and β are given by:

$$\alpha = \left(1.0 - 0.5\sqrt{n}\right)\alpha_{y,plan}; \tag{3.140}$$

$$\beta = \frac{1+n}{1.0 - n^{\left(\alpha_{z,plan} - 0.5\right)}}, \tag{3.141}$$

$\alpha_{y,plan}$ and $\alpha_{z,plan}$ are given by equation (3.137) for $N + M_y$ and $N + M_z$, respectively.

For rectangular hollow cross sections subjected to $N + M_y + M_z$, equation (3.138) also applies, with the parameters α_y and α_z given by (Villette, 2004):

$$\alpha = \beta = \frac{1.7}{1 - 1.13\,n^2} \qquad \left(\text{if } n < 0.8\right); \tag{3.142}$$

$$\alpha = \beta = 6 \qquad \left(\text{if } n \geq 0.8\right). \tag{3.143}$$

Bi-axial bending may be treated as a particular case of the previous interaction formulas, by taking $N_{Ed} = 0$.

3.7.3.2. Design resistance

Clause 6.2.9 provides several interaction formulae between bending moment and axial force, in the plastic range and in the elastic range. These are applicable to most cross sections.

i) *Class 1 or 2 sections*

In class 1 or 2 cross sections, the following condition should be satisfied (clause 6.2.9.1(2)):

$$M_{Ed} \leq M_{N,Rd}, \tag{3.144}$$

where M_{Ed} is the design bending moment and $M_{N,Rd}$ represents the design plastic moment resistance reduced due to the axial force N_{Ed}.

For rectangular solid sections under uni-axial bending and axial force, $M_{N,Rd}$ is given by (clause 6.2.9.1(3)):

$$M_{N,Rd} = M_{pl,Rd}\left[1-\left(\frac{N_{Ed}}{N_{pl,Rd}}\right)^2\right], \tag{3.145}$$

illustrated by the solid line in Figure 3.80. This figure also indicates, qualitatively, the normal stress diagrams for several combinations of M_{Ed} and N_{Ed}, where f_y is the yield strength, $M_{el,Rd}$ is the elastic resistance to bending moment and the remaining symbols were defined above.

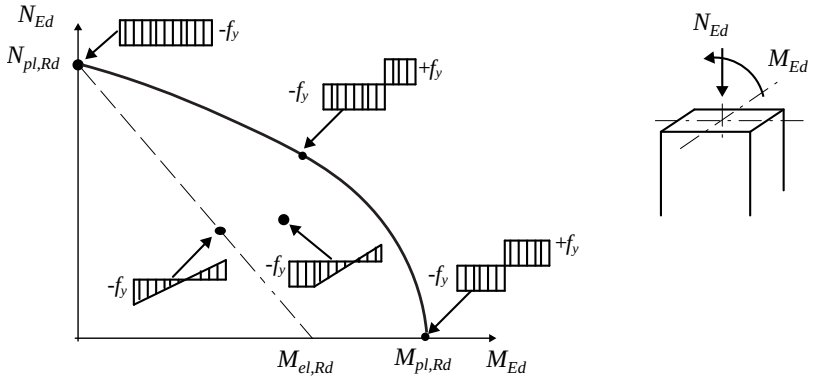


Figure 3.80 – $M + N$ interaction diagram in a rectangular solid section

For low values of axial force, the reduction of the plastic moment resistance is not significant, as can be seen in Figure 3.80. For doubly symmetric I or H sections, clause 6.2.9.1(4) states that:

> it is not necessary to reduce the plastic moment resistance about y if the two following conditions are satisfied:
>
> $$N_{Ed} \le 0.25\, N_{pl,Rd} \quad \text{and} \quad N_{Ed} \le 0.5\, h_w\, t_w\, f_y / \gamma_{M0}. \tag{3.146}$$

– it is not necessary to reduce the plastic moment resistance about z if the following condition is verified:

$$N_{Ed} \le h_w\, t_w\, f_y \big/ \gamma_{M0}\,, \tag{3.147}$$

where h_w and t_w are the height and the thickness of the web, respectively.

For I or H sections, rolled or welded, with equal flanges and where fastener holes are not to be accounted for, the reduced plastic moment resistances, $M_{N,y,Rd}$ and $M_{N,z,Rd}$ about the y and z axis respectively can be obtained from clause 6.2.9.1(5):

$$M_{N,y,Rd} = M_{pl,y,Rd}\frac{1-n}{1-0.5a} \quad \text{but} \quad M_{N,y,Rd} \le M_{pl,y,Rd}; \tag{3.148}$$

$$M_{N,z,Rd} = M_{pl,z,Rd} \qquad \text{if } n \le a; \tag{3.149a}$$

$$M_{N,z,Rd} = M_{pl,z,Rd}\left[1-\left(\frac{n-a}{1-a}\right)^2\right] \qquad \text{if } n > a, \tag{3.149b}$$

where $a = \left(A - 2\,b\,t_f\right)\big/A$, but $a \le 0.5$.

For circular hollow sections:

$$M_{N,Rd} = M_{pl,Rd}\left(1-n^{1.7}\right). \tag{3.150}$$

For rectangular hollow sections of uniform thickness and for welded box sections with equal flanges and equal webs and where fastener holes are not to be accounted for, the reduced plastic moment resistances, can also be obtained from clause 6.2.9.1(5):

$$M_{N,y,Rd} = M_{pl,y,Rd}\frac{1-n}{1-0.5a_w} \quad \text{but} \quad M_{N,y,Rd} \le M_{pl,y,Rd}; \tag{3.151}$$

$$M_{N,z,Rd} = M_{pl,z,Rd}\frac{1-n}{1-0.5a_f} \quad \text{but} \quad M_{N,z,Rd} \le M_{pl,z,Rd}, \tag{3.152}$$

where $a_w \le 0.5$ and $a_f \le 0.5$ are the ratios between the area of the webs and of the flanges, respectively, and the gross area of the cross section.

In a cross section under bi-axial bending and axial force, the $N + M_y + M_z$ interaction can be checked by the following condition:

$$\left[\frac{M_{y,Ed}}{M_{N,y,Rd}}\right]^{\alpha} + \left[\frac{M_{z,Ed}}{M_{N,z,Rd}}\right]^{\beta} \leq 1.0, \tag{3.153}$$

where α and β are parameters that depend on the shape of the cross section and $M_{N,y,Rd}$ and $M_{N,z,Rd}$ are the reduced plastic moments resistances around y and z, respectively, evaluated as previously described. The values of α and β are given as follows in clause 6.2.9.1(6):

- I or H sections $\alpha = 2; \beta = 5n,$ but $\beta \geq 1;$
- circular hollow sections $\alpha = \beta = 2;$
- rectangular hollow sections $\alpha = \beta = \frac{1.66}{1 - 1.13\,n^2},$ but $\alpha = \beta \leq 6.$

ii) *Class 3 or 4 cross sections*

In class 3 or 4 cross sections, the interaction between bending and axial force requires that the following condition be checked:

$$\sigma_{x,Ed} \leq \frac{f_y}{\gamma_{M0}}, \tag{3.154}$$

where $\sigma_{x,Ed}$ is the design value of the local longitudinal stress due to bending moment and axial force, taking into account the fastener holes where relevant. This stress is evaluated by an elastic stress analysis, based on the gross cross section for class 3 cross sections, and on a reduced effective cross section for class 4 sections. Additionally, in class 4 cross sections the bending moments due to the shift of the centroidal axis on the reduced effective cross section should be taken into account, see clause 6.2.9.3(2).

The calculation of the effective area in class 4 cross sections should be in accordance with EC3-1-5.

iii) *Interaction of bending, axial and shear force*

The interaction between bending, axial and shear force should be checked as follows (clause 6.2.10):

- When $V_{Ed} \leq 50$ % of the design plastic shear resistance $V_{pl,Rd}$, no reduction need be made in the bending and axial force resistances obtained from clause 6.2.9.
- When $V_{Ed} > 50$ % of $V_{pl,Rd}$, then the design resistance to the combination of bending moment and axial force should be calculated using a reduced yield strength for the shear area. This reduced strength is given by $(1-\rho)f_y$, where $\rho = \left(2V_{Ed}/V_{pl,Rd} - 1\right)^2$.

3.7.4. Buckling resistance

3.7.4.1. Theoretical background

For a member under bending and compression, besides the first-order moments and displacements (obtained based on the undeformed configuration), additional second-order moments and displacements exist ("*P-δ*" effects); these should be taken into account. Figure 3.81 illustrates the behaviour of a member, with an initial bow imperfection defined by a transverse displacement e_0, subject to bending moment and axial compression; the bending moment diagram includes the first order moments and the second order moments that result from the lateral deformation.

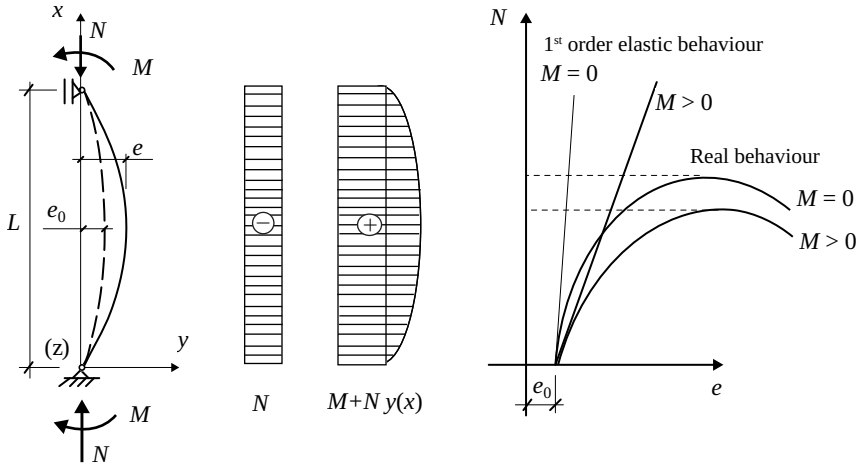


Figure 3.81 – Behaviour of a member subjected to bending and compression

In the past, various interaction formulae have been proposed to represent this situation over the full slenderness range. The present approach of EC3-1-1 is based on a linear-additive interaction formula, illustrated by expression (3.155). According this approach, the effects of the axial compression and the bending moments are added linearly and the non-linear effects of the axial compression are taken into account by specific interaction factors.

$$f\left(\frac{N}{N_u},\frac{M_y}{M_{uy}},\frac{M_z}{M_{uz}}\right)\leq 1.0, \tag{3.155}$$

where N, M_y and M_z are the applied forces and N_u, M_{uy} and M_{uz} are the design resistances, that take in due account the associated instability phenomena.

The development of the design rules, and in particular those adopted by EC3-1-1, is quite complex, as they have to incorporate two instability modes, flexural buckling and lateral-torsional buckling (or a combination of both), different cross sectional shapes and several shapes of bending moment diagram, among other aspects. These formulae, based on second-order theory, have to incorporate several common concepts, such as that of equivalent moment, the definition of buckling length and the concept of amplification. These formulae were mainly based on doubly-symmetric cross sections, although recent investigations (Kaim, 2004) have shown that they could give good approximate solutions for mono-symmetric sections.

Following Boissonade *et al* (2006), for a member under N_{Ed} + $M_{y,Ed}$ + $M_{z,Ed}$, disregarding the complex coupling between instabilities in both principal planes, the elastic flexural stability in both planes (*x*-*y* plane and *x*-*z* plane) can be expressed by the following expressions:

$$\frac{N_{Ed}}{\chi_y N_{pl,Rd}}+\mu_y\left[\frac{C_{my}M_{y,Ed}}{\left(1-\frac{N_{Ed}}{N_{cr,y}}\right)M_{el,y,Rd}}+\frac{C_{mz}M_{z,Ed}}{\left(1-\frac{N_{Ed}}{N_{cr,z}}\right)M_{el,z,Rd}}\right]\leq 1.0; \tag{3.156}$$

$$\frac{N_{Ed}}{\chi_z N_{pl,Rd}} + \mu_z \left[\frac{C_{my} M_{y,Ed}}{\left(1 - \frac{N_{Ed}}{N_{cr,y}}\right) M_{el,y,Rd}} + \frac{C_{mz} M_{z,Ed}}{\left(1 - \frac{N_{Ed}}{N_{cr,z}}\right) M_{el,z,Rd}} \right] \leq 1.0, \quad (3.157)$$

where C_{my} and C_{mz} are the equivalent moment factors relating to the M_y and M_z diagrams respectively and μ_y and μ_z are parameters defined by the following equations:

$$\mu_y = \frac{1 - N_{Ed} / N_{cr,y}}{1 - \chi_y N_{Ed} / N_{cr,y}}; \quad (3.158)$$

$$\mu_z = \frac{1 - N_{Ed} / N_{cr,z}}{1 - \chi_z N_{Ed} / N_{cr,z}}. \quad (3.159)$$

The general formulae expressed by (3.156) and (3.157) are based on elastic second-order theory, so are only valid for class 3 cross sections. Class 1 and class 2 cross sections may buckle in an elasto-plastic flexural buckling mode, leading to the following modified expressions:

$$\frac{N_{Ed}}{\chi_y N_{pl,Rd}} + \mu_y \left[\frac{C_{my} M_{y,Ed}}{\left(1 - \frac{N_{Ed}}{N_{cr,y}}\right) C_{yy} M_{pl,y,Rd}} + \alpha^* \frac{C_{mz} M_{z,Ed}}{\left(1 - \frac{N_{Ed}}{N_{cr,z}}\right) C_{yz} M_{pl,z,Rd}} \right] \leq 1.0; \quad (3.160)$$

$$\frac{N_{Ed}}{\chi_z N_{pl,Rd}} + \mu_z \left[\beta^* \frac{C_{my} M_{y,Ed}}{\left(1 - \frac{N_{Ed}}{N_{cr,y}}\right) C_{zy} M_{pl,y,Rd}} + \frac{C_{mz} M_{z,Ed}}{\left(1 - \frac{N_{Ed}}{N_{cr,z}}\right) C_{zz} M_{el,z,Rd}} \right] \leq 1.0, \quad (3.161)$$

where C_{yy} , C_{yz} , C_{zy} and C_{zz} are parameters introduced to simulate plasticity effects and α^* and β^* are factors that depend on the material's non-linear behaviour.

The formulae given above represent the behaviour of members in which the potential failure mode is flexural buckling in one of the principal planes. This would be the case in thin-walled closed sections and sections with lateral restraint. In members of open section without lateral restraint, lateral-torsional buckling is a potential failure mode. Consider an I or H section of doubly-symmetric cross section, with support conditions as shown in Figure 3.62 (the "standard case"), subject to axial compression and uniform bending moment $M_{y,Ed}$. Assuming a lateral sinusoidal bow imperfection, see equation (3.81), and a first yield failure criterion, the buckling formula is the following (Kaim, 2004):

$$\frac{N_{Ed}}{N_{pl,Rd}}+\frac{M_y}{\left(1-\frac{N_{Ed}}{N_{cr,y}}\right)M_{y,Rd}}+ \\ \frac{1}{\left(1-\frac{M_{y,Ed}^2}{M_{cr}^2}\right)}e_{0,d}\left(\frac{N_{Ed}}{\left(1-\frac{N_{Ed}}{N_{cr,z}}\right)M_{z,Rd}}+\frac{N_{cr,z}}{M_{z,Rd}}\frac{M_{y,Ed}^2}{M_{cr(N)}^2}+\frac{N_{cr,z}^2\frac{h}{2}}{M_{z,Rd}}\frac{M_{y,Ed}}{M_{cr(N)}^2}\right)\le 1.0, \tag{3.162}$$

where $M_{cr(N)}$ is the critical lateral-torsional buckling moment under the additional effect of the axial compression (Boissonnade *et al*, 2006), $M_{y,Rd}$ and $M_{z,Rd}$ are the elastic resistance moments about y and z respectively, and the remain symbols are as defined before.

Expression (3.162) describes theoretically the lateral-torsional buckling mode of a member under axial compression and in-plane M_y bending moment. This needs to be simplified into a more appropriate format for design. Expressions (3.155) to (3.162) are the basis for the two design approaches for beam-columns given in EC3-1-1. In developing these, some simplifications have been made and several parameters calibrated by numerical and experimental investigations. The two approaches, termed Method 1 and Method 2, are described in the following sub-section.

3.7.4.2. Design resistance

In sub-chapter 2.3, several procedures provided in EC3-1-1 were described for the verification of the global stability of a steel structure,

including the different ways of considering the second order effects (local P-δ effects and global P-Δ effects). Local P-δ effects are generally taken into account according to the procedures given in clause 6.3; global P-Δ effects are either directly considered in the global analysis of the structure, or they are indirectly considered, by an appropriate increase of the buckling lengths of the members.

The instability of a member of doubly symmetric cross section, not susceptible to distortional deformations, and subject to bending and axial compression, can be due to flexural buckling or to lateral torsional buckling. Therefore, clause 6.3.3(1) considers two distinct situations:

- Members not susceptible to torsional deformation, such as members of circular hollow section or other sections restrained from torsion. Here, flexural buckling is the relevant instability mode.
- Members that are susceptible to torsional deformations, such as members of open section (I or H sections) that are not restrained from torsion. Here, lateral torsional buckling tends to be the relevant instability mode.

Consider a single span member of doubly symmetric section, with the "standard case" end conditions shown in Figure 3.62. The member is subject to bending moment and axial compression. The following conditions should be satisfied:

$$\frac{N_{Ed}}{\chi_y N_{Rk}/\gamma_{M1}} + k_{yy}\frac{M_{y,Ed}+\Delta M_{y,Ed}}{\chi_{LT} M_{y,Rk}/\gamma_{M1}} + k_{yz}\frac{M_{z,Ed}+\Delta M_{z,Ed}}{M_{z,Rk}/\gamma_{M1}} \le 1.0; \qquad (3.163a)$$

$$\frac{N_{Ed}}{\chi_z N_{Rk}/\gamma_{M1}} + k_{zy}\frac{M_{y,Ed}+\Delta M_{y,Ed}}{\chi_{LT} M_{y,Rk}/\gamma_{M1}} + k_{zz}\frac{M_{z,Ed}+\Delta M_{z,Ed}}{M_{z,Rk}/\gamma_{M1}} \le 1.0; \qquad (3.163b)$$

where: N_{Ed}, $M_{y,Ed}$ and $M_{z,Ed}$ are the design values of the axial compression force and the maximum bending moments along the member about y and z , respectively;

$\Delta M_{y,Ed}$ and $\Delta M_{z,Ed}$ are the moments due to the shift of the centroidal axis on a reduced effective class 4 cross section;

χ_y and χ_z are the reduction factors due to flexural buckling about y and z, respectively, evaluated according to clause 6.3.1 or in sub-chapter 3.5;

χ_{LT} is the reduction factor due to lateral-torsional buckling, evaluated according to clause 6.3.2 or in sub-chapter 3.6 (χ_{LT} = 1.0 for members that are not susceptible to torsional deformation);

k_{yy}, k_{yz}, k_{zy} and k_{zz} are, interaction factors that depend on the relevant instability and plasticity phenomena, obtained through Annex A (Method 1) or Annex B (Method 2);

$N_{Rk} = f_y A_i$, $M_{i,Rk} = f_y W_i$ and $\Delta M_{i,Ed}$ are evaluated according to Table 3.10, depending on the cross sectional class of the member.

Table 3.10 – Values for the calculation of N_{Rk}, $M_{i,Rk}$ and $\Delta M_{i,Ed}$

Class	1	2	3	4
A_i	A	A	A	A_{eff}
W_y	$W_{pl,y}$	$W_{pl,y}$	$W_{el,y}$	$W_{eff,y}$
W_z	$W_{pl,z}$	$W_{pl,z}$	$W_{el,z}$	$W_{eff,z}$
$\Delta M_{y,Ed}$	0	0	0	$e_{N,y} N_{Ed}$
$\Delta M_{z,Ed}$	0	0	0	$e_{N,z} N_{Ed}$

In EC3-1-1 two methods are given for the calculation of the interaction factors k_{yy}, k_{yz}, k_{zy} and k_{zz}; Method 1, developed by a group of French and Belgian researchers, and Method 2, developed by a group of Austrian and German researchers (Boissonnade *et al*, 2006).

In members that are not susceptible to torsional deformation, it is assumed that there is no risk of lateral torsional buckling. The stability of the member is then verified by checking against flexural buckling about *y* and about *z*. This procedure requires application of expressions (3.163a) (flexural buckling around *y*) and (3.163b) (flexural buckling around *z*), considering χ_{LT} = 1.0 and calculating the interaction factors k_{yy}, k_{yz}, k_{zy} and k_{zz} for a member not susceptible to torsional deformation.

In members that are susceptible to torsional deformation, it is assumed that lateral torsional buckling is more critical. In this case, expressions (3.163a) and (3.163b) should be applied, with χ_{LT} evaluated according to clause 6.3.2 or sub-chapter 3.6, and calculating the interaction factors for a member susceptible to torsional deformation.

According to Method 1, a member is not susceptible to torsional deformations if $I_T \geq I_y$, where I_T and I_y are the torsion constant and the second

moment of area about *y*, respectively. If the section is such that $I_T < I_y$, but there are lateral restraints along the member, this situation could still be considered as not susceptible to torsional deformations, if the following condition is verified:

$$\overline{\lambda}_0 \le 0.2\sqrt{C_1}\sqrt[4]{\left(1-\frac{N_{Ed}}{N_{cr,z}}\right)\left(1-\frac{N_{Ed}}{N_{cr,T}}\right)}, \tag{3.164}$$

where C_1 is a coefficient that depends on the shape of the bending moment diagram between laterally braced sections (obtained according to sub-section 3.6.2.2 or Table 3.12), $N_{cr,z}$ and $N_{cr,T}$ represent the elastic critical loads for flexural buckling about *z* and for torsional buckling, respectively, and $\overline{\lambda}_0$ is the non dimensional slenderness coefficient for lateral torsional buckling, assessed for a situation with constant bending moment. If condition (3.164) is not satisfied, the member must be considered as a member susceptible to torsional deformations.

Next, the following tables from Annex A of EC3-1-1 are presented, for the calculation of the interaction factors according to Method 1. In Table 3.11 the values of the interaction factors k_{ij} are indicated.

Table 3.11 – Interaction factors k_{ij} according to Method 1

Interaction factors	Elastic sectional properties (Class 3 or 4 sections)	Plastic sectional properties (Class 1 or 2 sections)
k_{yy}	$C_{my}C_{mLT}\dfrac{\mu_y}{1-\dfrac{N_{Ed}}{N_{cr,y}}}$	$C_{my}C_{mLT}\dfrac{\mu_y}{1-\dfrac{N_{Ed}}{N_{cr,y}}}\dfrac{1}{C_{yy}}$
k_{yz}	$C_{mz}\dfrac{\mu_y}{1-\dfrac{N_{Ed}}{N_{cr,z}}}$	$C_{mz}\dfrac{\mu_y}{1-\dfrac{N_{Ed}}{N_{cr,z}}}\dfrac{1}{C_{yz}}0.6\sqrt{\dfrac{w_z}{w_y}}$
k_{zy}	$C_{my}C_{mLT}\dfrac{\mu_z}{1-\dfrac{N_{Ed}}{N_{cr,y}}}$	$C_{my}C_{mLT}\dfrac{\mu_z}{1-\dfrac{N_{Ed}}{N_{cr,y}}}\dfrac{1}{C_{zy}}0.6\sqrt{\dfrac{w_z}{w_y}}$
k_{zz}	$C_{mz}\dfrac{\mu_z}{1-\dfrac{N_{Ed}}{N_{cr,z}}}$	$C_{mz}\dfrac{\mu_z}{1-\dfrac{N_{Ed}}{N_{cr,z}}}\dfrac{1}{C_{zz}}$

In Table 3.12 some auxiliary terms are given. The information includes the calculation of factors C_{yy}, C_{yz}, C_{zy} and C_{zz}; these depend on the degree of plasticity in the cross section at collapse of the member.

These terms assume distinct values, depending on whether the member is susceptible or not to torsional deformations.

Table 3.12 – Auxiliary terms for the calculation of the interaction factors k_{ij} of the previous table

Auxiliary terms:
$\mu_y = \dfrac{1-\dfrac{N_{Ed}}{N_{cr,y}}}{1-\chi_y \dfrac{N_{Ed}}{N_{cr,y}}}$; $\mu_z = \dfrac{1-\dfrac{N_{Ed}}{N_{cr,z}}}{1-\chi_z \dfrac{N_{Ed}}{N_{cr,z}}}$; $w_y = \dfrac{W_{pl,y}}{W_{el,y}} \le 1.5$; $w_z = \dfrac{W_{pl,z}}{W_{el,z}} \le 1.5$. $n_{pl} = \dfrac{N_{Ed}}{N_{Rk}/\gamma_{M1}}$; $a_{LT} = 1 - \dfrac{I_T}{I_y} \ge 0$; C_{my} and C_{mz} are factors of equivalent uniform moment, determined by Table 3.13. For class 3 or 4, consider $w_y = w_z = 1.0$.
$C_{yy} = 1 + \left(w_y - 1\right)\left[\left(2 - \dfrac{1.6}{w_y} C_{my}^2 \overline{\lambda}_{\max} - \dfrac{1.6}{w_y} C_{my}^2 \overline{\lambda}_{\max}^2\right) n_{pl} - b_{LT}\right] \ge \dfrac{W_{el,y}}{W_{pl,y}}$, where $b_{LT} = 0.5\, a_{LT} \overline{\lambda}_0^2 \dfrac{M_{y,Ed}}{\chi_{LT} M_{pl,y,Rd}} \dfrac{M_{z,Ed}}{M_{pl,z,Rd}}$. $C_{yz} = 1 + \left(w_z - 1\right)\left[\left(2 - 14 \dfrac{C_{mz}^2 \overline{\lambda}_{\max}^2}{w_z^5}\right) n_{pl} - c_{LT}\right] \ge 0.6 \sqrt{\dfrac{w_z}{w_y}} \dfrac{W_{el,z}}{W_{pl,z}}$, where $c_{LT} = 10\, a_{LT} \dfrac{\overline{\lambda}_0^2}{5 + \overline{\lambda}_z^4} \dfrac{M_{y,Ed}}{C_{my} \chi_{LT} M_{pl,y,Rd}}$. $C_{zy} = 1 + \left(w_y - 1\right)\left[\left(2 - 14 \dfrac{C_{my}^2 \overline{\lambda}_{\max}^2}{w_y^5}\right) n_{pl} - d_{LT}\right] \ge 0.6 \sqrt{\dfrac{w_y}{w_z}} \dfrac{W_{el,y}}{W_{pl,y}}$, where $d_{LT} = 2 a_{LT} \dfrac{\overline{\lambda}_0}{0.1 + \overline{\lambda}_z^4} \dfrac{M_{y,Ed}}{C_{my}\, \chi_{LT}\, M_{pl,y,Rd}} \dfrac{M_{z,Ed}}{C_{mz} M_{pl,z,Rd}}$.

Table 3.12 (cont.) – Auxiliary terms for the calculation of the interaction factors k_{ij} of the previous table

Auxiliary terms (continuation):

$$C_{zz} = 1 + \left(w_z - 1\right)\left[\left(2 - \frac{1.6}{w_z} C_{mz}^2 \overline{\lambda}_{\max} - \frac{1.6}{w_z} C_{mz}^2 \overline{\lambda}_{\max}^2\right) - e_{LT}\right] n_{pl} \geq \frac{W_{el,z}}{W_{pl,z}},$$ [4]

where $e_{LT} = 1.7\, a_{LT} \dfrac{\overline{\lambda}_0}{0.1 + \overline{\lambda}_z^4} \dfrac{M_{y,Ed}}{C_{my}\, \chi_{LT}\, M_{pl,y.Rd}}$.

$\overline{\lambda}_{\max} = \max\left(\overline{\lambda}_y, \overline{\lambda}_z\right)$;

$\overline{\lambda}_0 =$ non dimensional slenderness for lateral torsional buckling due to uniform bending moment, that is, taking $\Psi_y = 1.0$ in Table 3.13;

$\overline{\lambda}_{LT} =$ non dimensional slenderness for lateral torsional buckling;

If $\overline{\lambda}_0 \leq 0.2\sqrt{C_1}\sqrt[4]{\left(1 - \dfrac{N_{Ed}}{N_{cr,z}}\right)\left(1 - \dfrac{N_{Ed}}{N_{cr,T}}\right)}: C_{my} = C_{my,0};\ C_{mz} = C_{mz,0};\ C_{mLT} = 1.0;$

If $\overline{\lambda}_0 > 0.2\sqrt{C_1}\sqrt[4]{\left(1 - \dfrac{N_{Ed}}{N_{cr,z}}\right)\left(1 - \dfrac{N_{Ed}}{N_{cr,T}}\right)}:\ C_{my} = C_{my,0} + \left(1 - C_{my,0}\right)\dfrac{\sqrt{\varepsilon_y}\, a_{LT}}{1 + \sqrt{\varepsilon_y}\, a_{LT}};$

$$C_{mz} = C_{mz,0}; C_{mLT} = C_{my}^2 \frac{a_{LT}}{\sqrt{\left(1 - \dfrac{N_{Ed}}{N_{cr,z}}\right)\left(1 - \dfrac{N_{Ed}}{N_{cr,T}}\right)}} \geq 1;$$

$\varepsilon_y = \dfrac{M_{y,Ed}}{N_{Ed}} \dfrac{A}{W_{el,y}}$ for class 1, 2 or 3 cross sections;

$\varepsilon_y = \dfrac{M_{y,Ed}}{N_{Ed}} \dfrac{A_{eff}}{W_{eff,y}}$ for class 4 cross sections;

$N_{cr,y}$ is the elastic critical load for flexural buckling about y;

$N_{cr,z}$ is the elastic critical load for flexural buckling about z;

$N_{cr,T}$ is the critical load for torsional buckling;

I_T is the constant of uniform torsion or St. Venant's torsion;

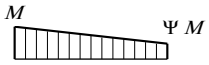
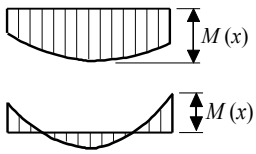
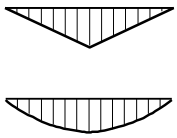
I_y is the second moment of area about y;

$C_1 = \left(\dfrac{1}{k_c}\right)^2$ where k_c is taken from Table 3.8.

[4] The corresponding formula which is presented in EC3-1-1 contained incorrections that were corrected in Corrigendum N1620E to EN 1993-1-1.

In Table 3.13, the $C_{mi,0}$ factors are given, which allows one to obtain the equivalent uniform moment factors, C_{mi}, as described in Table 3.12; these coefficients should be assessed based on the corresponding bending moment diagrams (about *y* or about *z*), between braced sections.

Table 3.13 – Equivalent uniform moment factors $C_{mi,0}$

Diagram of moments	$C_{mi,0}$
	$C_{mi,0} = 0.79 + 0.21\Psi_i + 0.36\left(\Psi_i - 0.33\right)\frac{N_{Ed}}{N_{cr,i}}$
	$C_{mi,0} = 1 + \left(\frac{\pi^2 E I_i \lvert\delta_x\rvert}{L^2 \lvert M_{i,Ed}(x)\rvert} - 1\right)\frac{N_{Ed}}{N_{cr,i}}$ $M_{i,Ed}(x)$ is the maximum moment $M_{y,Ed}$ or $M_{z,Ed}$ according to the first order analyses; $\lvert\delta_x\rvert$ is the maximum lateral deflection δ_z (due to $M_{y,Ed}$) or δ_y (due to $M_{z,Ed}$) along the member.
	$C_{mi,0} = 1 - 0.18\frac{N_{Ed}}{N_{cr,i}}$ $C_{mi,0} = 1 + 0.03\frac{N_{Ed}}{N_{cr,i}}$

According to Method 2, the following members may be considered as not susceptible to torsional deformation:

- members with circular hollow sections;
- members with rectangular hollow sections but, according to some authors (Kaim, 2004), only if $h/b \le 10/\overline{\lambda}_z$, where *h* and *b* are the depth and width of the cross section respectively, and $\overline{\lambda}_z$ is the non dimensional slenderness relative to the *z* axis);
- members with open cross section, provided that they are torsionally and laterally restrained. According to Boissonnade *et al*, (2006) a member with open I or H section, restrained by continuous restraints, may be classified as not susceptible to torsional deformation if the conditions predicted in the Annex BB.2 of EC3-1-1 are fulfilled; other situations must be demonstrated (Boissonnade *et al*, (2006).

Members of open section, such as I or H sections, are considered as members susceptible to torsional deformations if they are not adequately torsionally and laterally restrained. Laterally restrained means that the cross section is laterally restrained at the compression level.

For the calculation of the interaction factors according to Method 2, tables from Annex B of EC3-1-1 are presented. Tables 3.14 and 3.15 indicate the interaction factors k_{ij}. Table 3.16 indicates the equivalent uniform moment factors, C_{mi}, evaluated from the diagram of bending moments between braced sections.

Table 3.14 – Interaction factors k_{ij} in members not susceptible to torsional deformations according to Method 2

Interaction factors	Type of section	Elastic sectional properties (Class 3 or 4 sections)	Plastic sectional properties (Class 1 or 2 sections)
k_{yy}	I or H sections and rectangular hollow sections	$C_{my}\left(1+0.6\overline{\lambda}_y\frac{N_{Ed}}{\chi_y N_{Rk}/\gamma_{M1}}\right)$ $\le C_{my}\left(1+0.6\frac{N_{Ed}}{\chi_y N_{Rk}/\gamma_{M1}}\right)$	$C_{my}\left(1+\left(\overline{\lambda}_y-0.2\right)\frac{N_{Ed}}{\chi_y N_{Rk}/\gamma_{M1}}\right)$ $\le C_{my}\left(1+0.8\frac{N_{Ed}}{\chi_y N_{Rk}/\gamma_{M1}}\right)$
k_{yz}	I or H sections and rectangular hollow sections	k_{zz}	0.6 k_{zz}
k_{zy}	I or H sections and rectangular hollow sections	0.8 k_{yy}	0.6 k_{yy}
k_{zz}	I or H sections	$C_{mz}\left(1+0.6\overline{\lambda}_z\frac{N_{Ed}}{\chi_z N_{Rk}/\gamma_{M1}}\right)$	$C_{mz}\left(1+\left(2\overline{\lambda}_z-0.6\right)\frac{N_{Ed}}{\chi_z N_{Rk}/\gamma_{M1}}\right)$ $\le C_{mz}\left(1+1.4\frac{N_{Ed}}{\chi_z N_{Rk}/\gamma_{M1}}\right)$
	rectangular hollow sections	$\le C_{mz}\left(1+0.6\frac{N_{Ed}}{\chi_z N_{Rk}/\gamma_{M1}}\right)$	$C_{mz}\left(1+\left(\overline{\lambda}_z-0.2\right)\frac{N_{Ed}}{\chi_z N_{Rk}/\gamma_{M1}}\right)$ $\le C_{mz}\left(1+0.8\frac{N_{Ed}}{\chi_z N_{Rk}/\gamma_{M1}}\right)$
In I or H sections and rectangular hollow sections under axial compression and uniaxial bending ($M_{y,Ed}$), k_{zy} may be taken as zero.			

To illustrate the calculation of the equivalent uniform moment factors C_{mi} (Table 3.16), consider a member under bi-axial bending and axial compression, with the support sections restrained from rotating around its axis (fork conditions) and laterally braced at some intermediate sections. It is assumed that the intermediate bracings prevent not only torsional deformation, but also transverse displacements of the cross sections where they are applied. In this case, the factor C_{my} should be assessed based on the bending moment diagram M_y along the total length of the member; and factors C_{mz} and C_{mLT} should be assessed based on the bending moment diagrams M_z and M_y respectively, between laterally braced sections.

Table 3.15 – Interaction factors k_{ij} in members susceptible to torsional deformations according to Method 2

Interaction factors	Elastic sectional properties (Class 3 or 4 sections)	Plastic sectional properties (Class 1 or 2 sections)
k_{yy}	k_{yy} of Table 3.15	k_{yy} of Table 3.15
k_{yz}	k_{yz} of Table 3.15	k_{yz} of Table 3.15
k_{zy}	$\left[1-\frac{0.05\bar{\lambda}_z}{(C_{mLT}-0.25)}\frac{N_{Ed}}{\chi_z N_{Rk}/\gamma_{M1}}\right]$ $\geq\left[1-\frac{0.05}{(C_{mLT}-0.25)}\frac{N_{Ed}}{\chi_z N_{Rk}/\gamma_{M1}}\right]$	$\left[1-\frac{0.1\bar{\lambda}_z}{(C_{mLT}-0.25)}\frac{N_{Ed}}{\chi_z N_{Rk}/\gamma_{M1}}\right]$ $\geq\left[1-\frac{0.1}{(C_{mLT}-025)}\frac{N_{Ed}}{\chi_z N_{Rk}/\gamma_{M1}}\right]$ for $\bar{\lambda}_z<0.4:\ k_{zy}=0.6+\bar{\lambda}_z$ $\leq 1-\frac{0.1\bar{\lambda}_z}{(C_{mLT}-0.25)}\frac{N_{Ed}}{\chi_z N_{Rk}/\gamma_{M1}}$
k_{zz}	k_{zz} of Table 3.15	k_{zz} of Table 3.15

Table 3.16 – Equivalent uniform moment factors C_{mi}

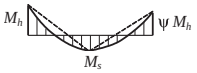
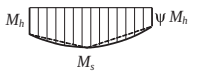
Diagram of moments	Range		C_{my}, C_{mz} and C_{mLT}	
			Uniform loading	Concentrated load
	$-1 \leq \Psi \leq 1$		$0.6 + 0.4\Psi \geq 0.4$	
 $\alpha_h = M_S / M_h$	$0 \leq \alpha_s \leq 1$	$-1 \leq \Psi \leq 1$	$0.2 + 0.8\ \alpha_s \geq 0.4$	$0.2 + 0.8\ \alpha_s \geq 0.4$
	$-1 \leq \alpha_s < 0$	$0 \leq \Psi \leq 1$	$0.1 - 0.8\ \alpha_s \geq 0.4$	$-0.8\ \alpha_s \geq 0.4$
		$-1 \leq \Psi < 0$	$0.1(1-\Psi) - 0.8\alpha_s \geq 0.4$	$0.2(-\Psi) - 0.8\alpha_s \geq 0.4$

Table 3.16 (cont.) – Equivalent factors of uniform moment C_{mi}

 $\alpha_h = M_h / M_s$	$0 \le \alpha_h \le 1$	$-1 \le \Psi \le 1$	$0.95 + 0.05\,\alpha_h$	$0.90 + 0.10\,\alpha_h$
	$-1 \le \alpha_h < 0$	$0 \le \Psi \le 1$	$0.95 + 0.05\,\alpha_h$	$0.90 + 0.10\,\alpha_h$
		$-1 \le \Psi < 0$	$0.95 + 0.05\,\alpha_h\,(1 + 2\Psi)$	$0.90 + 0.10\,\alpha_h(1 + 2\Psi)$
In the calculation of α_s or α_h parameters, a hogging moment should be taken as negative and a sagging moment should be taken as positive.				
For members with sway buckling mode, the equivalent uniform moment factor should be taken as $C_{my} = 0.9$ or $C_{mz} = 0.9$, respectively.				
Factors C_{my}, C_{mz} and C_{mLT} should be obtained from the diagram of bending moments between the relevant braced sections, according to the following:				

Moment factor	bending axis	points braced in direction
C_{my}	*y-y*	*z-z*
C_{mz}	*z-z*	*y-y*
C_{mLT}	*y-y*	*y-y*

3.7.5. Worked examples

Example 3.15: Consider column A-B that supports a steel cantilever B-C, represented in Figure 3.82. The column is fixed at section A, while the top section (B) is free to rotate, but restrained from horizontal displacements in both directions. The column has a rectangular hollow section SHS 200×150×8 mm in S 355 steel (E = 210 GPa and G = 81 GPa). Assuming that the indicated loading is already factored for ULS, verify the column according to EC3-1-1.

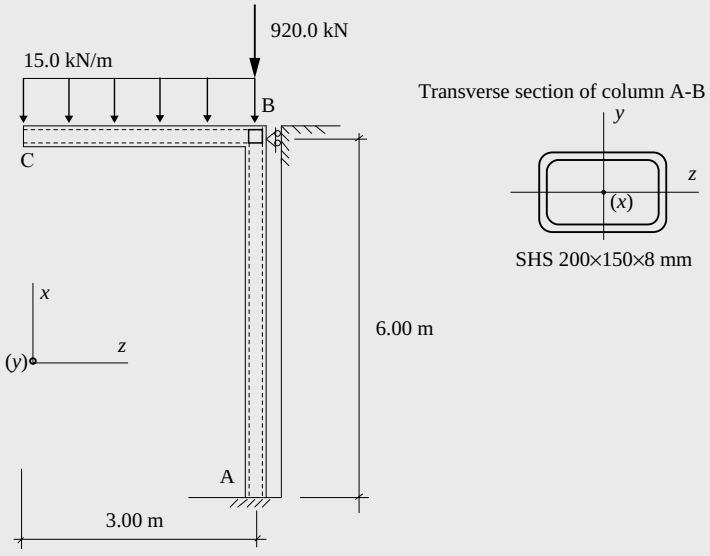


Figure 3.82 – Hot-finished rectangular hollow section structure

i) *Internal force diagrams*

For the given design loading, the internal force diagrams are represented in Figure 3.83.

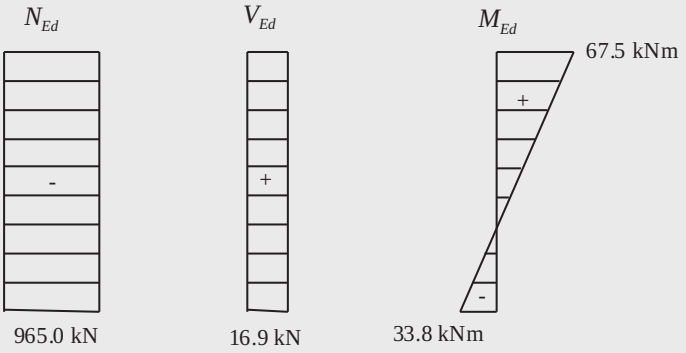


Figure 3.83 – Internal force diagrams

ii) *Verification of the cross section resistance*

The relevant geometrical characteristics of a SHS 200x150x8 mm are the following: A = 52.75 cm^2, $W_{pl,y}$ = 358.8 cm^3, $W_{el,y}$ = 297.1 cm^3, I_y = 2971 cm^4, i_y = 7.505 cm, $W_{pl,z}$ = 293.7 cm^3, $W_{el,z}$ = 252.6 cm^3, I_z = 1894 cm^4, i_z = 5.992 cm and I_T = 3643 cm^4.

As the cross section of the member is already known, the verification of its class is carried out according to clause 5.5. For a member subjected to varying bending and compression, the class of the cross section may vary along the member. While this does not introduce any type of difficulty in the verification of the cross section resistance (each section is designed according to its own class), it is more difficult to define the class of the cross section for the verification of the member's stability, as this is a global verification. In this example, a simplified approach is adopted, whereby the class of the cross section is verified for the most unfavourable situation (compressed section only). Thus, for the longer side, according to Table 2.21 (Table 5.2 in EC3-1-1),

$$c/t \approx \left(b-3t\right)/t = \left(200-3\times 8\right)/8 = 22.0 < 33\varepsilon = 33\times 0.81 = 26.7. \quad \text{(Class 1)}$$

The cross section is class 1 in compression and can be treated as a class 1 cross section for any other combination of stresses.

The resistance to bending about the *y* axis, combined with the axial force, is obtained from equation (3.151), according to clause 6.2.9.1(5):

$$M_{N,y,Rd} = M_{pl,y,Rd}\frac{1-n}{1-0.5\,a_w} \le M_{pl,y,Rd}.$$

For the critical cross section (top of the column), subjected to N_{Ed} = 965.0 kN and $M_{y,Ed}$ = 67.5 kNm,

$$n = \frac{N_{Ed}}{N_{pl,Rd}} = \frac{965}{52.75\times10^{-4}\times355\times10^{3}/1.0} = 0.52;$$

$$a_w = \frac{A-2b\,t}{A} = \frac{52.75-2\times15\times0.8}{52.75} = 0.55 > 0.5 \Rightarrow a_w = 0.5;$$

$$M_{pl,y,Rd} = 358.8\times10^{-6}\times\frac{355\times10^{3}}{1.0} = 127.4 \text{ kNm}.$$

The reduced design plastic moment resistance is given by:

$$M_{N,y,Rd} = 127.4\times\frac{1-0.52}{1-0.5\times0.5} = 81.5 \text{ kNm} < M_{pl,y,Rd}$$
$$\Rightarrow M_{N,y,Rd} = 81.5 \text{ kNm}.$$

so that,

$$M_{Ed} = 67.5 \text{ kNm} < M_{N,y,Rd} = 81.5 \text{ kNm}.$$

Shear must be verified in any cross section, since the member is under constant shear. From clause 6.2.6(3):

$A_v = \frac{A\,h}{b+h} = \frac{52.75\times20}{15+20} = 30.14 \text{ cm}^2$, leading to:

$$V_{pl,Rd} = \frac{A_v\,f_y}{\gamma_{M0}\sqrt{3}} = \frac{30.14\times10^{-4}\times355\times10^{3}}{1.0\times\sqrt{3}} = 617.7 \text{ kN}.$$

As $V_{Ed} = 16.9 \text{ kN} < V_{pl,Rd} = 617.7 \text{ kN}$, the resistance to shear is satisfactory.

For the verification of the shear buckling of the web, according to clause 6.2.6(6), with η = 1,

$$h_w/t_w \approx (h-3t)/t = (200-3\times8)/8 = 22.0 < 72\varepsilon/\eta = 58.3,$$

and so verification is not required.

The verification of the interaction of bending and compression with shear, according to clause 6.2.8, must be done for cross section B. As

$$V_{Ed} = 16.9 \text{ kN} < 0.50 \times V_{pl,Rd} = 0.5 \times 617.7 = 308.9 \text{ kN},$$

it is not necessary to reduce the resistance of the section due to this interaction.

iii) *Verification of the stability of the member*

For the beam-column subject to uniaxial bending (about *y*) and compression, using a class 1 section, according to expressions (3.163) the following conditions must be verified:

$$\frac{N_{Ed}}{\chi_y N_{Rk}/\gamma_{M1}} + k_{yy}\frac{M_{y,Ed}}{\chi_{LT} M_{y,Rk}/\gamma_{M1}} \le 1.0;$$

$$\frac{N_{Ed}}{\chi_z N_{Rk}/\gamma_{M1}} + k_{zy}\frac{M_{y,Ed}}{\chi_{LT} M_{y,Rk}/\gamma_{M1}} \le 1.0.$$

The interaction factors k_{yy} and k_{zy} can be obtained using one of the methods given in clause 6.3.3, Method 1 or Method 2; for the sake of comparison, both are used in this example.

iii-1) *Method* 1

Since the member has a rectangular hollow section with I_T = 3643 cm^4 > I_y = 2971 cm^4, the member is not susceptible to torsional deformation, so flexural buckling constitutes the relevant instability mode. Therefore it is not necessary to verify lateral-torsional buckling and χ_{LT} = 1.0 in expressions (3.163). The following steps are required to calculate the interaction factors k_{yy} and $k_{zy.}$

- *Step* 1: characteristic resistance of the section

$$N_{Rk} = A f_y = 52.75 \times 10^{-4} \times 355 \times 10^3 = 1872.6 \text{ kN};$$
$$M_{y,Rk} = W_{pl,y} f_y = 358.8 \times 10^{-6} \times 355 \times 10^3 = 127.4 \text{ kNm}.$$

- *Step* 2: reduction coefficients due to flexural buckling, χ_y and χ_z

Plane *xz* (buckling about *y*):

$L_{E,y} = 0.7 \times 6.0 = 4.2$ m;

$$\overline{\lambda}_y = \frac{L_{E,y}}{i_y}\frac{1}{\lambda_1} = \frac{4.2}{7.505 \times 10^{-2}} \times \frac{1}{93.9 \times 0.81} = 0.74;$$

$\alpha = 0.21$ Curve *a* (Table 6.2 of EC3-1-1);

$\phi = 0.83$ $\Rightarrow \chi_y = 0.83$.

Plane *xy* (buckling about *z*):

$L_{E,z} = 0.7 \times 6.0 = 4.2$ m;

$$\overline{\lambda}_z = \frac{L_{E,z}}{i_z}\frac{1}{\lambda_1} = \frac{4.2}{5.992 \times 10^{-2}} \times \frac{1}{93.9 \times 0.81} = 0.92;$$

$\alpha = 0.21$ Curve *a* (Table 6.2 of EC3-1-1);

$\phi = 1.00$ $\Rightarrow \chi_z = 0.72$.

- *Step* 3: calculation of the auxiliary terms, including factors C_{yy} and C_{zy} (factors that depend on the degree of plasticity of the section in the collapse situation), defined in Table 3.12 (Table A.1 of EC3-1-1).

$$N_{cr,y} = \frac{\pi^2 E\, I_y}{L_{E,y}^2} = \frac{\pi^2 \times 210 \times 10^6 \times 2971 \times 10^{-8}}{4.2^2} = 3490.8 \text{ kN};$$

$$N_{cr,z} = \frac{\pi^2\, E\, I_z}{L_{E,z}^2} = \frac{\pi^2 \times 210 \times 10^6 \times 1894 \times 10^{-8}}{4.2^2} = 2225.4 \text{ kN};$$

$$\mu_y = \frac{1 - \dfrac{N_{Ed}}{N_{cr,y}}}{1 - \chi_y \dfrac{N_{Ed}}{N_{cr,y}}} = \frac{1 - \dfrac{965}{3490.8}}{1 - 0.83 \times \dfrac{965}{3490.8}} = 0.94;$$

$$\mu_z = \frac{1 - \dfrac{N_{Ed}}{N_{cr,z}}}{1 - \chi_z \dfrac{N_{Ed}}{N_{cr,z}}} = \frac{1 - \dfrac{965}{2225.4}}{1 - 0.72 \times \dfrac{965}{2225.4}} = 0.82;$$

$$w_y = \frac{W_{pl,y}}{W_{el,y}} = \frac{358.8}{297.1} = 1.21 \ \left(< 1.5\right);$$

$$w_z = \frac{W_{pl,z}}{W_{el,z}} = \frac{293.7}{252.6} = 1.16 \ \left(< 1.5\right);$$

$$n_{pl} = \frac{N_{Ed}}{N_{Rk}/\gamma_{M1}} = \frac{965}{1872.6/1.0} = 0.52;$$

$$\overline{\lambda}_{\max} = \max\left(\overline{\lambda}_y, \overline{\lambda}_z\right) = \max\left(0.74; 0.92\right) = 0.92.$$

As the member is not susceptible to torsional deformations, in accordance with Table 3.12, the equivalent uniform moment factors are defined by $C_{my} = C_{my,0}$ and $C_{mLT} = 1.0$, where $C_{my,0}$ is the factor obtained based on Table 3.13 (Table A.2 of EC3-1-1). For a linear bending moment diagram, with $M_{y,Ed,base} = -33.8$ kNm and $M_{y,Ed,top} = 67.5$ kNm,

$$\Psi_y = M_{y,Ed,base}/M_{y,Ed,top} = -33.8/67.5 = -0.50;$$

$$C_{my,0} = 0.79 + 0.21\Psi_y + 0.36\left(\Psi_y - 0.33\right)\frac{N_{Ed}}{N_{cr,y}} =$$

$$= 0.79 + 0.21 \times \left(-0.5\right) + 0.36 \times \left(-0.50 - 0.33\right) \times \frac{965}{3490.8} = 0.60;$$

$$C_{my} = C_{my,0} = 0.60.$$

As $I_T > I_y \ \Rightarrow a_{LT} = 0 \ \Rightarrow b_{LT} = d_{LT} = 0$, factors C_{yy} and C_{zy} are given by:

$$C_{yy} = 1 + \left(w_y - 1\right)\left[\left(2 - \frac{1.6}{w_y}C_{my}^2\overline{\lambda}_{\max} - \frac{1.6}{w_y}C_{my}^2\overline{\lambda}_{\max}\right)n_{pl}\right] \geq \frac{W_{el,y}}{W_{pl,y}} \Leftrightarrow$$

$$C_{yy} = 1 + \left(1.21 - 1\right) \times \left[\left(2 - \frac{1.6}{1.21} \times 0.60^2 \times 0.92 - \frac{1.6}{1.21} \times 0.60^2 \times 0.92^2\right) \times 0.52\right] =$$

$$= 1.13 \qquad \left(> W_{el,y}/W_{pl,y} = 297.1/358.8 = 0.83\right);$$

$$C_{zy} = 1 + \left(w_y - 1\right)\left[\left(2 - 14\frac{C_{my}^2\overline{\lambda}_{\max}^2}{w_y^5}\right)n_{pl}\right] \geq 0.6\sqrt{\frac{w_y}{w_z}}\frac{W_{el,y}}{W_{pl,y}} \Leftrightarrow$$

$$C_{zy} = 1 + \left(1.21 - 1\right) \times \left[\left(2 - 14 \times \frac{0.60^2 \times 0.92^2}{1.21^5} \right) \times 0.52 \right] = 1.04$$

$$\left(> 0.6 \sqrt{\frac{w_y}{w_z}} \frac{W_{el,y}}{W_{pl,y}} = 0.6 \times \sqrt{\frac{1.21}{1.16}} \times \frac{297.1}{358.8} = 0.51 \right).$$

- *Step* 4: interaction factors k_{yy} and k_{zy}

Based on all the calculated auxiliary terms, considering that the cross section is class 1, expressions in Table 3.11, give the following interaction factors k_{yy} and k_{zy}:

$$k_{yy} = C_{my} C_{mLT} \frac{\mu_y}{1 - \frac{N_{Ed}}{N_{cr,y}}} \frac{1}{C_{yy}} = 0.60 \times 1.0 \times \frac{0.94}{1 - \frac{965.0}{3490.8}} \times \frac{1}{1.13} = 0.69;$$

$$k_{zy} = C_{my} C_{mLT} \frac{\mu_z}{1 - \frac{N_{Ed}}{N_{cr,y}}} \frac{1}{C_{zy}} 0.6 \sqrt{\frac{w_y}{w_z}} =$$

$$= 0.60 \times 1.0 \times \frac{0.82}{1 - \frac{965.0}{3490.8}} \times \frac{1}{1.04} \times 0.6 \times \sqrt{\frac{1.21}{1.16}} = 0.40.$$

Finally, expressions (3.163) yield:

$$\frac{N_{Ed}}{\chi_y N_{Rk} / \gamma_{M1}} + k_{yy} \frac{M_{y,Ed}}{\chi_{LT} M_{y,Rk} / \gamma_{M1}} =$$

$$= \frac{965.0}{0.83 \times 1872.6 / 1.0} + 0.69 \times \frac{67.5}{1.0 \times 127.4 / 1.0} = 0.99 < 1.0;$$

$$\frac{N_{Ed}}{\chi_z N_{Rk} / \gamma_{M1}} + k_{zy} \frac{M_{y,Ed}}{\chi_{LT} M_{y,Rk} / \gamma_{M1}} =$$

$$= \frac{965.0}{0.72 \times 1872.6 / 1.0} + 0.40 \times \frac{67.5}{1.0 \times 127.4 / 1.0} = 0.93 < 1.0.$$

The rectangular hollow section 200×150×8 mm in S 355 steel is verified according to Method 1.

iii-2) *Method* 2

As the member has a rectangular hollow section, due to its high lateral bending and torsional stiffness the verification of lateral torsional buckling is not required, and χ_{LT} = 1.0. Because Method 2 only differs from Method 1 with respect to the interaction factors, the calculation of these factors is done directly.

As the member is not susceptible to torsional deformations, the interaction factors must be obtained from Table 3.14 (Table B.1 of EC3-1-1).

For a linear bending moment diagram, with $M_{y,Ed,base}$= -33.8 kNm and $M_{y,Ed,top}$= 67.5 kNm,

$$\Psi_y = M_{y,Ed,base} / M_{y,Ed,top} = -33.8/67.5 = -0.50.$$

Table 3.16 (Table B.3 of EC3-1-1) gives:

$$C_{my} = 0.6 + 0.4 \times (-0.50) = 0.40 \quad (\geq 0.40).$$

Based on the previous calculations for Method 1 and for a class 1 section, interaction factors k_{yy} and k_{zy} are given by:

$$k_{yy} = C_{my}\left[1 + (\bar{\lambda}_y - 0.2)\frac{N_{Ed}}{\chi_y N_{Rk}/\gamma_{M1}}\right] =$$

$$= 0.40 \times \left[1 + (0.74 - 0.2) \times \frac{965.0}{0.83 \times 1872.6/1.0}\right] = 0.53;$$

$$\text{as } k_{yy} = 0.53 < C_{my}\left[1 + 0.8\frac{N_{Ed}}{\chi_y N_{Rk}/\gamma_{M1}}\right] = 0.60,$$

$$k_{yy} = 0.53.$$

According to Method 2, for a rectangular hollow section subject to compression and uniaxial bending about *y*, may be assumed k_{zy} = 0. Expressions (3.163) become:

$$\frac{965.0}{0.83 \times 1872.6/1.0} + 0.53 \times \frac{67.5}{1.0 \times 127.4/1.0} = 0.90 < 1.0;$$

$$\frac{965.0}{0.72 \times 1872.6/1.0} = 0.72 < 1.0.$$

so that the rectangular hollow section 200×150×8 mm in S 355 steel is also verified by Method 2. It is noted that, for this case, Method 2 yields less conservative results than Method 1.

Example 3.16: Verify the safety of column A-B of a typical industrial building, illustrated in Figure 3.84. The column' section is an IPE 360 (E = 210 GPa and G = 81 GPa) in S 355 steel. For a given load combination, the column is subjected to the factored design internal forces shown in Figure 3.84. It can be assumed that shear is small enough to be neglected in the verification of the member. The structure is assumed to be a sway frame. So, in accordance with the second method described in 2.3.2.1 (5.2.2(7)b of EC3-1-1), the design internal forces (given in Figure 3.84) were obtained from a second order analysis and the buckling length in the plane of the framework (plane *xz*) to be used in the design checks is given by $L_{E,y}$ = 6.0 m, equal to the real length. For the buckling length in the *xy* plane, consider that the column is braced at the bottom, at mid-height and at the top.

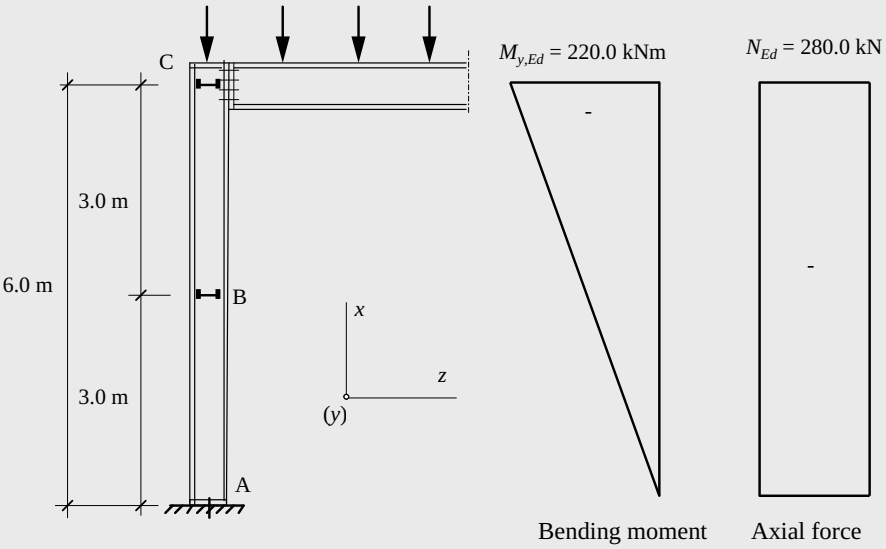


Figure 3.84 – Column subjected to major-axis bending and compression

---

Geometrical characteristics of the IPE 360: A = 72.73 cm^2, h = 360 mm, b = 170 mm, $W_{el,y}$ = 903.6 cm^3, $W_{pl,y}$ = 1019 cm^3, I_y = 16270 cm^4, i_y = 14.95 cm, $W_{el,z}$ = 122.8 cm^3, $W_{pl,z}$ = 191.1 cm^3, I_z = 1043 cm^4, i_z = 3.79 cm, I_T = 37.32 cm^4 and I_w = 313.6x10^3 cm^6.

i) *Cross section classification*

EC3-1-1 does not provide criteria for the definition of the cross sectional class to be considered in the verification of the stability of a member, for the common case in which the class varies along the member as a consequence of varying internal forces. Following the guidance from the SEMI-COMP+ project (Greiner *et al*, 2011), the classification for member buckling design may be established as an equivalent class based on the cross section with maximum first-order utilization factor. In this case, since the utilization factor is maximum at cross section C (UF = 0.608), the classification of the beam-column for member buckling design corresponds to the cross sectional class of section C. As this section is subjected to bending and compression, the position of the neutral axis for the situation of complete plastification of the section, which is necessary for the classification of the web, depends on the relation between the bending moment and the axial force. According to sub-chapter 2.4, equation (2.27b) may be used to estimate the position of the neutral axis, for fully plastic stress distributions, giving:

$$\alpha = \frac{1}{2} + \frac{\left|-220\right|}{-280} \times \left(\frac{1}{298.6 \times 10^{-3}} - \frac{1}{2 \times 298.6 \times 10^{-3}} \times \right.$$

$$\left. \times \sqrt{\left(298.6 \times 10^{-3} \times \frac{-280}{-220} \right)^2 + \frac{\left(-280\right)^2 \times \left(4 \times 1019 \times 10^{-6} - \left(298.6 \times 10^{-3} \right)^2 \times 8 \times 10^{-3} \right)}{\left(-220\right)^2 \times 8 \times 10^{-3}}} + 4 \right)$$

$$= 0.759.$$

For the web in bending and compression,

$$c/t = 298.6/8 = 37.3 < \frac{396\varepsilon}{13\alpha - 1} = \frac{396 \times 0.81}{13 \times 0.759 - 1} = 36.17 . \qquad \text{(not of Class 1)}$$

$$c/t = 298.6/8 = 37.3 < \frac{456\varepsilon}{13\alpha - 1} = \frac{456 \times 0.81}{13 \times 0.759 - 1} = 41.66 . \qquad \text{(Class 2)}$$

Compressed flange,

$$c/t = \left(170/2 - 8/2 - 18\right)/12.7 = 5.0 < 9\varepsilon = 9 \times 0.81 = 7.3. \qquad \text{(Class 1)}$$

Therefore, the section is class 2. Note that if the cross section class were established based on the internal forces at section A (compression only), the class of the member for the stability check would be 4.

ii) *Verification of the cross section resistance*

Based on the internal force diagrams, section C is the critical cross section, with $M_{y,Ed}$ = 220.0 kNm and N_{Ed} = 280.0 kN. Since

$$N_{pl,Rd} = f_y A/\gamma_{M0} = 355 \times 7273/1.0 = 2581.9 \text{ kN}$$

$$N_{Ed} = 280 \text{ kN} \le 0.25 N_{pl,Rd} = 645.5 \text{ kN},$$

and

$$N_{Ed} = 280.0 \text{ kN} \le 0.5\, h_w\, t_w\, f_y/\gamma_{M0} = 475.1 \text{ kN},$$

according to clause 6.2.9.1(4) it is not necessary to reduce the plastic bending resistance, which is therefore given by:

$$M_{pl,y,Rd} = W_{pl,y} \frac{f_y}{\gamma_{M0}} = 361.7 \text{ kNm} > M_{y,Ed} = 220.0 \text{ kNm}.$$

It is further noted that strictly speaking the resistance of the cross section A should also be checked; however, as the design axial force, N_{Ed} = 280 kN is very small compared with the cross section capacity (utilization factor of 0.11) and also as the analysis of cross section of class 4 is outside of the scope of this publication, this verification is not performed here.

iii) *Verification of the stability of the member*

In this example only Method 2 is applied. As the member is susceptible to torsional deformations (thin-walled open cross section), it is assumed that lateral-torsional buckling constitutes the relevant instability mode. Since $M_{z,Ed}$ = 0, the following conditions must be verified:

$$\frac{N_{Ed}}{\chi_y N_{Rk}/\gamma_{M1}} + k_{yy}\frac{M_{y,Ed}}{\chi_{LT} M_{y,Rk}/\gamma_{M1}} \le 1.0;$$

$$\frac{N_{Ed}}{\chi_z N_{Rk}/\gamma_{M1}} + k_{zy}\frac{M_{y,Ed}}{\chi_{LT} M_{y,Rk}/\gamma_{M1}} \le 1.0.$$

The following steps are required to calculate the interaction factors k_{yy} and $k_{zy.}$

- *Step* 1: characteristic resistance of the section

$$N_{Rk} = A f_y = 72.73\times10^{-4}\times355\times10^{3} = 2581.9 \text{ kN};$$

$$M_{y,Rk} = W_{pl,y} f_y = 1019\times10^{-6}\times355\times10^{3} = 361.7 \text{ kNm}.$$

- *Step* 2: reduction coefficients due to flexural buckling, χ_y and χ_z

Plane *xz* - $L_{E,y}$ = 6.0 m.

$$\overline{\lambda}_y = \frac{L_{E,y}}{i_y}\frac{1}{\lambda_1} = \frac{6}{14.95\times10^{-2}}\times\frac{1}{93.9\times0.81} = 0.53;$$

α = 0.21 Curve *a* (Table 6.2 of EC3-1-1);

$\phi = 0.68 \quad \Rightarrow \chi_y = 0.90.$

Plane *xy* - $L_{E,z}$ = 3.0 m, assuming that secondary beams prevent displacements of the braced cross sections in the *y* direction.

$$\overline{\lambda}_z = \frac{L_{E,z}}{i_z}\frac{1}{\lambda_1} = \frac{3.0}{3.79\times10^{-2}}\times\frac{1}{93.9\times0.81} = 1.04;$$

α =0.34 Curve *b* (Table 6.2 of EC3-1-1);

$\phi = 1.18 \quad \Rightarrow \chi_z = 0.58.$

- *Step* 3: calculation of the χ_{LT} using the alternative method applicable to rolled or equivalent welded sections (clause 6.3.2.3)

The length between braced sections is *L* = 3.0 m. Using equation (B.1) and Table B.5 for a member subjected to unequal end moments, gives:

$\beta = -0.50 \Rightarrow \alpha_m = 1.30 \Rightarrow M_{cr} = 644.9 \text{ kNm} \Rightarrow \overline{\lambda}_{LT} = 0.75.$

As $\alpha_{LT} = 0.49$ (rolled I or H sections with $h/b > 2 \Rightarrow$ curve *c* and, from clause 6.3.2.3, taking $\overline{\lambda}_{LT,0} = 0.4$ and, β = 0.75, gives:

$\phi = 0.80 \quad \Rightarrow \chi_{LT} = 0.79.$

The correction factor k_c, according to Table 3.8 (Table 6.6 of EC3-1-1), with Ψ = 0.50, is given by:

$$k_c = \frac{1}{1.33 - 0.33\Psi} = 0.86.$$

From equation (3.133),

$$f = 1 - 0.5 \times \left(1 - 0.86\right) \times \left[1 - 2.0 \times \left(0.75 - 0.8\right)^2\right] = 0.93,$$

The modified lateral-torsional buckling reduction factor is obtained:

$\chi_{LT,\text{mod}} = 0.79/0.93 = 0.85.$

- *Step* 4: interaction factors k_{yy} and k_{zy}.

Because the member is susceptible to torsional deformations, the interaction factors are obtained from Table 3.15 (Table B.2 of EC3-1-1).

First, the equivalent uniform moment factors C_{my} and C_{mLT} are obtained based on the bending moment diagram, between braced sections according to the *y* direction in case of C_{my} and in the *z* direction in case of C_{mLT}. The factor C_{my} is taken for a non-sway structure, in accordance with the second method described in 2.3.2.1 (5.2.2(7)b of EC3-1-1), that was adopted in this example. Assuming a member braced in *z* direction and laterally at the base, mid-height and top, the factor C_{mLT} must be calculated based on the bending moment diagram in the upper half of the column (most unfavourable), while C_{my} is calculated based on the bending moment diagram M_y along the total length of the member; since the bending moment diagram is linear, defined by $M_{y,Ed,base}$ = 0, $M_{y,Ed,1/2height}$ = -110 kNm and $M_{y,Ed,top}$ = -220 kNm, based on Table 3.16,

$$\Psi = M_{v,Ed,base} \big/ M_{v,Ed,top} = (0) \big/ (-220) = 0;$$

$$C_{my} = 0.60 + 0.4 \times (0) = 0.60 \quad (> 0.40).$$

and

$$\Psi = M_{y,Ed,1/2height} \big/ M_{v,Ed,top} = (-110) \big/ (-220) = 0.5;$$

$$C_{mLT} = 0.60 + 0.4 \times (0.5) = 0.80 \quad (> 0.40).$$

The interaction factors k_{yy} and k_{zy} are given by:

$$k_{yy} = C_{my} \left[1 + (\bar{\lambda}_y - 0.2) \frac{N_{Ed}}{\chi_y N_{Rk} / \gamma_{M1}} \right] =$$

$$= 0.60 \times \left[1 + (0.53 - 0.2) \times \frac{280.0}{0.90 \times 2581.9 / 1.0} \right] = 0.624;$$

$$\text{as } k_{yy} = 0.624 \le C_{my} \left[1 + 0.8 \frac{N_{Ed}}{\chi_y N_{Rk} / \gamma_{M1}} \right] = 0.658;$$

giving $k_{yy} = 0.624$.

$$k_{zy} = \left[1 - \frac{0.1 \bar{\lambda}_z}{(C_{mLT} - 0.25)} \frac{N_{Ed}}{\chi_z N_{Rk} / \gamma_{M1}} \right] =$$

$$= \left[1 - \frac{0.1 \times 1.04}{(0.8 - 0.25)} \times \frac{280}{0.58 \times 2581.9 / 1.0} \right] = 0.966$$

$$\text{as } k_{zy} = 0.966 \ge \left[1 - \frac{0.1}{(C_{mLT} - 0.25)} \frac{N_{Ed}}{\chi_z N_{Rk} / \gamma_{M1}} \right] = 0.947,$$

then $k_{zy} = 0.966$.

Finally, the verification of expressions (3.163) yields:

$$\frac{280.0}{0.9 \times 2581.9 / 1.0} + 0.624 \times \frac{220.0}{0.85 \times 361.7 / 1.0} = 0.56 < 1.0;$$

$$\frac{280.0}{0.58\times 2581.9/1.0}+0.966\times\frac{220.0}{0.85\times 361.7/1.0}=0.88<1.0.$$

It is concluded that the IPE 360 is adequate.

Example 3.17: Consider the beam-column of Figure 3.85, whose section is an IPE 500 profile in S 275 steel. Assume that the end sections are restrained from rotating around the axis of the member. The design loading consists of a concentrated load P_{Ed} = 320 kN, support reactions of 160 kN, an axial compressive force N_{Ed} = 520 kN and two pairs of equal end moments $M_{y,Ed}$ = 160 kNm and $M_{z,Ed}$ = 17.5 kNm, as shown in Figure 3.85. Verify the member according to EC3-1-1.

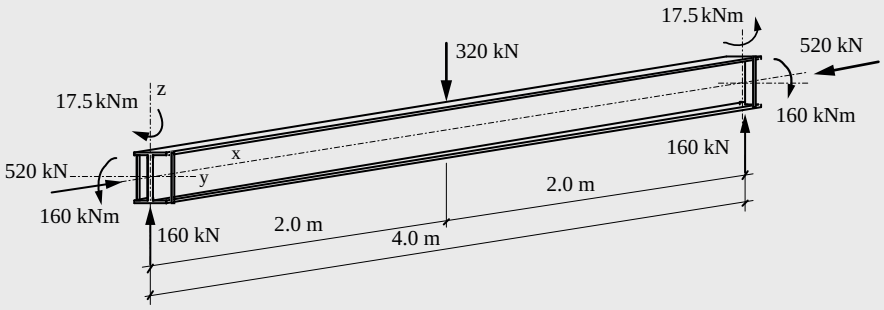


Figure 3.85 – Member under bi-axial bending and compression

The required geometrical properties of the IPE 500 section are the following: A = 115.5 cm^2, A_{vz} = 59.87 cm^2, h = 500 mm, b = 200 mm, $W_{el,y}$ = 1928 cm^3, $W_{pl,y}$ = 2194 cm^3, I_y = 48200 cm^4, i_y = 20.43 cm, $W_{el,z}$ = 214.2 cm^3, $W_{pl,z}$ = 335.9 cm^3, I_z = 2142 cm^4, i_z = 4.31 cm, I_T = 89.29 cm^4 and I_w = 1249x10^3 cm^6.

i) *Internal force diagrams*

For the design loading, the internal force diagrams are represented in the Figure 3.86.

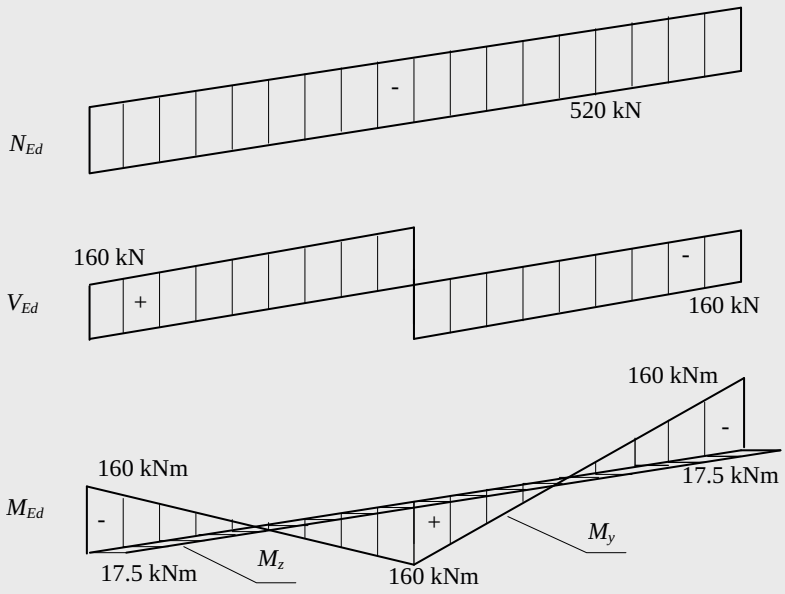


Figure 3.86 – Diagrams of internal forces

ii) *Classification*

Noting that a IPE 500 in steel S 275 is class 1 in pure bending and class 4 in compression, it is required to check the cross sectional class along the length of the member since it is subject to a varying bending moment M_y. Figure 3.87, obtained using the SEMICOMP+ Member Design software (Greiner *et al*, 2011), illustrates the calculation of the utilization factor in 10 equally-spaced cross sections along the member. It can be seen that the cross sectional class varies from 2 to 3, while the highest utilization factor is 0.64 for a cross section class 3.

For that critical cross section, for the web in bending and compression, the value of ψ is given by:

$\Psi = 0.03,$

so that

$$c/t = \frac{426}{10.2} = 41.8 < \frac{42\varepsilon}{0.67 + 0.33\psi} = \frac{42 \times 0.92}{0.67 + 0.33 \times 0.03} = 56.83. \qquad \text{(Class 3)}$$

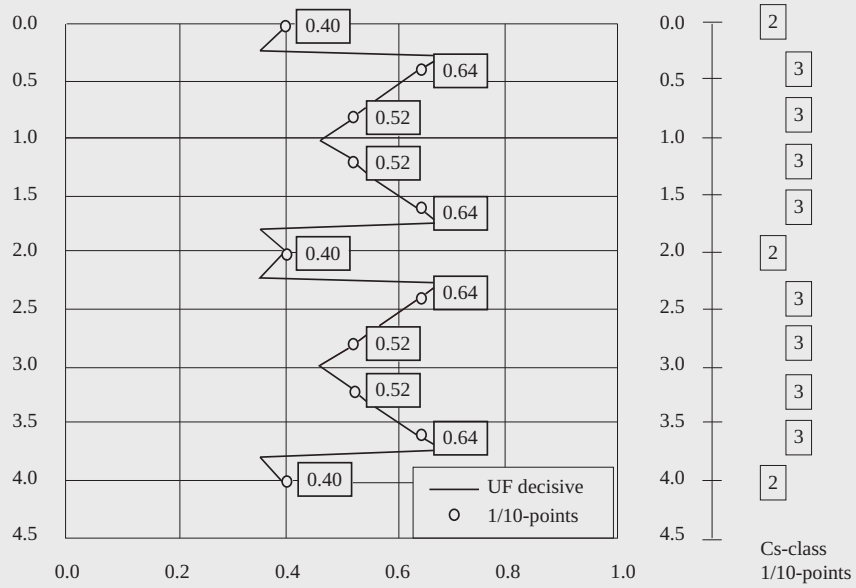


Figure 3.87 – Variation of utilization factor along the member

Compressed flange,

$$c/t = \left(200/2 - 10.2/2 - 21\right)/16.0 = 4.6 < 9\varepsilon = 9 \times 0.92 = 8.28. \qquad \text{(Class 1)}$$

Therefore, the classification for member buckling design is class 3.

iii) *Verification of the cross section resistance*

According to the internal force diagrams, the critical sections are adjacent to the end and mid-span sections, subjected to forces N_{Ed} = 520 kN (compression), V_{Ed} = 160 kN, $M_{y,Ed}$ = 160 kNm and $M_{z,Ed}$ = 17.5 kNm. First, the cross section resistance of the end and mid-span sections (cross sectional class 2) are checked according to the following steps.

- *Step* 1: shear resistance

As $A_{vz} = 59.87\ \text{cm}^2$, the shear resistance is given by:

$$V_{pl,Rd} = \frac{A_{vz}\, f_y}{\gamma_{M0}\sqrt{3}} = \frac{59.87 \times 10^{-4} \times 275 \times 10^3}{1.0 \times \sqrt{3}} = 950.6\ \text{kN},$$

so that,

$V_{Ed} = 160 \text{ kN} < V_{pl,Rd} = 950.6 \text{ kN}.$

According to clause 6.2.6(6), with η = 1, there is no need to calculate the shear buckling resistance of the web since,

$h_w / t_w = 468/10.2 = 45.9 < 72\varepsilon/\eta = 72 \times 0.92/1.0 = 66.2.$

- *Step* 2: bending resistance

The bending moment and compression with shear force interaction must be verified at the end or mid-span sections.

$V_{Ed} = 160 \text{ kN} < 0.50 \times V_{pl,Rd} = 0.50 \times 950.6 = 475.3 \text{ kN}.$

Hence, when considering the combination of bending moment with axial force, it is not necessary to reduce the resistance of the cross section due to shear.

The plastic axial force is given by:

$N_{pl,Rd} = A f_y / \gamma_{M0} = 115.5 \times 10^{-4} \times 275 \times 10^3 = 3176.3 \text{ kN}.$

As $N_{Ed} = 520 \text{ kN} \le 0.25 N_{pl,Rd} = 794.1 \text{ kN},$

and with h_w = 468 mm and t_w = 10.2 mm,

$N_{Ed} = 520 \text{ kN} \le 0.5\, h_w\, t_w\, f_y / \gamma_{M0} = 656.4 \text{ kN},$

it is concluded from clause 6.2.9.1(4) that it is not necessary to reduce the design plastic moment resistance about the *y* axis due to the axial force, so:

$$M_{N,y,Rd} = M_{pl,y,Rd} = 2194 \times 10^{-6} \times \frac{275 \times 10^3}{1.0} = 603.4 \text{ kNm}.$$

Similarly, as

$N_{Ed} = 520 \text{ kN} \le h_w\, t_w f_y / \gamma_{M0} = 1312.7 \text{ kN},$

it is also not necessary to reduce the design plastic moment resistance about the *z* axis, so:

$$M_{N,z,Rd} = M_{pl,z,Rd} = 335.9 \times 10^{-6} \times \frac{275 \times 10^3}{1.0} = 92.4 \text{ kNm}.$$

Bi-axial bending and compression according to expression (3.153):

$$\left[\frac{M_{y,Ed}}{M_{N,y,Rd}}\right]^{\alpha}+\left[\frac{M_{z,Ed}}{M_{N,z,Rd}}\right]^{\beta}\le 1.0.$$

As $n=\frac{N_{Ed}}{N_{pl,Rd}}=\frac{520}{3176.3}=0.16$ and for a IPE:

$$\alpha=2,\ \beta=5n=5\times 0.16=0.80\le 1\ \Rightarrow \beta=1.$$

so that expression (3.153) yields, for the left end section of the beam-column:

$$\left[\frac{160}{603.4}\right]^{2}+\left[\frac{17.5}{92.4}\right]^{1}=0.26<1.0,$$

Additionally, because of the variation of the cross sectional class, the sections adjacent to the end and mid-span sections also need to be checked for the combined action of N_{Ed} = 520 kN (compression), $M_{y,Ed}$ = 96 kNm and $M_{z,Ed}$ = 17.5 kNm. In this case, application of equation (3.2) leads to:

$$\frac{N_{Ed}}{N_{Rd}}+\frac{M_{y,Ed}}{M_{y,Rd}}+\frac{M_{z,Ed}}{M_{z,Rd}}=\frac{520}{3176.84}+\frac{96}{530.18}+\frac{17.5}{58.9}=0.64<1.$$

The IPE 500 section in S 275 steel has sufficient cross sectional capacity to resist the applied forces.

iv) *Verification of the stability of the member*

For the member subject to a combination of bi-axial bending with compression, and with a class 3 cross section, expressions (3.163) must be verified:

$$\frac{N_{Ed}}{\chi_y N_{Rk}/\gamma_{M1}}+k_{yy}\frac{M_{y,Ed}}{\chi_{LT}M_{y,Rk}/\gamma_{M1}}+k_{yz}\frac{M_{z,Ed}}{M_{z,Rk}/\gamma_{M1}}\le 1.0;$$

$$\frac{N_{Ed}}{\chi_z N_{Rk}/\gamma_{M1}}+k_{zy}\frac{M_{y,Ed}}{\chi_{LT}M_{y,Rk}/\gamma_{M1}}+k_{zz}\frac{M_{z,Ed}}{M_{z,Rk}/\gamma_{M1}}\le 1.0.$$

The interaction factors k_{yy} k_{yz}, k_{zy} and k_{zz} can be obtained from either Method 1 or Method 2; in this example both methods are applied.

iv-1) *Method* 1

As the member has a thin-walled open section with I_T = 89.29 cm^4 < I_y = 48200 cm^4 and there is no lateral bracing along the member, the section is susceptible to torsional deformations. Therefore, lateral-torsional buckling must be considered as the relevant instability mode. The following steps are required to calculate the interaction factors k_{yy}, k_{yz}, k_{zy} and k_{zz}.

- *Step* 1: characteristic resistance of the cross section

The characteristic resistances of the cross section are given by:

$$N_{Rk} = A f_y = 115.5\times10^{-4}\times275\times10^{3} = 3176.3\ \text{kN};$$

$$M_{y,Rk} = W_{el,y} f_y = 1928\times10^{-6}\times275\times10^{3} = 530.2\ \text{kNm};$$

$$M_{z,Rk} = W_{el,z} f_y = 214.2\times10^{-6}\times275\times10^{3} = 58.9\ \text{kNm}.$$

- *Step* 2: reduction coefficients due to flexural buckling χ_y and χ_z

Plane *xz* (buckling around *y*):

$L_{E,y}$ = 4.00 m;

$$\overline{\lambda}_y = \frac{L_{E,y}}{i_y}\frac{1}{\lambda_1} = \frac{4.00}{20.43\times10^{-2}}\times\frac{1}{93.9\times0.92} = 0.23;$$

$\alpha = 0.21$ Curve *a* (Table 3.3 or Table 6.2 of EC3-1-1);

$\phi = 0.53$ $\Rightarrow \chi_y = 0.99.$

Plane *xy* (buckling around *z*):

$L_{E,z}$ = 4.00 m;

$$\overline{\lambda}_z = \frac{L_{E,z}}{i_z}\frac{1}{\lambda_1} = \frac{4.00}{4.31\times10^{-2}}\times\frac{1}{93.9\times0.92} = 1.07;$$

$\alpha = 0.34$ Curve *b* (Table 3.3 or Table 6.2 of EC3-1-1);

$\phi = 1.22$ $\Rightarrow \chi_y = 0.55.$

- *Step* 3: calculation of the auxiliary terms, including factors C_{yy} and C_{zy}, defined in Table 3.12 (Table A.1 of EC3-1-1)

$$N_{cr,y} = \frac{\pi^2 E I_y}{L_{E,y}^2} = \frac{\pi^2 \times 210 \times 10^6 \times 48200 \times 10^{-8}}{4.00^2} = 62437.6 \text{ kN};$$

$$N_{cr,z} = \frac{\pi^2 E I_z}{L_{E,z}^2} = \frac{\pi^2 \times 210 \times 10^6 \times 2142 \times 10^{-8}}{4.00^2} = 2774.7 \text{ kN};$$

$$\mu_y = \frac{1 - \frac{N_{Ed}}{N_{cr,y}}}{1 - \chi_y \frac{N_{Ed}}{N_{cr,y}}} = \frac{1 - \frac{520}{62437.6}}{1 - 0.99 \times \frac{520}{62437.6}} = 1.00;$$

$$\mu_z = \frac{1 - \frac{N_{Ed}}{N_{cr,z}}}{1 - \chi_z \frac{N_{Ed}}{N_{cr,z}}} = \frac{1 - \frac{520}{2774.7}}{1 - 0.55 \times \frac{520}{2774.7}} = 0.91;$$

$$w_y = w_z = 1.0;$$

$$n_{pl} = \frac{N_{Ed}}{N_{Rk} / \gamma_{M1}} = \frac{520}{3176.3 / 1.0} = 0.16;$$

$$\overline{\lambda}_{\max} = \max\left(\overline{\lambda}_y, \overline{\lambda}_z\right) = \max\left(0.23, 1.07\right) = 1.07.$$

The critical moment for a uniform moment ("standard case") is given by:

$$M_{cr}^E = \frac{\pi}{L} \sqrt{G I_T E I_z \left(1 + \frac{\pi^2 E I_w}{L^2 G I_T}\right)} \Leftrightarrow$$

$$M_{cr}^E = \frac{\pi}{400} \times \sqrt{81 \times 10^6 \times 89.29 \times 10^{-8} \times 210 \times 10^6 \times 2142 \times 10^{-8}}$$

$$\times \sqrt{\left(1 + \frac{\pi^2 \times 210 \times 10^6 \times 1249 \times 10^{-9}}{4.00^2 \times 81 \times 10^6 \times 89.29 \times 10^{-8}}\right)} = 806.0 \text{ kNm}.$$

The coefficient of non-dimensional slenderness concerning lateral-torsional buckling with uniform moment ("standard case"), is calculated using the following equation:

$$\overline{\lambda}_0 = \sqrt{\frac{W_{el,y} f_y}{M_{cr}^E}} = \sqrt{\frac{1928\times10^{-6}\times275\times10^3}{806.0}} = 0.811.$$

The critical torsional buckling critical, $N_{cr,T}$, is obtained from equation (3.79):

$$N_{cr,T} = \frac{1}{i_C^2}\left(G\,I_T + \frac{\pi^2 E\,I_w}{L_{ET}^2}\right), \text{ where } i_C^2 = y_C^2 + \left(I_y + I_z\right)\Big/A.$$

Since y_C = 0, because the centroid coincides with the shear centre of the cross section and L_{ET} = 4.00 m, gives:

$$i_C^2 = 0.0 + \left(48200 + 2142\right)\Big/115.5 = 435.86 \text{ cm}^2;$$

$$N_{cr,T} = \frac{1}{435.86\times10^{-4}}\times$$

$$\times\left(81\times10^6\times89.29\times10^{-8} + \frac{\pi^2\times210\times10^6\times1249\times10^{-9}}{4.00^2}\right) = 5371.4 \text{ kN}.$$

For the applied bending moment diagram, represented in Figure 3.86, the coefficient of moments (taken as coefficient α_m defined in Table B.5) takes the value C_1 = 1.71. The verification of the condition:

$$\overline{\lambda}_0 = 0.81 > 0.2\sqrt{C_1}\sqrt[4]{\left(1-\frac{N_{Ed}}{N_{cr,z}}\right)\left(1-\frac{N_{Ed}}{N_{cr,T}}\right)}$$

$$= 0.2\times\sqrt{1.71}\times\sqrt[4]{\left(1-\frac{520}{2774.7}\right)\times\left(1-\frac{520}{5371.4}\right)} = 0.24,$$

shows that the beam-column is constituted by a cross section that is susceptible of undergoing torsional deformations; this determines the way of quantifying the equivalent uniform moment factors C_{mi}.

For the design bending moment diagrams, factors $C_{my,0}$ and $C_{mz,0}$ are obtained from Table 3.13 (Table A.2 of EC3-1-1), as follows:

$$\left|\delta_x\right| = \delta_z = 1.05 \text{ mm};$$

$$\left|M_{i,Ed}\left(x\right)\right| = \left|M_{y,Ed}\right| = 160 \text{ kNm};$$

$$\Psi_z = 17.5/17.5 = 1.00;$$

$$C_{my,0} = 1 + \left(\frac{\pi^2 E I_y \left|\delta_x\right|}{L^2 \left|M_{i,Ed}\left(x\right)\right|} - 1 \right) \frac{N_{Ed}}{N_{cr,y}} =$$

$$= 1 + \left(\frac{\pi^2 \times 210 \times 10^6 \times 48200 \times 10^{-8} \times 1.05 \times 10^{-3}}{4.00^2 \times 160} - 1 \right) \times \frac{520}{62437.6} = 1.00;$$

$$C_{mz,0} = 0.79 + 0.21\Psi_z + 0.36\left(\Psi_z - 0.33\right)\frac{N_{Ed}}{N_{cr,z}} =$$

$$= 0.79 + 0.21 \times 1.00 + 0.36 \times \left(1.00 - 0.33\right) \times \frac{520}{2774.7} = 1.05.$$

Next, the uniform moment equivalent factors C_{my}, C_{mz} and C_{mLT} are calculated according to Table 3.12 (Table A.1 of EC3-1-1), considering a member susceptible to torsional deformations.

As $M_{y,Ed}$ = 160 kNm (maximum absolute value of the bending moment along the member) and considering that this is a member that has a class 3 cross section, gives:

$$a_{LT} = 1 - \frac{I_T}{I_y} = 1 - \frac{89.29 \times 10^{-8}}{48200 \times 10^{-8}} = 1.00 \quad \left(> 0\right);$$

$$\varepsilon_y = \frac{M_{y,Ed}}{N_{Ed}} \frac{A}{W_{el,y}} = \frac{160}{520} \times \frac{115.5 \times 10^{-4}}{1928 \times 10^{-6}} = 1.84;$$

$$C_{my} = C_{my,0} + \left(1 - C_{my,0}\right) \frac{\sqrt{\varepsilon_y}\, a_{LT}}{1 + \sqrt{\varepsilon_y}\, a_{LT}}$$

$$= 1.00 + \left(1 - 1.00\right) \times \frac{\sqrt{1.84} \times 1.00}{1 + \sqrt{1.84} \times 1.00} = 1.00;$$

$$C_{mz} = C_{mz,0} = 1.05;$$

$$C_{mLT} = C_{my}^2 \frac{a_{LT}}{\sqrt{\left(1-\frac{N_{Ed}}{N_{cr,z}}\right)\times\left(1-\frac{N_{Ed}}{N_{cr,T}}\right)}}$$

$$= 1.00^2 \frac{1.00}{\sqrt{\left(1-\frac{520}{2774.7}\right)\times\left(1-\frac{520}{5371.4}\right)}} = 1.17 \quad (>1).$$

The critical bending moment and the slenderness coefficient $\overline{\lambda}_{LT}$, obtained based on equation (3.120), assuming that the load is applied 104 mm above the shear centre, are given by:

$M_{cr} = 788.0$ kNm,

$$\overline{\lambda}_{LT} = \sqrt{\frac{W_{el,y} f_y}{M_{cr}}} = \sqrt{\frac{1928\times10^{-6}\times275\times10^3}{788.0}} = 0.82.$$

Because this is an I rolled section, with $h/b > 2$, the imperfection coefficient is given by α_{LT} = 0.49 (curve *c*); by applying the alternative method for rolled or equivalent welded sections that is referred in clause 6.3.2.3, we obtain:

$$\phi_{LT} = 0.5\left[1+\alpha_{LT}\left(\overline{\lambda}_{LT}-\overline{\lambda}_{LT,0}\right)+\beta\,\overline{\lambda}_{LT}^2\right] =$$

$$= 0.5\times\left[1+0.49\times\left(0.88-0.4\right)+0.75\times0.88^2\right] = 0.86.$$

$$\chi_{LT} = \frac{1}{\phi_{LT}+\left(\phi_{LT}^2-\beta\,\overline{\lambda}_{LT}^2\right)^{0.5}} = \frac{1}{0.86+\left(0.86^2-0.75\times0.82^2\right)^{0.5}} = 0.75.$$

The correction factor k_c, according to Table 3.8 (Table 6.6 of EC3-1-1) , is given by:

$k_c = 0.77$.

From equation (3.133),

$$f = 1-0.5\times\left(1-0.77\right)\times\left[1-2.0\times\left(0.82-0.8\right)^2\right] = 0.89.$$

The modified lateral-torsional buckling reduction factor is obtained:

$\chi_{LT,\mathrm{mod}} = 0.75/0.89 = 0.84.$

Based on the previously calculated auxiliary terms, with a class 3 cross section, through the expressions mentioned in Table 3.11 (Table A.1 of EC3-1-1), the interaction factors k_{yy}, k_{yz}, k_{zy} and k_{zz} are given by:

$$k_{yy} = C_{my} C_{mLT} \frac{\mu_y}{1 - \frac{N_{Ed}}{N_{cr,y}}} = 1.00 \times 1.17 \times \frac{1.00}{1 - \frac{520}{62437.6}} = 1.17;$$

$$k_{yz} = C_{mz} \frac{\mu_y}{1 - \frac{N_{Ed}}{N_{cr,z}}} = 1.05 \times \frac{1.00}{1 - \frac{520}{2774.7}} = 1.29;$$

$$k_{zy} = C_{my} C_{mLT} \frac{\mu_z}{1 - \frac{N_{Ed}}{N_{cr,y}}} = 1.00 \times 1.17 \times \frac{0.91}{1 - \frac{520}{62437.6}} = 1.06;$$

$$k_{zz} = C_{mz} \frac{\mu_z}{1 - \frac{N_{Ed}}{N_{cr,z}}} = 1.05 \times \frac{0.91}{1 - \frac{520}{2774.7}} = 1.17.$$

Based on the determined parameters, expressions (3.163) give:

$$\frac{N_{Ed}}{\chi_y N_{Rk}/\gamma_{M1}} + k_{yy} \frac{M_{y,Ed}}{\chi_{LT} M_{y,Rk}/\gamma_{M1}} + k_{yz} \frac{M_{z,Ed}}{M_{z,Rk}/\gamma_{M1}} \le 1.0 \Leftrightarrow$$

$$\frac{520}{0.99 \times 3176.3/1.0} + 1.17 \times \frac{160}{0.84 \times 530.2/1.0} + 1.29 \times \frac{17.5}{58.9/1.0} = 0.96 < 1.0;$$

$$\frac{N_{Ed}}{\chi_z N_{Rk}/\gamma_{M1}} + k_{zy} \frac{M_{y,Ed}}{\chi_{LT} M_{y,Rk}/\gamma_{M1}} + k_{zz} \frac{M_{z,Ed}}{M_{z,Rk}/\gamma_{M1}} \le 1.0 \Leftrightarrow$$

$$\frac{520}{0.55 \times 3176.3/1.0} + 1.06 \times \frac{160}{0.84 \times 530.2/1.0} + 1.17 \times \frac{17.5}{58.9/1.0} = 1.02 < 1.0.$$

A IPE 500 in S 275 steel is not verified, according to Method 1.

iv-2) *Method* 2

$$\Psi_y = \frac{-160}{-160} = 1.00;\ \alpha_s = \frac{M_s}{M_h} = \frac{160}{-160} = -1.0;$$

As the beam-column has a cross section that is susceptible to torsional deformations (thin-walled open section, not laterally restrained), the stability of the member depends exclusively of its resistance to lateral-torsional buckling. As Method 2 only differs from Method 1 in the calculation of the interaction factors, the calculation of these factors is done directly.

The equivalent uniform moment factors are calculated from Table B.3 of EC3-1-1 or from Table 3.16. For the bending moment diagram around *y*:

$$\Rightarrow C_{my} = -0.8\alpha_s = -0.8\times(-1.0) = 0.8 \quad (>0.4).$$

For the bending moment diagram around *z*:

$$\Psi_z = \frac{17.5}{17.5} = 1.00;$$

$$\Rightarrow C_{mz} = 0.60 + 0.4\Psi_z = 0.6 + 0.4\times 1.00 = 1.0 \ (>0.40).$$

Coefficient C_{mLT} is given by:

$$C_{mLT} = C_{my} = 0.8.$$

Based on the previous parameters and on the parameters that were obtained in the application of Method 1, the interaction factors k_{yy}, k_{yz}, k_{zy} and k_{zz} are calculated from Table 3.15 (Table B.2 of EC3-1-1), through the following equations:

$$k_{yy} = C_{my}\left[1 + 0.6\overline{\lambda}_y \frac{N_{Ed}}{\chi_y N_{Rk}/\gamma_{M1}}\right] =$$

$$= 0.8\times\left[1 + 0.6\times 0.23\times\frac{520}{0.99\times 3176.3/1.0}\right] = 0.82;$$

$$\text{as } k_{yy} = 0.82 < C_{my}\left[1 + 0.6\frac{N_{Ed}}{\chi_y N_{Rk}/\gamma_{M1}}\right] = 0.88,$$

then $k_{yy} = 0.82$.

$$k_{zz} = C_{mz}\left[1+0.6\overline{\lambda}_z \frac{N_{Ed}}{\chi_z N_{Rk}/\gamma_{M1}}\right] =$$

$$= 1.0\times\left[1+0.6\times 1.07\times\frac{520}{0.55\times 3176.3/1.0}\right] = 1.18;$$

as $k_{zz} = 1.18 \le C_{mz}\left[1+0.6\frac{N_{Ed}}{\chi_z N_{Rk}/\gamma_{M1}}\right] = 1.18,$

then k_{zz} = 1.18.

$k_{yz} = k_{zz}$ = 1.18.

$$k_{zy} = \left[1-\frac{0.05\overline{\lambda}_z}{\left(C_{mLT}-0.25\right)}\frac{N_{Ed}}{\chi_z N_{Rk}/\gamma_{M1}}\right] =$$

$$= \left[1-\frac{0.05\times 1.07}{\left(0.8-0.25\right)}\times\frac{520}{0.55\times 3176.3/1.0}\right] = 0.97;$$

as $k_{zy} = 0.97 \ge \left[1-\frac{0.05}{\left(C_{mLT}-0.25\right)}\frac{N_{Ed}}{\chi_z N_{Rk}/\gamma_{M1}}\right] = 0.97,$

then k_{zy} = 0.97.

Expressions (3.163) give:

$$\frac{N_{Ed}}{\chi_y N_{Rk}/\gamma_{M1}} + k_{yy}\frac{M_{y,Ed}}{\chi_{LT} M_{y,Rk}/\gamma_{M1}} + k_{yz}\frac{M_{z,Ed}}{M_{z,Rk}/\gamma_{M1}} \le 1.0 \Leftrightarrow$$

$$\frac{520}{0.99\times 3176.3/1.0} + 0.82\times\frac{160}{0.84\times 530.2/1.0} + 0.85\times\frac{17.5}{58.9/1.0} = 0.81 < 1.0.$$

$$\frac{N_{Ed}}{\chi_z N_{Rk}/\gamma_{M1}} + k_{zy}\frac{M_{y,Ed}}{\chi_{LT} M_{y,Rk}/\gamma_{M1}} + k_{zz}\frac{M_{z,Ed}}{M_{z,Rk}/\gamma_{M1}} \le 1.0 \Leftrightarrow$$

$$\frac{520}{0.55\times 3176.3/1.0} + 0.95\times\frac{160}{0.84\times 530.2/1.0} + 1.18\times\frac{20}{58.0/1.0} = 0.99 < 1.0.$$

A IPE 500 in S 275 steel is verified according to Method 2.

Chapter 4

ELASTIC DESIGN OF STEEL STRUCTURES

4.1. INTRODUCTION

The first step in the design of a steel structure is the evaluation of internal forces and displacements for the various load combinations. It was seen in chapter 2 that, according to EC3-1-1, structural analysis can be elastic or take into account the nonlinear behaviour of steel. Depending on the method of analysis, EC3-1-1 gives specific requirements regarding second-order effects and the consideration of imperfections. It is the purpose of this chapter to present and discuss procedures for the design of steel structures within the framework of elastic analysis, complemented by the presentation of a real design example.

For most steel structures, elastic analysis is the usual method of analysis. This is in great part the result of the widespread availability of software that can easily perform linear elastic analysis. Furthermore, given current computer processing power and the user-friendliness of structural analysis software, 3D linear elastic analysis has become the standard in most design offices. This chapter therefore develops the design example using this approach.

Elastic design of steel structures comprises the following design steps: i) conceptual design, including the pre-design stage during which the structural members and joints are approximately sized; and ii) comprehensive verification and detailing, when systematic checks on the safety of all structural members and joints are carried out using more sophisticated procedures.

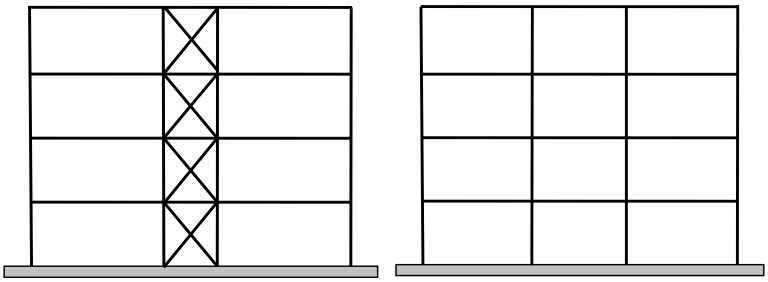
In the past, preliminary design was often based on simplified structural models. A typical methodology for non-seismic regions was to pre-design the

beams as simply-supported for gravity loading and to pre-design the columns for simplified sub-frames and a wind-based load combination using, for example, the wind-moment method (Hensman and Way, 2000), a very popular method in the UK. Nowadays, it is much more efficient to generate a more sophisticated structural model that already represents the entire structure or part of it and to carry out a linear elastic analysis, even with a crude assignment of cross sections. The implementation from the beginning of a realistic structural model that is good enough for the second stage of design (only with the addition of further detailing) results in increased speed and a significant reduction in uncertainties from a very early stage. The conceptual pre-design is therefore reduced to a very early search for the best structural system, at a stage when the modular basis of the architectural layout is still being defined. This should ideally be carried out with hand sketches and hand calculations, in what is often referred to as "calculations on the back of an envelope". Alternatively, very efficient pre-design tools exist that allow speedy estimates of alternative solutions, including cost estimates and member sizes.

A crucial conceptual decision in the design of multi-storey steel-framed buildings is the structural scheme to resist horizontal forces and to provide overall stability. In general, resistance to horizontal forces may be provided by frame action, resulting in moment-resisting frames. Alternatively, vertical bracing schemes, consisting of diagonal members acting in tension or shear walls, can be used. Provisions for vertical bracing need to be considered at the conceptual stage, particularly to avoid potential conflict with the fenestration (Lawson *et al*, 2004). Bracing in often located in the service cores to overcome this, but bracing in other areas is often necessary for the stability of the structure. Cross-flats provide a neat solution for residential buildings because they can be contained in the walls, and tubular struts may be used as an architectural feature in open areas (Lawson *et al*, 2004). In addition, a horizontal bracing system is also required to carry the horizontal loads to the vertical bracing. According to Brown *et al* (2004), usually the floor system will be sufficient to act as a horizontal diaphragm, without the need for additional horizontal steel bracing. All floor solutions involving permanent formwork, such as metal decking fixed by through-deck welding to the beams, with in-situ concrete infill, provide an excellent rigid diaphragm to carry horizontal loads to the bracing system. Floor systems involving precast concrete planks require proper consideration to ensure adequate load transfer.

Thorough guidance for the detailing of bracing systems for multi-storey buildings can be found in Brown *et al* (2004).

If a frame with bracing can be considered as laterally fully-supported, both systems (frame and bracing) can be analyzed separately. Each system is then analyzed under its own vertical loads, and all the horizontal loads are applied on the bracing system. Otherwise, the frame and any bracing should be analyzed as a single integral structure. Figure 4.1 illustrates a braced and an unbraced frame.



a) Braced frame b) Unbraced frame

Figure 4.1 – Braced and unbraced frames

It is therefore required to classify a structure as braced or unbraced. It is generally accepted that a structure is defined as braced if the following condition is satisfied:

$$S_{br} \geq 5 S_{unbr}\,, \tag{4.1}$$

where S_{br} is the global lateral stiffness of the structure with the bracing system and S_{unbr} is the global lateral stiffness of the structure without the bracing system. Usually, a braced structure is not sensitive to global 2nd order (P-Δ) effects.

4.2. SIMPLIFIED METHODS OF ANALYSIS

4.2.1. Introduction

The influence of second-order effects was extensively discussed in chapter 2. Rigorous assessment of the behaviour of steel structures requires a

full second-order analysis that takes into account *P*-δ and *P*-Δ effects. It was also established that the relevance of second-order effects may be indirectly assessed using the elastic critical load multiplier of the structure. Using elastic analysis, the consideration of second-order effects is mandatory whenever:

$$\alpha_{cr} = F_{cr} / F_{Ed} \leq 1.0 , \tag{4.2}$$

where F_{cr} and F_{Ed} were defined in chapter 2, section 2.3.2.

Simplified methods of analysis that approximate non-linear effects are often used. They allow the analysis of a structure based on linear elastic analyses, require less sophisticated software and are less time-consuming. In the context of elastic design of steel structures, two simplifications may be considered: i) simplified treatment of plasticity using linear elastic analysis (in particular cases where second-order effects are not relevant); ii) simplified consideration of second-order effects using linear elastic analysis (where plastic redistribution is not allowed):

i) Limited plastic redistribution of moments may be allowed in continuous beams. If, following an elastic analysis, some peak moments exceed the plastic bending resistance by up to 15 % (clause 5.4.1(4)B), the parts in excess of the bending resistance may be redistributed in any member, provided that:

- the internal forces and moments remain in equilibrium with the applied loads;
- all the members in which the moments are reduced have class 1 or class 2 cross sections;
- lateral torsional buckling of the members is prevented.

Example 3.5 (chapter 3) illustrates this limited plastic redistribution.

ii) Several simplified methods based on linear elastic analysis provide sufficiently accurate internal forces and displacements while taking into account second-order effects. The theoretical basis of these methods was explained in sub-section 2.3.2.3. EC3 describes the two following methods: a) the amplified sway-moment method; and b) the sway-mode buckling length method. A brief description of the two methods is presented in the following sections.

4.2.2. Amplified sway-moment method

The amplified sway-moment method (Boissonnade *et al*, 2006) is one that uses linear elastic analysis coupled with the amplification of the so-called sway moments by a sway factor. This depends on the ratio of the design vertical applied load and the lowest elastic critical load associated with global sway instability. The linear elastic analysis must include the horizontal external loads and the equivalent horizontal loads representing frame imperfections. Subsequently, the resistance and the stability of both the frame and its components are checked. For the stability checks, the non-sway effective lengths are used for the columns. For simplicity and as a conservative option, the real length of each column is usually taken as its non-sway buckling length. Finally, out-of-plane stability also has to be checked.

The amplified sway moment method comprises the following steps (Demonceau, 2008):

i) a linear elastic analysis is carried out for a modified frame with horizontal supports at all floor levels (Figure 4.2a); it results in a distribution of bending moments in the frame and reactions at the horizontal supports;

ii) a second linear elastic analysis is carried out for the original frame subjected to the horizontal reactions obtained in the first step (Figure 4.2b); the resulting bending moments are the "sway" moments;

iii) approximate values of the second-order internal forces *M*, *V* and *N* and displacements *d* are obtained by adding the results from the two elastic analyses according to equations (4.3):

$$d_{ap}^{II} = d_{NS}^{I} + \frac{1}{1-\frac{1}{\alpha_{cr.S}}} d_{S}^{I}; \tag{4.3a}$$

$$M_{ap}^{II} = M_{NS}^{I} + \frac{1}{1-\frac{1}{\alpha_{cr.S}}} M_{S}^{I}; \tag{4.3b}$$

$$V_{ap}^{II} = V_{NS}^{I} + \frac{1}{1-\frac{1}{\alpha_{cr.S}}} V_{S}^{I}; \tag{4.3c}$$

$$N_{ap}^{II} = N_{NS}^{I} + \frac{1}{1-\frac{1}{\alpha_{cr.S}}} N_{S}^{I}, \tag{4.3d}$$

where $\alpha_{cr.S}$ is the critical load multiplier for the lowest sway buckling mode;

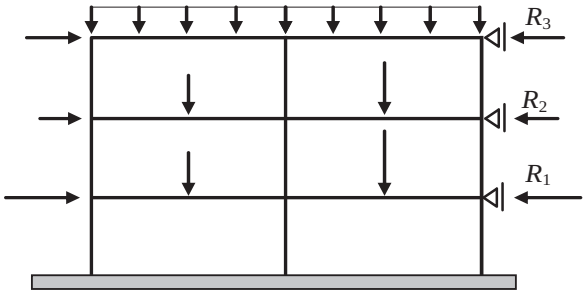
iv) finally, the maximum elastic resistance of the frame is reached with the formation of the first plastic hinge.

In normative terms, this approach is summarized in clause 5.2.2(4). For frames where the first sway buckling mode is predominant, first order elastic analysis should be carried out with subsequent amplification of relevant action effects (e.g. bending moments) by appropriate factors. For single storey frames designed on the basis of elastic global analysis (clause 5.2.2(5)), second order sway effects due to vertical loads may be calculated by increasing the horizontal loads H_{Ed} (e.g. wind) and equivalent loads $V_{Ed}\phi$ due to imperfections and other possible sway effects according to first order theory, by the factor:

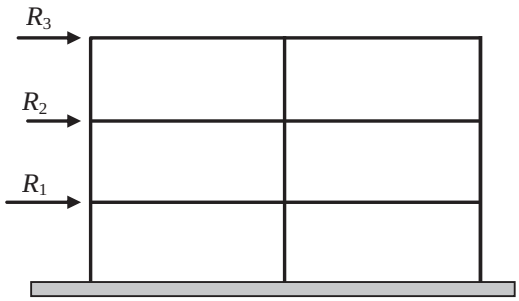
$$\frac{1}{1-\frac{1}{\alpha_{cr}}}, \tag{4.4}$$

provided that $\alpha_{cr} \geq 3.0$, where α_{cr} may be calculated according to Horne's method (equation (2.11), clause 5.2.1(4)B). This is provided that the axial compression in the beams or rafters is not significant. For multi-storey frames, second order sway effects may be calculated in a similar way provided that all storeys have a similar distribution of vertical loads, horizontal loads and frame stiffness with respect to the applied storey shear forces (clause 5.2.2(6)).

Example 4.1 illustrates the application of the amplified sway moment method.



a) Modified no-sway frame with horizontal supports (NS)



b) Original sway frame subjected to the horizontal reactions (S)

Figure 4.2 – Amplified sway moment method

4.2.3. Sway-mode buckling length method

The sway-mode buckling length method (Boissonnade *et al*, 2006) verifies the overall stability of the frame and the local stability of its members by column stability checks. These use buckling lengths appropriate to the global sway buckling mode for the whole structure. The method is based on the following two (conservative) assumptions: i) all the columns in a storey buckle simultaneously and ii) the global frame instability load corresponds to the stability load of the weakest storey in the frame. Because the method does not explicitly consider the increase in moments at the ends of the beams and in the beam-to-column joints arising from second-order effects, an amplification of the sway moments is usually considered for these parts of the structure.

The sway-mode buckling length method comprises the following steps (Demonceau, 2008):

i) a first-order elastic analysis is carried out for the frame;
ii) the sway moments in the beams and beam-to-column joints are amplified by a nominal factor of 1.2;
iii) the columns are checked for in-plane buckling using the sway mode buckling length, usually obtained from equation (2.12) and Figure 2.52. It must also be remembered to check out-of-plane buckling.

In normative terms, this approach is summarized in clause 5.2.2(8), where the stability of a frame is to be assessed by a check with the equivalent column method according to clauses 6.3. The buckling length values should be based on a global buckling mode of the frame accounting for the stiffness behaviour of members and joints, the presence of plastic hinges and the distribution of compressive forces under the design loads. In this case, internal forces to be used in resistance checks are calculated according to first order theory without considering imperfections.

Example 4.1 illustrates the application of the sway-mode buckling length method.

4.2.4. Worked example

Example 4.1: Consider the steel frame of example 2.4 (E = 210 GPa) subjected to the unfactored loads illustrated in Figure 4.3, where:

AP – permanent load (γ_G = 1.35);

AV_1 – imposed load (γ_Q = 1.50, $\psi_{0,1}$ = 0.7, $\psi_{1,1}$ = 0.5, $\psi_{2,1}$ = 0.3);

AV_2 – wind load (γ_Q = 1.50, $\psi_{0,2}$ = 0.6, $\psi_{1,2}$ = 0.2, $\psi_{2,2}$ = 0.0).

Assume rigid connections between the beams and the columns, column bases fully restrained and an elastic analysis. Calculate the design internal forces for the verification of the Ultimate Limit State (ULS), using the following simplified methods of analysis:

a) amplified sway-moment method;
b) sway-mode buckling length method (equivalent column method).

The results are presented for the critical cross sections in Figure 4.4.

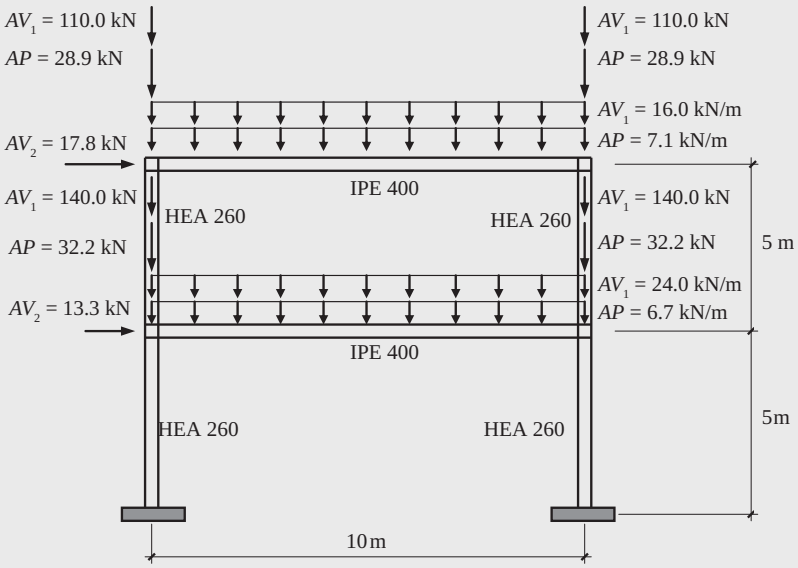


Figure 4.3 – Steel frame

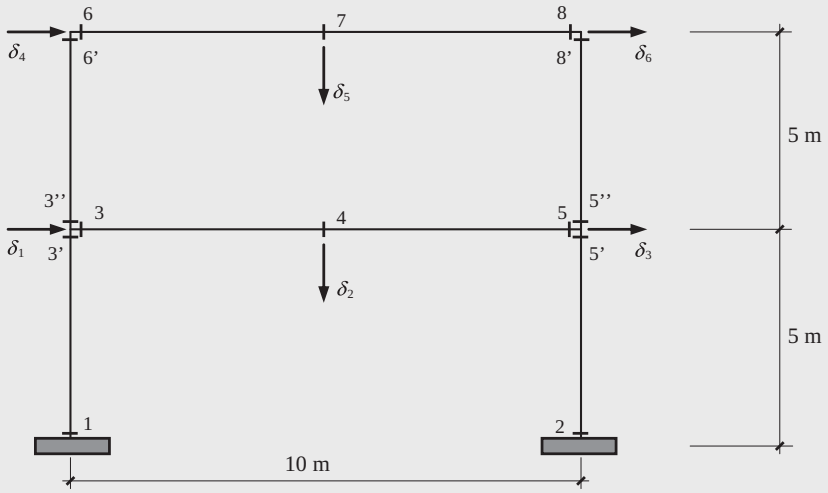


Figure 4.4 – Critical cross sections

a) Amplified sway-moment method

The two load combinations, corresponding to the two independent variable loads AV_1 and AV_2, with global imperfections already included, were defined in example 2.4 (Figures 2.59 and 2.60).

In example 2.4, α_{cr} was calculated for both load combinations, leading to the following values:

Load combination 1 - α_{cr} =7.82.

Load combination 2 - α_{cr} =10.25.

For load combination 1, as α_{cr} is less than 10, a 2nd order elastic analysis is required. For load combination 2, as α_{cr} is larger than 10, the design forces and moments may be obtained directly by a linear elastic analysis. Consequently, analysis using the amplified sway-moment method will be carried out for load combination 1 only.

The first step of this method consists of a linear elastic analysis of a modified frame with horizontal supports at each floor level, as shown in Figure 4.5; in this case, the horizontal reactions are equal to the horizontal loads as the vertical loads have no horizontal effects. The resulting internal forces are summarized in Table 4.1.

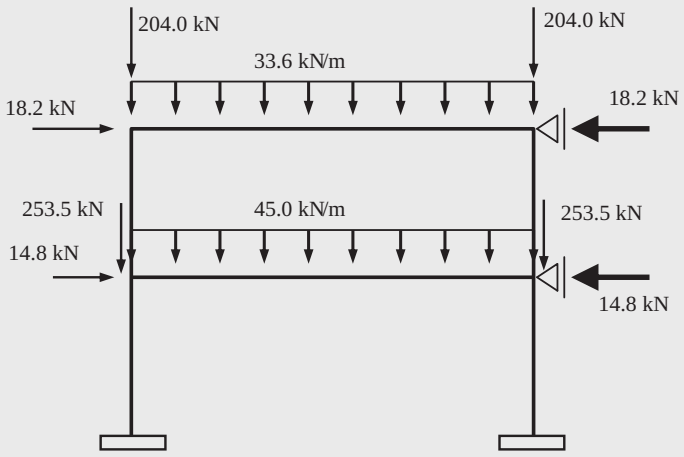


Figure 4.5 – Modified no-sway frame and load arrangement for load combination 1

In a second step, the sway moments (and other internal forces) are calculated by performing a linear elastic analysis on the original (sway) frame loaded by the horizontal reactions obtained in the previous step (Figure 4.6). The resulting internal (sway) forces are summarized in Table 4.1.

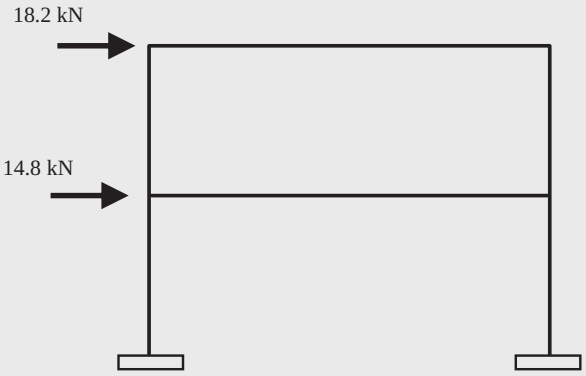


Figure 4.6 – Original sway frame subjected to the horizontal reactions (load comb. 1)

The approximate values of the second-order internal forces are obtained by adding the results from the first step (see Figures 2.61 to 2.63) with the results of the second step (see Figures 2.64 to 2.66) amplified by the following factor (expression (4.4)):

$$\frac{1}{1-1/\alpha_{cr}} = \frac{1}{1-1/7.82} = 1.15.$$

Table 4.1 and Figures 4.7 to 4.9 illustrate the final results.

Table 4.1 – Bending moments and axial forces at the critical cross sections (ASM)

	No-sway		Sway		2nd Order	
	M_y (kNm)	N_x (kN)	M_y (kNm)	N_x (kN)	M_y (kNm)	N_x (kN)
1	60.3	-850.5	-49.2	15.8	3.7	-832.3
2	-60.3	-850.5	-49.1	-15.8	-116.8	-868.7
3	-309.0	41.9	52.3	-7.4	-248.9	33.4
3’	-119.9	-850.5	33.4	15.8	-81.5	-832.3
3’’	189.0	-372.0	-18.9	5.3	167.3	-365.9
4	253.5	41.9	0	-7.4	253.5	33.4
5	-309.0	41.9	-52.2	-7.4	-369.0	33.4
5’	119.9	-850.5	33.3	-15.8	158.2	-868.7
5’’	-189.0	-372.0	-18.9	-5.3	-210.7	-378.1
6	-200.9	-78.0	26.6	-9.1	-170.3	-88.5
6’	-200.9	-372.0	26.6	5.3	-170.3	-365.9
7	219.1	-78.0	0	-9.1	219.1	-88.5
8	-200.9	-78.0	-26.6	-9.1	-231.5	-88.5
8’	200.9	-372.0	26.6	-5.3	231.5	-378.1

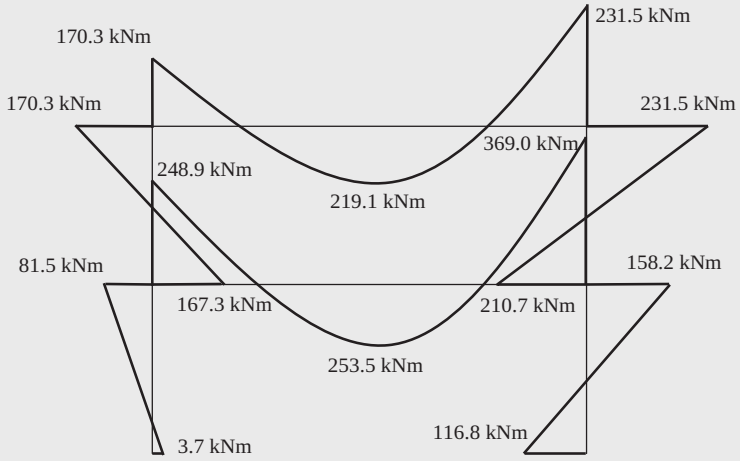


Figure 4.7 – Design bending moment diagram (ASM)

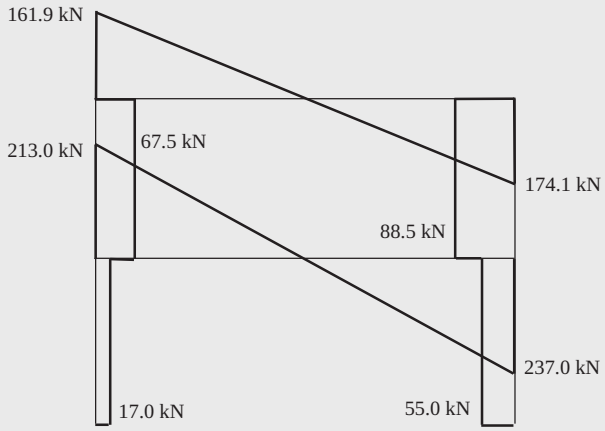


Figure 4.8 – Design shear force diagram (ASM)

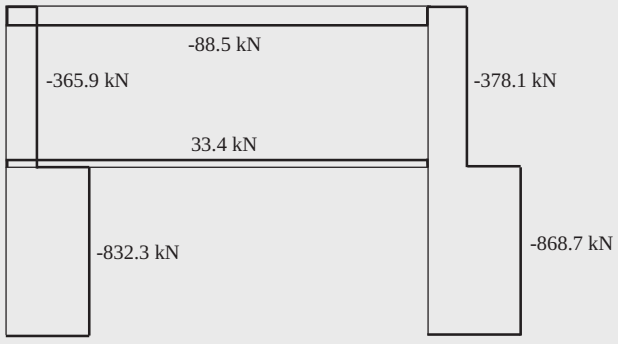


Figure 4.9 – Design axial force diagram (ASM)

b) Sway-mode buckling length method (SMBL)

According to this method, the internal forces to be used in the resistance checks of the columns are calculated according to first order theory, without considering imperfections. Figure 4.10 shows the resulting load arrangement for load combination 1. The second and third columns in Table 4.2 summarize the corresponding internal forces.

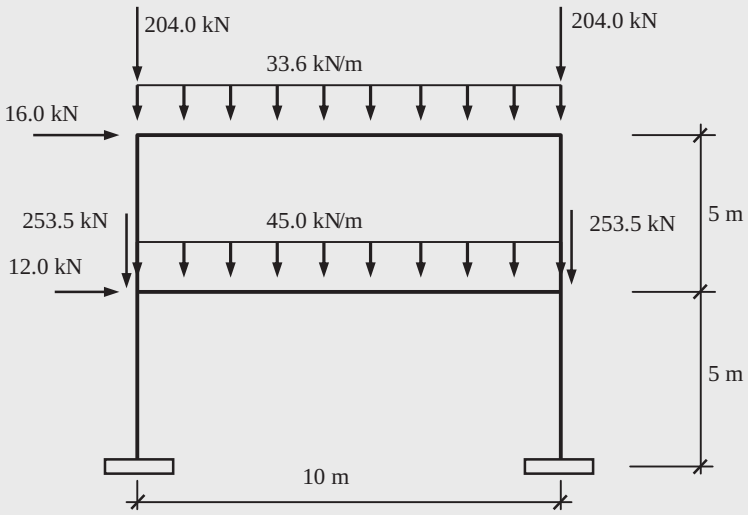


Figure 4.10 – Load arrangement for load combination 1

In a second step the sway moments and the other sway internal forces on the beams and joints are obtained as for the amplified sway moment method (Figure 4.11).

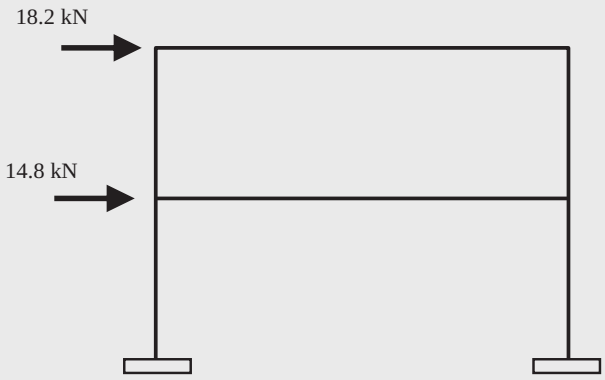


Figure 4.11 – Original frame subjected to the horizontal reactions (load comb. 1)

Finally the design internal forces on beams and beam-to-column joints are obtained by adding the internal forces obtained by a first-order analysis for the load arrangement, excluding horizontal loads, represented in Figure 4.10, to the amplified sway moments and other sway effects (obtained from Figure 4.11) by a nominal factor of 1.2.

Table 4.2 and Figures 4.12 to 4.14 represent the design internal forces for the columns (1st Order - Original frame) and the beams and beam-to-column joints (2nd Order).

Table 4.2 – Bending moments and axial forces at the critical cross sections

	1st Order - Original frame		Sway		2nd Order	
	M_y (kNm)	N (kN)	M_y (kNm)	N (kN)	M_y (kNm)	N (kN)
1	-18.4	-836.9	-	-	18.4	-836.9
2	-102.0	-864.1	-	-	-102.0	-864.1
3	-264.0	36.0	52.3	-7.4	-201.2	27.1
3’	-91.7	-836.9	-	-	-91.7	-836.9
3’’	172.3	-367.3	-	-	172.3	-367.3
4	253.6	36.0	0	-7.4	253.6	27.1
5	-353.9	36.0	-52.2	-7.4	-416.5	27.1
5’	148.1	-864.1	-	-	148.1	-864.1
5’’	-205.8	-376.7	-	-	-205.8	-376.7
6	-177.6	-86.0	26.6	-9.1	-145.7	-96.9
6’	-177.6	-367.3	-	-	-177.6	-367.3
7	219.1	-86.0	0	-9.1	219.1	-96.9
8	-224.1	-86.0	-26.6	-9.1	-256.0	-96.9
8’	224.1	-376.7	-	-	224.1	-376.7

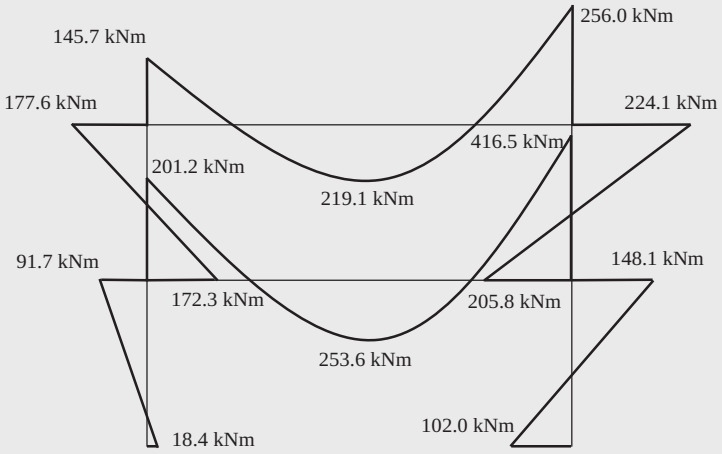


Figure 4.12 – Design bending moment diagram for load combination 1 (SMBL)

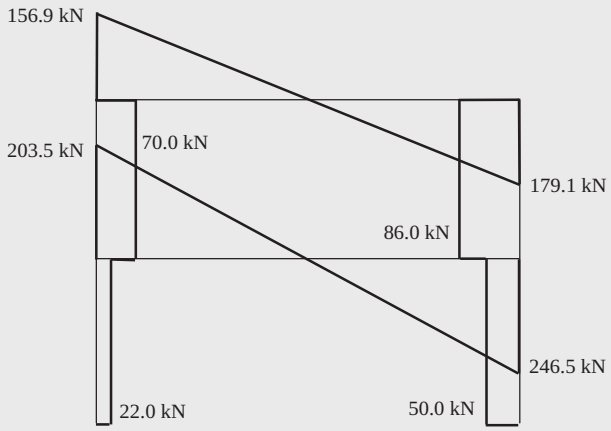


Figure 4.13 – Design shear force diagrams for load combination 1 (SMBL)

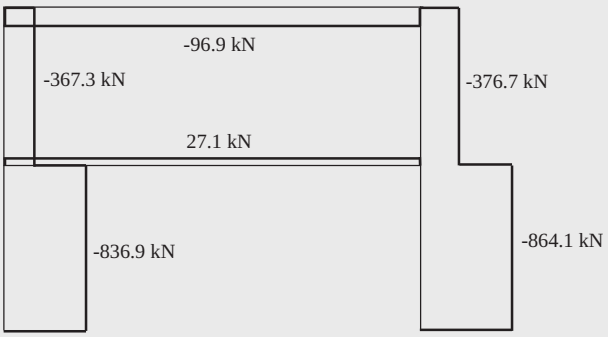


Figure 4.14 – Design axial force diagrams for load combination 1 (SMBL)

In the third step, the columns are checked for in-plane buckling using the sway mode buckling length. Figure 4.15 illustrates the shape of the lowest buckling mode and the numbering of the columns.

Considering Wood's equivalent frame (sub-section 2.3.2.2) for a frame with lateral displacements (Figure 2.52b), the stiffness coefficients for the columns are given by:

$$K_c = \frac{I_c}{L_c} = \frac{10450}{500} = 20.9;$$

$$K_1 \left(\text{or } K_2\right) = \frac{I_c}{L_c} = \frac{10450}{500} = 20.9,$$

where I_c is the in-plane second moment of area (I_y = 10450 cm^4 for HEA 260) of the columns of the columns and L_c is the length of the column.

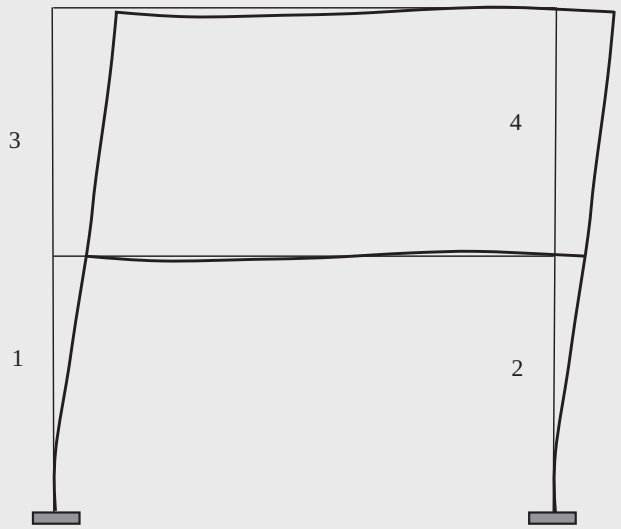


Figure 4.15 – Lowest sway buckling mode

The effective stiffness coefficients of the adjacent beams are given by (Table 2.19):

$$K_{12} = K_{22} = 1.5\frac{I_b}{L_b} = 1.50 \times \frac{23130}{1000} = 34.70,$$

where I_b is the in-plane second moment of area (I_y = 23130 cm^4 for IPE 400) of the beam and L_b is the length of the beam.

The distribution coefficients for the upper (η_1) and lower (η_2) ends of columns 1 and 2 are given by (eqs. (2.12)):

$$\eta_1 = \frac{K_c + K_1}{K_c + K_1 + K_{12}} = \frac{20.9 + 20.9}{20.9 + 20.9 + 34.70} = 0.55;$$

$\eta_2 = 0$ (fixed base).

From Figure 2.52b: $\frac{L_E}{L} \approx 1.26 \Rightarrow L_E \approx 1.26 \times 5.00 = 6.30$ m.

Similarly, the distribution coefficients for the upper (η_1) and lower (η_2) ends of columns 3 and 4 are given by (eqs. (2.12)):

$$\eta_1 = \frac{K_c}{K_c + K_{12}} = \frac{20.9}{20.9 + 34.70} = 0.38;$$

$$\eta_2 = \frac{K_c + K_2}{K_c + K_2 + K_{22}} = \frac{20.9 + 20.9}{20.9 + 20.9 + 34.70} = 0.55.$$

From Figure 2.52b: $\frac{L_E}{L} \approx 1.40 \Rightarrow L_E \approx 1.40 \times 5.00 = 7.00$ m.

Finally, the columns would be checked according to clause 6.3.3 for the internal forces represented in Figures 4.12 to 4.14, and the equivalent lengths L_E, calculated above.

Table 4.3 compares the approximate second-order results obtained using both methods with the results of an "exact" second-order elastic analysis.

Table 4.3 – Comparative synthesis of results

	Linear elastic	2nd Order	Amplified sway method		Sway mode buckling length method	
	M_y (kNm)	M_y (kNm)	M_y (kNm)	Δ (%)	M_y (kNm)	Δ (%)
1	11.0	2.9	3.7	+27.6	18.4	+534.5
2	-109.3	-115.1	-116.8	+1.5	-102.2	-11.2
3	-256.4	-244.0	-248.9	+2.0	-201.2	-17.5
3’	-86.4	-78.3	-81.5	+4.1	-91.7	+17.1
3’’	170.0	165.8	167.3	+0.9	172.3	+3.9
4	253.5	257.2	253.5	-0.8	253.6	-1.4
5	-360.9	-363.6	-369.0	+1.5	-416.5	+14.5
5’	153.1	156.4	158.2	+1.2	148.1	-5.3
5’’	-207.8	-207.2	-210.7	+1.7	-205.8	-0.7
6	-174.1	-168.7	-170.3	+0.9	-145.7	-13.6
6’	-174.1	-168.7	-170.3	+0.9	-177.6	+5.3
7	219.0	225.3	219.1	-2.5	219.1	-2.8
8	-227.3	-227.9	-231.5	+1.6	-256.0	+12.3
8’	227.3	227.9	231.5	+1.6	224.1	-1.7

4.3. MEMBER STABILITY OF NON-PRISMATIC MEMBERS AND COMPONENTS

4.3.1. Introduction

Chapter 3 has dealt with the resistance of prismatic members to instability under the usual combinations of applied loads. However, steel structures may include non-prismatic members and members with intermediate partial restraint. These are neither directly covered by the stability checks described in chapter 3 nor in clauses 6.3.1 to 6.3.3 of EC3-1-1. Since these situations are commonly used in conjunction with elastic analysis, the following section describes specific procedures for non-prismatic members and members with intermediate partial restraint. Subsequently, the General Method (clause 6.3.4) is described and discussed. It is a general procedure for lateral and lateral-torsional buckling of structural components such as: i) single members which may be built-up or have complex support conditions and ii) plane frames or sub-frames composed of such members subject to compression and/or in-plane bending, but which do not contain rotating plastic hinges.

4.3.2. Non-prismatic members

The verification of the stability of non-prismatic members is more complex than for prismatic members for the two following reasons: i) analytical expressions for the elastic critical loads are not readily available; and ii) the choice of the critical section for the application of the buckling resistance formulae is not straightforward.

Consider the beam-column of Figure 4.16, composed of a non- prismatic member with L = 7.0 m, simply-supported at the ends with fork supports (the “standard case”, see Figure 3.62). The welded cross section varies from an equivalent IPE 360 at one end to a cross section with similar flange width and thickness, equal web thickness and a total depth of 200 mm. S 235 steel grade was assumed. The uniformly distributed loading is applied at the shear centre of the cross section.

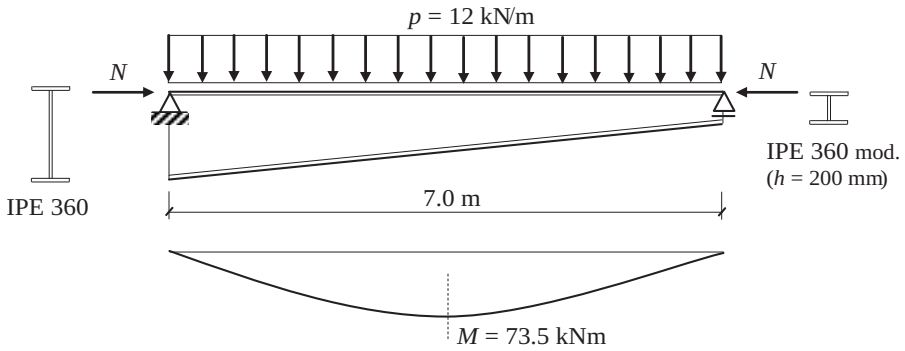


Figure 4.16 – Double-symmetric tapered I section beam

Table 4.4 and Figure 4.17 compare the "exact" numerical results from a linear eigenvalue analysis (LEA) with analytical results obtained using the classical elastic critical load formulae for prismatic members. Table 4.4 presents lower and upper bound results for the smaller and larger cross sections, respectively. Maximum differences of -50 % and +88 % are noted for flexural buckling about the *y* axis.

Table 4.4 – Elastic critical loads

Buckling mode		Numerical (LEA)	Analytical	
			A_{min} (x = 7 m)	A_{max} (x = 0 m)
Compression N_{cr} (kN)	Flexural *yy*	3489.7	1754.4 (-49.7 %)	6566.3 (88.2 %)
	Flexural *zz*	438.5	440.2 (0.4 %)	440.5 (0.5 %)
	Torsional	1976.8	2755.3 (39.4 %)	1546.6 (-21.8 %)
Bending M_{cr} (kNm)	Lateral-torsional	104.7	118.6 (13.2 %)	143.5 (37.0 %)

Table 4.5 compares the numerical results from a geometrical and material nonlinear analysis with imperfections (GMNIA) against the analytical results obtained using the beam-column interaction formulae (expressions (3.163)), evaluated using the "exact" values (numerical LEA) for the elastic critical loads

and the properties of the cross sections for the following locations along the length of the member: $x = \{0; L/2; L\}$; and $x = 3.92$ m (position of the critical cross section from a 3D GMNIA calculation). For all cases, the reference loading is $N_{Ed} = 80$ kN and $M_{y,Ed} = M_{y,max} = 73.5$ kNm. χ_{LT} is calculated according to the General Case from EC3-1-1 (see section 3.6.3) and Method 1 (Annex A) is adopted. Even using the "exact" values for the elastic critical loads, a maximum difference of -41 % is noted.

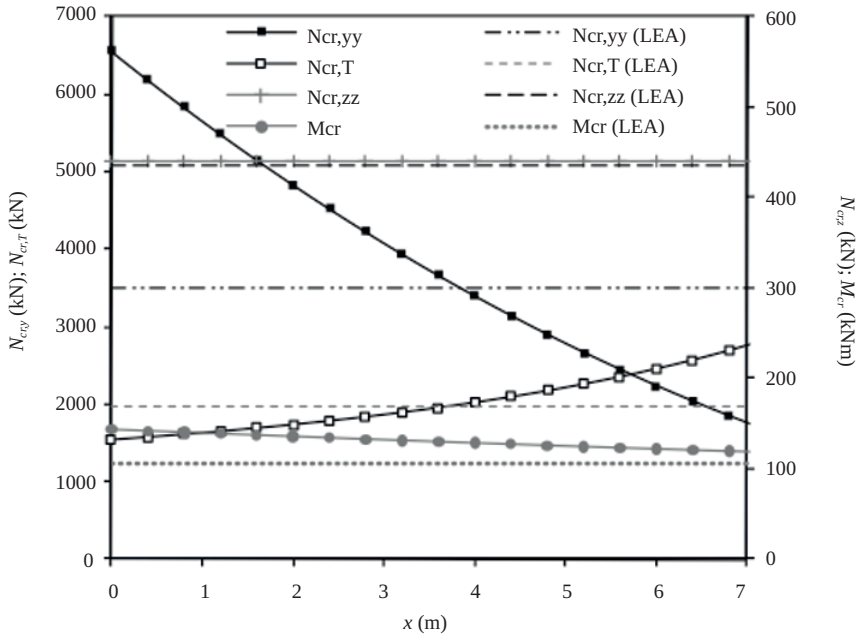


Figure 4.17 – Variation of the elastic critical loads with reference cross section

Table 4.5 – Buckling resistance

Case	Numerical (GMNIA)	Analytical (clause 6.3.3)			
		x=0 m	x=3.5 m	x=3.92 m	x=7.0 m
expression (3.163 a))	1.14	0.74 (-35.6 %)	0.77 (-33.0 %)	0.76 (-33.8 %)	0.67 (-41.4 %)
expression (3.163 b))	1.14	0.72 (-37.3 %)	1.10 (-4.0 %)	1.09 (-4.8 %)	0.99 (-13.8 %)

The utilization ratio α of a member is defined as the ratio between the applied internal forces and the resistance evaluated according to the various procedures, always assuming proportional loading. α corresponds to the inverse of the buckling resistance, i.e., α = 1/*Buckling Resistance*. Figure 4.18 illustrates the variation of the utilization ratio α along the member for the 3D GMNIA calculation and for each buckling mode, using clause 6.3.3 considering the applied internal forces at each position and the "exact" values for the elastic critical loads.

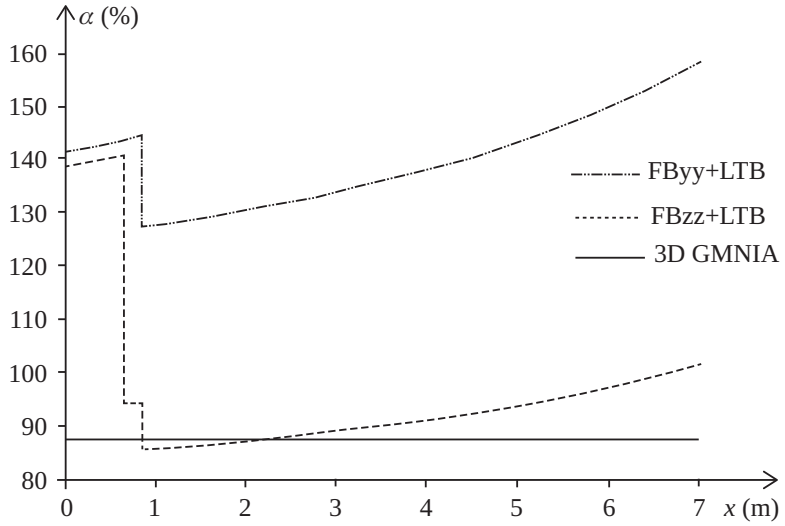


Figure 4.18 – Utilization ratio α (%) for the relevant modes

Nowadays, several possibilities exist to evaluate the elastic critical load of non-prismatic steel members: i) the use of tables for standard cases; ii) methods that approximate the elastic critical load using formulae for prismatic members with an appropriate equivalent cross section or equivalent length and iii) numerical calculations by performing a linear eigenvalue analysis.

For a range of web-tapered I-section steel columns, commonly used in elastically designed portal frames (Figure 4.19b), illustrated in Figure 4.19, Hirt and Crisinel (2001) present expressions for the elastic critical load of axially loaded non-prismatic members of double symmetric cross section.

Flexural buckling about the strong axis of the cross section occurs for:

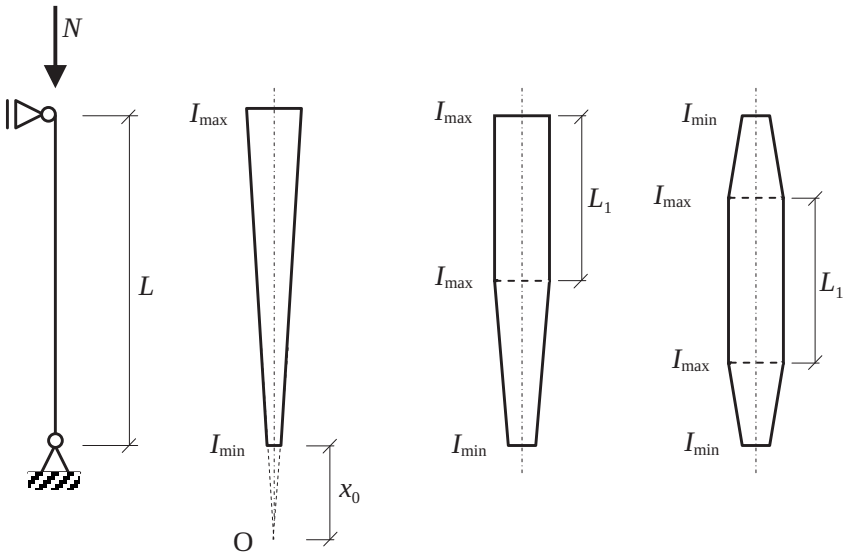
$$N_{cr} = \frac{\pi^2 E I_{y,eq}}{L^2}, \tag{4.5}$$

where

$$I_{eq,y} = C I_{y,\max}, \tag{4.6}$$

and C is a coefficient that depends on the parameter r, defined as the ratio between the minimum and the maximum moments of inertia of the column,

$$r = \sqrt{I_{y,\min} / I_{y,\max}}. \tag{4.7}$$



a) b) c) d)

Figure 4.19 – Non-prismatic I-section columns (b, t_f and t_w are all constant)

For a tapered column (Figure 4.19b),

$$C = 0.08 + 0.92r. \tag{4.8}$$

For the column shown in Figure 4.19c,

$$C = \left(0.08 + 0.92r\right) + \left(0.32 + 4\sqrt{r} - 4.32r\right)\left(\frac{L_1}{L}\right)^2 \quad \left(L_1 < 0.5L\right), \tag{4.9}$$

while for the column shown in Figure 4.19d,

$$C = \left(0.17 + 0.33r + 0.5\sqrt{r}\right) + \left(0.62\sqrt{r} - 1.62r\right)\left(\frac{L_1}{L}\right) \quad \left(L_1 < 0.5L\right). \tag{4.10}$$

According to Galea (1986), the elastic critical moment of beams subjected to a uniform bending moment and fork supports (the "standard case", see Figure 3.62) may be obtained using the expression for prismatic beams (equation (3.119)) as long as equivalent geometrical properties are used, given by:

$$h_{eq} = h_{\max}\sqrt{0.283 + 0.434\gamma + 0.283\gamma^2}\ , \tag{4.11}$$

where $h_{\max}$ is the maximum depth of the member and $\gamma (= h_{\min}/h_{\max})$ is the tapering ratio, and

$$I_{z,eq} = I_z\ , \tag{4.12a}$$

315

$$I_{T,eq} = \frac{I_{T,\max} + I_{T,\min}}{2}. \tag{4.12b}$$

This procedure is equally valid for non uniform bending moment distributions by modifying the uniform elastic critical moment using adequate coefficients (see chapter 3). For fully-restrained rotation about the weak axis of the cross section at the ends of the member, equation (4.11) should be replaced by:

$$h_{eq} = h_{\max}\sqrt{0.34 + 0.40\gamma + 0.26\gamma^2}\ . \tag{4.13}$$

Trahair (1993) provides expressions for the elastic critical moment of tapered and stepped beams.

Finally, performing a linear eigenvalue analysis is nowadays relatively simple and free software is available (LTBeam, 2010; LTBeamN, 2015; Li and Schafer, 2010).

Example 4.2 illustrates the evaluation of the buckling resistance of a non-prismatic member.

4.3.3. Members with intermediate restraints

Figure 4.20 illustrates the common situation of a member with partial bracing that only prevents transverse displacements of the tension flange. These partial bracings are very effective in increasing the resistance to out-of-plane buckling.

Following King (2001a), for prismatic members with a mono-symmetric cross section (minor-axis) (Figure 4.20a), the elastic critical load for pure compression in a torsional mode is given by:

$$N_{crT} = \frac{1}{i_s^2}\left(\frac{\pi^2 EI_z a^2}{L_t^2} + \frac{\pi^2 EI_w}{L_t^2} + GI_T\right), \tag{4.14}$$

in which

316

$$i_s^2 = i_y^2 + i_z^2 + a^2, \tag{4.15}$$

where:

I_T, I_z and I_w are, respectively, the torsional constant, the second moment of area with respect to the minor axis of the cross section and the warping constant;

i_y and i_z are the radius of gyration with respect to the y and z axes, respectively;

L_t is the length of the segment between effectively braced sections (laterally and torsional restrained, similar to fork supports), see Figure 4.20;

a is the distance between the restricted longitudinal axis (for example, the centroid of the purlins) and the shear centre of the beam (see Figure 4.21).

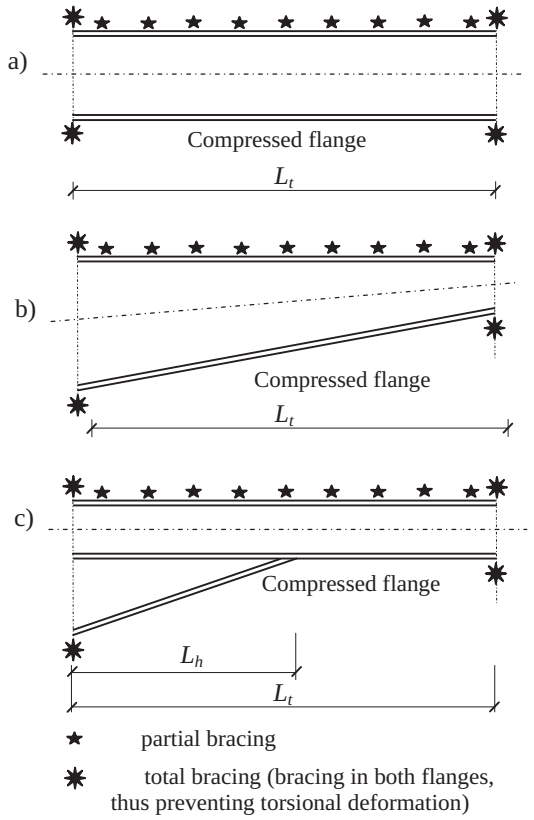


Figure 4.20 – Partial and total bracing

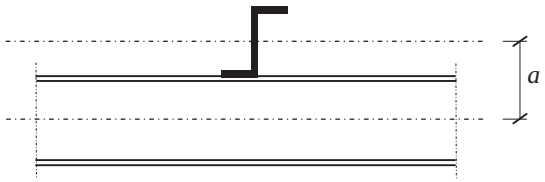


Figure 4.21 – Reference and bracing axes

The elastic critical moment for lateral-torsional buckling, M_{cr0}, for an uniform moment and standard bracing conditions at each end of the segment (no transverse displacement, no rotation around the longitudinal axis and free rotation in plan) is given by:

$$M_{cr0} = \left(\frac{i_s^2}{2a} \right) N_{crT}, \tag{4.16}$$

where N_{cr} is the elastic critical load in a torsional mode (equation (4.14).

For mono-symmetric cross sections with uniform flanges, the elastic critical moment for an arbitrary bending moment diagram is given by:

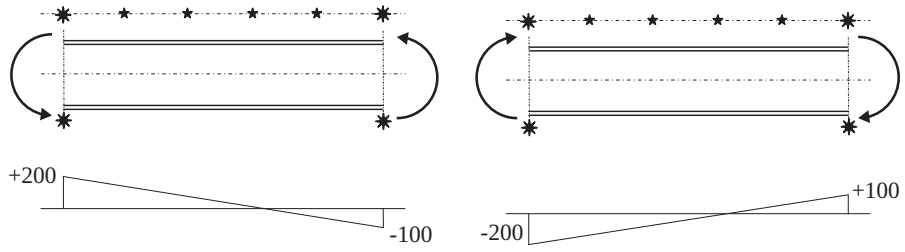
$$M_{cr} = \left(\frac{1}{m_t c^2} \right) M_{cr0}, \tag{4.17}$$

where m_t is the equivalent uniform moment factor and c is the equivalent cross section factor. In case of a linear variation of the bending moment diagram, m_t depends on the ratio β_t between the smaller and the larger bending moments acting at the ends of the member (sagging moment positive), defined according to Figure 4.22 and the ratio η, defined as,

$$\eta = \frac{N_{crE}}{N_{crT}}, \tag{4.18}$$

where, N_{crT}, is given by the equation (4.14) and N_{crE} is defined by the following equation:

$$N_{crE} = \frac{\pi^2 E I_z}{L_t^2}. \tag{4.19}$$



$$\beta_t = \frac{-100}{+200} = -0.5 \qquad \beta_t = \frac{-200}{+100} = -2$$

but $\beta_t \geq -1.0$ so $\beta_t = -1.0$

Figure 4.22 – Value of β_t

Table 4.6 defines m_t as a function of β_t, where β_t is the ratio between the lower and the higher values of the end moments (when $\beta_t < -1$, $\beta_t = -1.0$) and $y = \sqrt{\eta}$.

Table 4.6 – Equivalent uniform moment factor m_t

β_t \ y	0	0.1	0.2	0.3	0.4	0.5	0.6	0.7	0.8	0.9	1.0	1.1	1.2
-1.0	1.0	0.76	0.61	0.51	0.44	0.39	0.35	0.31	0.28	0.26	0.24	0.22	0.21
-0.9	1.0	0.78	0.63	0.52	0.45	0.40	0.36	0.32	0.30	0.28	0.26	0.24	0.23
-0.8	1.0	0.80	0.64	0.53	0.46	0.41	0.37	0.34	0.32	0.30	0.28	0.27	0.26
-0.7	1.0	0.81	0.66	0.55	0.47	0.42	0.39	0.36	0.34	0.32	0.30	0.29	0.28
-0.6	1.0	0.83	0.67	0.56	0.49	0.44	0.40	0.38	0.36	0.34	0.33	0.32	0.31
-0.5	1.0	0.85	0.69	0.58	0.50	0.46	0.42	0.40	0.38	0.37	0.36	0.35	0.34
-0.4	1.0	0.86	0.70	0.59	0.52	0.48	0.45	0.43	0.41	0.40	0.39	0.38	0.37
-0.3	1.0	0.88	0.72	0.61	0.54	0.50	0.47	0.45	0.44	0.43	0.42	0.41	0.41
-0.2	1.0	0.89	0.74	0.63	0.57	0.53	0.50	0.48	0.47	0.46	0.45	0.45	0.44
-0.1	1.0	0.90	0.76	0.65	0.59	0.55	0.53	0.51	0.50	0.49	0.49	0.48	0.48
0.0	1.0	0.92	0.78	0.68	0.62	0.58	0.56	0.55	0.54	0.53	0.52	0.52	0.52
0.1	1.0	0.93	0.80	0.70	0.65	0.62	0.59	0.58	0.57	0.57	0.56	0.56	0.56
0.2	1.0	0.94	0.82	0.73	0.68	0.65	0.63	0.62	0.61	0.61	0.60	0.60	0.60
0.3	1.0	0.95	0.84	0.76	0.71	0.69	0.67	0.66	0.65	0.65	0.65	0.64	0.64
0.4	1.0	0.96	0.86	0.79	0.75	0.72	0.71	0.70	0.70	0.69	0.69	0.69	0.69
0.5	1.0	0.97	0.88	0.82	0.78	0.76	0.75	0.75	0.74	0.74	0.74	0.74	0.74
0.6	1.0	0.98	0.91	0.85	0.82	0.81	0.80	0.79	0.79	0.79	0.79	0.79	0.79
0.7	1.0	0.98	0.93	0.89	0.87	0.85	0.85	0.84	0.84	0.84	0.84	0.84	0.84
0.8	1.0	0.99	0.95	0.92	0.91	0.90	0.90	0.89	0.89	0.89	0.89	0.89	0.89
0.9	1.0	1.00	0.98	0.96	0.95	0.95	0.95	0.95	0.95	0.94	0.94	0.94	0.94
1.0	1.0	1.00	1.00	1.00	1.00	1.00	1.00	1.00	1.00	1.00	1.00	1.00	1.00

The equivalent section factor, c, is equal to 1.0 for prismatic members.

For all the other cases, namely when the variation of the bending moment is not linear (Figure 4.23), the factor m_t is given by Singh (1969):

$$m_t = \frac{1}{12}\left(\frac{M_{c,Rd}}{M_{y,Ed}}\right)_{\min}\left(\frac{M_{y,Ed1}}{M_{c,Rd1}} + 3\frac{M_{y,Ed2}}{M_{c,Rd2}} + 4\frac{M_{y,Ed3}}{M_{c,Rd3}} + 3\frac{M_{y,Ed4}}{M_{c,Rd4}} + \right.$$
$$\left. + \frac{M_{y,Ed5}}{M_{c,Rd5}} + 2\mu_{SE}\right\}, \qquad (4.20)$$

where,

$$\mu_{SE} = \left(\frac{M_{y,EdS}}{M_{c,RdS}} - \frac{M_{y,EdE}}{M_{c,RdE}} \right). \tag{4.21}$$

$M_{y,EdS} / M_{c,RdS}$ is the maximum of $\frac{M_{y,Ed2}}{M_{c,Rd2}}, \frac{M_{y,Ed3}}{M_{c,Rd3}}, \frac{M_{y,Ed4}}{M_{c,Rd4}}$

and

$M_{y,EdE} / M_{c,RdE}$ is the maximum of $\frac{M_{y,Ed1}}{M_{c,Rd1}}, \frac{M_{y,Ed5}}{M_{c,Rd5}}$.

Note that only positive values of μ_{SE} are considered. In equation (4.20), $M_{y,Edi}$ and $M_{c,Rdi}$ represent the applied bending moments and the corresponding resistance moments at 5 equally-spaced cross sections along the segment, as shown in Figure 4.23.

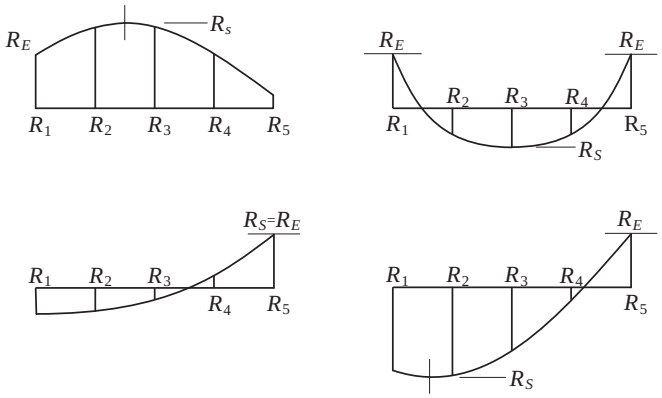


Figure 4.23 – Definition of the cross sections for non linear moment variation

In case of tapered or haunched members (Figures 4.20b and c) with prismatic flanges, equations (4.14) to (4.21) remain valid with the following changes:

- a is defined at the smallest cross section, whenever $\overline{\lambda}_{LT} \leq 1.0$; otherwise, the largest cross section should be used;

- M_{cr0} is calculated using the properties of the smallest cross section;
- for $\overline{\lambda}_{LT} \leq 1.0$, and for tapered members (Figure 4.20b), $c = c_0$, where c_0 is given by Table 4.7 (Horne *et al*, 1979). r is the ratio between the minimum distance and the maximum distance between the centroids of the flanges, t_f is the average thickness of the two external flanges and D is the minimum height of the cross section;

Table 4.7 – Equivalent section factor, c_0

D/t_f	r			
	1.5	2.0	2.5	3.0
20	1.162	1.271	1.355	1.425
22	1.128	1.219	1.290	1.350
24	1.108	1.186	1.249	1.304
26	1.094	1.164	1.222	1.272
28	1.084	1.149	1.202	1.249
30	1.077	1.137	1.187	1.232
32	1.072	1.128	1.176	1.219
34	1.067	1.121	1.167	1.208
36	1.064	1.115	1.160	1.200
38	1.061	1.110	1.154	1.193
40	1.059	1.106	1.149	1.187
42	1.057	1.103	1.144	1.182
44	1.055	1.100	1.141	1.178

- in the case of haunched members,

$$c = 1 + \left(c_0 - 1\right)\sqrt{q}\,, \tag{4.22}$$

where q is the ratio between the length of the haunch, L_h, and the total length of the member, L_t;

- for $\overline{\lambda}_{LT} > 1.0$, c = 1.0 and the maximum value of $\overline{\lambda}_{LT}$ should be used; this usually occurs at the largest cross section;
- for members with a third flange (internal), equations (4.14) to (4.21) must be determined with I_w and I_z calculated ignoring that internal flange; I_T, however, should include that flange.

Example 5.2 (chapter 5) illustrates the application of this procedure to a haunched member in a pitched-roof portal frame.

4.3.4. General method

The general method given in clause 6.3.4(1) concerns the overall resistance to out-of-plane buckling. It applies to any structural component such as: i) single members which may be built-up or have complex support conditions and ii) plane frames or sub-frames composed of such members and subject to compression and/or in-plane bending, but which do not contain rotating plastic hinges. The resistance can be verified by ensuring that (6.3.4(2)):

$$\chi_{op}\alpha_{ult,k}/\gamma_{M1} \geq 1, \tag{4.23}$$

$\alpha_{ult,k}$ is the minimum factor on the design loads needed to reach the characteristic resistance of the most critical cross section of the structural component, considering its in-plane behaviour. No account is taken of lateral or lateral-torsional buckling. Account is taken of all effects due to in-plane geometrical deformation and imperfections, global and local, where relevant. For example where $\alpha_{ult,k}$ is determined by a cross section check:

$$1/\alpha_{ult,k} = \frac{N_{Ed}}{N_{Rk}} + \frac{M_{y,Ed}}{M_{y,Rk}}, \tag{4.24}$$

χ_{op} is the reduction factor for the non-dimensional slenderness to take into account lateral and lateral-torsional buckling and γ_{M1} is the partial safety factor for instability effects (adopted as 1.0 in most National Annexes).

The global non dimensional slenderness $\overline{\lambda}_{op}$ for the structural component, used to find the reduction factor χ_{op} in the usual way using an appropriate buckling curve, should be determined from (clause 6.3.4(3)):

$$\overline{\lambda}_{op} = \sqrt{\alpha_{ult,k} / \alpha_{cr,op}}\,, \tag{4.25}$$

where $\alpha_{cr,op}$ is the minimum factor on the in-plane design loads needed to reach the elastic critical resistance of the structural component with respect to lateral or lateral-torsional buckling. No account is taken in-plane flexural buckling.

In the determination of $\alpha_{cr,op}$ and $\alpha_{ult,k}$, finite element analysis may be used.

According to clause 6.3.4(4), χ_{op} may be taken either as: i) the minimum value of χ (for lateral buckling, according to clause 6.3.1) or χ_{LT} (for lateral-torsional buckling, according to clause 6.3.2); or ii) an interpolated value between χ and χ_{LT} (determined as in i)), by using the formula for $\alpha_{ult,k}$ corresponding to the critical cross section. It is noted that ECCS TC8 (2006) recommends the use of the first option only. Further information on the application of i) and ii) is given in EC3-1-1, by Notes in clause 6.3.4(4).

The method uses a Merchant-Rankine type of empirical interaction expression to uncouple the in-plane effects and the out-of-plane effects. Conceptually, the method is an interesting approach because it deals with the structural components using a unique segment length for the evaluation of the stability with respect to the various buckling modes (Müller, 2003). In addition, for more sophisticated design situations that are not covered by code rules but need finite element analysis, the method simplifies this task. It is noted that EN 1993-1-6 (CEN, 2007) specifies a similar approach, the MNA/LBA approach, that may be seen as a generalisation of the stability reduction factor approach used throughout many parts of Eurocode 3 (Rotter and Schmidt, 2013).

Apart from the doctoral thesis of Müller (2003), this method was not widely validated and there is scarce published background documentation to establish its level of safety. Within Technical Committee 8 of ECCS, the need to explore deeply the field and limits of the application of the General

method was widely recognized (Snijder *et al*, 2006; Boissonnade *et al*, 2006). In particular, several examples have been carried out at the University of Graz (Greiner and Offner, 2007; Greiner and Lechner, 2007), comparing advanced finite element analyses (GMNIA) using beam elements with the general method. Simões da Silva *et al* (2010a) have demonstrated analytically that the method yields the same result as the application of clause 6.3.2 for the lateral-torsional buckling resistance of beams and approximately the same level of safety for prismatic columns and beam-columns.

For the General Method, the following options are possible:

i) for the evaluation of the in-plane resistance, either: (i.1) to use clause 6.3.3 (expression (3.163a)) with χ_{LT} = 1, for both Methods 1 and 2 and the cross section interaction formulae from clause 6.2.9 for the check of the end sections of the member; or i.2) to carry out constrained in-plane GMNIA numerical calculations (beam or shell elements);

ii) for the evaluation of the out-of-plane elastic critical load, either: ii.1) to use available theoretical results. For beam-columns with constant bending moment[1], Trahair (1993) proposes the following equation:

$$\left(\frac{M_{y,\max}}{M_{cr}}\right)^2 = \left(1-\frac{N_{\max}}{N_{cr,z}}\right)\left(1-\frac{N_{\max}}{N_{cr,T}}\right), \qquad (4.26)$$

where M_{cr} is the elastic critical bending moment, $N_{cr,z}$ is the elastic critical compressive buckling force in a bending mode about the z-z axis and $N_{cr,T}$ is the elastic critical compressive buckling force in a torsional mode; or ii.2) to perform a numerical LEA (beam or shell elements).

Figure 4.24 summarizes the various options.

Example 4.2 illustrates the application of the General Method to a non-prismatic member.

[1] For other bending moment diagrams, see Trahair (1993).

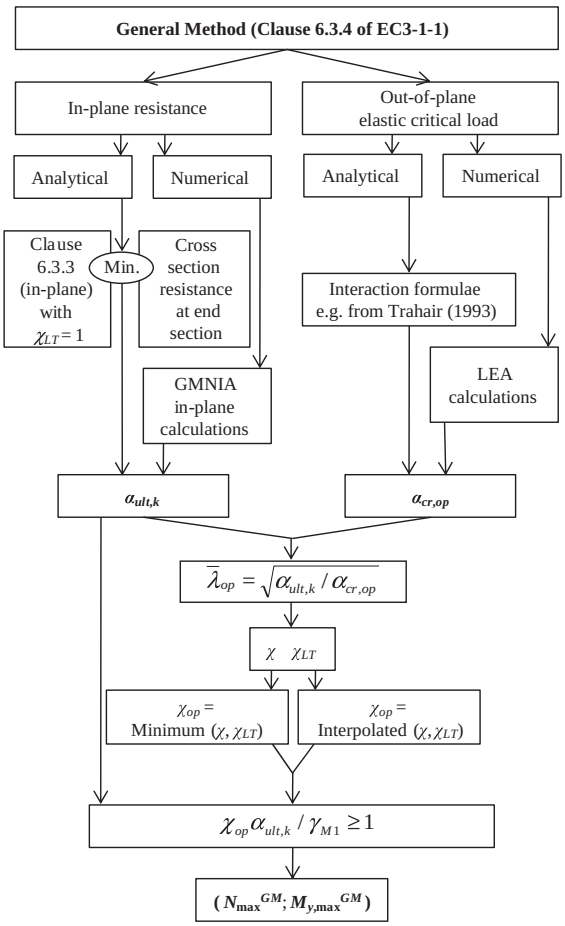


Figure 4.24 – Flowchart for the application of the General Method

4.3.5. Worked example

Example 4.2: Consider the beam-column of Figure 4.25. Assume a welded cross section that varies from an equivalent IPE 360 at one end to a cross section with similar flange width and thickness, equal web thickness and a total depth of 200 mm at the other end. Consider simply-supported ends with fork supports (the "standard case", see Figure 3.62). Assume steel grade S 235. A uniformly distributed load is applied at the shear centre. For simplicity of calculation of the cross sectional properties, the throat thickness of the welds is neglected. Assuming that the loading is already factored for ULS, verify the safety of the beam-column using the following procedures:

a) Clause 6.3.3

a.1) considering the properties of the cross section at x_{cr} according to the cross section resistance verification, except for the calculation of the critical loads, where an appropriate equivalent cross section is considered, see equations (4.5) to (4.13);
a.2) considering the properties of the cross section at the following locations along the length of the member: $x = \{0; x_{cr}; L\}$.

b) General Method (clause 6.3.4)

b.1) analytical approach: considering the properties of the cross section at the critical position, x_{cr}, according to the cross section resistance verification;
b.2) numerical approach.

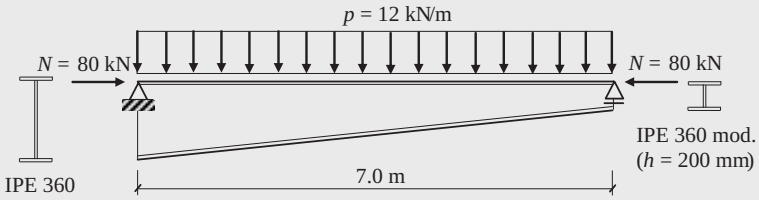


Figure 4.25 – Double-symmetric tapered I section beam

The internal force diagrams, the classification of the cross sections and the verification of the cross section resistance are identical for all design procedures. These verifications are presented in items i) to iii).

i) *Internal force diagrams*

The internal force diagrams are represented in Figure 4.26.

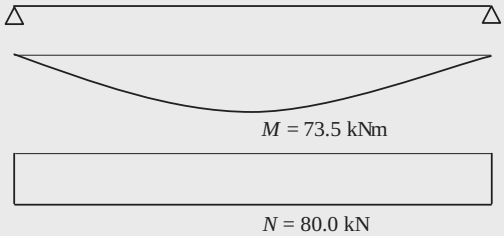


Figure 4.26 – Design internal force diagrams

ii) *Cross section classification*

Geometrical characteristics of an equivalent welded IPE 360: A = 69.95 cm^2, h = 360 mm, b = 170 mm, $W_{el,y}$ = 862.4 cm^3, $W_{pl,y}$ = 973 cm^3, I_y = 15524 cm^4, i_y = 14.90 cm, $W_{el,z}$ = 122.5 cm^3, $W_{pl,z}$ = 188.9 cm^3, I_z = 1041 cm^4, i_z = 3.86 cm, I_T = 28.93 cm^4 and I_w = 313.6×10^3 cm^6.

Geometrical characteristics of an equivalent welded modified IPE 360 with a total depth of 200 mm: A = 57.15 cm^2, h = 200 mm, b = 170 mm, $W_{el,y}$ = 414.8 cm^3, $W_{pl,y}$ = 465 cm^3, I_y = 4148 cm^4, i_y = 8.52 cm, $W_{el,z}$ = 122.4 cm^3, $W_{pl,z}$ = 186.3 cm^3, I_z = 1041 cm^4, i_z = 4.27 cm, I_T = 26.2 cm^4 and I_w = 91.2×10^3 cm^6.

The cross section is classified according to clause 5.5 of EC3-1-1 and Tables 2.21 and 2.22, neglecting the welds at the web-flange junction. Figure 4.27 illustrates the variation of the cross sectional class along the member.

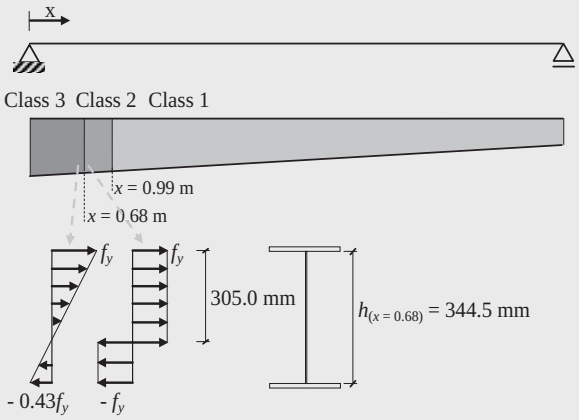


Figure 4.27 – Cross section classification

iii) *Verification of the cross section resistance*

The cross sectional resistance is checked using clauses 6.2.8 (bending and shear) and 6.2.9 (bending and axial force). For example, for x > 0.68 m (class 1 or 2 cross sections), the interaction diagram for bending and axial force, obtained from equation (3.148) (clause 6.2.9.1(5)), is illustrated in Figure 4.28:

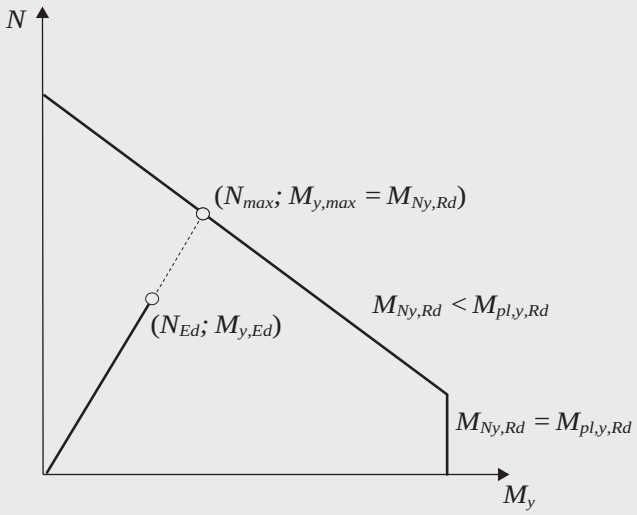


Figure 4.28 – Cross section plastic interaction diagram

The pair of forces (N_{max}; $M_{y,max}$) in Figure 4.28 are obtained by solving the following system of equations (equation (3.148)):

$$\begin{cases} M_{y,\max} = M_{N,y,Rd} = M_{pl,y,Rd}\dfrac{1-N_{\max}/N_{pl}}{1-0.5a} \le M_{pl,y,Rd}; \\ \dfrac{N_{\max}}{M_{y,\max}} = \dfrac{N_{Ed}}{M_{y,Ed}}. \end{cases}$$

From Figure 4.28, the utilization factor U_F of the cross section is given by the ratio between the norm of the applied internal forces and the norm of the bending and axial force resistance along the same load vector:

$$\frac{\sqrt{N_{Ed}^2 + M_{y,Ed}^2}}{\sqrt{N_{\max}^2 + M_{y,\max}^2}} \le 1.$$

For a class 3 cross section, the utilization factor U_F of the cross sections is given by

$$U_F = \frac{N_{Ed}}{Af_y} + \frac{M_{y,Ed}}{W_{el,y}f_y} \le 1\,.$$

Figure 4.29 shows the resulting variation of the utilization factor along the length of the member. The critical cross section is located at x = 4.14 m with a value of 0.46 (≤ 1).

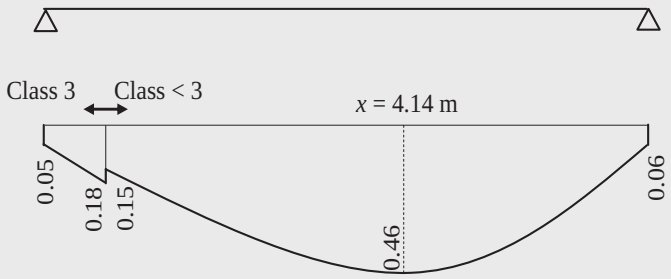


Figure 4.29 – Variation of the utilization factor along the length of the member

iv) *Verification of the buckling resistance of the member*

a) *Clause* 6.3.3

a.1) Considering cross section properties at x_{cr} and equivalent cross section properties for critical loads

The critical position was chosen according to the cross section verification, i.e. x_{cr} = 4.14 m. The properties of the cross section (class 1) at this position are: A = 62.38 cm^2, h = 265.4 mm, b = 170 mm, $W_{el,y}$ = 589.4 cm^3, $W_{pl,y}$ = 661 cm^3, I_y = 7819 cm^4, i_y = 11.20 cm, $W_{el,z}$ = 122.5 cm^3, $W_{pl,z}$ = 187.4 cm^3, I_z = 1041 cm^4, i_z = 4.09 cm, I_T = 27.3 cm^4 and I_w = 166.0x10^3 cm^6.

Considering the properties at x_{cr}, the values of the characteristic resistance are given by (class 1 or 2 cross sections):

$$N_{Rk} = Af_y = 1465.9 \text{ kN};$$

$$M_{y,Rk} = W_{pl,y}f_y = 155.3 \text{ kNm}.$$

Flexural buckling

The equivalent second moment of area about the strong axis is given by equations (4.6) to (4.8):

$$\begin{cases} r = \sqrt{I_{y,\min}/I_{y,\max}} = 0.517; \\ C = \left(0.08 + 0.92r\right) = 0.08 + 0.92 \times 0.517 = 0.555; \\ I_{y,eq} = CI_{y,\max} = 0.555 \times 15524 = 8624 \text{ cm}^4, \end{cases}$$

leading to

$$N_{cr,y} = \frac{\pi^2 EI_{y,eq}}{L^2} = \frac{\pi^2 \times 210 \times 10^6 \times 8624 \times 10^{-8}}{7.0^2} = 3647.88 \text{ kN}.$$

The flexural buckling reduction factor χ_y about the *y* axis is given by:

$$\overline{\lambda}_y = \sqrt{N_{pl,Rd}/N_{cr,y}} = 0.634;$$

$$\alpha = 0.34 \qquad \left(\text{Curve } b\right);$$

$$\phi = 0.77 \qquad \Rightarrow \chi_y = 0.820.$$

The flexural buckling reduction factor χ_z about the *z* axis is given by:

$$N_{cr,z} = \frac{\pi^2 EI_{z,\min}}{L^2} = \frac{\pi^2 \times 210 \times 10^6 \times 1041 \times 10^{-8}}{7.0^2} = 440.2 \text{ kN};$$

$$\overline{\lambda}_z = \sqrt{N_{pl,Rd}/N_{cr,z}} = 1.825;$$

$$\alpha = 0.49 \quad \left(\text{Curve } c\right);$$

$$\phi = 2.56 \quad \Rightarrow \chi_z = 0.229.$$

Lateral-torsional buckling

The equivalent cross sectional properties are obtained considering the following equivalent depth of the member (equation (4.11)):

$$\begin{cases} h_{eq} = h_{\max}\sqrt{0.283 + 0.434\gamma + 0.283\gamma^2}; \\ \gamma = 200/360 = 0.56; \qquad \rightarrow h_{eq} \approx 281.5 \text{ mm}. \\ h_{\max} = 360 \text{ mm}; \end{cases}$$

From equation (4.12),

$$I_T = I_{T,eq} = \frac{I_{T,\max} + I_{T,\min}}{2} = \frac{26.19 + 28.93}{2} = 27.56\ \text{cm}^4\ .$$

Considering $I_z = I_{z,min}$, and $I_w = f\ (h_{eq})$, the elastic critical moment (using equation B.1) is

$$M_{cr} = \alpha_m M_{cr,E} = 1.13 \times \left[\frac{\pi}{L} \sqrt{GI_T EI_Z \left(1 + \frac{\pi^2 EI_w}{L^2 GI_T} \right)} \right] = 130.30\ \text{kNm.}$$

From equation (3.130) and Table 3.6 the lateral-torsional buckling reduction factor χ_{LT} is given by:

$$\bar{\lambda}_{LT} = \sqrt{M_{pl,y,Rd} / M_{cr}} = 1.092;$$

$$\alpha = 0.49 \qquad (\text{Curve } c);$$

$$\phi = 1.31 \qquad \Rightarrow \chi_{LT} = 0.489.$$

Finally, also considering equivalent cross section properties from Galea (1986) (equations (4.11) and (4.12), $N_{cr,T}$ is obtained. For this calculation, $I_y = f\ (h_{eq})$:

$$N_{cr,T} = \frac{A}{I_y + I_z} \left(GI_T + \frac{\pi^2 EI_w}{L^2} \right) = 1929.7\ \text{kN.}$$

Buckling resistance – application of the interaction formulae

The design forces for the verification of the buckling resistance are N_{Ed} = 80 kN and $M_{y,Ed} = M_{y,max}$ = 73.5 kNm.

– Auxiliary terms (Table 3.12):

$$\mu_y = \frac{1 - \dfrac{N_{Ed}}{N_{cr,y}}}{1 - \chi_y \dfrac{N_{Ed}}{N_{cr,y}}} = \frac{1 - \dfrac{80.0}{3647.88}}{1 - 0.820 \times \dfrac{80.0}{3647.88}} = 0.996;$$

$$\mu_z = \frac{1 - \dfrac{N_{Ed}}{N_{cr,z}}}{1 - \chi_z \dfrac{N_{Ed}}{N_{cr,z}}} = \frac{1 - \dfrac{80.0}{440.18}}{1 - 0.229 \times \dfrac{80.0}{440.18}} = 0.854;$$

$$w_y = \frac{W_{pl,y}}{W_{el,y}} = \frac{660.69}{589.28} = 1.121 \quad (\leq 1.5);$$

$$w_z = \frac{W_{pl,z}}{W_{el,z}} = \frac{187.35}{122.46} = 1.530 \quad (> 1.5 \Rightarrow w_z = 1.5).$$

– $C_{my,0}$ factor (for a uniformly distributed load):

$$C_{my,0} = 1 + 0.03\frac{N_{Ed}}{N_{cr,y}} = 1 + 0.03 \times \frac{80.0}{3647.88} = 1.00.$$

Because I_T = 27.3 cm^4 < I_y = 7819 cm^4, the member is susceptible to lateral-torsional buckling.

$$M_{cr,0} \equiv M_{cr,E} = 115.31 \text{ kNm};$$

$$\overline{\lambda}_0 = 1.160.$$

Because y_c = 0 (distance between the shear centre and the centroid of the cross section), $N_{cr,TF} \equiv N_{cr,T}$ =1929.7 kN. Since C_1=1.12 (Table 3.5), from expression (3.164):

$$\overline{\lambda}_{0,\lim} = 0.2\sqrt{C_1}\sqrt[4]{\left(1 - \frac{N_{Ed}}{N_{cr,y}}\right)\left(1 - \frac{N_{Ed}}{N_{cr,TF}}\right)} =$$

$$= 0.2 \times \sqrt{1.12} \times \sqrt[4]{\left(1 - \frac{80.0}{3647.9}\right) \times \left(1 - \frac{80.0}{1929.7}\right)} = 0.20.$$

As $\overline{\lambda}_{0,\lim} = 0.20 < \overline{\lambda}_0 = 1.160$, lateral-torsional buckling has to be taken into account.

$$a_{LT} = 1 - \frac{I_T}{I_y} = 0.997 \geq 0;$$

$$\varepsilon_y = \frac{M_{y,Ed}}{N_{Ed}}\frac{A}{W_{El,y}} = \frac{73.5}{80} \times \frac{62.38 \cdot 10^{-4}}{589.28 \times 10^{-6}} = 9.73;$$

$$C_{my} = C_{my,0} + \left(1 - C_{my,0}\right)\frac{\sqrt{\varepsilon_y}\, a_{LT}}{1 + \sqrt{\varepsilon_y}\, a_{LT}} =$$

$$= 1.0 + \left(1.0 - 1.0\right) \times \frac{\sqrt{9.73} \times 0.997}{1 + \sqrt{9.73} \times 0.997} = 1.0;$$

$$C_{mLT} = C_{my}^2 \frac{a_{LT}}{\sqrt{\left(1 - \frac{N_{Ed}}{N_{cr,y}}\right)\left(1 - \frac{N_{Ed}}{N_{cr,TF}}\right)}} =$$

$$= 1.0^2 \times \frac{0.997}{\sqrt{\left(1 - \frac{80.0}{3647.9}\right) \times \left(1 - \frac{80.0}{1929.7}\right)}} = 1.126 \geq 1;$$

$$n_{pl} = \frac{N_{Ed}}{N_{Rk} / \gamma_{M1}} = \frac{80.0}{1465.88 / 1.0} = 0.055;$$

$$\overline{\lambda}_{\max} = \max \begin{cases} \overline{\lambda}_y = 0.63 \\ \overline{\lambda}_z = 1.82 \end{cases} = 1.82;$$

$$C_{yy} = 1 + \left(w_y - 1\right)\left[\left(2 - \frac{1.6}{w_y} C_{my}^2 \overline{\lambda}_{\max} - \frac{1.6}{w_y} C_{my}^2 \overline{\lambda}_{\max}^2\right) n_{pl}\right] \geq \frac{W_{el,y}}{W_{pl,y}} \Leftrightarrow$$

$$C_{yy} = 1 + \left(1.16 - 1\right)\left[\left(2 - \frac{1.6}{1.12} \times 1.0^2 \times 1.82 - \frac{1.6}{1.12} \times 1.0^2 \times 1.82^2\right) \times 0.05\right] =$$

$$= 0.965 \qquad \left(\geq W_{el,y} / W_{pl,y} = 589.28 / 660.69 = 0.892\right);$$

$$C_{zy} = 1 + \left(w_y - 1\right)\left[\left(2 - 14 \frac{C_{my}^2 \overline{\lambda}_{\max}^2}{w_y^5}\right) n_{pl}\right] \geq 0.6 \sqrt{\frac{w_y}{w_z}} \frac{W_{el,y}}{W_{pl,y}} \Leftrightarrow$$

$$C_{zy} = 1 + \left(1.16 - 1\right) \times \left[\left(2 - 14 \times \frac{1.0^2 \times 1.82^2}{1.12^2}\right) \times 0.05\right] =$$

$$= 0.839 \qquad \left(\geq 0.6 \sqrt{\frac{w_y}{w_z}} \frac{W_{el,y}}{W_{pl,y}} = 0.6 \times \sqrt{\frac{1.12}{1.5}} \times \frac{589.28}{660.69} = 0.462\right).$$

– Interaction factors (class 1 cross section): From Table 3.11,

$$k_{yy} = C_{my} C_{mLT} \frac{\mu_y}{1 - \frac{N_{Ed}}{N_{cr,y}}} \frac{1}{C_{yy}} = 1.0 \times 1.126 \times \frac{0.996}{1 - \frac{80.0}{3647.88}} \times \frac{1}{0.965} = 1.19;$$

$$k_{zy} = C_{my} C_{mLT} \frac{\mu_z}{1 - \frac{N_{Ed}}{N_{cr,y}}} \frac{1}{C_{zy}} 0.6 \sqrt{\frac{w_y}{w_z}} =$$

$$= 1.0 \times 1.126 \times \frac{0.854}{1 - \frac{80.0}{3647.88}} \times \frac{1}{0.839} \times 0.6 \times \sqrt{\frac{1.121}{1.5}} = 0.61.$$

– Interaction formulae:

The interaction formulae (3.163) give:

$$\frac{N_{Ed}}{\chi_y N_{Rk} / \gamma_{M1}} + k_{yy} \frac{M_{y,Ed}}{\chi_{LT} M_{y,Rk} / \gamma_{M1}} =$$

$$= \frac{80}{0.82 \times 1465.9 / 1.0} + 1.19 \times \frac{73.5}{0.49 \times 155.3 / 1.0} = 1.22 > 1;$$

334

$$\frac{N_{Ed}}{\chi_z N_{Rk} / \gamma_{M1}} + k_{zy} \frac{M_{y,Ed}}{\chi_{LT} M_{y,Rk} / \gamma_{M1}} =$$

$$== \frac{80}{0.23 \times 1465.9 / 1.0} + 0.61 \times \frac{73.5}{0.49 \times 155.3 / 1.0} = 0.83 < 1.$$

It is concluded that the beam-column does not satisfy safety using this procedure.

a.2) Using the properties at the locations $x = \{0; x_{cr}; L\}$

The design forces for verification of the buckling resistance are N_{Ed} = 80 kN and $M_{y,Ed} = M_{y,max}$ = 73.5 kNm. The plastic resistance is considered at $x = \{x_{cr}; L\}$ (class 1 cross sections), while at x = 0 m, the elastic resistance is considered (class 3 cross section).

For the verification of the buckling resistance, the process is analogous to a.1). However, critical loads are calculated considering the properties of the cross sections at the specified locations. The application of the interaction formulae give:

– Design at x = 0 m:

$$\frac{N_{Ed}}{\chi_y N_{Rk}/\gamma_{M1}} + k_{yy}\frac{M_{y,Ed}}{\chi_{LT} M_{y,Rk}/\gamma_{M1}} =$$

$$= \frac{80}{0.88\times 1643.8/1.0} + 1.15\times\frac{73.5}{0.38\times 202.7/1.0} = 1.15 > 1;$$

$$\frac{N_{Ed}}{\chi_z N_{Rk}/\gamma_{M1}} + k_{zy}\frac{M_{y,Ed}}{\chi_{LT} M_{y,Rk}/\gamma_{M1}} =$$

$$= \frac{80}{0.21\times 1643.8/1.0} + 0.98\times\frac{73.5}{0.38\times 202.7/1.0} = 1.16 > 1.$$

– Design at $x = x_{cr}$ = 4.14 m:

$$\frac{N_{Ed}}{\chi_y N_{Rk}/\gamma_{M1}} + k_{yy}\frac{M_{y,Ed}}{\chi_{LT} M_{y,Rk}/\gamma_{M1}} =$$

$$= \frac{80}{0.80\times 1465.9/1.0} + 1.19\times\frac{73.5}{0.48\times 155.3/1.0} = 1.23 > 1;$$

$$\frac{N_{Ed}}{\chi_z N_{Rk}/\gamma_{M1}} + k_{zy}\frac{M_{y,Ed}}{\chi_{LT} M_{y,Rk}/\gamma_{M1}} =$$

$$= \frac{80}{0.23\times 1465.9/1.0} + 0.61\times\frac{73.5}{0.48\times 155.3/1.0} = 0.84 < 1.$$

– Design at $x = L$ = 7 m:

$$\frac{N_{Ed}}{\chi_y N_{Rk}/\gamma_{M1}} + k_{yy}\frac{M_{y,Ed}}{\chi_{LT} M_{y,Rk}/\gamma_{M1}} =$$

$$= \frac{80}{0.68\times 1343.0/1.0} + 1.19\times\frac{73.5}{0.56\times 109.4/1.0} = 1.51 > 1;$$

$$\frac{N_{Ed}}{\chi_z N_{Rk}/\gamma_{M1}} + k_{zy}\frac{M_{y,Ed}}{\chi_{LT} M_{y,Rk}/\gamma_{M1}} =$$

$$= \frac{80}{0.25\times 1343.0/1.0} + 0.62\times\frac{73.5}{0.56\times 109.4/1.0} = 0.98 < 1.$$

These results are also unsafe.

b) *General Method*

b.1) Analytical approach: using the properties at the critical cross section, x_{cr}
In-plane buckling resistance

The analytical expressions for in-plane buckling are evaluated using the properties of the cross section at x = 4.14 m. To calculate $\alpha_{ult,k}$, clause 6.3.3 is considered (expression (3.163a)) with χ_{LT} = 1 (see Figure 4.24); to calculate χ_{op}, χ_{LT} is calculated according to the General Case (clause 6.3.2.2) and Method 1 (Annex A) is adopted.

The application of the interaction formulae gives:

$$\alpha_{ult,k} = \left(\frac{N_{Ed}}{\chi_y N_{Rk}/\gamma_{M1}} + k_{yy}\frac{M_{y,Ed}}{\chi_{LT} M_{y,Rk}/\gamma_{M1}}\right)^{-1} =$$

$$= \left(\frac{80}{0.80\times 1465.9/1.0} + 1.02\times\frac{73.5}{155.3/1.0}\right)^{-1} = \frac{1}{0.55} = 1.819.$$

Out-of-plane elastic critical load

Figure 4.30 compares the “exact” numerical results from a linear eigenvalue analysis with the analytical results obtained using equation (4.26). The analytical results are calculated considering the bending moment corresponding to each position and the maximum bending moment at $x = L/2$. For the evaluation of $\alpha_{cr,op}$, the numerical value is considered, as equation (4.26) is not simple to apply.

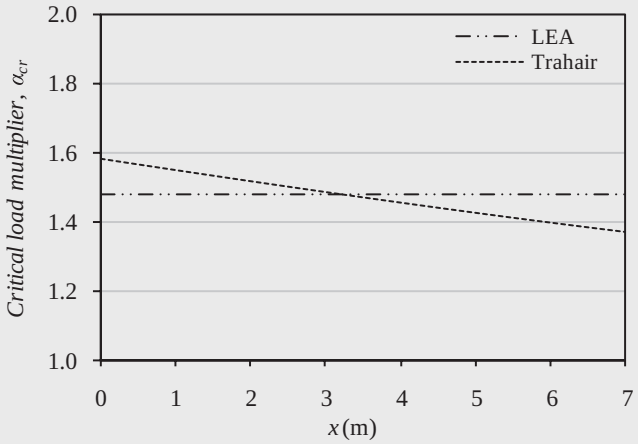


Figure 4.30 – Elastic critical load multiplier

The load multiplier of the numerical model is $\alpha_{cr,op}$=1.482, which results in

$$\left(N_{\max};M_{y,\max}\right)=\alpha_{cr,op}\times\left(N_{num};M_{y,num}\right)$$

$$=1.482\times\left(80\text{ kN};73.5\text{ kNm}\right)=\left(118.6\text{ kN};108.9\text{ kNm}\right).$$

Buckling resistance

The non linear in-plane load multiplier and the out-of-plane elastic critical load multiplier are $\alpha_{ult,k}$ = 1.819 and $\alpha_{cr,op}$ = 1.482, respectively. The global non dimensional slenderness $\overline{\lambda}_{op}$ is (see equation (4.25)):

$$\overline{\lambda}_{op}=\sqrt{\alpha_{ult,k}/\alpha_{cr,op}}=1.108.$$

For x = 4.14 m, both the buckling curves for lateral-torsional buckling and out-of-plane flexural buckling are c (Table 3.6):

$$\overline{\lambda}_{op}\left\langle\begin{array}{l}\text{curve } c\rightarrow\chi_z=0.480\\ \text{curve } c\rightarrow\chi_{LT}=0.480\end{array}\right. .$$

χ_{op} is calculated as:

$$\chi_{op}=\text{minimum}\left(\chi_z;\chi_{LT}\right)\equiv\text{interpolated}\left(\chi_z;\chi_{LT}\right)=0.480.$$

Application of expression (4.23) gives:

$\chi_{op}\alpha_{ult,k}/\gamma_{M1} \geq 1 \rightarrow 0.480 \times 1.819/1 = 0.873 < 1.$

Therefore, according to this method, the buckling resistance is not verified. The utilization ratio is 1/0.873=1.15, i.e., 15 % higher than permitted.

b.2) Numerical approach

Considering the applied loads, the load multipliers for in-plane GMNIA and LEA calculations are $\alpha_{ult,k}$ = 1.993 and $\alpha_{cr,op}$ = 1.482, respectively. The global non dimensional slenderness $\overline{\lambda}_{op}$ is (see equation (4.25)):

$$\overline{\lambda}_{op} = \sqrt{\alpha_{ult,k}/\alpha_{cr,op}} = 1.160.$$

The buckling curve for flexural buckling out-of-plane is always *c* along the member, while for lateral-torsional buckling the buckling curve is *d* at *x* = [0; 0.88] m and *c* at *x* = [0.88; 7.0] m (at *x* = 0.88 m, *h/b* = 2). Although the position of the critical cross section for an in-plane GMNIA calculation is *x* = 4.13 m, both buckling curves for lateral-torsional buckling are considered for comparison. The reduction factors χ and χ_{LT} are given by:

– Curve *c* for FB_{zz} and curve *c* for LTB:

$$\overline{\lambda}_{op} \left\langle \begin{array}{l} \text{curve } c \rightarrow \chi_z = 0.454 \\ \text{curve } c \rightarrow \chi_{LT} = 0.454 \end{array} \right. .$$

– Curve *c* for FB_{zz} and curve *d* for LTB:

$$\overline{\lambda}_{op} \left\langle \begin{array}{l} \text{curve } c \rightarrow \chi_z = 0.454 \\ \text{curve } d \rightarrow \chi_{LT} = 0.393 \end{array} \right. .$$

χ_{op} is calculated as:

– Curve *c* for FB_{zz} and curve *c* for LTB:

$$\chi_{op} = \text{minimum}\left(\chi_z;\chi_{LT}\right) \equiv \text{interpolated}\left(\chi_z;\chi_{LT}\right) = 0.454.$$

– Curve *c* for FB_{zz} and curve *d* for LTB:

$$\chi_{op} = \text{minimum}\left(\chi_z;\chi_{LT}\right) = 0.393,$$

or

$$\chi_{op} = \text{interpolation}\left(\chi_z ; \chi_{LT}\right) = \frac{\phi + 1}{\phi / \chi_z + 1 / \chi_{LT}} = 0.398,$$

where ϕ is obtained from (the cross section is class 1):

$$\phi = \frac{N_{Rk} / N_{Ed}}{M_{y,Rk} / M_{y,Ed}} = \frac{N_{pl,Rd} / N_{Ed}}{M_{pl,y,Rd} / M_{y,Ed}} 0.115.$$

The derivation of the formulae presented above for the interpolated value between χ and χ_{LT} can be found in Simões da Silva *et al* (2010b).

Finally, the application of expression (4.23) leads to:

– Curve *c* for FB_{zz} and curve *c* for LTB:

$$\chi_{op} \alpha_{ult,k} / \gamma_{M1} \geq 1 \rightarrow 0.454 \times 1.9972 / 1 = 0.904 < 1.$$

– Curve *c* for FB_{zz} and curve *d* for LTB:

Considering χ_{LT} = minimum (χ_{LT} ; χ_{LT}),

$$\chi_{op} \alpha_{ult,k} / \gamma_{M1} \geq 1 \rightarrow 0.393 \times 1.9927 / 1 = 0.783 < 1.$$

Or considering χ_{LT} = interpolation (χ_{LT} ; χ_{LT}),

$$\chi_{op} \alpha_{ult,k} / \gamma_{M1} \geq 1 \rightarrow 0.393 \times 1.9927 / 1 = 0.794 < 1.$$

For all alternatives, the buckling resistance is not verified.

v) *Comparison of results*

Table 4.8 summarizes the results from the several methods and compares them to a full 3D GMNIA calculation. Firstly, all methods yield conservative results when compared to the "exact" GMNIA calculation. Secondly, the location of the cross section for consideration of geometrical properties has significant influence in results – the utilization ratio varies from 116 % to 151 %. Regarding the General Method, it is much simpler to apply and does not suffer from using inconsistent geometrical properties in the verification. Finally, the difficult choice of the buckling curve for tapered members results in a great scatter of results.

Table 4.8 – Comparison of results

Method			Utilization ratio	Diff. (%)
GMNIA			0.88	-
Clause 6.3.3	$x = x_{cr}$ + Equivalent properties for critical loads		1.22	39.0
	$x = 0$		1.16	32.8
	$x = x_{cr}$		1.23	40.8
	x = L		1.51	72.7
General Method (theoretical) - x_{cr}			1.15	30.8
General Method (numerical)	ZZ – curve *c*; LT – curve *c*		1.11	26.4
	ZZ – curve *c*; LT – curve *d*	Minimum	1.28	45.9
		Interpolated	1.26	43.9

This example highlights the large scatter of results that may be obtained by the use of application rules that are not validated for non-prismatic members. In such cases, it is up to the designer to use his/her engineering judgment and properly implement verification procedures that do not violate the principles in EC3-1-1.

4.4. DESIGN EXAMPLE 1: ELASTIC DESIGN OF BRACED STEEL FRAMED BUILDING

4.4.1. Introduction

The building analyzed in this case study is based in the steel-framed structure shown in Figure 4.31, a building used as a test facility and erected at Cardington (UK), in 1993. The structure was designed as a typical modern multi-storey office building.

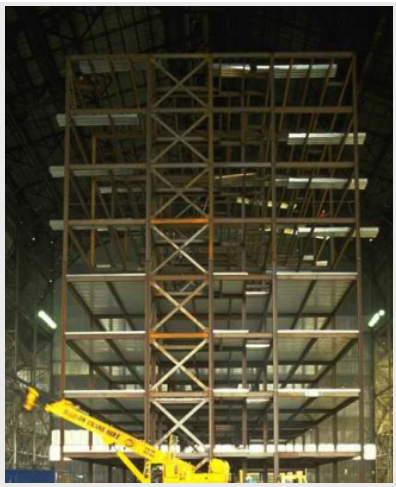


Figure 4.31 – Side elevation view

The building has an area of 21 m by 45 m and a total height of 33 m. Along the length, there are 5 bays, each 9 m long. Across the width there are 3 bays of 6 m, 9 m and 6 m. The building has 8 storeys. The height of the first storey is 4.335 m from the ground floor to the top-of-steel height. All the other storeys have a height of 4.135 m from top-of-steel to top-of-steel.

On the south elevation there is a two storey ground floor atrium, 9 m × 8 m. At each side of the building there is a 4 m × 4.5 m void, to provide fireman's access and an escape stairwell. Additionally, on the west side, there is another 4 m × 2 m void, for a goods lift. In the middle of the building there's a central lift core, 9 m × 2.5 m. Figure 4.32 represents the typical floor plan of the building. All slabs are lightweight composite slabs with a thickness of 130 mm.

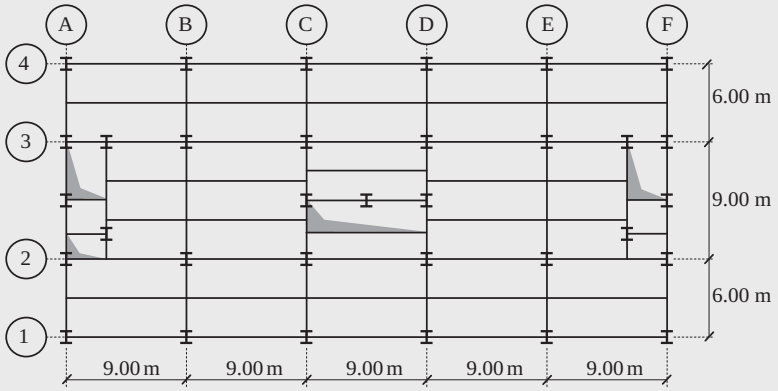


Figure 4.32 – Plan of the 3rd to 7th floor

4.4.2. Description of the structure

The structure is designed as a braced frame with lateral restraint provided by cross bracing of flat steel plates, around the three vertical access shafts. Figure 4.33 to 4.35 and Tables 4.9 to 4.11 represent the various structural floor plans and the geometry of the beams.

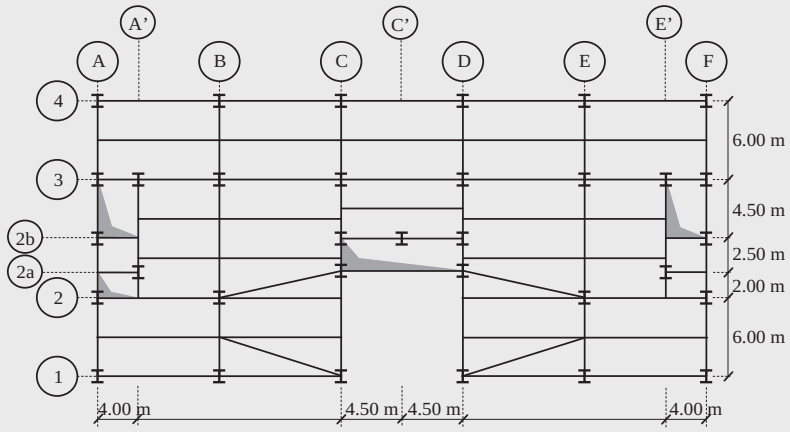


Figure 4.33 – Plan of the 1st floor

Table 4.9 – Geometric characteristics of the beams (1st floor)

Beams	Cross section	Steel grade
A1 – F1, A4 – F4	IPE 400	S 355
A1 – A4, B1 – B2, B3 – B4, C2a – C4, D2a – D4, E1 – E2, E3 – E4, F1 – F4	IPE 400	S 355
C1 – C2a, D1 – D2a	IPE 600	S 355
B2 – B3, E2 – E3	IPE 600	S 355
A2 – B2, A2a – A'2a, A2b – A'2b, A3 – A'3, A'2 - A'3	IPE 400	S 355
E'2a – E'3, E'2b – F2b, E'3 – F3	IPE 400	S 355
C2a – D2a, C2b – D2b, C3 – D3	IPE 400	S 355
All others secondary beams	IPE 360	S 355

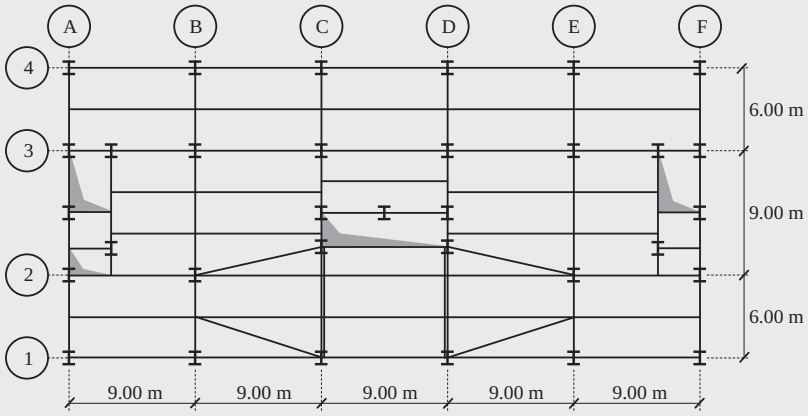


Figure 4.34 – Plan of the 2nd floor

Table 4.10 – Geometric characteristics of the beams (2nd floor)

Beams	Cross section	Steel grade
A1 – F1, A4 – F4	IPE 400	S 355
A1 – A4, B1 – B2, B3 – B4, C2a – C4, D2a – D4, E1 – E2, E3 – E4, F1 – F4	IPE 400	S 355
C1 – C2a, D1 – D2a	2 x HEA 700	S 355
B2 – B3, E2 – E3	IPE 600	S 355
A2 – B2, A2a – A'2a, A2b – A'2b, A3 – A'3, A'2 - A'3	IPE 400	S 355
E'2a – E'3, E'2b – F2b, E'3 – F3	IPE 400	S 355
C2a – D2a, C2b – D2b, C3 – D3	IPE 400	S 355
All others secondary beams	IPE 360	S 355

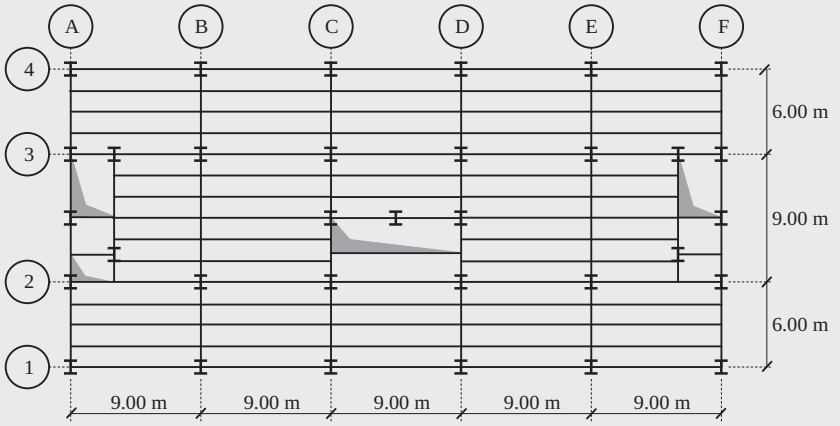


Figure 4.35 – Plan of the 8th floor

Table 4.11 – Geometric characteristics of the beams (3rd to 8th floors)

Beams	Cross section	Steel grade
A1 – F1, A4 – F4	IPE 400	S 355
A1 – A4, B1 – B2, B3 – B4, C1 – C4, D1 – D4, E1 – E2, E3 – E4, F1 – F4	IPE 400	S 355
B2 – B3, E2 – E3	IPE 600	S 355
A2 – B2, A2a – A'2a, A2b – A'2b, A3 – A'3, A'2 - A'3	IPE 400	S 355
E'2a – E'3, E'2b – F2b, E'3 – F3	IPE 400	S 355
C2a – D2a, C2b – D2b, C3 – D3	IPE 400	S 355
All others secondary beams	IPE 360	S 355

Table 4.12 details the geometrical characteristics of the columns (S 355).

Table 4.12 – Geometric characteristics of the columns

Columns	Ground floor – 2nd floor	2nd floor – 5th floor	5th floor – 8th floor
B2, C2, D2, E2, C2b, C'2b, D2b, B3, C3, D3, E3	HEB 340	HEB 320	HEB 260
	Ground floor – 4th floor	4th floor – 8th floor	
B1, C1, D1, E1, A2, F2, A3, F3, B4, C4, D4, E4, A'2a, A2b, A'3, E'2a, F2b, E'3	HEB 320	HEB 260	
	Ground floor – 8th floor		
A1, A4, F1, F4	HEB 260		

4.4.3. General safety criteria, actions and combinations of actions

4.4.3.1. General safety criteria

Actions are classified, according to EN 1990, by their variation in time as: i) permanent actions (*G*) (e.g. self-weight), ii) variable actions (*Q*) (e.g. imposed loads on buildings floors, wind loads, snow loads) and iii) accidental actions (*A*) (e.g. explosions).

The actions considered in this design example are described in the following paragraphs. All actions are quantified according to the relevant parts of EN 1991. In addition, the recommended values are always adopted whenever the specific choice is left to the National Annexes.

4.4.3.2. Permanent actions

The permanent actions include the self-weight of the structural elements and also the non-structural elements, such as coverings, partitions, thermal insulation, etc.

The self-weight of the structural elements includes the weight of the steel structure (78.5 kN/m^3) and the self-weight of a lightweight concrete slab (12.5 kN/m^3) with a constant thickness of 130 mm.

4.4.3.3. Imposed loads

The characteristic value of the imposed load depends of the category of the loaded area of the building. For an office building and according to Table 6.1 of EN 1991-1-1 (CEN, 2002b), the category of the loaded area is B, the corresponding characteristic values being given by: q_k = 2.0 to 3.0 kN/m^2 and Q_k = 1.5 to 4.5 kN. q_k is intended for the determination of global effects and Q_k for local effects. According to EN 1991-1-1, the characteristic value of the imposed load is given by the National Annexes; however, the recommended values are underlined.

Accessible roofs with occupancy according to category B are categorized according to clause 6.3.4.1 (Table 6.9) as category I. In this case, the imposed load for the roof is given in Table 6.2 for the category of loaded area B: q_k = 2.0 to 3.0 kN/m^2 and Q_k = 1.5 to 4.5 kN.

In buildings with fixed partitions, their self-weight should be taken into account as a permanent load. In the case of movable partitions, and provided that the floor allows for lateral distribution of loads, their self-weight may be taken into account as a uniformly distributed load, q_k, that must be added to the imposed load on the floor (clause 6.3.1.2 (8) of EN 1991-1-1). In this design example, the partition walls were considered to be movable with a self-weight less than 1 kN/m per wall length, so that the value of the corresponding uniformly distributed load is 0.5 kN/m^2 (clause 6.3.1.2(8) of EN 1991-1-1).

4.4.3.4. Wind actions

i) Wind forces

The quantification of the wind actions on the building follows EN 1991-1-4 (CEN, 2005e). Two main directions are assumed for the wind: $\theta = 0^o$ and $\theta = 90^o$. According to clause 5.3(3), the wind forces are calculated by the vectorial summation of the external forces, $F_{w,e}$, and the internal forces, $F_{w,i}$, given by equations (4.27) and (4.28), respectively

$$F_{w,e} = c_s c_d \sum_{surfaces} w_e A_{ref} \tag{4.27}$$

and

$$F_{w,i} = \sum_{surfaces} w_i A_{ref}\,, \tag{4.28}$$

where $c_s c_d$ is the structural factor, A_{ref} is the reference area of the individual surfaces, and w_e and w_i are the external and internal pressures on the individual surfaces at reference heights z_e and z_i, respectively for external and internal pressures, given by the following equations:

$$w_e = q_p\left(z_e\right) c_{pe} \tag{4.29}$$

and

$$w_i = q_p\left(z_i\right) c_{pi}\,, \tag{4.30}$$

$q_p(z)$ is the peak velocity pressure, and c_{pe} and c_{pi} are the pressure coefficients for the external and internal pressures, respectively.

The structural factor $c_s c_d$ is defined in clause 6.1(1). For multistory steel buildings with rectangular plan layout and vertical external walls, with regular distribution of stiffness and mass, the structural factor, $c_s c_d$, may be taken from Annex D of EN 1991-1-4. For h = 33 m and b = 21 m ($\theta = 0^o$), $c_s c_d$ = 0.95 and for b = 45 m ($\theta = 90^o$), $c_s c_d$ = 0.89.

ii) Calculation of reference height

The reference heights, z_e, for vertical windward walls of rectangular plan buildings (side D in Figures 4.38 and 4.39) depend on the aspect ratio h/b and are always the upper heights of the different parts of the walls (clause 7.2.2(1)). For $\theta = 0^o$ (see Figure 4.38), b = 21 m < h = 33 m < 2b = 42 m,

therefore the height of the building may be considered in two parts, comprising a lower part extending upwards from the ground to a height equal to *b* and an upper part consisting of the remainder. The resulting shape of the velocity pressure profile is shown in Figure 4.36.

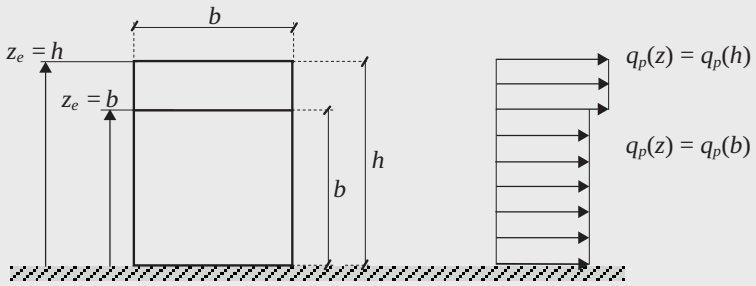


Figure 4.36 – Velocity pressure distribution on face D ($\theta = 0^o$)

For $\theta = 90^o$ (see Figure 4.39), h = 33 m < b = 45 m, and the shape of the velocity pressure profile is shown in Figure 4.37 and should be considered to be one part.

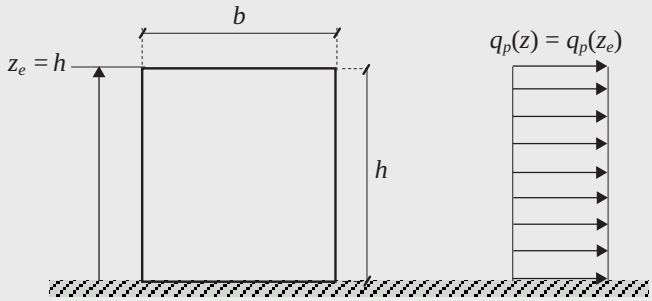


Figure 4.37 – Velocity pressure distribution on face D ($\theta = 90^o$)

For the determination of the velocity pressure distribution for the leeward wall and sidewalls (faces A, B, C and E) the reference height may be taken as the height of the building.

iii) Calculation of external and internal pressure coefficients

External and internal pressure coefficients are determined according to clause 7.2 of EN 1991-1-4. Internal and external pressures shall be considered to act at the same time (clause 7.2.9). The worst combination of external and internal pressures shall be considered.

According to clause 7.2.2(2), the façades are divided in different pressure zones, defined as a function of e, where e is the lesser of b or $2h$. For wind direction $\alpha = 0^o$ (see Figure 4.38):

$$e = \min(21\,;66) = 21\text{ m} < d = 45\text{ m}$$

and for wind direction $\alpha = 90^o$ (see Figure 4.39):

$$e = \min(45\,;66) = 45\text{ m} > d = 21\text{ m}.$$

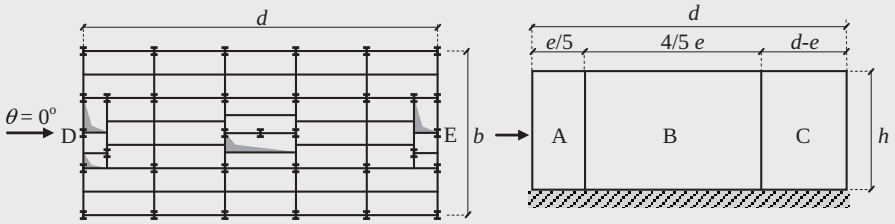


Figure 4.38 – Pressure zones for wind direction $\theta = 0^o$

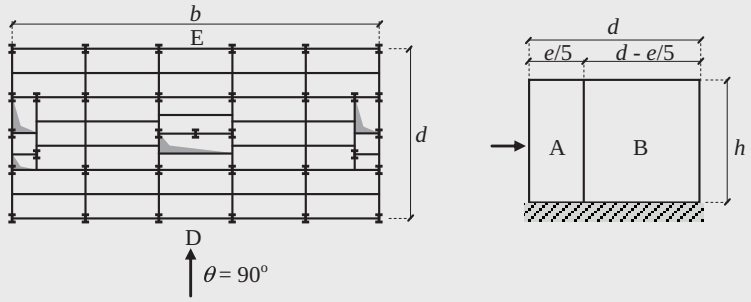


Figure 4.39 – Pressure zones for wind direction $\theta = 90^o$

The resulting external pressure coefficients, c_{pe}, for zones A, B, C, D and E are obtained from Table 7.1 of EN 1991-1-4 and are represented in Table 4.13.

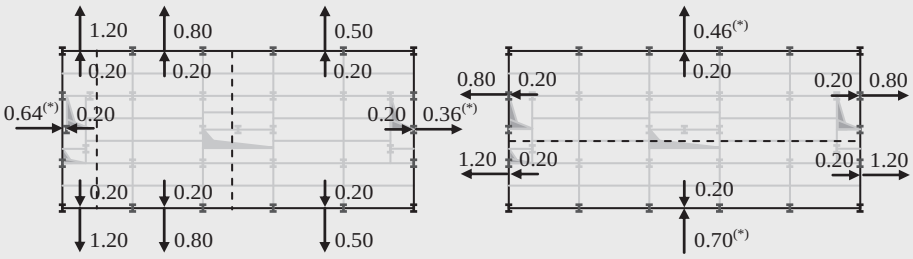
Table 4.13 – External pressure coefficients c_{pe}

	zone	A	B	C	D	E
$\theta = 0^o$	h/d = 0.73	-1.20	-0.80	-0.50	+0.76	-0.43
$\theta = 90^o$	h/d = 1.57	-1.20	-0.80	-	+0.80	-0.53

According to clause 7.2.2(3), the lack of correlation of wind pressures between the windward and leeward sides may be taken into account by multiplying the resulting force by a factor, *f*, that depends on the relation *h/d* for each case. Therefore, by linear interpolation between $f = 1.0$ for $h/d \geq 5$ and $f = 0.85$ for $h/d \leq 1$, the following factors are obtained: for $\theta = 0^o$, $f = 0.84$ and for $\theta = 90^o$, $f = 0.87$.

The internal pressure coefficients, c_{pi}, depend on the size and distribution of the openings in the building envelope. For buildings without a dominant face and where it is not possible to determine the number of openings, then c_{pi} should be taken as the more onerous of +0.2 and -0.3.

Considering the values for external pressure coefficients from Table 4.13, the external and internal pressure coefficients are represented in Figure 4.40a and b, respectively, for $\theta = 0^o$ and $\theta = 90^o$, according to the worst case for each face of the building.



a) $\theta = 0^o$ b) $\theta = 90^o$

Figure 4.40 – External and internal coefficients

(*) the values for faces D and E are obtained by multiplying the external coefficient by $f = 0.84$ for $\theta = 0^o$ and $f = 0.87$ for $\theta = 90^o$.

iv) Calculation of the peak velocity pressure $q_p(z)$

The peak velocity pressure $q_p(z)$, at height *z*, is given by the following equation (clause 4.5):

$$q_p(z) = \left[1 + 7I_v(z)\right]\frac{1}{2}\rho\, v_m^2(z) = c_e(z)q_b, \qquad (4.31)$$

where $I_v(z)$ is the turbulence intensity, ρ is the air density, $v_m(z)$ is the mean wind velocity, $c_e(z)$ is the exposure factor and q_b is the basic velocity

pressure. Both options in equation (4.31) may be used to calculate the peak velocity pressure. In this design example only the first will be applied, because EN 1991-1-4 only provides one graph for a limited range of cases for the direct determination of the exposure factor.

The air density ρ depends on the altitude, temperature and barometric pressure to be expected in the region during wind storms. EN 1991-1-4 recommends the value 1.25 kg/m^3.

v) Calculation of mean wind velocity (v_m)

The mean wind velocity is given by (clause 4.3.1),

$$v_m(z) = c_r(z)c_o(z)v_b, \tag{4.32}$$

where $c_r(z)$ is the roughness factor and $c_o(z)$ is the orography factor, taken as 1.0 unless otherwise specified in clause 4.3.3, and v_b is the basic wind velocity. The roughness factor is specified in clause 4.3.2 and is given by:

$$\begin{cases} c_r(z) = k_r \ln\left(\dfrac{z}{z_0}\right) \Leftarrow z_{\min} \le z \le z_{\max} \\ c_r(z) = c_r(z_{\min}) \Leftarrow z \le z_{\min} \end{cases}, \tag{4.33}$$

$z_{\max}$ may be taken as 200, $z_{\min}$ is the minimum height, z_0 is the roughness length, both defined in Table 4.1 of EN 1991-1-4 as a function of the terrain category, and k_r is the terrain factor, depending on the roughness length z_o and given by:

$$k_r = 0.19\left(\frac{z_0}{z_{0,II}}\right), \tag{4.34}$$

where $z_{0,II}$ = 0.05 m. The basic wind velocity v_b is calculated from (clause 4.2):

$$v_b = c_{dir}c_{season}v_{b,0}, \tag{4.35}$$

where c_{dir} and c_{season} are directional and seasonal factors, respectively, which may be given by the National Annexes. The recommended value, for each case, is 1.0. The fundamental value of the basic wind velocity, $v_{b,0}$, is also

given in the National Annexes as a function of the regional wind maps. Assuming $v_{b,0}$ = 30 m/s, then $v_b = v_{b,0}$ = 30 m/s.

Assuming a terrain of category II (i.e., area with low vegetation and isolated obstacles), from Table 4.1 of EN1991-1-4, $z_o = z_{0,II}$ = 0.05 and z_{min} = 2 m, thus k_r = 0.19. From equations (4.33), with $z_{min} < z = 33 < z_{max}$,

$$c_r\left(z=33\right)=0.19\times\ln\left(\frac{33}{0.05}\right)=1.23$$

and from equation (4.32),

$$v_m\left(z=33\right)=1.23\times1.00\times30=36.9\,\text{m/s}.$$

For $z_{min} < z = 21 < z_{max}$,

$$c_r\left(z=21\right)=0.19\times\ln\left(\frac{21}{0.05}\right)=1.15$$

and from equation (4.32),

$$v_m\left(z=21\right)=1.15\times1.00\times30=34.5\,\text{m/s}.$$

vi) Calculation of turbulence intensity (I_v)

The turbulence intensity is given by (clause 4.4(1)):

$$\begin{cases} I_v=\dfrac{k_I}{c_0\left(z\right)\ln\left(\dfrac{z}{z_0}\right)} \Leftarrow z_{min}\le z\le z_{max} \\ I_v=I_v\left(z_{min}\right)\Leftarrow z<z_{min} \end{cases}, \qquad (4.36)$$

where k_I is the turbulence factor.

The recommended value for k_I is 1.0, thus for $z_{min} < z = 33 < z_{max}$,

$$I_v=\frac{1.0}{1.0\times\ln\left(\dfrac{33}{0.05}\right)}=0.15$$

and for $z_{min} < z = 21 < z_{max}$,

$$I_v = \frac{1.0}{1.0 \times \ln\left(\frac{21}{0.05}\right)} = 0.17 .$$

Finally, from equation (4.31), for z = 33 m and z = 21 m:

$$q_p(z=33) = \left[1+7\times 0.15\right] \times \frac{1}{2} \times 1.25 \times 36.9^2 = 1744.56 \text{ N/m}^2 = 1.74 \text{ kN/m}^2 ;$$

$$q_p(z=21) = \left[1+7\times 0.17\right] \times \frac{1}{2} \times 1.25 \times 34.5^2 = 1629.16 \text{ N/m}^2 = 1.63 \text{ kN/m}^2 .$$

vii) Calculation of external and internal pressures

The external and internal pressures are obtained from equations (4.29) and (4.30) and are indicated in Table 4.14. Note that external pressures are already multiplied by the structural factor, $c_s c_d$, from equation (4.27). In Figures 4.41 and 4.42 the resulting values are represented for $\theta = 0^o$ and $\theta = 90^o$.

Table 4.14 – External and internal pressures

$c_s c_d$		A	B	C	D		E
					$z < 21$	$z > 21$	
$\theta = 0^o$	$c_s c_d \cdot w_e$	- 1.98	- 1.32	- 0.83	+ 0.99	+ 1.06	- 0.60
	w_i	+ 0.35	+ 0.35	+ 0.35	+ 0.33	+ 0.35	+ 0.35
$\theta = 90^o$	$c_s c_d \cdot w_e$	- 1.85	- 1.24	-	+ 1.08		- 0.71
	w_i	+ 0.35	+ 0.35	-	+ 0.35		+ 0.35

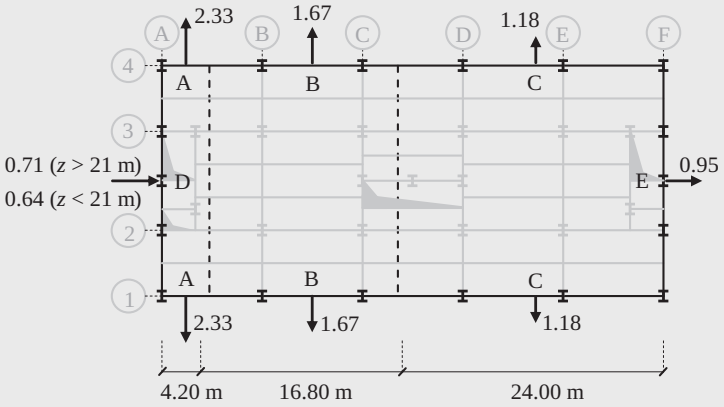


Figure 4.41 – Wind pressures (kN/m^2) on walls, $\theta = 0^o$

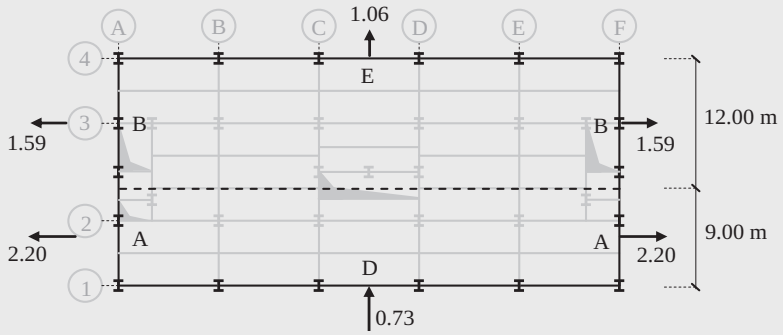


Figure 4.42 – Wind pressures (kN/m^2) on walls, $\theta = 90^o$

4.4.3.5. Summary of basic actions

The resulting actions for this design example are summarized in Table 4.15.

Table 4.15 – Summary of actions

Action no.	Description	Type	Value
LC1	Self-weight of structural elements	Permanent action	varies
LC2	Imposed load on office buildings (Cat. B)	Variable action	q_k^1 = 3.0 kN/m^2
LC3	Movable partitions	Variable action	q_k^2 = 0.5 kN/m^2
LC4	Wind direction $\theta = 0^o$	Variable action	varies (see Figure 4.40)
LC5	Wind direction $\theta = 90^o$	Variable action	varies (see Figure 4.41)

4.4.3.6. Frame imperfections

Frame imperfections are considered as equivalent horizontal loads, according to clause 5.3.2 of EN 1993-1-1. Thus, global initial sway imperfections are given by (equation (2.18)):

$$\phi = \phi_0 \, \alpha_h \, \alpha_m ,$$

where: $\phi_0 = 1/200$;

α_h is the reduction factor for height *h*, given by $\alpha_h = 2/\sqrt{h}$ but $2/3 \le \alpha_h \le 1.0$;

h is the height of the structure (m);

α_m is the reduction factor for the number of columns in a row, given by:

$$\alpha_m = \sqrt{0.5\left(1+\frac{1}{m}\right)};$$

and m is the number of columns in a row.

Hence, for this structure, h = 33 m and α_h = 0.67. The number of columns changes according to the frame considered. In Table 4.16, the initial imperfection (ϕ) for each frame is presented (see Figure 4.33).

Table 4.16 – Initial imperfections

Frame	m	ϕ
A	7	0.00253
B	4	0.00265
C	5.5	0.00258
D	5.5	0.00258
E	4	0.00265
F	7	0.00253
1	6	0.00256
2	8	0.00251
2b	5	0.00259
3	8	0.00251
4	6	0.00256

The equivalent horizontal load at each floor is given by (Figure 2.54):

$$H_{Ed} = V_{Ed}\,\phi\,, \tag{4.37}$$

where V_{Ed} is the total design vertical load in each floor. The design vertical load in each floor is given by LC1 and LC2 + LC3. The relevant values, in each direction, are listed in Tables 4.17 to 4.18. These values are added to the relevant combinations.

Table 4.17 – Equivalent horizontal forces in transversal frames

Frame		kN	1st floor	2nd floor	3rd - 7th floor	8th floor
A	L1	V_{Ed}	165.1	218.1	206.8	214.8
		H_{Ed}	0.42	0.55	0.52	0.54
	LC2+LC3	V_{Ed}	208.7	269.2	264.9	241.2
		H_{Ed}	0.53	0.68	0.67	0.61
B	L1	V_{Ed}	406.9	387.8	373.4	390.6
		H_{Ed}	1.08	1.03	0.99	1.04
	LC2+LC3	V_{Ed}	682.6	648.4	636.3	511.5
		H_{Ed}	1.81	1.72	1.69	1.36
C	L1	V_{Ed}	254.4	412.3	373.2	401.4
		H_{Ed}	0.66	1.06	0.96	1.04
	LC2+LC3	V_{Ed}	355.4	582.5	540.9	477.4
		H_{Ed}	0.92	1.50	1.40	1.23
D	L1	V_{Ed}	254.4	412.3	362.3	401.3
		H_{Ed}	0.66	1.06	0.93	1.05
	LC2+LC3	V_{Ed}	355.2	582.2	563.6	476.9
		H_{Ed}	0.92	1.50	1.45	1.23
E	L1	V_{Ed}	406.6	388.1	374.0	391.6
		H_{Ed}	1.08	1.03	0.99	1.04
	LC2+LC3	V_{Ed}	682.9	649.8	638.4	514.5
		H_{Ed}	1.81	1.72	1.69	1.36
F	L1	V_{Ed}	179.5	228.9	217.0	224.6
		H_{Ed}	0.45	0.58	0.55	0.57
	LC2+LC3	V_{Ed}	238.2	299.7	294.1	265.1
		H_{Ed}	0.60	0.76	0.74	0.67

According to clause 5.3.2(8), the initial sway imperfections should be applied in all relevant horizontal directions, but they need only be considered in one direction at a time.

Table 4.18 – Equivalent horizontal forces in longitudinal frames

Frame		kN	1st floor	2nd floor	3rd - 7th floor	8th floor
1	L1	V_{Ed}	265.1	560.6	301.7	314.6
		H_{Ed}	0.68	1.44	0.77	0.81
	LC2+LC3	V_{Ed}	383.2	832.1	474.9	400.9
		H_{Ed}	0.98	2.13	1.22	1.03
2	L1	V_{Ed}	554.4	506.4	553.9	629.9
		H_{Ed}	1.39	1.27	1.39	1.58
	LC2+LC3	V_{Ed}	833.7	757.1	914.2	810.5
		H_{Ed}	2.09	1.90	2.29	2.03
2b	L1	V_{Ed}	98.1	121.0	227.3	200.6
		H_{Ed}	0.25	0.31	0.59	0.52
	LC2+LC3	V_{Ed}	117.7	120.8	295.9	212.8
		H_{Ed}	0.30	0.31	0.77	0.55
3	L1	V_{Ed}	454.7	558.2	514.1	567.3
		H_{Ed}	1.14	1.40	1.29	1.42
	LC2+LC3	V_{Ed}	726.0	852.3	806.2	667.5
		H_{Ed}	1.82	2.14	2.02	1.68
4	L1	V_{Ed}	294.6	301.5	298.6	311.8
		H_{Ed}	0.75	0.77	0.76	0.80
	LC2+LC3	V_{Ed}	462.2	469.7	470.0	394.8
		H_{Ed}	1.18	1.20	1.20	1.01

4.4.3.7. Load combinations

The rules and methods for the definition of the load combination are given in Annex A1 of EN 1990.

The recommended values of the reduction factors ψ for the actions considered are indicated in Table 4.19 according to clause A1.2.2.

Table 4.19 – Reduction factors ψ

Type of action	ψ_0	ψ_1	ψ_2
Imposed load in buildings: category B	0.7	0.5	0.3
Wind loads on buildings	0.6	0.2	0.0

Thus, the following load combinations are considered for the Ultimate Limit State (ULS) of resistance:

i) Combination 1

$E_d1 = 1.35 \times LC1 + 1.5\ [(LC2 + LC3) + 0.6 \times LC4]$.

ii) Combination 2

$E_d2 = 1.35 \times LC1 + 1.5\ [(LC2 + LC3) + 0.6 \times LC5]$.

iii) Combination 3

$E_d3 = 1.00 \times LC1 + 1.5 \times LC4$.

iv) Combination 4

$E_d4 = 1.00 \times LC1 + 1.5 \times LC5$.

v) Combination 5

$E_d5 = 1.35 \times LC1 + 1.5\ [LC4 + 0.7 \times (LC2 + LC3)]$.

vi) Combination 6

$E_d6 = 1.35 \times LC1 + 1.5\ [LC5 + 0.7 \times (LC2 + LC3)]$.

Other combinations for ULS may have been considered, however, they were not critical for the structure.

Regarding the serviceability limit states, limits for vertical deflections and sway are considered under the frequent values of the load combinations, considering a reversible limit state (Annex A1 of EN 1990):

i) Combination 7

$E_d7 = 1.00 \times LC1 + 0.5 \times (LC2 + LC3)$.

ii) Combination 8

$E_d8 = 1.00 \times LC1 + 0.2 \times LC4$.

iii) Combination 9

$E_d9 = 1.00 \times LC1 + 0.2 \times LC5$.

iv) Combination 10

$E_d10 = 1.00 \times LC1 + 0.2 \times LC4 + 0.3 \times (LC2 + LC3)$.

v) Combination 11

$E_d11 = 1.00 \times LC1 + 0.2 \times LC5 + 0.3 \times (LC2 + LC3)$.

Additional load combinations should be considered for accidental design situations such as fire. Although the fire resistance of this building is not treated in this volume of the ECCS Eurocode Design Manuals, load combinations 12 to 14 would be required for the fire design of the structure, using the frequent value for the dominant variable action:

i) Combination 12

E_d12 = LC1 + 0.5 × (LC2 + LC3).

ii) Combination 13

E_d13 = LC1 + 0.2 × LC4 + 0.3 × (LC2 + LC3).

iii) Combination 14

E_d14 = LC1 + 0.2 × LC5 + 0.3 × (LC2 + LC3).

A forthcoming volume of this collection (Franssen and Vila Real, 2015) deals specifically with the fire design of buildings.

4.4.3.8. Load arrangement

According to clause 6.2.1(1) of EN 1991-1-1, for the design of a floor structure within one storey or a roof, the imposed load shall be taken into account as a free action applied at the most unfavourable part of the influence area of the action effects considered. Figure 4.43 represents the most unfavourable load arrangement for the imposed loads.

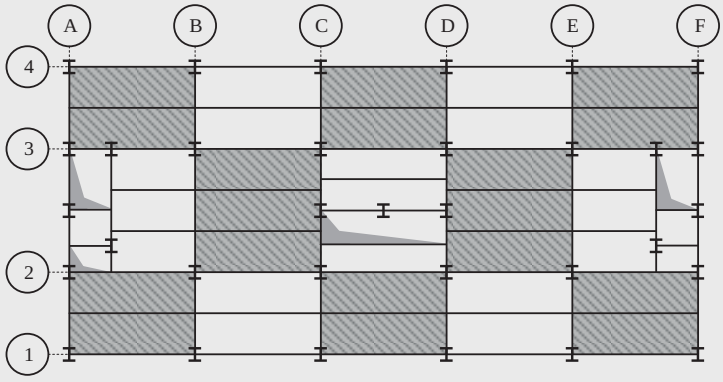


Figure 4.43 – Load arrangement for the analysis of the shadow areas

The distribution of the load to the secondary beams is represented in Figure 4.44.

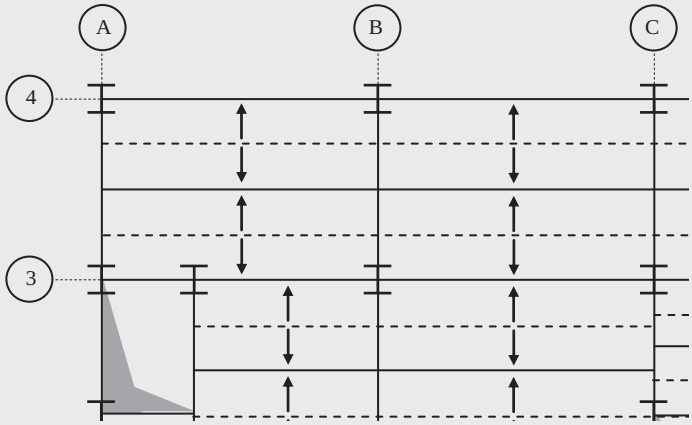


Figure 4.44 – Load distribution in the secondary beams

For the design of the columns or the walls, loaded by several storeys, the total imposed loads on the floor of each storey should be assumed to be distributed uniformly over the whole floor area, but the total value may be reduced by a factor α_n according to the following equation (clause 6.3.1.2(11) of EN 1991-1-1)

$$\alpha_n = \frac{2+(n-2)\times\psi_0}{n} = \frac{2+(8-2)\times 0.70}{8} = 0.775, \qquad (4.38)$$

where n is the number of storeys (>2) and ψ_0 is given according to Annex A1 (Table A1.1) of EN 1990.

4.4.4. Structural analysis

4.4.4.1. Structural model

The structural model for the analysis is a 3D model, represented in Figure 4.45. All steel elements (columns, bracing elements and beams) are defined by beam elements. The main direction of the structure is in plane *zy*. Beams in plane *zy* are rigidly connected to the steel columns. Beams in plane *zx* are hinged at both ends. Elements defining the bracing system are also hinged at both ends.

Although the steelwork is the main supporting structure, the concrete slab has a strong influence on the global stiffness of the structure, as will be discussed over the next paragraphs.

There are several ways of modeling the concrete slab, as it was shown in example 2.3. If the software allows the use of shell elements together with beam elements, then the slab can be modeled by those elements. However, proper attention needs to be given to the real behaviour of the composite structure; whether or not composite action arises through connection of the slab to the steel beams. If there is no composite action then the slab can be modeled by a horizontal bracing system, using beam elements connecting the main columns. The cross section of these elements needs to be equivalent to the stiffness provided by the real concrete slab. This simplified procedure was adopted in the example.

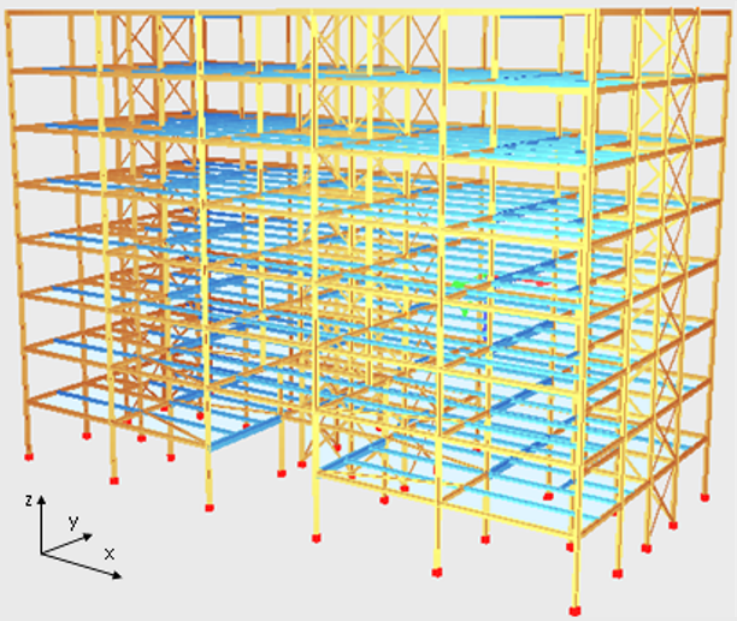


Figure 4.45 – 3D structural model

4.4.4.2. Linear elastic analysis

The linear elastic analysis was performed with a commercial structural analysis program, Sofistik® (2008), and the internal forces and moments were determined.

4.4.4.3. Susceptibility to 2nd order effects: elastic critical loads

For design purposes, the internal forces and moments should be determined using a 2nd order analysis if relevant. Thus, the classification of the structure must be checked first. This is done by computing the elastic critical load factor (α_{cr}), as discussed in chapter 2. Second-order effects must be considered whenever $\alpha_{cr} \leq 10$.

Numerical calculation of α_{cr}

In Table 4.20, the values of the first 5 elastic critical loads factors α_{cr} are indicated for each combination.

Table 4.20 – Elastic critical load factors

	α_{cr} 1	α_{cr} 2	α_{cr} 3	α_{cr} 4	α_{cr} 5
Combination 1	7.96	8.22	8.28	8.40	8.67
Combination 2	8.01	8.08	8.48	8.57	8.66
Combination 3	21.11	25.15	28.28	28.62	29.38
Combination 4	13.14	14.21	18.56	18.84	19.98
Combination 5	9.87	10.16	10.23	10.39	10.62
Combination 6	8.58	9.37	10.07	10.14	10.17

For combinations 1, 2, 5 and 6 the values of α_{cr} are smaller than 10. According to clause 5.2.1, the frame requires a second-order analysis for load combinations 1, 2, 5 and 6. As a result, the 2nd order sway effects must be taken into consideration in the design and analysis. Moreover, combinations 1, 2 and 6 exhibit more than one buckling mode with a critical load factor lower than 10.

Figure 4.46 represents the 1st buckling mode for combination 1. The first buckling mode is clearly a local bucking mode. The same happens to the other critical load factors indicated in Table 4.20, although not represented graphically. This indicates that the structure is not very susceptible to 2nd order effects. Nevertheless, a 2nd order elastic analysis is performed to prove this statement.

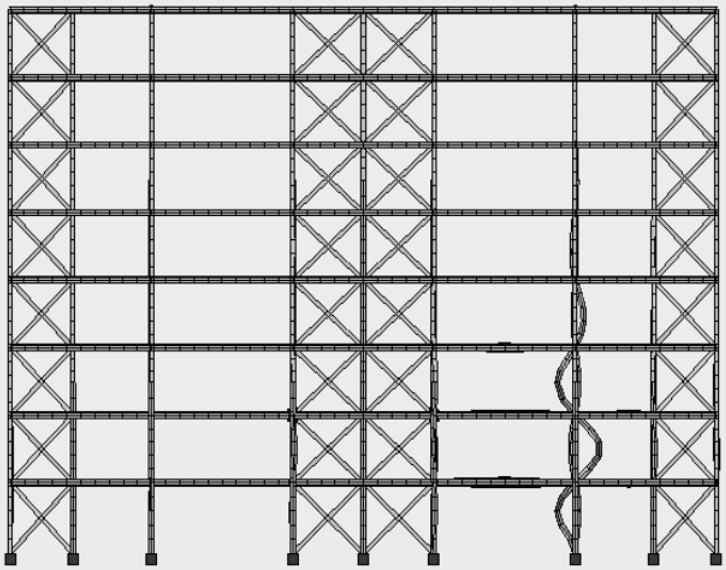


Figure 4.46 – 1st buckling mode for combination 1 – frontal view

4.4.4.4. 2nd order elastic analysis

Second order effects are calculated by a numerical analysis. In Table 4.21, the results obtained for load combination 1, using a 1st order and a 2nd order numerical analysis, are compared for column E1. For the bending moments, the moments at both ends of the elements are indicated.

Table 4.21 – Comparative results for column E1 (combination 1)

	1st Order		2nd Order			
	M_{Ed} (kNm)	N_{Ed} (kN)	M_{Ed} (kNm)	Δ (%)	N_{Ed} (kN)	Δ (%)
1st floor	25/14	1699	25/11	0/-21.4	1704	+ 0.3
2nd floor	62/47	1492	74/55	19.4/17.0	1496	+ 0.3
3rd floor	69/28	1261	69/29	0/3.6	1262	+ 0.1
4th floor	51/25	1052	54/28	5.9/12.0	1053	+ 0.1
5th floor	53/27	841	56/29	5.7/7.4	841	0
6th floor	54/29	630	57/32	5.6/10.3	630	0
7th floor	55/26	417	59/30	7.3/15.4	417	0
8th floor	69/63	201	72/66	4.3/4.8	201	0

The same comparison in made for beam E1 to E4 in 4th floor, and the results are indicated in Table 4.22.

Table 4.22 – Comparative results for beam E1 to E4 (combination 1)

	1st Order		2nd Order			
	M_{Ed} (kNm)	N_{Ed} (kN)	M_{Ed} (kNm)	Δ (%)	N_{Ed} (kN)	Δ (%)
E1-E2	+114/-106	61	+114/-111	0/4.7	39	-36.1
E2-E3	+168/-269	155	+163/-256	-3.0/-4.8	139	-10.3
E3-E4	+113/-105	61	+114/-110	0.9/4.8	50	-18.0

Tables 4.21 and 4.22 show that 2nd order effects are indeed negligible.

4.4.5 Design checks

4.4.5.1. General considerations

The design checks on all members and joints, under all load combinations, are the last step in a structural design procedure. In this design example, the following checks are made, for the ultimate limit state:

i) cross section resistance;
ii) stability of beams;
iii) stability of columns.

Although an essential design check, the joints are not checked in this example because the design of joints is outside the scope of this manual. A companion volume (Jaspart, 2010) deals in detail with the design of joints. In this case, although all the structure was verified, the design checks are illustrated for two members only: column E1 (see Figure 4.47 and Table 4.23) and beam E1-E4 on the 4th floor (see Figure 4.48 and Table 4.24) for load combination 1.

Column E1 has a total height of 33.28 m, comprising all the floors of the building, and it is composed of a HEB 320 from the ground floor to the 4th floor and a HEB 260 from the 4th floor to the 8th floor.

The selected beam has two side spans with a length of 6.00 m and an IPE 400 cross section, and a central span with a length of 9.00 m and an IPE 600 cross section.

Taking the 2nd order results from Tables 4.21 and 4.22, the design internal forces (N_{Ed}, $V_{z,Ed}$ and $M_{y,Ed}$) for the selected members are represented in Figures 4.47 and 4.48.

The following paragraphs present the checks according to EC3-1-1 for the selected members. For the sake of simplification, the detailed calculations are omitted. However, the detailed procedures have been presented in chapter 3.

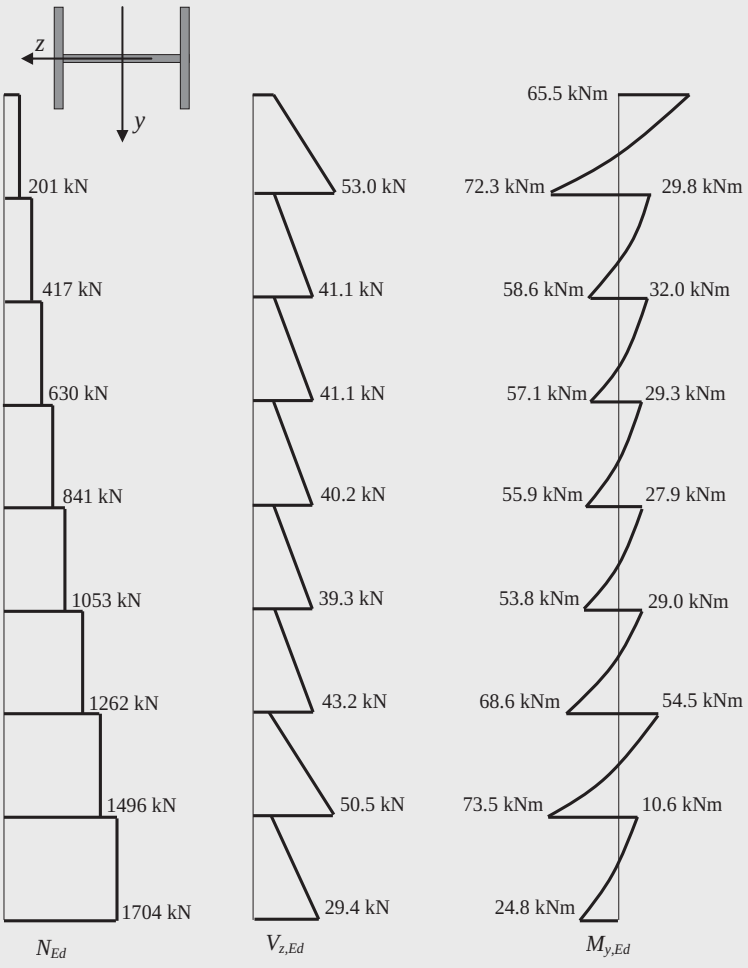


Figure 4.47 – Internal forces on column E1 for load combination 1 (local axes)

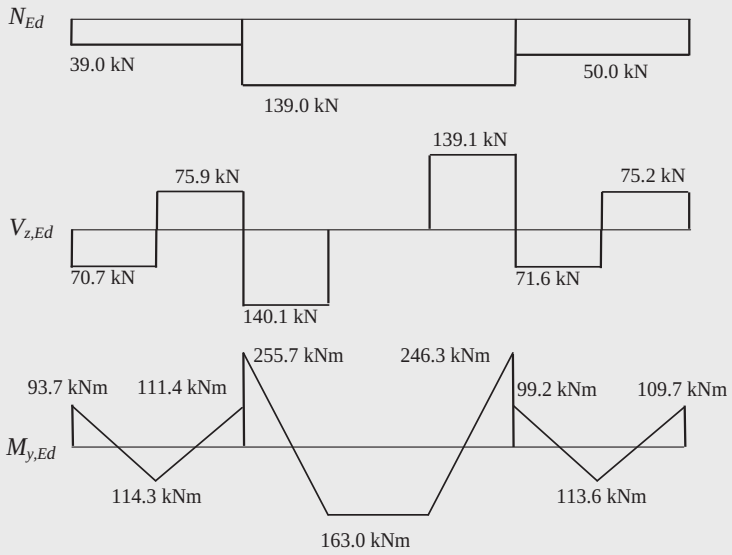


Figure 4.48 – Internal forces on beam E1-E4 in the 4th floor for load combination 1

4.4.5.2. Cross section resistance

The utilization levels for the applied forces are summarized in Table 4.23 for the critical sections (class 1) along column E1. The values of $V_{z,Ed}$ are such that the interaction N_{Ed}+$M_{y,Ed}$+$V_{z,Ed}$ can be neglected.

Table 4.23 – Utilization levels for column E1

	1st floor	2nd floor	3rd floor	4th floor	5th floor	6th floor	7th floor	8th floor
	HEB 320	HEB 320	HEB 320	HEB 320	HEB 260	HEB 260	HEB 260	HEB 260
N_{Ed}	0.30	0.26	0.22	0.18	0.20	0.15	0.10	0.05
$M_{y,Ed}$	0.03	0.10	0.09	0.07	0.12	0.13	0.13	0.16
$V_{z,Ed}$	0.03	0.05	0.04	0.04	0.05	0.05	0.05	0.07
N_{Ed}+$M_{y,Ed}$	0.04	0.11	0.10	0.08	0.14	0.13	0.13	0.15

Table 4.24 indicates the utilization levels for the cross section of beam E1-E4 (class 1) on the 4th floor. Again, the values of $V_{z,Ed}$ are such that the interaction N_{Ed}+$M_{y,Ed}$+$V_{z,Ed}$ can be neglected.

Table 4.24 – Utilization levels for beam E1-E4

	1st span (L = 6.00 m)	2nd span (L = 9.00 m)	3rd span (L = 6.00 m)
	IPE 400	IPE 600	IPE 400
N_{Ed}	0.01	0.03	0.02
$M_{y,Ed}$	0.25	0.21	0.24
$V_{z,Ed}$	0.09	0.08	0.09
$N_{Ed}+M_{y,Ed}$	0.25	0.21	0.24

4.4.5.3. Buckling resistance of beams

For the lateral torsional buckling check, beam E1-E4 is assumed to be lateral restrained by secondary beams, every 3.00 m. Table 4.25 gives the LTB resistance ratios for beam E1-E4.

Table 4.25 – Beam E1-E4 LTB ratios

	1st span (L = 6.00 m)	2nd span (L = 9.00 m)	3rd span (L = 6.00 m)
	IPE 400	IPE 600	IPE 400
LTB ratio	0.32	0.26	0.33

4.4.5.4. Buckling resistance of columns and beam-columns

For the buckling check, it is assumed that column E1 is restrained at each floor level. According to the analysis procedures carried out in this example, a buckling length equal to the distance between floors (system length) were adopted, although lower values would be permitted. In Table 4.26, the buckling resistance ratios for column E1 are presented. The column was assumed to be “susceptible to torsional deformations”.

Table 4.26 – Column E1 buckling ratios

	1st floor	2nd floor	3rd floor	4th floor	5th floor	6th floor	7th floor	8th floor
	HEB 320	HEB 320	HEB 320	HEB 320	HEB 260	HEB 260	HEB 260	HEB 260
Buckling ratio	0.46	0.42	0.39	0.32	0.42	0.35	0.28	0.23

Chapter 5

PLASTIC DESIGN OF STEEL STRUCTURES

5.1. GENERAL PRINCIPLES OF PLASTIC DESIGN

5.1.1. Introduction

The mechanical properties of steel to EN 10025-1 (CEN, 2004b) and EN 10210-1 (CEN, 2006a) make it particularly suitable for the use of plastic design: a long yield plateau, guaranteed ultimate strains of 15 % ($\varepsilon_u \geq 15\varepsilon_y$), a minimum over-strength of f_u / $f_y \geq 1.10$ (clause 3.2.2) and a behaviour that reasonably approximates to an elastic-plastic constitutive law. It is therefore usually possible to assess the cross section resistance assuming total yielding. For many a structure it is also possible to evaluate the global resistance by taking advantage of its redundancy and the progressive formation of plastic hinges until a mechanism is reached. This possibility results in more economical structures.

Plastic design of steel structures may assume different degrees of complexity and sophistication (Hill, 1950; Neal, 1977; Horne and Morris, 1981). In this chapter, only methods of analysis and structural models based on beam theory are presented. In addition, the plastic design methods are framed in the context of the general principles of EC3-1-1. Consequently, although the use of advanced analysis methods is possible, a two-step procedure is assumed: structural analysis followed by code checks concerning the cross section resistance and member stability.

Plastic analysis of structures can be carried out with different levels of sophistication. In practical terms, the chosen approach depends on purpose:

for preliminary design or a quick check on a project, manual methods are preferable, using a calculator and/or a excel worksheet; whereas for thorough verification, computational methods and structural analysis programs are used. In the first case, methods of plastic limit analysis are invariably used, as they allow non-computational approaches, while in the second case the analysis is usually non linear elastic-plastic. However, a good knowledge of the basic principles of plastic analysis is relevant in both cases, and so these principles are briefly presented in the following paragraphs.

As bending predominates, plastic collapse corresponds to the formation of a mechanism due to the progressive appearance of plastic hinges. In a hyperstatic structure, failure occurs (unless some partial mechanism is formed) after the formation of $r+1$ plastic hinges, where r is the degree of redundancy of the structure. In addition, classical theory assumes that at collapse, the following conditions are satisfied: i) an equilibrium condition and ii) a yield condition. Equilibrium requires that a statically admissible distribution of bending moments is achieved. The yield condition requires that at all sections the bending moment does not exceed the plastic moment of resistance.

The methods of plastic analysis can be based on: i) the static theorem or maximum principle, leading to a lower bound (safe) estimate of the plastic collapse load because the formation of a mechanism is not enforced; or ii) the kinematic theorem or minimum principle, leading to an upper bound (unsafe) estimate of the plastic collapse load of the structure, because a statically admissible moment distribution is not enforced. The interested reader may find further information on this matter in Heyman (1971), Neal (1977) or Horne (1979).

5.1.2. Plastic limit analysis: method of mechanisms

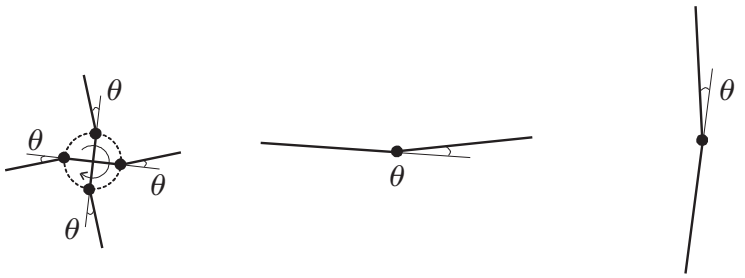
The method of mechanisms is an upper bound method that allows an expeditious determination of the plastic collapse load for a given mechanism. The method uses the principle of virtual work to establish the equation of equilibrium between the total external work produced by external forces and the internal work at the sections where plastic hinges are formed. The virtual work equation is generically shown in equation (5.1):

$$\alpha_p \sum F_i \delta_i = \sum M_p \theta \,. \tag{5.1}$$

where F_i represents the external loading, δ_i is the corresponding displacement at the point of load application i, M_p is the plastic moment, θ is the corresponding plastic rotation and α_p is the load multiplier that corresponds to failure of the structure.

Being an upper bound method, this approach requires the consideration of all possible mechanisms to ensure that the correct plastic collapse load is obtained. Since the search for all possible mechanisms in a larger structure can prove itself difficult, a way of minimizing this difficulty consists in the systematic search of all possible mechanisms through the combination of elementary mechanisms (Horne and Morris, 1981).

Elementary mechanisms can be defined as those that result in a single displacement, either a beam mechanism or a "sway" mechanism. In a systematic way, three types of elementary mechanisms are identified: node mechanisms, beam mechanisms and frame mechanisms. A node mechanism, illustrated in Figure 5.1a, consists on the rotation of the node with hinges at the ends of the elements that converge in that node. A beam mechanism is the one that involves at least one hinge along the length of the bar without any axial displacement of its nodes, as illustrated in Figure 5.1b. Finally, a frame mechanism is that which implies the sway displacement of some of the nodes of the frame (Figure 5.1c).



a) Node b) Bar c) Frame

Figure 5.1 – Elementary mechanisms

In a general way, if r is the degree of redundancy of the structure and p is the total number of potential locations of plastic hinges, the number of elementary mechanisms, m, is given by:

$$m = p - r \,. \tag{5.2}$$

Several alternative sets of linearly independent elementary mechanisms are possible. However, whenever three or more members

converge into one node, it is necessary to include node mechanisms in the set of elementary mechanisms. The total number of global potential mechanisms is given by:

$$C_{r+1}^{p} = \frac{p!}{(r+1)!(p-r-1)!}. \tag{5.3}$$

Pitched-roof portal frames represent a common type of structure that is usually designed using plastic analysis. To illustrate the method, consider the example in Figure 5.2, reproduced from Davies and Brown (1996).

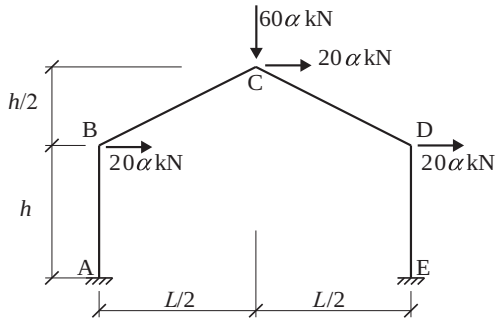


Figure 5.2 – Pitched-roof portal frame

370

Since the degree of redundancy of the structure is r = 3 and the total number of potential plastic hinge locations is p = 5, the number of elementary mechanisms is m = 2 (given by equation (5.2)). Hence the total number of global potential mechanisms is $C_{r+1}^{p} = 5$ (given by equation (5.3)).

A valid potential mechanism is represented in Figure 5.3 with plastic hinges at points B, C, D and E.

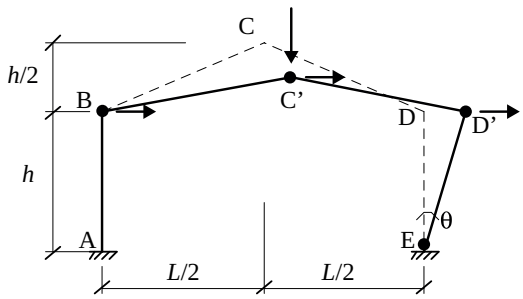


Figure 5.3 – Mechanism 1

Considering M_p = 300 kNm leads to the following virtual work equation:

$$20\alpha\frac{h}{2}\theta + 60\alpha\frac{L}{2}\theta + 20\alpha\, h\,\theta = 300\left(\theta + 2\theta + 2\theta + \theta\right),$$

and $\alpha^{(1)} = \dfrac{60}{h+L}$.

The second potential mechanism, illustrated in Figure 5.4, consists of plastic hinges at points A, C, D and E.

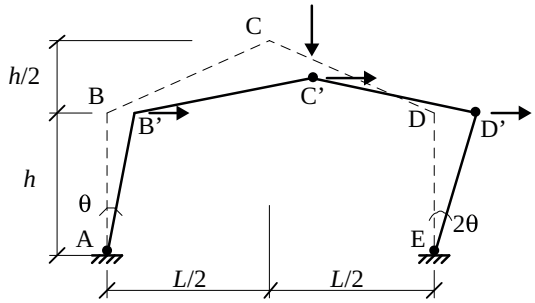


Figure 5.4 – Mechanism 2

The virtual work equation is:

$$20\alpha\, h\,\theta + 20\alpha\frac{L}{2}\theta + 60\alpha\frac{L}{2}\theta + 20\alpha\left(\frac{L+h}{2}\right)\theta = 300\left(\theta + 2\theta + 3\theta + 2\theta\right),$$

and $\alpha^{(2)} = \dfrac{240}{3h+5L}$.

Finally, the third potential mechanism presents plastic hinges at points A, B, D and E (Figure 5.5). The virtual work equation is:

$$20\alpha h\,\theta = 300\left(\theta + \theta + \theta + \theta\right),$$

and $\alpha^{(3)} = \dfrac{20}{h}$.

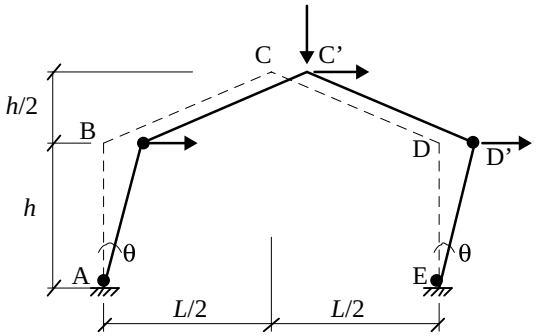


Figure 5.5 – Mechanism 3

Note that, by symmetry, there would be two mechanisms identical to (1) and (2), in which the plastic hinge would be formed at point A (or B), instead of E (or D), respectively. Assuming h = 6 m and L = 18 m, the critical mechanism is mechanism (2), as it leads to the lowest load factor, $\alpha^{(2)} = 2.22$, which corresponds to the bending moment diagram of Figure 5.6.

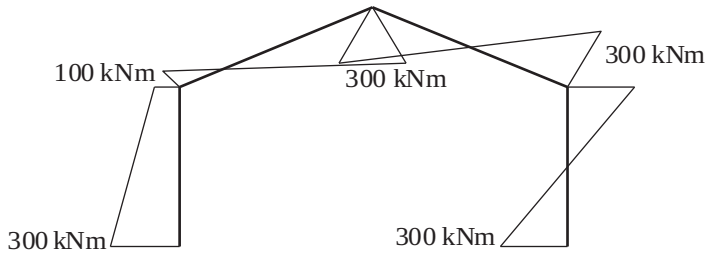


Figure 5.6 – Bending moment diagram at collapse

5.1.3. Code requirements for plastic analysis

The use of plastic global analysis must comply with several requirements. In contrast to elastic global analysis, plastic global analysis can only be used (clause 5.4.1(3)) where the structure exhibits sufficient rotation capacity at the plastic hinge locations. These may occur either in the members or in the connections and should allow the necessary re-distributions of bending moments (clause 5.4.3(2)). In addition, plastic global analysis can only be used where the stability of the members at plastic hinges is assured (clause 5.4.3(3)).

Where a plastic hinge occurs in a member, the cross section of the member should be doubly symmetrical or monosymmetrical but with the plane of symmetry coincident with the plane of rotation of the plastic hinge (clause 5.4.1(3)). Note that this restriction results from insufficient validation of solutions with asymmetric sections. In addition, at plastic hinge locations, the cross section of the member that contains the plastic hinge should have a rotation capacity that is not less than the corresponding required rotation at the plastic hinge location (clause 5.6(1)).

By adopting the concept of a discrete plastic hinge, cross sections must also fulfil the following additional requirements (clauses 5.6(2) to (5)) in order to ensure an adequate capacity for plastic re-distribution of forces:

i) for a prismatic member, it can be assumed that the rotation capacity at a plastic hinge is adequate if:
   - the member has a class 1 cross section at the plastic hinge location;
   - where a transverse force that exceeds 10 % of the shear resistance of the cross section is applied to the web at the plastic hinge location, web stiffeners must be provided within a distance along the member of $h/2$ from the plastic hinge location, where h is the depth of the cross section at this location.

ii) for non-prismatic members, the following additional criteria must be satisfied:
   - adjacent to plastic hinge locations, the thickness of the web should not be reduced for a distance each way along the member from the plastic hinge location of at least $2d$, where d is the clear depth of the web at the plastic hinge location;
   - adjacent to plastic hinge locations, the compression flange should be Class 1 for a distance each way along the member from the plastic hinge location of not less than the greater of:
     - $2d$, where d is the clear depth of the web at the plastic hinge location;
     - the distance to the adjacent point at which the moment in the member has fallen to 0.8 times the plastic moment resistance at the point concerned;

- elsewhere in the member the compression flange should be class 1 or class 2 and the web should be class 1, class 2 or class 3.

iii) for all members, any fastener holes in tension adjacent to plastic hinge locations should satisfy expression (5.4) or clause 6.2.5(4) for a distance each way along the member from the plastic hinge defined in the previous paragraph:

$$\frac{A_{f.net}\,0.9 f_u}{\gamma_{M2}} \geq \frac{A_f f_y}{\gamma_{M0}}. \tag{5.4}$$

In cases where methods of global plastic analysis are used that consider the real stress and strain behaviour along the member, including the combined effect of local, member and global stability, it is not necessary for cross sections to fulfil the above requirements from clauses 5.6(2) to (5) (clause 5.6(6)).

When the plastic hinge occurs in a joint, the joint should either have sufficient strength to ensure the hinge remains in the member (full strength joint) or should exhibit sufficient rotation capacity (clause 5.4.1(3)). In this latter case, part 1-8 of EC3 specifies the general principles for the determination of the rotation capacity of a joint between I and H sections (see EC3-1-8, clause 6.4). In addition, it establishes that the rotation capacity of a joint does not need to be verified whenever the moment resistance of the connection, M_{jRd}, is at least 1.2 times higher than the plastic moment resistance of the cross section of the connected member.

As was already mentioned in section 5.1.1, plastic global analysis can show several levels of sophistication in the incorporation of the effects of material non-linearity. In clause 5.4.3(1), the following methods are explicitly foreseen:

- elastic-plastic analysis with plastified sections and/or joints as plastic hinges;
- non-linear plastic analysis considering the partial plastification of members in plastic zones;
- rigid plastic analysis neglecting the elastic behaviour between hinges.

In all cases, for the steel grades specified in section 3 of EC3-1-1 it is possible to use the bilinear stress-strain relationship of Figure 5.7 (clause 5.4.3(4)). Alternatively, more precise stress-strain relationships can be adopted (EC3-1-5, clause C.6).

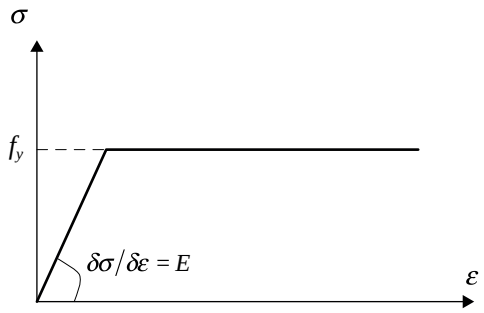


Figure 5.7 – Bilinear stress-strain relation

Plastic global analysis should also account for significant second order effects and the global stability of the structure (clause 5.4.3(6)), as already discussed in sub-chapter 2.3. This aspect will be further discussed in sub-chapter 5.2. Note that rigid-plastic analysis can only be applied in the cases where the second order effects do not have to be considered (clause 5.4.3(5)).

Finally, Table 5.1 summarizes the normative references to EC3 Part 1-1 specifically concerning global plastic analysis.

Table 5.1 – Normative references

Clauses	Description
5.4.1(3), 5.4.3(2), 5.4.3(3)	General requirements
5.2.1(3), 5.4.3(1), 5.4.3(5)-(6)	Types of analysis
5.4.3(4), 1-5-C.6	Properties of steel
5.4.1(3), 5.6(1), 5.6(4)-5.6(6), 6.2.5(4)	Cross section requirements for global plastic analysis
5.6(2)	Prismatic members
5.6(3)	Non-prismatic members

5.2. METHODS OF ANALYSIS

5.2.1. Introduction

Plastic analysis of structures is mostly used for low-rise buildings. This follows from the requirements described in paragraph 5.1.3 that necessitate geometrically and materially non-linear elastic-plastic analysis with imperfections (usually denoted GMNIA) whenever the structure shows significant susceptibility to second order effects. This is more likely as the number of storeys increases. Second-order analysis is essential whenever the effects of the deformed geometry significantly increase the forces or displacements or significantly modify the structural behaviour (clause 5.2.1(2)).

Plastic design of steel structures is often used in the design of pitched-roof portal frames. It was this type of structures that made plastic analysis of structures popular in the UK from 1950's onwards, with the publication of "The Steel Skeleton" (Baker *et al*, 1956). Throughout this chapter, without loss of generality, this type of structure is used to exemplify the relevant aspects of plastic design of steel structures, always with reference to EC3. Firstly, in this sub-chapter, procedures for the plastic analysis of pitched-roof portal frames are given, in which the global analysis is first order. The problem is thus simplified since it deals only with material non-linearity, either from a pre-design point of view using simple approximate methods, or in the context of an incremental elastic-plastic computational analysis. Secondly, procedures for the incorporation of second order effects (geometric non-linearity) are presented and discussed. Reference is made to simplified methods and to more thorough computational analysis, illustrated with simple examples.

5.2.2. Approximate methods for pre-design

Pitched-roof portal frames are characterized by a small degree of redundancy and a small number of members, therefore being particularly suitable for manual methods of analysis. Following Davies and Brown (1996), a pre-design method that can be easily programmed in an Excel worksheet is briefly presented in this section.

Consider the portal frame of Figure 5.8, in which, for ease of presentation, the loading is assumed in a simplified manner.

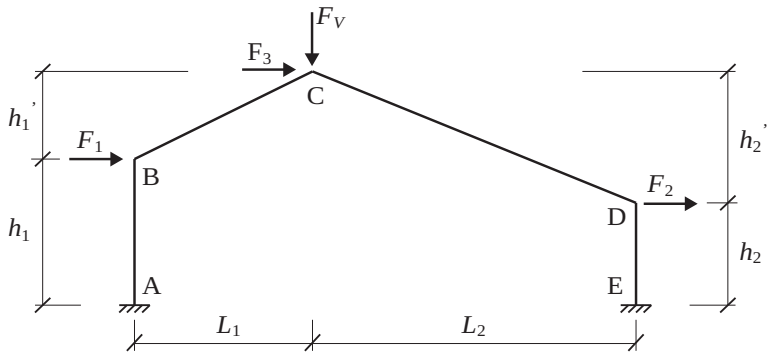
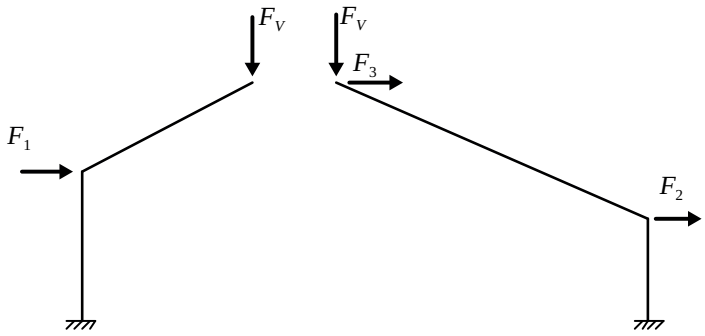
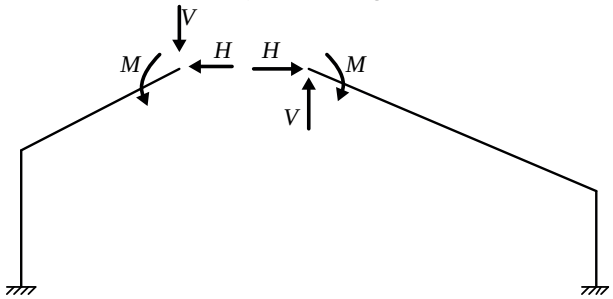


Figure 5.8 – Structural model

Consider the equivalent statically determinate structure of Figure 5.9, in which *M*, *V* and *H* represent the statically redundant unknown internal forces of the frame.



a) Real loading



b) Statically redundant unknown internal forces

Figure 5.9 – Equivalent statically determinate structure

The corresponding internal force diagrams are shown in Figure 5.10.

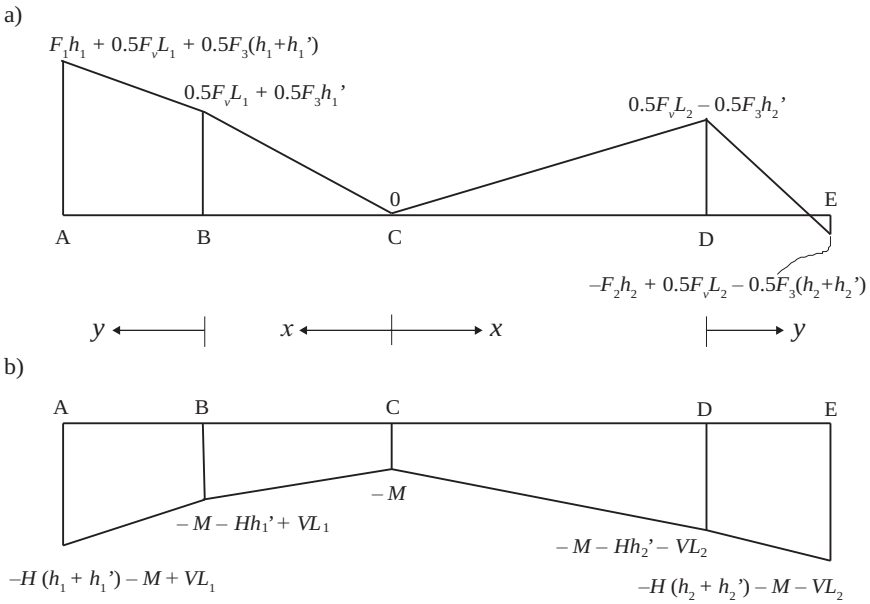


Figure 5.10 – Internal force diagrams: a) real loading; b) statically redundant internal forces

Knowing the applied loads and the statically redundant internal forces *M*, *V* and *H*, the real internal force diagrams are obtained as the sum of the diagrams of Figure 5.10. In the context of a plastic analysis, the plastic mechanism requires four plastic hinges. Assuming that the structure is formed of the same steel profile throughout, with a plastic bending moment resistance M_p, the real bending moment diagram should show four cross sections at M_p and all the other cross sections with lower values. Here, the method differs from elastic analysis by the force method, as it is not necessary to impose conditions of compatibility of deformations, but only to ensure the verification of the plastic mechanism. According to the topology of the structure (4 elements) and the applied loads (concentrated loads acting exclusively in the nodes of the structure), there are only 5 potential locations for the plastic hinges, while the necessary number of plastic hinges will be 4 (degree of redundancy + 1). Thus, the number of mechanisms is given by (equation 5.3):

$$C_4^5 = \frac{5!}{4!(5-4)!} = 5,$$

which are illustrated in Figure 5.11.

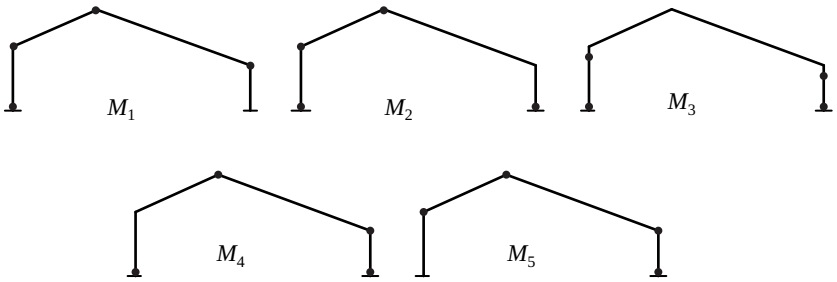


Figure 5.11 – Potential mechanisms

Equations (5.5) represent the values of the bending moment as a function of *M*, *V* and *H* for all possible locations of the plastic hinges:

$$\begin{cases} A:\ M_A = F_1 h_1 + 0.5F_V L_1 + \left(0.5F_3 - H\right)\left(h_1 + h_1^{'}\right) - M + VL_1 \\ B:\ M_B = 0.5F_V L_1 + 0.5F_3 h_1^{'} - M - Hh_1^{'} + VL_1 \\ C:\ M_C = -M \\ D:\ M_D = 0.5F_V L_2 - 0.5F_3 h_2^{'} - M - Hh_2^{'} - VL_2 \\ E:\ M_E = -F_2 h_2 + 0.5F_V L_2 - \left(0.5F_3 + H\right)\left(h_2 + h_2^{'}\right) - M - VL_2 \end{cases} . \quad (5.5)$$

Assuming that mechanism 4 is the real mechanism, equations (5.5) yield:

$$\begin{cases} A:\ F_1 h_1 + 0.5F_V L_1 + \left(0.5F_3 - H\right)\left(h_1 + h_1^{'}\right) - M + VL_1 = M_p \\ C:\ -M = -M_p \\ D:\ 0.5F_V L_2 - 0.5F_3 h_2^{'} - M - Hh_2^{'} - VL_2 = M_p \\ E:\ -F_2 h_2 + 0.5F_V L_2 - \left(0.5F_3 + H\right)\left(h_2 + h_2^{'}\right) - M - VL_2 = -M_p \end{cases} . \quad (5.6)$$

It is noted that, for a compatible mechanism, the signs attached to M_p should always alternate for consecutive plastic hinges. Assuming

$L_1 = L_2 = 23.5$ m, $h_1 = h_2 = 7$ m, $h_1' = h_2' = 2.88$ m, $F_V = 110$ kN, $F_1 = F_2 = F_3 = 55$ kN, equations (5.6) give the required minimum plastic moment resistance, without considering the influence of other internal forces, namely axial force.

$$\begin{cases} M_p = 551.3 \text{ kNm} \\ M = 551.3 \text{ kNm} \\ H = 75.0 \text{ kN} \\ V = -4.5 \text{ kN} \end{cases} . \tag{5.7}$$

It is further required to check that the plastic moment is not exceeded at B.

$$M_B = 0.5F_V L_1 + 0.5F_3 h_1' - M - Hh_1' + VL_1 = 498.9 \text{ kNm} < 551.3 \text{ kNm} . \tag{5.8}$$

If mechanism 2 was chosen instead as the critical mechanism, the required minimum plastic moment would be

$$M_p = 288.7 \text{ kNm} , \tag{5.9}$$

but the verification

$$M_D = 0.5F_V L_2 - 0.5F_3 h_2' - M - Hh_2' - VL_2 = -1292.5 \text{ kNm} > M_p , \tag{5.10}$$

shows that the yield criterion is violated, and mechanism 2 is not the true failure mechanism.

In practical terms, pitched-roof portal frames commonly consist of different cross sections for the columns and for the rafters, with haunched segments in the rafters next to the eaves and apex connections. Loads act through purlins and sheeting rails, rather than directly onto the frame, and two distinct combinations of actions usually need to be considered. Consider therefore the typical pitched-roof portal frame of Figure 5.12, where the parameters c_i represent the positions of the purlins. Also assume that the plastic moment of the column is β times larger than that of the rafter.

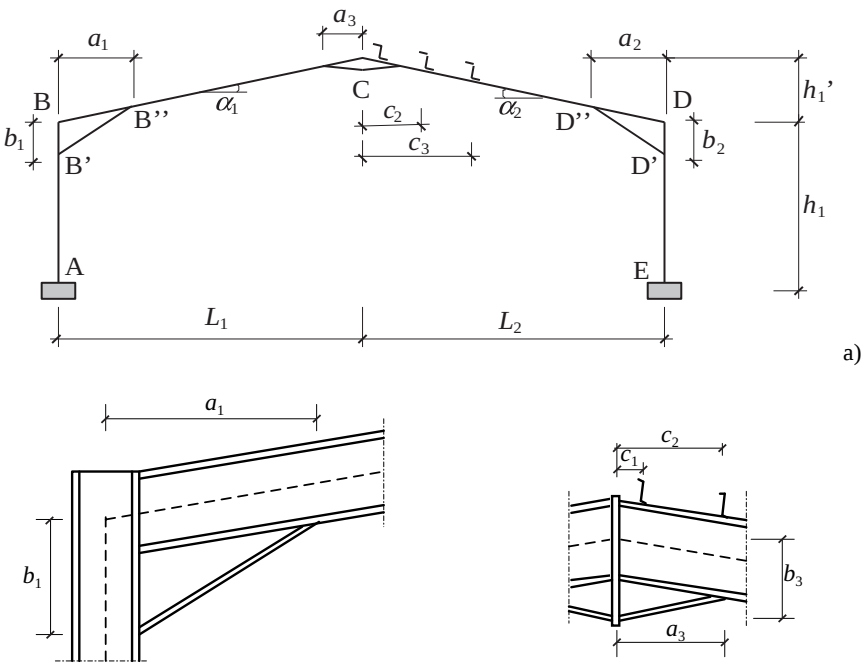


Figure 5.12 – Structural model

For this frame, the possible positions of the plastic hinges are represented in Figure 5.13.

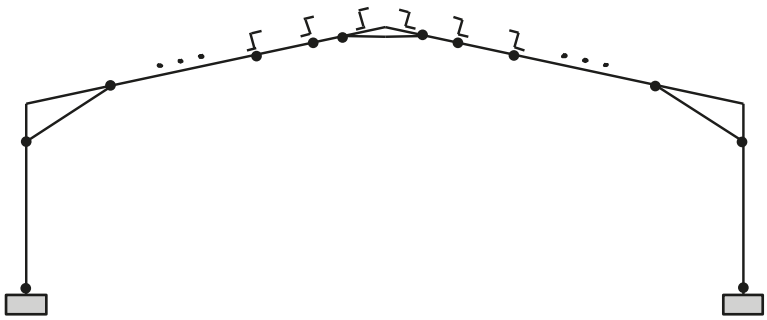


Figure 5.13 – Potential locations of plastic hinges

Consider, firstly, the symmetrical loading indicated in Figure 5.14. It represents the load combination where the leading variable action is the imposed load (or, alternatively, the snow load, in case it is more critical).

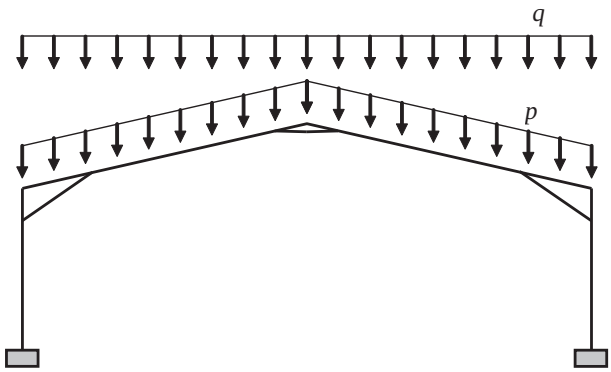


Figure 5.14 – Load combination where the leading variable action is the imposed loading

Using the same equivalent statically determinate system as the previous case, Figure 5.15 shows the resulting bending moment diagrams for the real loading and the statically indeterminate unknown internal forces:

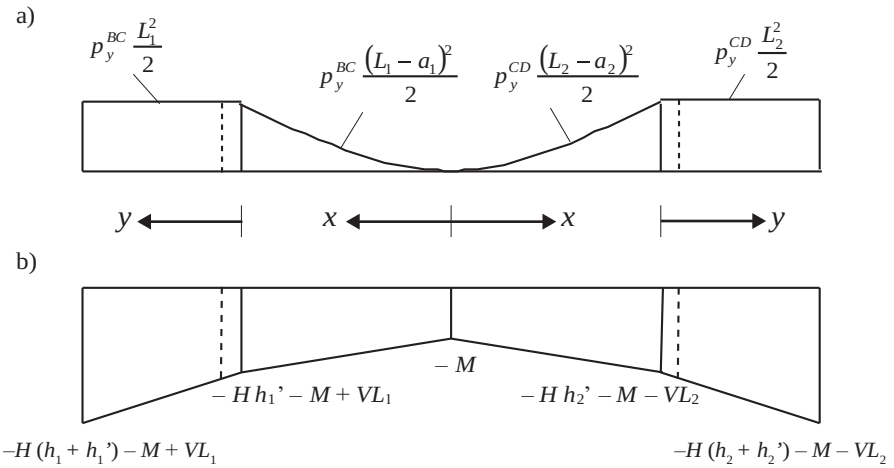


Figure 5.15 – Bending moment diagrams: a) real loading; b) statically indeterminate unknown internal forces

Equations (5.11) summarize the total bending moment for all the potential locations of the plastic hinges:

$$\begin{cases} M_A = p_y^{BC}\dfrac{L_1^2}{2} - M - H\left(h_1 + h_1^{'}\right) + VL_1 \\ M_B^{'} = p_y^{BC}\dfrac{L_1^2}{2} - M - H\left(b_1 + h_1^{'}\right) + VL_1 \\ M_B = p_y^{BC}\dfrac{L_1^2}{2} - M - Hh_1^{'} + VL_1 \\ M_B^{''} = p_y^{BC}\dfrac{\left(L_1 - a_1\right)^2}{2} - M - Hh_1^{'}\dfrac{\left(L_1 - a_1\right)}{L_1} + V\left(L_1 - a_1\right) \\ M_x^{BC} = p_y^{BC}\dfrac{x^2}{2} - M - Hh_1^{'}\dfrac{x}{L_1} + Vx \\ M_C = -M \end{cases}, \tag{5.11}$$

where p_y^{BC} and p_y^{CD} correspond to uniformly distributed gravity loads[1] in members BC and CD, respectively. Assuming, $L_1 = L_2$, $h_1 = h_2$, $h_1' = h_2'$ and that the plastic hinges are formed in A, B' and in segment B″-C′, leads to (where, by symmetry, $V = 0$):

$$\begin{cases} M_A = p_y^{BC}\dfrac{L_1^2}{2} - M - H\left(h_1 + h_1^{'}\right) = M_p^{col} \\ M_B^{'} = p_y^{BC}\dfrac{L_1^2}{2} - M - H\left(b_1 + h_1^{'}\right) = -M_p^{col} \\ M_x^{BC} = p_y^{BC}\dfrac{x^2}{2} - M - Hh_1^{'}\dfrac{x}{L_1} = M_p^{raft} \end{cases}, \tag{5.12}$$

where

$$M_p^{raft} = \frac{p_y^{BC}\left(L_1^2 - x^2\right)}{2\left[\left(\beta - 1\right) - \dfrac{2\beta}{b_1}\left(h_1 + h_1^{'}\left(1 - \dfrac{x}{L_1}\right)\right)\right]}. \tag{5.13}$$

[1] Per projected length.

The position of the plastic hinge can be obtained by minimization of M_p^{raft} with respect to x,

$$\frac{dM_p^{raft}}{dx} = 0\,, \tag{5.14}$$

leading to (with L_1 = 23.5 m, h_1 = 7 m, h_1' = 2.88 m, a_1 = 4.5 m, b_1 = 1.2 m, a_3 = 1.5 m , b_3 = 0.8 m, β = 1.0 e $p_y^{BC} = p_y^{CD}$ = 15.64 kN/m)

$$x = 4.50 \text{ m}\,. \tag{5.15}$$

Of the two solutions of equation (5.14), one is normally negative, and so only the other will be relevant. As the position of the plastic hinge should coincide with the location of a purlin, the final definition of the plastic hinge is easily established by inspection. Assuming that the spacing between the purlins is 2.2 m leads to:

$$\begin{cases} M_p^{raft} = 1059.47 \text{ kNm} \\ M_p^{col} = 1398.50 \text{ kNm} \\ M = 951.85 \text{ kNm} \\ H = 482.29 \text{ kN} \end{cases}, \tag{5.16}$$

and the corresponding bending moment diagram of Figure 5.16.

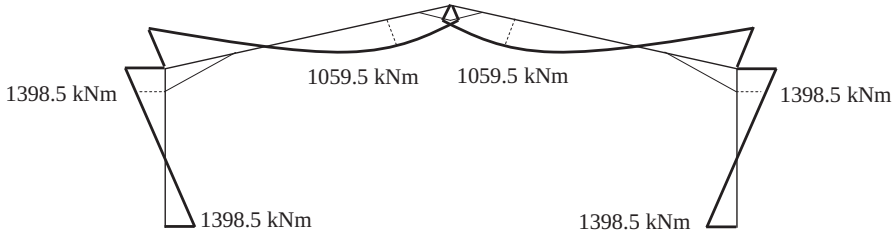


Figure 5.16 – Bending moment diagram at collapse

Consider next the load combination where the leading variable action is wind, typically represented in Figure 5.17. The actions to be considered in each member are summarized in equations (5.17), where x and y represent the global coordinates of the structure,

$$\begin{cases} p_x^{AB} = p_n^{(AV)} \\ p_y^{AB} = p_y^{(AP)} \end{cases} \qquad \begin{cases} p_x^{DE} = -p_n^{(AV)} \\ p_y^{DE} = p_y^{(AP)} \end{cases} \tag{5.17}$$

$$\begin{cases} p_x^{BC} = p_n^{(AV)} \operatorname{tg}\alpha_1 \\ p_y^{BC} = \dfrac{p_y^{(AP)}}{\cos\alpha_1} + p_n^{(AV)} \end{cases} \qquad \begin{cases} p_x^{CD} = -p_n^{(AV)} \operatorname{tg}\alpha_2 \\ p_y^{CD} = \dfrac{p_y^{(AP)}}{\cos\alpha_2} + p_n^{(AV)} \end{cases}$$

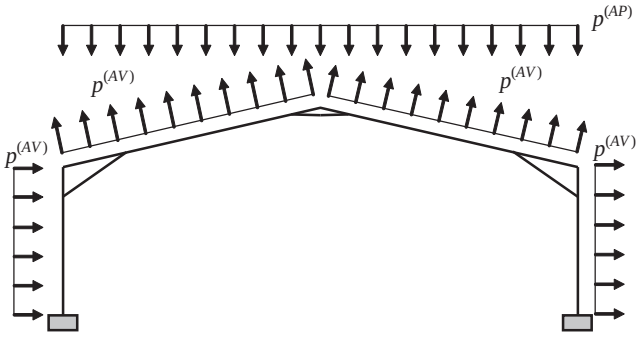


Figure 5.17 – Load combination where the leading variable action is wind

In this case, the bending moment diagrams for the equivalent statically determinate structure are represented in Figure 5.18, leading to the following expressions for the potential locations of the plastic hinges:

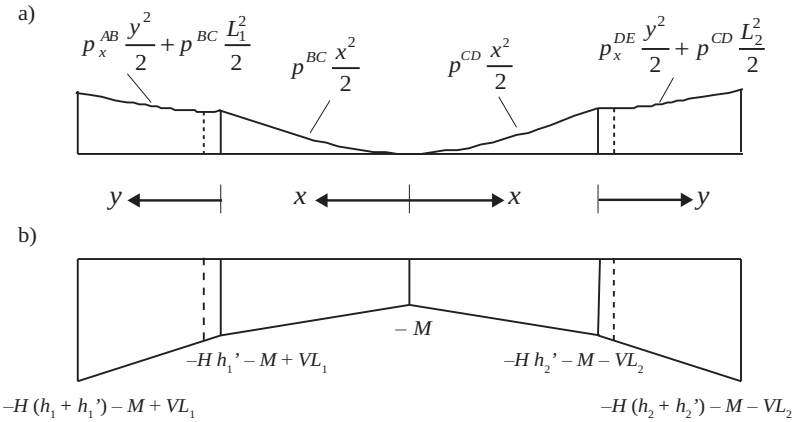


Figure 5.18 – Bending moment diagrams: a) real loading; b) statically indeterminate unknown internal forces

$$
\begin{cases}
M_A = p_x^{AB}\dfrac{h_1^2}{2} + p^{BC}\dfrac{L_1^2}{2} - M - H\left(h_1 + h_1^{'}\right) + VL_1 \\
M_y^{AB} = p_x^{AB}\dfrac{y^2}{2} + p^{BC}\dfrac{L_1^2}{2} - M - H\left(y + h_1^{'}\right) + VL_1 \\
M_B^{'} = p_x^{AB}\dfrac{b_1^2}{2} + p^{BC}\dfrac{L_1^2}{2} - M - H\left(b_1 + h_1^{'}\right) + VL_1 \\
M_B = p^{BC}\dfrac{L_1^2}{2} - M - Hh_1^{'} + VL_1 \\
M_B^{''} = p^{BC}\dfrac{\left(L_1 - a_1\right)^2}{2} - M - Hh_1^{'}\dfrac{L_1 - a_1}{L_1} + V\left(L_1 - a_1\right) \\
M_x^{BC} = p^{BC}\dfrac{x^2}{2} - M - Hh_1^{'}\dfrac{x}{L_1} + Vx \\
M_C = -M \\
M_x^{CD} = p^{CD}\dfrac{x^2}{2} - M - Hh_1^{'}\dfrac{x}{L_1} - Vx \\
M_D^{''} = p^{CD}\dfrac{\left(L_2 - a_2\right)^2}{2} - M - Hh_2^{'}\dfrac{L_2 - a_2}{L_2} - V\left(L_2 - a_2\right) \\
M_D = p^{CD}\dfrac{L_2^2}{2} - M - Hh_2^{'} - VL_2 \\
M_D^{'} = p_x^{DE}\dfrac{b_2^2}{2} + p^{CD}\dfrac{L_2^2}{2} - M - H\left(b_2 + h_2^{'}\right) - VL_2 \\
M_y^{DE} = p_x^{DE}\dfrac{y^2}{2} + p^{CD}\dfrac{L_2^2}{2} - M - H\left(y + h_2^{'}\right) - VL_2 \\
M_E = p_x^{DE}\dfrac{h_2^2}{2} + p^{CD}\dfrac{L_2^2}{2} - M - H\left(h_2 + h_2^{'}\right) - VL_2
\end{cases}
. \qquad (5.18)
$$

where,

$$
\begin{aligned}
p^{BC} &= p_x^{BC}\sin\alpha_1 + p_y^{BC}\cos\alpha_1 \\
p^{CD} &= p_x^{CD}\sin\alpha_2 + p_y^{CD}\cos\alpha_2
\end{aligned}
. \qquad (5.19)
$$

Whenever the gravity load combination is critical it is useful to check what is the load multiplier that corresponds to the plastic collapse of the structure, for the wind combination, instead of calculating the required

plastic moment. Applying a load factor α to the wind actions (only to the wind action because the gravity loading is favourable), and assuming plastic hinges at B′, C, D″ and E, the following system of equations is obtained:

$$\begin{cases} M_B^{'} = \alpha_p p_x^{AB} \dfrac{b_1^2}{2} + \left(\alpha_p p_x^{BC} \sin\alpha_1 + \left(\dfrac{p_y^{(AP)}}{\cos\alpha_1} + \alpha_p p_n^{(AV)} \right) \cos\alpha_1 \right) \dfrac{L_1^2}{2} \\ \qquad - M - H\left(b_1 + h_1^{'}\right) + VL_1 = M_p^{col} \\ M_C = -M = M_p^{raft} \\ M_D^{''} = \left(\alpha_p p_x^{CD} \sin\alpha_2 + \left(\dfrac{p_y^{(AP)}}{\cos\alpha_2} + \alpha_p p_n^{(AV)} \right) \cos\alpha_2 \right) \dfrac{\left(L_2 - a_2\right)^2}{2} \\ \qquad - M - Hh_2^{'} \dfrac{L_2 - a_2}{L_2} - V\left(L_2 - a_2\right) = M_p^{raft} \\ M_E = \alpha_p p_x^{DE} \dfrac{h_2^2}{2} + \left(\alpha_p p_x^{CD} \sin\alpha_2 + \left(\dfrac{p_y^{(AP)}}{\cos\alpha_2} + \alpha_p p_n^{(AV)} \right) \cos\alpha_2 \right) \dfrac{L_2^2}{2} \\ \qquad - M - H\left(h_2 + h_2^{'}\right) - VL_2 = M_p^{col} \end{cases} . \quad (5.20)$$

For $p_x^{AB} = p_x^{DE} = 10.26$ kN/m, $p_x^{BC} = -0.40$ kN/m, $p_x^{CD} = 1.71$ kN/m, $p_y^{AB} = p_y^{DE} = 0$, $p_y^{BC} = 1.25$ kN/m and $p_y^{CD} = -9.42$ kN/m, the following results are obtained:

$$\begin{cases} \alpha_p = 8.87 \\ M = -1247 \text{ kNm} \\ V = -542.0 \text{ kN} \\ H = -790.9 \text{ kN} \end{cases} . \quad (5.21)$$

This means that the structure is safe for the wind load combination and the wind loads have to be 8.87 times the design values to cause collapse using the M_p values from equations (5.16).

The final choice of the cross sections should take into account the axial force. From the values of M_p given by equations (5.16), to compensate

for the detrimental influence of the axial force, the bending and axial force plastic interaction equations (3.148) and (3.149) for I or H-sections (clause 6.2) can be used,

$$M_{N,y,Rd} = M_{pl,y,Rd}\frac{1-n}{1-0.5a} \quad \text{but} \quad M_{N,y,Rd} \le M_{pl,y,Rd}; \tag{5.22a}$$

$$\begin{cases} M_{N,z,Rd} = M_{pl,z,Rd} & n \le a; \\ M_{N,z,Rd} = M_{pl,z,Rd}\left[1-\left(\dfrac{n-a}{1-a}\right)^2\right] & n > a, \end{cases} \tag{5.22b}$$

where $n = N_{Ed} / N_{pl,Rd}$ and $a = (A - 2b\,t_f) / A$, but $a \le 0.5$, where A represents the area of the cross section, b is the width of the flanges and t_f is the thickness of the flange. Approximately, the required minimum plastic moment resistance is obtained by replacing the value of plastic moment given by equations (5.16) and solving for $M_{pl,y,Rd}$ from equation (5.22a).

Finally, it must be pointed out that there are speedy procedures for the plastic pre-design of pitched-roof portal frames, either as tables (Salter *et al*, 2004), or as very simple sequential procedures, using nomograms.

5.2.3. Computational analysis

Material non linear analysis (MNA) with an elastic-plastic constitutive law (Figure 5.7) requires an incremental procedure whereby a load factor is progressively increased from a reference loading, for each load combination, until a maximum is reached. For each load increment, an iterative procedure usually based on a Newton-Raphson scheme is required to ensure convergence of the results to the "true" solution. Figure 5.19 illustrates schematically the analysis procedure.

Consequently, the plastic analysis of a structure using computational methods requires a careful interpretation of the results and it often does not lead to the same results as manual methods. This latter aspect, apparently surprising, results mainly from the two following reasons: i) the numerical nature of computational methods inevitably leads to numerical errors and ii) manual methods normally assume, a priori, a set of simplifications that are not present in computational methods.

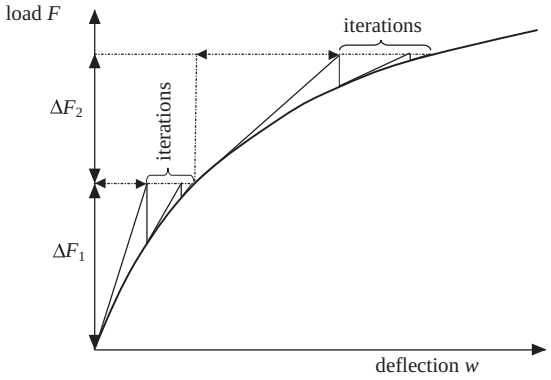


Figure 5.19 – Incremental non linear procedure

This first aspect is better understood by realising that, numerically, the assessment of the plastification of a section is a discontinuous process, depending on the discretization of the structure into elements. Figure 5.20 illustrates this statement. The bending moment diagram for the trapezoidal load illustrated in Figure 5.20 is given by:

$$M(x) = -\frac{p}{6L}x^3 - \frac{p}{2}x^2 + \frac{34pL}{40}x - \frac{22pL^2}{120}. \qquad (5.23)$$

Considering L = 10 m and a plastic moment resistance of M_p = 60 kNm, the analytical solution predicts the formation of a plastic hinge for a load level of p = 5.348 kN/m at a distance x = 6.432 m.

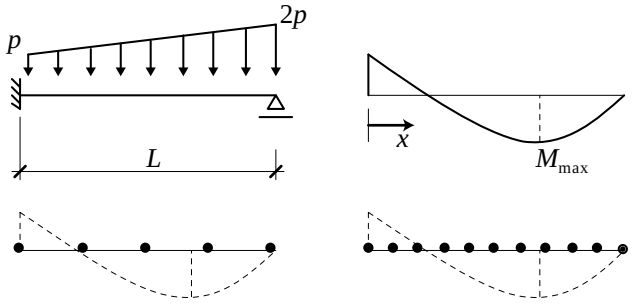


Figure 5.20 – Plastic analysis of a hinged fixed-ended beam

The numerical solution with a 4 element mesh discretization locates the plastic hinge at x = 5.00 m and a load factor α^{pl} = 1.00, whereas a mesh discretization of 10 elements provides x = 6.00 m and α^{pl} = 0.90. This small

example highlights the importance of adequately assessing the sensitivity of the results to mesh discretization.

Concerning the second aspect, the yield criterion (von Mises, Tresca, etc.) can be implemented: i) directly from the stress state at all points along the depth of a cross section, thus dealing properly with an arbitrary three-dimensional stress distribution, such as biaxial bending and axial compression or ii) indirectly through generalized force-displacement relations that reproduce more closely manual analysis. This latter situation is normally implemented in commercial codes through bilinear or non-linear spring elements, which have the additional disadvantage of requiring the previous knowledge of the potential locations of plastic hinges. The simple plane frame of Figure 5.21 can be used to compare these two situations. Considering L = 15 m, h = 10 m, S 275 steel, a plastic moment resistance of M_p^{col} = 118.1 kNm and M_p^{b} = 60.7 kNm, in the columns and in the beam respectively, and $V = 10H$, the analytical solution using elastic-plastic analysis leads to the formation of the first two plastic hinges for α_1 = 3.125 in points A and D and the collapse mechanism for α_p = 3.576 with two additional plastic hinges in B and C (frame mechanism).

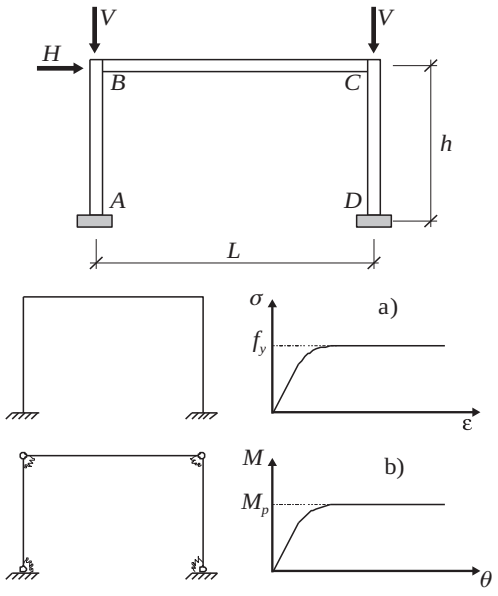


Figure 5.21 – Alternative implementations of yield criteria

Numerically, using beam non-linear finite elements and the von Mises' yield criterion (Figure 5.21a), defined through a generalized

stress-strain relation, the plastic hinges are formed sequentially for load factors α_1 = 3.38 and M_D = 110.2 kNm (N_D =346.9 kN), α_2 = 3.385 and M_A = 110.9 kNm (N_A = 331.2 kN), α_3 = 3.475 and M_B = 60.6 kNm (N_B = 17.3 kN), whereas the collapse load is reached for a load factor α_p = 3.479 and M_C = 60.6 kNm (N_C = 17.4 kN), again with the formation of a frame mechanism. Alternatively, using bilinear spring elements and an equivalent moment-rotation relation (Figure 5.21b), the first plastic hinges are formed for a load factor α_1 = 3.125 and M_A = M_D = 118.1 kNm (N_A = 307.4 kN and N_D = 317.6 kN), whereas the collapse load is reached for a load factor α_p = 3.575 and M_B = M_C = 60.7 kNm (N_B = N_C = 17.9 kN). Note that the analytical solution coincides almost exactly with the numerical solution with spring elements. Secondly, comparing both numerical solutions, identified as (1) and (2), the load factor α is different, for the formation of the first hinge ($\alpha_1^{(1)} = 3.38$ *vs* $\alpha_1^{(2)} = 3.125$), and for the plastic collapse of the structure ($\alpha_p^{(1)} = 3.479$ *vs* $\alpha_p^{(2)} = 3.575$). The same conclusion is reached by comparing the plastic moments at points A and D, where the bending and axial force interaction is significant ($M_D^{(1)} = 110.2$ kNm *vs* $M_D^{(2)} = 118.1$ kNm).

An additional difficulty with computational analysis is to ensure that "false" mechanisms are not formed that may lead to wrong plastic collapse loads. Firstly, it is frequent that some programs lead to wrong mechanisms, particularly for symmetric loadings, in which the direction of rotation of one of the plastic hinges is opposite to the bending moment that causes it. This error can be easily avoided, as long as the program checks that the product of the bending moment at the plastic hinge location and its corresponding rotation is always positive[2]. Secondly, in case transitory plastic hinges[3] occur, the behaviour of the plastic hinge during unloading must be elastic and maintain the residual plastic rotation, as is shown in Figure 5.22.

[2] That is, the rotation must always have the same direction of the bending moment

[3] That is, the situation in which somewhere along the analysis, the plastic hinge inverts the direction of the rotation

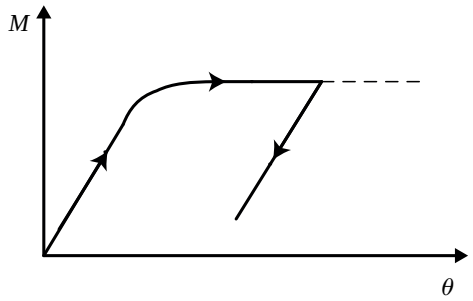


Figure 5.22 – Behaviour of plastic hinge in the unloading

To illustrate this last aspect, consider the two-span continuous beam of Figure 5.23, with a section of plastic moment of 6.75 kNm, area A = 80 cm^2 and second moment of area I = 40 cm^4, reproduced from Davies and Brown (1996).

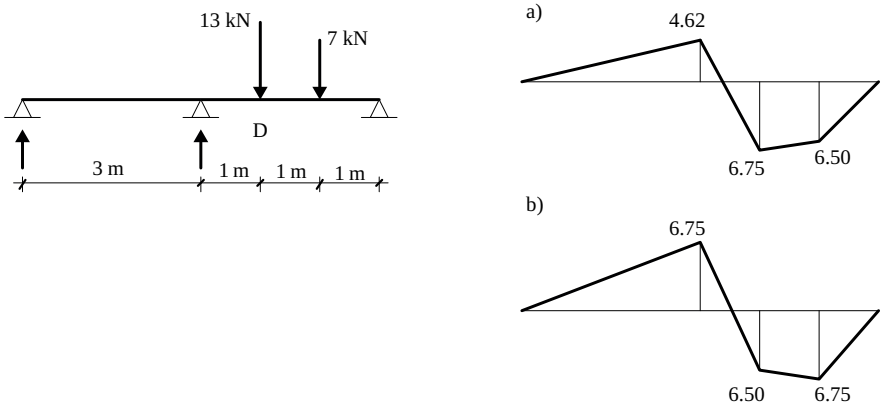


Figure 5.23 – Continuous beam with transitory plastic hinge

Figure 5.24 illustrates the analytical result for this case, which gives the first plastic hinge at D for a load factor α = 0.893. That hinge unloads elastically so that the correct collapse mechanism can be reached for a load factor of 1.0. All the non-linear finite element commercial programs that were tested by the authors led to the wrong result of the false mechanism of Figure 5.24.

The several aspects of computational analysis will be illustrated and discussed in detail in the context of a design example in sub-chapter 5.4.

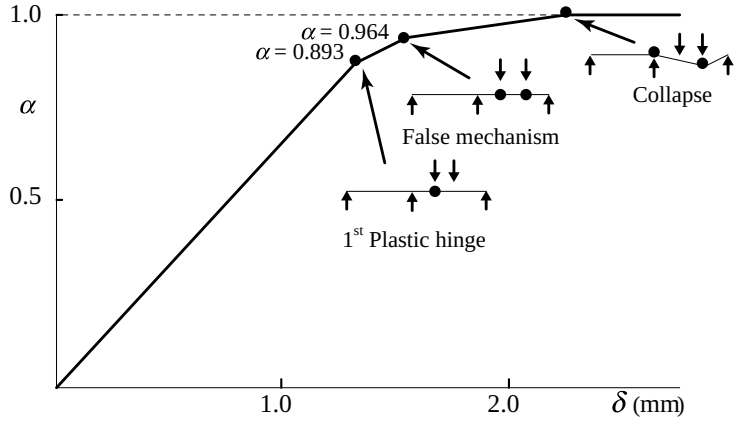


Figure 5.24 – Load factor-vertical displacement diagram

5.2.4. 2nd Order effects

5.2.4.1. Introduction

Sub-chapter 2.3 highlighted the need to account for 2nd order effects. Plastic design of steel structures normally leads to optimized and, consequently, slender structures. Therefore, it is often required to verify the global stability of the structure using a 2nd order analysis and considering imperfections (clause 5.2.2(2)). This requirement is compulsory for plastic analysis whenever (clause 5.2.1(3)):

$$\alpha_{cr} = F_{cr} / F_{Ed} \leq 15 . \tag{5.24}$$

It is noted that in the determination of the 2nd order effects a computational 2nd order analysis can always be used and there are approximate methods of more limited scope available in the literature.

Because the sensitivity of a structure to 2nd order effects is assessed indirectly from the elastic critical load of the structure, F_{cr}, the following sub-section presents approximate expressions for the elastic critical load of pitched-roof portal frames. Subsequently, some considerations on computational second-order analysis of steel frames are also presented. Finally, simplified approximate methods are also briefly described.

5.2.4.2. Elastic critical load

As already discussed in sub-section 2.3.2.2, the elastic critical load of a structure plays an important role in evaluating the sensitivity of a structure to 2nd order effects. In case of pitched-roof portal frames, Horne's and Wood's methods are not adequate as the axial force in the rafter is usually sufficient to affect significantly the stability of the frame. According to King (2001b), the critical load of single-span pitched-roof portal frames can be estimated, for hinged column-bases, by:

$$\alpha_{cr} = \frac{1}{\left(\frac{N_{raft}}{N_{raft.cr.E}}\right) + \left(4 + 3.3R\right)\left(\frac{N_{col}}{N_{col.cr.E}}\right)}; \tag{5.25}$$

and

$$L_{raft} = \frac{L}{\cos\alpha} \qquad R_I = \frac{I_{col}}{I_{raft}} \qquad R_L = \frac{L_{raft}}{L_{col}}, \tag{5.26}$$

where:

L_{col} is the length of the column;

L_{raft} is the real length of the rafter (span between columns measured along the rafter);

R is the ratio between the stiffness of the column and the stiffness of the rafter, given by:

$$R = R_I \, R_L; \tag{5.27}$$

N_{col} is the compressive force in the column;

N_{raft} is the compressive force in the rafter;

$N_{col.cr.E}$ is the elastic critical Euler load of the column;

$$N_{col.cr.E} = \frac{\pi^2 E I_{col}}{L_{col}^2}; \tag{5.28}$$

$N_{raft.cr.E}$ is the elastic critical Euler load of the rafter (equation 5.28, replacing column by rafter).

In case of nominally hinged column-bases, where a rotational stiffness of 10 % of the column's stiffness is assumed, the elastic critical load of the structure is given by:

$$\alpha_{cr} = \frac{1+0.1R}{\left(\frac{N_{raft}}{N_{raft.cr.E}}\right)+\left(2.9+2.7R\right)\left(\frac{N_{col}}{N_{col.cr.E}}\right)}, \tag{5.29}$$

whereas in the case of nominally rigid column-bases, where the rotational stiffness is equal to the column's stiffness, the following equation should be used:

$$\alpha_{cr} = \frac{\left(1+0.08R\right)}{\left(\frac{N_{raft}}{N_{raft.cr.E}}\right)+\left(0.8+0.52R\right)\left(\frac{N_{col}}{n_{col.cr.E}}\right)}. \tag{5.30}$$

Note that, in case the pitched-roof portal frame is asymmetric, the elastic critical load must be taken as the lowest of the critical loads for the two sets column-rafter, left or right. Similarly, Silvestre *et al* (2000) derived alternative expressions for the lowest critical loads in symmetric and anti-symmetric modes that include the flexibility of the connections. For the common case of rigid eaves and apex connections, the lowest critical loads are given by (Nogueiro, 2000):

$$\alpha_{cr} = \left[\left(\frac{N_{col}}{\rho_{col.0}N_{col.cr.E}}\right)^{C}+\left(\frac{N_{raft}}{\rho_{raft.0}N_{raft.cr.E}}\right)^{C}\right]^{-1/C}; \tag{5.31}$$

$$C = \frac{1.6S+1.2}{S+1}, \tag{5.32}$$

and $\rho_{col,0}$ and $\rho_{raft,0}$ are given by:

$$\rho_{col.0} = \begin{cases} \dfrac{S\left(R+3\right)+3}{10R+12+S\left(4R+3\right)} & \text{when } AS \\ \dfrac{4.8+12R\left(1+R_H\right)+S\left(1+4.8R+4.2RR_H\right)}{2.4+12R\left(1+R_H\right)+7R^2R_H^2+S\left(2.4R+2R^2R_H^2\right)} & \text{when } S \end{cases}; \tag{5.33}$$

$$\rho_{raft.0} = \begin{cases} \dfrac{4+S\left(2R+4\right)}{4+S\left(R+4\right)} & \text{when } AS \\ \dfrac{12R+8.4RR_H+S\left(4R+4.2RR_H+R^2R_H^2\right)}{12R+4+S\left(4R+2\right)} & \text{when } S \end{cases}, \qquad (5.34)$$

and

$$S = \frac{K_1 L_{col}}{EI_{col}}; \qquad (5.35)$$

$$R_H = R_L \sin\alpha\,, \qquad (5.36)$$

where K_1 is the stiffness of the column-base connection.

Table 5.2 compares both methods (equations (5.25) to (5.36)) with numerical results, for a frame with L = 15 m, IPE 450 rafters, HEB 280 columns, h = 5.0 m, h' = 1.58 m, for gravity loading (see Figure 5.14). The following cases are compared: (A) hinged column-bases and real rotational stiffness of the eaves and apex connections; (B) semi-rigid column-bases, with $S_{j,ini}$ = 5000 kNm/rad and the remaining connections as in (A); (C) rigid column-bases and remaining connections as in (A); and (D) all the connections rigid.

Table 5.2 – "Exact" and approximate elastic critical loads

Behaviour of connections	"Exact" (numerical)		Approximate (analytical)	
	α_{cr}^{ASM}	α_{cr}^{SM}	α_{cr}^{ASM}	α_{cr}^{SM}
A	22.98	49.23	21.45	55.45
B	35.18	46.52	31.94	53.00
C	43.57	39.32	44.59	40.51
D	43.63	42.92	44.59	40.51

In case of pitched-roof portal frames with multiple spans, approximate formulae can be found in King (2001b) or Silvestre and Camotim (2000).

5.2.4.3. 2nd order computational analysis

Geometrical non linear analysis (GNA) presents the additional complexity of potential unstable behaviours, typically represented in Figure 5.25. This unstable behaviour results from the bifurcational nature of stability problems. Numerically, unstable behaviours require more sophisticated numerical algorithms such as the arc-length method. This requires the specification of convergence criteria that define when equilibrium is reached. These criteria may be specified in terms of displacements, strains, forces, stresses or work. The selection of the proper convergence criterion is extremely important. Tolerances that are too small can result in an unnecessary number of iterations, while tolerances that are too slack can lead to wrong results. In general, in geometrically non linear analysis, narrow tolerances are necessary, such as to maintain the solution in the correct equilibrium path, while in the case of predominantly materially non linear problems, wider tolerances are preferable, as it can be necessary to tolerate locally high residuals.

The 2nd order elastic-plastic analysis of a structure using computational methods directly provides the values of forces and displacements for the verifications of safety for the structure.

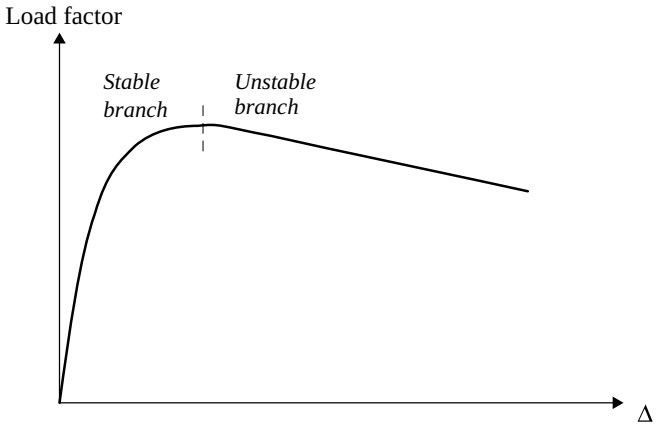


Figure 5.25 – Unstable behaviour

5.2.4.4. Simplified methods for analysis

Simplified methods of analysis that approximate material and geometrical non linear effects constitute a common choice for designers. They allow the analysis of a structure based on first-order methods.

The Merchant-Rankine method is a simplified approach that assesses the ultimate load factor of a structure through a formula that takes into account the interaction between plasticity (α_p) and stability (α_{cr}) in an empirical way.

$$\frac{1}{\alpha_f} = \frac{1}{\alpha_p} + \frac{1}{\alpha_{cr}} . \tag{5.37}$$

In practical terms, the Merchant-Rankine method can be used (Horne, 1963) to obtain an estimate of the 2nd order effects in global plastic analysis using a 1st order elastic-plastic approach with amplification of the total applied loading by:

$$\frac{1}{1-\frac{1}{\alpha_{cr}}} . \tag{5.38}$$

It is noted that this approach is not equivalent to the amplification described in sub-section 2.3.2.3, as it amplifies the totality of the loading and not just the sway components. Secondly, the Merchant-Rankine method requires the additional verification of out-of-plane stability.

Recently, Demonceau (2008) proposed a promising simplified method of analysis that consists on the use of an Ayrton-Perry formulation to assess the ultimate load factor of steel and composite frames. In contrast to the Merchant-Rankine method, it recognizes the fact that the different types of plastic mechanisms are not affected in the same way by the second-order effects developing in a structure, therefore leading to a better agreement with the true behaviour of the frame.

In the context of pitched-roof portal frames, the axial compression in the rafters is often significant (recall clause 5.2.1(4)B), and the structure usually presents two similar critical loads, corresponding to symmetric and anti-symmetric buckling modes (Figure 5.26).

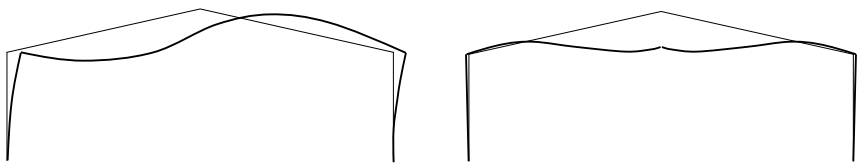


Figure 5.26 – Symmetric and anti-symmetric buckling modes in pitched-roof portal frames

In this case, the simplified procedure for 2nd order elastic analysis described in sub-section 2.3.2.3 and equations (2.17) is not valid and the elastic amplification must be done for both modes, as illustrated in Figure 5.27.

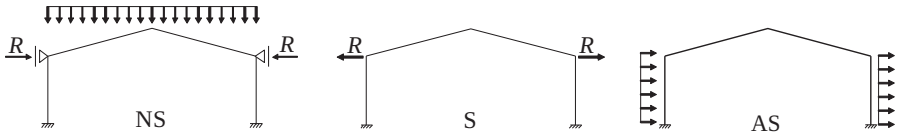


Figure 5.27 – Amplification in the symmetric and anti-symmetric modes

The 2nd order effects are given by:

$$d^{II} = d^{I}_{NS} + \left(1 - \frac{1}{\alpha_{cr.S}}\right)^{-1} d^{I}_{S} + \left(1 - \frac{1}{\alpha_{cr.AS}}\right)^{-1} d^{I}_{AS}; \qquad (5.39a)$$

$$M^{II} = M^{I}_{NS} + \left(1 - \frac{1}{\alpha_{cr.S}}\right)^{-1} M^{I}_{S} + \left(1 - \frac{1}{\alpha_{cr.AS}}\right)^{-1} M^{I}_{AS}; \qquad (5.39b)$$

$$V^{II} = V^{I}_{NS} + \left(1 - \frac{1}{\alpha_{cr.S}}\right)^{-1} V^{I}_{S} + \left(1 - \frac{1}{\alpha_{cr.AS}}\right)^{-1} V^{I}_{AS}; \qquad (5.39c)$$

$$N^{II} = N^{I}_{NS} + \left(1 - \frac{1}{\alpha_{cr.S}}\right)^{-1} N^{I}_{S} + \left(1 - \frac{1}{\alpha_{cr.AS}}\right)^{-1} N^{I}_{AS}, \qquad (5.39d)$$

where indexes *NS*, *S* and *AS* denote, respectively, no-sway, sway in a symmetric mode and sway in an anti-symmetric mode.

For pitched-roof portal frames, Silvestre and Camotim (2005) report that amplification only with the anti-symmetric mode (equations (2.17)) underestimate the 2nd order effects by 10 %. The more rigid the column-base connections are, the greater the error. In contrast, the evaluation of the 2nd order effects using equations (5.39) usually overestimates results by less than 3.5 %. Example 5.1 compares the "exact" 2nd order elastic results (numerical) with approximate results (amplified).

In the case of plastic global analysis, the amplification defined by equations (5.39) is more complex, as the separation of the 1st order moments into sway and no-sway (or symmetrical and anti-symmetrical) components is not obvious.

5.2.5. Worked example

Example 5.1: Consider the pitched-roof portal frame of Figure 5.28 (S 355 steel), subject to the indicated loading (already factored), which was already pre-designed (Figure 5.16) in section 5.2.2. Determine the design forces and displacements of the structure for the following situations:

a) 1st order elastic analysis;
b) Elastic analysis considering 2nd order effects (P–Δ)
  b.1) exact;
  b.2) approximate;
c) 1st order elastic-plastic analysis;
d) Elastic-plastic analysis considering 2nd order effects (P–Δ);
  d.1) exact;
  d.2) approximate;
e) Elastic-plastic analysis considering 2nd order effects (P–δ and P–Δ)

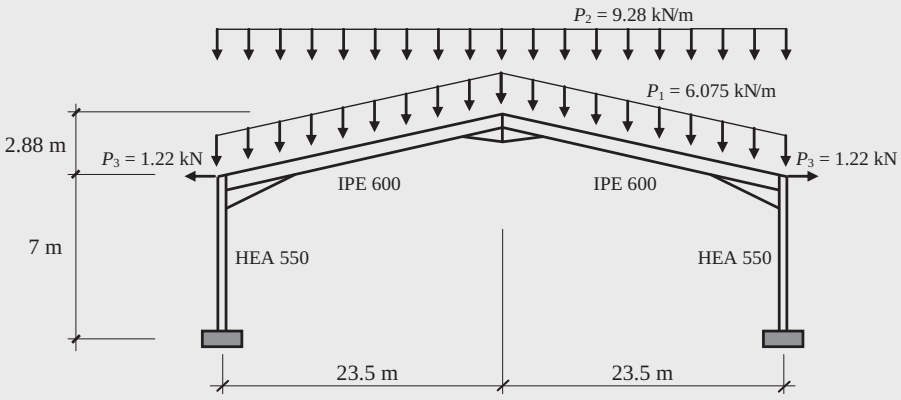


Figure 5.28 – Pitched-roof portal frame

a) *1st order elastic analysis*

Figures 5.29 to 5.31 represent the internal force diagrams for the indicated loading. Note that, for the chosen cross sections, the plastic moments in the columns and rafters are, respectively.

$M_p^{raft} = 1246.8\,\text{kNm}$ and $M_p^{col} = 1640.0\,\text{kNm}$.

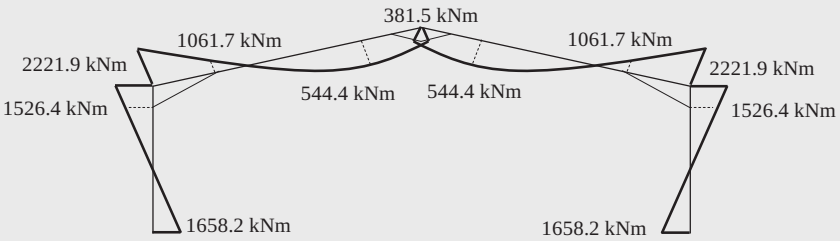


Figure 5.29 – Bending moment diagram, linear elastic analysis

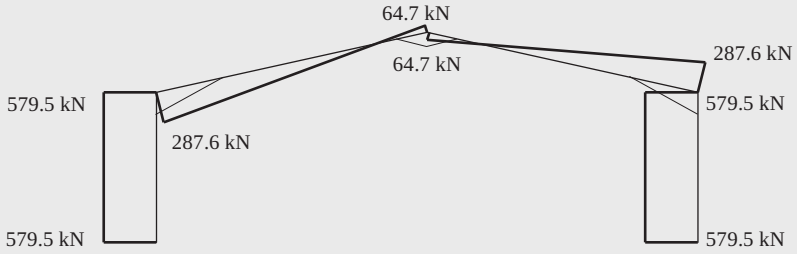


Figure 5.30 – Shear force diagram, linear elastic analysis

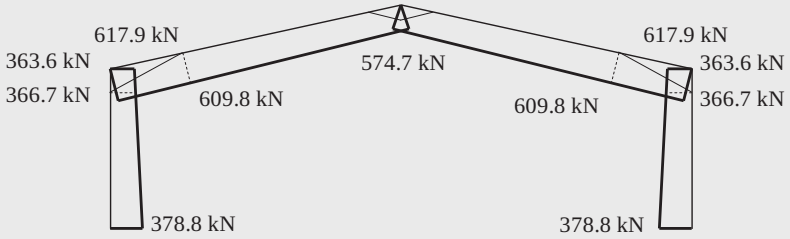


Figure 5.31 – Axial force diagram, linear elastic analysis

Figure 5.32 represents the deformation for the same loading.

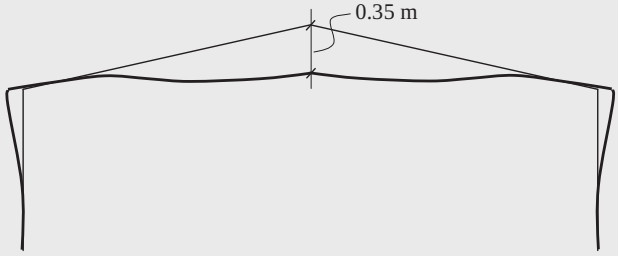


Figure 5.32 – Displacements in the structure, linear elastic analysis

b.1) *Elastic analysis considering 2nd order effects in an "exact" way*

An eigenvalue analysis leads to the critical loads of Table 5.3. For comparison, results obtained using the approximate equations (5.30) and (5.31) are also presented.

Table 5.3 – Critical loads

	α_{cr}^{1}	α_{cr}^{2}	α_{cr}^{3}	α_{cr}^{4}	α_{cr}^{5}
"Exact"	7.32	10.14	18.82	20.95	28.25
Eq. 5.30	6.48	-	-	-	-
Eq. 5.31	7.98	8.73	-	-	-

The corresponding buckling modes are illustrated in Figure 5.33.

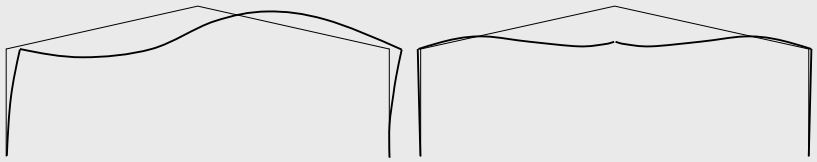


Figure 5.33a – 1st (ASM) and 2nd (SM) buckling modes

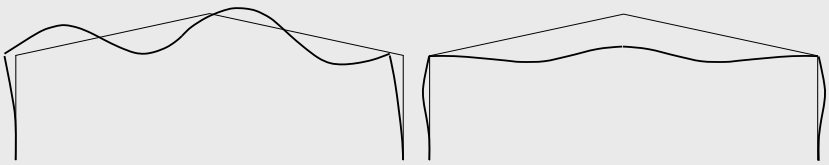


Figure 5.33b – 3rd and 4th buckling modes

The lowest critical loads indicate that the structure is sensitive to 2nd order effects. A 2nd order computational analysis leads to the results of Figure 5.34.

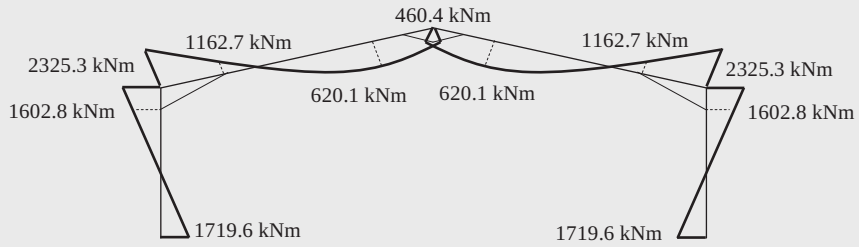


Figure 5.34 – Bending moment diagram; 2nd order "exact" elastic analysis

b.2) *Elastic analysis considering 2nd order effects in an approximate way*

According to equations (2.17), it is necessary to decompose the internal forces in the sway component and an anti-symmetric mode. However, in this case, the applied loading causes a deformation that is similar to the symmetric buckling mode, and so the amplified bending moment diagram coincides with the 1st order bending moment diagram (Figure 5.35):

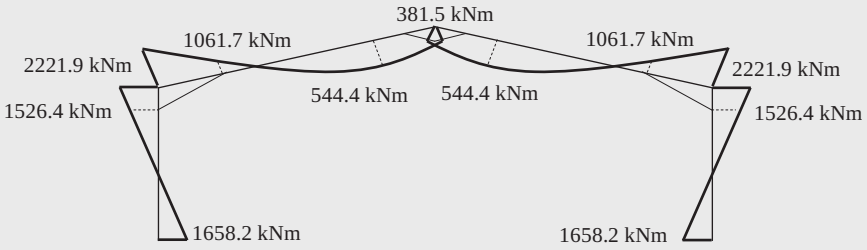


Figure 5.35 – Amplified bending moment diagram (equations (2.17))

Alternatively, according to equations (5.39), both symmetric and anti-symmetric modes must be amplified. The no-sway diagrams (Figure 5.36) are obtained from an elastic analysis considering the real loading of the structure, but fixing the horizontal displacement of nodes B and D.

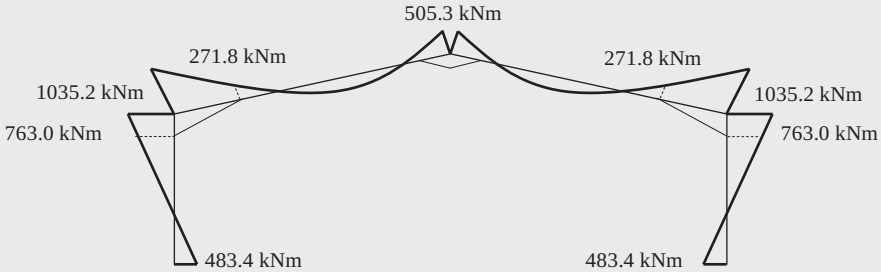


Figure 5.36 – 1st order bending moment diagram, M^{I}_{NS}

By applying the value of the horizontal reactions to the portal frame, the symmetric component of the bending moment diagram is obtained, represented in Figure 5.37. As stated before, the anti-symmetric component is zero because of the symmetry of the structure and of the loading.

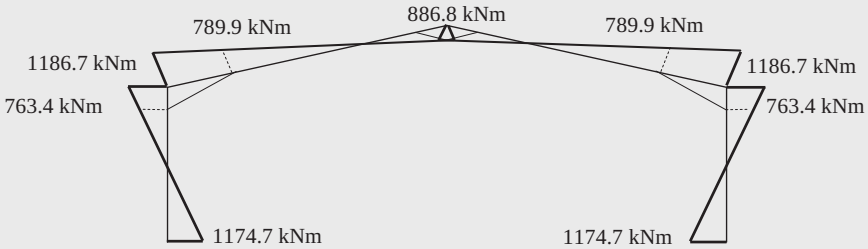


Figure 5.37 –1st order bending moment diagram, M_s^I

Amplifying the bending moment diagrams of Figure 5.36 and 5.37 according to equations (5.39) gives the results of Table 5.4 that also summarizes the "exact" results, for comparison.

Table 5.4 – 2nd order effects

M_y (kNm)	Exact	Eqs. 2.17	Error (%)	Eqs. 5.39	Error (%)
A	1719.57	1658.15	-3.57	1786.67	3.90
B'	1602.75	1526.44	-4.76	1609.97	0.45
B	2325.31	2221.86	-4.45	2387.87	2.69
B''	1162.67	1061.73	-8.68	1148.15	-1.25
C	460.44	381.51	-17.14	478.52	3.93
D''	1162.67	1061.73	-8.68	1148.15	-1.25
D	2325.31	2221.86	-4.45	2387.87	2.69
D'	1602.75	1526.44	-4.76	1609.97	0.45
E	1719.57	1658.15	-3.57	1786.67	3.90

c) *1st order elastic-plastic analysis*

The bending moment diagram that corresponds to the formation of the first plastic hinge is represented in Figure 5.38. Table 5.5 summarizes the values corresponding to the formation of each plastic hinge; the locations referred to in Table 5.5 are shown in Figure 5.12(a).

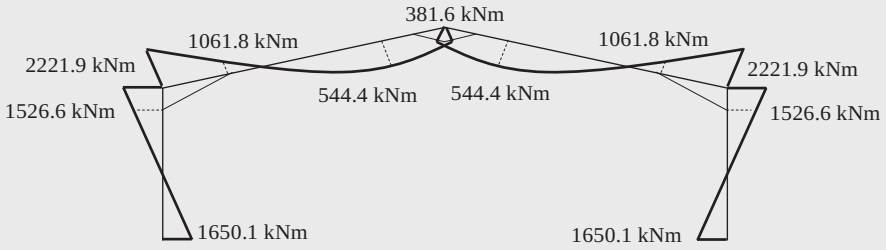


Figure 5.38 – Bending moment diagram that corresponds to the formation of the first plastic hinge (α =1.00), 1st order elastic-plastic analysis

Table 5.5 – 1st order elastic-plastic analysis

M_y (kNm)	α = 1.000	α = 1.070
A	1650.10	1612.06
B’	1526.56	1653.50
B	2221.92	2392.49
B’’	1061.76	1144.94
C	381.58	425.57
D’’	1061.76	1144.94
D	2221.92	2392.49
D’	1526.56	1653.50
E	1650.10	1612.06

The collapse mechanism is represented in Figure 5.39.

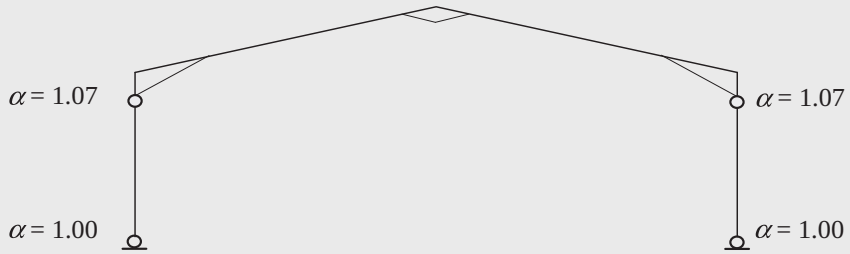


Figure 5.39 – Collapse mechanism and sequence of formation of the plastic hinges

Careful examination of the bending moments at sections A and E for a load factor α =1.00 or sections B’ and D’ for load factor α = 1.07 reveals that the moments are, respectively, 1650 kNm and 1653 kNm instead of the plastic moment of the column section given earlier as 1640 kNm. This difference might very easily result from lack of convergence, as was discussed in

sections 5.2.3 and 5.2.4 or from the extrapolation from the "exact" Gauss point results to nodal results. However, in this case, because of the presence of a compressive axial force, the plastic moment is modified by the bending-axial force plastic interaction. Secondly, it is noted that the moment at A and E go down between a load level of 1.00 and 1.07 because of unloading occurring at A and E.

d.1) *Elastic-plastic analysis, considering 2nd order effects in an "exact" way*

A 2nd order elastic-plastic analysis leads to the results represented in Figures 5.40 and 5.41.

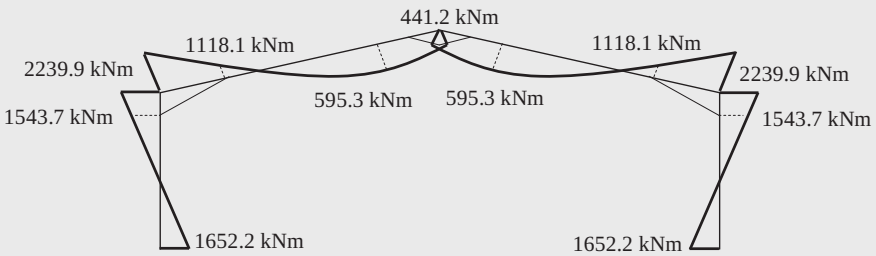


Figure 5.40 –Bending moment diagram that corresponds to the formation of the first plastic hinge (α = 0.965), 2nd order elastic-plastic analysis

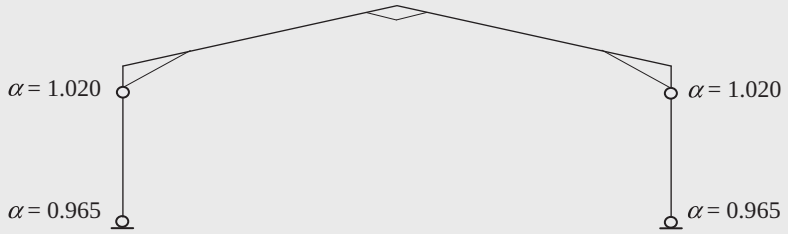


Figure 5.41 – Collapse mechanism with the indication of the load factors that correspond to formation of the plastic hinges

Table 5.6 summarizes the results for the two load levels that correspond to the formation of plastic hinges. Similarly to the previous case, the plastic moment is modified by the bending-axial force plastic interaction and unloading occurs at A and E.

Table 5.6 – 2nd order elastic-plastic analysis

M_y (kNm)	$\alpha = 0.965$	$\alpha = 1.020$
A	1652.20	1612.58
B’	1543.71	1654.53
B	2239.91	2386.79
B’’	1118.05	1195.33
C	441.18	485.73
D’’	1118.05	1195.33
D	2239.91	2386.79
D’	1543.71	1654.53
E	1652.20	1612.58

d.2) *Elastic-plastic analysis considering 2nd order effects in an approximate way (Merchant-Rankine method)*

From sub-section 5.2.4.4, with load amplification from expression (5.38), the plastic hinges are found to form as shown in Figure 5.42. Table 5.7 compares the detailed results with the “exact” values.

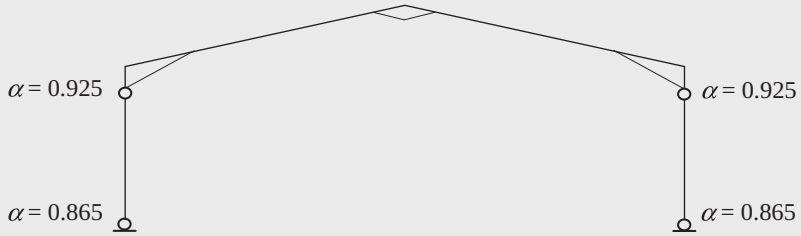


Figure 5.42 – Collapse mechanism and load factors corresponding to the formation of the plastic hinges

Table 5.7 – Approximate 2nd order elastic-plastic analysis

M_y (kNm)	Exact		Eqs. 5.39			
	1st hinge ($\alpha = 0.965$)	2nd hinge ($\alpha = 1.020$)	1st hinge ($\alpha = 0.865$)	Error (%)	2nd hinge ($\alpha = 0.925$)	Error (%)
A	1652.20	1612.58	1646.19	-0.36	1612.06	-0.03
B’	1543.71	1654.53	1529.51	-0.92	1652.79	-0.11
B	2239.91	2386.79	2226.11	-0.62	2395.84	0.38
B’’	1118.05	1195.33	1063.74	-4.86	1146.53	-4.08
C	441.18	485.73	382.24	-13.36	426.41	-12.21
D’’	1118.05	1195.33	1063.74	-4.86	1146.53	-4.08
D	2239.91	2386.79	2226.11	-0.62	2395.84	0.38
D’	1543.71	1654.53	1529.51	-0.92	1652.79	-0.11
E	1652.20	1612.58	1646.19	-0.36	1612.06	-0.03

Similarly to the two previous cases, the plastic moment is modified by the bending-axial force plastic interaction and unloading occurs at A and E. Figure 5.43 shows the variation in horizontal displacement at the apex of the frame with load factor. A decrease of about 5 % in the resistance of the frame is observed due to 2nd order effects. The different responses show that plastic analysis can result in a significant economy in terms of quantity of steel, when compared to an elastic analysis.

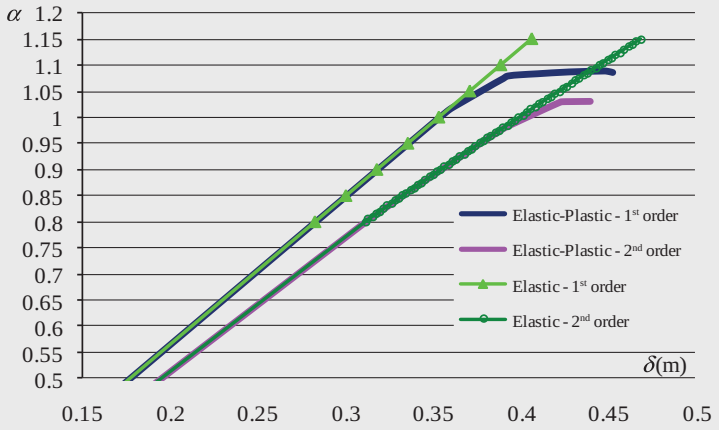


Figure 5.43 – Load factor-horizontal displacement diagram at the apex

Finally, Table 5.8 summarizes the results for all the analysis at a load factor α = 1, corresponding to ULS.

Table 5.8 – Comparative summary of results

	Elastic 1st Order	Elastic 2nd Order	Elastic-Plastic 1st Order		Elastic-Plastic 2nd Order	
			α = 1.00		α = 1.00	
	M_y (kNm)	M_y (kNm)	M_y (kNm)	N (kN)	M_y (kNm)	N (kN)
A	1658.15	1719.57	1650.10	371.68	1613.18	357.58
B’	1526.44	1602.75	1526.56	365.86	1614.49	363.74
B_{col}	2221.86	2325.31	2221.92	363.55	2331.64	362.22
B_{raft}				617.86		636.83
B’’	1061.73	1162.67	1061.76	609.72	1166.23	623.40
C	381.51	460.44	381.58	574.65	467.56	591.91
D’’	1061.73	1162.67	1061.76	609.72	1166.23	623.40
D_{raft}	2221.86	2325.31	2221.92	617.86	2331.64	636.83
D_{col}				363.55		362.22
D’	1526.44	1602.75	1526.56	365.86	1614.49	363.74
E	1658.15	1719.57	1650.10	371.68	1613.18	357.58

e) *2nd order elastic-plastic analysis, considering both P–δ and P–Δ, 2nd order effects*

In order to explicitly include in the analysis the local bow imperfections (*P–δ* effects), it is necessary to calculate first the equivalent horizontal forces, according to section 2.3.3 and Table 2.20, represented in Figure 5.44.

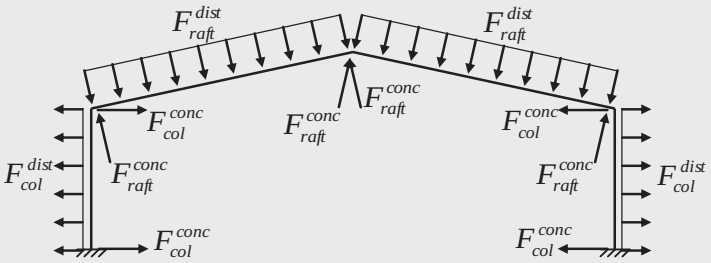


Figure 5.44 – Equivalent local bow imperfections

where,

$F_{raft}^{dist} = 0.82\ \text{kN/m}$, $F_{raft}^{conc} = 9.76\ \text{kN}$, $F_{col}^{dist} = 1.70\ \text{kN/m}$ and $F_{col}^{conc} = 5.95\ \text{kN}$.

Table 5.9 compares the results of 2nd order elastic-plastic analyses with and without *P-δ* effects, considered as equivalent horizontal forces. Increased bending moments are observed at the eaves of the frame, the collapse mechanism being formed for a load factor of 1.00.

Table 5.9 – Comparative results for 2nd order elastic-plastic analyses

	Elastic-Plastic 2nd Order (*P*-Δ)		Elastic-Plastic 2nd Order (*P*-δ and *P*-Δ)	
	$\alpha = 1.00$		$\alpha = 1.00$	
	M_y (kNm)	N (kN)	M_y (kNm)	N (kN)
A	1613.18	357.58	1612.00	384.95
B’	1614.49	363.74	1646.85	363.90
B_{col}	2331.64	362.22	2364.17	360.80
B_{raft}		636.83		650.10
B’’	1166.23	623.40	1164.95	628.05
C	467.56	591.91	420.65	597.08
D’’	1166.23	623.40	1164.95	628.05
D_{raft}	2331.64	636.83	2364.17	650.10
D_{col}		362.22		360.80
D’	1614.49	363.74	1646.85	363.90
E	1613.18	357.58	1612.00	384.95

5.3. MEMBER STABILITY AND BUCKLING RESISTANCE

5.3.1. Introduction

In the context of the two-step analysis and verification procedure that still constitutes standard design practice for most steel structures, the previous sub-chapter (5.2) presented methods of analysis that provide realistic and adequate estimates of the design internal forces and displacements. The aim of the present sub-chapter is to describe the verification procedures for members and components that contain potential plastic hinges, being an essential feature of plastic design.

The verification phase embodies all the effects that result from geometric non-linearities and imperfections, enabling the verification of the cross section resistance. The verification of the stability of members and components includes out-of-plane buckling. Because of the complexity of such verifications and potential loss of resistance and therefore economy, a common procedure is to prevent out-of-plane buckling by the use of adequate bracings. General criteria for the verification of the stability of members with plastic hinges, as well as rules for bracings, are presented below. Subsequently, the detailed procedures for the verification of the stability of members with plastic hinges are presented. Finally, at the end of this sub-chapter, the several procedures are illustrated through worked examples.

5.3.2. General criteria for the verification of the stability of members with plastic hinges

The verification of safety of members or components containing plastic hinges addresses:

- prismatic and non-prismatic members;
- the presence of bracings that restrict only some displacements or part of the cross section.

Normally, the stability of a member is checked as a series of effectively braced segments, considering the internal force diagrams along

each segment. Figure 5.45 typifies the typical situation of a prismatic column in a single-storey building, being designed using plastic analysis. The column length shown contains one plastic hinge. Side rails and other components provide intermediate bracing of varying effectiveness.

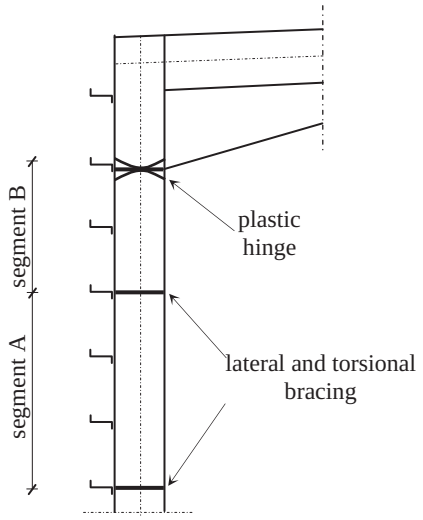


Figure 5.45 – Generic member containing one plastic hinge and bracings

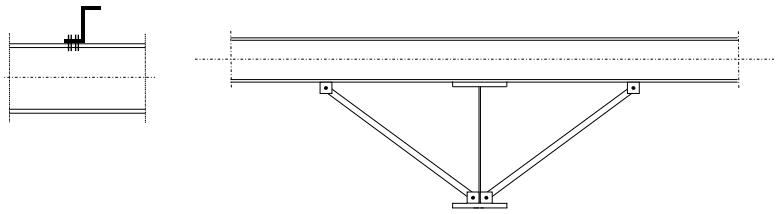
The verification procedure distinguishes between segments not containing plastic hinges (segment A), already discussed in section 3.7.3 and sub-chapter 4.3, and segments containing plastic hinges (segment B) that are discussed in section 5.3.4 below. Additionally, as already mentioned in section 5.1.3, plastic design requires bracing at the plastic hinge locations to prevent out-of-plane rotation of the plastic hinge. This issue is discussed next in section 5.3.3.

5.3.3. Bracings

In plastic design it is customary to guarantee that out-of-plane buckling is prevented through adequate bracing. The bracing must provide effective restraint to lateral displacements of the compressed flange about the minor axis of the cross section, and should prevent the rotation of the cross section about the longitudinal axis of the member. Three types of bracing can contribute to avoiding out-of-plane buckling:

- lateral bracing, which prevents transverse displacements (with respect to the minor axis of the cross section) of the compression flange;
- torsional bracing, which prevents the rotation of a cross section around its longitudinal axis;
- partial bracing, of the tension flange, which, although not fully preventing out-of-plane buckling, is equivalent to an elastic support.

In practical terms, bracings can be achieved using purlins and side-rails. Figure 5.46 illustrates typical bracing solutions: (a) lateral bracing, provided by a purlin bolted to the compression flange and (b) lateral and torsional bracing of a member.



a) Lateral b) Lateral and torsional

Figure 5.46 – Typical bracing

Bracing can also be achieved by a slab connected to the compression flange, as illustrated in Figure 5.47. In this case, the bracing is continuous along the member and it simultaneously prevents the transverse displacement and the torsional rotation of the cross section.

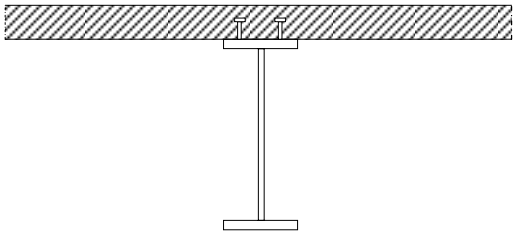


Figure 5.47 – Typical lateral and torsional bracing of the compression flange by a slab

At each rotating plastic hinge, the cross section should have effective lateral and torsional restraint with appropriate resistance to lateral forces and torsion induced by local plastic deformations of the member at this location

(clause 6.3.5.2(1)). According to clause 6.3.5.2(2), effective restraint should be provided according to the following rules:

- for members carrying either bending moment or bending and axial force, by lateral restraint to both flanges. This may be provided by lateral restraint to one flange and a stiff torsional restraint to the cross section preventing the lateral displacement of the compression flange relative to the tension flange, as illustrated in Figure 5.46b;
- for members carrying either bending moment alone or bending and axial tension in which the compression flange is in contact with a floor slab, by lateral and torsional restraint to the compression flange (e.g. by connecting it to a slab, as shown in Figure 5.47). For cross sections that are more slender than rolled I and H cross sections the distortion of the cross section should be prevented at the plastic hinge location (e.g. by means of a web stiffener also connected to the compression flange with a stiff joint from the compression flange into the slab).

In case it is not practicable to provide effective restraint at the plastic hinge location, it should be placed within a distance of $h/2$ along the length of the member, where h is its overall depth at the plastic hinge location (clause 6.3.5.2(4)).

The design of bracing systems must satisfy the requirements of clauses 6.3.5.2(3) and (5), as well as the provisions in clause 5.3.3 concerning imperfections, already presented in section 2.3.3. Firstly, the bracing system must resist the effects of local forces Q_m applied at each stabilized member at the plastic hinge locations, given by:

$$Q_m = 1.5\alpha_m \frac{N_{f,Ed}}{100}, \tag{5.40}$$

where $N_{f,Ed}$ is the axial force in the compression flange of the stabilized member at the plastic hinge location and α_m is defined in clause 5.3.3(1) as:

$$\alpha_m = \sqrt{0.5\left(1+\frac{1}{m}\right)}, \tag{5.41}$$

where m is the number of members to be restrained. In this verification all the external forces acting directly on the bracings should also be included (clause

5.3.3(5)). Secondly, at each plastic hinge location, the connection (e.g. bolts) of the compression flange to the resisting element at that point (e.g. purlin), and any intermediate element (e.g. diagonal brace) should be designed to resist a local force of at least 2.5 % of $N_{f,Ed}$ (defined in 6.3.5.2(5)B), transmitted by the flange in its plane and perpendicular to the web plane, without any combination with other loads. As a practical rule, a secondary member will have adequate rigidity to work as bracing as long as the depth of the cross section is at least 25 % of the depth of the braced member (Salter *et al*, 2004).

5.3.4. Verification of the stability of members with plastic hinges

5.3.4.1. Introduction

The verification of the stability of a segment containing plastic hinges requires adequate rotation capacity. This can be achieved by limiting the slenderness of the cross sections adjacent to the plastic hinge in order to avoid premature out-of-plane instability (lateral buckling). Note that the direct application of the methodology presented in section 3.7.3 and in sub-chapter 4.3 is not possible in this case, as the presence of plastic hinges was not contemplated in the underlying research (Horne *et al*, 1979).

According to EC3, the plastic design of structures is possible if out-of-plane buckling is prevented (clause 6.3.5.1) through:

- bracings at the points where rotating plastic hinges are formed that fulfil the conditions described in the previous section 5.3.3;
- guaranteed stability of the segments adjacent to plastic hinges.

This requirement can be stated in the following way:

$$L_{segment} \leq L_{stable} . \tag{5.42}$$

This verification leads to more restrictive results than the evaluation of the out-of-plane stability of segments not containing plastic hinges due to the additional requirement of adequate rotation capacity at the cross section where the plastic hinge is formed. Note that it is still necessary to verify the in-plane stability of the member or component (expressions (3.163), with $\chi_{LT} = 1.0$, as for members not containing plastic hinges.

In the particular case of prismatic segments with I or H cross section, in which $h/t_f \leq 40\varepsilon$, subjected to a linearly varying bending moment and without significant axial force ($N_{Ed} \leq 0.05N_{pl,Rd}$), the stable length is given by (clause 6.3.5.3(1)):

$$L_{stable} = \begin{cases} 35\varepsilon i_z & 0.625 \leq \psi \leq 1 \\ (60 - 40\psi)\varepsilon i_z & -1 \leq \psi \leq 0.625 \end{cases}, \tag{5.43}$$

where,

$$\psi = \frac{M_{Ed,\min}}{M_{pl.Rd}}. \tag{5.44}$$

Equation (5.43) is very easily applicable but, besides its restricted scope of application, it leads to quite conservative results. In the following sub-sections, more general procedures for the verification of expression (5.42) are presented, according to Annex BB.3.

5.3.4.2. Prismatic members constituted by hot-rolled or equivalent welded I sections

In the case of prismatic members formed of hot-rolled or equivalent welded I-sections, the stable length L_{stable} of expression (5.42) is given by (clause BB.3.1.1(1)):

$$L_m = \frac{38 i_z}{\sqrt{\frac{1}{57400}\left(\frac{N_{Ed}}{A}\right) + \frac{1}{756 \times C_1^2}\left(\frac{W_{pl,y}^2}{A I_t}\right)\left(\frac{f_y}{235}\right)^2}}, \tag{5.45}$$

where:

- N_{Ed} is the design value of the axial force in the member (in kN);
- i_z is the radius of gyration;
- C_1 is a factor that depends on the loading and on the conditions of support (indicated in section 3.7.4);
- A is the area of the cross section (in m^2);
- $W_{pl,y}$ is the plastic modulus of the section around the major axis (in m^3);
- I_T is the torsion constant (in m^4);
- f_y is the yield stress of steel, in MPa.

This expression is valid as long as the segment is braced at the plastic hinge location and the other end fulfils one of the following conditions concerning bracings:

- lateral bracing of the compression flange, with that flange is in compression all along the length of the segment;
- torsional bracing.

As there are many situations in which partial bracings exist along the tension flange, it is possible to take advantage of that situation to achieve longer stable lengths. In this case, and with reference to Figure 5.48, it is necessary to cumulatively satisfy the following criteria:

$$L_2 \leq L_m ; \tag{5.46a}$$

$$L_{segment} \leq L_s , \tag{5.46b}$$

that is, the distance of the plastic hinge to the first bracing of the tension flange (L_2) should be smaller than the stable length L_m defined in equation (5.45) and the total length of the segment should be smaller than the stable length L_s, as long as there is at least one intermediate partial bracing (bracing to the tension flange).

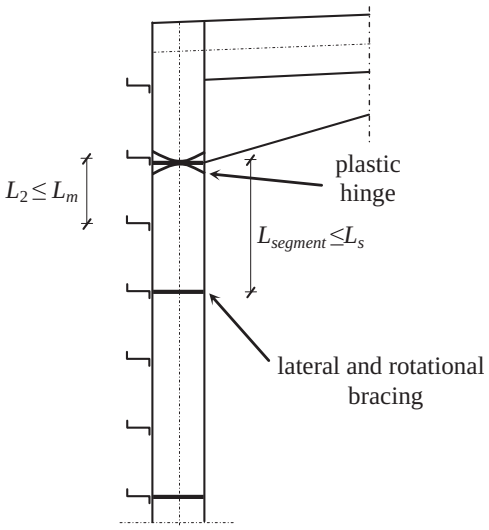


Figure 5.48 – Definition of stable length with partial bracings

The stable length L_s is, in case of a uniform bending moment acting along the segment, given by (clause BB.3.1.2(1)):

$$L_k = \frac{\left(5.4 + \frac{600 f_y}{E}\right)\left(\frac{h}{t_f}\right) i_z}{\sqrt{5.4\left(\frac{f_y}{E}\right)\left(\frac{h}{t_f}\right)^2 - 1}}, \tag{5.47}$$

where h is the depth of the cross section. In case of a bending moment with a linear gradient and a compressive axial force acting along the segment, L_s is given by (clause BB.3.1.2(2)):

$$L_s = \sqrt{C_m} L_k \left(\frac{M_{pl,y,Rk}}{M_{N,y,Rk} + aN_{Ed}} \right), \tag{5.48}$$

where:

- C_m is the modification factor for a linear moment gradient (defined in sub-section 5.3.4.4);
- a is the distance between the centroid of the member where the plastic hinge is formed and the centroid of the restraint member.

Finally, in the case of a bending moment with a non-linear gradient and a compressive axial force acting along the segment, L_s is given by (clause BB.3.1.2(3)):

$$L_s = \sqrt{C_n} L_k, \tag{5.49}$$

where C_n is the modification factor for a non-linear moment gradient (defined in sub-section 5.3.4.4). Note that generally $L_s > L_m$.

5.3.4.3. Haunched or tapered members made of rolled sections or equivalent welded I sections

In the case of haunched or tapered members made of rolled sections or equivalent welded I sections, the procedure is analogous to the previous case. The maximum stable length L_{stable} of expression (5.42) is given by (clause BB.3.2.1(1)), for a three flange haunch:

$$L_m = \frac{38 i_z}{\sqrt{\frac{1}{57400}\left(\frac{N_{Ed}}{A}\right) + \frac{1}{756 \times C_1^2}\left(\frac{W_{pl,y}^2}{AI_t}\right)\left(\frac{f_y}{235}\right)^2}}, \qquad (5.50)$$

whereas for a two flange haunch, L_m is given by:

$$L_m = 0.85 \frac{38 i_z}{\sqrt{\frac{1}{57400}\left(\frac{N_{Ed}}{A}\right) + \frac{1}{756 \times C_1^2}\left(\frac{W_{pl,y}^2}{AI_t}\right)\left(\frac{f_y}{235}\right)^2}}, \qquad (5.51)$$

where:

N_{Ed} is the design value of the axial force in the member (in kN)

i_z is the minimum radius of gyration in the segment;

C_1 is a factor that depends on the loading and on the conditions of support (indicated in section 3.7.4);

$W_{pl,y}^2 / AI_t$ is the maximum value in the segment;

A is the cross section area (in m^2) at the point where $W_{pl,y}^2 / AI_t$ is maximum for the tapered member;

$W_{pl,y}$ is the major axis plastic section modulus of the member (in m^3);

I_t is the torsion constant of the member (in m^4);

f_y is the yield stress of steel, in MPa.

These expressions are valid as long as the bracing fulfils the requirements given in 5.3.4.2 above for expression (5.45) to be valid.

In case of partial bracings along the tension flange, the procedure is similar to that given above in 5.3.4.2, both expressions (5.46) being required. In this case, and referring to Figures 5.49 and 5.50, the stable length L_s, in case of a moment with or without linear gradient and a compressive axial force acting along the segment, is given by (clause BB.3.2.2(1)):

for a three flange haunch,

$$L_s = \frac{\sqrt{C_n} L_k}{c}, \qquad (5.52)$$

whereas for a two flange haunch,

$$L_s = 0.85\frac{\sqrt{C_n}L_k}{c}, \tag{5.53}$$

where:

C_n is the modification factor for a non-linear moment gradient (defined in sub-section 5.3.4.4);

L_k is the length derived for a prismatic member with a cross section equal to the shallowest cross section, given by equation (5.47);

c is the taper factor (defined in sub-section 5.3.4.4).

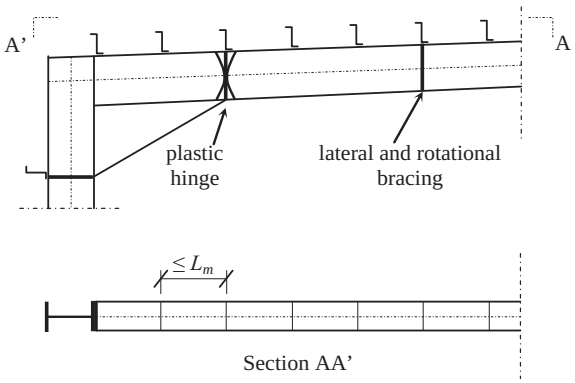


Figure 5.49 – Three flange haunch

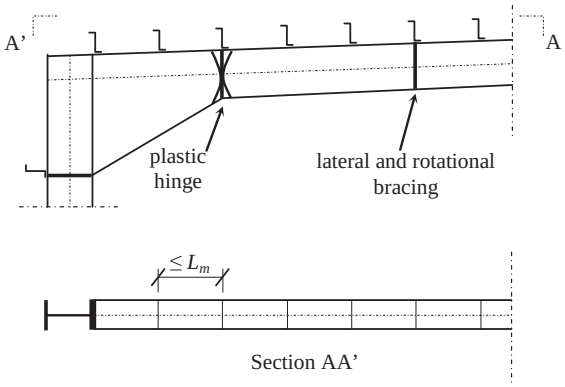


Figure 5.50 – Two flange haunch

Note that, according to clause 6.3.5.3(2)B, where a rotated plastic hinge location occurs immediately adjacent to one end of a haunch, the

tapered segment need not be treated as a segment adjacent to a plastic hinge location if the following criteria are satisfied:

- the restraint at the plastic hinge location should be within a distance *h*/2 along the length of the tapered segment, not the uniform segment;
- the compression flange of the haunch remains elastic throughout its length.

5.3.4.4. Modification factors for moment gradients in members laterally restrained along the tension flange

In the case of members along laterally restrained the tension flange, the modification factor for linear moment gradients is given by (clause BB.3.3.1):

$$C_m = \frac{1}{B_0 + B_1\beta_t + B_2\beta_t^2}, \tag{5.54}$$

where β_t is is the ratio of the algebraically smaller end moment to the larger end moment as illustrated in Figure 5.51, and:

$$B_0 = \frac{1+10\eta}{1+20\eta}; \tag{5.55a}$$

$$B_1 = \frac{5\sqrt{\eta}}{\pi+10\sqrt{\eta}}; \tag{5.55b}$$

$$B_2 = \frac{0.5}{1+\pi\sqrt{\eta}} - \frac{0.5}{1+20\eta}, \tag{5.55c}$$

η is defined as:

$$\eta = \frac{N_{crE}}{N_{crT}}, \tag{5.56}$$

where N_{crT}, is given by equation (4.14) and N_{crE} is defined by equation (4.19).

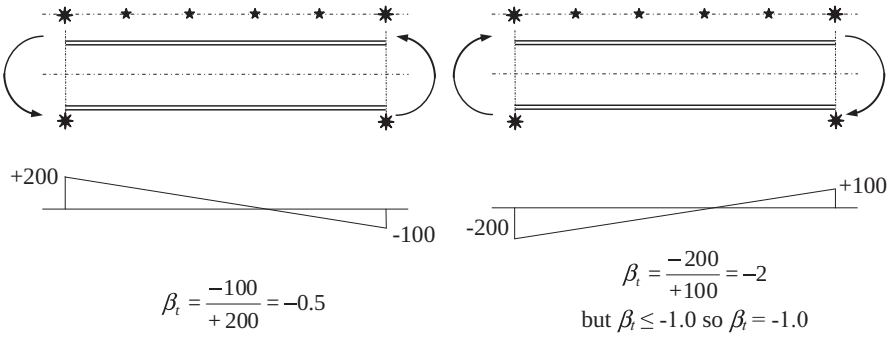


Figure 5.51 – Value of β_t

The modification factor for non linear moment gradients is given by (clause BB.3.3.2):

$$C_n = \frac{12}{\left[R_1 + 3R_2 + 4R_3 + 3R_4 + R_5 + 2\left(R_S - R_E\right)\right]}, \tag{5.57}$$

where the values of R_i (i = 1,...,5) are calculated at the ends, quarter points and mid-length of the segment and are given by:

$$R_i = \frac{M_{y,Ed} + aN_{Ed}}{f_y W_{pl,y}}, \tag{5.58}$$

where a has the same meaning as in equation (5.48) and the index i denotes 5 equally-spaced cross sections along the segment, as shown in Figure 5.52.

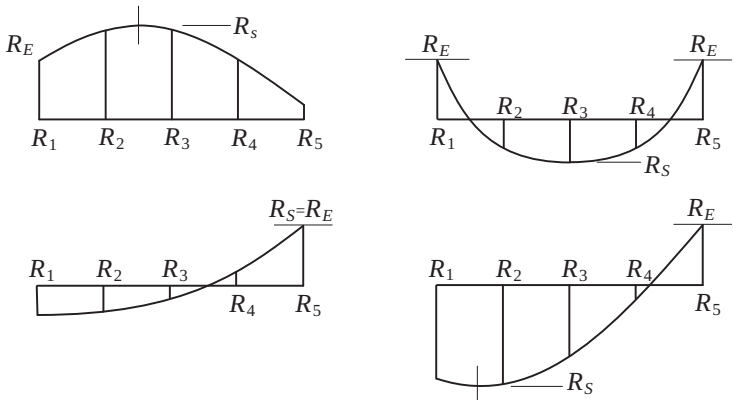


Figure 5.52 – Definition of the cross sections for a non linear moment variation

Only positive values of R_i should be included as well as only positive values of ($R_S - R_E$). R_E is the greater of R_1 or R_5 and R_S is the maximum value of R_i anywhere in the length L.

The taper factor is given by (clause BB.3.3.3), for tapered members or segments (Figure 5.53a):

$$c = 1 + \frac{3}{\frac{h}{t_f} - 9}\left(\frac{h_{\max}}{h_{\min}} - 1\right)^{2/3}, \tag{5.59}$$

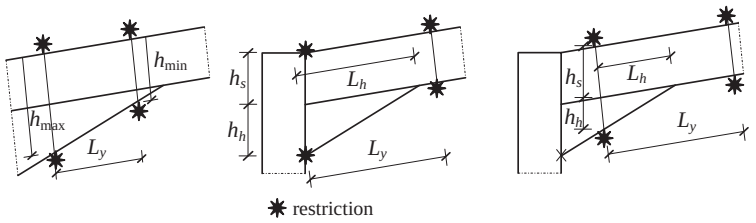
whereas for haunched members or segments (Figure 5.53b or c):

$$c = 1 + \frac{3}{\frac{h}{t_f} - 9}\left(\frac{h_h}{h_s}\right)^{2/3}\sqrt{\frac{L_h}{L_y}}, \tag{5.60}$$

where, according to Figure 5.53:

h_h is the additional (vertical) depth of the haunch or taper;
$h_{\max}$ is the maximum depth of cross section within the length L_y;
$h_{\min}$ is the minimum depth of cross section within the length L_y;
h_s is the vertical depth of the un-haunched section;
L_h is the length of haunch within the length L_y;
L_y is the length between points at which the compression flange is laterally restrained.

The quotient h/t_f must be calculated for the cross section with the shallowest depth. Note that equations (5.59) and (5.60) are only valid for members with prismatic flanges for which $h \geq 1.2\ b$ and $h / t_f \geq 20$ (clause BB.3.3.3(1)B).

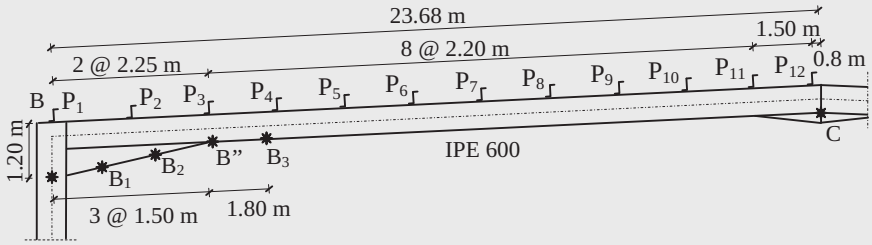


a) Tapered segment b) Haunched segment c) Haunched segment

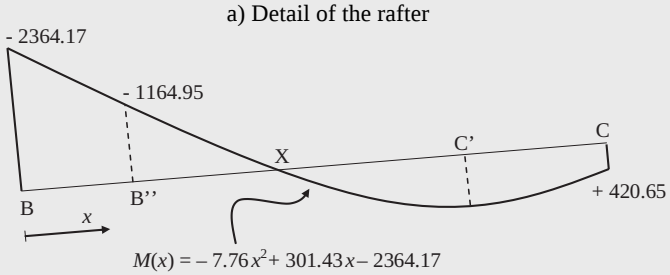
Figure 5.53 – Dimensions for the definition of the taper factor

5.3.5. Worked examples

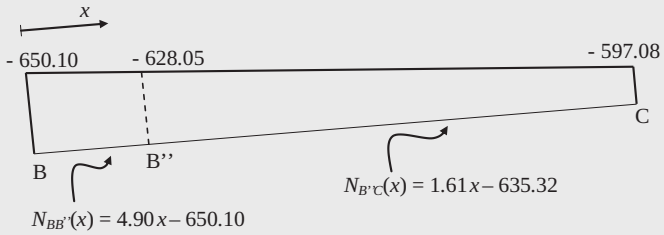
Example 5.2: Consider the rafter in Figure 5.54a (S 355 steel), subject to the design internal force diagrams indicated in Figure 5.54b. These forces are already factored and include the P-Δ and P–δ 2nd order effects. Assume that the purlins consist of Z sections with a depth of 200 mm, connected to the top flange of the rafter by a connection with two bolts and with the layout indicated in Figure 5.54. Verify the safety of the rafter.



a) Detail of the rafter



b1) Bending moment diagram



b2) Axial force diagram

Figure 5.54 – Rafter

The relevant geometrical properties of the cross section with the shallowest depth (IPE 600) are as follows: A = 156.0 cm^2, A_{vz} = 83.78 cm^2, h = 600 mm, b = 220 mm, t_w = 12 mm, t_f = 19 mm, I_y = 92080 cm^4, i_y = 24.3 cm,

$W_{el,y}$ = 3069 cm^3, $W_{pl,y}$ = 3512 cm^3, I_z = 3387 cm^4, i_z = 4.66 cm, $W_{el,z}$ = 307.9 cm^3, $W_{pl,z}$ = 485.6 cm^3, I_T = 165.4 cm^4 and I_w = 2846×10^3 cm^6. Note also that an IPE 600 is a class 1 cross section in pure bending.

For the internal force diagrams of Figure 5.54b, the rafter does not contain any plastic hinge (as $M_{y,Ed} < M_{pl,y,Rd}$), and so its stability should be verified according to sub-chapter 4.3. Examination of the bending moment diagram shows that the compression flange is laterally restrained between points X and C, whereas between points B and X the lateral bracing is only partial, provided by the connection of the purlins to the tension flange.

Also note that for rafters, according to Salter *et al* (2004), the point of zero moment X (x = 10.91 m) can be assumed as a virtually braced section, as the following conditions are verified: i) the rafter is an IPE (IPE 600); ii) the connections between the purlins and the rafter have at least two bolts and iii) the depth of the purlin is greater than 25 % of the depth of the rafter (0.2 m > 0.25 × 0.6 = 0.15 m).

i) *Verification of the in-plane stability*

According to King (2001b), in pitched-roof portal frames, the rafters resist: i) a relatively low compressive axial force and ii) relatively high bending moments. The latter occur far from the mid-span of the member where the amplification of the moment by the axial force is maximum, so the verification of in-plane buckling is not critical. Besides, because the forces presented in Figure 5.54b correspond to the results of the analysis already considering the P–δ and P–Δ 2nd order effects (see example 5.1, case *e*), it is only necessary to check the cross sectional resistance.

The classification of the cross sections must be done in bending and axial force, leading to the results in Table 5.10.

Table 5.10 – Classification of the cross sections

	B	B''	C'	C
$M_{y,Ed}$ (kNm)	2364.17	1164.95	561.88	420.65
N_{Ed} (kN)	650.10	628.05	604.07	597.08
Classification	Class 3	Class 2	Class 2	Class 2

Cross section B is class 3 because of the web, whereas the flanges are class 1; so, according to clause 5.5.2(11), the cross section can be classified as class 2, as long as an effective cross section is considered. The calculation of the effective cross section implies an iterative procedure according to clause 6.2.2.4; however, in this example the plastic neutral axis of the effective cross section is assumed to be located at the level of the intermediate flange. Hence, the effective cross section is represented in Figure 5.55. Neglecting the contribution of the intermediate flange gives A_{eff} = 205 cm^2 and $W_{eff,pl,y}$ = 8257 cm^3, and therefore $M_{pl,y,Rd}$ = 2931.10 kNm. The verification of the cross section resistance of cross section B using equation (3.148) leads to:

$$M_{N,y,Rd} = M_{pl,y,Rd}\frac{1-n}{1-0.5a} = 3542.75 \text{ kNm},$$

however, as $M_{N,y,Rd} > M_{pl,y,Rd}$ then, $M_{N,y,Rd} = M_{pl,y,Rd}$ = 2931.10 kNm.

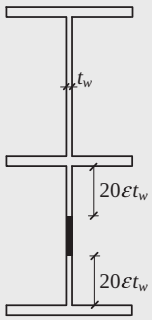


Figure 5.55 – Effective class 2 cross section

Table 5.11 summarizes the results for the other critical cross sections.

Table 5.11 – Cross section resistance

	B	B''	C'	C
$M_{N,y,Rd}$ (kNm)	2931.10	1246.76	1246.76	1246.76

ii) *Verification of the out-of-plane stability*

The verification of the out of plane stability can take advantage of the partial bracing provided by the purlins. Between points B and X, the purlins prevent lateral displacements of the tension flange only, so that it is necessary to restrain the compression flange. Adopting the bracing positions detailed in

Figure 5.54a, six distinct segments must be considered: BB_1, B_1B_2, B_2B'', $B''B_3$, B_3X and XC, with lengths $L_t^{BB_1} = L_t^{B_1B_2} = L_t^{B_2B^*} = 1.50$ m, $L_t^{B^*B_3} = 1.80$ m, $L_t^{B_3X} = 4.61$ m and $L_t^{XC} = 12.77$ m, respectively. Considering firstly the segment between points B and B_1, in which there are partial bracings to the tension flange and the segment is tapered with a varying depth between 1.20 m and 1.00 m, it is necessary, first, to determine the elastic critical loads for the compression force in a bending mode and in a torsional mode. Equations (4.19), (4.15) and (4.14) give, successively (considering the properties of the shallowest cross section):

$$N_{crE} = \frac{\pi^2 EI_z}{L_t^2} = \frac{\pi^2 \times 210 \times 10^6 \times 3393 \times 10^{-8}}{1.5^2} = 31255.96 \text{ kN};$$

$$i_s^2 = i_y^2 + i_z^2 + a^2 = 38.44^2 + 4.08^2 + 60^2 = 5094 \text{ cm}^2;$$

$$N_{crT} = \frac{1}{i_s^2}\left(\frac{\pi^2 EI_z a^2}{L_t^2} + \frac{\pi^2 EI_w}{L_t^2} + GI_t\right) =$$

$$= \frac{1}{5094 \times 10^{-4}} \times \frac{\pi^2 \times 210 \times 10^6}{1.5^2} \times \left(3393 \times 10^{-8} \times 0.6^2 + 8112 \times 10^{-9}\right) +$$

$$+ \frac{80.77 \times 10^6 \times 188 \times 10^{-8}}{5094 \times 10^{-4}} = 37057.20 \text{ kN}.$$

Next, the critical moment is calculated through equations (4.16) and (4.17). The elastic critical moment for lateral-torsional buckling for a uniform bending moment and standard bracing conditions (equation (4.16)) is given by:

$$M_{cr0} = \left(\frac{i_s^2}{2a}\right) N_{cr} = \left(\frac{0.5094}{2 \times 0.6}\right) \times 37057.20 = 15730.99 \text{ kNm}.$$

The elastic critical moment for the applied loading (non linear variation of bending moment) implies the subdivision of the segment into 4 sections of equal length, such as indicated in Figure 5.56,

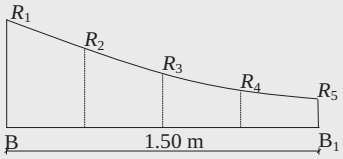


Figure 5.56 – Bending moment diagram in segment BB_1

and the determination of the applied bending moments and the bending resistance at those sections, summarized in Table 5.12.

Table 5.12 – Applied bending moments and bending resistance

	R_1	R_2	R_3	R_4	R_5
$M_{y,Edi}$	2364.20	2252.20	2142.50	2034.90	1929.50
$M_{c,Rdi}$	2931.10	2807.55	2686.34	2567.45	2441.30
$M_{y,Edi}/M_{c,Rdi}$	0.807	0.802	0.798	0.793	0.790

Equations (4.20) and (4.21) lead to:

$$\mu_{SE} = \left(\frac{M_{y,EdS}}{M_{c.RdS}} - \frac{M_{y,EdE}}{M_{c.RdE}} \right) = 0.802 - 0.807 = -0.005 ,$$

but as $\mu_{SE} < 0$, this term is neglected.

$$m_t = \frac{1}{12} \left(\frac{M_{c.Rd}}{M_{y,Ed}} \right)_{\min} \left(\frac{M_{y,Ed1}}{M_{c.Rd1}} + 3\frac{M_{y,Ed2}}{M_{c.Rd2}} + 4\frac{M_{y,Ed3}}{M_{c.Rd3}} + 3\frac{M_{y,Ed4}}{M_{c.Rd4}} + \right.$$

$$\left. + \frac{M_{y,Ed5}}{M_{c.Rd5}} \right) = 0.989.$$

From Table 4.7, by interpolation, $c = c_0 = 1.015$, leading to:

$$M_{cr} = \left(\frac{1}{m_t c^2} \right) M_{cr0} = \left(\frac{1}{0.989 \times 1.015^2} \right) \times 15730.99 = 15441.10 \text{ kNm} .$$

The lateral-torsional buckling resistance of the rafter is verified according to clause 6.3.2, with $L_t^{BB_1} = 1.50 \text{ m}$ and $M_{cr}^{BB_1} = 15441.10 \text{ kNm}$. Hence:

$$\overline{\lambda}_{LT} = \sqrt{\frac{W_{eff,pl,y} \times f_y}{M_{cr}}} = 0.44 \Rightarrow \quad \chi_{LT} = 0.91 ;$$

$$\Rightarrow M_{b,Rd} = \chi_{LT\, eff,pl,y} \times W_{eff,pl,y} \times f_y / \gamma_{M1} = 2672.16 \text{ kNm} > 2364.20 \text{ kNm} .$$

Table 5.13 summarizes the verification of the lateral-torsional buckling resistance for the other segments.

Table 5.13 – Verification of the lateral-torsional buckling resistance

	L_t	N_{crT}	M_{cr0}	M_{cr}	λ_{LT}	χ_{LT}	$M_{b,Rd}$	$M_{Ed}/M_{b,Rd}$
B_1B_2	1.50	36125.2	12686.7	12585.0	0.45	0.91	2289.0	0.84
B_2B''	1.50	35023.0	9684.1	10313.9	0.42	0.92	1690.2	0.91
$B'B_3$	1.80	24506.1	6776.1	8182.9	0.39	1.00	1246.9	0.93
B_3X	4.61	4248.0	1174.6	2542.1	0.70	0.78	977.0	0.79

The flexural buckling resistance of the rafter is given by equation (3.101):

$$N_{b.Rd.z} = \chi_z A_{eff} f_y / \gamma_{M1} .$$

However, since $N_{Ed}/N_{cr} < 0.04$ (clause 6.3.1.2(4)), flexural buckling can be neglected. The same condition applies for segments BB_1, B_1B_2, B_2B'' and $B''B_3$. For segment B_3X, $N_{Ed}/N_{cr} > 0.04$, so that

$$\overline{\lambda_z} = \sqrt{\frac{A \times f_y}{N_{cr,z}}} = 1.29 \Rightarrow \chi_z = 0.43 \Rightarrow$$

$$N_{b.Rd.z} = \chi_z \times A \times f_y / \gamma_{M1} = 2378.04 \text{ kN} > 632.93 \text{ kN} .$$

In this case, the buckling resistance considering the combined effect of bending and axial force (expression (3.163b)), with $k_{zy} = 0.92$, yields:

$$\frac{N_{Ed}}{\chi_z N_{Rk}/\gamma_{M1}} + k_{zy} \frac{M_{y,Ed}}{\chi_{LT} M_{y,Rk}/\gamma_{M1}} = \frac{632.93}{2378.40} + 0.92 \times \frac{773.29}{976.96} = 0.99 \le 1.0 .$$

For segment XC the situation is simpler, as the purlins provide total bracing and it is only required to check the out-of-plane stability between purlins ($L_{z,E}^{BX} = 2.2$ m). The maximum moment $M_{\max}$ = 561.88 kNm, occurs at x = 19.41 m, between purlins P_9 (x = 17.7 m) and P_{10} (x =19.9 m). Then, considering the sub-segment between purlins P_9 and P_{10}, application of equations (4.19), (4.16) and (4.17) leads to:

N_{crT} = 16604.5 kN; M_{cr0} = 4591.27 kNm; M_{cr} = 4635.30 kNm

$$\overline{\lambda}_{LT} = \sqrt{\frac{W_{pl,y} \times f_y}{M_{cr}}} = 0.52 \Rightarrow \quad \chi_{LT} = 0.88$$

$\Rightarrow M_{b,Rd} = \chi_{LT,pl,y} \times W_{pl,y} \times f_y / \gamma_{M1} = 1092.11 \text{ kNm} > 561.88 \text{ kNm}$.

Similarly, the flexural buckling resistance of the sub-segment is given by:

$\overline{\lambda_z} = 0.62 \Rightarrow \chi_z = 0.83 \Rightarrow$

$N_{b.Rd.z} = \chi_z \times A \times f_y / \gamma_{M1} = 4584.99 \text{ kN} > 610.93 \text{ kN}.$

Finally, the buckling resistance considering the combined effect of bending and axial force, with k_{zy} = 0.99, is obtained from:

$$\frac{N_{Ed}}{\chi_z N_{Rk}/\gamma_{M1}} + k_{zy} \frac{M_{y,Ed}}{\chi_{LT} M_{y,Rk}/\gamma_{M1}} = \frac{610.93}{4584.99} + 0.99 \times \frac{561.88}{1092.11} = 0.62 \le 1.0.$$

Example 5.3: Consider the column in Figure 5.57 (steel grade S 355), subject to the design forces shown; these are already factored. Verify the safety of the column.

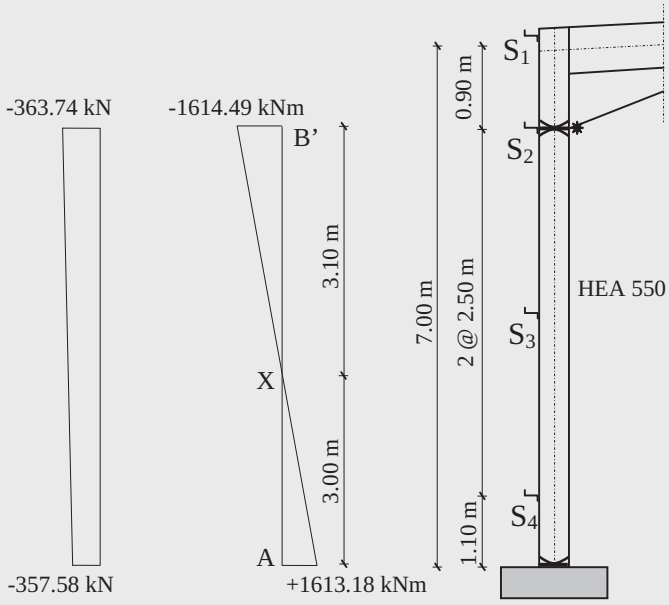


Figure 5.57 – Detail of the column

The relevant geometrical properties of the cross section (HEA 550) are the following: A = 211.8 cm^2, A_{vz} = 83.72 cm^2, h = 540 mm, b = 300 mm, t_w = 12.5 mm, t_f = 24 mm, I_y = 111900 cm^4, i_y = 22.99 cm, $W_{el,y}$ = 4146 cm^3, $W_{pl,y}$ = 4622 cm^3, I_z = 10820 cm^4, i_z = 7.15 cm, $W_{el,z}$ = 721.3 cm^3, $W_{pl,z}$ = 1107 cm^3, I_T = 351.5 cm^4 and I_w = 7189x10^3 cm^6. Also note that a HEA 550 is a class 1 cross section in pure bending. According to the internal force diagrams of Figure 5.57 (see example 5.1), the column contains two plastic hinges, one at each end of the member, and so its stability should be verified according to section 5.3.4. Examination of the bending moment diagram shows that the compression flange is braced by S_4 between points A and X, whereas between points X and B' the lateral bracing is only partial, provided by the connection of the side-rails to the tension flange.

The verification of the in-plane stability is performed using expressions (3.163), with χ_{LT} = 1. As the column cross section is class 1, $\Delta M_{y,Ed}$ = 0.

$$\frac{N_{Ed}}{\chi_y N_{Rk}/\gamma_{M1}} + k_{yy}\frac{M_{y,Ed}}{M_{y,Rk}/\gamma_{M1}} \le 1.0\,;$$

$$\frac{N_{Ed}}{\chi_z N_{Rk}/\gamma_{M1}} + k_{zy}\frac{M_{y,Ed}}{M_{y,Rk}/\gamma_{M1}} \le 1.0\,.$$

However, for both expressions, N_{Ed}/N_{cr} < 0.04, and so it is not necessary to check the in-plane buckling resistance of the column, but only the cross sectional resistance. Application of equation (3.148) gives: at cross section A: $M_{N,y,Rd}$ = $M_{pl,y,Rd}$ = 1640.81 kNm; and at cross section B': $M_{N,y,Rd}$ = $M_{pl,y,Rd}$ = 1640.81 kNm.

The verification of the out-of-plane stability can take advantage of the partial bracing provided by the side-rails, according to expressions (5.46). Specifically,

$$L_2 = 2.50\ \text{m} \le L_m\,;$$

$$L_{segment} = 6.10\ \text{m} \le L_s\,.$$

where L_m and L_s are given by equations (5.45) and (5.48), respectively. Equation (5.45) gives:

$$L_m = \frac{38 i_z}{\sqrt{\frac{1}{57400}\left(\frac{N_{Ed}}{A}\right) + \frac{1}{756 \times C_1^2}\left(\frac{W_{pl,y}^2}{A I_t}\right)\left(\frac{f_y}{235}\right)^2}} =$$

$$= \frac{38 \times 0.0715}{\sqrt{\frac{1}{57400} \times \left(\frac{363.74}{0.02118}\right) + \frac{1}{756 \times 2.45^2} \times \left(\frac{\left(4.622 \times 10^{-3}\right)^2}{0.02118 \times 3.515 \times 10^{-6}}\right) \times \left(\frac{355}{235}\right)^2}}$$

$= 4.08 \text{ m} > 2.50 \text{ m}.$

For the calculation of L_s, it is first necessary to determine C_m; applying equations (4.19), (4.15), (4.14), (5.56) and (5.55) in succession gives:

$$N_{crE} = \frac{\pi^2 E I_z}{L_t^2} = \frac{\pi^2 \times 210 \times 10^6 \times 10820 \times 10^{-8}}{6.1^2} = 6026.8 \text{ kN};$$

$$i_s^2 = i_y^2 + i_z^2 + a^2 = 22.99^2 + 7.15^2 + 37^2 = 1949 \text{ cm}^2;$$

$$N_{crT} = \frac{1}{i_s^2}\left(\frac{\pi^2 E I_z a^2}{L_t^2} + \frac{\pi^2 E I_w}{L_t^2} + G I_t\right) =$$

$$= \frac{1}{0.1949} \times \frac{\pi^2 \times 210 \times 10^6}{6.1^2} \times \left(10820 \times 10^{-8} \times 0.37^2 + 7189 \times 10^{-9}\right) +$$

$$+ \frac{80.77 \times 10^6 \times 351.5 \times 10^{-8}}{0.1949} = 7745.8 \text{ kN};$$

$$\eta = \frac{N_{crE}}{N_{crT}} = \frac{6666.4}{8411.8} = 0.78;$$

$$B_0 = \frac{1 + 10\eta}{1 + 20\eta} = \frac{1 + 10 \times 0.79}{1 + 20 \times 0.79} = 0.530;$$

$$B_1 = \frac{5\sqrt{\eta}}{\pi + 10\sqrt{\eta}} = \frac{5 \times \sqrt{0.79}}{\pi + 10 \times \sqrt{0.79}} = 0.369;$$

$$B_2 = \frac{0.5}{1 + \pi\sqrt{\eta}} - \frac{0.5}{1 + 20\eta} = \frac{0.5}{1 + \pi \times \sqrt{0.79}} - \frac{0.5}{1 + 20 \times 0.79} = 0.102.$$

According to Figure 5.51,

$\beta_t = -1.0,$

and, from equation (5.54),

$$C_m = \frac{1}{B_0 + B_1\beta_t + B_2\beta_t^2} = \frac{1}{0.529 + 0.370 \times (-1) + 0.102 \times (-1)^2} = 3.80.$$

From expression (5.47),

$$L_k = \frac{\left(5.4 + \frac{600 f_y}{E}\right)\left(\frac{h}{t_f}\right) i_z}{\sqrt{5.4\left(\frac{f_y}{E}\right)\left(\frac{h}{t_f}\right)^2 - 1}} = \frac{\left(5.4 + \frac{600 \times 355}{210000}\right) \times \left(\frac{0.54}{0.024}\right) \times 0.0715}{\sqrt{5.4 \times \left(\frac{355}{210000}\right) \times \left(\frac{0.54}{0.024}\right)^2 - 1}} = 5.42.$$

Finally, from equation (5.48),

$$L_s = \sqrt{C_m} L_k \left(\frac{M_{pl,y,Rk}}{M_{N,y,Rk} + aN_{Ed}}\right) =$$

$$= \sqrt{3.80} \times 5.42 \times \left(\frac{1640.8}{1640.8 + 0.37 \times 363.74}\right) = 9.76 \text{ m} > 6.10 \text{ m}.$$

Note that the use of equation (5.43) would lead to the more conservative result of L_{stable} = 3.49 m < 6.10 m so that this calculation would show the structural arrangement to be inadequate. Also, with N_{Ed} / $N_{pl,Rd}$ = 4.8 % ≈ 5 % and $h/\varepsilon t_f$ = 27.65 < 40, the use of equation (5.43) is at the limit of the scope of application.

5.4. DESIGN EXAMPLE 2: PLASTIC DESIGN OF INDUSTRIAL BUILDING

5.4.1. Introduction

The plastic design of a typical single-span pitched-roof portal frame industrial building is presented in this design example. This is a type of structure that is particularly suitable for the application of plastic analysis and well illustrates all the aspects presented in this chapter. The design example focuses only on

the design of a representative transverse frame as a plane frame. The design of secondary members such as sheeting, purlins and side-rails and the longitudinal stability of the building are not treated in this example.

In the presentation of this example, the following design sequence is adopted:

– General description, where the geometrical requirements for the structure are established.
– Quantification of actions, load combinations and general safety criteria, where the self-weight of the structure is estimated and all the other permanent actions, imposed loads, snow, wind and temperature actions are quantified.
– Pre-design, where the dimensions of the structural members are defined and the details are presented.
– Structural analysis, where the various relevant analyses are presented in detail, with a particular emphasis on plastic analysis of the structure.
– Code checks, where the normative requirements of EN 1993-1-1 are thoroughly verified.
– Synthesis, where the design results are summarized and a summary of the bill of quantities is presented.

5.4.2. General description

The industrial building is 140 m long, has a span (centre to centre) of 47 m, a height of 7 m, a rafter slope of $\alpha = 7^o$ and a spacing between frames of 7.5 m, as illustrated in Figure 5.58. The steel cross sections consist of hot-rolled I-sections.

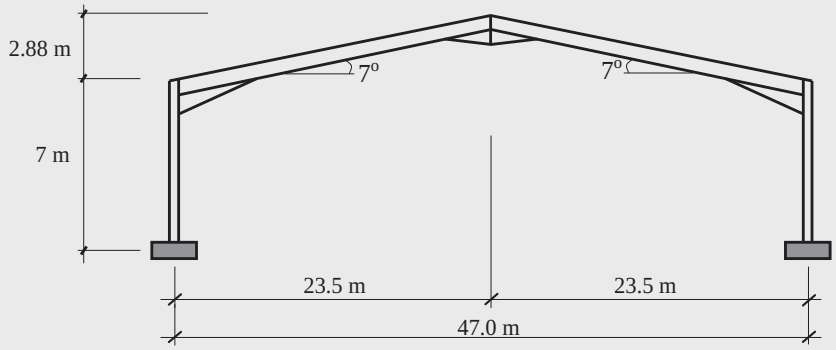


Figure 5.58 – Portal frame

The rafters include 4.5 m long eaves haunches and 1.5 m long haunches close to the apex connection. The column bases are assumed rigid and full-strength. The steel used is S 355J2 according to EN 10025-2 (CEN, 2004c). The building is located at an altitude of 610 m. Assume a basic wind velocity of $v_{b,0}$ = 37.27 m/s.

5.4.3. Quantification of actions, load combinations and general safety criteria

5.4.3.1. General criteria

The quantification of the actions and their combinations was made according to EN 1990 (CEN, 2002a), EN 1991-1-1 (CEN, 2002b), EN 1991-1-3 (CEN, 2003) and EN 1991-1-4 (CEN, 2005e), considering the permanent actions that correspond to the self-weight of the structure and non-structural members, the variable actions corresponding to imposed loads, snow and wind and the imperfections.

5.4.3.2. Permanent actions

In quantifying the permanent actions, not only is the self-weight of structural members considered, but also the self-weight of the purlins and that of the roof sheeting, which are estimated as 0.35 kN/m^2. Additionally, a permanent action that corresponds to permanent suspended equipment with a value of 0.25 kN/m^2 is also considered. For each frame, considering the spacing of 7.5m, a total value of 4.5 kN/m is obtained.

5.4.3.3. Imposed loads

The imposed load on the roof is given according to EN 1991-1-1. Considering that the roof is not accessible, except for repairing/maintenance operations (H category), the characteristic value of the uniformly distributed imposed load q_k, (defined in the National Annexes), must be between 0.0 kN/m^2 and 1.0 kN/m^2, in horizontal plan (clause 6.3.4.2). In this case, taking a value of q_k = 0.5 kN/m^2, and considering the spacing between frames of 7.5 m, a total value of 3.75 kN/m is obtained.

5.4.3.4. Snow loads

According to EN 1991-1-3, the quantification of the snow action is given by (clause 5.2.):

$$S = \mu_1 C_e C_t S_k, \tag{5.61}$$

where μ_1 is the snow load shape coefficient, C_e is the exposure coefficient, C_t is the thermal coefficient and S_k is the characteristic value of the snow action, at the level of the ground, for a given location. For the Iberian Peninsula, S_k is given by:

$$S_k = \left(0.498Z - 0.209\right)\left[1 + \left(\frac{A}{452}\right)^2\right], \tag{5.62}$$

where Z is a coefficient that depends on the location of the building and A is the altitude above the sea level (in metres). In this case, μ_1 = 0.8 (since 0º < α < 30º); C_e = 1.0; C_t = 1.0; Z = 1.0 and as A = 610 m, S = 0.65 kN/m^2 in horizontal plan. Considering the distance between frames of 7.5 m, a total value of 4.875 kN/m is obtained.

5.4.3.5. Wind loads

The quantification of wind forces in the building is made according to EN 1991-1-4. According to clause 5.3(3), the wind forces are calculated by the vectorial summation of external forces, $F_{w,e}$, and internal forces, $F_{w,i}$, given by equations (4.27) and (4.28),

$$F_{w,e} = c_s c_d \sum_{surfaces} W_e A_{ref},$$

and

$$F_{w,i} = \sum_{surfaces} W_i A_{ref},$$

where $c_s c_d$ is the structural factor, A_{ref} is the reference area of the individual surface, and W_e and W_i are the external and internal pressures on the individual surface at reference heights z_e and z_i, for external and internal pressures respectively, given by the equations (4.29) and (4.30):

$$W_e = q_p\left(z_e\right) c_{pe},$$

and

$$W_i = q_p\left(z_i\right) c_{pi},$$

$q_p(z)$ is the peak velocity pressure, and c_{pe} and c_{pi} are the pressure coefficients for the external and internal pressures, respectively.

The structural factor ($c_s c_d$) is given by clause 6.2(1), and in case of buildings with a height lower than 15 m this coefficient can be taken as 1 (clause 6.2(1)).

i) Calculation of the peak velocity pressure of the wind ($q_p(z)$)

The peak velocity pressure of the wind is given by equation (4.31), (clause 4.5 and equation (4.8) of EN 1991-1-4):

$$q_p\left(z\right) = c_e\left(z\right) q_b,$$

where $c_e(z)$ is the exposure factor and q_b is the basic velocity pressure of wind, given by:

$$q_b = \frac{1}{2}\rho\, v_b^2, \tag{5.63}$$

in which ρ is the density of the wind air (recommended value of 1.25 kg/m^3) and v_b is the basic wind velocity. The latter is calculated according to clause 4.2 and expression (4.1) of EN 1991-1-4 (equation (4.35)):

$$v_b = c_{dir}\; c_{season}\; v_{b,0},$$

where c_{dir} and c_{season} are directional and season factors, respectively, which may be given by the National Annexes. The recommended value, for each case, is 1. The fundamental value of the basic wind velocity, $v_{b,0}$, is also given in the National Annexes and in this case, it is given as $v_{b,0}$ = 37.27 m/s for this location. Equation (4.35) gives v_b = $v_{b,0}$ = 37.27 m/s. The basic velocity pressure follows from equation (5.70)[4],

$$q_b = 0.87\ \mathrm{kN/m^2}.$$

The exposure factor $c_e(z)$ is function of the terrain category and the height above the terrain, z. Since z = 7 m, considering a flat terrain where

[4] 1 N = 1 kg·m/s^2

$c_0(z)$ = 1.0 (clause 4.3.3) and terrain category II (area with low vegetation such as grass and isolated obstacles (trees, buildings) with separations of at least 20 obstacle heights), the value of $c_e(z)$ can be taken from Figure 4.2 of EN 1991-1-4 as $c_e(z)$ = 2.1.

Finally, from equation (4.31), the peak velocity pressure is given by $q_p(z)$ = 1.827 kN/m^2.

ii) Calculation of the external pressure coefficients (c_{pe})

External pressure coefficients change according to the direction of the wind and the area of the wall or roof, as illustrated in Figures 5.59 and 5.60.

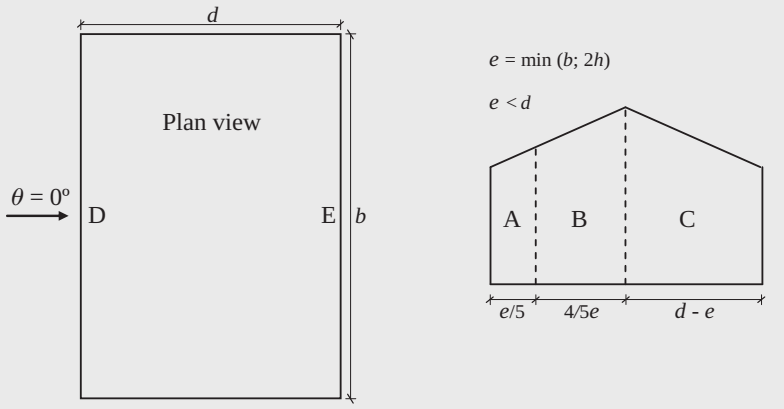


Figure 5.59 – Pressure zones on the walls

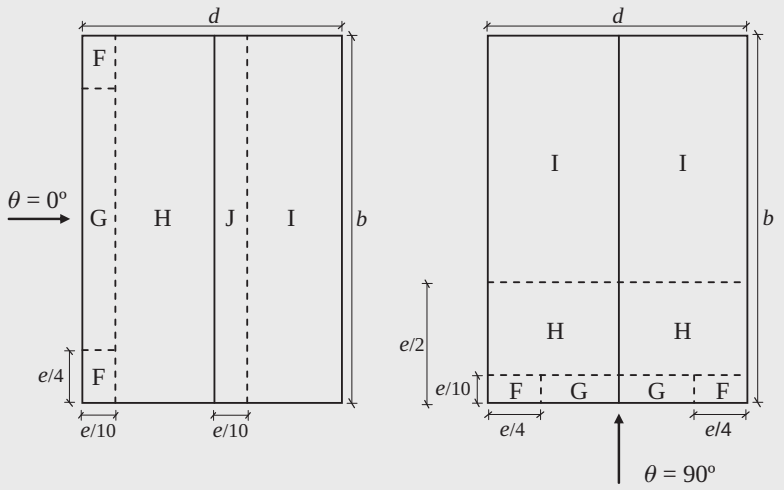


Figure 5.60 – Pressure zones on the roof

The external pressure coefficients (clause 7.2.2) depend on the relation between the height, h, of the building and the length, b. In this case, with $h = 7$ m $< b = 140$ m, the reference height z_e is equal to h and, as the ratio between the height of the building and the width, $d = L = 47$ m, $h/d \leq 0.25$, the pressure coefficients indicated in Table 5.14 are obtained:

Table 5.14 – External pressure coefficients on the walls (c_{pe})

	A	B	C	D	E
c_{pe}	-1.20	-0.80	-0.50	+0.70	-0.30

The external pressure coefficients on the roof are given by clause 7.2.5 and depend on the slope α, of the roof. For a slope of 7°, the pressure coefficients are obtained by interpolation and are indicated in Table 5.15 for the transverse wind direction ($\theta = 0°$) and for the longitudinal wind direction ($\theta = 90°$):

Table 5.15 – External pressure coefficients on the roof (c_{pe})

$\alpha = 7°$	F	G	H	I	J
$\theta = 0°$	-1.54/0.04	-1.12/0.04	-0.54/0.04	-0.56/-0.48	-0.04/-0.48
$\theta = 90°$	-1.54	-1.30	-0.68	-0.58	-

From Table 5.15, there are two possible situations for transverse wind, which are represented in Figure 5.61 (a_1 and a_2). For the longitudinal wind, consider a current frame in zone I (b).

The internal pressure coefficients (c_{pi}) depend on the dimensions of the openings in the building and on the distribution of those openings along the building. Assuming a uniform distribution of the openings, according to clause 7.2.9, we can assume for the value of c_{pi}, and for any direction of the wind, the most unfavourable situation between the value of + 0.2 and – 0.3. The external and internal pressures must act simultaneously. From the analysis of the previous coefficients the most unfavourable situation is considered for each direction of the wind, leading to the final coefficients given in Figure 5.62.

iii) Calculation of wind forces

These coefficients lead to the forces represented in Figure 5.63, for both wind directions, calculated from equations (4.27) and (4.30):

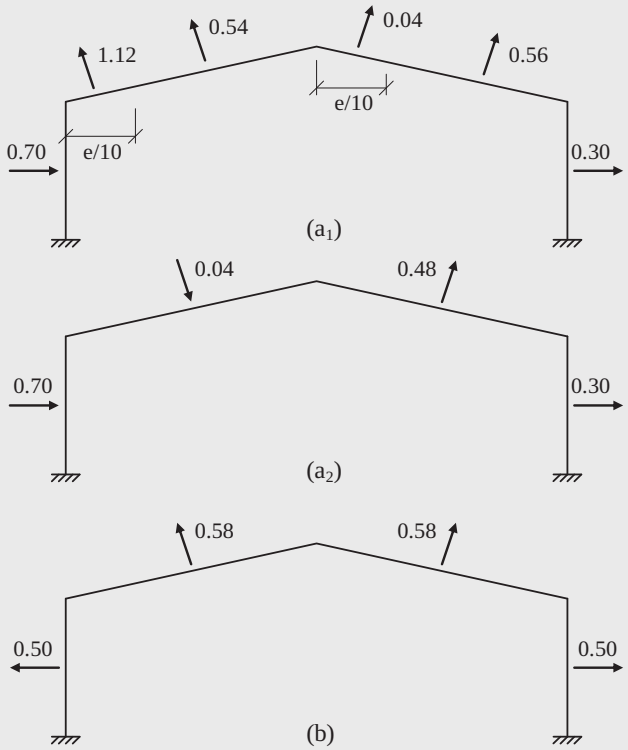


Figure 5.61 – External pressure coefficients on the walls and roofs: (a) wind in transverse direction (θ = 0°); (b) wind in longitudinal direction (θ = 90°).

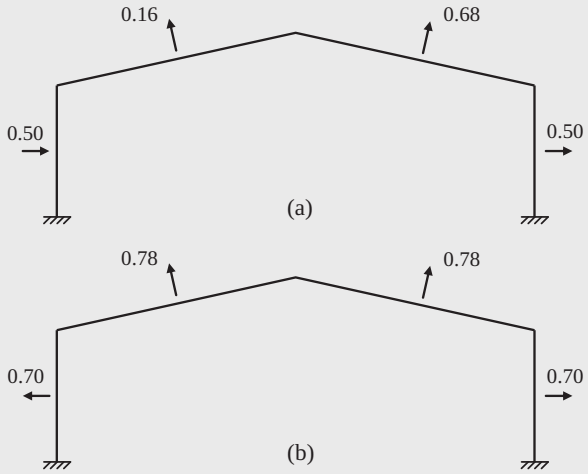


Figure 5.62 – Final pressure coefficients: (a) wind in transverse direction (θ = 0°); (b) wind in longitudinal direction (θ = 90°)

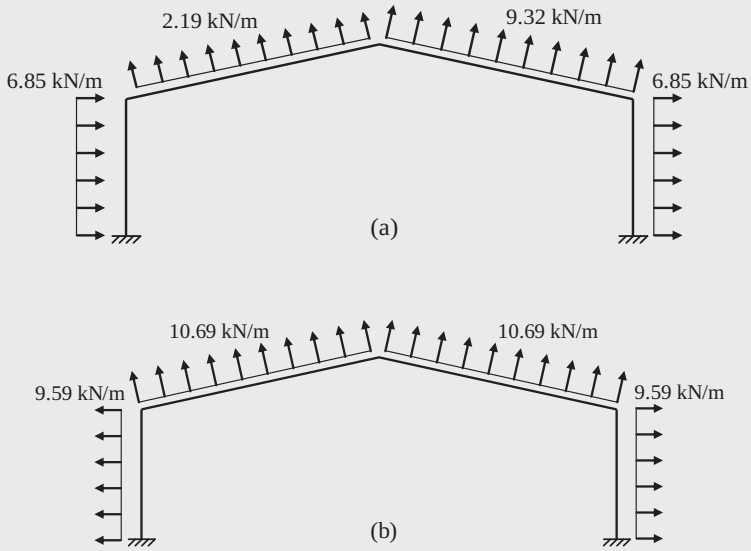


Figure 5.63 – Wind force: (a) in transverse direction (θ = 0°); (b) in longitudinal direction (θ = 90°)

5.4.3.6. Summary of basic actions

The resulting actions for this design example are summarized in Table 5.16.

Table 5.16 – Summary of actions

Action no.	Description	Type	Value
LC1	Self-weight of structural elements	Permanent action	p = 4.5 kN/m
LC2	Imposed load on roof	Variable action	q_k = 3.750 kN/m
LC3	Snow load	Variable action	q_k = 4.875 kN/m
LC4	Wind direction θ = 0º	Variable action	varies (see Figure 5.63a)
LC5	Wind direction θ = 90º	Variable action	varies (see Figure 5.63b)

5.4.3.7. Imperfections

The global imperfections are considered as equivalent horizontal forces. From equation (2.18), with ϕ_0 = 1/200, α_h = 0.756 and α_m = 0.866, ϕ = 0.003273. Hence, F_i = 0.30 kN for loadcase 1 (LC1). The equivalent

horizontal forces are applied at the top of the columns in the most unfavourable direction. Table 5.17 summarizes the imperfections for the remaining loadcases.

Table 5.17 – Values of imperfections by loading

	LC2	LC3	LC4	LC5
F_i (kN)	0.22	0.32	0.45	0.65

5.4.3.8. Load combinations

The design values of the applied forces are obtained from the fundamental combinations, given by (EN 1990, 2002):

$$E_d = \gamma_{G,j} \times G_{k,j} + \gamma_g \times P + \gamma_{Q,1} \times Q_{k,1} + \sum_{i=2}^{n} \gamma_{Q,i} \times \psi_{0,i} \times Q_{k,i}. \qquad (5.64)$$

The values of $\gamma_{G,j}$ and γ_g are taken as 1.35 or 1.0 for the unfavourable or favourable permanent actions, respectively. In case of variable actions, $\gamma_{Q,i}$ is always taken as 1.5. Reduced values of variable actions are obtained by multiplying the characteristic values by the corresponding reduction coefficients, $\psi_{0,i}$. In case of an imposed load on a roof, the reduction coefficients are $\psi_{0,i} = 0$. For snow, considering the altitude H ≤ 1000 in CEN Member States (except Finland, Iceland, Norway and Sweden), the reduction coefficients are $\psi_0 = 0.5$, $\psi_1 = 0.2$ and $\psi_2 = 0.0$. In case of wind the reduction coefficients are: $\psi_0 = 0.6$, $\psi_1 = 0.2$ and $\psi_2 = 0.0$. As the imposed and the snow loads have the same direction, only the imposed load will be used as the leading variable action, because it is more unfavourable. In this case, three leading variable actions are considered: imposed load ($Q_{imposed}$), transverse wind ($Q_{wind,tranv.}$) and longitudinal wind ($Q_{wind,long.}$), leading to three fundamental combinations. According to CEN (2002a):

Combination 1 – Imposed load as leading variable action

In this case, because the longitudinal or the transverse wind pressures are favourable for this combination, the corresponding reduced values are zero:

$$Ed_1 = 1.35 \times P + 1.50 \times Q_{imposed} + 1.50 \times 0.50 \times Q_{snow}. \qquad (5.65)$$

Combination 2 – Transverse wind as leading variable action

In this case, as the permanent actions have a favourable effect, $\gamma_G = 1.0$:

$$Ed_2 = 1.00 \times P + 1.50 \times Q_{wind,tranv}. \quad (5.66)$$

Combination 3 – Longitudinal wind as leading variable action

Also in this case, the permanent actions have a favourable effect, $\gamma_G = 1.0$:

$$Ed_3 = 1.00 \times P + 1.50 \times Q_{wind,long}. \quad (5.67)$$

Figures 5.64 to 5.66 illustrate the three load combinations.

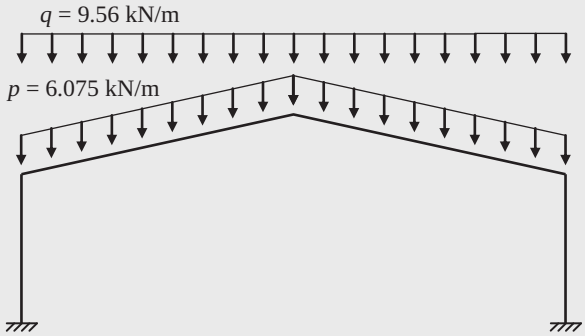


Figure 5.64 – Load combination 1

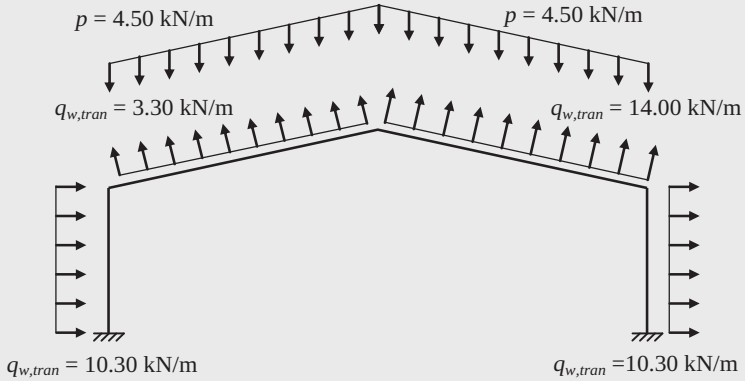


Figure 5.65 – Load combination 2

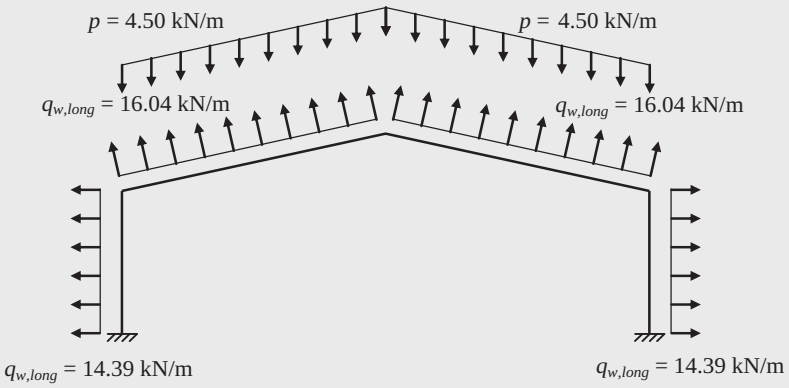


Figure 5.66 – Load combination 3

Additionally, a load combination 4 for the verification of the serviceability limit states (SLS) is also considered:

$$Ed_4 = 1.0 \times P \ + 1.0 \times Q_{imposed}. \tag{5.68}$$

5.4.4. Pre-design

The pre-design follows the methodology presented in section 5.2.2. Firstly, only load combinations 1 and 2 need to be considered as, by inspection, combination 3 is less severe than combination 2. In addition, the following assumptions are made:

- the plastic moment of the column, $M_{p.col}$, is 1.32 times the plastic moment at the rafter, $M_{p.raft}$ (arbitrary choice, corresponding to usual ratios between plastic moment of the column and rafter, respectively);
- the haunch at the eaves connection has a length (a_1) of 4.5 m and a depth (b_1) of 1.2 m, see Figure 5.12;
- the haunch at the apex connection has a total length ($2 \times a_3$) of 3.0 m and a depth (b_3) of 0.80 m, see Figure 5.12.

Considering first load combination 1 (without imperfections), the resulting factored vertical loads are (see Figure 5.14):

$$p_y^{BC} = p_y^{CD} = 15.40 \text{ kN/m}.$$

Introducing these values in equations (5.11) leads to the bending moment diagram of Figure 5.67.

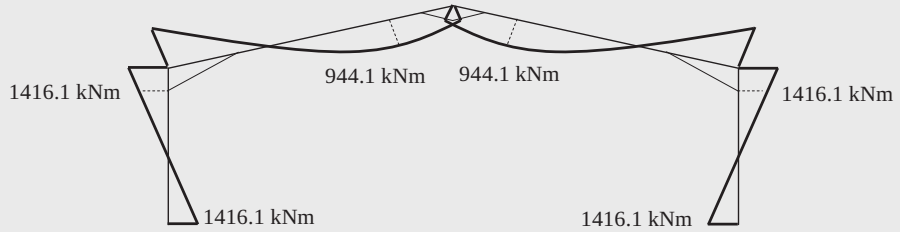


Figure 5.67 – Diagram of collapse moments

The minimum plastic moments for the columns and rafters are, respectively, $M_{p.col}$, = 1416.1 kNm and $M_{p.raft}$, = 944.1 kNm, leading to the selection of HEA 550 and IPE 600 cross sections in S 355 steel for the columns and rafters, respectively.

Similarly, for load combination 2 (without imperfections), the resulting factored member loads (equations (5.17)) are:

$$\begin{cases} p_x^{AB} = 10.26 \\ p_y^{AB} = 0 \end{cases} \qquad \begin{cases} p_x^{DE} = 10.26 \\ p_y^{DE} = 0 \end{cases}$$

$$\begin{cases} p_x^{BC} = -0.40 \\ p_y^{BC} = 1.25 \end{cases} \qquad \begin{cases} p_x^{CD} = 1.71 \\ p_y^{CD} = -9.42 \end{cases}$$

Introducing these values in equations (5.18) and solving for the load factor, gives:

$$\begin{cases} \alpha_p = 8.87 \\ M = -1247 \text{ kNm} \\ V = -542.0 \text{ kN} \\ H = -790.0 \text{ kN} \end{cases},$$

so this combination is not critical.

Note that, for both combinations, the axial force is very low (< 5 % of N_{pl}), so that the bending and axial force plastic interaction is negligible.

For a simplified assessment of 2nd order effects, equations (5.31) to (5.36) are first evaluated to provide the lowest elastic critical loads for the symmetric and anti-symmetric modes, for load combination 1:

$$\alpha_{cr}{}^{1} = 7.98$$

$$\alpha_{cr}{}^{2} = 8.73$$

The 2nd order effects can be accounted for as described in sub-section 5.2.4.4. Amplifying the 1st order bending moments according to expression (5.38),

$$M^{II} = \left(1 - \frac{1}{7.98}\right)^{-1} M^{I},$$

and solving again equations (5.18), now with respect to the load factor, yields:

$$\alpha_p^{II} = 1.04 > 1.0.$$

Table 5.18 summarizes the plastic resistances of the chosen cross sections.

Table 5.18 – Plastic resistance of the cross sections

Cross section	A (m^2)	$W_{pl,y}$ (m^3)	$M_{pl,y}$ (kNm)	N_{pl} (kN)	V_{pl} (kN)
HEA 550	211.8E-4	4622E-6	1640.8	7518.9	1715.9
IPE 600	156E-4	3512E-6	1246.8	5538.0	1717.1

Having pre-designed the cross sections, it is necessary to detail the positioning of the purlins, side-rails, lateral and torsional bracings and connections. Figure 5.68 illustrates the detailing of column AB and rafter BC.

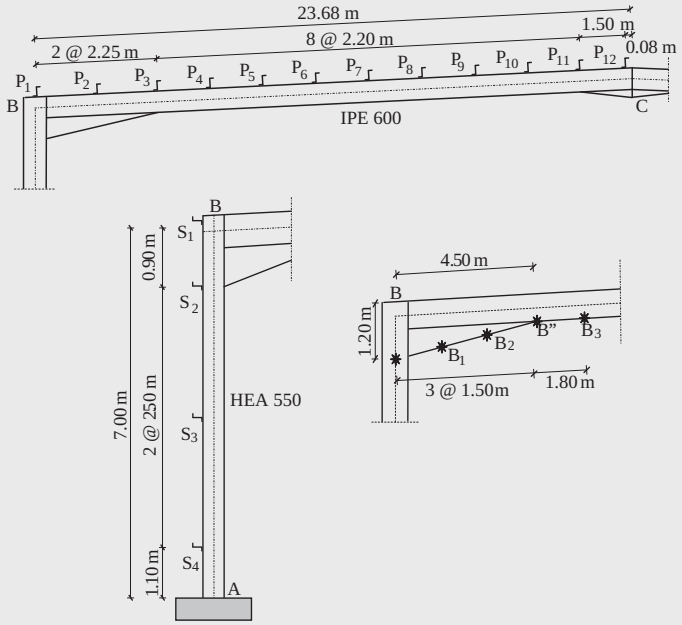


Figure 5.68 – Detailing of column AB, rafter BC and position of additional effective restraints

5.4.5. Structural analysis

5.4.5.1. Linear elastic analysis

Linear elastic analysis is carried out initially for the ULS load combinations to provide a reference solution and preclude gross errors. The three load combinations defined for the ultimate limit states (ULS), as well as the load combination for the serviceability limit state (SLS), lead to the 1st order elastic bending moment diagrams of Figures 5.69 to 5.72 (see example 5.1 for detailed results of the several types of analysis for load combination 1).

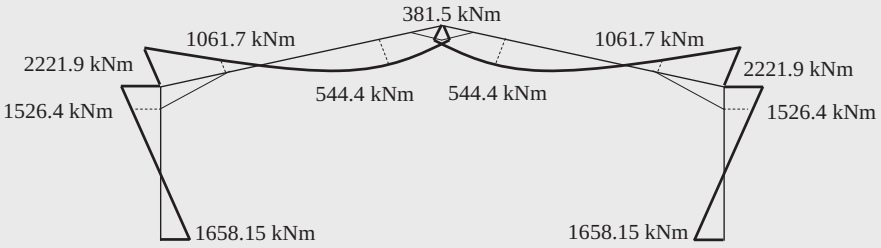


Figure 5.69 – Bending moment diagram (LEA) for C1

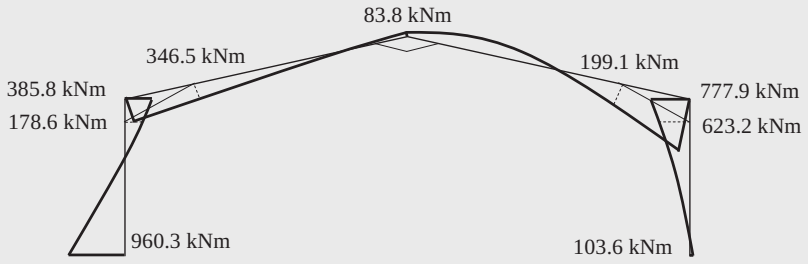


Figure 5.70 – Bending moment diagram (LEA) for C2

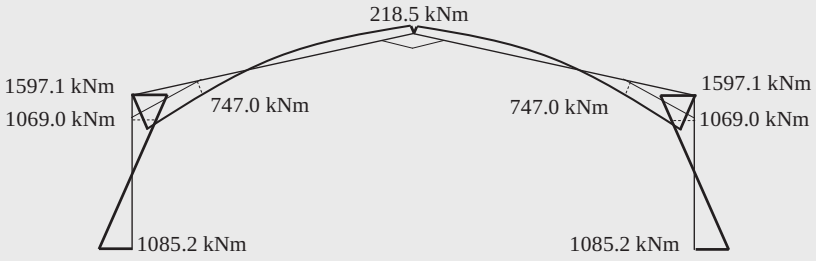


Figure 5.71 – Bending moment diagram (LEA) for C3

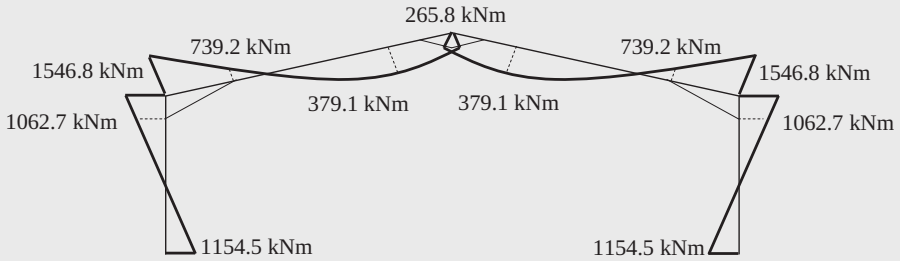


Figure 5.72 – Bending moment diagram (LEA) for C4

Similarly, Figures 5.73 to 5.76 represent the deformations for the four load combinations.

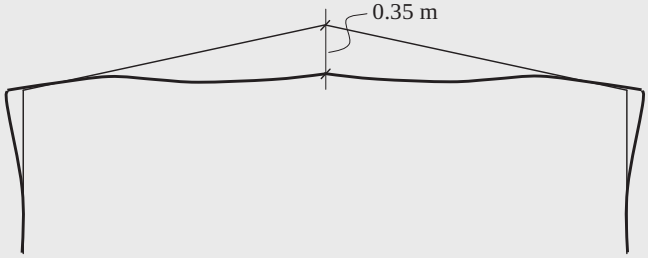


Figure 5.73 – Displacements (LEA) for C1

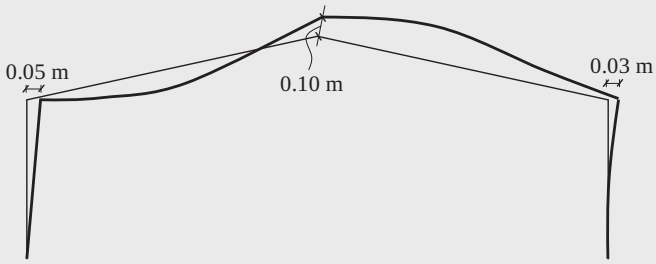


Figure 5.74 – Displacements (LEA) for C2

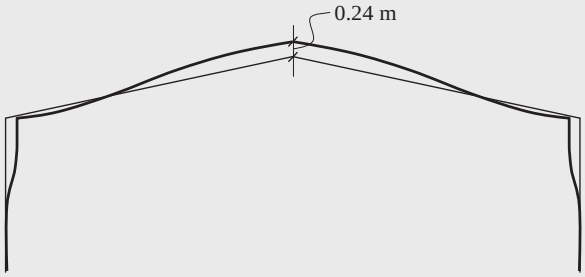


Figure 5.75 – Displacements (LEA) for C3

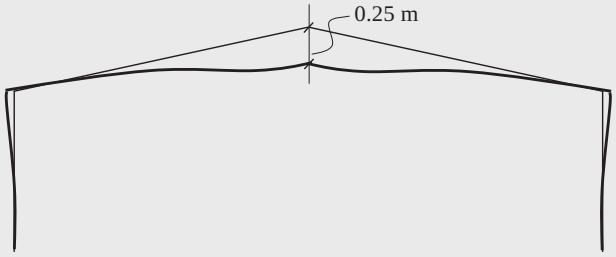


Figure 5.76 – Displacements (LEA) for C4

Table 5.19 summarizes the results for all load combinations and relevant cross section locations:

Table 5.19 – Results from the 1st order elastic analyses

	Combination 1		Combination 2		Combination 3		Combination 4	
	M_y (kNm)	N_x (kN)	M_y (kNm)	N_x (kN)	M_y (kNm)	N_x (kN)	M_y (kNm)	δ (mm)
A	1658.2	378.8	960.3	11.2	1085.2	255.2	1154.5	0
B’	1526.4	366.7	178.6	23.4	1069.0	267.3	1062.7	26.7
B_{col}	2221.9	363.6	385.8	26.5	1597.1	270.4	1546.8	27.3
B_{raft}		617.9		168.4		478.7		
B’’	1061.7	609.8	346.5	170.8	747.0	481.1	739.2	30.1
$C_{B''}$	381.5	574.7	83.8	181.1	218.5	491.4	265.8	246
$C_{D''}$		574.7		167.6		491.4		
D’’	1061.7	609.8	199.1	157.3	747.0	481.1	739.2	30.1
D_{raft}	2221.9	617.9	777.9	154.9	1597.1	478.7	1546.8	27.3
D_{col}		363.6		167.0		270.4		
D’	1526.4	366.7	623.2	163.9	1069.0	267.3	1062.7	26.7
E	1658.2	378.8	103.6	151.8	1085.2	255.2	1154.5	0

Table 5.19 shows that on the basis of elastic analysis, the frame would be under-designed (the applied bending moment at A, for load combination 1, is 1658 kNm, higher than the plastic moment resistance of 1640 kNm).

5.4.5.2. 2nd Order effects

The determination of the critical loads is reproduced in Table 5.20. These results indicate that the structure is sensitive to 2nd order effects since (equation (5.24)):

$$\alpha_{cr}^{\min} = 7.32 < 15.$$

Consequently, 2nd order effects must be considered.

Table 5.20 – Critical loads

	α_{cr}^{1}	α_{cr}^{2}	α_{cr}^{3}	α_{cr}^{4}	α_{cr}^{5}
C1	7.32	10.14	18.82	20.95	28.25
C2	24.42	30.81	55.71	65.44	75.04
C3	9.40	12.58	24.19	27.63	41.72

Table 5.21 summarizes the results of the 2nd order elastic analysis (described in detail in example 5.1 for load combination 1).

Table 5.21 – Results of the 2nd order elastic analysis

	Combination 1		Combination 2		Combination 3		Combination 4	
	M_y (kNm)	N_x (kN)	M_y (kNm)	N_x (kN)	M_y (kNm)	N_x (kN)	M_y (kNm)	δ (mm)
A	1719.6	379.8	953.5	11.3	1049.6	254.4	1183.4	0
B’	1602.8	366.6	181.3	24.7	1034.1	266.9	1097.8	27.2
B_{col}	2325.3	362.8	387.6	27.6	1548.1	270.3	1594.6	27.7
B_{raft}		641.9		170.3		466.8		
B’’	1162.7	627.9	340.7	170.0	700.2	471.5	785.8	31.0
$C_{B''}$	460.4	596.5	76.8	180.9	184.4	483.4	301.9	267.0
$C_{D''}$		596.5		168.5		483.4		
D’’	1162.7	627.9	192.5	157.7	700.2	471.5	785.8	31.0
D_{raft}	2325.3	641.9	763.0	149.8	1548.1	466.8	1594.6	27.7
D_{col}		362.8		166.9		270.3		
D’	1602.8	366.6	608.4	164.2	1034.1	266.9	1097.8	27.2
E	1719.6	379.8	94.5	151.2	1049.6	254.4	1183.4	0

5.4.5.3. Elastic-plastic analysis

The 1st order elastic-plastic analysis leads to the results of Table 5.22, for α= 1.0. As the 2nd order effects are not negligible, the design forces correspond to the results of the 2nd order elastic-plastic analysis, summarized in Table 5.23. Finally, in Table 5.24 the history of the formation of plastic hinges is summarized, for each combination.

Table 5.22 – Results of the 1st order elastic-plastic analysis (α = 1.0)

	Combination 1		Combination 2		Combination 3	
	M_y (kNm)	N_x (kN)	M_y (kNm)	N_x (kN)	M_y (kNm)	N_x (kN)
A	1650.1	371.7	960.3	15.2	1085.2	259.1
B’	1526.6	365.9	178.6	24.2	1069.0	268.1
B_{col}	2221.9	363.6	385.8	26.5	1597.1	270.4
B_{raft}		617.9		168.4		478.7
B’’	1061.8	609.7	346.6	170.8	747.0	481.1
$C_{B''}$	381.6	574.7	83.8	181.1	218.5	491.4
$C_{D''}$		574.7		167.6		491.4
D’’	1061.8	609.7	199.1	157.3	747.0	481.1
D_{raft}	2221.9	617.9	777.9	154.9	1597.1	478.7
D_{col}		363.6		167.0		270.4
D’	1526.6	365.9	623.2	164.7	1069.0	268.1
E	1650.1	371.7	103.6	155.7	1085.2	259.1

Table 5.23 – Results of the 2nd order elastic-plastic analysis (α= 1.0)

	Combination 1		Combination 2		Combination 3	
	M_y (kNm)	N_x (kN)	M_y (kNm)	N_x (kN)	M_y (kNm)	N_x (kN)
A	1613.2	357.6	953.5	15.3	1049.6	258.4
B’	1614.5	363.7	181.3	25.5	1034.1	267.7
B_{col}	2331.6	362.2	387.6	27.6	1548.1	270.3
B_{raft}		636.8		170.3		466.8
B’’	1166.2	623.4	340.7	170.0	700.2	471.5
$C_{B''}$	467.6	591.9	76.8	180.9	184.4	483.4
$C_{D''}$		591.9		168.5		483.4
D’’	1166.2	623.4	192.5	157.7	700.2	471.5
D_{raft}	2331.6	636.8	763.0	149.8	1548.1	466.8
D_{col}		362.2		166.9		270.3
D’	1614.5	363.7	608.4	165.0	1034.1	267.7
E	1613.2	357.6	94.5	155.2	1049.6	258.4

Table 5.24 – Formation of plastic hinges

	Combination 1	Combination 2	Combination 3
1st plastic hinge	α = 0.965 (A/E)	α = 1.75 (A)	α = 1.605 (A/E)
2nd plastic hinge	α = 1.020 (B’/D’)	α = 2.75 (D’)	α = 1.635 (B’/D’)
3rd plastic hinge	-	(*)	-

(*) Note that for Combination 2 there was not numerical convergence

5.4.6. Code checks

5.4.6.1. General considerations

The verifications to carry out for each load combination (ULS) are the following:

i) cross sectional resistance;
ii) buckling resistance of the rafters;
iii) buckling resistance of the columns.

5.4.6.2. Cross section resistance

It is first noted that the cross sectional resistance to bending (clause 6.2.5) was guaranteed a *priori* by the 2nd order elastic-plastic analysis. According to the results of Table 5.22, the critical load combination is combination 1, for all cross sections. Consequently, it suffices to verify the resistance of the cross sections for this combination. The cross section resistance for load combination 1 was checked in examples 5.2 and 5.3, for the rafter and for the column, respectively. Note that, for all cases, $V_{Ed} < 0.5\ V_{pl,Rd}$, and so the verification of the combined action of the axial force, bending moment and shear force is not necessary (clause 6.2.10).

5.4.6.3. Buckling resistance of the rafters

From Figures 5.69 to 5.71, it is observed that the bending moments for combination 1 have opposite signs when compared to those from combinations 2 and 3. The verification of the buckling resistance of the rafters for combination 1 was performed in example 5.2. The verification of the buckling resistance of the rafters for the other combinations follows a similar procedure. Only the results for combination 3 are presented, being the most unfavourable combination.

The cross section classification depends on the applied forces given in Table 5.23. These lead to the classification and the cross sectional resistances indicated in Table 5.25.

Table 5.25 – Classification of cross sections for combination 3

	B_{trav}	B''	C'	C
$M_{y,Ed}$ (kNm)	1548.1	700.2	383.3	184.4
N_{Ed} (kN)	466.8	471.5	479.8	483.4
Classification	2(*)	1	1	1
$M_{pl,y,Rd}$ (kNm)	2712.6	1246.8	1246.8	1246.8
$N_{pl,Rd}$ (kN)	7099.3	5538.0	5538.0	5538.0

(*) based on the effective section

The verifications of the in plane stability of the rafters, for this combination, can be done as in example 5.2 or based on expressions (3.163). Considering that the rafter corresponds to a non-prismatic member, expressions (3.163) are not strictly applicable. However, they can be safely applied as follows.

First, determine the reduction coefficients for buckling by compression in both bending modes, χ_y and χ_z. In a conservative manner, assume a prismatic cross section (IPE 600), the maximum axial force, N_{Ed} = 483.4 kN, and a buckling length L_y = 23.7 m (total length of the rafter) and L_z = 2.20 m (maximum distance between purlins). According to clause 6.3.1, the following reduction coefficients are obtained:

$$\chi_y = 0.48 \quad \text{and} \quad \chi_z = 1.0.$$

Then, determine the interaction coefficients k_{yy} and k_{zy} (see Annex B.2 of EC 3-1-1).

$$k_{yy} = 1.03 \quad \text{and} \quad k_{zy} = 0.62.$$

Finally, apply expressions (3.163) at two distinct cross section locations: at section C', where the maximum negative moment occurs in the rafter (x = 17.93 m) and at section B'', where the maximum positive moment occurs in the prismatic part of the rafter (see Figure 5.68 and Figure 5.77).

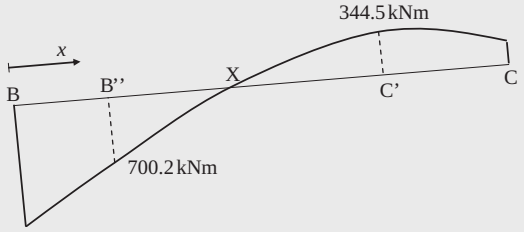


Figure 5.77 – Bending diagram in the rafter for Combination 3

For the first case $\left(M_{y,Ed}^{C'} = 344.5 \text{ kNm and } M_{y,Rk}^{C'} = 1246.8 \text{ kNm}\right)$:

$$\frac{N_{Ed}}{\chi_y N_{Rk}/\gamma_{M1}} + k_{yy}\frac{M_{y,Ed}}{M_{y,Rk}/\gamma_{M1}} = \frac{480.3}{0.48\times 5538.0/1} + 1.03\times\frac{344.5}{1246.8/1} = 0.47 \le 1.0;$$

$$\frac{N_{Ed}}{\chi_z N_{Rk}/\gamma_{M1}} + k_{zy}\frac{M_{y,Ed}}{M_{y,Rk}/\gamma_{M1}} = \frac{480.3}{1.00\times 5538.0/1} + 0.62\times\frac{344.5}{1246.8/1} = 0.26 \le 1.0;$$

whereas for the second case $\left(M_{y,Ed}^{B''} = 700.2 \text{ kNm e } M_{y,Rk}^{B''} = 1246.8 \text{ kNm}\right)$,

$$\frac{N_{Ed}}{\chi_y N_{Rk}/\gamma_{M1}} + k_{yy}\frac{M_{y,Ed}}{M_{y,Rk}/\gamma_{M1}} = \frac{471.5}{0.48\times 5538.0/1} + 1.03\times\frac{700.2}{1246.8/1} = 0.76 \le 1.0;$$

$$\frac{N_{Ed}}{\chi_z N_{Rk}/\gamma_{M1}} + k_{zy}\frac{M_{y,Ed}}{M_{y,Rk}/\gamma_{M1}} = \frac{471.5}{1.00\times 5538.0/1} + 0.62\times\frac{700.2}{1246.8/1} = 0.43 \le 1.0$$

and so in-plane buckling is verified.

The verification of the out of plane stability can take advantage of the partial bracing provided by the purlins. From the analysis of the bending moment diagram (Figure 5.77 and Figure 5.68), it can be seen that the compressed flange is laterally braced between points B and X, whereas between points X and C the lateral bracing is only partial, provided by the connection of the purlins to the tension flanges. Thus, from the analysis of the detailing of the rafter, six distinct segments must be considered: segments BP_2, P_2B'', $B''P_4$, P_4P_5, P_5,X and XC, with lengths $L_t^{BP_2} = L_t^{P_2B''} = 2.25$ m, $L_t^{B''P_4} = L_t^{P_4P_5} = 2.20$ m, $L_t^{P_5X} = 1.04$ m and $L_t^{XC} = 13.74$ m, respectively.

From equations (4.14) to (4.19) the results summarized in Table 5.26 are obtained. Note that segment XC had to be divided into two new segments XC' and C'C, with additional bracing at the compression flange, in order to satisfy the buckling verification. For simplicity, the bracing is positioned at C', at the point of maximum moment of the initial segment, as illustrated in Figure 5.78.

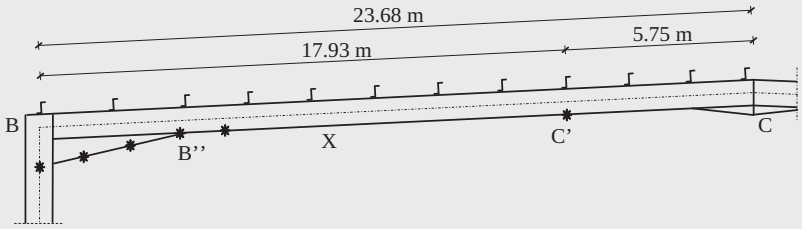


Figure 5.78 – Final detailing of rafter BC

Table 5.26 – Lateral-torsional buckling verification

	L_t	N_{crT}	M_{cr0}	M_{cr}	λ_{LT}	χ_{LT}	M_{br}	M_{Ed}/M_{br}
BP_2	2.25	15901.1	6387.8	6681.3	0.63	0.82	2185.5	0.71
P_2B''	2.25	15901.1	4396.8	4678.9	0.64	0.82	1574.1	0.69
$B'P_4$	2.20	16604.5	4591.3	5072.7	0.60	0.84	1540.3	0.45
P_4P_5	2.20	16604.5	4591.3	7305.3	0.41	0.92	1148.2	0.33
P_5X	1.04	72204.1	19964.9	40761.4	0.17	1.00	1246.9	0.09
XC'	7.99	1817.1	502.4	742.0	1.30	0.43	534.5	0.72
C'C	5.75	2946.3	814.7	978.7	1.13	0.52	646.2	0.59

In segments BP_2, P_2B'', $B''P_4$, P_4P_5 and P_5X, $N_{Ed}/N_{cr} < 0.04$ and, according to clause 6.3.1.2(4), buckling by compression can be neglected. For segments XC' and C'C, the buckling resistance considering the combined effect of bending and axial force is given by expression (3.163b), leading to values of 0.98 and 0.80, respectively, so that structural adequacy is confirmed.

5.4.6.4. Buckling resistance of the columns

According to the results of Table 5.23, the critical combination is combination 1, for all cross sections. It suffices to verify the buckling resistance of the columns for this combination. The buckling resistance of the columns for combination 1 was verified in example 5.3.

5.4.7. Synthesis

The adopted solution corresponds to the use of 25.3 kg/m^2 of steel in the main structure of the building, not including, therefore, purlins, side-rails and longitudinal bracing. For each frame, this density of steel corresponds to 189.75 kg/m or, in terms of total quantities of the used steel, to 8.92 ton/frame.

Annex A

FORMULAS FOR COMMON TORSIONAL CASES

A.1. CROSS SECTIONAL PROPERTIES FOR TORSION

Table A.1 lists expressions for the shear centre, torsional constant and warping constant for typical thin-walled cross sections

Table A.1 – Shear centre, torsion constant and warping constant for typical cross sections

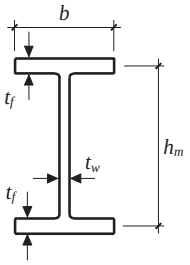
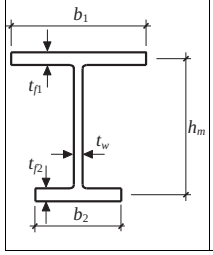
	e	I_T	I_w
	0	$\frac{2t_f^3\, b + t_w^3\, h_m}{3}$	$\frac{t_f\, h_m^2\, b^3}{24}$
	$\frac{t_{f1} b_1^3 h_m}{t_{f1} b_1^3 + t_{f2} b_2^3}$	$\frac{t_{f2}^3 b_2 + t_{f2}^3 b_2 + t_w^3 h_m}{3}$	$\frac{h_m^2}{12} \frac{t_{f1} t_{f2} b_1^3 b_2^3}{t_{f1} b_1^3 + t_{f2} b_2^3}$

Table A.1 (cont.) – Shear centre, torsion constant and warping constant for typical cross sections

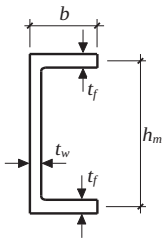
	e	I_T	I_w
	$\frac{3b^2}{h_m+6b}$	$\frac{2t_f^3 b+t_w^3 h_m}{3}$	$\frac{t_f b^3 h_m^2}{12}\frac{3bt_f+2h_m t_w}{6bt_f+h_m t_w}$
Circular	0	$\frac{\pi}{2}\left[\left(\frac{d_e}{2}\right)^4-\left(\frac{d_i}{2}\right)^4\right]$	0
Rectangular hollow	0	$\frac{2t_w t_f b_m^2 h_m^2}{t_w b+t_f h-t_w^2-t_f^2}$	≈ 0
			≈ 0

Table A.2 describes the warping function ω and the static function with respect to the warping function for typical thin-walled open cross section.

Table A.2 – Warping function and static function with respect to the warping function for typical cross sections

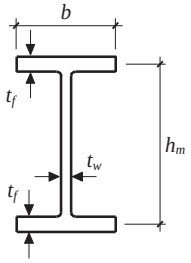
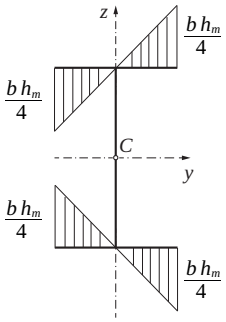
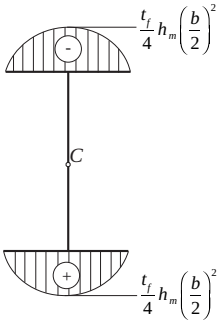
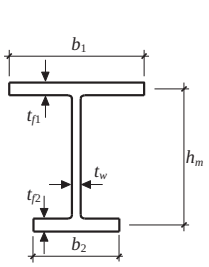
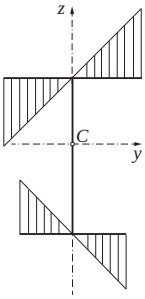
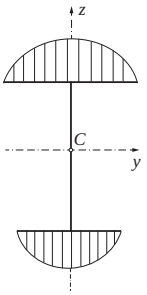
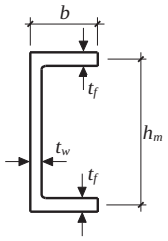
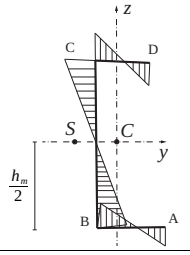
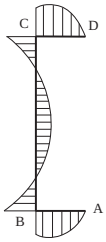
	ω	S_ω
		

Table A.2 (cont.) – Warping function and static function with respect to the warping function for typical cross sections

	ω	S_ω
		
		

A.2. SOLUTION OF DIFFERENTIAL EQUATION FOR TORSION

A.2.1. Concentrated torsional moment

The solution of the differential equation for a concentrated torsional moment (equation (3.35)) is given by equation (3.38a). Alternatively (Roark and Young, 1976), it may be written as (Figure A.1):

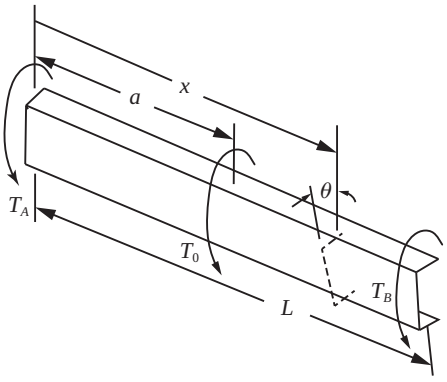


Figure A.1 – Generic open cross section beam subject to concentrated torsional moment

$$\varphi(x)=\varphi_A+\frac{\varphi_A^{'}}{k}\sinh kx+\frac{\varphi_A^{''}}{k^2}\left(\cosh kx-1\right)+\frac{T_A}{k^3EI_w}\left(\sinh kx-kx\right)+$$
$$+\frac{T_0}{k^3EI_w}\left(\sinh k\left\langle x-a\right\rangle-k\left\langle x-a\right\rangle\right) \tag{A.1a}$$

$$\frac{d\varphi(x)}{dx}=\varphi_A^{'}\cosh kx+\frac{\varphi_A^{''}}{k}\sinh kx+\frac{T_A}{k^2EI_w}\left(\cosh kx-1\right)+$$
$$+\frac{T_0}{k^2EI_w}\left\langle x-a\right\rangle^0\left[\cosh k\left(x-a\right)-1\right] \tag{A.1b}$$

$$\frac{d^2\varphi(x)}{dx^2}=\varphi_A^{'}k\sinh kx+\varphi_A^{''}\cosh kx+\frac{T_A}{kEI_w}\sinh kx+$$
$$+\frac{T_0}{kEI_w}\sinh k\left\langle x-a\right\rangle \tag{A.1c}$$

$$\frac{d^3\varphi(x)}{dx^3}=\varphi_A^{'}k^2\cosh kx+\varphi_A^{''}k\sinh kx+\frac{T_A}{EI_w}\cosh kx+$$
$$+\frac{T_0}{EI_w}\left\langle x-a\right\rangle^0\cosh k\left(x-a\right) \tag{A.1d}$$

with

$$T=T_A+T_0\left\langle x-a\right\rangle^0 \tag{A.2}$$

$$k=\sqrt{\frac{GI_t}{EI_w}} \tag{A.3}$$

The bimoment and the warping and St. Venant torsional moments are given by:

$$B_w=-EI_w\frac{d^2\varphi}{dx^2}=$$
$$=-EI_w\left(\varphi_A^{'}k\sinh kx+\varphi_A^{''}\cosh kx+\frac{T_A}{kEI_w}\sinh kx+\frac{T_0}{kEI_w}\sinh k\left\langle x-a\right\rangle\right) \tag{A.4a}$$

$$T_w = -EI_w \frac{d^3\varphi}{dx^3} = -EI_w \left(\varphi_A^{'} k^2 \cosh kx + \varphi_A^{''} k \sinh kx + \frac{T_A}{EI_w} \cosh kx + \right.$$
$$\left. + \frac{T_0}{EI_w} \langle x-a \rangle^0 \cosh k(x-a) \right) \tag{A.4b}$$

$$T_t = GI_t \frac{d\varphi}{dx} = GI_t \left(\varphi_A^{'} \cosh kx + \frac{\varphi_A^{''}}{k} \sinh kx + \frac{T_A}{k^2 EI_w} (\cosh kx - 1) + \right.$$
$$\left. + \frac{T_0}{k^2 EI_w} \langle x-a \rangle^0 \left[\cosh k(x-a) - 1 \right] \right) \tag{A.4c}$$

Table A.3 presents the formulas for cantilevers with two distinct boundary conditions subject to a concentrated torsional moment applied at the free end of the cantilever.

Table A.3 – Formulas for thin-walled elastic cantilevers under a concentrated torsional moment T_0

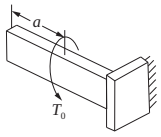
	Concentrated Moment T_0 at an intermediate section with free warping at the free end and zero torsional rotation and zero warping at the built-in end
$\varphi_A^{''} = 0$ $\varphi_B = \varphi_B^{'} = 0$	
$T_A = 0 \qquad T_B = -T_0$ $\varphi_A = \frac{T_0}{k^3 EI_w} \left(\frac{\sinh kl \cosh k(L-a) - 1}{\cosh kl} - \left(\sinh k(L-a) - k(L-a) \right) \right)$ $\varphi_A^{'} = -\frac{T_0}{k^2 EI_w} \left(\frac{\cosh k(L-a) - 1}{\cosh kL} \right)$	
$B_w(x) = -EI_w \left(\varphi_A^{'} k \sinh kx + \frac{T_0}{kEI_w} \sinh k\langle x-a \rangle \right)$ $T_w(x) = -EI_w \left(\varphi_A^{'} k^2 \cosh kx + \frac{T_0}{EI_w} \langle x-a \rangle^0 \cosh k(x-a) \right)$	

Table A.3 (cont.) – Formulas for thin-walled elastic cantilevers under a concentrated torsional moment T_0

$$T_t(x) = GI_t\left(\varphi_A' \cosh kx + \frac{T_0}{k^2 EI_w}\langle x-a\rangle^0\left[\cosh k(x-a)-1\right]\right)$$

Section A ($x = 0$):

$$B_w = 0 \qquad T_w = T_0\left(\frac{\cosh k(L-a)-1}{\cosh kL}\right) \qquad T_t = -T_0\left(\frac{\cosh k(L-a)-1}{\cosh kL}\right) = -T_w$$

Section 0 ($x = a$):

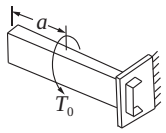
$$B_w = -EI_w\left(\varphi_A' k \sinh ka\right)$$

$$T_w = -EI_w\left(\varphi_A' k^2 \cosh ka\right)$$

$$T_t = GI_t\left(\varphi_A' \cosh ka\right)$$

Section B ($x = L$):

$$B_w = \frac{T_0}{k}\left(\frac{\cosh k(L-a)-1}{\cosh kL}\sinh kL - \sinh k(L-a)\right) \qquad T_w = -T_0 \qquad T_t = 0$$



Concentrated Moment T_0 at the free end with free warping at the free end and zero torsional rotation and free warping at the built-in end

$$\varphi_A'' = 0$$

$$\varphi_B = \varphi_B'' = 0$$

$$T_A = 0 \qquad T_B = -T_0$$

$$\varphi_A = \frac{T_0}{k^3 EI_w}(L-a)$$

$$\varphi_A' = -\frac{T_0}{k^2 EI_w}\frac{\sinh k(L-a)}{\sinh kL}$$

Table A.3 (cont.) – Formulas for thin-walled elastic cantilevers under a concentrated torsional moment T_0

$$B_w(x) = -EI_w\left(\varphi_A' k\sinh kx + \frac{T_0}{kEI_w}\sinh k\langle x-a\rangle\right)$$

$$T_w(x) = -EI_w\left(\varphi_A' k^2\cosh kx + \frac{T_0}{EI_w}\langle x-a\rangle^0\cosh k(x-a)\right)$$

$$T_t(x) = GI_t\left(\varphi_A'\cosh kx + \frac{T_0}{k^2EI_w}\langle x-a\rangle^0\left[\cosh k(x-a)-1\right]\right)$$

Section A ($x = 0$):

$$B_w = 0 \qquad T_w = T_0\frac{\sinh k(L-a)}{\sinh kL} \qquad T_t = -T_0\frac{\sinh k(L-a)}{\sinh kL}$$

Section 0 ($x = a$):

$$B_w = \frac{T_0}{k}\frac{\sinh k(L-a)}{\sinh kL}\sinh ka$$

$$T_w = T_0\frac{\sinh k(L-a)}{\sinh kL}\cosh ka$$

$$T_t = -T_0\frac{\sinh k(L-a)}{\sinh kL}\cosh ka$$

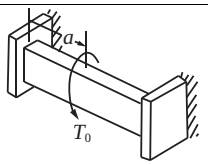
Section B ($x = L$):

$$B_w = 0 \qquad T_w = T_0\left(\frac{\sinh k(L-a)}{\sinh kL}\cosh kL - \cosh k(L-a)\right)$$

$$T_t = T_0\left(\frac{-\sinh k(L-a)}{\sinh kL}\cosh kL + \cosh k(L-a) - 1\right)$$

Table A.4 presents the formulas for simply-supported beams with two distinct boundary conditions subject to a concentrated torsional moment applied at an intermediate cross section.

Table A.4 – Formulas for thin-walled elastic double-supported beams under a concentrated torsional moment

	Concentrated Moment T_0 at an intermediate section with zero torsional rotation and zero warping at the ends

$$\varphi_A = \varphi_A^{'} = 0$$

$$\varphi_B = \varphi_B^{'} = 0$$

$$T_A = -T_0 \frac{\sinh kL\left(\sinh k\left(L-a\right)-k\left(L-a\right)\right)-\left(\cosh kL-1\right)\left(\cosh k\left(L-a\right)-1\right)}{\sinh kL\left(\sinh kL-kL\right)-\left(\cosh kL-1\right)^2}$$

$$T_B = -T_0 - T_A$$

$$\varphi_A^{"} = \frac{T_0}{kEI_w} \frac{\left(\cosh kL-1\right)\left(\sinh k\left(L-a\right)-k\left(L-a\right)\right)-\left(\sinh kL-kL\right)\left(\cosh k\left(L-a\right)-1\right)}{\sinh kL\left(\sinh kL-kL\right)-\left(\cosh kL-1\right)^2}$$

$$B_w\left(x\right) = -EI_w\left(\varphi_A^{"}\cosh kx + \frac{T_A}{kEI_w}\sinh kx + \frac{T_0}{kEI_w}\sinh k\left\langle x-a\right\rangle\right)$$

$$T_w\left(x\right) = -EI_w\left(\varphi_A^{"}k\sinh kx + \frac{T_A}{EI_w}\cosh kx + \frac{T_0}{EI_w}\left\langle x-a\right\rangle^0\cosh k\left(x-a\right)\right)$$

$$T_t\left(x\right) = GI_t\left(\frac{\varphi_A^{"}}{k}\sinh kx + \frac{T_A}{k^2EI_w}\left(\cosh kx-1\right) + \frac{T_0}{k^2EI_w}\left\langle x-a\right\rangle^0\left[\cosh k\left(x-a\right)-1\right]\right)$$

Section A ($x = 0$):

$$B_w = -EI_w\varphi_A^{"} \qquad T_w = -T_A \qquad T_t = 0$$

Section 0 [1] ($x = a$):

$$B_w = -EI_w\left(\varphi_A^{"}\cosh ka + \frac{T_A}{kEI_w}\sinh ka\right)$$

$$T_w = -EI_w\left(\varphi_A^{"}k\sinh ka + \frac{T_A}{EI_w}\cosh ka\right)$$

Table A.4 (cont.) – Formulas for thin-walled elastic double-supported beams under a concentrated torsional moment

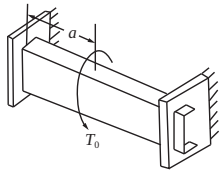
$$T_t = GI_t\left(\frac{\varphi_A^{"}}{k}\sinh ka + \frac{T_A}{k^2EI_w}\left(\cosh ka - 1\right)\right)$$

Section B ($x = L$):

$$B_w = -EI_w\left(\varphi_A^{"}\cosh kL + \frac{T_A}{kEI_w}\sinh kL + \frac{T_0}{kEI_w}\sinh k\left(L-a\right)\right)$$

$$T_w = -EI_w\left(\varphi_A^{"}k\sinh kL + \frac{T_A}{EI_w}\cosh kL + \frac{T_0}{EI_w}\cosh k\left(L-a\right)\right)$$

$$T_t = GI_t\left(\frac{\varphi_A^{"}}{k}\sinh kL + \frac{T_A}{k^2EI_w}\left(\cosh kL - 1\right) + \frac{T_0}{k^2EI_w}\left[\cosh k\left(L-a\right) - 1\right]\right)$$



Concentrated Moment T_0 at an intermediate section with zero torsional rotation and free warping at the ends

$$\varphi_A = \varphi_A^{"} = 0$$
$$\varphi_B = \varphi_B^{"} = 0$$

$$T_A = -T_0\left(1 - \frac{a}{L}\right) \qquad T_B = -T_0\frac{a}{L}$$

$$\varphi_A^{'} = \frac{T_0}{k^2EI_w}\left(1 - \frac{a}{L} - \frac{\sinh k\left(L-a\right)}{\sinh kL}\right)$$

$$B_w\left(x\right) = -EI_w\left(\varphi_A^{'}k\sinh kx + \frac{T_A}{kEI_w}\sinh kx + \frac{T_0}{kEI_w}\sinh k\left\langle x-a\right\rangle\right)$$

$$T_w\left(x\right) = -EI_w\left(\varphi_A^{'}k^2\cosh kx + \frac{T_A}{EI_w}\cosh kx + \frac{T_0}{EI_w}\left\langle x-a\right\rangle^0\cosh k\left(x-a\right)\right)$$

$$T_t\left(x\right) = GI_t\left(\varphi_A^{'}\cosh kx + \frac{T_A}{k^2EI_w}\left(\cosh kx - 1\right) + \frac{T_0}{k^2EI_w}\left\langle x-a\right\rangle^0\left[\cosh k\left(x-a\right) - 1\right]\right)$$

Table A.4 (cont.) – Formulas for thin-walled elastic double-supported beams under a concentrated torsional moment

Section A:

$$B_w = 0 \qquad T_w = T_A - T_t \qquad T_t = T_0\left(1 - \frac{a}{L} - \frac{\sinh k\left(L-a\right)}{\sinh kL}\right)$$

Section 0:

$$B_w = -EI_w\left(\varphi_A' k \sinh ka + \frac{T_A}{kEI_w}\sinh ka\right)$$

$$T_w = EI_w\left(\varphi_A' k^2 \cosh ka + \frac{T_A}{EI_w}\cosh ka\right)$$

$$T_t = GI_t\left(\varphi_A' \cosh ka + \frac{T_A}{k^2 EI_w}\left(\cosh ka - 1\right)\right)$$

Section B ($x = L$):

$$B_w = 0 \qquad T_w = T_A - T_t \qquad T_t = T_0\left(1 - \frac{a}{L} - \frac{\sinh k\left(L-a\right)}{\sinh kL}\right)$$

A.2.2. Distributed torsional moment

The solution of the differential equation for a uniformly distributed torsional moment (equation (3.37)) is given by equation (3.38b). Alternatively (Roark and Young, 1976), it may be written as (Figure A.2):

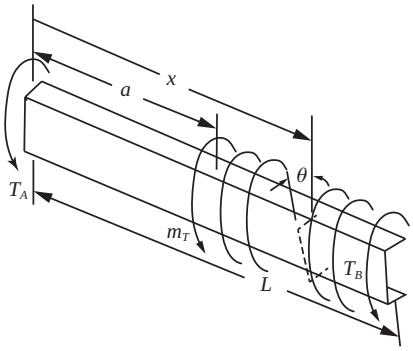


Figure A.2 – Generic open cross section beam subject to a uniformly distributed torsional moment

$$\varphi(x)=\varphi_A+\frac{\varphi_A^{'}}{k}\sinh kx+\frac{\varphi_A^{''}}{k^2}\left(\cosh kx-1\right)+\frac{T_A}{k^3EI_w}\Big[\langle x-a\rangle^0 \left(\cosh k\left(x-a\right)-1\right)-\frac{k^2}{2}\langle x-a\rangle^2\Big]+\frac{m_T(x)}{k^4EI_w}\left(\sinh k\langle x-a\rangle-k\langle x-a\rangle\right) \tag{A.5a}$$

$$\frac{d\varphi(x)}{dx}=\varphi_A^{'}\cosh kx+\frac{\varphi_A^{''}}{k}\sinh kx+\frac{T_A}{k^2EI_w}\left(\cosh kx-1\right)+\frac{m_T(x)}{k^3EI_w}\left(\sinh k\langle x-a\rangle-k\langle x-a\rangle\right) \tag{A.5b}$$

$$\frac{d^2\varphi(x)}{dx^2}=\varphi_A^{'}k\sinh kx+\varphi_A^{''}\cosh kx+\frac{T_A}{kEI_w}\sinh kx+\frac{m_T(x)}{k^2EI_w}\langle x-a\rangle^0\left[\cosh k\left(x-a\right)-1\right] \tag{A.5c}$$

$$\frac{d^3\varphi(x)}{dx^3}=\varphi_A^{'}k^2\cosh kx+\varphi_A^{''}k\sinh kx+\frac{T_A}{EI_w}\cosh kx+\frac{m_T(x)}{kEI_w}\sinh k\langle x-a\rangle \tag{A.5d}$$

with

$$T=T_A+m_T\langle x-a\rangle \tag{A.6}$$

$$k=\sqrt{\frac{GI_t}{EI_w}} \tag{A.7}$$

The bimoment and the warping and St. Venant torsional moments are given by:

$$B_w=-EI_w\frac{d^2\varphi}{dx^2}=-EI_w\left(\varphi_A^{'}k\sinh kx+\varphi_A^{''}\cosh kx+\frac{T_A}{kEI_w}\sinh kx+\frac{m_T(x)}{k^2EI_w}\langle x-a\rangle^0\left[\cosh k\left(x-a\right)-1\right]\right) \tag{A.8a}$$

$$T_w = -EI_w \frac{d^3\varphi}{dx^3} = -EI_w \left(\varphi_A' k^2 \cosh kx + \varphi_A'' k \sinh kx + \frac{T_A}{EI_w} \cosh kx + \right.$$
$$\left. + \frac{m_T(x)}{kEI_w} \sinh k\langle x-a \rangle \right) \tag{A.8b}$$

$$T_t = GI_t \frac{d\varphi}{dx} = GI_t \left(\varphi_A' \cosh kx + \frac{\varphi_A''}{k} \sinh kx + \frac{T_A}{k^2 EI_w} (\cosh kx - 1) + \right.$$
$$\left. + \frac{m_T(x)}{k^3 EI_w} (\sinh k\langle x-a \rangle - k\langle x-a \rangle) \right) \tag{A.8c}$$

Table A.5 presents the formulas for cantilevers with two distinct boundary conditions subject to a uniformly distributed torsional moment.

Table A.5 – Formulas for thin-walled elastic cantilevers under uniformly distributed torsional moment

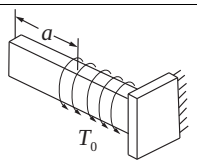
	Concentrated Moment T_0 at an intermediate section with free warping at the free end and zero torsional rotation and zero warping at the built-in end
$\varphi_A'' = 0$ $\varphi_B = \varphi_B' = 0$	
$T_A = 0 \qquad T_B = -T_0$ $\varphi_A = \frac{m_T}{k^4 EI_w} \left(\frac{\sinh kL(\sinh k(L-a) - k(L-a))}{\cosh kL} - (\cosh k(L-a) - 1) + \frac{k^2}{2}(L-a)^2 \right)$ $\varphi_A' = -\frac{m_T}{k^3 EI_w} \left(\frac{\sinh k(L-a) - k(L-a)}{\cosh kL} \right)$	
$B_w(x) = -EI_w \left(\varphi_A' k \sin kx + \frac{T_A}{kEI_w} \sinh kx + \frac{m_T}{k^2 EI_w} \langle x-a \rangle^0 (\cosh k(x-a) - 1) \right)$ $T_w(x) = -EI_w \left(\varphi_A' k^2 \cosh kx + \frac{T_A}{EI_w} \cosh kx + \frac{m_T}{kEI_w} \sinh k\langle x-a \rangle \right)$	

Table A.5 (cont.) – Formulas for thin-walled elastic cantilevers under uniformly distributed torsional moment

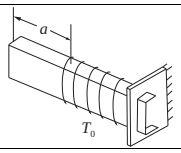
<table>
<tr><td colspan="2">$$T_t(x)=GI_t\left(\varphi_A^{'}\cosh kx+\frac{T_A}{k^2EI_w}\left(\cosh kx-1\right)+\frac{m_T}{k^3EI_w}\left(\sinh k\langle x-a\rangle-k\langle x-a\rangle\right)\right)$$</td></tr>
<tr><td colspan="2">Section A ($x = 0$):
$$B_w=0 \quad T_w=\frac{m_T}{k}\left(\frac{\sinh k(L-a)-k(L-a)}{\cosh kL}\right) \quad T_t=-\frac{m_T}{k}\left(\frac{\sinh k(L-a)-k(L-a)}{\cosh kL}\right)$$
Section 0 ($x = a$):
$$B_w=\frac{m_T}{k^2}\left(\frac{\sinh k(L-a)-k(L-a)}{\cosh kL}\sinh ka\right)$$
$$T_w=\frac{m_T}{k}\left(\frac{\sinh k(L-a)-k(L-a)}{\cosh kL}\cosh ka\right) \qquad T_t=-T_w$$</td></tr>
<tr><td colspan="2">Section B ($x = L$):
$$B_w=\frac{m_T}{k^2}\left(\frac{\sinh k(L-a)-k(L-a)}{\cosh kL}\sinh kL-\cosh k(L-a)+1\right)$$
$$T_w=-m_T(L-a) \qquad T_t=0$$</td></tr>
<tr><td> 
</td><td>Concentrated Moment T_0 at the free end with free warping at the free end and zero torsional rotation and free warping at the built-in end</td></tr>
<tr><td colspan="2">$$\varphi_A^{''}=0$$
$$\varphi_B=\varphi_B^{''}=0$$</td></tr>
<tr><td colspan="2">$$T_A=0 \qquad T_B=-T_0(L-a)$$
$$\varphi_A=\frac{m_T}{2k^2EI_w}(L-a)^2$$
$$\varphi_A^{'}=-\frac{m_T}{k^3EI_w}\left(\frac{\cosh k(L-a)-1}{\sinh kL}\right)$$</td></tr>
</table>

Table A.5 (cont.) – Formulas for thin-walled elastic cantilevers under uniformly distributed torsional moment

$$B_w(x) = -EI_w\left(\varphi_A' k\sin kx + \frac{T_A}{kEI_w}\sinh kx + \frac{m_T}{k^2EI_w}\langle x-a\rangle^0\left(\cosh k(x-a)-1\right)\right)$$

$$T_w(x) = -EI_w\left(\varphi_A' k^2\cosh kx + \frac{T_A}{EI_w}\cosh kx + \frac{m_T}{kEI_w}\sinh k\langle x-a\rangle\right)$$

$$T_t(x) = GI_t\left(\varphi_A'\cosh kx + \frac{T_A}{k^2EI_w}\left(\cosh kx-1\right) + \frac{m_T}{k^3EI_w}\left(\sinh k\langle x-a\rangle - k\langle x-a\rangle\right)\right)$$

Section A ($x = 0$):

$$B_w = 0 \qquad T_w = \frac{m_T}{k}\left(\frac{\cosh k(L-a)-1}{\sinh kL}\right) \qquad T_t = -T_w$$

Section 0 ($x = a$):

$$B_w = \frac{m_T}{k^2}\left(\frac{\cosh k(L-a)-1}{\sinh kL}\sinh ka\right)$$

$$T_w = \frac{m_T}{k}\left(\frac{\cosh k(L-a)-1}{\sinh kL}\cosh ka\right) \qquad T_t = -T_w$$

Section B ($x = L$):

$$B_w = 0$$

$$T_w = \frac{m_T}{k}\left(\frac{\cosh k(L-a)-1}{\sinh kL}\cosh kL - \sinh k(L-a)\right)$$

$$T_t = -\frac{m_T}{k}\left(\frac{\cosh k(L-a)-1}{\sinh kL}\cosh kL - \left(\sinh k(L-a) - k(L-a)\right)\right)$$

Table A.6 presents the formulas for simply-supported beams with two distinct boundary conditions subject to a uniformly distributed torsional moment.

Table A.6 – Formulas for thin-walled elastic double-supported beams under uniformly distributed torsional moment

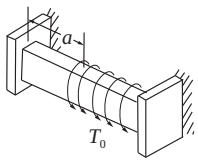
	Concentrated Moment T_0 at an intermediate section with zero torsional rotation and zero warping at the ends
$\varphi_A = \varphi_A^{'} = 0$ $\varphi_B = \varphi_B^{'} = 0$	
$T_A = -\frac{m_T}{k}\frac{\sin kL\left(\cosh k(L-a)-1-\frac{k^2}{2}(L-a)^2\right)-(\cosh kL-1)\left(\sinh k(L-a)-k(L-a)\right)}{\sinh kL(\sinh kL-kL)-(\cosh k(L-a)-1)^2}$ $= -\frac{m_T}{k}A_1$ $T_B = -T_0 - T_A$ $\varphi_A^{''} = \frac{m_T}{k^2 EI_w}\frac{(\cosh kL-1)\left(\cosh k(L-a)-1-\frac{k^2}{2}k(L-a)^2\right)-(\sinh kL-kL)\left(\sinh k(L-a)-k(L-a)\right)}{\sinh kL(\sinh kL-kL)-(\cosh k(L-a)-1)^2}$ $= \frac{m_T}{k^2 EI_w}A_2$	
$B_w(x) = -EI_w\left(\varphi_A^{''}\cosh kx + \frac{T_A}{kEI_w}\sinh kx + \frac{m_T(x)}{k^2 EI_w}\langle x-a\rangle^0\left[\cosh k(x-a)-1\right]\right)$ $T_w(x) = -EI_w\left(\varphi_A^{''}k\sinh kx + \frac{T_A}{EI_w}\cosh kx + \frac{m_T(x)}{kEI_w}\sinh k\langle x-a\rangle\right)$ $T_t(x) = GI_t\left(\frac{\varphi_A^{''}}{k}\sinh kx + \frac{T_A}{k^2 EI_w}(\cosh kx-1) + \frac{m_T(x)}{k^3 EI_w}\left(\sinh k\langle x-a\rangle - k\langle x-a\rangle\right)\right)$	
Section A ($x = 0$): $B_w = -\frac{m_T}{k^2}A_2 \qquad T_w = -T_A \qquad T_t = 0$	

Table A.6 (cont.) – Formulas for thin-walled elastic double-supported beams under uniformly distributed torsional moment

Section 0 ($x = a$)[l]:

$$B_w = -\frac{m_T}{k^2}\left(A_2 \cosh ka - A_1 \sinh ka\right)$$

$$T_w = -\frac{m_T}{k}\left(A_2 \sinh ka - A_1 \cosh ka\right)$$

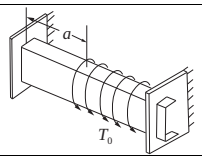
$$T_t = \frac{m_T}{k}\left(A_2 \sinh ka - A_1\left(\cosh ka - 1\right)\right)$$

Section B ($x = L$):

$$B_w = -\frac{m_T}{k^2}\left(A_2 \cosh kL - A_1 \sinh kL + \left(\cosh k\left(L-a\right) - 1\right)\right)$$

$$T_w = -\frac{m_T}{k}\left(A_2 \sinh kL - A_1 \cosh kL + \sinh k\left(L-a\right)\right)$$

$$T_t = \frac{m_T}{k}\left(A_2 \sinh kL - A_1\left(\cosh kL - 1\right) + \left(\sinh k\left(L-a\right) - k\left(L-a\right)\right)\right)$$



Concentrated Moment T_0 at an intermediate section with zero torsional rotation and free warping at the ends

$$\varphi_A = \varphi_A'' = 0$$

$$\varphi_B = \varphi_B'' = 0$$

$$T_A = -\frac{m_T}{2L}\left(L-a\right)^2 \qquad \varphi_A' = \frac{m_T}{k^3 EI_w}\left(\frac{k}{2L}\left(L-a\right)^2 - \frac{\cosh k\left(L-a\right) - 1}{\sinh kL}\right)$$

$$B_w = -EI_w\left(\varphi_A' k \sinh kx + \frac{T_A}{kEI_w}\sinh kx + \frac{m_T\left(x\right)}{k^2 EI_w}\left\langle x-a\right\rangle^0\left[\cosh k\left(x-a\right) - 1\right]\right)$$

$$T_w = -EI_w\left(\varphi_A' k^2 \cosh kx + \frac{T_A}{EI_w}\cosh kx + \frac{m_T\left(x\right)}{kEI_w}\sinh k\left\langle x-a\right\rangle\right)$$

$$T_t = GI_t\left(\varphi_A' \cosh kx + \frac{T_A}{k^2 EI_w}\left(\cosh kx - 1\right) + \frac{m_T\left(x\right)}{k^3 EI_w}\left(\sinh k\left\langle x-a\right\rangle - k\left\langle x-a\right\rangle\right)\right)$$

Table A.6 (cont.) – Formulas for thin-walled elastic double-supported beams under uniformly distributed torsional moment

Section A ($x = 0$):

$$B_w = 0 \qquad T_w = -\frac{m_T}{k}\left(\frac{k}{2L}(L-a)^2 - \frac{\cosh k(L-a)-1}{\sinh kL} - \frac{k}{2}\frac{(L-a)^2}{L}\right)$$

$$T_t = \frac{m_T}{k}\left(\frac{k}{2L}(L-a)^2 - \frac{\cosh k(L-a)-1}{\sinh kL}\right)$$

Section 0 (x = a):

$$B_w = -\frac{m_T}{k}\left(\left(\frac{k}{2L}(L-a)^2 - \frac{\cosh k(L-a)-1}{\sinh kL}\right)\sinh ka - \frac{k(L-a)^2}{2L}\sinh ka\right)$$

$$T_w = -\frac{m_T}{k}\left(\left(\frac{k}{2L}(L-a)^2 - \frac{\cosh k(L-a)-1}{\sinh kL}\right)\cosh ka - \frac{k(L-a)^2}{2L}\cosh ka\right)$$

$$T_t = \frac{m_T}{k}\left(\left(\frac{k}{2L}(L-a)^2 - \frac{\cosh k(L-a)-1}{\sinh kL}\right)\cosh ka - \frac{k(L-a)^2}{2L}(\cosh ka - 1)\right)$$

Section B ($x = L$):

$$B_w = 0$$

$$T_w = -\frac{m_T}{k}\left(\left(\frac{k}{2L}(L-a)^2 - \frac{\cosh k(L-a)-1}{\sinh kL}\right)\cosh kL - \right.$$
$$\left. - \frac{k}{2L}(L-a)^2\cosh kL + \sinh k(L-a)\right)$$

$$T_t = \frac{m_T}{k}\left(\left(\frac{k}{2L}(L-a)^2 - \frac{\cosh k(L-a)-1}{\sinh kL}\right)\cosh kL - \right.$$
$$\left. - \frac{k}{2L}(L-a)^2(\cosh kL - 1) + \sinh k(L-a) - k(L-a)\right)$$

Annex B

ELASTIC CRITICAL MOMENT

B.1. ABACUS TO CALCULATE THE COEFFICIENTS C_1, C_2 AND C_3

Obtained from the ECCS publication nº 119 (Boissonade *et al*, 2006)

B.1.1. Elastic critical moment in beams submitted to end moments simultaneously with transverse loads

In equation (3.120) the coefficients C_1 and C_2 are obtained from Figures B1 to B8 depending on the parameters Ψ and μ, for double-symmetric cross sections.

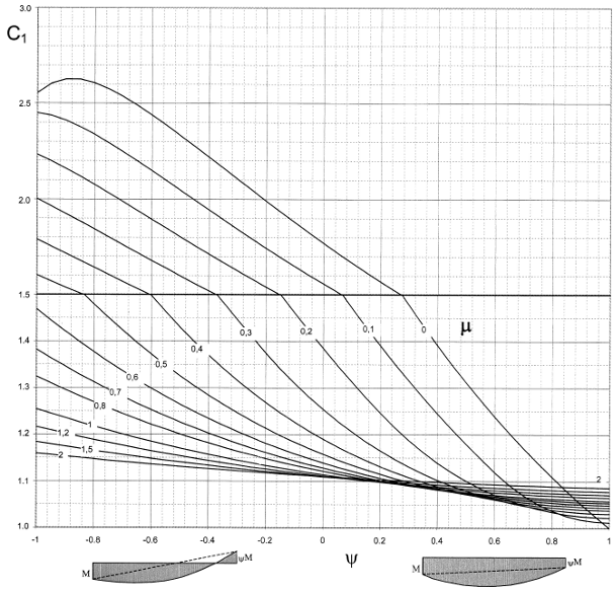


Figure B1 – C_1 coefficient for end moment and uniform load, with $\mu > 0$

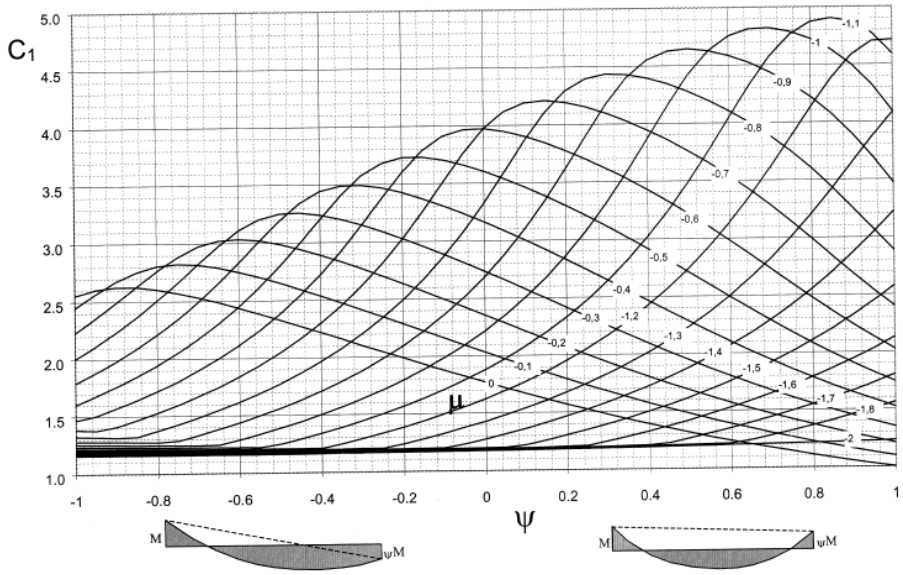


Figure B2 – C_1 coefficient for end moment and uniform load, with $\mu < 0$

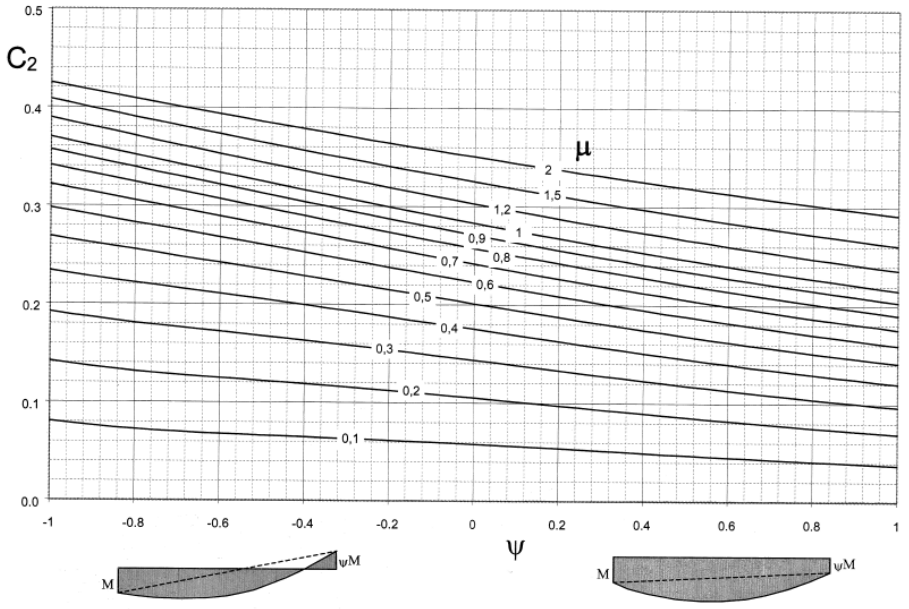


Figure B3 – C_2 coefficient for end moment and uniform load, with $\mu > 0$

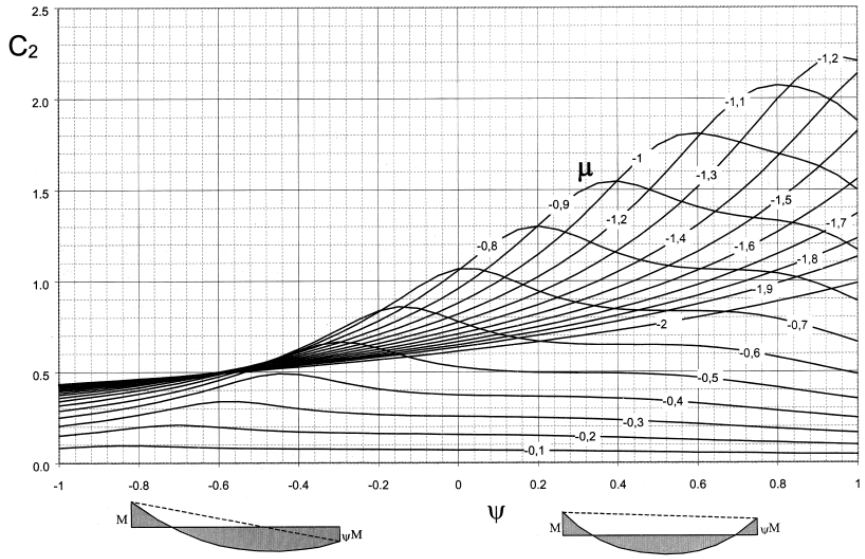


Figure B4 – C_2 coefficient for end moment and uniform load, with $\mu < 0$

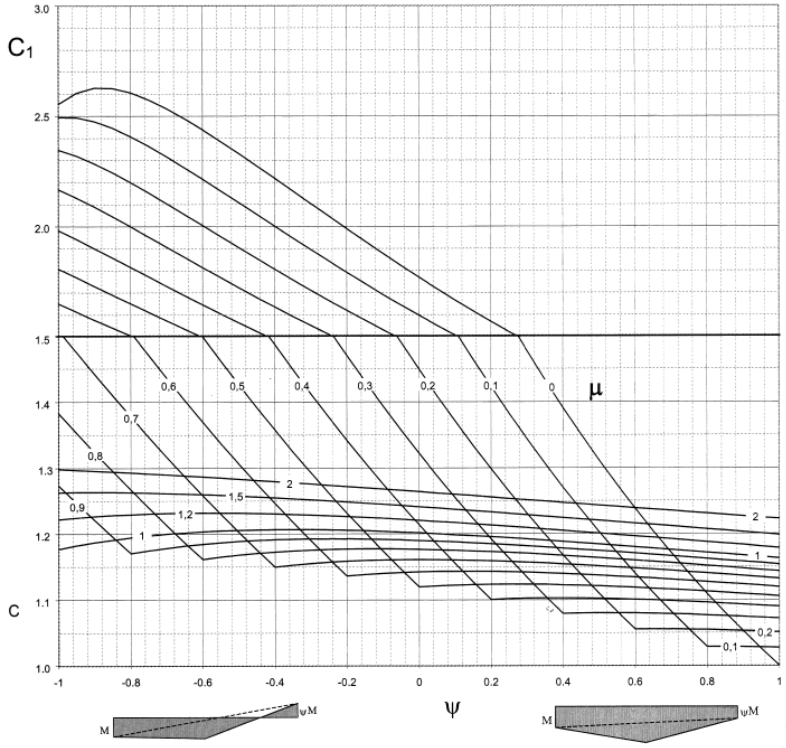


Figure B5 – C_1 coefficient for end moment and point load at mid span, with $\mu > 0$

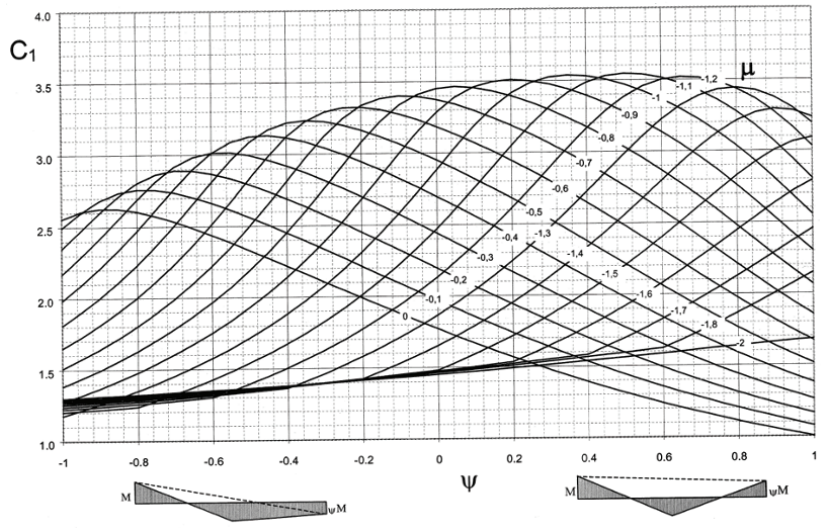


Figure B6 – C_1 coefficient for end moment and point load at mid span, with $\mu < 0$

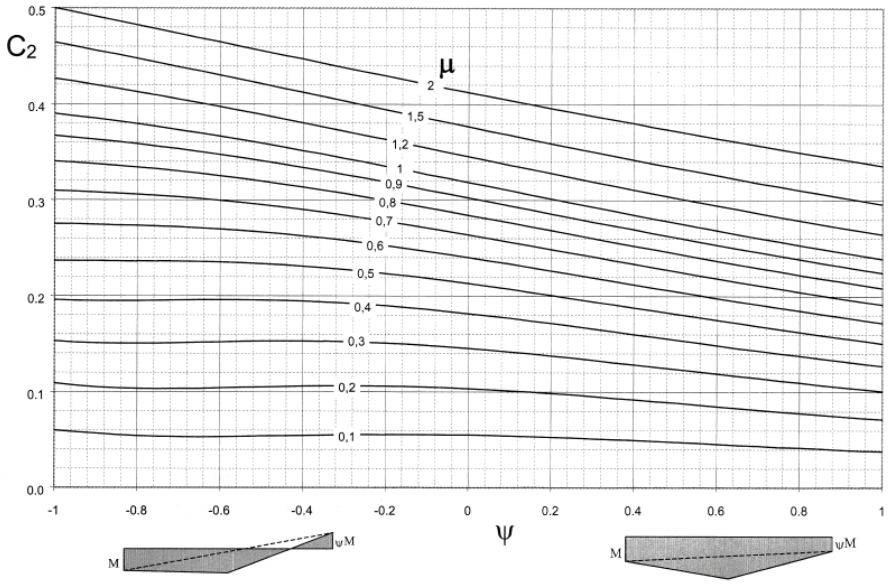


Figure B7 – C_2 coefficient for end moment and point load at mid span, with $\mu > 0$

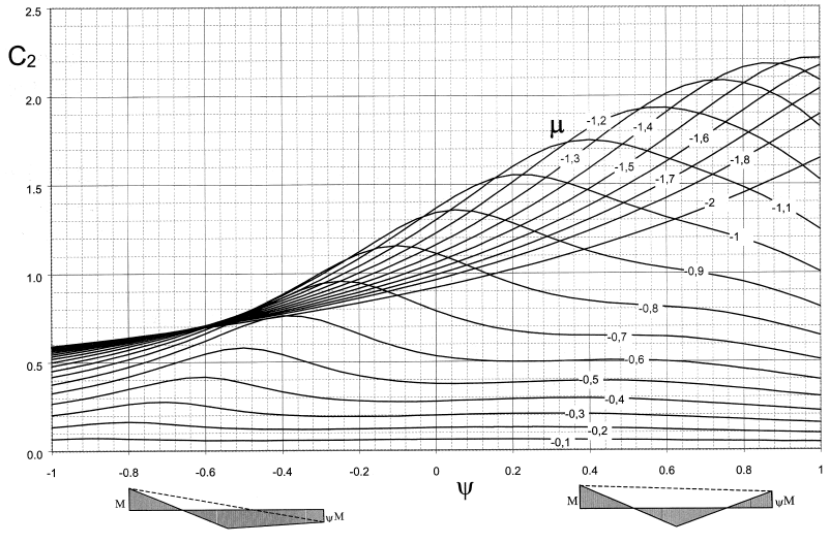


Figure B8 – C_2 coefficient for end moment and point load at mid span, with $\mu < 0$

B.1.2. Elastic critical moment of unbraced cantilevers

In equation (3.120) the effective length factors k_z and k_w are equal to 2 and 1 respectively in both cases. The solution is limited to the range $0.1 \le \overline{K} \le 2.5$, where:

$$\overline{K} = \frac{\pi}{L}\sqrt{\frac{EI_z h_s^2}{4GI_t}}$$

– **Cantilever with warping prevented at the fixed end**

Table B.1 – Values of C_1 and C_2 for cantilevers with warping prevented at the fixed end

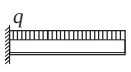
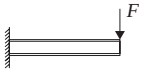
Loading	**Values of coefficients**		
	C_1	C_2	
		Top flange loading	**Bottom flange loading**
	$\frac{2.462}{\sqrt{1+\overline{K}^2}}+\frac{2.383\overline{K}}{\sqrt{1+\overline{K}^2}}$	$0.380+2.092\overline{K}-0.318\overline{K}^2$	$0.512+0.370\overline{K}-0.033\overline{K}^2$
	$\frac{3.962}{\sqrt{1+\overline{K}^2}}+\frac{5.531\overline{K}}{\sqrt{1+\overline{K}^2}}$	$1.130+1.539\overline{K}-0.176\overline{K}^2$	$1.049+0.234\overline{K}+0.020\overline{K}^2$

Table B.2 – Values of C_3 for cantilevers with warping prevented at the fixed end

Loading		Values of coefficients
		C_3
	**Top flange loading**	$1.520 - 1.342\psi_f - 0.010\psi_f^2 - 0.424\psi_f^3 + \left(0.162 + 2.419\psi_f + 0.875\psi_f^2 + 0.400\psi_f^3\right)\overline{K} + (0.148 - 0.623\psi_f - 0.216\psi_f^2 + 0.141\psi_f^3)\overline{K}^2$
	Shear center loading	$1.808 - 0.944\psi_f + 0.299\psi_f^2 - 0.061\psi_f^3 + \left(0.060 + 1.235\psi_f - 0.574\psi_f^2 - 0.337\psi_f^3\right)\overline{K} + \left(0.128 - 0.409\psi_f + 0.047\psi_f^2 + 0.237\psi_f^3\right)\overline{K}^2$
	Bottom flange loading	$1.966 - 0.792\psi_f + 0.139\psi_f^2 - 0.341\psi_f^3 + \left(0.061 + 0.549\psi_f + 0.077\psi_f^2 - 0.206\psi_f^3\right)\overline{K} + \left(0.064 - 0.135\psi_f - 0.050\psi_f^2 + 0.058\psi_f^3\right)\overline{K}^2$
	**Top flange loading**	$2.441 - 1.589\psi_f + 0.176\psi_f^2 - 0.658\psi_f^3 + \left(-0.412 + 2.442\psi_f + 0.635\psi_f^2 + 0.261\psi_f^3\right)\overline{K} + \left(0.273 - 0.601\psi_f - 0.140\psi_f^2 + 0.205\psi_f^3\right)\overline{K}^2$
	Shear center loading	$2.609 - 1.801\psi_f + 0.552\psi_f^2 + 0.461\psi_f^3 + \left(-0.445 + 2.251\psi_f - 0.620\psi_f^2 - 0.1443\psi_f^3\right)\overline{K} + \left(0.244 - 0.701\psi_f - 0.044\psi_f^2 + 0.611\psi_f^3\right)\overline{K}^2$
	Bottom flange loading	$2.793 - 1.235\psi_f + 0.428\psi_f^2 - 0.630\psi_f^3 + \left(-0.495 + 1.008\psi_f - 0.134\psi_f^2 - 0.095\psi_f^3\right)\overline{K} + \left(0.194 - 0.263\psi_f - 0.003\psi_f^2 + 0.060\psi_f^3\right)\overline{K}^2$
ψ_f is limited to the range $-0.8 \le \psi_f \le 0.8$.		

– Cantilever with warping free at the fixed end

Table B.3 – Values of C_1 and C_2 for cantilevers with warping free at the fixed end

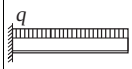
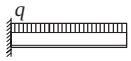
Loading	Values of coefficients		
	C_1	C_2	
		Top flange loading	Bottom flange loading
	$\frac{2.437}{\sqrt{1+\overline{K}^2}}+\frac{0.613\overline{K}}{\sqrt{1+\overline{K}^2}}-\frac{0.105\overline{K}^2}{\sqrt{1+\overline{K}^2}}$	$0.409+1.444\overline{K}+0.070\overline{K}^2$	$0.529+0.234\overline{K}+0.149\overline{K}^2$
	$\frac{3.840}{\sqrt{1+\overline{K}^2}}+\frac{1.496\overline{K}}{\sqrt{1+\overline{K}^2}}-\frac{0.247\overline{K}^2}{\sqrt{1+\overline{K}^2}}$	$0.987+1.420\overline{K}+0.165\overline{K}^2$	$1.028+0.388\overline{K}+0.150\overline{K}^2$

Table B.4 – Values of C_3 for cantilevers with warping free at the fixed end

Loading		Values of coefficients
		C_3
	**Top flange loading**	$1.732-0.648\psi_f-0.062\psi_f^2+0.059\psi_f^3+$ $+\left(0.066+1.539\psi_f+0.520\psi_f^2-0.032\psi_f^3\right)\overline{K}+$ $+\left(0.446+0.221\psi_f-0.037\psi_f^2+0.066\psi_f^3\right)\overline{K}^2$
	Shear center loading	$2.021+0.361\psi_f+0.176\psi_f^2-0.655\psi_f^3+$ $+\left(0.242+0.120\psi_f-0.426\psi_f^2+0.891\psi_f^3\right)\overline{K}+$ $+\left(0.337+0.052\psi_f-0.198\psi_f^2-0.099\psi_f^3\right)\overline{K}^2$
	Bottom flange loading	$2.156-0.055\psi_f+0.101\psi_f^2-0.079\psi_f^3+$ $+\left(0.435+0.168\psi_f-0.083\psi_f^2+0.077\psi_f^3\right)\overline{K}+$ $+\left(0.238-0.022\psi_f-0.011\psi_f^3-0.030\psi_f^3\right)\overline{K}^2$

Table B.4 (cont.) – Values of C_3 for cantilevers with warping free at the fixed end

Loading		Values of coefficients
		C_3
	**Top flange loading**	$2.669 - 0.815\psi_f + 0.071\psi_f^2 - 0.066\psi_f^3 + \left(0.113 + 1.812\psi_f + 0.359\psi_f^2 + 0.007\psi_f^3\right)\overline{K} + \left(0.499 + 0.289\psi_f + 0.043\psi_f^2 + 0.081\psi_f^3\right)\overline{K}^2$
	Shear center loading	$3.036 + 0.310\psi_f + 0.306\psi_f^2 - 0.888\psi_f^3 + \left(0.066 + 0.036\psi_f - 0.585\psi_f^2 + 1.180\psi_f^3\right)\overline{K} + \left(0.462 + 0.098\psi_f - 0.227\psi_f^2 - 0.123\psi_f^3\right)\overline{K}^2$
	Bottom flange loading	$3.277 - 0.350\psi_f + 0.348\psi_f^2 - 0.263\psi_f^3 + \left(0.190 + 0.348\psi_f - 0.195\psi_f^2 - 1.137\psi_f^3\right)\overline{K} + \left(0.395 + 0.071\psi_f - 0.009\psi_f^2 + 0.009\psi_f^3\right)\overline{K}^2$
ψ_f is limited to the range $-0.8 \le \psi_f \le 0.8$.		

B.2. ALTERNATIVE EQUATIONS FOR THE DETERMINATION OF THE ELASTIC CRITICAL MOMENT

According to Trahair (1993), the critical moment between laterally braced cross sections of beams of doubly symmetric transverse section, such as I or H sections, subject to bending around the strong axis (y axis), for several types of loadings applied at the shear centre of the cross sections, can be estimated by multiplying the elastic critical moment for constant bending moment (M_{cr}^E obtained from equation (3.119)) by a factor α_m defined in Table B.5:

$$M_{cr} = \alpha_m M_{cr}^E . \tag{B.1}$$

Equation (B.1) assumes that the extreme sections (supports or other laterally braced cross sections) prevent lateral displacements and twisting but allow warping and bending rotations around the cross sectional axes (*y* and *z*). In case of enhanced support conditions that are totally or partially

restrained against lateral bending or warping, the critical moment can also be conservatively obtained using equation (B.1).

The point of application of the loads relatively to the shear centre of the cross section has a significant influence in the value of the critical moment. In the case of simply supported I or H beams, with concentrated loads at half-span or uniformly distributed loads then, according to Trahair (1993), the critical moment can be estimated through the following equation:

$$M_{cr} = \alpha_m M_{cr}^E \left\{ \sqrt{1 + \left(\frac{0.4\alpha_m y_Q}{M_{cr}^E / N_{cr,z}} \right)^2} + \frac{0.4\alpha_m y_Q}{M_{cr}^E / N_{cr,z}} \right\}, \qquad \text{(B.2)}$$

where α_m is given by α_m = 1.35 for a central concentrated load and α_m = 1.13 for a uniform distributed load, y_Q is the distance between the point of application of the loads and the centroid (in this case it coincides with the shear centre), and $N_{cr,z} = \pi^2 E I_z / L^2$, where I_z the second moment of area in relation to z and L is the distance between laterally braced sections. For gravity loads, the y_Q distance must be taken as negative or positive depending on the loads being applied above or below the shear centre.

Table B.5 – Factors for the calculation of the critical moment in spans of beams with length L and doubly symmetric section

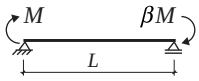
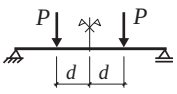
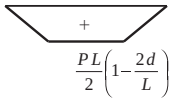
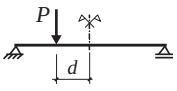
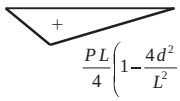
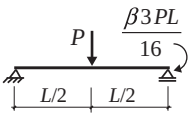
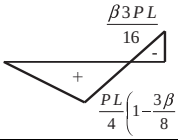
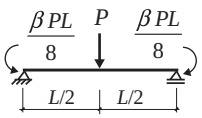
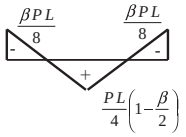
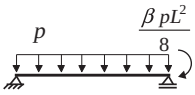
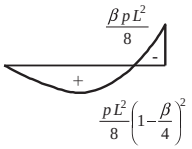
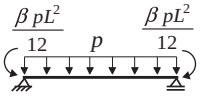
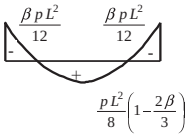
Member	Diagram of moments	α_m	Validity limits
		$1.75 + 1.05\beta + 0.3\beta^2 \le 2.5$	$-1 \le \beta \le 1$
		$1.0 + 0.35\left(1 - 2d/L\right)^2$	$0 \le \dfrac{2d}{L} \le 1$
		$1.35 + 0.4\left(2d/L\right)^2$	$0 \le \dfrac{2d}{L} \le 1$
		$1.35 + 0.15\beta$	$0 \le \beta \le 0.89$
		$-1.2 + 3\beta$	$0.89 \le \beta \le 1$

Table B.5 (cont.) – Factors for the calculation of the critical moment in spans of beams with length L and doubly symmetric section

Member	Diagram of moments	α_m	Validity limits
		$1.35+0.36\beta$	$0 \le \beta \le 1$
		$1.13+0.10\beta$	$0 \le \beta \le 0.7$
		$-1.25+3.5\beta$	$0.7 \le \beta \le 1$
		$1.13+0.12\beta$	$0 \le \beta \le 0.75$
		$-2.38+4.8\beta$	$0.75 \le \beta \le 1$

In cantilever beams under a concentrated load at the free end or under a linearly distributed load along the span, the elastic critical moment can be estimated from equations (B.3) and (B.4), respectively (Trahair, 1993).

$$M_{cr} = 11\frac{\sqrt{EI_z GI_T}}{L}\left[1+\frac{1.2\varepsilon}{\sqrt{1+1.44\varepsilon^2}}\right]+ 4\left(K-2\right)\frac{\sqrt{EI_z GI_T}}{L}\left[1+\frac{1.2\left(\varepsilon-0.1\right)}{\sqrt{1+1.44\left(\varepsilon-0.1\right)^2}}\right]; \quad \text{(B.3)}$$

$$M_{cr} = 27\frac{\sqrt{EI_z GI_T}}{L}\left[1+\frac{1.4\left(\varepsilon-0.1\right)}{\sqrt{1+1.96\left(\varepsilon-0.1\right)^2}}\right]+ 10\left(K-2\right)\frac{\sqrt{EI_z GI_T}}{L}\left[1+\frac{1.3\left(\varepsilon-0.1\right)}{\sqrt{1+1.69\left(\varepsilon-0.1\right)^2}}\right]; \quad \text{(B.4)}$$

where the parameters ε and K are defined by:

$$\varepsilon = \frac{2y_Q}{h_m}\frac{K}{\pi} \quad \text{and} \quad K = \sqrt{\frac{\pi^2 E\, I_W}{G\, I_T\, L^2}} \tag{B.5}$$

and h_m is the distance between the centres of the flanges, see Figure 3.37 and the remaining symbols are as defined previously.

REFERENCES

Allen HG, Bulson PS (1980). *Background to Buckling*, McGraw-Hill, Maidenhead, Berkshire, England.

Baker JF, Horne MR, Heyman J (1956). *The Steel Skeleton*, Vol. II, Cambridge University Press.

Beg D, Kuhlmann U and Davaine L (2010). *Design of plated structures*, ECCS Eurocode Design Manuals, ECCS Press / Ernst&Sohn.

Bjorhovde R (2004). Development and use of high performance steel, *Journal of Constructional Steel Research*, 60, 393-400.

Boissonnade N, Greiner R, Jaspart JP, Lindner J (2006). *New design rules in EN 1993-1-1 for member stability*, ECCS Technical Committee 8 – Structural Stability, P119, European Convention for Constructional Steelwork, Brussels.

Brown DG, King CM, Rackham JW, Way AGJ (2004). *Design of multi-storey braced frames*, P334, SCI.

BSI (2000). BS 5950-1:2000: Structural use of steelwork in building - Code of Practice for Design: rolled and welded sections, *British Standards Institution*, UK.

CEN (1990). EN 10045-1:1990 – Metallic materials – Charpy impact test. Part 1: Test method, *European Committee for Standardization*, Brussels.

CEN (1993). EN 10034:1993 – Structural steel I and H sections - Tolerances on shape and dimensions, *European Committee for Standardization*, Brussels.

CEN (2000). EN 10020: 2000 – Definition and classification of grades of steel, *European Committee for Standardization*, Brussels.

CEN (2002a). EN 1990:2002 – Eurocode, Basis of Structural Design, *European Committee for Standardization*, Brussels.

CEN (2002b). EN 1991-1-1:2002 – Eurocode 1: Actions on Structures – Part 1-1: General Actions – Densities, self-weight, imposed loads for buildings, *European Committee for Standardization*, Brussels.

CEN (2003). EN 1991-1-3: 2002 – Eurocode 1: Actions on Structures – Part 1-3: General Actions – Snow loads, *European Committee for Standardization*, Brussels.

CEN (2004a). EN 1998-1:2004 - Eurocode 8: Design of Structures for Earthquake Resistance – Part 1: General rules, seismic actions and rules for buildings, *European Committee for Standardization*, Brussels.

CEN (2004b). EN 10025-1:2004 – Hot rolled products of structural steels – Part 1: General technical delivery conditions, *European Committee for Standardization*, Brussels.

CEN (2004c). EN 10025-2:2004 – Hot rolled products of structural steels – Part 2: Technical delivery conditions for non-alloy structural steels, *European Committee for Standardization*, Brussels.

CEN (2004d). EN 10164:2004 – Steel products with improved deformation properties perpendicular to the surface of the product – Technical delivery conditions, *European Committee for Standardization*, Brussels.

CEN (2005a). EN 1993-1-1:2005 – Eurocode 3: Design of Steel Structures, Part 1-1: General rules and rules for buildings, *European Committee for Standardization*, Brussels.

CEN (2005b). EN 1993-1-8:2005 – Eurocode 3: Design of Steel Structures, Part 1.8: Design of joints, *European Committee for Standardization*, Brussels.

CEN (2005c). EN 1993-1-9:2005 – Eurocode 3: Design of Steel Structures, Part 1.9: Fatigue, *European Committee for Standardization*, Brussels.

CEN (2005d). EN 1993-1-10:2005 – Eurocode 3: Design of Steel Structures, Part 1.10: Material toughness and through-thickness properties, *European Committee for Standardization*, Brussels.

CEN (2005e). EN 1991-1-4:2005 – Eurocode 1: Actions on Structures – Part 1-4: General Actions – Wind actions, *European Committee for Standardization*, Brussels.

CEN (2006a). EN 10210-1:2006 – Hot finished structural hollow sections of non-alloy and fine grain steels – Part 1: Technical delivery conditions, *European Committee for Standardization*, Brussels.

CEN (2006b). EN 10219-1:2006 – Cold formed welded structural hollow sections of non-alloy and fine grain steels – Part 1: Technical delivery conditions, *European Committee for Standardization*, Brussels.

CEN (2006c). EN 1993-1-5:2006 – Eurocode 3: Design of Steel Structures, Part 1.5: Plated structural elements, *European Committee for Standardization*, Brussels.

CEN (2006d). EN 1993-2:2006 – Eurocode 3: Design of Steel Structures, Part 2: Steel bridges, *European Committee for Standardization*, Brussels.

CEN (2006e). EN 1993-1-11:2006 – Eurocode 3: Design of Steel Structures, Part 1-11: Design of structures with tension components, *European Committee for Standardization*, Brussels.

CEN (2007). EN 1993-1-6:2007, Eurocode 3: Design of Steel Structures, Part 1.6: General rules – Strength and stability of shell sructures, *European Committee for Standardization*, Brussels.

CEN (2009). EN ISO 6892-1, Metallic materials - Tensile testing - Part 1: Method of test at room temperature (ISO 6892-1:2009), *European Committee for Standardization*, Brussels.

CEN (2011). EN 1090-2:2008+A1:2011, Execution of steel structures and aluminium structures - Part 2: Technical requirements for steel structures, *European Committee for Standardization*, Brussels.

Cerfontaine F (2003). *Bending moment and axial force interaction in bolted joints*, PhD Thesis, Université de Liège.

Chen WF, Atsuta T (1977). *Theory of Beam Columns: Space Behavior and Design*, Vol. 2, McGraw-Hill

Chen WF, Lui EM (1987). *Structural Stability, Theory and Implementation*, Elsevier, New York.

Clark JW, Hill HN (1960). Lateral Buckling of Beams, *Proceedings ASCE, Journal of the Structural Division*, vol. 68, nº ST7.

Davies JM, Brown BA (1996). *Plastic Design to BS 5950*, The Steel Construction Institute, Blackwell, London.

Demonceau J-F (2008). *Steel and composite building frames: sway response under conventional loading and development of membranar effects in beams further to an exceptional action*, PhD Thesis, Université de Liège.

Dowling PJ (1992). EC3: the new Eurocode for steel structures, *IABSE Conference: Structural Eurocodes*, Davos, 159-166.

ECCS (1976). *Manual on stability of steel structures*, 2nd Edition, P022, ECCS Technical Committee 8 – Structural Stability, European Convention for Constructional Steelwork, Brussels.

ECCS (1977). *European recommendations for steel construction*, P023, European Convention for Constructional Steelwork, Brussels.

Franssen JM, Vila Real P (2015). *Fire design of steel structures – second edition*, ECCS Eurocode Design Manuals, ECCS Press / Ernst&Sohn.

Galéa Y (1981). Abaques de Deversement Pour Profilés Laminés, *Construction Métallique*, 4, 39-51.

Galéa Y (1986). Deversement des barres à section en I bissymétriques et hauteur d'âme bilinéairement variable, *Construction Métallique*, 23(2), 50-54.

Gardner L, Nethercot DA (2005). *Designers' Guide to EN 1993-1-1, Eurocode 3: Design of steel structures – General rules and rules for buildings*, Thomas Telford, SCI.

Gervásio H, Santos P, Simões da Silva L and Gameiro Lopes A (2010). "Influence of thermal insulation on the energy balance between embodied energy and operational energy in light-steel residential buildings", *Advanced Steel Construction*, 6(2), pp. 742-766 (2010).

Ghali A, Neville AM (1997). *Structural Analysis – A unified classical and matrix approach*, 4th edition, E&F Spon.

Gjelsvik A (1981). *The theory of thin walled bars*. New York: John Wiley & Sohns.

Gonçalves JM (2000). *Imperfeições "locais" em estruturas de aço – conceitos, resultados e reflexões (in Portuguese)*, MSc Thesis, Universidade Técnica de Lisboa, Portugal.

Greiner R, Lechner A (2007). Comparison of General Method with traditional methods – Part 2 – Example of a sway frame with the free unrestrained corners, *ECCS TC8 Stability*, TC8-2007-013, Brussels.

Greiner R, Ofner R (2007). Comparison of General Method with traditional methods – Example of a sway frame with lateral restraints, *ECCS TC8 Stability*, TC8-2007-006, Brussels.

Greiner R, Lechner A, Kettler M, Jaspart J-P, Weynand K, Ziller C, Oerder R, Herbrand M, Simões da Silva L and Dehan V. (2011). Design guidelines for cross-section and member design according to Eurocode 3 with particular focus on semi-compact sections, *Valorisation Project SEMI-COMP+*: *"Valorisation action of plastic member capacity of semi-compact steel sections – a more economic approach"*, RFS2-CT-2010-00023, Brussels.

Hensman JS, Way AGJ (2000). *Wind-moment design of unbraced composite frames*, P264, SCI.

Heyman (1971). *Plastic design of frames, Vol. 2*, Cambridge University Press, Cambridge.

Hill R (1950). *The mathematical theory of plasticity*, Oxford University Press.

Hirt MA, Bez R, Nussbaumer A (2006). *Construction Métallique – Notions Fondamentales et Méthodes de Dimensionnement*, Traité de Génie Civil, vol. 10, Presses Polytechniques et Universitaires Romandes, Lausanne.

Hirt MA, Crisinel M (2001). *Charpentes Métalliques – Conception et Dimensionnement des Halles et Bâtiments*, Traité de Génie Civil, vol. 11, Presses Polytechniques et Universitaires Romandes, Lausanne.

Horne MR (1963). Elastic-plastic failure loads of plane frames, *Proceedings of the Royal Society*, Vol. A, Part 274, 343-364.

Horne MR (1975). An Approximate Method for Calculating the Elastic Critical Loads of Multistorey Plane Frames, *The Structural Engineer*, Vol. 53, nº 6 (p.242).

Horne MR (1979). *Plastic Theory of Structures*, 2nd Ed., Pergamon Press.

Horne MR (1985). An Approximate Method for Calculating the Elastic Critical Loads of Multistorey Plane Frames, *The Structural Engineer*, Vol. 53, nº 6 (p.242).

Horne MR, Morris LJ (1981). *Plastic Design of Low-Rise Frames*, Constrado Monographs, Collins, London.

Horne MR, Shakir-Khalil H, Akhtar S (1979). The stability of tapered and haunched beams, *Proceedings of the Institution of Civil Engineers*, Part 2, 67, 677-694.

IPQ (2010). NA EN-1993-1-1:2005 – Eurocode 3: Design of Steel Structures, Part 1-1: General rules and rules for buildings, Portuguese National Annex. *Instituto Português da Qualidade*, Lisbon.

ISO/DIS 10137 (2006). Basis for design of structures – Serviceability of buildings against vibration, *International Organization for Standardization*.

Jaspart J-P (1991). *Etude de la semi-rigidité des noeuds poutre-colonne et son influence sur la resistance et la stabilité des ossatures en acier (in french)*. PhD Thesis, Université de Liège, Belgium.

Jaspart J-P, Weynand K (2016). *Design of joints in steel and composite structures*, ECCS Eurocode Design Manuals, ECCS Press / Ernst&Sohn.

Jordão S, Simões da Silva L, Simões R (2013). Behaviour of welded beam-to-column joints with beams of unequal depth, *Journal of Constructional Steel Research*, 91, 42-59, doi: 10.1016/j.jcsr.2013.07.023.

Kaim P (2004). *Spatial buckling behaviour of steel members under bending and compression*, PhD Thesis, Graz University of Technology, Austria.

King CM (2001a). *Design of steel portal frames for Europe*, P164, The Steel Construction Institute.

King CM (2001b). *In-plane stability of portal frames to BS 5950-1:2000*, P292, The Steel Construction Institute.

Kollbrunner CF and Basler K (1969). *Torsion in Structures*, Springer Verlag, Berlin.

Landolfo R, Mazzolani, F, Dubina D, Simões da Silva L and D'Aniello M (2016). *Design of steel structures for buildings in seismic areas*, ECCS Eurocode Design Manuals, ECCS Press / Ernst&Sohn.

Lawson RM, Ogden RG, Rackham JW (2004). *Steel in multi-storey residential buildings*, P332, SCI.

Lescouarc'h Y (1977). Capacité de résistance d'une section soumise à divers types de sollicitations, *Construction Métallique*, 23(2), 50-54.

Li Z, Schafer BW (2010). Buckling analysis of cold-formed steel members with general boundary conditions using CUFSM: conventional and constrained finite strip methods, *Proceedings of the 20th Int;l. Spec. Conf. on Cold-Formed Steel Structures*, St. Louis, MO. November, 2010.

Livesley RK, Chandler DB (1956). *Stability functions for structural steelworks*, Manchester University Press.

LTBeam (2010). *Lateral Torsional Buckling of Beams*, LTBeam version 1.0.11, CTICM, France.

LTBeamN (2015). *Lateral Torsional Buckling of Beam Columns*, LTBeamN version 1.0.1, CTICM, France.

Maquoi R, Rondal J (1978). Mise en équation des nouvelles courbes Européennes de flambement, *Construction Métallique*, (1), 17-30.

Mirambel E, Bordallo J, Real E (2016). Torsion and its interaction with other internal forces in EN 1993-1-1. A new approach, *Steel Construction – Design and Research 9* (2016), No. 3.

Müller C (2003). *Zum Nachweis ebener Tragwerke aus Stahl gegen seitliches Ausweichen*, PhD Thesis, RWTH Aachen, Germany.

Nadai A (1950). *Theory of Flow and Fracture of Solids*, McGraw-Hill.

Nakai H, Yoo CH (1988). *Analysis and Design of Curved Steel Bridges*, McGraw-Hill Book Company, New York.

Neal BG (1977). *The Plastic Methods of Structural Analysis*, Chapman and Hall.

Nogueiro P (2000). *Influence of the real behaviour of connections in pitch roof steel portal frames (in Portuguese)*, MSc Thesis, Universidade de Coimbra, Portugal.

OJ L 040 (1989). Construction Products Directive – Council Directive 89/106/EEC of 21 December 1988, *Official Journal of the European Union*, Brussels, 11/02/1989, 0012 – 0026.

OJ L 088 (2013). Construction Products Regulation – Council Directive 305/2011 of 09 March 2011, *Official Journal of the European Union*, Brussels, 04/04/2011, L 88/5 – L 88/43.

Roark RJ, Young WC (1976). *Formulas for Stress and Strain*, *5th edition*, McGraw-Hill.

Rotter JM, Schmidt H (2013). *Buckling of Steel Shells European Design Recommendations – 5th Edition- Revised second impression*, ECCS Press - P125-2, Brussels.

Salter PR, Malik AS, King CM (2004). *Design of single-span steel portal frames to BS 5950-1:2000*, P252, SCI.

Sedlacek G, Muller C (2006). The European standard family and its basis, *Journal of Constructional Steel Research*, 62, 1047–1059, doi:10.1016/j.jcsr. 2006.06.027.

Silvestre N, Camotim D (2005). Second order analysis and design of pitched-roof steel frames, in Shen ZY, Li GQ, Chan SL (eds.), *Advances in Steel Structures*, Elsevier, 225-232.

Silvestre N, Camotim D, (2000). In-plane stability and 2nd order effects in multi-bay pitched-roof steel frames. *Proceedings of SSRC 2000 Annual Technical Session and Meeting*. Memphis. 2000. p. 89–103.

Silvestre N, Mesquita A, Camotim D, Simões da Silva L (2000). In-Plane Buckling Behavior of Pitched-Roof Steel Frames with Semi-Rigid Connections, Frames with Partially Restrained Connections (Structural Stability Research Council (SSRC) 1998 Theme Conference Workshop Volume), Atlanta, pp. 21-34, 21-23 de September (1998), 2000.

Simões da Silva L (2005). "Current and future trends in steel construction: research and practice", Keynote Paper, in Hoffmeister, B. and Hechler, O. (eds.), *Eurosteel 2005 – 4th European Conference on Steel and*

Composite Structures - Research - Eurocodes - Practice, Druck und Verlagshaus Mainz GmbH, Aachen, vol. A, pp. 0.35-42.

Simões da Silva L (2008). Towards a consistent design approach for steel joints under generalized loading, *Journal of Constructional Steel Research*, 64(9), 1059-1075 (2008), doi: 10.1016/j.jcsr.2008.02.017.

Simões da Silva L, Lima L, Vellasco P, Andrade S (2004). Behaviour of flush end-plate beam-to-column joints subjected to bending and axial force, *International J. of Steel and Composite Structures* 4(2), 77-94.

Simões da Silva L, Rebelo C, Nethercot D, Marques L, Simões R and Vila Real P (2010a), Statistical evaluation of the lateral-torsional buckling resistance of steel I-beams - Part 2: Variability of steel properties, *Journal of Constructional Steel Research*, 65(4), pp. 832-849.

Simões da Silva, L., Marques, L. and Rebelo, C., (2010b). Numerical validation of the general method in EC3-1-1: lateral, lateral-torsional and bending and axial force interaction of uniform members, *Journal of Constructional Steel Research*, 66, pp. 575-590.

Sing KP (1969). *Ultimate behaviour of laterally supported beams*, University of Manchester.

Smith AL, Hicks SJ and Devine PJ (2007). *Design of floors for vibration*, P354, SCI.

Snijder B, Greiner R and Jaspart, J P (2006). Fields and limits of the application of the General Method, *ECCS TC8 Stability*, TC8-2006-015, Brussels.

Sofistik (2008). *SOFiSTik Aktiengesellschaft*, "ASE – General static analysis of finite element structures", version 01/2008, SOFiSTik AG, Oberschleissheim.

Strating J and Vos H (1973). Simulation sur ordinateur de la courbe CECM de flambement à l'aide de la méthode de Monte-Carlo, *Construction Métallique*, 2, 23-39.

Timoshenko S (1956). *Strength of Materials – Part II: Advanced*, International Student Editions, Van Nostrand Reinhold, 3rd edition.

Timoshenko S, Gere JM (1961). *Theory of Elastic Stability*, International Student Editions, McGraw-Hill.

Trahair, NS (1993). *Flexural-Torsional Buckling of Structures*, E & FN SPON, London.

Villette M (2004). *Analyse critique du traitement de la barre comprimée et fléchie et proposition de nouvelles formulations (in french)*. PhD Thesis, Université de Liège, Belgium.

Weaver W, Gere JM (1990). *Matrix analysis of framed structures*, Van Nostrand Reinhold, 3rd edition.

Weynand K, Jaspart JP, Steenhuis M (1995). The Stiffness Model of Revised Annex J of Eurocode 3, In: *Connections in Steel Structures III*, *Proceedings of the 3rd International Workshop on Connections* (eds.: Bjorhovde R, Colson A, Zandonini R), Trento, Italy, May 8-31, 441-452.

Weynand K, Oeder R, Jaspart J-P (2014). *COP – The Connection Program*, Program to design steel and composite joints in accordance with EC3 and EC4, Version 1.7.2, Feldmann + Weynand GmbH, Germany, http://cop.fw-ing.com.

Wood RH (1974). Effective Lengths of Columns in Multi-Storey Buildings, *The Structural Engineer*, Vol. 52, nº 7 (p.235), nº 8 (p.295), nº 9 (p.241).